Order Number 8804154

Structural style of the Laramide orogeny, Wyoming foreland. (Volumes I and II)

Brown, William Gregor, Ph.D.

University of Alaska Fairbanks, 1987

U·M·I
300 N. Zeeb Rd.
Ann Arbor, MI 48106

STRUCTURAL STYLE OF THE LARAMIDE OROGENY, WYOMING FORELAND

A

THESIS

Presented to the Faculty of the University of Alaska

in Partial Fulfillment of the Requirements

for the Degree of

DOCTOR OF PHILOSOPHY

By

William G. Brown, B.S., M.S.

Fairbanks, Alaska

May 1987

STRUCTURAL STYLE OF THE LARAMIDE OROGENY, WYOMING FORELAND

RECOMMENDED:

Chairman, Advisory Committee

Department Head

APPROVED:

Dean College of Natural Sciences

Director of Graduate Programs

15 April 1987

Date

ABSTRACT

This study documents the styles of Laramide structures of the Wyoming foreland, and presents an integrated synthesis of foreland development. Theoretical data and experimental results are compared to field observations, subsurface well control, and geophysical data to judge their application to the foreland.

The direction of collision (N40-50E) between the North American and Farallon plates represents the direction of maximum compressive stresses during the Laramide orogeny. A "tectonic front" progressed from west to east across the foreland during Campanian to middle Eocene time.

No single model of uplift applies throughout the foreland. Dips of basement faults vary with changes in strike (i. e. northwest strike: 20-45 degrees; north to north-northwest strike: 45-60 degrees; east to northeast strike: 60 degrees to vertical). Northwest-trending uplifts are fold-thrust structures exhibiting dual fault systems and rotated flanks. North-northwest trending uplifts are thrust uplift structures bounded by single reverse faults. East- and northeast-trending uplifts are drape folds and upthrust structures along which displacements were dominantly vertical.

The forms of Laramide structures were controlled by upward movement of basement forcing blocks, arrangement of lithology into mechanical packages, and deformational mechanisms which were determined by dominant lithology, applied stresses, and depth of burial. "Crowd" structures (i. e. back-limb, cross-crestal, and rabbit-ear folds) developed as volumetric adjustments in upward-tightening, parallel-folded synclines.

There is no consistent relationship between basement fabric and northwest-trending Laramide structures; however, reactivated Precambrian-age zones of weakness controlled east- and northeast-trending compartmental faults, which intersect and segment other trends. As a result, northwest-trending thrust and fold-thrust structures may change directions of asymmetry, be offset, or even replaced by other structural styles, while maintaining overall structural balance.

This study has documented approximately 30 miles of crustal shortening (representing 15% strain), which was pervasive and uniform across the foreland.

TABLE OF CONTENTS

Page

Page

LIST OF FIGURES

All figures are in Volume 2; page numbers coincide with figure numbers.

LIST OF TABLES

LIST OF APPENDICES

1.0 INTRODUCTION

1.1 Purpose

It is my intent to describe the style of the structures developed during the Laramide orogeny and which are best depicted in outcrop and in the subsurface of Wyoming. Therefore the purpose of this dissertation is four-fold:

1) The primary purpose is to demonstrate that the prevailing style of the northwest-trending Laramide structures follows the fold-thrust model of Berg (1962).

2) The second purpose is to document the controlling influence of certain structural features of the Precambrian basement rocks, on the development and geometry of foreland structures.

3) The third purpose is to describe and document the geometry of Laramide structures in the sedimentary section resulting from flexural slip fold mechanisms.

4) The final purpose is to present a geologically unified interpretation of the Laramide structural history of the Wyoming foreland. The predominantly northwest-trending thrust and fold-thrust structures, as well as the east and northeast-trending drape fold and upthrust structures, are all developed within a regional compressional system during the Laramide orogeny. I will demonstrate the compatibility of development of the upthrust and drape fold models of the vertical uplift

concept, with the thrust and fold-thrust models of horizontal compression.

All cross sections presented in this dissertation are "true scale", with the horizontal and vertical scales being equal, unless noted otherwise.

1.2 Definition of Wyoming Foreland

The term "Wyoming foreland" as used here refers to the area of basement-involved structures formed during the Laramide orogeny, lying east of the Wyoming overthrust belt, but excluding the Black Hills uplift (fig. 1; Lowell, 1974). The Wyoming foreland is a part of the larger Rocky Mountain foreland (fig. 2; Woodward, 1976) which includes the Precambrian-involved mountain ranges of Colorado, Montana, New Mexico, and Utah.

1.3 Definition of the Laramide Orogeny

The Laramide orogeny was first mentioned by Dana (1896) wherein he related it to the Laramie Formation, a coal-bearing sequence which is transitional from the marine Cretaceous rocks, indicating the early stage of uplift of the Rocky Mountains. The Uppermost Cretaceous Laramie Formation is overlain unconformably by Tertiary rocks. Jenkins (1943) defined the Laramide revolution (orogeny) as "a period of mountain building and erosion in

the Rocky Mountain region that began in Late Cretaceous time and ended in early Tertiary time."

Armstrong (1968) has shown that there was an overlap in timing of what he called the "Sevier orogeny" and the classic Laramide orogeny (fig. 3). Burchfiel and Davis (1975) have discussed concurrent development of Laramide age thin-skin thrusting in Mexico and basement-involved uplift in Wyoming. The time equivalency of these diverse structural styles is important to the understanding that there must be a common origin of these features. There is also an overlap of thin-skin and basement-involved deformation in space (e.g. in the Jackson Hole region of western Wyoming). For purposes of discussion, I will limit the term "Laramide" to those basement-involved features which developed in Late Cretaceous to Eocene time, and the subsidiary features related to them.

1.4 Methods of Investigation

My investigation of the Wyoming foreland began in 1958 when I was employed by the company which is now Chevron USA, and was assigned to study stratigraphic changes in the Upper Cretaceous, Paleocene, and Eocene rocks across Wyoming. Structural reconnaissance and surface mapping followed these initial stratigraphic studies. Since then I have completed numerous additional

projects in the area. These involved surface mapping and detailed photogeologic studies with associated field checking, detailed mapping of local structural features, and subsurface investigations.

I began my study of the structural style of the Laramide orogeny in an exploration project in the Bighorn basin of Wyoming for Chevron in the late 1960's. This project consisted of detailed observations of structural trends at all stratigraphic levels from the Precambrian basement to the Eocene.

In subsequent studies with Chevron, analysis was concentrated on areas where structural features might be potential traps for hydrocarbon accumulation. In recent years, surface work has been directed at areas where specific aspects of the structural style could be demonstrated. Problems which have been studied most recently have involved the geometry of the Precambrian-Cambrian contact on the downthrown side of basement-involved faults, and the relationships between major northwest-trending Laramide structures and the east or northeast trends along which they are abruptly terminated.

Subsurface structural interpretations using electrical well logs and reflection seismic data were conducted in areas of interest, concurrently with surface studies. Potential methods, primarily gravity data, were

also used whenever possible to place constraints on structural interpretations.

A variety of published reflection seismic lines will be presented in this dissertation, along with my interpretation of the data. Unpublished data will be utilized in structural interpretations where possible, and is included in the dissertation with permission of the owner of the data.

In the following sections, structural styles are displayed on true-scale, structural cross sections. The methods of downplunge viewing and plunge projection of structural geometry are employed to bridge the gap from basic data to the interpretation. Diagrammatic sections are used to discuss a concept with actual examples for documentation.

1.5 Acknowledgments

I wish to take this opportunity to thank Dr. Lewis H. Shapiro, Department of Geology and Geophysics, University of Alaska-Fairbanks, Chairman of my committee, who has offered many suggestions to improve the quality of this dissertation, and has been my encourager over the years. I also wish to express my appreciation to the other members of the committee. These are: Drs. Daniel B. Hawkins, R. Keith Crowder, and David B. Stone, all of the Depart-

ment of Geology and Geophysics, University of Alaska-Fairbanks, and Dr. John H. Spang, of Texas A&M University, the non-resident member. I wish to thank each of these gentlemen for their time and assistance in completing this dissertation.

It is almost impossible in a study which has developed over a long period of time like this, to acknowledge the input of all persons who have contributed and to thank them individually. Nevertheless, I feel a strong sense of indebtedness to a large number of people, and thus I will attempt to acknowledge those who have made a significant contribution to my interest in structural geology and this study in particular.

First and foremost I wish to acknowledge the assistance in the field, encouragement at home and forbearance given me by my wife Claretta. Without her constant love and support I would never have accomplished this personal goal, nor survived the long and tedious process of completing this degree. Also I express appreciation to my children, Cheryl, Pam, and Mike, who have spent numerous vacations "looking at rocks", and having made many trips to the airport in sending me to, and welcoming me home from numerous field trips. They have always believed that I could accomplish this goal.

Professionally I have worked with many fine geologists and geophysicists who have all made contributions to

various concepts developed over the years. I hereby express my deep appreciation for the many who have influenced my thoughts. Particular acknowledgment must be made to three men who were co-workers in the field in the beginning stages of this study. The first is David Keefer, now of the U. S. Geological Survey, who was a summer field assistant; the second is G. C. Young of Chevron who mapped many of the structures on aerial photographs. Special thanks go to F. A. Petersen, now retired from Chevron, who was not only a field partner, but a contributor of many ideas to concepts developed through-out the years. His contribution to my overall professional growth has been significant and is greatly appreciated.

A special acknowledgment must go to Dr. C. D. A. Dahlstrom, the first coordinator of the Standard Oil Company of California (Chevron) Structural Seminar which I attended in 1966. Clint was the one who made me aware of many basic principles of structural geology and kindled my interest in systematic structural investigations. Others who I wish to thank specifically are listed by name only, but this should in no way detract from the significance of their contributions to my overall work. These are, in alphabetical order: Thomas L. Kingery, Paul R. Lamerson, Frank Royse, and Peter Verrall, all of Chevron.

During the course of field work, a geologist comes into contact with landowners, in order to obtain per-

mission for access to outcrops on their land. Very few times have I been refused such access. There are three landowners in the Bighorn basin area for whom I have developed a special fondness over these many years. These are: Mr. Homer Renner, north of Tensleep, Wyoming; the Hampton family, south of Tensleep; and Mr. Perley Brooks of Owl Creek Road, west of Thermopolis, Wyoming.

I cannot adequately thank the many professors with whom I have had professional contact in different ways over the years, but those who standout in my memory are: Dr. Donald Blackstone, University of Wyoming; Dr. L. T. Grose, Colorado School of Mines; and Drs. Robert Berg, John Logan and John Spang, of Texas A&M University.

I wish to thank the corporate management of Chevron, USA, Inc. for initial permission to pursue this dissertation and the original approval of the topic. Needless to say, without the encouragement of scientific pursuit in conjunction with the search for hydrocarbon reserves, this study would never have resulted. I also thank the local management of Chevron in Denver, as well as the Corporate management in San Francisco for allowing me to present these ideas, and I take full responsibility for all statements made in this dissertation.

I wish to thank Baylor University, the Department of Geology, and the Ben Williams Scholarship Committee for providing financial assistance during the summers of 1982,

1983, and 1984. This financial assistance allowed me to complete the final field work and do the early writing on this dissertation.

The following individuals and/or companies are acknowledged for their contributions of electric logs, maps, seismic data, and other information included in this study. In alphabetical order:

1) AMOCO Production Company, Denver, Colorado
2) CHEVRON USA, Inc., Denver, Colorado
3) Robbie Rice Gries, independent geologist, Denver, Colorado
4) T. L. Kingery, of Chevron USA, Inc., Denver, Colorado
5) Donald S. Stone, president, Sherwood Exploration Company, Denver, Colorado
6) K. A. Weiler, Chevron USA, Inc., Denver, Colorado.

I am grateful for the support given me by students and fellow faculty at Baylor University during the years I have been there. They have had faith in my ability to finish this program. Finally, I want to thank Robert Cervenka, Jay Hightower, Jon Krystinik, and Bryce McKee for their assistance in the preparation of figures, tables, and photographs for this dissertation. I also appreciate the grant from the Geology Faculty Development Fund, which paid for preparation of the figures.

1.6 Personal Dedication

I wish to acknowledge my belief in the Creator of the Earth which I study, and my dependence upon Him for strength to continue with this program and to see it through. To this end, I dedicate this work to Him.

> In the beginning God created the heaven and the earth. And the earth was without form, and void; and darkness was upon the face of the deep. And the spirit of God moved upon the face of the waters (Genesis 1:1-2 KJV). All things were made by him; and without him was not any thing made that was made (John 1:3 KJV). I will lift up mine eyes into the hills, from whence cometh my help? My help cometh from the Lord, which made heaven and earth (Psalm 121:1-2 KJV). I can do all things through Christ, which strengtheneth me (Philippians 4:13 KJV). O Come, let us worship and bow down: let us kneel before the Lord our maker (Psalm 95:6 KJV).

2.0 HISTORICAL REVIEW OF WYOMING FORELAND STRUCTURAL INTERPRETATIONS

2.1 Introduction

In this section, studies which have significantly influenced the present structural interpretations of the Wyoming foreland will be reviewed, with emphasis on the chronological development of the various concepts. This will be achieved by dividing the discussion into four categories: 1) early geologic studies, which were concerned with the general geology of the foreland (1867-1919), 2) development of the earliest foreland structural concepts (1920-1940), 3) development of modern structural models (1941-1970), and 4) continued debate of the various structural models, which was brought into sharp focus by new well control and better seismic data which have been obtained recently (1971-Present).

2.2 Early Geologic Studies (1867-1919)

The period of initial geologic exploration of the Rocky Mountain region during the 1800's was also the time during which the science of geology was becoming well established in the United States. Earliest work in the region was carried out in conjunction with the initial military and topographic surveys, as the frontier moved west.

The F. V. Hayden Survey moved into Wyoming in 1868, and worked in the Snowy Range of southeastern Wyoming and in the Yellowstone-Teton-Jackson Hole area until 1873 (Dockery, 1972). The King Survey, led by Clarence King (who later became head of the U. S. Geological Survey), worked eastward from California, along the 40th Parallel, and reached Ft. Bridger, in southwestern Wyoming, in 1871. The Yale Scientific Expedition, directed by O. C. Marsh, and guided by William F. ("Buffalo Bill") Cody, moved into the Bighorn basin region in 1870. The Expedition was the first to recognize the potential for oil and gas accumulations in the Bighorn region (Dockery, 1972). A geological reconnaissance in northwest Wyoming was published by Eldridge in 1894.

In 1895, N. H. Darton was transferred to the Hydrologic Branch of the U. S. Geological Survey in the Rocky Mountain region, and began his work in the Black Hills of North and South Dakota. Darton worked in the Bighorn Mountains, the Owl Creek Mountains, and the Laramie basin of southeastern Wyoming. Most significant to future foreland interpretations was the publication of Darton's work as USGS Professional Paper 51, entitled "Geology of the Bighorn Mountains", Folio 141 (Bald Mountain and Dayton quadrangles), and Folio 142 (Cloud Peak and Ft. Mckinney quadrangles) in 1906.

D. F. Hewett and Charles T. Lupton (1917) published USGS Bulletin 656, entitled "Anticlines in the southern part of the Bighorn basin, Wyoming" (personal note: Mr. Homer Renner, landowner north of Tensleep, Wyoming [section 1.5], was a teamster for Charles Lupton in the Bighorn region). Other workers published on the water, mineral resources, and stratigraphy of the Rocky Mountain region, and the area of the Wyoming foreland in particular, during this same period of time. By the end of this period, the general stratigraphic section was well understood, the major tectonic features of the region were outlined and detailed mapping had been completed on some of the mountain uplifts and basin margin folds.

Many of the present-day giant oil fields such as Elk Basin Field, Grass Creek Field, Hamilton Dome Field, Little Buffalo Basin Field, and Oregon Basin Field (all in the Bighorn basin); Lander Field, and Pilot Butte Field (all in the Wind River basin); and Rangely Field in northwest Colorado were first drilled and discoveries made during this period of time. The studies mentioned above provided basic geologic data used by later workers in the interpretation of the Wyoming foreland.

2.3 Development of Earliest Foreland Structural Concepts (1920 to 1940)

W. H. Bucher, W. T. Thom, and R. T. Chamberlain conducted geologic studies in the Yellowstone-Beartooth-Bighorn region during the early part of this period. All three published significant works based upon their studies in the region. Bucher (1920) published on a mechanical interpretation of joints, which was the forerunner for later studies trying to determine the style and mechanisms of basement deformation in the foreland. Thom (1923) described the relationship of structural features to deepseated faults of central Montana, and Chamberlain (1925) postulated his "wedge theory" of diastrophism, as related to mountain building in the foreland. He postulated that the mountain uplifts were bounded by reverse faults which resulted in a triangular or wedge shape in cross section. His theory was to influence later research into structural geology, both in the Wyoming foreland and elsewhere.

Wilson (1934) studied the Five Springs area located on the western flank of the Bighorn Mountains, and recognized a surface dip of only five degrees on the Five Springs thrust fault (but interpreted the average dip to be 10-20 degrees). He interpreted the Five Springs thrust in terms of the "wedge uplift" process (Chamberlain,

1925), which elevated the Bighorn Mountains through a combination of tangential stresses and isostatic adjustments. Wilson also conducted detailed studies on the Precambrian basement fractures exposed in the area. His observations were used by later workers to explain basement deformation of other Laramide structures and will be discussed in later sections on possible basement folding mechanisms (section 5.32) and the fold-thrust foreland model (section 7.24).

The surface observation of low-dipping reverse faults which crop out in the sedimentary section along the steep flanks of the uplifts, combined with the "wedge theory" of tectonics greatly influenced the structural interpretations of this period because it fit the field observations. Both were in agreement with the concept of horizontal compression as the active stress system during the Laramide orogeny. Other geologists (Beckwith, 1938; Fanshawe, 1939; Blackstone, 1940) published interpretations of foreland structures, utilizing low angle reverse faults bounding the uplifts. Fanshawe (1939) used this model to interpret the east-trending Owl Creek Mountains (fig. 1) as having been thrust southward over the adjacent Wind River basin along a reverse fault dipping 30 degrees to the north. Blackstone (1940) interpreted the monoclinal folds of the Pryor Mountains (southern Montana) to have

been created by movement on curved, concave upward, reverse faults, in response to horizontal compression.

2.4 Development of Modern Structural Models (1941 to 1970)

Many changes in the basic concepts of the foreland structural style were made during the period from 1941 to 1970. The concept of low angle reverse faults bounding the major foreland uplifts continued to prevail in the early years of this period (Beckwith; 1941, 1942; Demorest, 1941). Classic foreland areas such as Elk Mountain in south-central Wyoming, were interpreted in this manner (Beckwith 1941). Blackstone (1947, 1948, 1949, 1951, 1956, 1963, 1970) continued his studies of local foreland structures and the regional aspects of foreland deformation. Nelson and Church (1943) described the geometry of foreland reverse faults as having the concave upward shape of "sled runners", and applied the name "trapdoor" faults to the resulting structures. Chamberlain (1945) continued his studies on the deformation of basement rocks and adopted the concept of localization of large Laramide uplifts as being controlled by Precambrian structures.

Beginning in the post-war years, and continuing to the present, an increasing number of maps and papers dealing with the regional geology of the foreland and specific structural features, have been published by the U. S. Geological Survey. Most notable is the work of J. D. Love, whose publications span the time from the late 1930's until the present (Love and Christiansen, 1985) and cover the entire area of the foreland. Keefer (1965, 1970) also made a significant contribution to the understanding of the development of foreland structures with his Professional Papers 495-A, D, on the Wind River basin.

Two significant research papers were published during the 1950's. The first paper (Hafner, 1951) presented the results of theoretical mathematical models of structural development--one of horizontal compression, and a second one of vertical uplift. The second paper (Sanford, 1959) presented the results of theoretical and experimental models of vertical uplift. Both of these works will be discussed in a later section on structural characteristics of basement rocks (5.23), and foreland structural models (7.20). During this same period, Bell (1956) postulated the transverse segmentation of fold systems created through compression, and described as compartmental deformation by this author (8.0).

A significant modification of the wedge uplift concept was introduced by Berg (1961, 1962b), and he called this idea the "fold-thrust" model, recognizing that a major component of folding must have accompanied the thrusting which developed the uplift. The model consisted of an uplift bounded by an overturned limb, rotated between two parallel, or subparallel low angle reverse faults. He had described this style of deformation by interpreting subsurface well control on several mountain fronts in Wyoming, and predicted this model to be the structural style of major foreland structures, such as the Wind River Mountains, which will be discussed in a later section (7.24).

The concept of horizontal compression as the deforming force was gradually replaced by that of "differential vertical uplift". The first "reinterpretation" of foreland structures using the vertical uplift models of Hafner (1951) and Sanford (1959) was published by Osterwald (1961). The terms "upthrust" and "drape folding", which are applied to most interpretations utilizing the vertical uplift concept today, were formalized by Prucha and others in 1965 and will be discussed in later sections (7.21; 7.22; 7.31). The publication of these works marked a departure from the prevailing model in the interpretation of the mode of uplift of foreland structural features.

During the 1960's, work continued toward determining the role which Precambrian basement rocks played in the development of Laramide structures (Hoppin, 1961; Hoppin and Palmquist, 1965; Hoppin and others, 1965; Palmquist, 1967; and Jennings, 1967). Hoppin and others (1965) demonstrated that Precambrian structures in the Bighorn Mountains (such as the Tensleep fault) had been reactivated during the Laramide orogeny. Their work also provided a large data base of specific structural features in the Bighorn Mountains. Similar detailed mapping was being done in the Beartooth Mountains (Foose and others, 1961). The role of fracturing as a basement deformation mechanism in foreland areas continued to be studied (Wise, 1963).

Sales (1968) created experimental models of various areas of the foreland using a medium of layered barite muds deformed in shear. The results reproduced the map patterns of many Wyoming foreland structures, and cross sections through the hardened models displayed the structural geometry often encountered in the subsurface. The concept of strike-slip or "wrench" tectonics was applied to the Wyoming foreland by Stone (1969, 1975), which introduced the possibility of large lateral offsets resulting from horizontal compression.

2.5 Continued Debate of the Various Structural Models (1971 to Present)

The idea that vertical uplift, which requires little or no crustal shortening, was dominant in foreland deformation, rather than horizontal compression and large-scale crustal shortening, received widespread acceptance during the early years of this time period. Stearns (1971) published his work on Rattlesnake Mountain anticline, near Cody, Wyoming, and interpreted this feature as a "drape fold". The various models for vertical uplift will be discussed in a later section (7.20). For the next decade, publications by Stearns (1975, 1978) either alone, or with his students (Stearns and Weinberg, 1975; Weinberg and Stearns, 1978; Stearns, Couples, and Stearns, 1978; Stearns and Stearns, 1978; Couples and Stearns, 1978; Cook and Stearns, 1975) dominated the literature on the structural style of the Wyoming foreland. A significant aspect of this work was the study of experiments in which rock slabs were deformed into drape folds under confining pressures simulating true depths of burial during the Laramide orogeny. These models display many of the features observed in outcrop.

The interpretation of the origin of foreland structures by vertical uplift reached a zenith with the publication of Geological Society of America Memoir 151, enti-

tled Laramide folding associated with basement block faulting in the Western United States, which was essentially a volume on vertical uplift. Modern seismic data published prior to Memoir 151 (Brock and Nicolaysen, 1975; Stearns and others, 1975) indicated that the quality of the available data was good enough to demonstrate the large amounts of crustal shortening postulated by the "compressionalists"; however these interpretations continued to apply the vertical uplift concept. My reinterpretation of some of these same seismic lines demonstrating a compressional model will be presented in a later section (10.0).

Publication of Memoir 151 served as the impetus for a group of compressionalists to hold a symposium entitled "Rocky Mountain Foreland Basement Tectonics". The symposium volume (Contributions to Geology, v. 19, no. 2) was dedicated to Dr. D. L. Blackstone, Jr., a long-time proponent of the horizontal compression model and contained a number of articles documenting the concept of horizontal compression as the deforming agent during the Laramide orogeny (Brown, 1981; Gries, 1981). The fold-thrust geometry encountered in wells drilled since Berg (1962b) formulated the model was documented by Gries (1981, 1983a). Brown (1983) documented the sequential development of Berg's fold-thrust model, and also presented a reverse fault interpretation of Rattlesnake

Mountain anticline (Brown, 1984a) as an alternative to the drape fold interpretation of Stearns (1971).

Modern seismic data has been published which interpretes the basement overhang present on many major uplifts (Gries, 1983a,b; Lowell, 1983; Skeen and Ray, 1983; and Sprague, 1983). The Consortium On Continental Reflection Profiling (COCORP) shot reflection seismic lines across the Wind River Mountains (Smithson and others, 1978), and the Laramie Range (Johnson and Smithson, 1985) in an attempt to obtain deep crustal data. The COCORP data establish the low angle nature of the bounding reverse faults for both mountain uplifts.

2.6 Summary

Early geologic studies of the Wyoming foreland were concerned with initial mapping of the major structural features, followed closely by studies of the water and mineral resources of the region. The early studies of the structural style of the Wyoming foreland concentrated on the major uplifts and the mode of deformation in the Precambrian basement rocks. Interpretations by early workers generally recognized horizontal compressive stresses as the cause of the major structural uplifts, and most mountain-bounding reverse faults were depicted as dipping at angles of less than 30 degrees.

Results of theoretical and experimental studies published during the 1950's contributed to a major change in the concept of formation of the structural uplifts, and the dips of the associated faults. Proponents of the concept of "differential vertical uplift" adopted the two basic models referred to as the "upthrust" and the "drape fold", which will be discussed more fully under the topic of foreland structural models (7.20). These two models received widespread acceptance by some geologists, while others continued to document mountain-bounding low angle reverse faults, major basement overhangs and the necessity of horizontal compression to form them, through the interpretation of seismic reflection data and subsurface well control.

The introduction of the fold-thrust model by Berg (1962b), followed by its documentation by well control and seismic data over a period of approximately two decades, has resulted in the recent publication of a number of studies which demonstrate crustal shortening across the Wyoming foreland and will be covered in later sections (9.0). This has led to a return to the earlier concept of horizontal compressive stress as the active agent in Laramide deformation, an interpretation which is compatible with the the modern understanding of plate tectonics, and recognition that horizontal compression may give rise to vertical movements in the earth's crust.

3.0 GENERAL GEOLOGY OF THE WYOMING FORELAND

The discussion of the general geology of the Wyoming foreland will provide a background for the topics which follow and is divided into three sections: 1) Precambrian basement complex, 2) Phanerozoic stratigraphic section, and 3) regional structure of the foreland.

3.1 Precambrian Basement Complex

3.11 Introduction

The Wyoming foreland is characterized by large mountain uplifts which expose the Precambrian basement in their eroded cores. The Precambrian "basement complex" of the Wyoming foreland is characterized by igneous and metamorphic rocks of varying ages and diverse structural orientations (figs. 4, 5). Additional discussion of the structural characteristics of the basement rocks will be covered in a later section (see Structural Characteristics of Basement Rocks, section 5.0).

3.12 Age of Precambrian rocks

The Precambrian rocks of the Wyoming foreland range in age from 900-1,200 m. y., to older than 3,000 m. y. (Hedge, 1972). The younger Precambrian rocks are represented by the slightly metamorphosed sedimentary sequences of the Uinta

Mountain Group and Belt Supergroup. These rocks were deposited in the Uinta and Belt embayments of Utah and Montana, and along the Precambrian continental margin west of the Wyoming foreland. The presence of up to 40,000 feet (1,200 m) of these sediments may indicate deposition in late Precambrian aulacogens.

The older Precambrian rocks of the Wyoming foreland are a series of igneous and metamorphic rocks which are older than 1,400 m. y. (fig. 4). The area of exposure of the oldest Precambrian rocks (older than 1,700 m. y.) is the Wyoming Province of Houston (1971) which represents the southwestern extension of the Superior Province of the Canadian shield. The oldest rocks exposed in the foreland (older than 2,900 m. y.) crop out in the Beartooth, Bighorn and Wind River uplifts, and are surrounded by rocks which date between 2,600 and 2,900 m. y.. The 2,600 m. y. and older complex is in tectonic contact with rocks of 1,700 m. y. and younger along the Mullen Creek-Nash Fork "shear zone" which is the southern boundary of the Wyoming Province in southeastern Wyoming (Houston and others, 1968).

3.13 Precambrian rock types

The basement complex includes plutonic, meta-igneous, meta-sedimentary, and meta-volcanic rocks of various types (fig. 5). The meta-sedimentary suite includes marble, quartzite, iron formation, meta-conglomerates, a variety of

granitic and felsic gneisses, and pelitic and graphitic schists. Houston (1971) presented a brief synthesis of regional relationships of the various Precambrian outcrops in Wyoming. Of significance to later discussions of the structural characteristics of foreland basement rocks (section 5.0), is the observation that approximately 22% of the foreland is not igneous rock, but is comprised of meta-sedimentary and meta-volcanic rocks. Table 1 is a compilation of the principal rock types exposed in each range.

3.14 Precambrian structural trends

Studies of Precambrian rocks exposed in the foreland reveal a predominance of east, northeast, and north trends of foliation, igneous dikes, faults, and fold axes (some of the more prominent features with these trends are listed in table 2 in section 3.32). Brown (1975) has documented the same trends for similar features in the northern Laramie Range.

Geologists working in the foreland have long speculated on the role which Precambrian "zones of weakness" may have played in controlling the development of Laramide structures (Houston, 1971). Laramide reactivation of Precambrian structures produced folds and associated faults in the overlying Phanerozoic sedimentary section, which display similar east, northeast, and north orientations. Several

TABLE 1. PRINCIPAL PRECAMBRIAN ROCK TYPES IN WYOMING MOUNTAIN RANGES.

MOUNTAIN RANGE	PRINCIPAL PRECAMBRIAN ROCK TYPES DESCRIBED	REFERENCE
Beartooth Range	granitized & metamorphosed quartzo-feldspathic, gneissic with rare interlayers of metasediments intruded by basaltic magmas	Poldevaart & Bentley (1958)
Bighorn Range a) Northern	granitic terrain with scattered bodies of quartz monzanite, quartz diorite, agmatite	Heimlich (1969)
b) Southern	gneiss terrain: plagioclase-quartz gneiss, augen gneiss, amphibolites, quartz diorite	Heimlich (1969)
c) Horn Area	metamorphic gneiss complex, granitic gneiss, quartzo-feldspathic banded igneous, garnetiferous gneiss, large lensoid bodies of conformable amphibolite, some marble, banded ironstone; characterized as supracrustal	Palmquist (1967) Hoppin, et al. (1965)
d) North of Tensleep Fault	massive gneisses; cross cutting amphibolite, characterized as infra-crustal	Hoppin, et al. (1965)
e) East Flank	quartz biotite-plagioclase gneiss & migmatite, minor hornblende gneiss & small ultramafic bodies	Hoppin (1961)
f) Deep Creek	dolerite dike striking N10-15E	Nichols (1965)
Granite	pelitic schist, quartzite, iron fm. granite. amphibolite	Love & Christiansen (1985)
Gros Venture	gneisses, serpentinite	Love & Christiansen (1985)
Laramie Range	granite, gneiss, amphibolite, syenite, thin quartzite layers, metasediments	Holden & Fleckenstein (1980)
Medicine Bow	gneiss & schists in NW part intruded by basaltic dikes & sills	Houston (1968)
Owl Creek	iron formation, graywacke suite, pegmatite intrusions	Houston (1971)
Seminole	iron formation, graywacke suite	Houston (1971)
Sierra Madre	granite, granodiorite, quartz diorite, metasediments, meta-volcanics	Love & Christiansen (1985)
Tetons	quartz monzanite, metasediments, meta-volcanics, meta-gabbro, mafic intrusions	Love & Christiansen (1985)
Washakie	granites	Love & Christiansen (1985)
Wind River	graphic schist, meta-conglomerates, meta-gabbro, iron formation, graywacke suite cut by granite and pegmatite	Houston (1971) Love & Christiansen (1985)

Precambrian structural features have been documented as having been reactivated during the Laramide Orogeny. The resulting Laramide structures with proven Precambrian control are: 1) the east-trending Tensleep fault and associated monocline in the sedimentary section (Hoppin and others, 1965), 2) the northeast-trending Tongue River zone, (Jennings, 1967; Hoppin and Jennings, 1971), and 3) the northeast-trending Mullen Creek-Nash Fork "shear zone" (Houston and others, 1968).

Some faults which were formed during Laramide are adjacent and/or parallel to features such as igneous dikes, foliation trends, changes in foliation trends, and axes of large folds in the basement rocks. A more detailed discussion of the possible relationships of Precambrian age structures to Laramide deformation is given in the section on "compartmental deformation" (section 8.0).

3.15 Summary

The basement of the Wyoming foreland is comprised of Precambrian igneous and metamorphic rocks. The basement rocks of the central portion of the foreland (Wyoming Province) have been dated as older than 1,700 m. y., while the basement rocks in southeastern Wyoming range in age from 1,400 m. y. to 1,700 m. y.. The Precambrian Mullen Creek-Nash Fork shear zone marks the tectonic contact between basement rocks in the two age groups in southeastern

Wyoming. Outcrops of structural features of Precambrian age trend predominantly east, northeast, and north. Several of these Precambrian features have been demonstrated to have been reactivated during Laramide deformation. Other Precambrian structural trends are parallel and adjacent to Laramide-age faults suggesting that these Laramide features may also have been formed by reactivation of Precambrian zones of weakness. This provides a possible explanation (see Relationship of Precambrian and Laramide Structures, section 5.12) for the multiple orientations of the less prominent Laramide structures which seem to transect the northwest-trending prominent Laramide uplifts.

3.2 Phanerozoic Sedimentary Section

3.21 Introduction

The sedimentary section involved in the Laramide orogeny ranges from Cambrian through Eocene in age. The structures exposed in the sedimentary section are the result of movements by segments of the Precambrian basement.

The Wyoming foreland was a stable platform of deposition from the time of the initial transgression of the Cambrian sea eastward onto the craton, until Late Cretaceous, as evidenced by a general absence of thickening into local basins, and thinning over uplifts. Sedimentary rocks accumulated with so little lateral variation that most

stratigraphic groups, and many individual formations, are easily recognizable between present-day basins.

Upper Cretaceous units which prograde eastward in response to uplift and erosion in the west, record the early stages of deformation of the Wyoming foreland. The sources of many Upper Cretaceous sands present on the foreland were the synorogenic conglomerates of the western Wyoming thrust belt (Royse and others, 1975). The appearance of local lakes in Late Cretaceous Lancian time signaled the subsidence in the beginning stages of the Laramide orogeny (Keefer, 1965).

The subsequent breakup of the foreland into individual structural uplifts and basin downwarps continued into the Tertiary. Local sediment source areas shed debris into adjacent basinal areas during Paleocene and Eocene times, filling the sites of Late Cretaceous lacustrine deposition (Keefer, 1965, 1970) and eventually buried the mountains in their own debris after cessation of mountain building in middle to late Eocene time. The present cycle of erosion is now exhuming the Laramide uplifts and has removed large volumes of sediment from the basins.

This section is divided under three headings: Paleozoic, Mesozoic and Cenozoic Erathems. This description of the stratigraphic section is presented as an aid in understanding the regional structure (section 3.3), and as background for the section on "structural stratigraphy"

(section 6.2). The discussion will cover the regional distribution, isopach thickness, and general lithology of each erathem. The distribution of lithologies, both areally and vertically, affected the overall structural response during the Laramide orogeny as indicated, in general, in this section. Detailed descriptions of mechanisms and structural styles are given in the sections on structural characteristics of the sedimentary section (6.2) and models of the Wyoming foreland (7.0).

Figure 6 is a montage of selected isopach and paleogeographic maps which display the regional distribution and variations in thicknesses of the Paleozoic, Mesozoic and early Cenozoic rocks, across the foreland. Figure 7 is a regional stratigraphic section across the Wyoming foreland showing general facies relationships and thickness distributions along an east-to-west line. Figure 8 is a stratigraphic column from the Bighorn basin, and is representative of most of the foreland.

3.22 Paleozoic Erathem

Rocks belonging to all systems of the Paleozoic Era, except the Silurian, are present within the Wyoming foreland. The Paleozoic stratigraphic section is characterized by general westward thickening from the stable craton into the Cordilleran miogeosynclinal wedge. The zero isopach lines of the lower Paleozoic units (fig. 6a,b,c) trend

northeasterly across central and southeastern Wyoming, and represent the erosional truncation of these units along the north flank of the Transcontinental arch trending northeast-southwest from northcentral South Dakota, to northwestern Arizona (Lochman-Balk, 1972), passing through northeastern Colorado.

The Cambrian section is composed of a basal sandstone, which is time-transgressive from west to east, overlain by several hundred feet of marine shale and an upper limestone. These facies change eastward into a section dominated by sand. This change occurs along a line which trends northeastward across south-central Wyoming, and through the Powder River Basin of eastern Wyoming (fig. 7). The presence of the Cambrian shales in all but the southeastern part of Wyoming places an incompetent, ductile unit between the Precambrian basement and the overlying Ordovician-through-Permian section. This has important implications for the structural development as discussed in the section on structural stratigraphy (see section 6.0).

The southwest-trending Transcontinental arch was slightly positive prior to the deposition of the Devonian (fig. 6c) stratigraphic section as demonstrated by (1) the absence of Silurian rocks on the foreland [with the possible exception of remnants found in collapsed Devonian diatremes in the Front Range of northern Colorado and southern Wyoming; Chronic and others (1969)], and (2) the truncation

of the Ordovician (fig. 6b) and Cambrian (fig. 6a) units along the north flank of the Transcontinental arch, in southeastern Wyoming and southwestern South Dakota. The Devonian System is also truncated along the same trend by pre-Mississippian erosion on the Transcontinental arch.

The isopach of the Mississippian System (fig. 6d) shows continued thickening to the west and southwest of the foreland, and rocks of this age overlap the older Paleozoic rocks to the east (fig. 7). Mississippian rocks are absent locally in the area of the Front Range of Colorado and the southern Laramie Range of southeastern Wyoming, as a result of erosion following the uplift of the Ancestral Rocky Mountains. The Laramide Sweetwater uplift (central Wyoming) was also a positive structural feature of the Ancestral Rocky Mountains as shown by thinning of isopachs of Mississippian rocks in that area.

The Ordovician, Devonian and Mississippian sections are predominantly carbonates. The Ordovician Bighorn Formation is a dolomite, while the Devonian Darby and Mississippian Madison Formations are mainly limestone, with some dolomite and thin, interbedded shales. This 500 to 1,500 feet (150 to 450 m) thick package of carbonate rock acts as the dominant competent member (Currie and others, 1962) of the Paleozoic section, in the development of Laramide folds (see section on structural characteristics of the sedimentary section 6.0).

The Pennsylvanian isopach map (fig. 6e) shows a thickness of approximately 500 feet (150 m) over much of the foreland, with thickening westward off the stable platform. This system of rocks is bounded at both top and bottom by unconformities (fig. 7); local areas of stratigraphic thinning represent sites of Ancestral Rocky Mountains structures. The Pennsylvanian section is usually divided into a lower red shale unit (Amsden Formation), which becomes dolomitic upward, and grades into the overlying sandstone of the Tensleep (or Quadrant) Formation. Pennsylvanian rocks are almost always folded in conformity with the underlying competent carbonate units.

The Permian isopach map (fig. 6f) indicates a return to normal stable platform deposition. Permian rocks thicken into the Cordilleran trough with a total thickness ranging up to 500 feet (150 m). Permian strata display a classic facies change from west to east across the foreland. In the western portion of the foreland and into the thrust belt, the Park City and Phosphoria Formations are comprised of cherts, phosphorites, dark shales and limestone. Eastward into central Wyoming, the phosphorites disappear, the cherts thin, and the predominant lithofacies is dark gray limestone. In a distance of less than 100 miles (160 km), this carbonate facies changes into red shale, siltstones, and evaporites of the Goose Egg Formation. While the Permian

section usually conforms to the underlying Paleozoic rocks in Laramide folds, disharmonic folding and faulting between Permian and Pennsylvanian units does occur locally.

3.23 Mesozoic Erathem

The Mesozoic stratigraphic section is composed predominatly of clastic rocks with a few thin limestones and evaporitic units present (figs. 7, 8). In most of the foreland, the Triassic is represented by the red shales, sandstones and siltstones of the Chugwater Formation (McLachlan, 1972), and a thin limestone marker bed (Alcova) which is continuous across much of the foreland and into the thrust belt of western Wyoming (Picard and others, 1969). The regional thickness of approximately 1,000 feet (300 m) in central Wyoming thins to 500 feet (150 m) in northern Wyoming, and increases to 2,000 feet (600 m) in the thrust belt of western Wyoming (fig. 6g).

The northern part of the foreland was tilted regionally toward the south and eroded prior to the start of deposition in the Jurassic Period. Triassic rocks are truncated under the pre-Jurassic unconformity (fig. 7). Jurassic rocks lie on progressively older rocks northward into Montana, where they are in contact with Mississippian rocks. The basal Jurassic unit is progressively younger from west to east, as it onlaps the foreland (fig. 7). In southwest and south-central Wyoming, the basal unit is the non-marine Nugget

Sandstone (Lower Jurrasic). In northcentral and northwestern Wyoming, it is the Gypsum Spring Formation (Middle Jurassic), composed of marine carbonate, red shales, and evaporites. To the east and northeast, the basal Jurassic is the Sundance Formation (Upper Jurrasic) which is mainly marine, and includes the green-gray Redwater Shale. The Redwater Shale is an important incompetent structural unit in the stratigraphic section, which controls the position of bedding plane detachment surfaces and faults observed both on the surface and in the subsurface (fig. 8; see Structural Stratigraphy, section 6.20). Late Jurassic is represented by siltstones, sandstones, conglomerates, and variegated shales of the Morrison Formation (fig. 7). Total Jurassic thickness ranges from 500 to 1000 feet (150 to 300 m; fig. 6h).

The Cretaceous stratigraphic section is characterized by thick sections of alternating sandstone and shale indicating multiple transgressions and regressions across the foreland. During Cretaceous time, the Western Interior Seaway trended north-south across the foreland, with sediment input from both the east and west during Early Cretaceous (McGooky, 1972).

The Lower Cretaceous stratigraphic section is composed of (in ascending order) the basal Cretaceous Cloverly Group (100-400 feet; 30-120 m), Thermopolis Shale, Muddy Sandstone, and Mowry Shale (figs. 7, 8). Most of the Lower

Cretaceous sand was derived from the synorogenic conglomerates originating in the western Wyoming thrust belt. These clastic sediments were transported eastward by streams, and reworked in the marine environment of the Western Interior Seaway. The marine Thermopolis and Mowry Shales are good subsurface marker horizons, readily recognizable on electric well logs. These two shales also were important zones of bedding plane slip and detachment faulting during Laramide deformation (see Structural Stratigraphy, section 6.20). The Lower Cretaceous isopach map (fig. 6i) shows a variation in thickness from 400 to 1,000 feet (300 m) in central Wyoming, to over 4,000 feet (1,200 m) at the breakover into the Cordilleran thrust belt.

The Upper Cretaceous stratigraphic section is characterized by four major transgressive and regressive cycles (McGookey, 1972) within an overall pattern of eastward migration of the shoreline through time (fig. 7). The lowermost Upper Cretaceous sandstone unit is the Frontier Formation (figs. 7, 8), which averages 500-600 feet (150-180 m) thick, and had its primary source in the west, both from the thrust belt and the Idaho batholith (McGooky, 1972; DeChadenes, 1975). Sandstones of the Frontier Formation served as a competent structural member between relatively thick shale sections.

The thick, marine Cody Shale (figs. 7, 8) overlies the Frontier Formation and grades upward into the nearshore

sandstones and lignitic beds of the lower Mesaverde Formation. The source area for the Mesaverde Formation was also the western Wyoming thrust belt; regionally the unit is a large deltaic complex which migrated eastward into the Cretaceous seaway (Asquith, 1975). The Mesaverde Formation (figs. 7, 8) is a series of interbedded sandstones and shales, which become non-marine upward; each sandstone wedge (up to 1,000 feet thick; 300 m) pinches out into marine shales in eastern Wyoming (fig. 7). Sandstones of the Mesaverde Formation form the topographic rims surrounding some of the major anticlines in the foreland. Present erosion through the Mesaverde Formation (into the underlying Cody Shale) results in development of topographic basins on anticlinal highs. The Mesaverde sandstones form a local competent structural unit during deformation.

The last marine invasion of the foreland is marked by the Lewis Shale (fig. 7) which is restricted to east and southeast Wyoming. The Meeteetse Formation (figs. 7, 8), is the non-marine equivalent of the Lewis Shale and contains numerous coal beds in the eastern Wind River and Bighorn basins. The uppermost Cretaceous unit is the Lance Formation (figs. 7, 8), a sequence made up of thick lacustrine shales and sandstones, with a high bentonite content. The latter are the first record of the long period of volcanism in the area north and west of the foreland.

The thickness of the total Upper Cretaceous section (fig. 6j) is approximately 6,000 to 8,000 feet (1,800 to 2,400 m) over most of the foreland, with thicknesses exceeding 16,000 feet (4,800 m) in what is now the Hanna basin of southcentral Wyoming, and in the western Wyoming thrust belt. Local thinning of up to 2,000 feet (600 m) in central Wyoming establishes the early growth of the present Wind River Mountains.

The sandstones of the Mesozoic Erathem respond as local dominant, competent structural units (Currie and others, 1962), while the shales react as the more ductile, incompetent units. As a result different portions of the Mesozoic section form disharmonic structures above the Paleozoic section (see section 6.0, Structural Characteristics of the Sedimentary Section).

3.24 Cenozoic Erathem

The Paleocene Fort Union Formation is present in all basins throughout the foreland, suggesting a continuation of regional depositional conditions following the end of the Cretaceous Period. However, paleogeographic maps of the Fort Union Formation (fig. 6k; Robinson, 1972) indicate the presence of local basinal areas and slightly positive areas, marginal to the basins. Conglomerates and sandstones were shed into these local basins from the adjacent rising uplifts (fig. 7). One of these local depositional areas was

the "Waltman Lake" which occupied the deeper north and east portions of the Wind River basin. Coarse clastics were first shed into the Waltman Lake from the Rattlesnake Hills and Wind River Mountains to the south and west in early Paleocene time. By late Paleocene time, clastic sediments were being shed from the Owl Creek uplift and the Southern Bighorn Mountains to the north and from the Casper arch to the east (Phillips, 1983). Keefer (1965, 1970) documented 5,500 feet (1.670 m) of structural downwarp along the northern edge of the Wind River basin, and 9,000 feet (2,700 m) of uplift of the Owl Creek Mountains immediately to the north, during Paleocene time.

The Paleocene marks the major breakup of the once stable foreland, into individual basins with intervening mountain ranges. Coal deposits of Paleocene age attest to the near sea level elevation of the foreland surface at this time. The Fort Union Formation crops out around the margins of most foreland basins and is locally thick immediately adjacent to uplifts such as the Beartooth Range (Gingerich, 1983). Synclinal structures along the rim of the Bighorn basin contain deeply infolded Paleocene rocks, which are locally overlapped by Eocene conglomerates, attesting to post-Paleocene deformation.

The general name "Wasatch Formation" is used for Eocene strata throughout the foreland, but its use should not imply continuity of deposition from one basin to another

(fig. 61). The Wasatch Formation is unconformable on nearly all underlying stratigraphic units at some point around the margins of the basins. The middle Eocene Tatman Formation contains oil shales which are preserved in the central Bighorn basin. Tatman oil shales are approximately time equivalents with much higher grade Green River oil shales of southwestern Wyoming, northwestern Colorado, and northeastern Utah. These fine grained, hydrocarbon-rich sediments verify the tectonic quiesence following the Laramide orogeny.

Post-Eocene sediments are arkosic sands, tuffaceous sands and shales, and some volcanic flows, indicating the continued erosion of the surrounding mountain ranges (fig. 61), and deposition during periods of volcanism.

3.25 Summary

The lateral consistency of the sedimentary section of the Wyoming foreland shows the stability of the foreland throughout the Paleozoic and most of the Mesozoic. Late Cretaceous and early Tertiary sedimentary units record the breakup and deformation of the once stable foreland, during the Laramide orogeny. The Phanerozoic stratigraphic section can generally be characterized as being comprised of a lower, ductile, incompetent zone (Cambrian shales), a middle competent unit (Ordovician through Permian) which is the dominant structural unit in the sedimentary section, and a

thick, upper "composite unit" of contrasting competent sandstones and incompetent shales of Mesozoic and early Tertiary age.

3.3 Regional Foreland Structure

3.31 Introduction

The objectives of this section are to describe the orientations of the Laramide structures in the foreland and relate them to the timing and sequence of deformation during the Laramide orogeny. Later sections (Compartmental Deformation, section 8.0) will discuss the significance of reactivation of older (Precambrian) faults and abrupt changes in the direction of asymmetry along strike of the same fold trends.

3.32 Orientations of Major Laramide Structures

There are four orientations of major structural trends in the Wyoming foreland. These are: 1) northwest, 2) northeast, 3) east-west, and 4) north-south. All of the above trends have been recognized during systematic studies of basement fractures in the cores of the major uplifts (Hodgson, 1965). Figure 9 is a montage showing the orientations of various Laramide structures in the Wyoming foreland. While each structural trend must be considered important to the overall development of the foreland, the northwest trends are here considered the primary Laramide

trends because the major uplifts and basins developed along them, as noted in the discussion of the plate tectonic setting of the Laramide orogeny (section 4.31). Major uplifts and basins are considered to be those which cover hundreds of square miles in area, and often are comprised of individual folds, and faults (Grose, 1972). The northwest trend appears to dominate in number, size, and length of structures (Hoppin and Jennings, 1971).

The major mountain ranges and intervening basins are typically asymmetric in profile; however, the direction of asymmetry varies from basin-to-basin, and range-to-range. The Powder River and Bighorn basins, in the northern half of Wyoming, have an asymmetry which places the basin axes close to the western margisn of the basins. The axis of the Wind River basin, however, lies along the northern and eastern margins, adjacent to the Owl Creek Mountains and Casper arch. The Green River basin axis lies to the east, under the basement overhang of the Wind River Mountains. The asymmetry of the mountain ranges changes abruptly along the strike of the individual ranges (see section 7.44, Fold-thrust Uplifts; section 8.0, Compartmental Deformation), and anticlinal structures within a basin often develop an asymmetry which is directed out-of-the-basin. The significance of out-of-the-basin asymmetry will be discussed in a later chapter (section 10.0 Structural Synthesis of the Wyoming Foreland).

The predominant Laramide structural features oriented northwest-southeast (fig. 9a) are: the Bighorn Mountains, northern Laramie Range, Casper arch, Beartooth Mountains, Medicine Bow Mountains, Teton-Gros Ventre Ranges, Washakie Range and EA thrust, Wind River Mountains, portions of the Owl Creek Range, the Derby-Winkleman line of folding, Immigrant Gap thrust and associated line of folding, and the axes of the Bighorn basin (northwest and southeast), Green River basin (central), Laramie Basin, Powder River basin, and Wind River basin (northwest and southeast).

Many northeast, east-west, and north-south structural trends are prominent features, but are secondary to the primary northwest trends, in that they are less numerous, and of smaller areal extent. The major Laramide structures which are oriented northeast-southwest (fig. 9b) are: Corral Creek fault, Deep Creek fault, Hartville fault zone, Mullen Creek-Nash Fork fault zone, Piney Creek "tear" faults, Tongue River fault zone, and buried fault zones such as the Bonanza-Zeisman zone and others discussed under the topic "Compartmental Deformation" (section 8.0).

The major Laramide structural features oriented east-west (fig. 9c) are: Boysen fault, Casper Mountain fault, North and South Owl Creek faults, Tensleep fault, those faults which bound the south ends of Buffalo Fork and Rawlins uplifts, and the axis of the central portion of the

Wind River basin. The major Laramide structures which are oriented north-south (fig. 9d) are: the East Beartooth fault, the north and south segments of the Bighorn Mountains, the southern Laramie Range, Moxa arch, and Rock Springs uplift, along with the axis of the central Green River basin.

Many of the northeast, east and north-trending faults and igneous dikes in the basement exposures do not penetrate the sedimentary section, and are thus clearly Precambrian in age (Brown, 1975). The northwest-striking faults exposed in the basement also affect overlying sedimentary rocks as young as Cretaceous and Tertiary, indicating that they are Laramide in origin. Mitra and Frost (1981) studied fault and shear zones in the Precambrian basement of the Wind River Mountains. They found that Early and Late Precambrian deformation zones do not cut overlying Cambrian sedimentary rocks. The deformation zones interpreted to be of Laramide origin are a series of five northwest striking (northeast dipping) fault or shear zones, and two northeast striking (northwest and southeast dipping) shear zones. All of these also cut the overlying Paleozoic (and younger) sedimentary rocks, indicating a Laramide origin.

Several northeast, east, and north-trending structural features can be shown to have Precambrian ancestry (table 2). Examples and references for documentation of Precambrian ancestry have already been given in the section on

Precambrian structural trends (section 3.14). Other Laramide features display remarkable parallelism to Precambrian trends (Luth, 1960). The Precambrian faults or shear zones which were reactivated during the Laramide orogeny offset the upper basement surface and form anticlinal folds in the overlying sedimentary section which are oriented parallel to the older basement faults. Plate tectonic reconstructions for North America (section 4.0) indicate that the orientation of the stress system across the foreland (as indicated by plate convergence directions) varied during the Sevier and Laramide orogenies (see section 4.20; 4.30). Reactivation of older basement faults during Laramide was accomplished by a stress field which is inferred to have been different than the one which created the original faults during the Precambrian, due to the age differences and intervening plate rotations. The superposition of a Laramide stress field across the trends of the older faults resulted in the reactivation of some of these.

The time of Laramide movement of the various faults (reactivated and newly formed) are considered to be essentially simultaneous in a local area. Thus, cross-cutting relationships indicated in map patterns do not indicate that multiple periods of movement in distinctly different orientations necessarily occurred in such areas. This relation-

TABLE 2. PRECAMBRIAN ANCESTRY OF LARAMIDE AGE STRUCTURES.

STRUCTURAL FEATURES	TREND OF FEATURE	DOCUMENTATION OF PRECAMBRIAN AGE
Tensleep Fault	East-West	Hoppin (1961); Palmquist (1978)
Boysen Normal Fault	East-West	strike and dip parallels foliation
Casper Mountain Fault	East-West	Brown (1975)
Corral Creek Fault	Northeast	Brown (1975)
East Flank Beartooth Range	North-South	Foose, et al. (1961)
Florence Pass Fault	East-West	Hodgson (1965)
Deep Creek Fault	N10E	Nichols (1965)
Bighorn Mountains: Tear Faults on East Flank	N15-20E N55-60E	Hoppin (1961)
Tongue River Alignment	N52E	Jennings (1967)
Five Springs Tear Faults	N42E	Hoppin (1970)

ship will be discussed more fully in the section on Compartmental Deformation (section 8.0).

3.33 Time of Development of Major Structures

It has been well established by the dating of syn-orogenic conglomerates, that the deformation in the Cordilleran overthrust belt of western Wyoming, Utah, and Idaho, progressed from west to east in time (Armstrong and Oriel, 1965; Royse and others, 1975). In the record of foreland deformation, the oldest basement involved features are the Targhee-Teton uplift (Love, 1977, 1982) and the Moxa arch (Gries 1983b; Wach, 1977) in western Wyoming. The time of formation of these features (fig. 10) is Campanian, coincident with the emplacement of the Absaroka thrust to the west (Lamerson, 1982). The latest movement on the easternmost thrust (Hogsback-Prospect) in the overthrust belt took place in Paleocene-early Eocene (Lamerson, 1982) and actually overrode the Moxa arch (Kraig and others, 1986; Royse, 1985; Murray, 1960). Evidence of uplift of the Wind River Mountains in Maestrichtian time (Gries, 1983b) is recorded by the presence of feldspar fragments in Paleocene Fort Union rocks in the Green River basin just west of the present Wind River Range (Brown, unpublished data). Paleocene rocks also overlap the uppermost Cretaceous Lance Formation (Maestrichtian) and Mesaverde Formation (Campanian) with angular unconformity on the northeast flank of the Wind

River Mountains, and dip gently to the northeast into the Wind River basin. The north margin of the Wind River basin was downwarped approximately 5,500 feet (1,670 m), during Maestrichtian time while the adjacent Owl Creek Range (to the north) was first uplifted during during Paleocene (Keefer, 1965).

Deformation culminated in the Bighorn basin in late Paleocene-early Eocene as documented by the deep infolding of Paleocene rocks in synclines around the flanks of the basin and the angular relationship with the gently dipping overlying Eocene rocks. Local areas, such as the northeast flank of the basin, were subjected to pulses of uplift in Maestrichtian time, as shown by the slight angularity between the Lance Formation and the Fort Union Formation in an area just west of Greybull, Wyoming. The latest stage of Laramide uplift is documented on the east flank of the Bighorn Mountains, just west of Buffalo, Wyoming, where early Eocene rocks are rotated to steep dip by middle or late Eocene uplift of the Bighorn Mountains.

The eastward progression of the onset of deformation was accompanied by continued deformation in the overthrust belt to the west, as indicated by the Triassic Nugget Sandstone which is thrust over Paleocene age rocks on the easternmost (Prospect) overthrust (Royse and others, 1975). There is much discussion whether this east vergent overthrust is younger, or older, than the southwest verging

foreland fault (Cache Creek) which bounds the Teton and Gros Ventre Ranges (Dunn, 1983; Royse and others, 1975).

3.4 Summary

Primary Laramide structural trends are generally northwest, with subordinate trends of northeast, east, and north, superimposed across the northwest structural grain. The superposition of these four structural orientations results in a block-like grid of faults and folds. Most of the prominent mountain ranges and intervening basins strike northwest, with flank structures oriented parallel to the basin axes, in most cases. The ranges are segmented by northeast and east-west striking faults. Many individual anticlinal folds display a blunted plunging end where the secondary east and northeast trends transect the fold (see The "Corner" Problem, section 8.5).

Many of these secondary trends appear to be controlled by older zones of weakness in the basement (which are Precambrian in age). The presence of four different trends of Laramide age, suggests that a variety of movement patterns (reverse dip slip, normal dip slip, oblique slip, and strike slip) may have taken place, causing folding in the sedimentary section, resulting in fold styles which may differ from trend to trend.

The sequence of deformation of the foreland has been shown to progress eastward in time along a tectonic front which probably had subtle, early deformation in front of it, and continued active deformation behind it. This eastward progression created unconformities which date the passage of the tectonic front (see section 3.33, Time of Development of Major Structures) by becoming progressively younger toward the east (i.e. Upper Cretaceous on the Moxa arch, pre-Paleocene on the northeast flank of the Wind River Mountains, and pre-Eocene in the Bighorn basin). The Wind River Mountains of central Wyoming were first uplifted in Maestrichtian time and the Big Horn Mountains and Casper arch were uplifted in Paleocene (Gries, 1983b).

4.0 PLATE TECTONIC SETTING OF THE LARAMIDE OROGENY

4.1 Introduction

The purpose of the following discussion is to outline the characteristics of western North America's plate tectonic history which directly affected the structural development of the Wyoming foreland during the Laramide orogeny. The primary factors to be considered are: 1) the relationship between the directions of plate convergence and maximum compressive stress, and 2) the possible relationship of the rate of convergence and the dip of the subduction zone to the change from the "thin skin" overthrusting of the Nevadan-Sevier orogenies, to basement-involved reverse faulting during the Laramide orogeny.

4.2 Sevier Orogeny

Armstrong (1968) proposed the name "Sevier orogeny" for a Cretaceous deformational episode, during which overthrust structures developed in the orogenic belt of Utah, Idaho, and western Wyoming (fig. 3). He particularly set these features apart from the basement-involved uplifts of the Wyoming foreland, which are typical of the Laramide orogeny.

According to Coney (1978), the direction of convergence between the North American and Farallon (Pacific)

plates during the Sevier orogeny, was along a line trending N72E (fig. 11a). The direction of convergence can be taken as the average or regional direction of the maximum compressive stress during the development of the generally north-south trending Utah-Idaho-Wyoming over-thrust belt. The structures which developed in the region at this time were a series of eastward verging thrust sheets which, as noted in section 3.33 (General Geology of the Wyoming Foreland), are interpreted as being older in the west than the east (Armstrong and Oriel, 1956). These thrusts are thought to be "thin-skinned", in contrast to the basement-involved features in central Wyoming. Recent reflection seismic data (Cook and others, 1979) obtained by the Consortium on Continental Reflection Profiling (COCORP) in the Appalachian Mountains (over-thrust belt) has established basement-involvement in that "thin-skinned" thrust belt, and arguments have been made that the basement may also be involved in the Sevier orogeny thrust sheets (Armstrong, 1968; Brown, 1985; Blackstone, 1977). It seems reasonable that the basement was shortened by an amount roughly equivalent to that of the overlying stratigraphic section, since there is no exposure of basement rock in the hinterland, denuded of the overlying sedimentary veneer.

4.3 Laramide Orogeny

Armstrong (1968) concluded that the Laramide orogeny began in Campanian time and ended in Eocene time (fig. 3). Coney's (1978) plate tectonic reconstruction for the period 80 to 40 m. y. ago (fig. 11b) effectively brackets this time range, and appears to fit reasonably well with a number of other published plate tectonic reconstructions (Smith and Briden, 1979; Smith and others, 1981). The sequential development of the Laramide orogeny across the Wyoming foreland (fig. 10) has been discussed previously (see section 3.33, Time of Development of Major Structures.)

4.31 Plate convergence and direction of compression

It is important to separate the direction of convergence from the direction of plate movement. An analogy of Western North America during the Laramide orogeny with the present-day Andean subduction model, shows that the compressive stress is parallel to the direction of plate convergence (Jordan and others, 1983; Burchfiel and Davis, 1976; Stauder, 1975). Stauder (1975) has shown that compressive stresses in the crust exist 400 to 500 miles (700 km) inland (east) of the Chile-Peru subduction zone today.

During the Laramide, the North American plate moved almost due west at a rate of 5 cm/year, while the Farallon plate moved northeastward at 12 cm/year (fig. 11b). The resulting direction of convergence during the Laramide orogeny was along a line trending N40E, which is essentially perpendicular to the major foreland structures. From the argument above, this indicates that the regional orientation of the maximum compressive stress is almost perpendicular to the northwest trending major Laramide crustal uplifts in the Wyoming foreland.

In addition to these large-scale inferences of the regional orientation of compression for the foreland, there are several features observable in the field which indicate a northeast-southwest orientation for the maximum compressive stress. They are listed in table 3.

Allison (1983) mapped numerous small-scale structural features (stylolites, slickensides, plumose structures and joint orientations) along the trend of the Tensleep fault (T.47 N, Rs.88 and 89 W.) in the Bighorn basin which individually and collectively indicate a northeasterly direction of compression (N48E to N61E).

Sandstone dikes cut across several anticlinal structures in the foreland. One of these dikes crosses the axis of Alkali anticline (T.54 N., R.95 W. in the northeastern Bighorn basin) along a trend of N65E. These sandstone dikes are syntectonic, soft-sediment features,

TABLE 3. FIELD EVIDENCE INDICATING A NORTHEAST DIRECTION OF LARAMIDE COMPRESSION.

STRUCTURAL FEATURE	REGION OR LOCATION	IMPLIED DIRECTION OF COMPRESSION	SOURCE OF DATA
Tertiary Igneous Dikes	Fourbear Anticline	N60E	Brown
	Winkleman Anticline	N40E	Brown
Tertiary Sandstone Dikes	Alkali Anticline	N65E	Brown
Slickensides	Tensleep Area	N45E	Allison 1983
	Sheep Mtn.		Brown
Stylolites	Tensleep Area	N59E	Allison 1983
Fold Axes	Tensleep Area	N30E	Allison 1983
	Wind River Mtn.	N50E	Brown
	Casper Arch	N50E	Brown
Joints	Tensleep Area	N50E; S80E-East	Allison 1983
Joint Plumes	Tensleep Area	N60E; S50-80E	Allison 1983
Gypsum Veins	Tensleep Area	N70E; S50E	Allison 1983

which apparently represent extension parallel to the axis of the fold, and perpendicular to the trend of the dike.

Numerous igneous dikes were also injected along northeast trends during the late stages of the Laramide orogeny (middle Eocene). These features cut across anticlines essentially at right angles to the axes of folds. In the Bighorn basin, one igneous dike has intruded along a fault plane which trends N55E across the southern end of Fourbear anticline (T.47 N., R.102 W.). In the Wind River basin, an igneous dike on the west side of Winkleman dome (secs. 24, 25 and 26, T.2 N., R.2 W.) cuts early or middle Eocene rocks along a trend of N40E. Although dike orientation does not yield a unique solution to the maximum compressive stress direction, it should be within the plane of the dike. These, and other dikes, trend to the northeast, indicating agreement with the small-scale features mapped by Allison (1983). The available data on stress direction during the Laramide orogeny, based on small-scale structures, agrees with the direction of plate convergence.

4.32 Rate of convergence and dip of subduction zone

The rate of plate convergence during the Sevier orogeny (fig. 11a) was 8 cm/year. During the Laramide, the rate of convergence nearly doubled (14 cm/year; fig. 11b).

The change from thin-skinned deformation during the Sevier orogeny, to that of basement-involved structures on the foreland during the Laramide orogeny represents the collapse of the basement-supported foreland. This time of collapse of the foreland coincides with the onset of rapid collision between the North American and Farallon plates, and the coincidence may indicate a fundamental relationship between the magnitude of orogenic forces and the associated rate(s) of the collision causing them. Other factors are probably involved in this change of structural style. Although the discussion which follows points out possible relationships between the rate of subduction, dip of the subduction zone, and possible thermal weakening of the cratonic crust, other factors (i.e. thickness of the sedimentary section as it relates to the depth of burial in the Cordilleran geosyncline versus the foreland; possible contrast in crustal types in the two areas, etc.) could also be of importance to the change from "thin-skinned" to "thick-skinned" deformation.

Flattening of the subduction zone has been postulated for the western margin of North America during the Laramide orogeny (Coney, 1978; Dickinson and Snyder, 1978; Lowell, 1977; Burchfiel and Davis, 1975) in response to the increased rate of convergence (Coney, 1978). It has

been used to explain several anomalous conditions associated with this orogenic period.

First, the so-called "magmatic gap" in the western United States (the absence of magmatic activity in an area directly opposite the Wyoming foreland) from Late Cretaceous to middle or late Eocene has been interpreted to be the result of a shallow dipping subduction zone, segmented and bounded by east-trending transform faults (fig. 12a). The shallow dip of the subduction zone would have shifted the high heat flow associated with the subduction zone inland for a distance of several hundred miles compared to areas north and south of the transform faults (fig. 12b).

Similar segmentation of the present-day Chile-Peru subduction zone has been demonstrated by Jordan and others (1983) and Barazangi and Isacks (1979), with a corresponding change from thin-skin to basement-involved tectonics along the trend of the orogenic belt (Allmendinger, personal communication, 1982). A direct correlation between low-dipping subduction zones and the absence of recent volcanism in the overlying plate by Barazangi and Isacks (1979) is similar to the Laramide magmatic gap in Western North America defined by Armstrong (1968).

The inland shift of volcanic-magmatic activity into Idaho, Montana, northwest Wyoming, and Colorado (Dickinson and Snyder, 1978) is envisioned as causing the thermal weakening of the foreland crust by concentration of high

heat flow under these areas (Coney, 1978). Thermal weakening of the deep crust of the foreland would facilitate the development of low angle thrust faults in the basement, such as those postulated by Hafner (1951) as the result of regional compression. The eastward dip of the thrusts on the west flank of the Wind River Mountains and Casper arch (Gries, 1981, Smithson and others, 1978, Berg, 1962b; Skeen and Ray, 1983) represent brittle yielding of the upper crust in contrast to the ductile shortening in the thermally weakened lower crust. The northwest trends of these features agree with the earlier conclusion that the N40E direction of plate convergence represents the regional direction of shortening.

4.4 Post-Laramide plate movements

The major structural development of the Laramide orogeny ceased in approximately early Eocene; however, deformed lower Eocene rocks in Wyoming attest to continued plate interaction along the west coast of North America during middle to late Eocene time. Coney (1978) shows a return of the direction of convergence to a direction of N60E during the time of 40 to 20 m. y. ago. A steepening of the subduction zone (Coney, 1978) probably accompanied the slowing of the rate of convergence to 8 cm/year.

The development of extensional tectonics in the Basin and Range, beginning as early as Eocene, and the initiation of transform movement along the San Andreas fault system at least by Oligocene time, are two factors which are related to the cessation of the Laramide orogeny to the east. Certainly the change from subduction to transform fault tectonics would have caused a reorientation of stresses in the crust, and compression would probably no longer be transmitted very far to the east, as during the Laramide orogeny.

4.5 Summary

The plate tectonic setting of Western North America during the Laramide orogeny can be compared to the present-day subduction zone along the Chile-Peru trench, and the Andean mountain belt. The direction of South American and Pacific plate convergence and the earthquake fault plane solutions are in agreement with an eastwardly directed compression.

Comparison of the present-day Andean model to Western North America in Late Cretaceous, may be made if later (Eocene-Present) extension (Basin and Range taphrogeny) is accounted for. Hamilton and Meyer (1966) contructed a palinspastic restoration of the Western United States to a time at the end of the Laramide orogeny. This reconstruc-

tion shows that the Wyoming foreland was approximately 500 to 700 miles (800 to 1,100 km) east of the subduction zone during the Laramide orogeny (fig. 13). This distance is comparable to that which the Andes are from the present-day Chile-Peru subduction zone. It is reasonable to conclude that the crustal compressive stresses generated during the Laramide orogeny would have reached inland to the Wyoming foreland.

The greatly increased rate of convergence at the onset of the Laramide orogeny apparently resulted in a flattening of the subduction zone, which shifted the areas of high heat flow hundreds of miles eastward under the crust of the Wyoming foreland. Displacement of the high heat flow under the foreland may have created a thermally weakened crust which yielded along low angle reverse faults when subjected to compressive forces. The major crustal structures which developed during the period of rapid convergence indicate that the direction of collision was the direction of compression. Therefore the Wyoming foreland was under compression which acted along a line trending about N40E during the Laramide orogeny. Data derived from mapping small scale structures in the field supports this conclusion.

5.0 STRUCTURAL CHARACTERISTICS OF BASEMENT ROCKS

Many foreland workers place major importance on the role which Precambrian basement has played in the development of the foreland structural style. Five characteristics of the basement will be discussed in light of how each affects the style of foreland deformation. These are: 1) structural fabric, 2) rock mechanical properties, 3) concept of folded basement, 4) geometry of faulted basement, and 5) basement fault orientations/attitudes.

5.1 Precambrian Basement Structures

5.11 Introduction

Basement outcrops of the Wyoming foreland display a complex structural fabric of Precambrian age, which may include any, or all, of the following: 1) foliation, 2) fold axes, 3) shear zones, and 4) igneous dikes. These same features may display a variety of geographic orientations, but the predominant directions of strike are northeast, east-west, and north-south. Table 4 is a listing of such Precambrian structures which have been recognized in the cores of various mountain ranges throughout the foreland. The listing is representative of the foreland, but is by no means comprehensive. Included in table 4 is a short description of the relationship of Precam-

TABLE 4. TRENDS OF PRECAMBRIAN AGE STRUCTURES IN THE WYOMING FORELAND.

MOUNTAIN RANGE	PRINCIPAL TRENDS OF PRECAMBRIAN AGE	RELATIONSHIP OF PRECAMBRIAN STRUCTURES TO NEARBY LARAMIDE STRUCTURES	REFERENCE
Beartooth Range T56N, R103-104W	south plunging folds, developed post-metamorphism	fold axes are parallel to adjacent north-south trending East Beartooth fault. Axes are at a high angle (>45 degrees) to the northwest trends of the Beartooth thrust	Foose, et al. (1961)
Bighorn Mtns. T47-52N R83-86W	gneisses have general NE trending fabric	strikes at high angle to overall northwest trend of mountain uplift, but parallel to Tongue River lineament	Osterwald (1959)
a) Horn Area T46N R83-84W	a large antiform with axial plane dipping 70 degrees, N49E	antiformal axis is parallel to Laramide Horn anticlinal structure, but at right angles to Laramide Tensleep fault, which cuts across north end of Horn	Palmquist (1978)
b) Tensleep Area T47N R84-85W	foliation strikes E/W and dips 50-70N	foliation is parallel to dip and strike of Laramide Tensleep fault, but at high angles to northwest trend of mountain uplift	Hoppin, et al. (1965)
	second foliation trends N50-65W and dips 60-70NE	foliation is at 35-40 degree angle to Tensleep fault and nearly parallel to overall northwest trend of mountain uplift	
c) Piney Creek Area T52-53N R84W	shear foliation strikes N10-15E	foliation is at high angle to northwest trend of mountain uplift; parallel to tear fault at south end of Piney Creek block	
d) Buffalo Area T50-51N R83-84W	foliation trends of N10E, N45E, and E/W	N10E foliation is parallel to some tear faults along front of mountain uplift. N45E foliation is parallel to other tear faults. E-W foliation is at high angles to northwest trend of mountain uplift	Hoppin (1961)
e) Five Springs Area T56N R92W	steep NE dipping foliation; strikes NNW	foliation strikes parallel to Five Springs thrust, and to Laramide fault which crops out in Precambrian rocks; dikes strike parallel and adjacent to East Medicine Butte fault (tear fault); at high angles to northwest trend of uplift	Hoppin (1970)

TABLE 4. (CONT'D)

f) Tongue River Area T55-56N R88-90W	Precambrian dikes and shear zones trend NE and ENE	dikes parallel northeast trending Tongue River lineament and east-northeast trending compartmental faults; at high angles to mountain uplift	Jennings (1968)
		shear zones are parallel to east-northeast trending compartmental faults	
	granites are in a north plunging synform	axis of synform strikes parallel to trend of uplift but at high angle to Tongue River lineament	
g) Deep Creek Area T41-44N R86-87W	Precambrian dolerite dike strikes N10E	dolerite dike is parallel and adjacent to the Laramide Deep Creek compartmental fault; at low angles to north-west trend of uplift	Nichols (1965)
h) Florence Pass Area	Precambrian normal (?) fault trends east-west	parallel to and coincident with Laramide Florence Pass fault	Hodgson (1965)
Casper Mtn. T32N R78-81W	east-west trending foliation	east trending dikes and shear zones are parallel to Casper Mountain fault along north side of uplift; north-northeast trending dikes parallel Hat Six fault on east side of Casper Mountain	Brown (1975)
	NNE trending dikes at northern edge of Laramie Range		
Laramie Range T30-32N R76-79W	lineament studies indicate NNE, E, and NE trends of dikes and shear zones	northeast trending dikes and shear zones are parallel to the Laramide Corral Creek fault	Brown (1975)
	NE trending foliation	parallel to northeast trending Corral Creek fault; at high angles to north-northwest trend of uplift	
Medicine Bow Range T14-17N R78-81W	Nash Fork Mullen Creek "shear zone" trends N70E	parallel and coincident with tear faults along east flank of uplift; cuts south end and provides south plunge of Quealy dome, in Laramie basin; parallel to strike of Hartville uplift and at high angles to Laramie Range	Houston, et al. (1968)
	Precambrian foliation trends N, NE	strikes at right angles to Laramide structures	

TABLE 4 (CONT'D)

Owl Creek Range a) North Flank T8N, R1E-1W	E-W trending foliation, dips north	parallels east-west trend of North Owl Creek fault	Brown
b) Wind River Canyon T5N, R6E	E-W trending foliation, dips south at 60 degrees	parallel to strike and dip of Boysen normal fault; parallel to strike of South Owl Creek fault	Brown
Shirley Mtns. T25-26N R82-83	NE trending igneous dikes	parallel to and coincident with northeast trending tear faults	Brown
Wind River Mtns.	Precambrian structures have NE trending axes	dikes parallel and project towards Laramide compartmental faults on Winkleman-Derby line of folding on northeast flank of uplift	Houston (1971)
	igneous dikes trend NE	dikes are at high angles to northwest trend of uplift	Brown
	NE and E-W trending Precambrian fault (deformation) zones	at high angles to, and cut by , northwest trending Laramide fault deformation zones	Mitra and Frost (1981)

brian structures to nearby Laramide structures. Precambrian structures are not pervasive throughout the foreland, but are significant in local areas, in that they appear to control the location and trend of selected Laramide structures, suggesting that some Laramide structures have been reactivated along Precambrian age structures.

Table 5 is a listing of percentages of various Precambrian rock types which have been described from structural uplifts across the foreland. The percentages were derived by visual estimation of the distribution of the rock types as shown in figure 5.

The basement rocks range from the typical granitic suite (granite, granite gneiss, and granodiorite) to quartz diorite and quartz monzonite, with anorthosite and meta-sedimentary/meta-volcanic rocks completing the distribution. The variety of rock types described throughout the foreland clearly indicates that the Precambrian foreland basement of Wyoming is not a single homogeneous igneous body, but rather a heterogeneous basement complex.

5.12 Relationship of Precambrian and Laramide Structures

The trends of Precambrian foliation are most often at high angles to the major northwest-trending Laramide

TABLE 5. APPROXIMATE PERCENTAGE OF BASEMENT ROCK TYPES IN PRECAMBRIAN OUTCROPS.

LARAMIDE UPLIFT	PERCENTAGE OF ROCK TYPES						
	GRANITE	GRANO-DIORITE	GRANITE-GNEISS	META-SED/ META-VOL.	META-MAFIC/ ULTRA MAFIC	QTZ. DIORITE/ QTZ. MONZO-	ANORTHO-SITE
Beartooth (in Wyoming)	—	—	100	—	—	—	—
Bighorn	—	—	50	—	—	50	—
Casper Mtn.	—	—	100	—	—	—	—
Granite	75	—	—	25	—	—	—
Gros Ventre	—	—	100	—	—	—	—
Hartville	100	—	—	—	—	—	—
Laramie	55	—	—	12	9	—	24
Medicine Bow	25	—	3	72	—	—	—
North Bighorn	—	—	—	—	—	100	—
Owl Creek	—	—	50	50	—	—	—
South Madre	30	—	30	40	—	—	—
South Bighorn	—	—	100	—	—	—	—
Teton	25	—	—	75	—	—	—
Washakie	100	—	—	—	—	—	—
Wind River	29	20	33	18	—	—	—

structures (Houston, 1971; Hoppin and Palmquist, 1965; e.g. Bighorn Mountains, Buffalo area, Laramie Range, Medicine Bow Range: table 4). This divergence of trends clearly indicates that foliation does not exert a primary control of the northwest-trending major Laramide features. However, there are several areas where Precambrian foliation appears to have controlled the orientation of east-, northeast-, and north-trending Laramide structures (e.g. Boysen fault, Casper Mountain fault, Corral Creek fault: table 4).

Precambrian-age fold axes exposed in the foreland trend in either a north-south direction (e.g. Beartooth Mountains, Tongue River and Horn areas: table 4), or a northeast direction (e.g. Wind River Mountains: table 4). Only in the Horn area (table 4) does there appear to be any direct relationship between a Precambrian-age anticline in the basement and a Laramide-age anticline in the sedimentary section. Laramide faults do strike parallel to the north-south trend of the Precambrian folds along the east flank of the Beartooth Mountains, and parallel to the basement structure in the Horn area.

Precambrian-age shear zones typically strike northeast or east-west in the foreland (e.g. Florence Pass fault, Nash Fork-Mullen Creek "shear", Piney Creek "tear" faults, Tensleep fault, Tongue River lineament: table 4). These same Precambrian shear zones are also recognized as

prominent Laramide fault zones (Houston and others, 1968; Hodgson, 1965; Hoppin and others, 1965), thus establishing Laramide reactivation of Precambrian shear zones.

Precambrian igneous dikes have a predominant strike direction to the northeast in the foreland (table 4). Several northeast-trending Laramide faults are parallel to, or close-by northeast-trending Precambrian igneous dikes (e.g. Corral Creek fault, Tongue River lineament, Derby-Winkleman compartmental faults: table 4). In other areas, Laramide faults (e.g. Deep Creek fault, Shirley Mountains and Five Springs "tear" faults: table 4) are immediately adjacent to Precambrian dikes.

The distribution of Precambrian rock-types in the basement of the foreland clearly establishes the regional heterogeniety of the basement complex. The contact between major rock units in the various uplifts does not appear to exert any significant control on the subsequent development of Laramide structures, as originally postulated by Thom (1923). The only significant (apparent) relationship between the location of Laramide-reactivated Precambrian faults and major changes in basement rock types are shown by the Tensleep fault and Nash Fork-Mullen Creek shear zone (tables 2 and 4; Hoppin, 1961; Houston and others, 1968). The ancestral (Precambrian) Tensleep fault sepa- rated distinctly different crustal rocks (Palmquist, 1978), as does the Nash Fork-Mullen Creek

zone. Other Laramide-reactivated Precambrian faults (e.g. Florence Pass, Tongue River) transect the Bighorn Mountain range, independent of boundaries between major basement rock types, although the Florence Pass zone is at a very small angle to the northeast-trending boundary between the granodiorite and quartz monzonite bodies of the central Bighorn Mountains (figs. 5, 122).

The presence of meta-sedimentary rocks in the Precambrian basement of approximately one-half of the mountain uplifts in Wyoming may be significant on more local scales. The role of these rocks in facilitating possible folding of basement will be discussed in a later section (5.32, Possible basement folding mechanisms).

5.13 Summary

The exposed basement in the Wyoming foreland is heterogeneous with respect to basement rock-types and orientation of structural fabric. The strike of Precambrian-age structural fabric ranges from northeast, to east-west, to north-south, with a strong preference for northeast. There is no consistent relationship between structural trends in the basement and the major northwest-trending Laramide uplifts. Likewise, there is no apparent controlling influence, exerted by variation in basement rock-types, on the orientation of most Laramide structures. In the light of these two factors, many foreland

workers have concluded that Laramide structures have no relationship to Precambrian trends (Houston, 1971).

However, a major understanding to be gained from a comparison of Precambrian and Laramide structural features is that several secondary Laramide structures, which trend northeast, east, and north, are controlled by faults which are apparently localized along Precambrian structures consisting primarily of shear zones and igneous dikes. Other Laramide structures show a strong parallelism locally to zones of Precambrian foliation and fold axes. Such evidence of control of Laramide faulting by Precambrian igneous dikes, and of reactivation of Precambrian shear zones, indicates the presence of important localized zones of weakness in the basement.

Laramide structures follow older (Precambrian) structural trends where these trends were favorably oriented during the Laramide orogeny. Reactivation of these ancient structures played a significant role in development of the foreland structural pattern, and in the maintenance of structural balance during deformation (see Section 8.0, Compartment Deformation).

5.2 Rock Mechanical Properties of Foreland Basement

As an outgrowth of studies in experimental rock deformation, the term mechanical basement has been introduced into interpretations of the Wyoming foreland (Stearns, 1971). According to Stearns, mechanical basement "...includes those rocks which are statistically homogeneous and isotropic, which behave in a brittle manner to depths of at least 50,000 feet (15,000 m), and below which layered rocks do not occur (1971, p. 125)."

In this section I will review the the characteristics of "mechanical" basement listed above and discuss evidence pertaining to them from the Wyoming foreland. I will alsc discuss application of theoretical and experimental results to the deformation of the foreland basement, as they relate to the concept and characteristics of mechanical basement. Finally, I will discuss the role which Precambrian basement structural fabric played in the localization of Laramide structures.

5.21 Characteristics of mechanical basement

Homogeneity is the first characteristic of mechanical basement to be considered here. Stearns (1971, p. 125) states that "Precambrian crystalline granitic rocks comprise most of the basement in the Wyoming Province." If one reads the sample descriptions of wells which have

been drilled into the Precambrian rocks of Wyoming, the term which is most frequently used is "granite". The geologist describing these samples is usually not an igneous petrologist, and the samples are in the form of cuttings which are essentially ground-up rock fragments. When a "soft rock" geologist sees quartz and feldspar together in cuttings, he calls the drilled-up rock granite. Occasionally Precambrian rock is cored, and the descriptions reported are therefore more reliable than those from cuttings. Terms such as schist and gneiss are then often reported. Data presented earlier (fig. 5; table 5) clearly demonstrate that, while the shallow foreland basement may be homogeneous in local areas, it is not dominated by crystalline granitic rocks.

The second characteristic of mechanical basement to be considered is whether the rocks are isotropic. Excluded from mechanical basement by this definition are all foliated and layered rocks and any igneous body (such as a sill) which might exist above layered rocks.

The earlier discussion on Precambrian structural fabric (section 5.12) demonstrated the presence of numerous structural discontinuities within the basement and the variation in Precambrian structural fabric on all scales, ranging from foliations to major shear zones. Large-scale discontinuities such as Precambrian shear zones and igneous dikes (section 5.12) have exerted control on the

location of major Laramide faults (i.e. Tensleep and Deep Creek faults). The presence of these large-scale discontinuities results in a heterogeneous mosaic of basement blocks which may be homogeneous individually, but are separated by distinct zones of weakness. Subsequent Laramide deformation selectively reactivated those discontinuites which were properly oriented in the stress field. Discussion of table 4 (in section 5.12) demonstrated that foliations and other small-scale features are of less importance, and probably do not significantly alter the homogeneity of the individual basement blocks.

The third characteristic of mechanical basement to be considered here is the requirement of brittle deformation down to depths of 50,000 feet (15,000 m) or more. This restriction rules out folding of the basement according to the definition given above. Discussion of this restriction will be covered in a later section on folded basement (5.3).

While the brittle nature of crystalline rocks under conditions simulating depths of burial of up to 75,000 feet (22,000 m) has been demonstrated under laboratory conditions (Borg and Handin, 1966), it is possible that ductile deformation of these rocks could occur over longer time spans. The Laramide orogeny spanned a period of approximately 30 m. y., which, when combined with the

higher heat flow postulated for the Laramide orogeny (discussed in section 4.32), makes ruling out ductile deformation in some of the basement rocks arbitrary.

My objection to the requirement for brittle deformation is that it excludes Precambrian rocks such as those schists and other highly foliated rocks exposed in the Owl Creek Mountains. In the Wind River canyon, the rocks beneath the Cambrian Flathead Sandstone are pink Precambrian granite pegmatites which would deform in the brittle manner. However, this granitic body intrudes the foliated rocks (fig. 15) which are widespread throughout the uplift.

The top of "brittle" basement would thus have to drop to unknown depths along the sharp local boundary at the edge of the intrusion where the highly foliated rocks are exposed, thus making application of the term "basement" difficult to apply, if restricted to brittle deformation only. Many of the anisotropies found in the basement represent brittle deformation on a local scale; however on the larger scale of the foreland, they allow the basement to deform in what appears to be a ductile manner.

It is my conclusion that while it is reasonable to exclude rocks such as the Belt and Uinta Groups, all of the rest of the Precambrian rocks exposed in the Wyoming foreland should be considered basement. I also conclude that the basement of the Wyoming foreland will deform by

several different modes, depending upon the rock type and the presence of various discontinuities, which renders the foreland basement anisotropic, overall.

5.22 Mechanical basement and theoretical/experimental models

The results of theoretical and experimental studies have exerted great influence on the interpretation of foreland structural styles. The results have been widely applied, but often with certain basic data omitted. It is important therefore to fully understand the assumptions, boundary conditions, and limitations of these models.

The most widely quoted works in support of models of foreland deformation are the theoretical works of Hafner (1951) and the theoretical and experimental work of Sanford (1959). Both Hafner and Sanford defined the material deformed in their models as homogeneous and isotropic, a reasonable condition for experimental and physical models, as the "simplest case" approach.

Hafner calculated stress trajectories for mathematical models of crustal blocks under both vertically oriented sinusoidal stresses (fig. 16a), and horizontal compressive stresses applied to their boundaries (fig. 17a). From these stress trajectories, he derived the geometry of potential fault planes (figs. 16b, 17b) which could develop under those specific conditions. His solutions for

the case of sinusoidal stress along the base of the block (fig. 16a) have been widely quoted as models for foreland upthrust fault profiles based upon the presence of high angle reverse faults above the points of stress reversal (Prucha and others, 1965). However, figure 16 shows that the uplifted portion of the model includes a pattern of normal faults which would allow extension on the front edge of the uplift. These faults are necessary for the concave downward upthrust fault geometry to develop. The change from no structural shortening on the vertical portion of the upthrust fault plane, to structural shortening (repetition) on the low-dipping, upper portion of the upthrust fault requires the progressive upward increase in extension.

Sanford studied two models of differential vertical uplift using a sandbox apparatus (fig. 18; note that the "layers" in the models are reference lines, and do not represent true stratigraphic layering). The models show the development of the characteristic concave downward shape of the upthrust fault bounding the uplifted blocks (Type II; figs. 18b, 19). However, the development of normal faults on the upthrown blocks, antithetic to the upthrusts, are clearly shown. These satisfy the requirement for extension mentioned above. In the Type I model (fig. 18a) extension is accommodated by the development of a "crestal graben", as predicted by Hafner's (1951) work.

Note that the extensional requirement is omitted in most published interpretations (Prucha and others, 1965), and will be discussed more fully in later sections (7.21; 7.22; 7.30) on models of foreland deformation. The signifcance of the contrast in style of extension between these two models is considered in a section on the application of the various models of foreland deformation (10.0; Structural Synthesis of the Wyoming Foreland).

For comparison, one of Hafner's solutions for horizontal compression is shown in figure 17. In this case, the predicted fault pattern consists of conjugate shears which, for the boundary stresses used in the calculation, dip between 25 and 40 degrees.

This case has been ignored by many foreland workers, but is used here to contrast the geometry of potential faults which might form under the two conditions (vertically oriented sinusoidal stress and horizontal compressive stress) assumed by different workers. It will be shown in the section on orientations of basement faults (see section 5.5), that a conjugate set of reverse faults does exist in the basement of the foreland. Recognition of this geometry suggests that the assumption of homogeneity (in Hafner's models) may also be applicable, at varying scales, to the foreland basement.

5.23 Summary

The shallow portion of the Wyoming foreland basement is broken into a series of blocks or plates, outlined by the northwest trend of the major Laramide uplifts and basins, and the generally northeast trend of secondary structures. Laramide deformation has been concentrated along the northwest trends by generally brittle yielding of the crust to horizontal compressive stresses which were at right angles to these structures. Deformation along the secondary structures resulted from reactivation of Precambrian zones of weakness which were properly oriented with respect to the northeast-directed Laramide compressive stress. Local deformation within the various blocks may have been controlled by small-scale inhomogeneities within the basement.

To illustrate this development, consider the crust in the foreland as a slab of homogeneous and isotropic material with a number of vertical "cuts", of various depths and lengths, all of which are oriented northwest-southeast and scattered ramdonly over the slab. If a stress is applied from the southwest (as in Laramide time), the cuts would close under the compression and the slab would deform as if the cuts were not present (i.e. as a homogeneous, isotropic material). The result would be some kind of folding at the upper surface of the slab (if the material was ductile), or a conjugate set of reverse faults

(if the material was brittle), all of which would trend northwest-southeast, perpendicular to the applied compressive stress.

Now consider the same slab, but this time the same cuts are oriented generally northeast-southwest. As before, the compressive stress is applied from the southwest. The result again would be a series of northwest-trending folds, or conjugate reverse faults, but this time some of the folds and reverse faults would be cut-off against northeast-trending "compartmental" faults (see section 8.0). In this case, the material between the northeast-trending cuts is homogeneous and isotropic, but the "cuts" will control the lengths of the folds and reverse faults along strike. These "cuts" represent anisotropies, or zones of weakness which were properly oriented to the applied stress, and therefore were "reactivated" during the deformation.

From the previous discussion the following conclusions may be made: 1) the assumption of homogeneous and isotropic conditions is acceptable in theoretical modeling, 2) the conjugate reverse faults observed in the Wyoming foreland may be related to a homogeneous mechanical basement, which was deformed by a horizontal compressive stress, 3) this homogeneous basement was segmented into discrete individual blocks by structural discontinuities inherited from the Precambrian history of the foreland,

and 4) small-scale Precambrian structural fabric exerted variable control on local Laramide structures.

5.3 Concept of Folded Basement

The term "folded basement" means different things to different geologists. To many geologists (and as used in this study), the term refers to the geometric shape of a fold (anticlinal or synclinal) displayed at the surface of the Precambrian basement. To others, the term implies folding by a flexural or ductile mechanism. An outgrowth of the application of the concept of mechanical basement is the argument that "basement" cannot fold, because it deforms in a brittle manner. This argument has become closely associated with the entire question of the structral style of the Wyoming foreland. The configuration of the upper basement surface is important to the understanding of the foreland structural style because it relates to the recognition of crustal shortening, and secondarily to the interpretation of the geometry of basement faulting.

Interpretations of foreland structures employing the definition of mechanical basement generally show the basement surface to be planar on both the upthrown and downthrown blocks of basement faults. Any dip on these planar surfaces is considered to be the consequence of

rigid-body rotation on curved fault surfaces. It will be shown, however, that the configuration of the upper basement surface may differ between the downthrown and upthrown blocks. Because the surface of the upthrown blocks are often visible, outcrops which expose the geometry of the downthrown block are of special interest.

5.31 Observations of basement surface

The configuration of the upper surface of the basement depends upon a number of factors. One is whether the basement rock actually buckle folds in a flexural (or ductile) type mechanism, or whether the configuration of the upper basement surface is controlled by cataclastic (brittle) deformation. Other factors are the shapes of fault planes within the basement, and the angles at which fault surfaces leave the basement.

Many uplifts within the Wyoming foreland display curved, antiformal shapes of the upper basement surface, which many geologists describe simply as "folds", without reference to possible fold mechanisms (e. g. Berg, 1962b). Other geologists object [citing experimental work such as that by Borg and Handin (1966)], to argue that the basement is rigid and non-folding, and deforms only by brittle mechanisms to great depths of burial (Stearns, 1971).

Several different configurations of the basement surface have been described in the foreland. These are:

1) broad, gently curved surfaces, usually several miles in extent, 2) anticlinal forms on the hanging walls of reverse faults, 3) synclinal curvature on the footwalls of reverse faults, 4) horizontal planar surfaces (most commonly on upthrown blocks), and 5) rotated planar dipping surfaces, also on upthrown blocks. Table 6 lists several examples of structures within the Wyoming foreland where the upper basement surface appears to be folded in conformity with the overlying sedimentary section.

5.32 Possible "folding" mechanisms

There are several mechanisms which may account for the apparent folding of the upper basement surface in the examples in table 6. These are: 1) cataclastic deformation, 2) macro-fracturing, 3) rigid-body rotation, and 4) flexural slip mechanisms.

Cataclastic deformation, as a mechanism for deforming the Precambrian basement in the cores of Laramide anticlines, has not been widely documented in the Wyoming foreland. The process of cataclasis is dominated by microfracturing and frictional sliding (Suppe, 1985). Stearns (1971) has discussed the apparent folding of the granite core of a small fold just west of Manitou Springs, Colorado. The fold has a vertical relief of 100 feet (30 m),

TABLE 6. STRUCTURES DISPLAYING FOLDED PRECAMBRIAN BASEMENT.

NAME	LOCATION	GEOMETRY OBSERVED
Sunshine Nose	T19N R70W	South plunging nose with Pennsylvanian Casper Formation on Precambrian basement
Richeau Dome	T21N R69W	Four-way closure at Pennsylvanian and Precambrian contact
La Prelle	T31N R72-74W	Faulted on South side with East plunging anticline at Precambrian and Pennsylvanian level on hanging wall
South Bighorn Range	T39-40N R86-88W	Cambrian/Precambrian contact in large antiform plunging SE towards Casper arch
Horn Area	T45-46N R83W	SE plunge stops; Cambrian/ Precambrian contact dips 50 to 80 degrees SW
Beaver Creek	T47N R83-84W	Reversal of flank dip at Cambrian/Precambrian level from 17 degrees East dip to 12 degrees dip then back to regional dip
Hunt Mountain	T54-55N R91W	Slight reversal of Cambrian Flathead Sandstone on hanging wall of reverse fault

TABLE 6. (CONT'D)		
Porcupine	T55-56N R91-92W	Synclinal curvature on downthrown block at Cambrian/Precambrian level
Deer Creek	T57N R92W	Same as at Porcupine (above)
Clarks Fork Canyon	T56N R103-104W	Anticlinal curvature on upthrown (West) block; synclinal (?) dip on downthrown side (East) at Cambrian/Precambrian level
North Owl Creek/ Anchor Area	T8N R1E-1W	50 degrees north dip of Flathead SS. and Precambrian; anticlinal shape plunges west
Sheep Ridge	T30N R96-97W	Anticlinal reversal at Cambrian/Precambrian contact on West plunging anticline
South Wind River Mtns.	T29-30N R96-97W	SE plunge end of range
Ferris Mountains	T30N R88W	Small anticlinal reversal on upthrown side (South) plunges West
Bald Mtn. Anticline	T25N R81W	Anticlinal reversal on hanging wall basement

with the basement granite conforming to the overlying Cambrian sandstones. The granite was broken and fragmented so that individual pieces are approximately one inch in diameter. The apparent folding resulted from the pieces of granite moving relative to each other like lead shot in a paper weight. Hudson (1955) concluded that the cataclasis preceded deposition of the Paleozoic sediments, but it is more likely that it is the result of Laramide deformation. The question also arises as to whether this mechanism can operate at scales large enough to account for much larger features present in the foreland.

Macro-fracturing (movement along closely spaced multiple fractures in the basement) is a second mechanism which is often suggested to explain curved basement surfaces (Prucha and others, 1965). The process is analogous to slip along the surfaces of a deck of cards where the cards are at a high angle to the horizontal. Initially horizontal reference lines on the deck can be deformed to the shape of an anticline by movement on the shear planes, with no contribution from flexural mechanisms. However, Stearns (1971) has shown that such a mechanism was not operative in the basement at Rattlesnake Mountain anticline, west of Cody, Wyoming. The spacing of the vertical fractures in the basement in that structure would require an average of eight inches of vertical displacement per fracture to account for the observed rotation of the

basement surface, but this amount of displacement is clearly not present.

Rigid-body rotation (the en masse rotation of a fault block with no accompanying internal rotation) is a third possible mechanism for forming "folds" at the basement surface. Fault surfaces must be portions of circular arcs for blocks to rotate without developing volume problems at depth (Prucha and others, 1965). Stearns (1975) used experimental models to demonstrate how rotation of blocks may occur on curved surfaces. Brown (1984a) has shown that rotated basement blocks can result from movement on a concave upward reverse fault, as at Rattlesnake Mountain anticline (see section 5.52, Fault cut-off angles).

Stearns and Weinberg (1975) applied the concept of rigid-body rotation to explain some of the observed basement geometries in the Wyoming foreland, and examples will be discussed in a later section (5.42) on downthrown fault blocks.

Flexural slip (the differential slip of one rock layer with respect to another as the result of flexing of the layers during compression) could be operative in the Precambrian Belt and Uinta Groups. It is less likely to be operative in older meta-sediments, where flexing and slippage must occur on original bedding planes, or metamorphic foliation. Several outcrops of igneous basement

rocks in the foreland display horizontal joints. In the Wind River canyon (T.6 N., R.6 E.) the granitic intrusion in the basement displays fracture surfaces parallel to the top of the Precambrian basement (fig. 20). These fractures represent sheeting joints which could have developed parallel to the Precambrian surface during erosion and unloading, prior to deposition of the basal Cambrian Flathead Sandstone. Several of these fractures contain material which may be the product of weathering, or may be fault gouge developed as granite has slipped past granite in an attempt to flex in response to the compressive stresses. Although not investigated in detail, exposures in Shell Creek canyon in the Bighorn Mountains (T.53 N., Rs.89 and 90 W.) also display numerous subhorizontal joints in the basement.

Sheeting joints would have been in the optimum position during the Laramide orogeny to act as pseudo bedding planes in the upper portion of the basement. Wilson (1934) reported slickensides on such features at Five Springs area, in the central Bighorn Mountains. Such joints would become less frequent downward, thus limiting any such flexural folding to the upper few tens of feet of the basement. While the initial development of the fractures would be brittle deformation, the Laramide folding would be a flexural slip process.

Another possible method of developing subhorizontal joints or fractures, can be found in the development of extension fractures parallel to the maximum compressive stress direction in compressional tests. If the maximum compressive stress is horizontal, and the minimum compressive stress is vertical, the resulting fracture set could include conjugate shears as low angle reverse faults, and horizontal extensional fractures. It would be difficult to identify horizontal extension fractures in sedimentary rocks, since the fractures would be parallel to the bedding planes. However, they might be observed in massive basement rocks such as granite bodies. These fractures would probably be restricted to shallow depths because they form only at low stresses normal to the fracture surface. Folding by this means would be a combination of brittle deformation and flexural slip.

5.4 Geometry of Faulted Basement

The forms which have been observed on faulted basement blocks (table 6) can be grouped into four general types: 1) horizontal planar upper basement surface, 2) rotated planar upper basement surface, 3) anticlinal curvature of the upper basement surface, and 4) synclinal curvature of the upper basement surface.

Horizontal planar basement surfaces represent either unfaulted areas, or blocks offset along planar, non-curved fault surfaces. Rotated planar basement surfaces achieve their orientation either by rotation along curved fault surfaces, or by rigid-body rotation between two faults surfaces.

Basement anticlinal curvature is generally observed on the upthrown (hanging wall) blocks of reverse faults, and the curvature originates as: a) "drag" effect along planar (?) fault surfaces, b) faulting of an already "folded" basement surface, or c) as a ramp anticline (Rich, 1934; Appendix A) by maintaining (during deformation) the cut-off angle between the fault and the basement surface (Brown, 1982) which is developed at the initiating of the faulting. The fault cut-off angle may be used to interpret the curvature and geometry of the fault plane deeper within the basement (see section 5.52, Basement fault cut-off angles).

5.41 Upthrown fault blocks

Dipping planar (rotated) basement surfaces on upthrown fault blocks are observed to outcrop in several areas throughout the foreland (table 6), and are frequently suggested in interpretations (Prucha and others, 1965; Stearns, 1971, 1975). An example crops out at Rattlesnake Mountain anticline (fig. 21), west of Cody, Wyo-

ming (T.52 N., R.103 W.), where the Precambrian basement surface dips approximately 13 degrees to the northeast (basinward). There are no exposures of Precambrian rocks on the downthrown side of the exposed fault, but the interpretation by Stearns (1971; 1975, his fig. 11; 1978) is that the basement surface on the downthrown side of the fault zone is horizontal and planar.

Many planar mountain flank dip slopes (having a sedimentary cover) have been cited to indicate that the underlying Precambrian surface is merely tilted by rigid-body rotation of the upthrown block, along a curved fault plane. An example is the gentle east-dipping east flank of Bald Mountain anticline (fig. 45) on the north flank of the Hanna basin. The rotation was caused by uplift along a curved fault on the west flank of Bald Mountain anticline.

Observations from areas such as Hunt Mountain, Porcupine Creek, and The Horn area (table 6) show instances where planar dip on the basement surface reverses direction and, for a short distance, dips into a major reverse fault, forming an anticline on the upthrown block (e.g. fig. 27). Detailed study of these and similar areas is needed to determine (if possible): (1) whether the anticlinal shape is the result of drag or faulting of a preexisting basement fold, (2) the type of basement rock

present, and (3) the "folding" mechanism which was operative at the time of deformation.

The Precambrian basement surface exposed in the canyon of the Clarks Fork River in the Beartooth Range (fig. 22), dips eastward toward the Bighorn basin on the upthrown block of the (East) Beartooth fault. Stearns (personal communication, 1982) has pointed out that evidence of cataclastic deformation, suggesting high angle faulting, is found in many of the erosional ravines in the face of the basement exposure. This suggests that the curvature of the basement surface may be the result of differential displacement and rotation along the high angle faults. However, the structural relief of this feature is 2,500 feet (760 m; approximately 1,000 feet, or 300 m, of relief is visible in the photo in figure 22) in a distance of two miles (3 km), and an estimate of the number of possible faults present (based on the number of major ravines) is approximately twenty. Therefore, an average displacement of 125 feet (38 m) per fault would be required to provide the 2,500 feet (760 m) of structural relief. Pierce (1965), has mapped faults farther up the canyon (to the west) which offset the basement by this magnitude, but he shows no such faults in this area, and a close examination of figure 22 shows that no offsets of the basement surface are apparent.

It is possible that the zones of cataclasis in the basement are the response to the attempted buckling of the basement rock brought about by horizontal compression. The anticlinal shape of the basement surface produced by the postulated buckling may represent an incipient Rich-model ramp anticline (Rich, 1934; see APPENDIX A). Basement-involved ramp anticlines should be able to form on the hanging wall blocks of reverse faults in the same manner as in overthrust belts, since the phenomenon is simply a geometric requirement of the fault shape. [An interpretation of a Rich-model ramp anticline has been published by Spang and others (1985) for the basement surface of Sage Creek anticline in the western Wind River basin (T.1 N., R.1 W., Wind River Meridian.)]. Recognition of such a step anticline on the basement surface would therefore imply a specific fault geometry in the subsurface. The tectonic significance of this geometry will be discussed in relation to the concept of compartmental deformation (see section 8.0).

The Precambrian basement in the Five Springs area (Wilson, 1934; and Hoppin, 1970) dips westward into the Five Springs thrust, in conformity with the overlying sedimentary section (fig. 23). A second reverse fault in the hanging wall of the Five Springs thrust is the upper boundary of the westward dipping segment of the basement, and in turn, has flat planar Precambrian basement on its

hanging wall. The role of flexural slip on sheeting joints in folding the basement has been discussed previously (see Possible Folding Mechanisms, section 5.32). It can be concluded that either the basement was folded by flexural slip and the resulting fold was later cut by the two faults of the Five Springs system, or that the basement was rotated between the two faults, and the rotation was, in part, accomplished by slip on the sheeting joints.

5.42 Downthrown fault blocks

The data needed to define the geometry of the Precambrian surface on downthrown fault blocks is seldom obtained from drilling or seismic exploration, the latter for reasons related to the seismic ray paths in that structural setting. Therefore, it is important to the interpretation of foreland structural styles to study those areas which are eroded deeply enough to expose the geometry of the basement surface on the downthrown block.

The basement surface exposed on the downthrown side of the Beartooth fault at Clarks Fork canyon dips 45 degrees eastward, in conformity with the overlying sedimentary section (fig. 24). It is not possible to determine whether the dip is due to rigid-body rotation on a deeper fault, or to flexure of the surface under compression. Either possibility is compatible with the formation of a

possible ramp anticline on the hanging wall, as discussed earlier (section 5.41). Stearns and Weinberg (1975) interpreted the dip of the basement surface seen here to be the result of rotation on a buried, curved fault. This geometry has not been verified in outcrop of the Wyoming foreland, but it is a valid method of accomplishing such rotations. Brown (1983) discussed the possibility that rotation on curved faults in footwall blocks may be responsible for the development and propagation of the lower reverse fault along the synclinal hinge, and will be covered in the discussion of the fold-thrust model of foreland deformation (see Model 4; section 7.24).

The reverse fault which controls the Porcupine Creek anticline (Bighorn Mountains) is exposed at basement level (fig. 25). The basement surface on the upthrown block is flat and planar (fig. 26a); however, on the downthrown block, the basement surface dips approximately 45 degrees westward in conformity with the overlying sedimentary section (fig. 25), and is interpreted to flatten westward into a shallow syncline on the footwall of the Porcupine fault, but still on the uplifted mountain block, as seen in figure 26b. This geometry suggests that the basement and sediments were folded, or rotated, together.

In the Hunt Mountain area, approximately four miles (6 km) southeast of Porcupine Creek cross section (fig. 25), the basement surface dips: (1) gently northeast away

from the faults, (2) westward, toward the fault on the upthrown block, and (3) westward, away from the fault on the downthrown block. This gives the appearance of an anticline which is faulted at (or very near) the crest of the structure at basement level. Maximum relief on this structure is approximately 4,500 feet (1,370 m) dip and fault offset). The fault displacement dies out to only a few hundred feet, along strike to the northwest (fig. 26a), but the anticlinal form is apparent with approximately 2,000 feet (600 m) of structural relief remaining. A lateral fault-to-fold interchange, such as this, is suggestive of sequential stages in the development of the fault. Some folding or rotation of the basement surface must have preceded propagation of the reverse fault upwards and out of the basement.

Note that the dipping basement surface on both hanging wall and footwall blocks represents a component of the total crustal shortening across the structure. The model of synclinal curvature on the footwall demonstrated here will be applied to interpretations discussed in later sections (5.52).

5.5 Orientations and Attitudes of Basement Faults

This section will explore the observed relationships between the strike of basement faults and the angle at

which they dip. This relationship has been mentioned briefly in an earlier section (3.32), as it applies to the diversity of movement patterns on Laramide faults resulting from reactivation of Precambrian faults.

5.51 Fault dip angles

The reported dips of fault planes in the Precambrian basement throughout the foreland range from 60 degrees to vertical for normal faults, and 20 to 60 degrees for reverse faults (table 7).

Low angle reverse faults. Figure 28 shows the location and trend of reported low angle (45 degrees or less), basement-involved reverse faults in the Wyoming foreland. To my knowledge, the first area in which there was sufficient well control to calculate the dip of a major subsurface reverse fault was the Waltman field, on the west flank of the Casper arch (Tps.36 and 37 N., Rs.85, 86, and 87 W.). There, the hanging wall of the northwest trending Casper arch thrust moved from northeast to southwest and subcrops under the Eocene Wind River Formation (fig. 29). Three wells drilled by 1960 had penetrated the thrust fault at the Upper Cretaceous level, and a three-point calculation yielded a dip of 20 degrees to the east-northeast. Later drilling (1979 to 1983) further east penetrated the Precambrian overhang, and data from three additional wells gave a dip of 43 degrees to the north-

TABLE 7. REPORTED DIP OF FAULTS IN PRECAMBRIAN ROCKS OF THE WYOMING FORELAND

AREA	FAULT DIP (DEG.)	STRIKE DIRECTION	TYPE OF FAULT	DOCUMENTATION
Arlington Fault	20	NW	Reverse	surface & seismic
Beartooth Fault	20-30	NW	Reverse	surface, seis., grav.
Cache Creek Flt.	30	NW	Reverse	seismic
Casper Arch	30-45	NW	Reverse	wells, seis.
EA thrust	20-30	NW	Reverse	wells, seis.
Elk Basin	30	NW	Reverse	wells, seis.
Five Springs	30	NW	Reverse	outcrop
Horn Area	45	NNW	Reverse	outcrop
Immigrant Tr.	20-30	NW	Reverse	wells, seis.
Laramie R.	30-45	N-S	Reverse	seismic
Owl Creek, N.	20	NW	Reverse	outcrop
Owl Creek, S.	30	E-W	Reverse	wells, seis.
Piney Creek	30-45	NNW	Reverse	wells, seis.
Porcupine	45-60	N-S	Reverse	outcrop
S. Granite	30	WNW	Reverse	wells, seis.
Uinta Mtns.	30	E-W	Reverse	wells, seis.
Wind River F.	20-30	NW	Reverse	wells, seis.
Beartooth,(East)	60-80	N-S	Reverse	outcrop
Beartooth,(Maurice)	80-90	NE	Tear Flt.	outcrop
Boysen	60	E-W	Normal	outcrop
Casper Mtn.	60-70	E-W	Reverse	outcrop
Corral Crk.	45-60	NE	Reverse	wells, seis.
Deep Crk.	70-80	NNE	Normal (?)	outcrop
Deer Crk.	45-60	N-S	Reverse	outcrop
Florence Pass	60-80	E-W	Reverse	outcrop
Mullen Crk. (Quealy fld.)	60-80	ENE	Normal	wells, seis.
Owl Crk., N.	60-80	E-W	Reverse	outcrop
Owl Crk., S. (deep)	?	E-W	Reverse	none
Piney Crk.	70-90	NE	Tear Flt.	outcrop
Tensleep Fault	60-80	E-W	Reverse	outcrop
Tongue River	70-90	NE	Tear; Rev.	outcrop

east on the thrust plane (fig. 30) at the base of the Precambrian overhang.

The change from a 20 degree dip in the sedimentary section, to a 43 degree dip in the basement is suggestive of the geometry of an upthrust fault (Prucha and others, 1965). However, Skeen and Ray (1983) and Sprague (1983), interpret seismic data as indicating that the Casper arch thrust flattens in the basement and dips very gently to the northeast for three to four miles (6 km) under the Casper arch, as shown in the seismic time-structure map of the thrust plane (fig. 31). Skeen and Ray also suggest that the process of steepening and flattening could be repeated further east, giving a stair-step appearance to the fault plane (fig. 29).

Another foreland feature which trends northwest, and is thrust to the southwest is the Wind River Mountain uplift of west-central Wyoming. In 1973, Husky Oil Company drilled through 6,247 feet (1,900 m) of Precambrian basement (fig. 32), cut a reverse fault, passed into upside-down Paleozoic rocks, and bottomed in overturned Pennsylvanian (?) rocks at a total depth of 12,944 feet (3,900 m), thus confirming the overhang and underturned flank of the fold-thrust model. The low angle form of the Wind River thrust is evident from industry seismic data (fig. 33).

In contrast to the previous examples of northwest trending foreland structures which have been thrust to the southwest, the Beartooth Mountains of southern Montana and northern Wyoming trend northwest, but have been thrust to the northeast on the southwest dipping Beartooth thrust fault. This conclusion is supported by Bonini and Kinard (1983) from analysis of a gravity profile across the northeast corner of the range (near Red Lodge, Montana). The results (fig. 34) indicate that the gravity data best fit a model of the Beartooth thrust dipping to the southwest at approximately 20 degrees, with an overhang of at least six miles (10 km).

The western Owl Creek Range is another northwest trending uplift (or series of small uplifts) which has been thrust to the northeast. The North Owl Creek fault, which bounds the northeast flank of this uplift, strikes northwest, from T.6 N., R.3 E., to T.8 N., R.1 E. (fig. 35a), where it is a low angle reverse fault which dips 20 degrees to the southwest, and places Cambrian through Pennsylvanian rocks on top of overturned Triassic beds (fig. 35b).

Other Laramide structures which have been documented by drilling, seismic data, and surface mapping, as being low angle reverse faults (less than 45 degrees) are summarized in table 7. It should be noted that all of the features discussed thus far are major northwest trending

Laramide uplifts controlled by reverse faults which dip gently to the northeast or southwest. These dip orientations are compatible with the mathematical models of Hafner (1951) and represent a conjugate reverse fault system.

Well exposed fault planes in the Precambrian basement of the foreland are rare. However, new road cuts through the hanging wall of the Five Springs thrust (fig. 23) have created several fresh exposures of the basement. Several small displacement reverse faults (fig. 36) can be seen dipping to the northeast at 30 degrees in the Precambrian basement.

High angle reverse faults. Figure 37 shows the location and trend of the known major high angle (greater than 45 degrees) reverse faults in the foreland (table 7). The North Owl Creek fault (described in the last section), which bounds the northeast flank of the Owl Creek uplift, changes strike in T.8 N., R.1 E. (fig. 35a), to become a west-trending fault which is upthrown on the south, bringing Precambrian and older Paleozoic rocks against upper Paleozoic and Triassic rocks (fig. 38). Field observations indicate this fault is a high angle reverse fault, dipping to the south. Other structural relationships relating to this fault will be discussed in a later section (see Evidence for the Various Models, section 7.4). Along the northeast side of the Beartooth Mountains

(in the vicinity of Red Lodge, Montana), Foose and others (1961) mapped two northeast-trending nearly vertical tear faults. Slickensides on the fault surfaces are subhorizontal, and the tear faults offset the Beartooth thrust.

The north-south trending Deer Creek fault (fig. 39) in the northern Bighorn Mountains, dips from 45 to 60 degrees to the east. It should be noted that the features discussed in this section strike to the east, northeast, and north, and several of the faults listed on table 7 have been shown to be reactivated Precambrian age zones of weakness (table 2). These are: the Casper Mountain, Corral Creek, Deep Creek, Mullen Creek-Nash Fork, Tensleep, and Tongue River faults; others have a high degree of parallelism with nearby Precambrian foliation and fold trends (table 4).

Synthesis. There is a consistent geometric relationship between the strike orientation and the dip angle of foreland faults. The major northwest-trending faults range in dip from 20 to 45 degrees to the northeast or southwest. They are perpendicular to the Laramide axis of maximum compression, and can be interpreted as a conjugate thrust system. Reverse faults which trend north, or north-northeast dip from 45 to 60 degrees. Those faults which trend east, or east-northeast (both reverse and normal) generally dip between 60 and 80 degrees and those

faults which strike northeast (parallel to the direction of maximum compression) are nearly vertical. The east and northeast trending faults described in this section display varying amounts of apparent lateral offset and oblique slip, and will be discussed further in section 9.0 (Crustal Shortening and Lateral Movements).

5.52 Basement fault cut-off angles

Dip angles of fault planes may be either increased or decreased by later rotation. Continued uplift of an anticline, or downwarp of a basin, as well as later faulting, may rotate a fault plane into a different position than at the time of formation. The initial dip of a basement-involved fault may be estimated from the angle included between the fault and the basement surface (assuming that the basement surface was originally horizontal). This angle is called the cut-off angle (fig. 40; Brown, 1982). Cut-off angles range from 20 to 90 degrees in the foreland, suggesting that there is a variety of inclinations of faults at the basement surface.

The importance of cut-off angles has been demonstrated by Brown (1984a) at Rattlesnake Mountain anticline. The cross section of Rattlesnake anticline (fig. 41) by Stearns (1971) was discussed concerning dipping planar basement surfaces (section 5.41). His section was drawn north of the Shoshone River canyon, the only expo-

sure of Precambrian on the anticline. The normal fault (A), which exposes the Precambrian in the Shoshone canyon, has been considered by many workers to be the major fault controlling the anticline. However, the small displacement on this fault indicates that it is more likely to represent crestal extension of a compressional fold, and to control the location of a broken off corner of the Precambrian forcing block. Stearns (1971) has described such a corner on a fold near Manitou Springs, Colorado (section 5.32).

Brown (1984a) interpreted Rattlesnake Mountain anticline (fig. 42), using a reverse fault model, with application of the synclinal basement configuration discussed previously (section 5.42). Note the synclinal curvature with upturned basement and sedimentary section (fig. 42) in the footwall of reverse fault (E). When the length of the Precambrian-Cambrian contact (X-X') is restored to its pre-deformation, subhorizontal position, the intersection of the fault and the basement surface (X') is seen to be at a point (X'') east of the crest of the anticline; thus a reverse fault dipping east at 65 degrees (reverse fault E), with a heave component of 2,250 feet (680 m), is required.

The cut-off angle of 52 degrees is determined from the cross section, by measuring between the top of the basement and the reverse fault (E). The dip on the base-

ment surface is 13 degrees to the northeast, and represents the difference between the present-day dip of the fault and the cut-off angle. This is equivalent to the rotation angle of the basement surface due to movement of the hanging wall block up the curved fault. If rotation of the basement surface produced by the curved fault is removed, the basement surface returns to its predeformational horizontal position (X-X"). Therefore the cut-off angle between fault (E) and the basement surface represents the actual dip of the fault at the original horizontal surface of the basement.

Lines drawn perpendicular to the fault plane (fig. 43) at the two dip positions of 65 degrees and 52 degrees, will intersect at a point which represents the pole of rotation for the arc of curvature of which the fault plane is a segment. The fault must be perpendicular to other "normals" also, and the controlling reverse fault must therefore flatten at depth to the northeast.

I have arbitrarily chosen to allow the fault in figure 43 to flatten down-dip until it reaches an angle of 30 degrees since this is the dip predicted for brittle shear failure for faults formed under horizontal compression (Hafner, 1951). Movement along this curved fault surface will produce the observed sense and magnitude of rotation (13 degrees) of the upper basement surface, as well as a

vertical fault-to-fold interchange (fault dies out upward into the sedimentary section) as shown in figure 42.

Many published structural interpretations would be altered dramatically if they were reinterpreted to account for the cut-off angles and footwall geometry. Rattlesnake Mountain anticline may now be placed into a scheme of regional compression, along with the other foreland features which have been listed and described as major (northwest oriented) Laramide structures (3.32). The reverse fault system of Rattlesnake Mountain anticline demonstrates that regional compression can produce a structure with relatively large vertical relief, small to moderate overhang, and basement rotation. Such an interpretation can explain the various structural features observed within the foreland in a manner which is consistent with the compressional development of the larger structures, such as the Wind River Mountains and Casper arch.

5.6 Summary

Data presented in the previous discussions demonstrate that the Precambrian basement of the Wyoming foreland is heterogeneous with respect to rock types and fabric orientation on the scale of individual outcrops. There is no consistent relationship between rock type and structural trends in the basement, and the northwest-

trending major Laramide uplifts. However, the presence of large-scale zones of weakness (major shear zones) in the basement have exerted a strong control on the location of many northeast-trending Laramide structural features. These structural features were reactivated during the Laramide orogeny because they were properly oriented with respect to the southwest-northeast direction of maximum compressive stress. Precambrian igneous dikes appear to have strongly influenced the location and trend of Laramide tear faults.

The data show that there is great variation in the Precambrian structural trends on all scales, ranging from foliations to major shear zones. The effect on Laramide structures of small-scale fabric elements such as foliation is minor.

Compatibility of the observed set of conjugate reverse faults in the basement with the fault trajectories in Hafner's (1951) solution for horizontal compressive stresses, suggests that the "homogeneity" assumed for the theoretical models, might also be applicable to the foreland basement in an overall sense. The foreland basement may be capable of deforming as an homogeneous body, while at the same time being broken into a heterogeneous pattern of blocks by reactivation of properly oriented zones of weakness in the Precambrian basement.

While the question of folding of the basement is not directly related to the development of the structural style, recognition of curved basement surfaces on both the hanging and footwall blocks is important because they present a part of the total crustal shortening involved in the compressive structural style. The published concept of mechanical basement (Stearns, 1978) requires brittle deformation and allows no folding of the basement. However, observations of the upper basement surface reveals several configurations which clearly indicate that the basement has been folded. This folding may have been created by several methods. These are: 1) cataclastic deformation, 2) macro-fracturing, 3) rigid-body rotation, and 4) flexural slip mechanisms. All of these mechanisms may have operated during Laramide deformation.

Flexural slip requires that either the rocks of the basement have properly oriented planar fabric elements such as foliation or joints, which can be activated as pseudo bedding planes, or such joints must form as extension joints parallel to the maximum compressive stress. Development of extension fractures would allow the flexing phenomenon to be active to the base of brittle basement, at which depths more plastic deformation would dominate. More study needs to be done throughout the foreland to determine which folding mechanisms may be predominant, and

to gather more data on possible horizontal extension joints.

The relationship of low angle reverse faults having varying magnitudes of overhang, and their common northwest trend, indicates that these reverse faults are primary conjugate shears, developed in a homogeneous basement, at right angles to the direction of maximum Laramide compressive stress. High angle reverse faults strike in the northeast quadrant, and have reverse oblique-slip, resulting in lateral offset (see Rattlesnake Mountain "Corner", section 8.52). These northeast trending features are controlled by basement zones of weakness of Precambrian age.

6.0 STRUCTURAL CHARACTERISTICS OF THE SEDIMENTARY SECTION

6.1 Introduction

The Precambrian basement complex is involved in many Laramide structures in the form of fault-bounded forcing blocks. A "forcing block" is any block of competent rock, which moves upward, forcing the overlying sedimentary section into folds which generally conform to the shape and size of the forcing block. The resulting structures in the overlying sedimentary section are dependent upon the mechanical properties of the rocks (structural stratigraphy) in each stratigraphic unit, the orientation of the principal stresses (compressional loading) in the sedimentary section, depth of burial, and pore pressure.

Bedding plane detachment is an important deformational mechanism in the folding process in the foreland. The presence of detachments in different stratigraphic units allows the development of secondary structures which do not involve the Precambrian basement.

6.2 Structural Stratigraphy

The term "structural stratigraphy" implies that stratigraphy (lithology) controls structural style. The stresses applied to the stratigraphic column during the

Laramide orogeny caused varying responses by different rock types, and also caused different responses by identical rock types which were located at increasing depths of burial. In the previous discussion on Paleozoic stratigraphy (section 3.32), it was noted that the Ordovician through Mississippian carbonate section has acted as the dominant structural member of the sedimentary section, and that the Pennsylvanian and Permian rocks have generally conformed to that dominant member.

However, the presence of incompetent, ductile Cambrian shales above the basement has resulted in the occasional complete detachment of the carbonate section from the underlying basement. In other instances, the carbonate section conforms to the pattern of basement deformation, with detachments in the Cambrian shales allowing some disharmonic folding to occur between the carbonates and the basement.

The Mesozoic section is comprised of sands and shales of differing thicknesses which react as "compound" structural units. The variable spacing and thickness of the competent sandstones (separated by incompetent shales), resulted in variations in responses to stress throughout the section, in contrast with the underlying Paleozoic section which deformed more consistently. Some of the changes in structural style observed at different stratigraphic levels in the Mesozoic section, are a direct

response to different depths of burial at the time of deformation.

The influence of stratigraphy upon structural style in the foreland has become better understood over the past several years. This is the result of theoretical and experimental work, and of detailed surface and subsurface analysis. Two concepts described in the next section have been developed based on this work; while both relate to stratigraphic control of structural style, they emphasize different aspects of the mechanisms involved.

6.21 Mechanical stratigraphy

The term mechanical stratigraphy has not been formally introduced into the published literature, but the concept has been discussed at length by Stearns (1978) and Weinberg (1978). The concept of mechanical stratigraphy is based on the experimental determination of the deformational mechanisms for various rock types at confining pressures simulating the probable depth of burial when the foreland was deformed.

Stearns (1971, 1978) and others have recognized sequences of stratigraphic units which respond to stress in a similar manner. These mechanical responses also include the idea of detachment faulting. Detachment faulting is a deformational mechanism which is dependent upon the me-

chanical stratigraphy which allows, or enhances bedding-plane slip.

The resulting form of foreland structures is controlled, in part, by the response and interactions of individual lithologies to the applied stress. These responses are summarized on table 8.

At the depths of burial postulated for the onset of the Laramide orogeny, igneous rocks, dolomites, quartz-cemented sandstones, and quartzites deform in a relatively brittle manner. Deformation of the sandstones depends upon depth of burial and pore pressure. Shallowly buried sandstones tend to deform by a brittle mechanism, such as fracturing or cataclasis, while deeply buried sandstones may deform in a more ductile manner. Limestones deform in a ductile manner with the development of calcite twin lamellae.

Shales have such variable mineralogy, that it is difficult to predict what deformational mechanism will be active. In general, shales with high quartz content deform in a more brittle fashion than shales which are clay-rich (Logan, 1982, personal communication). The clay-rich shales are the mechanical stratigraphic units which are most suceptible to the detachment process. In either case, the presence of well developed fissility enhances the development of bedding-plane slip, or detachment faulting.

TABLE 8. DEFORMATIONAL MECHANISMS FOR VARIOUS ROCK TYPES.

ROCK TYPE	DEFORMATION MECHANISM	CHARACTERISTICS OF DEFORMATION
IGNEOUS BASEMENT	brittle fracturing	macroscopic fractures "Rich-model" folding
METAMOR-PHIC BSMT.	flexure slip folding; brittle fracturing	on existing foliation or relict bedding
SHALES	bedding plane slip; ductile flow	thinning
LIMESTONE	ductile flow	flow until 30% deformation is achieved; twinning
SANDSTONE	cataclastic flow, (less ductile than limestone) brittle fracturing	granulation; rigid rotations of 15-20% before fracturing
DOLOMITE	brittle fracturing	in outcrop: macroscopic ductility can be achieved
QUARTZITE	brittle fracturing; cataclasis	macroscopic fractures complete granulation

Fanshawe (1971) has summarized the role which stratigraphy plays in localizing preferred zones of bedding-plane faulting or detachment within the sedimentary section. Figure 8 shows Fanshawe's grouping of the Bighorn basin sedimentary section into packages of relatively competent rocks (Cx); the bottom of each such unit is marked with an arrow labeled "DT" for a detachment horizon. He pointed out that all of the detachment horizons have also been described by other authors in relation to gravity induced sliding (such as in the Owl Creek Mountains; Wise, 1963; and the Heart Mountain and South Fork detachments; Pierce, 1957).

In addition to those horizons listed by Fanshawe, I have recognized several other stratigraphic horizons as being detachment-prone throughout the foreland. These units have been noted on figure 8 with the notation "DT-B". The various zones of detachments will be discussed in the section relating mechanical stratigraphy to the foreland (section 6.22).

Stearns (1978) has described three general categories of responses by the overall sedimentary section to forced folding in the foreland. These categories are: 1) nonwelded, nonthinning, 2) welded, nonthinning, and 3) welded, ductile.

1) Nonwelded, nonthinning stratigraphic units are ones in which the dominant competent unit deforms by brit-

tle mechanisms without thinning by ductile flow, and is separated from the forcing member by a ductile structural unit. In a welded, nonthinning section, the dominant competent unit is brittle under the conditions of deformation, and the ductile unit is absent, so that the dominant member is in depositional contact with the forcing member. Welded, ductile stratigraphic units differ from welded, nonthinning units only in that the dominant member is ductile under the conditions of deformation.

Nonwelded, nonthinning units are present in the lower Paleozoic stratigraphic section over much of the Wyoming foreland. The Ordovician to Mississippian carbonates, along with the Pennsylvanian sandstone and Permian carbonates, act as the dominant, nonthinning unit which controls the shapes and sizes of folds. The Cambrian shales and shaly limestones are the ductile units between the dominant carbonate unit and the underlying Precambrian basement forcing block.

An example of this type of stratigraphic section is exposed at Rattlesnake Mountain anticline (fig. 44) located near Cody, Wyoming. Stearns (1971, 1978) has pointed out that the Paleozoic carbonates have folded via the mechanism of rigid body rotation, with fixed hinges. He has also shown that the thickness of the Mississippian carbonates does not change appreciably across the fold. Fractures oriented at low angles to bedding in the car-

bonates indicate generally brittle deformation, and also (at least locally) that the principal stress was bedding parallel and perpendicular to strike. Numerous slickensides on carbonate bedding planes indicate that flexural slip has occurred.

2) The foreland stratigraphic section which demonstrates the welded, nonthinning condition is in south-central Wyoming, where the Cambrian shales have been replaced by thickening of the Flathead Sandstone, through a facies change (section 3.22). Only this thin sandstone unit separates the underlying Precambrian basement forcing block from the overlying dominant, controlling member. Folds such as Bald Mountain anticline (Blackstone, 1983; Prucha and others, 1965) on the north flank of the Hanna basin display this type of stratigraphic section. Folds formed in such areas show more brittle deformation, and are usually faulted through more of the sedimentary section, with less basement displacement than structures with the nonwelded, nonthinning stratigraphic section (Stearns, 1978).

At Bald Mountain (fig. 45), the steep flank of the structure is rotated into a nearly vertical position and highly imbricated, with numerous small displacement reverse faults. Bald Mountain is also one of the several features in the foreland which displays an anticlinal fold

on the hanging wall (Blackstone, 1983), which is mappable at the basement-sediment contact.

3) The welded, ductile stratigraphic section is present in southeastern Wyoming, where the lower Paleozoic section was removed by erosion of the Ancestral Rocky Mountains and the Pennsylvanian sandstone section was deposited directly on the Precambrian basement. The sandstone deforms by cataclastic flow, which causes extreme granulation of the grains (Suppe, 1985). During deformation, the sandstone is "forced" by the basement forcing block, deforms in a ductile manner, and at the same time, controls the shape and size of the fold in the sedimentary section (fig. 46).

The concept of mechanical stratigraphy provides a framework for subdividing the stratigraphic section in the foreland into "packages" which deform as discrete units. The mode of deformation for each package is dependendent upon the lithology of the controlling member.

6.22 Mechanical stratigraphy applied to the foreland

When the above mechanisms are correlated to the specific stratigraphic units of the Wyoming foreland, the relationships shown in table 9 should exist. The foreland stratigraphic section displays a variety of lithologies

TABLE 9. DEFORMATIONAL MECHANISMS APPLIED TO THE WYOMING FORELAND STRATIGRAPHIC SECTION.

PERIODS	FORMATION	DEFORMATIONAL MECHANISMS
TERTIARY	Fort Union	fracture; bedding plane slip
CRETACEOUS	Lance Mesaverde	bedding plane slip; fracture
	Cody	bedding plane slip; ductile flow
	Frontier Mowry-Thermopolis Cloverly	fracture; bedding plane slip; fracture
JURASSIC	Morrison Sundance	fracture; bedding plane slip
	Redwater Shale Mbr.	ductile flow, slip
	Gypsum Spring	fracture; bedding plane slip
TRIASSIC	Chugwater	
PERMIAN	Opeche Shale and Phosphoria Ls.	ductile flow; bedding plane slip
PENNSYLVANIAN	Tensleep Ss.	ductile flow up to 15-20% deformation by cataclastic deformation, then brittle failure
MISSISSIPPIAN	Amsden Sh.	ductile flow
	Madison Ls.	ductile flow up to 30% permenant deformation
DEVONIAN	Darby Ls.	bedding plane slip; detachment faulting
ORDOVICIAN	Big Horn Dolomite	brittle fracturing; macroscopic flow, via cataclasis

TABLE 9. (CONT'D)

CAMBRIAN	Gallatin Ls.	ductile flow
	Gros Ventre Sh.	generally ductile flow, some brittle deformation in "impure" shales
	Flathead Ss.	brittle deformation; cataclastic
PRECAMBRIAN	Igneous rock Metamorphic Rock	brittle deformation (?) flexural slip

grouped into "packages" which deform as coherent units. At the base, the basal Cambrian Flathead Sandstone is "welded" to the basement, and deforms in a brittle fashion as part of the forcing block.

There are shale units which are thick enough (several hundred feet) to be considered a single ductile package. Cambrian shales, when present, deform as a ductile, non-thinning unit, which allows the overlying stratigraphic section to deform somewhat independently and disharmonically with respect to the underlying basement forcing block. An example of a fold which forms from detachment in the Cambrian shales is discussed in a later section (see section 6.42, Paleozoic Section).

Other parts of the stratigraphic section form "mixed or compound" packages. The entire Paleozoic section above the Cambrian shales deforms as a very large package. The upper Cambrian limestones conform to the overlying carbonates of the Mississippian, Devonian, and Ordovician, which combine to control the overall shape and size of foreland structures as seen at Rattlesnake Mountain, Sheep Mountain, and Clarks Fork Canyon anticlines.

Deeply buried, thick limestone sequences deform by the calcite twinning mechanism. Dolomite on the other hand deforms by a brittle (fracture) mechanism at all depths. Presence of the Big Horn Dolomite in the stratigraphic

section causes the combined carbonate section to act as a forcing block.

Many carbonate units fold disharmonically above (or below) other carbonates, by virtue of detachment on very thin shale seams. Detachment faulting in the shaly limestones of the Devonian (fig. 8) causes structural repetition of the Mississippian limestones, and modification of the fold-form of the dominant carbonate member.

The Pennsylvanian Tensleep Formation typically conforms to the underlying Mississippian carbonates, with some disharmonic folding facilitated by detachment faulting in the Amsden Shale (fig. 8). The overlying Permian carbonates, and shale facies, deform in a more ductile manner than the Tensleep Sandstone; numerous bedding-plane detachment faults occur in this stratigraphic unit in the subsurface and in surface outcrops.

The sandstones, siltstones, and shales of the Triassic usually deform as a single package, with minor local variations if a thick sandstone or shale unit (fig. 8) is present. The Jurassic deforms in two units; the Gypsum Spring Formation deforms in continuity with the underlying Triassic Chugwater Formation, and the Morrison and upper Sundance Formations conform to the overlying basal Cretaceous package. The separation of the Jurassic

into two packages is in response to the ductile deformation and detachments in the Redwater Shale (fig. 8).

The Frontier Formation and Cloverly Group (basal Cretaceous) are both predominantly sandstones, while the intervening Mowry and Thermopolis Formations are shale; yet the section from the Frontier Sandstone down through the Cloverly Group typically deforms as a single compound unit, with minor influence exerted by the Mowry (fig. 8) and Thermopolis shales. The ductile response of the overlying Cody Shale (fig. 7) separates the Lance-Mesaverde and the Frontier-Cloverly "packages" into two different mechanical units. Detachment faulting in the Cody Shale (fig. 8) usually occurs in the upper portion, in the facies which are transitional with the Mesaverde Sandstone.

The Mesaverde Formation is predominantly sandstone with interbedded shales, while the overlying Lance and Meeteetse Formations (fig. 7) are about equally divided between sandstone and shale. These three formations (Mesaverde, Lance, and Meeteetse) usually deform as a single structural package, folding in parallel with one another. The Paleocene Fort Union Formation is included in the Lance-Mesaverde package in the Bighorn and eastern Wind River basins, where the Paleocene is conformable with the underlying Cretaceous rocks.

The presence of detachment-prone stratigraphic horizons has strong implications for the selection of the basic structural style of the Wyoming foreland. Cross sections presented in this study show many faults which clearly duplicate stratigraphic units at one level, and sole out in lower detachment zones. Superposition of such features in a single structure results in gentle or open anticlines (Fleuty, 1964) which tighten downward to a detachment zone, and possibly return to gentle open folds beneath the detachment.

6.23 Summary

The forms of Laramide structures are controlled by three factors which interact during the time of deformation. These are: 1) the upward movement of a basement forcing block, 2) the deformational mechanisms active in the sedimentary section which are controlled by lithology, depth of burial, and pore pressure, and 3) arrangement of the various lithologies into "packages". These packages may be of the same lithology (and same deformational mechanism), or of different lithologies which may combine into "compound packages", in which the preferred deformational mechanism is determined by the dominant lithology. The resulting structural configuration(s) will thus display a variety of geometries (fig. 47). The Precambrian basement forcing block is typically faulted up

into the overlying Cambrian rocks, forming a large, relatively simple anticline in the overlying Paleozoic section. The form of the fold is controlled by the dominant member of the Paleozoic package, which is composed of the Ordovician through Mississippian carbonates. Adjustments in fold shape are accomplished by detachments in the shaly limestone of Devonian age and the Pennsylvanian-Mississippian Amsden Shale, which develop as volume adjustments out of the adjacent synclines.

Overlying the Paleozoic rocks will be a fold in the Mesozoic rocks which becomes more broadly folded upward through the section, and which displays numerous subsidiary folds, which are again the result of volumetric crowding in the adjacent synclines. Multiple detachments allow the anticline to tighten downward, detach and then return to a more open fold, often changing directions of asymmetry as it does so. Further implications of these structural configurations will be discussed in later sections (see Structures Related to Synclinal Adjustments, section 6.33; and Fold-thrust Uplifts, section 7.44).

6.3 Compressive Loading of the Sedimentary Section

6.31 Introduction

In this section I discuss the geometries which result from compressive loading of the sedimentary section. This loading may be a primary loading, related to the regional compression forming the major structures, or it may be a secondary compressive loading related to volume problems created by the development of other structures. The folding is described as parallel or "concentric", and is typified by anticlines which tighten downwards, and synclines which tighten upward, along their axial surfaces.

6.32 Foreland examples of flexural slip folding

In the foreland, folding is dominated by flexural slip. Characteristics of parallel folding (generated by flexural slip) are covered in APPENDIX B. Slip is on bedding surfaces, with the direction of slip from the synclinal hinge toward the anticlinal hinge (see APPENDIX fig. B-2).

Large scale foreland structures show characteristics of flexural slip. Slickensides have been observed on bedding planes in structures such as Rattlesnake Mountain (section 6.21) and Sheep Mountain anticlines. The sense of movement on bedding-plane slip on the steep eastern limb of Sheep Mountain anticline is parallel to the dip of the bedding in the Mississippian carbonates (fig. 48a).

Reverse faults on the same limb, verge toward the anticlinal crest, and can be observed to sole-out downward onto bedding planes, indicating a genetic relationship between bedding-plane slip and some reverse faults (see fig. 48b). Subsidiary drag folds (6.33) have formed near the crest of Sheep Mountain anticline (fig. 49) as a result of upward transfer of displacement from bedding-plane slip, to reverse faults, to folding (Hennier and Spang, 1983).

Wildhorse Butte anticline (fig. 50a) is a structure which becomes more tightly folded down the axial plane to the point where volumetric (bedlength) problems develop (APPENDIX B). The core of the anticline exposes Permian limestones in two tightly folded anticlines which are thrust from the east (out-of-the-syncline), on a series of imbricate faults (fig. 50b). The presence of thrusts and tight folds (fig. 51a) in the core of this structure indicates that the basal detachment is just below ground level. The role of fracturing as a folding mechanism is shown by the Permian carbonates in the core of this tight fold (fig. 51b).

West Mud Creek anticline (fig. 52), displays a zone of basal detachment, below which the Permian limestones are folded in a gentle anticline (APPENDIX fig. B-3). The downward continuation of anticlines across zones of detachment allows for a greater vertical propogation (with

depth) than would be predicted by the characteristics of parallel folding. The repeated process of detachment and fold propogation leads to the concept of "multiple detachments" (Dahlstrom, 1970; APPENDIX fig. B-10), which will be discussed more fully in the next section (6.33).

Synclinal "upper detachments" (Dahlstrom, 1969a; APPENDIX figs. B-6, B-10) can be seen in outcrops of the Lower Cretaceous Mowry and Thermopolis Shales (fig. 53a) at Goose Egg anticline on the east flank of the Bighorn basin. The syncline is developed between the main axis of the Goose Egg anticline (right) and a subsidiary fold on the northeast (left) flank (fig. 53b). Volumetric adjustments in the syncline can be seen as tightly folded anticlines and synclines, and small reverse faults, outlined on the photograph. Above these tight folds, the shales of the Mowry display a broad, flat-bottomed synclinal form, with the overlying Frontier Sandstone preserved as a synclinal remnant. The Mowry Shale is also folded isoclinally (APPENDIX fig. B-3) in the core of the subsidiary anticline (fig. 53b). The characteristic downward tightening of the anticline indicates that the "basal detachment" (APPENDIX fig. B-5) should be just below ground level, as shown in the subsurface interpretation of Goose Egg anticline (fig. 54). The subsidiary fold appears as a large "Z" fold on the flank of Goose Egg anticline. Subsidiary "drag" folds are

developed by flexural slip movements on the flanks of synclines. Typical "S" and "Z" drag folds (APPENDIX B) have formed on different foreland structures at almost every stratigraphic level of the foreland sedimentary section.

6.33 Structures related to synclinal adjustments

Based upon my work in the foreland, I have recognized three styles of structures which result from deformation related to the volumetric adjustments (out-of-the-syncline crowding) required by parallel folding. I have named these: 1) BACK-LIMB FOLDS, 2) CROSS-CRESTAL STRUCTURES, and 3) RABBIT-EAR FOLDS (fig. 55 a,b,c). The geometry and mechanism of formation of these types of structures will be discussed in the following three sections. Recognition of these structural styles is critical to accurate interpretation of subsurface well control and seismic reflection data. In addition, all of these structures may develop on a scale large enough to be of economic importance in the exploration for hydrocarbons.

Back-limb folds (originally called crowd structures, Brown, 1982) are essentially large-scale "Z" or "S" drag folds and thrust faults, which develop in response to the volumetric problems created in upward tightening synclines. When stratigraphic layers are flexed in the parallel folding of a syncline (APPENDIX B), bedding-plane

slip occurs which is directed away from the constricted synclinal hinge, and up the flanks of the structure. A back-limb fold (fig. 55a) will develop on the gentle back limb of an adjacent anticline (as an "S" or "Z" drag fold), but may also form on the gentle flank of a basin, and seemingly have no relationship to an underlying anticline. The initial movement is usually along a detachment as bedding-plane slip. The displacement may remain confined to the bedding plane but become "blind" (or die out) in the direction of slip, and fold the overlying layers, with the bedding plane serving as the basal detachment. It will more commonly cut upsection in one or more ramps, giving rise to anticlines as shown (fig. 55a).

An example of this ramping style is displayed on the gentle back limb of the Virgin anticline in southwestern Utah (fig. 56). The displacement along the fault which occupies the synclinal axial plane (lower right) transfers material from the hinge zone of the syncline, up the gentle flank of the structure, removing excess volume from the trough of the fold. Similar features are developed at a larger scale at Spring Creek anticline (fig. 57; Petersen, 1983). The existence of back-limb folds is shown by interpretation from well control and outcrop data. An unpublished reflection seismic line located along the line of this cross section shows that the Frontier Sandstone on

the gentle flank of the syncline is undisturbed, substantiating the interpretation that the fault encountered in the well control on the left dies out at the synclinal hinge.

The surface map of the Horse Center and Half Moon anticlines (Pierce, 1970; fig. 58), displays the west-verging Half Moon thrust which cuts the Frontier Sandstone along the surface trace of the thrust. The geometry of the Half Moon fault can be determined from logs of wells drilled in the Half Moon oil field (fig. 59). The fault plane soles out in the Jurassic Redwater Shale (fig. 8) on the west flank of the Dry Creek syncline. Unpublished reflection seismic data along the line of cross section confirm that the fault remains confined in the Redwater Shale eastward to the synclinal hinge under the Horse Center surface anticline. The geometry is essentially the same as that on the Virgin anticline in Utah (fig. 56), but the slip surface can be traced over a distance of approximately four miles (6 km) in this example.

Examples of large scale back-limb folds are found on the northeast flank of the Wind River Mountains. The northwest Wind River basin becomes more tightly constricted toward its northwest end, as the west-trending Owl Creek uplift converges on the northwest-trending Wind River Mountains. Volumetric problems in the Wind River

basin have been relieved through the development of the Wind Ridge thrust, which verges to the southwest.

The Windrock Ranch anticline (fig. 60a) can be interpreted as a back-limb fold on the northeast dipping flank of the Wind River Mountains. It is a tight fold at the stratigraphic level of the Jurassic Sundance Formation, suggesting that the anticline is detached from the underlying Paleozoic strata. The depth-to-detachment calculation (APPENDIX D) for this anticline, when plotted on the cross section (fig. 60b), indicates that the detachment surface is in the Jurassic Redwater Shale, or possibly as deep as the Triassic Chugwater Formation.

Downdip (northeast) into the Wind River basin, a northeast-trending seismic reflection line reveals a similar anticlinal structure under Tertiary rocks (fig. 61). The prominent reflections are as indicated on the figure (basal Cretaceous sandstone section, near the top of the Triassic Chugwater Formation, and near the top of the Mississippian carbonate section).

The basal detachment for the anticline is apparently in the Jurassic Redwater Shale. Bedding plane slip in this horizon has been translated updip into a reverse fault, which dies out into the fold at the base of the Cretaceous section. The details of the faulting can not be clearly discerned from the reflection data, because the structural thickening in the core of the anticline,

resulting from the reverse faulting, appears to have affected the local velocity distribution (as indicated by the "break up" of the deep Mississippian reflections under the steep forelimb of the anticline). The scale and location of both the Windrock anticline and the uried fold described above, suggest they represent large scale back-limb folds, related to the crowding resulting from the folding of the Wind River basin. These features are located so far up the regional flank of the basin, that they can not realis- tically be the result of local compressional forces related to the uplift of the Owl Creek or Wind River Mountains. The wide range of scales displayed by back-limb folds indicates that this mechanism of volumetric compensation is an important fold style in the Wyoming foreland.

Cross-crestal structures (fig. 55b; Brown, 1982) are created by the same volume problem and fold mechanism as back-limb folds, and originate where bedding-plane slip on the gentle flank of the syncline, overrides the axial plane of the adjacent anticline, shifting the crest. While the trajectory of the bedding-plane slip is depicted in the diagram as remaining confined to a single bed until the crest of the anticline is encountered, this is not a rigid requirement. The initial bedding-plane slip may ramp upsection in the direction of tectonic transport, creating ramp anticlines (Rich, 1934; APPENDIX A) as in

the case of the back-limb folds. In either case, the fault eventually cuts across bedding when it reaches the axial plane and repetition of stratigraphic units increases in the direction of transport (unless the fault dies out into fold displacement). This can be illustrated diagrammatically (fig. 62) by a series of wells arranged in a transverse section of an anticline. The stratigraphic throw (repetition or vertical displacement) decreases progressively from well #1 to well #5. This decrease in the vertical component suggests that the fault plane is passing downward into bedding-plane slip. As the vertical offset of the layers decreases, the electric log no longer displays recognizable repetition of the log pattern; however, the electric log curve may exhibit a more smooth, rounded, and "stretched" character, indicating the disruption of the bedding planes.

Petersen (1983) recognized the cross-crestal nature of subsurface faults in Pitchfork anticline in the Big Horn basin (fig. 63). The detachment in the Jurassic Redwater Shale extends from the syncline at the northeast side of the cross section along a horizontal distance of 16,000 feet (4,800 m) and cuts upsection as a reverse fault on the flank of Pitchfork anticline. Stratigraphic duplication across the fault reaches 250 feet (75 m) where the fault crosses the deeper structure, shifting the shallow crest approximately 1,000 feet (300 m) to the west.

A surface example of a cross-crestal structure is shown on the map of Horse Center anticline (fig. 64a) which is shown in the "down-plunge" viewing orientation (north to the bottom). The crestal line of the anticline is deflected where it crosses through the outcrop of Jurassic rocks. Field observations establish that the fault which offsets the Cretaceous Frontier Formation, also offsets the Cloverly and Morrison Formations (KJcm), becomes parallel to bedding in the Jurassic Redwater Shale, and cannot be traced any further to the northeast (fig. 64b). The schematic cross section (fig. 65) shows that the fault overrides the deeper crest of the anticline.

Rabbit-ear folds (Tomlinson, 1952; fig. 55c) are created by the same synclinal volume problems and fold mechanism as back-limb folds, and cross-crestal structures. Rabbit-ear folds serve the same purpose on the steep limb of anticlines, as the back-limb folds do on the gentle limb. Rabbit-ear folds are so-named for the appearance in both map and cross section view as that of a "long-eared" subsidiary fold on the steep flank of an anticline (fig. 66; see Foreland Examples of Flexural Slip, section 6.32).

Bedding-plane slip, which originates at the hinge of the syncline, transfers excess rock volume upwards, along the steep limb of the adjacent anticline. At the axial

plane (axial trace in cross section) the movement continues upward toward the direction of least stress, rather that following along the bedding planes over the crest of the structure. Field observations confirm that the original trajectory of the motion of the bedding-plane slip, is maintained by the reverse faulting.

Description of the geometry and formation of the rabbit-ear fold will be presented through a discussion of four examples from the foreland. 1) A small rabbit-ear fold exposed in the Permian Goose Egg Formation on Big Trails anticline in the southern end of the Bighorn basin (fig. 67a) is faulted through the top of the Pennsylvanian Tensleep Sandstone. The fault dies out upward into the Permian Goose Egg Formation, which is folded into an "L" shaped syncline on the east side of the structure. The down-plunge view of the structure to the northwest (fig. 67b) shows a rabbit-ear fold outlined by the white gypsum bed. The rabbit ear is projected up-plunge (dashed bedding in figure 67a), to show the overall relationship of the structure. The tightly folded units in the core of the rabbit-ear (at ground level in fig. 67b) suggest that the principal detachment is just below the ground surface, and has died out upward by fault-fold interchange.

2) The geometry of the lower portion of an "L" shaped syncline is exposed on a large scale in the Mississippian Madison Formation of the Wind River Mountains (fig. 68).

The syncline at this outcrop is highly asymmetric, with the gentle limb dipping away from the mountain uplift. The basinward dip of the gentle flank of the syncline concentrates the bedding-plane slip on the steep limb, as it is easier to move up the flank (toward direction of less stress) than to shove material down dip, and the best exposed rabbit ears have this geometry. Bedding plane slip which occurs in the shaly carbonates, changes to recognizable reverse faulting at the position of the anticlinal axial trace, as shown by the duplicated Mississippian limestone beds on the steep flank of the structure. In most exposures of rabbit-ear structures, the reverse fault dies out upward by fault/fold interchange. In this example, erosion has removed any evidence of such a fold. The fault-fold interchange (fig. 55c) gives the appearance of the "rabbit ear". Often the plunge of the main anticline is greater than the plunge of the "ear" accentuating the map pattern of the rabbit ear (fig. 69).

3) The aerial view in figure 70a shows the rabbit-ear fold developed on the steep forelimb of Rattlesnake Mountain anticline. The Ordovician Big Horn Dolomite has been repeated on that steep limb of the anticline (fig. 70b) by a reverse fault which dies out upward into a rabbit-ear fold in the Mississippian limestones (fig. 71a). The out-of-the-syncline reverse fault was generated

by volumetric constriction of the adjacent syncline (fig. 71b).

4) A down plunge view of Sheep Mountain anticline (fig. 72) shows the development of a rabbit ear on the steep flank of that structure. This example clearly demonstrates the downward sole-out of the reverse fault into bedding plane slip in Jurassic rocks.

Spring Creek anticline (fig. 57) demonstrates that rabbit-ear folds can develop on the steep limb of a syncline while back-limb folds develop on the gentle limb of the same syncline. Both structures originate from, and solve, the same synclinal volume problem.

The creation of multiple detachments (Dahlstrom, 1970; APPENDIX B) in foreland structures causes the formation of multiple rabbit-ear folds which are "stacked", or superimposed over one another at locations determined by the positions of the detachment prone horizons (fig. 8). The development of multiple rabbit-ear folds is shown schematically in figure 73. The asymmetry developed by the basement forcing block (facing right) forms a continuous "L"-shaped syncline at deep stratigraphic levels. Bedding-plane slip created by the volumetric constriction in this syncline causes numerous detachment faults which move up the steep flank (toward the left) of the main anticline. Each of these detachments will die out upward into a rabbit-ear fold

which will be asymmetric (left facing) in the direction of tectonic transport, but opposite to the major structure. Thus each rabbit-ear will create a secondary syncline, (a small scale version of the major "L"-shaped syncline) which will be located almost directly over the crest of the main anticline. The secondary synclines will develop volume problems which are accommodated by bedding-plane slip directed up the short flank of the underlying rabbit-ear fold (toward the right), which will develop a secondary rabbit-ear fold. Asymmetry of the secondary rabbit-ear folds will be in the same direction as the basement forcing block and major syncline. The interaction of multiple rabbit ears produces an alternation in the direction of fold asymmetry, up through the sedimentary section. I have called this arrangement of oppositely vergent rabbit-ear folds "ping-pong structure" (Brown, 1982).

An example of multiple rabbit-ear folds and "ping pong structure" is shown by Chabot anticline (in the southeast end of the Bighorn basin). The anticline is eroded into Upper Cambrian limestones (fig. 74) exposing a tight fold, with an interlimb angle of approximately 30 degrees. The fold plunges to the northwest at approximately 14 degrees (as determined by a stereonet plot of surface dips and strikes). The east-facing asymmetry of the fold at the top of the Pennsylvanian Tensleep For-

mation is indicated in a down-plunge aerial view of the structure (fig. 75).

The syncline visible in the Mesozoic stratigraphic units (fig. 74) projects to depth at the base of the steep limb exposed in the Pennsylvanian Tensleep Formation. Bedding plane slip in the Permian Goose Egg Formation (figs. 75, 76a), directed up the forelimb of the anticline is replaced by reverse faulting, which places the Permian Goose Egg Formation over Triassic Chugwater Formation (fig. 76b). The faulting is replaced upward by a rabbit-ear fold expressed in the basal Jurassic Gypsum Spring Formation (figs. 75, 77a). The direction of asymmetry of the rabbit-ear fold at the Gypsum Spring horizon is opposite to the direction of asymmetry of the fold expressed in the Pennsylvanian Tensleep Formation (fig. 75).

The reversal of asymmetry outlined by the Jurassic Gypsum Spring Formation creates a syncline which is secondary to the main syncline on the east flank (fig. 75). Bedding plane slip is moved toward the east, out of this secondary syncline, resulting in another change of asymmetry expressed in the Lower Cretaceous Thermopolis Shale (figs. 75, 77b). Detachments in the Lower Cretaceous stratigraphic section are directed westward, out of the main syncline to the east. The disharmonic relationship between the west-verging fold in the Mowry

Shale, and the east-verging fold in the underlying Thermopolis Shale is exposed down the plunge (figs. 75, 77b).

The cross section of Chabot anticline (fig. 78) shows the relationship of all of the detachments and rabbit-ear folds, and looks very similar to the schematic section (fig. 73) shown earlier.

6.34 Summary

Compressive loading of the sedimentary section, either by regional or local stresses, causes flexural slip folding, which creates parallel folds. A distinctive characteristic of parallel folds is the development of basal detachments beneath anticlines and upper detachments above synclines. Detachments are created by bedding plane slip which occurs as the rocks flex during folding. Volumetric constriction of parallel synclines causes bedding-plane slip to move away from the synclinal axis, and up the flanks of the fold.

Bedding-plane slip translates into reverse faults which cut upsection in the direction of tectonic transport, and die out upward by fault-fold interchange. The structures which result from this process are called:

1) back-limb folds (on the gentle back-limb), 2) cross-crestal structures, (which offset the crest of the adjacent anticline), and 3) rabbit-ear folds (which form

on the steep forelimb of anticlines).

Back-limb folds have been observed at several different scales and represent one of the major structural styles in the foreland. Because of the potential for large offsets of anticlinal crests, a recognition of cross-crestal geometry is very important to proper mapping of deep structures, based upon shallow well control and seismic data.

The opportunity for multiple changes in direction of asymmetry within a single foreland fold, through the development of multiple rabbit ears, urges caution when comparing directions of asymmetry between different structures.Such comparisons made between different structures, should be at the same stratigraphic level since most detachment horizons are present in all of the major foreland structures.

Duplication of strata on the steep limb of foreland anticlines as a result of out-of-the-syncline crowding, rather than extension or thinning of the rock layers, suggests that horizontal compression is more likely to have generated these structures than the process of differential vertical uplift.

6.4 Structural Observations at Different Stratigraphic Levels

6.41 Introduction

Structures displayed in the sedimentary section are strongly influenced by the movements of the underlying Precambrian basement forcing block. The typical foreland anticline is asymmetric, and contributes to the generation of subsidiary folds which move out of the adjacent synclines as volumetric adjustments (section 6.33).

Structural configurations in the sedimentary section change with depth and variations in lithology, as indicated in the discussion of structural stratigraphy (section 6.20). The foreland sedimentary section may be divided into "mechanical" packages (see Mechanical Stratigraphy Applied to the Foreland; section 6.22) which are controlled by the thickness of the dominant member, and by its mechanical response to applied stress. Some packages are monolithologic and have a common deformational mechanism, while others are compound packages (multilithologic), and are controlled by the deformational mechanism of the dominant member (with minor variations due to the presence of other lithologies).

This section will discuss the structures observed at different stratigraphic levels throughout the foreland, and the changes which take place in fold forms as a func-

tion of the deformational characteristics of the various mechanical packages discussed earlier (see Structural Stratigraphy, section 6.2; and Compressive Loading of the Sedimentary Section, section 6.3). Refer to figures 6 and 7 for the regional distribution of the stratigraphic units across the foreland, and to figure 8 for reference to recognized detachment-prone stratigraphic horizons (see Mechanical Stratigraphy, section 6.21).

6.42 Paleozoic section

The basal Cambrian sandstone is welded to the basement (see Mechanical Stratigraphy, sections 6.21; and 6.22), and can be traced over and around many Laramide folds, outlining the anticlinal shape. Many of these folds are faulted at their crests, and fault offset of the basal sandstone is easily determined. Examples of this are: West Billy Creek anticline (Brown, 1983); Bald Mountain anticline (Blackstone, 1983); southeast plunge of Porcupine Creek anticline (Brown, unpublished data); Sunshine "nose" (east flank of the Laramie Range; Love and Christiansen, 1985); Sheep Mountain anticline (southwest Wind River basin; Gooldy, 1947); and the northwest plunge end of the Ferris Mountain anticline (Brown, unpublished data). Occurrences of anticlinal forms such as these has led to the concept that the top of the Precambrian basement is "folded". The possible methods of such folding

have been discussed previously (see Possible Folding Mechanisms, section 5.32).

The ductile Cambrian shales have served as the detachment horizon for Lodge Grass Creek anticline in the northern Bighorn Mountains (fig. 79). This is an example of a fold where this process has detached the upper limestone unit of the Cambrian and the Ordovician Big Horn Dolomite, from the underlying basal Cambrian sandstone and Precambrian basement. Another example of detachment in the ductile Cambrian shales is displayed at the up-plunge exposure of Anchor anticline (fig. 80). Here the limestones within the Cambrian shale section are folded disharmonically with respect to underlying units, and with the overlying upper Cambrian Gallatin Limestone. The upper limestone unit is not separated from the overlying Ordovician Big Horn Dolomite by a detachment surface or ductile zone, and thus becomes part of the controlling carbonate member.

The Mississippian through Ordovician carbonate section generally folds into anticlines and synclines as a single unit, with some minor disharmonic folding caused by the presence of occasional shales, which act as local detachment zones (see Mechanical Stratigraphy, sections 6.21 and 6.22). Because the Paleozoic carbonate layers act as dominant members of the deforming rock package, and usually fold as a single unit, they may be thought of as a

"structural strut" (Stearns, 1978). This strut is the main resistance to Laramide stresses in the sedimentary section; as such the configuration which the strut takes on during deformation greatly influences the form of the structure in the overlying stratigraphic section.

On the outcrop, this carbonate section forms impressive dip slopes on the gentle flanks of the uplifts, and massive flatirons on the steep flanks. Anticlines eroded to the top of the Mississippian carbonate are long and linear. The narrow hinges of the folds are often well-displayed in almost circular shapes (fig. 81). The anticlines exposed at this level are typically asymmetric, with the steep limb facing the adjacent mountain uplift. If the erosion level is near the base of the Mississippian section, the hinge of the syncline adjacent to the steep flank, is exposed in the form of an "L", as the steep limb flattens to a gentle dip (see figs. 68, 82). Local detachments also form along the bedding planes of the Mississippian carbonates (fig. 48), resulting in the formation of disharmonic drag folds (rabbit-ears) in the carbonates (fig. 49).

The Devonian shaly limestones often act as a local detachment horizon within the Mississippian-Ordovician mechanical package (dominant member). In the subsurface of Horse Center anticline (fig. 59), reverse faults, which are interpreted to sole-out in the Devonian shaly lime-

stones, repeat the Pennsylvanian and Mississippian section (fig. 83).

The Ordovician Big Horn Dolomite typically forms tight anticlinal hinges, such as at Shell Canyon (fig. 84). The synclinal hinges are often broadly folded into the form of an "L" (fig. 79, Lodge Grass Creek). In a few areas, the Big Horn Dolomite can be observed to be structurally duplicated by reverse faulting (which originated in the Cambrian shales) on the steep limb of Rattlesnake Mountain anticline (fig. 70b; Structures Related to Synclinal Adjustments, section 6.33).

The Permian and Pennsylvanian structural package usually conforms to the underlying Mississippian-Ordovician dominant member. However, in some structures such as West Mud Creek anticline (fig. 52) the Permian limestones tighten progressively downward and detach in the core of the structure along local bedding planes. Chabot anticline (figs. 74, 75, 76) is a classic example in which the red shales of the Goose Egg Formation act as detachment prone horizons. Subsurface well control shows the triplication of the limestone of the Goose Egg Formation in the core of Iron Creek anticline (fig. 85), located on Casper arch. Stricker (1984) reported the presence of subsidiary rabbit ear folds in the Permian Goose Egg Formation, localized on the steep flank of the Zeisman-Brokenback anticlinal trend (T.48 N., R.89 W.) as

the result of crowding out of the adjacent syncline by bedding-plane slip.

The Pennsylvanian sandstone unit is often exposed in large, closely folded anticlines along the mountain flanks. These folds are typically asymmetric away from the axis of the adjoining basin. Occasionally, the Pennsylvanian-Mississippian Amsden Shale acts as a detachment horizon, allowing the overlying Pennsylvanian to become folded disharmonically with respect to the underlying Mississippian-Ordovician carbonate package. An example appears on the flank of the Shell Canyon flexure at Red Canyon, on the west side of the Bighorn Mountains (fig. 86). Wildhorse Butte anticline (figs. 50 and 56) is another example where the structure is detached in the Amsden Shale, and the Permian-Pennsylvanian section is folded disharmonically above the Mississippian.

The limestones of the Permian Phosphoria Formation often conform to the shape of the structure in the underlying Pennsylvanian Tensleep Sandstone. At Anchor anticline, the upper surface of the Tensleep Sandstone is reverse faulted in the core of the structure (fig. 87). The overlying Phosphoria limestones are not faulted as they pass over the crest of the structure, creating a vertical fault-to-fold interchange.

6.43 Mesozoic section

The Triassic stratigraphic section deforms in conformity with the underlying Permian (and Pennsylvanian) rocks, as well as the overlying basal Jurassic section. The Jurassic has been divided into two structural packages which deform independently of one another. The basal Jurassic Gypsum Spring Formation deforms in conformity with the underlying Triassic red beds (section 6.22). The Redwater Shale is one of the prominent, detachment-prone stratigraphic horizons (fig. 8), and has been shown to be the detachment horizon for the Windrock anticline (fig. 60; Structures Related to Synclinal Adjustments, section 6.33), and the cross crestal structure at Pitchfork anticline (fig. 63). A cross section of the Cottonwood Creek field (fig. 88) shows the same relationships.

Anticlines exposed in the Lower Cretaceous Frontier-Cloverly package are more elongate and somewhat narrower than those in the Upper Cretaceous, and consequently the asymmetry is more pronounced. Also, changes in direction of fold asymmetry occur in the Lower Cretaceous rocks (Chabot, section 6.33; fig. 77b). I have observed changes in asymmetry in similar exposures on the Lander-Hudson anticline in the Wind River basin (T.2 N., R.1 E.). Small-scale structures are more numerous in the Lower Cretaceous section because, as the anticlines tighten downward, the volume problem becomes more acute and more

subsidiary folds form to solve the space problem. Such a fold is exposed in the Frontier Formation on the southwest flank of Maverick Springs anticline (fig. 89a; T.5 N., R.1 W.) and in the Mowry Shale on the northeast flank of Horse Center anticline (fig. 89b). Numerous rabbit ear folds are controlled by detachment in intervening Mowry and Thermopolis Shales. An example of this is Spring Creek anticline in T.50 N., R.102 W. (fig. 57).

The Upper Cretaceous through Paleocene stratigraphic section has been described as deforming as a single package above the ductile Cody shale. Detachments which are present in the upper Cody Shale are responsible for the problems encountered in trying to use thicknesses of the Cody Shale (measured on the surface) to tie the Mesaverde-Cody contact into subsurface well control (Brown, unpublished data). The Mesaverde, Lance, and Meeteetse Formations are exposed in broad, open anticlinal folds above the narrower fold in the Lower Cretaceous package described above. The characteristics of parallel folding (Appendix B) dictates that the synclines in the Upper Cretaceous formations, adjacent to these broad anticlines, will be tightly folded, as the upper detachment is encountered.

6.44 Cenozoic section

In the Bighorn basin, the Fort Union Formation is tightly folded into synclines adjacent to Laramide structures such as Grass Creek anticline (fig. 90). Studies of variations of surface dips across some of these synclines involving Paleocene rocks indicate that dip angles increase upward in the stratigraphic section toward the axis of the syncline, which is a characteristic of parallel or "concentric" folding. In some synclines (fig. 90a) zones of upward tightening are overlain by beds with lower dips. This reflects the presence of bedding plane slip along an upper detachment which is required by volumetric constraints associated with the mechanism of parallel folding (Dahlstrom, 1969a). An example of this geometry can be seen in a syncline southeast of Grass Creek anticline (fig. 90b).

Eocene age rocks in most basins within the foreland are unconformable on Paleocene (or older) rocks. Structures expressed in the Eocene rocks are gentle, broad, low-relief folds. The pre-Eocene unconformity may be clas- sified as a "disconformity" in the center of the foreland basins, but is typically an "angular unconformity" around the margins of the basins. Around the flanks of many of the Rocky Mountain basins, the Eocene rocks dip away from the mountain uplifts at angles up to

40 degrees, indicating continued middle to late Eocene uplift and/or basinal subsidence.

In summary, observations of folds at various stratigraphic levels clearly indicate that anticlines become more tightly folded down the axial surface (fig. 60a), while synclines become more tightly folded upward (fig. 60b). This process is seen to occur regardless of the lithologies involved. Much of the repetition observed in outcrop and interpreted from electric logs is related to tightening of the folds.

Volumetric adjustments represented by multiple folds and reverse fault repetition are displayed in the cores of anticlines. Several anticlines have been shown to detach at the base of these volumetric adjustments and are underlain by planar regional dip (Lodge Grass Creek anticline); however, other folds (Iron Creek anticline) continue below the detachment as broad anticlines, which again repeat the downward-tightening process.

Synclines tighten upward and develop an upper detachment in the higher portion of the fold. When the upper detachment is exposed by erosion, the rock layers above the detachment are typically folded into an open synclinal form, while below the detachment the form is tight, with many subsidiary folds. The upper detachment allows the continuation of the parallel syncline above the detachment.

Published examples of subsidiary folds in the Mississippian carbonates on the steep limb of Sheep Mountain anticline (fig. 61) indicate the presence of bedding plane slip out of the adjacent syncline (Hennier and Spang, 1983). The presence of bedding plane slip, reverse faults (fig. 53), and subsidiary folds on the steep limb, suggests an inter-relationship.

Asymmetry of the anticline forces the adjacent syncline to become more tightly folded, resulting in volumetric problems. Bedding-plane slip occurs as part of the folding process and synclinal volume problems are resolved by the formation of subsidiary "drag" folds near the crest of the anticline. These relationships have led to the conclusion that the basic fold mechanism operating in the foreland sedimentary section during the Laramide orogeny was that of the flexural slip process.

6.5 Summary

The forms of Laramide structures are controlled by three factors which interact during the time of deformation. These are: 1) the upward movement of a basement forcing block, 2) the deformational mechanisms active in the sedimentary section which are controlled by lithology, depth of burial, and pore pressure, and 3) arrangement of the various lithologies into "packages" which are of the same, or of different lithologies. The preferred defor-

mational mechanism of these packages is determined by the dominant lithology.

Adjustments in fold shape are accomplished by detachments in the shales and shaly limestones. Compressive loading of the sedimentary section, either by regional or local stresses, causes flexural slip folding, which creates parallel folds. A distinctive characteristic of parallel folds is the development of basal detachments beneath anticlines and upper detachments above synclines. Multiple detachments allow anticlines to tighten downward, detach and return to more open folds, often changing directions of asymmetry as they do so. The opportunity for multiple changes in direction of asymmetry within a single foreland fold urges caution when comparing directions of asymmetry between different structures, and any such comparison should be made at the same stratigraphic level, since most of the detachment horizons are present in the majority of foreland structures.

Bedding plane slip translates into reverse faults which cut upsection in the direction of tectonic transport, and die out upward by fault-fold interchange. Structures which result from this process are called 1) back-limb folds (on the gentle back-limb), 2) cross-crestal structures, (which offset the crest of the adjacent anticline), and 3) rabbit-ear folds (which form on the steep forelimb of anticlines).

Duplication of strata on the steep limb of an anticline, rather than extension or thinning, suggests that a model utilizing horizontal compression is more likely to have generated these subsidiary structures than one using vertical uplift. The scale and location of the Windrock anticline suggest folds such as this represent large scale back-limb folds, generated by volumetric crowding resulting from the compressional folding of the Wind River basin.

7.0 MODELS OF THE STRUCTURAL STYLE OF THE WYOMING FORELAND

7.1 Introduction

Models applied to the origin of the major uplifts and folds of the Wyoming foreland reflect the choice between two basic concepts for the cause of deformation: vertical uplift, or horizontal compression (see Geologic Studies, 1941-1970, section 2.40). This section will present the characteristics of the four basic models which are applied to the foreland area, and will discuss the strengths and weaknesses of each model. A comparison of the two concepts (vertical uplift and horizontal compression) will be made by contrasting interpretations which have been applied to the same foreland areas by different workers. Finally, evidence will be presented which will demonstrate the viability of each model, and how they should be applied to the Wyoming foreland.

In the past, the adoption of models pertaining to either of the two major concepts, has led to the mutual exclusion of all other models. This has resulted in the publication of widely divergent interpretations of the same Laramide structures, which allows a direct comparison and evaluation of the different models in a number of areas.

7.20 Basic Models Of Foreland Deformation

The basic models for the origin of the foreland uplifts and folds (fig. 91) are: 1) uplift on vertical faults, with draping of the sedimentary section, 2) upthrust on faults which steepen with depth, 3) thrust uplift, and 4) fold-thrust uplifts. The first two are models of the vertical uplift concept, and the last two are models of the concept of horizontal compression. An additional model, wrench faulting, has been proposed by Stone (1969), and will be discussed in later sections (see Compartmental Deformation, section 8.0; Crustal Shortening and Lateral Movements, section 9.0).

7.21 Model 1: Uplift on vertical faults (with drape folding)

Characteristics of the model: The model of uplift on vertical faults with drape folding was formally introduced by Prucha and others in 1965. The name implies that the sedimentary section "drapes" passively over the edge of a vertically rising, rigid basement block (fig. 91a). Note that there is no equirement for crustal (basement) shortening. Application of the drape fold model, without proper regard to necessary extensional mechanisms on the upthrown block, generally results in a structural (volumetric and line length) imbalance (APPENDIX B) between the

sedimentary section and the basement surface. For example, in the presentation of the draping mechanism by Prucha and others (fig. 91a), compare the length of the sedimentary section as portrayed by line ab before deformation, to line a'b' after deformation. The length of the line has obviously increased, but the bed thickness has remained the same.

Drape folds must exist in the Wyoming foreland if the vertical uplift model is to be a valid one. Monoclinal bends are exposed in the sedimentary rocks along the fronts of mountain uplifts. The existence of vertical faults in the basement has not been adequately documented for most of these features. If the model is to be applied to these structures, it must be documented that these monoclines have been formed by some mechanism of drape folding.

Prucha and others (1965, p.983) discussed the problem of the volumetric adjustments which should be present in the drape fold model. They concluded that "The mechanism by which this is accomplished is ... not known, although thinning of beds in the flexure probably is common." An example of this mechanism is illustrated in figure 92a. A second possible mechanism for maintaining structural balance is extension of the of the sedimentary section through normal faulting (fig. 92b).

Stearns (1971) proposed a third mechanism based on his study of the of Rattlesnake Mountain anticline (fig. 41). He found that there was insufficient extension by normal faulting and/or thinning of the Paleozoic carbonate section to maintain structural balance. Therefore he proposed the development of a detachment above the basement surface in the sedimentary section (fig. 92c). According to this hypothesis, the detachment formed during the vertical movement of the basement block. The thickness of the sedimentary section was maintained by sliding of the section toward the area of the drape fold, bringing additional section into the area. Stearns postulated that the detachment would develop on the steep limb of the fold and extend into the adjacent syncline. This would allow the movement of the sedimentary section towards the steep flank of the anticline, and the result would be the removal of the entire sedimentary section (above the detachment plane) from an area (the "void") equal in volume to the rock needed to maintain structural balance.

Discussion of the model: Prucha and others (1965) postulated that drape folds developed as intermediate stages in the process of uplift by "upthrust", the other model of vertical uplift. Thus, it is possible that numerous drape folds were formed and subsequently destroyed by continued uplift. It is also possible that some drape folds have been so deeply eroded that the only

evidence to confirm such an interpretation would be the mapping of a vertical fault in the basement.

If the vertical uplift/drape fold model is to be applied, it is necessary to establish that the sedimentary section is sufficiently thinned or extended by normal faults to preserve bed volume. Hennings and Spang (1985) have described thinning of the Paleozoic carbonate section exposed on the steep flank of Dry Fork anticline, northeast Bighorn Mountains. They interpret the controlling high angle reverse fault (76 degrees east dip) to flatten at a depth of approximately 5.5 miles (9 km). However, I know of no published interpretations of "drape" folds in the foreland which have documented sufficient thinning of the carbonate section (see for example Brock and Nicolaysen, 1975; Matthews and Work, 1978; and Stearns and Stearns, 1978) with the possible exception of Rattlesnake Mountain anticline (Stearns, 1971), which will be discussed more fully below. If bed volume is not maintained through thinning or extension by faulting, then the detachment accommodation (fig. 63c) postulated by Stearns (1971) must be shown to apply. This requires a void of proper proportions, to exist west of the steep limb of the anticline, unless there has been concomitant shortening of the basement to the west.

Stearns (1971) has shown that a detachment surface which is located just above the base of the Ordovician Big

Horn Dolomite, was activated on the steep limb of Rattlesnake anticline, apparently during the folding process. This detachment surface is the same one utilized by the Heart Mountain gravity slide which formed at a later time (Pierce, 1949). The stratigraphic section needed for structural balance at Rattlesnake Mountain must have come from the area west of the syncline which is opposite the steep limb of the anticline (it is unlikely that it could have moved into the steep limb from the top of the fold, since the Paleozoic carbonate section is continuous across the fold; fig. 81).

The area west of the anticline is now covered with middle to late Eocene volcanic rocks. These rest on glide blocks (involved in the Heart Mountain gravity slide) of Paleozoic rocks which have slid over early Eocene sedimentary rocks which, in turn, are unconformable on Upper Cretaceous Cody Shale.

Well control 12 miles (19 km) west of the syncline establishes the presence (below the Eocene volcanics) of a normal stratigraphic section below the Eocene sedimentary rocks, from Cretaceous Cody Shale down through Pennsylvanian Tensleep Sandstone (fig. 7). It is not known whether the full stratigraphic section is present in the entire area between the well and the steep flank of the anticline (although unpublished seismic data suggests that it is). However, if it is there, then structural balance

cannot be satisfied by the detachment method. Thus, balance must have been maintained by some other (unknown) mechanism, or the vertical uplift/drape fold model does not apply to this structure.

If the void does exist it could have formed in two ways. First, it may have formed by the detachment mechanism during the uplift of Rattlesnake Mountain anticline, as suggested by Stearns (1971). Secondly, it may have formed by the development of "break-away" areas related to later implacement of the Heart Mountain gravity slide. Whatever the answer, this area of detached blocks of Paleozoic rocks is a unique situation, occurring only in this isolated portion of the Bighorn region.

The application of this detachment accommodation to folds in other structural settings is also questionable. Some Laramide folds are asymmetric toward one another, so that the void in the section would be required to develop in the area between the two folds (fig. 93a). This should be readily detected by reflection seismic surveys, surface mapping, and well control. An example of a structural arrangement of opposed asymmetries is present on the Casper arch, where the steep limbs of the Emigrant Gap and Oil Mountain anticlines face each other (fig. 65). No such void exists between these folds (Brown, 1975) as shown by the Cretaceous rocks on the surface, which are older than

the folding, nor has any void been documented between any other anticlines in the foreland with opposing asymmetries.

In the northeastern portion of the Bighorn basin, a series of parallel, northwest trending anticlines, all asymmetric toward the mountains, are developed successively up the flank of the basin (fig. 93b). If structural balance is maintained by detachment/sliding, then each succeeding fold must have derived its compensating bed volume from the backlimb of the next fold toward the mountains. Again, the resulting voids should be clearly detectable on surface data and seismic data, but such evidence is entirely lacking (see section 10.0; also fig. 166).

It is tempting perhaps, to account for the needed volume of rock in the example above, by pulling the sedimentary section off the tops of the nearest mountain range and thus exposing the Precambrian core by the detachment/sliding mechanism, rather than by erosion. However, traverses across the Bighorn Mountains along the Montana-Wyoming state line (T.58 N., Rs.88 through 95 W.) reveal a continuous Paleozoic cover over the mountain uplift. The area of Precambrian basement exposures is too small to account for the sedimentary section needed to balance a series of uplifts such as the Pryor Mountains, and Fran-

nie, Sage Creek, and Elk Basin anticlines. A similar condition exists in the southern portion of the Bighorn Mountains, south of the Tensleep fault.

Conclusions: The only known location in the Wyoming foreland where the detachment/sliding mechanism might be applied is at Rattlesnake Mountain anticline, and it is unproven there. It should be made clear that uplift on vertical faults with drape folding may be possible. However, in the absence of direct observation of the basement faults, one or more of the bed length accommodations noted above must be demonstrated, in order to account for the required extension of the sedimentary section. If this cannot be done, then a different model of deformation should be applied to the structure.

7.22 Model 2: Upthrust structures

Characteristics of the model: Prucha and others (1965) presented a model of differential vertical uplift of rigid basement blocks which they called the "upthrust" model (fig. 91b). This model differs from Model 1, in that the faults which bound the uplifted block are interpreted as concave downward. Thus gently dipping thrust faults near the surface steepen downward toward vertical in the basement. In this way, the model accounts for the observed low angle thrust faults at the surface along some of the uplifts, and agrees with the theoretical

studies of Hafner (1951) and Sanford (1959), as well as the results of Sanford's sandbox experiments.

Note that the shape of the upthrust implies that the shallow sedimentary section is shortened (duplicated) along the low dipping portion of the upthrust, while the basement is not shortened, but merely offset. The discrepancy between the lengths of the basement and sedimentary section must be balanced by extension of the shallow sedimentary section, on the upthrown side of the upthrust. Theoretical studies of vertical uplift by Hafner (1951) and Sanford (1959; figs. 18, 21) show that the upthrust geometry requires extensional mechanisms, such as normal faults, on the hanging wall (see Mechanical basement and experimental models, section 5.23). The upthrust model has been applied to many foreland interpretations without recognizing the need for these extensional features in the interpretation (see Model 1, section 7.21).

Discussion of the model: Lack of evidence of extension on the upthrown block will result in a structural imbalance between the sedimentary section and the basement; the sedimentary section being longer than the basement surface (fig. 91b). The problems encountered in attempting to balance the structure by sliding the section on a detachment above the basement (Stearns, 1971) have already been discussed in relation to Model 1 (section

7.21). Also, if drape folds represent an intermediate stage in the development of upthrusts, as suggested by Prucha and others (1965), then the steep limb will be faulted as part of the process. If thinning of the section were the mechanism of extension, then evidence may be preserved on either the hanging wall, the footwall, or both.

Interpretations of upthrust structures have been published by: 1) Prucha and others (1965) for Bald Mountain area, Wyoming (T.25 N., R.81 W.); 2) Osterwald (1961) for Soda Lakes area, Colorado (T.55 N., R.69 W.); 3) Stearns and Weinberg (1975) for the Owl Creek Mountains, Wyoming (Tps.5 and 6 N., R.6 E., Wind River Meridian), and 4) Stearns and others (1978) for the Wind River Mountains, Wyoming.

The interpretation of the Wind River Mountains by Stearns and others (1978) shows extension by normal faulting on the upthrown block which is postulated to be present, but has not been documented. Only the interpretation across the Owl Creek Mountains (Stearns and Weinberg, 1975) demonstrates structural balance with substantiated extension on the hanging wall. It should be noted, for later discussion, that this feature is oriented east-west, while the other three examples trend north, or northwest.

The process of development of upthrusts in Sanford's (1959) sandbox models (fig. 21) has shown that the initial

stage of vertical uplift resulted in "...tensile cracks at the upper boundary and shear fractures at the lower boundary" (Sanford, 1959, p.43). The progressive uplift, upward propagation, and flattening of the upthrust fault was then accompanied by the development of normal faults on the hanging wall. The final event in the process was the development of a steeply dipping, conspicuous normal fault which extended from the upper to the lower boundary of the uplifted block, almost intersecting the vertical lower portion of the upthrust (fig. 21). The sequential development of the normal faulting provided the extension to accommodate the extension of the uplifting block.

The location of the major extensional features on the hanging wall is also of significance. In the sandbox experiments (Sanford, 1959), the principal normal faults were situated on the hanging wall and either directly over the vertical portion of the upthrust, or farther inboard of the vertical segment of the fault on the uplifted block, and not over the shallow dipping portion of the upthrust.

In contrast to his upthrust models, Sandford (1959) also created models of a broadly curved antiformal structure (fig. 95), using a sinusoidal vertical displacement on the bottom of the block. The fracture pattern which developed was described as "...a complex zone of normal faults which taper inward toward the axis of the fold and

die out at depth" (Sanford, 1959, p.19). In the foreland, normal faults are found in this position at the crests of large, broadly arched anticlines, such as West Poison Spider field in the Wind River basin (fig. 96). They tend to die out downward in the Cretaceous shales (Clark, 1978).

Thus the fracture pattern developed during the upthrusting, is one of concentrated fractures over the deep vertical fault, with deep penetration of the conspicuous normal faults. If the model studies are representative of the actual process, then the deep penetration of these normal faults would indicate that they may still be present in the older rocks on the hanging wall of deeply eroded upthrusts; it is possible that in very deeply eroded upthrusts, the faults will be exposed only in Precambrian basement rocks.

Conclusions: There are both theoretical and experimental results to support the validity of the upthrust model. However, it requires compensation for bed length changes, in order to maintain structural balance between the sedimentary section and the basement. This compensation is most likely to be achieved through extension by normal faulting. Mapping the location of these extensional normal faults may be a key to separating the upthrust structures from structures which were generated by compression.

7.23 Model 3: Thrust uplift

Characteristics of the model: In many older studies of foreland structure the boundaries of the uplifts were interpreted to be low angle thrust faults, which carry the basement and sedimentary rocks over the adjacent basins. The Five Springs area (T.56 N., R.92 W.) in the Bighorn Mountains was interpreted by Wilson (1934) to be bound by a single, low angle reverse fault. Berg (1962b) used the term "thrust uplift" for those structures which are believed to have attained their great vertical relief by this mechansim (fig. 91c). The structural style implies an origin in a compressional regime. According to the model, the overthrust block moves as a relatively rigid body, with only minor internal deformation (Berg, 1962b). In contrast to Models 1 and 2 (sections 7.21; 7.22), a thrust uplift will be in structural balance, because no changes in bed length or volume occur during formation of the structure. Note that this model can result in structures with large structural overhangs. The Arlington, Bradley Peak, and Shirley Mountain thrusts (south and south-central Wyoming) have been interpreted by Blackstone (1983) as thrust uplifts.

Discussion of the model: Some faults on the State Geologic Map of Wyoming (Love and Christiansen, 1985) are

shown with the fault planes oriented at low angles to both the sedimentary layers and the basement surface. These faults thrust basement and Paleozoic rocks over right-side up Mesozoic rocks. The down-plunge view (fig. 97) demonstrates this geometry on the south flank of the Sweetwater uplift. In addition, a back-thrust is also displayed, giving the appearance of a "wedge uplift" (Chamberlin, 1925). This occurrence suggests the geometry which is seen in physical rock models (Morse, 1977) of thrust faults which flatten at depth, resulting in a ramp geometry (Rich, 1934; APPENDIX A).

Conclusion: The thrust uplift model implies horizontal compression as the mode of formation. This model maintains structural balance more readily than vertical uplift models, by moving all the rocks over the same fault geometry. The anticipated low angle of the thrust, combined with significant displacement, may result in the development of mountain front overhangs, while faults with lesser displacement may form unfaulted folds in the sedimentary section via fault-to-fold interchange.

7.24 Model 4: Fold-thrust uplift

Characteristics of the model: The fold-thrust model of foreland deformation (fig. 91d) was postulated by Berg (1961) based upon evidence from four wells which had penetrated basement overhangs in the foreland. The model was

used to interpret the structure of the Wind River Mountains.

The major problem Berg encountered in developing the fold-thrust theory was determining a deformational mechanism for the basement which would allow the postulated folding of the upper basement surface. Berg concluded that movement on secondary joints, as at the Five Springs area in the Bighorn Mountains (Wilson, 1934), would have allowed the basement to fold. Mechanisms of basement deformation have already been discussed in detail (section 5.32).

Berg described a three stage sequence of formation of the fold thrust. The first stage is progressive internal deformation of the basement and folding of the sedimentary section involved on the steep flank of a faulted asymmetric anticline (fig. 98a). The anticline was shown to be controlled by a basement-involved reverse fault which was located high on the flank of the structure and died out upward (fault-fold interchange).

The second stage (fig. 98b) is characterized by continued movement of this reverse fault so that it eventually breaks upward through the sedimentary section. A second reverse fault then develops basinward of the first and occupies the trace of the synclinal axis. This second fault is seen in outcrop to die out downward into the syncline (Brown, 1983). The sedimentary section encased be-

tween the these two faults (dual fault zone; Brown 1983) dips steeply to overturned, and eventually becomes thinned through internal rotation. The overturning is a partial response to the continued downwarping of the adjacent basin. The zone of deformation on the steep flank (between the faults) is referred to as the rotated flank (Brown, 1983).

The third stage of Berg's sequence is the formation of the overhang (fig. 98c) by large movement on the mountain bounding thrusts with little or no additional folding. Wells drilled through such overhangs (Berg, 1962b; Gries, 1983a) have penetrated inverted sedimentary section which has been thinned in the dual fault zone. The recognizable parts of the sections are the more competent units such as the limestones, dolomites, and sandstones. The less competent shaley units are deformed to the extent that they are often missing or cannot be identified.

The dual fault zone dips between 20 and 40 degrees under the uplifts, as determined from well control and seismic data. The low dip of the bounding fault zone allows development of basement overhangs of large areal extent (fig. 98c). The amount of overhang is a minimum measure of the crustal shortening (see section 9.0) involved in the fold-thrust.

The distance traveled by the overthrust Precambrian basement block may be great enough to override Late Cre-

taceous and early Paleocene synorogenic congolmerates. Both seismic data and well control document the fact that the basinal rocks continue to dip under the basement overhang for ten miles (16 km) or more, so that the synclinal axis may actually be under the gentle backlimb of the uplift.

The presence of the overturned and rotated flank in the dual fault zone, convinced Berg that the process was one of folding and thrusting, and not block uplift, or simple thrust uplift.

Discussion of the model: Berg (1962b) is often credited with being the first of the modern-day proponents of large scale Laramide crustal shortening. However he initially attributed the development of fold-thrust features to dominantly vertical movements; the overturned limb was interpreted as due to local compressive forces marginal to the great uplifts. Berg's interpretation of the Wind River Mountains as a major fold-thrust (fig. 99) shows the Wind River thrust zone to have approximately 10 miles (16 km) of heave. The two thrusts which comprise the dual fault zone are shown as steepening toward the vertical, rather abruptly at an elevation of approximately 20,0000 feet (6100 m) below sea level. This gives the Wind River uplift the form of an upthrust.

More recent reflection seismic data (fig. 33) shows that the fault zone does not steepen, but continues to dip

gently to the east end of the seismic section. The COCORP (Consortium for Continental Reflection Profiling) seismic line (Smithson and others, 1978) indicates that the length of overhang (and thus heave; fig. 100), is approximately 13-14 miles (20 to 22 km). Proponents of a compressional origin for the foreland uplifts point out that it is doubtful that such large scale crustal shortening could be generated through vertical uplift. My interpretation of the fold-thrust model (Brown, 1983) includes the COCORP seismic data so that the uplift rides on a low angle thrust fault, which does not steepen with depth (as is shown by Berg, 1962b).

A depth to detachment (Appendix D) calculated for the Bighorn Mountains (Petersen, 1983), plots at a depth of 50,000 feet (15,000 m) below sea level, suggesting that there are zones of intra-crustal detachment (Schmidt and others, 1985).

There are several differences between the thrust uplift and fold-thrust uplift models. The most obvious is in the development of the dual fault zone and rotated flank in the fold-thrust. Another difference is the folding of the upper basement surface necessitated by the fold-thrust model. Penetrative deformation of the basement rock in the fold-thrust permits the "folding" of the upper basement surface (section 5.32). Both models permit extensive crustal shortening; however, the

fold-thrust mechanism can account for more shortening with less thrusting because of the shortening involved in the initial folding of the structure. More work needs to done to separate and document those features which may be thrust uplifts from those which are fold-thrust structures. Detailed surface mapping of structures with different orientations needs to be done to determine the presence (or absence) of dual fault zones, rotated flanks, and internal basement deformation. Interpretation of seismic data might also help determine whether the dual fault zone and rotated flank (sedimentary section) is present.

After Berg first postulated the fold-thrust model (1961), most of the published interpretations of foreland structures (until 1982) involved vertical movements. With the increase in hydrocarbon exploration in the mid-70's, better seismic data became available and many new wells were drilled in more structurally complex areas. Twenty-four years after Berg published his model, 21 wells have been drilled through basement overhangs in the foreland province Gries (1983a) has tabulated (table 10) the presence or absence of the dual fault system and overturned sedimentary section in all the wells which have drilled the Precambrian overhang. Two wells (nos. 5 & 7) shown as not having drilled a "subthrust fault sliver" (dual fault zone and rotated flank), drilled into a normal strati-

TABLE 10. Well data regarding sub-thrust penetrations along Laramide mountain fronts in the Wyoming foreland. (Modified from Gries, 1983a).

	Well Name and Operator	Location	Thrust	Spud Date	Compl. Date	Subthrust Fault Sliver Thickness ft (m)	Formation Beneath Fault Sliver	TD ft (m)
1.	Carter 1 Unit	Sec. 32, 30N, 93W Fremont Co., Wyo.	Emigrant Trail	1-12-50	6-7-50	880 (268)	Cretaceous Thermopolis	6,591 (2,009)
2.	Shell 1 Govt.	Sec. 9, 42N, 105W Fremont Co., Wyo.	E A	6-29-56	12-6-56	820 (250)	Cretaceous Mowry	10,689 (3,258)
3.	Tennessee Gas 1 USA Margie Hicks-A	Sec. 3, 3N, 103W Moffat Co., Colo.	Uinta Mountain	9-22-60	1-28-61	370 (113)	Triassic Moenkopi	9,371 (2,856)
4.	Atlantic Refining 1 Ice Slough	Sec. 9, 29N, 93W Fremont Co., Wyo.	Emigrant Trail	11-3-60	12-18-60	520 (158)	Cretaceous Thermopolis	6,552 (1,997)
5.	Sinclair 1 Cooper Creek	Sec. 19, 28N, 90W Fremont Co., Wyo.	Emigrant Trail	4-22-61	9-15-61	none	–	12,224 (3,726)
6.	Shell 21X-9 Dahlgreen Creek	Sec. 9, 2N, 14E Summit Co., Utah	Uinta Mountain	11-17-67	10-8-68	2,083 (635)	Cretaceous Mesaverde	17,100 (5,212)
7.	Mountain Fuel 1 Dickey Springs	Sec. 24, 27N, 101W Fremont Co., Wyo.	Wind River	6-14-70	10-3-70	none	–	12,282 (3,744)
8.	True & Rainbow Res. Shaffer Fed. 41-6	Sec. 6, 32N, 75W Converse Co., Wyo.	Northern Laramie Range	3-14-71	4-17-71	1,450 Overturned Cret. Cody (442)	Cretaceous Cody	7,898 (2,407)
9.	True 31-6 Hakalo	Sec. 6, 32N, 75W Converse Co., Wyo.	Northern Laramie Range	7-8-71	8-17-71	2,590 (789)	Cretaceous Cody	7,675 (2,339)
10.	Husky 8-2 Federal	Sec. 2, 29N, 106W Sublette Co., Wyo.	Wind River	5-29-73	10-2-73	unknown	unknown	12,944 (3,945)
11.	American Quasar 1 Skinner Fed.	Sec. 32, 28N, 101W Fremont Co., Wyo.	Uinta Mountain	9-27-74	11-6-75	3,900 (1,189)	Cretaceous Mesaverde	15,040 (4,584)
12.	Champlin Fed. 31-19 (Bear Springs)	Sec. 19, 11N, 102W Moffat Co., Colo.	Uinta Mountain	8-30-75	4-10-76	none	–	13,810 (4,209)
13.	West Coast Oil 1 Skinner Fed.	Sec. 9, 27N, 101W Fremont Co., Wyo.	Wind River	9-12-76	1-22-77	unknown	–	9,700 (2,957)
14.	Mobil C-1 McCormick Fed.	Sec. 11, 21S, 22E Grand Co., Utah	Uncom-pahgre	2-3-77	12-1-77	unknown	unknown	19,270 (5,873)
15.	Supron Energy 1 F-28-30-93	Sec. 28, 30N, 93W Fremont Co., Wyo.	Emigrant Trail	9-12-80	11-3-80	450 (137)	Triassic Chugwater	7,769 (2,368)
16.	Moncrief 16-1 Tepee Flats	Sec. 16, 37N, 86W Natrona Co., Wyo.	Casper Arch	10-18-79	1-15-81	2,373 (723)	Cretaceous Cody?	19,733 (6,015)

graphic section, with Tertiary rocks immediately under the Precambrian. These two wells were located along the leading edge of the fold-thrust and did not penetrate the overturned section which other wells, drilled further up on the uplift, did encounter. Two other wells (nos. 8 & 9) were drilled by True Oil Company along the northeast-trending Corral Creek fault, which bounds the northern edge of the Laramie Range. Gries (1983a) shows these wells (table 10) as having drilled steeply dipping Cretaceous rocks in the footwall, immediately under the Precambrian, but does not interpret this as a "subthrust fault sliver" in cross section (her fig. 11). Two wells (nos. 6 & 12) were drilled on the east-west trending Uinta Mountain (north flank) thrust. One, the Shell Dahlgreen (no. 6) is shown as having drilled a subthrust sliver, while the Champlin Federal (no. 12) did not (Gries, 1983a). More needs to be known about the timing and history of the Uinta Mountains before an explanation of why this east-west trending fault seemingly displays different fault relationships along trend.

Conclusions: The fold-thrust model of foreland deformation is characterized by the thrusting of Precambrian basement rocks over overturned Paleozoic or Mesozoic rocks which in turn, are thrust over right-side up Mesozoic or Cenozoic rocks. This model accomodates the great-

est crustal shortening and basement overhang of any foreland model.

The differences between the fold-thrust and thrust uplift models is primarily the absence of the dual fault zone, rotated flank, and penetrative brittle deformation and folding of the basement, in the thrust uplift. Surface mapping, well control, and seismic data offer greater documentation for the fold-thrust, than for any of the other models.

7.3 Comparison Of Vertical Uplift and Compressional Models

Interpretations of the same foreland structures have been published which allow direct comparison of the models as applied in each case. Three examples are reviewed in the following section.

7.31 Soda Lakes area, Colorado

Osterwald (1961) and Berg (1962a) have published interpretations of the Soda Lakes area, of the Colorado Front Range (fig. 101) which contrast the upthrust and fold-thrust models. Both authors recognize the presence of the overturned sedimentary sequence and the two reverse faults which encase it. The major differences between these interpretations are the attitudes of the reverse

faults and geometry of the top of the crystalline basement in the vicinity of the faults.

In Osterwald's interpretation (fig. 101a) based on the upthrust model, the high angle reverse faults in the sedimentary section join and steepen into a single fault which is almost vertical in the basement. The basement surface is drawn into the fault planes without significant curvature. Berg applied his fold-thrust model (fig. 101b), keeping the two faults separate through the sedimentary section and into the basement. He indicates that they steepen at depth, as he did in the interpretation of the Wind River Mountains (fig. 99). Folding preceding faulting is indicated by the curvature at the basement surface on both the hanging and footwall blocks. The difference in crustal shortening between the two interpretations is readily apparent from the difference in the length of the basement surface in the two interpretations.

The application of the principle of "structural balance" (see Appendix C) to these two interpretations (fig. 102) will demonstrate which is more likely to be correct. Assuming parallel folding, constant bed volume, and consistent fault cut-off relationships, the difference in length between the Cretaceous Dakota (Cloverly) Group (Kd) and the Precambrian basement surface can be taken to represent the extent to which each interpretation is out

of volumetric (structural) balance. On Osterwald's section, the basement is approximately 25% shorter than the Dakota Group, while on Berg's section it is only 5% shorter.

The difference in length between the basement surface and the Dakota Group may have been created in three ways: 1) the basement surface may have been shortened by removal of material during the deformation, 2) the sedimentary section may have been lengthened during the deformation by thinning or normal faulting, or 3) the extra length of sedimentary section may have been brought in from outside the immediate area. It is not likely that basement rock has been destroyed during deformation, so this possibility may be ruled out. There is no indication that the sedimentary section has been lengthened or extended by normal faulting. The extension by normal faulting can be seen from the figures to be minimal. Finally, the problems related to detachment of the sedimentary section above the basement and sliding rocks into the area has already been discussed (section 7.21). Therefore, the failure of Osterwald's section to satisfy balance requirements may indicate that the wrong model was used in the interpretation.

The lack of bed thinning or extension in the data makes it difficult, if not impossible, to modify Osterwald's interpretation to bring it into structural

balance and still maintain the vertical uplift model. Experience has shown that the methods used to bring such an interpretation into balance are the same as those which would be used to interpret the structure in terms of a fold-thrust model, so that the interpreted length of the basement section is increased. The reverse fault(s) should be flattened all the way into the basement, and not joined, to give room for a longer basement length under the overhang. The curvature of the basement surface on the hanging wall and footwall blocks, as well as in the dual fault zone also increases the length of the basement surface. Note that even if Osterwald had used the log from the easternmost well (Great Basins well on fig. 101) when he did his study, it would likely not have changed his interpretation, because that part of the section is acceptable.

A small adjustment in the angle of faulting or the curvature on the basement surface in Berg's interpretation would bring that interpretation into structural balance.

7.32 Belleview Dome, Colorado

Matthews and Work (1978) interpreted Belleview dome structure (T.8 N, R.69 W., Colorado) as a vertical uplift, with drape folding (fig. 103 a,b) in which the basement fault does not break through the sedimentary section. My interpretation (Brown, 1983) of the same structure (fig.

103c), is that of the thrust uplift, or early stage fold-thrust uplift, in which the basement fault is interpreted as dipping to the east to represent an out of the basin thrust. Folding of the basement surface is restricted to the footwall as seen in other areas (section 5.4, Geometry of faulted basement; fig. 27). Comparison of the length of the top of the basement and the restored sedimentary layers in figure 103 (b,c) shows that, as in the Soda Lakes area, the basement surface in the vertical uplift drape fold model is too short. However, the fold-thrust interpretation is in structural balance.

7.33 Rattlesnake Mountain Anticline, Wyoming

Stearns'(1978) cross section of Rattlesnake Mountain anticline represents the most popular view of the drape fold interpretation (fig. 104). My interpretation (fig. 105; Brown, 1984a) has already been discussed (section 5.52). Both of these interpretations were drawn along the same surface profile. Stearns interprets the structure as being controlled by normal fault B which splays into reverse faults B', C, and D near the surface. The upward convergence of the sedimentary section toward the faulted face of the basement results in the truncation and disappearance of the Cambrian Pilgrim Limestone and adjacent beds. The drape fold interpretation of Rattlesnake Mountain anticline requires that the sedimentary section be

extended more than can be accounted for by the normal faults at the surface. Stearns (1971) showed that the Paleozoic carbonates are continuous over the fold, and that thinning of the section is insignificant. He therefore proposed the mechanism of sliding the necessary section into the area (from the syncline to the west) along a detachment surface. The problems associated with this mechanism were discussed above (see Model 1, section 7.21).

In order to compare the two interpretations by structural balance (see APPENDIX C), three bedding surfaces in the sedimentary section (top Mississippian; top Ordovician Big Horn; and top Cambrian Pilgrim) and the Precambrian basement surface were measured (figs. 106 and 107). In the drape fold interpretation, the Mississippian and Ordovician Big Horn are 5,000 feet (1500 m) longer than the basement, and 2,000 feet (600 m) longer than the Cambrian Pilgrim Limestone. The difference in lengths between the sedimentary section and the basement surface implies that the drape fold displays none of the proper bed length adjustments, and the section is not balanced.

The difference in the lengths of the Mississippian and the Pilgrim may be surprising, since most applications of the vertical uplift/drape fold model show the units above the basement in general structural balance. The difference in this case results from the absence of the

Pilgrim Limstone between faults C and D, and D and B. This gap implies that the Pilgrim Limestone has been pulled to the left, away from the structure; the fault-terminated ends of the Pilgrim should restore to meet one another.

Brown's (1984a) reverse fault interpretation (fig. 107a) displays a near perfect structural balance of all the layers. The basement surface is almost identical in length with the overlying sedimentary section (fig. 107b).

It appears from figure 104, that it was necessary to omit the Pilgrim Limestone because of the interpreted shape of the basement fault (B); whereas in figure 105 the use of a reverse fault (E) and overhang provides the space in the footwall of fault C to accommodate the extra length of Pilgrim Limestone needed to balance the section.

The Cambrian beds are also cut by two sets of small displacement faults which extend the section. One set is nearly horizontal, with a slight dip to the east, while the second set dips strongly to the west (fig. 108). Off-set on both sets is too small to account for bed length extension necessitated by the drape fold interpretation, but may represent stretching over the edge of the broken-off block corner (section 5.52).

7.4 Evidence For The Various Models

7.41 Uplift on vertical faults (with drape folding)

The general lack of observed ductile stretching and normal fault extension on the steep limbs of Laramide anticlines suggests that there are fewer drape folds in the foreland than would be expected based on published work (see Model 1, section 7.21), or else the model has not been properly applied. Theoretical and experimental data suggest that drape folds should be formed where the component of tectonic transport is primarily vertical, with the controlling fault dying out upward in the overlying folded sedimentary rocks.

The foreland structural trends which offer the best possibility for the development of the required differential vertical uplift are along faults which are oblique (east-west) or transverse (northeast) to the northwest trending major Laramide structures (see Precambrian Structural Trends, section 3.14; and Orientation of Major Laramide Structures, section 3.32). One such feature (discussed earlier in Fault Dip Angles, section 5.51) is the east-west trending high angle reverse fault zone which bounds the north side of the Owl Creek Mountains (T.8 N., Rs.1 E and 1W.) in the southwestern portion of the Bighorn basin (figs. 35a, 38). Northwest-trending, basement-cored, anticlinal folds on the upthrown side (south) are

terminated along the (North) Owl Creek fault zone, the maximum differential vertical uplift is at the crest of these structures where Precambrian basement rocks are juxtaposed against Triassic rocks.

Preliminary field study (Brown, unpublished field notes) suggests that several of the stratigraphic units involved in the faulting and near vertical uplift of the north flank of the Owl Creek Mountains have been thinned approximately 30%. This may provide all or part of the necessary bed length accommodation for drape folding along this trend. Unfortunately, the areas which need to be studied in detail to confirm the thinning are within the Wind River Indian Reservation, and access is presently prohibited. It appears that this east-west line of faulting may have originated as a drape fold, at least in its earliest development. However, the juxtaposition of Triassic rocks against Precambrian basement and a vertical offset of approximately 4,000 feet (1,200 m), suggests that this feature may have undergone considerably more deformation than a passive draping of the sedimentary section could accommodate. This trend will be discussed further in the next section (Upthrust Structures, section 7.42).

Few of the east and northeast structural trends in the foreland have been mapped in the detail necessary to determine whether drape folds are present. However, the

State Geologic Map of Wyoming (Love and Christiansen, 1985) shows several locations where the question might be answered if there are sufficient exposures. For example, in the Owl Creek Mountains (T.7 N., Rs.2 and 3 E.), the southeast plunge of Phlox Mountain anticline (fig. 109) is cut by the easterly trending high angle Stagner fault, with the north side upthrown (Long, 1959). The southeast striking sedimentary section wraps around the west end of this transverse fault and dips steeply south. Study of the stratigraphic section on the steep plunge should provide data concerning possible thinning which might indicate drape folding over the nearly vertical rise of the Precambrian basement rocks on the north side of the Stagner fault.

An area where normal faulting observed in the sedimentary section may represent extension associated with drape folds, is at Zeisman dome (T.49 N., R.89 W.) in the Bighorn basin. The normal fault at Zeisman dome (Stricker, 1984) trends east-west, and is on the upthrown side of the (deeper) nearly vertical fault which controls the steep north plunge of the dome (fig. 110; see Compartmental Deformation, section 8.0).

Another structural setting where drape folds might develop is in the fault-to-fold interchange along a high angle fault as it dies out along strike by progressive loss of displacement (fig. 111a). A series of cross

sections spaced along the trend of such a structure could show the time sequential development of a drape fold into a faulted drape fold (fig. 111b).

Lateral fault-to-fold interchange is present along the major east-west and northeast trending faults which transect the Bighorn Mountains. For example, the Tensleep fault (T.47 N., Rs.83 through 89 W.; see Precambrian shear zones, section 5.13) dips 60 to 70 degrees to the north and passes into a fold (at the Triassic stratigraphic level) westward into the Bighorn basin (fig. 112). Reconstruction from surface and subsurface data indicates that the fault changes displacement from Precambrian against Ordovician at the crest of the range (fig. 112a), to Precambrian against lower Cambrian, approximately 16 miles (25 km) to the west (fig. 112b), and is interpreted to die out into a monoclinal flexure on the basement surface deeper into the Bighorn basin (fig. 112c). The Tensleep fault may represent the development of a drape fold over a reverse fault, rather than over a normal fault depicted in the models (Prucha and others, 1965). Substantiation for the drape fold interpretation (bed thinning) cannot be demonstrated here because of the absence of detailed studies which compare thicknesses of similar stratigraphic section along the trend of the fault, and the removal of any evidence in the sedimentary section (on the upthrown

side) by erosion at the crest of the Bighorn Mountains, where the displacement is the greatest (Allison, 1983).

In summary, the evidence of the possible occurrence of drape folds in the foreland is generally localized on structures which trend east-west, or northeast-southwest, and are thus oblique or subparallel to the northeast direction of regional shortening, because the maximum differential vertical uplift occurs along these trends.

7.42 Upthrust structures

As discussed earlier (see section 7.22, Model 2) Prucha and others (1965) envisioned upthrust faulting to be a further development of the vertical uplift (drape fold) model. It should be anticipated that the structural trends which offer the best possibility for the development of the upthrust are the same ones which were discussed under the evidence for the drape fold (section 7.41). The same problems for documentation of the drape fold model exist for the upthrust model, and many of the same features (where drape folding has been postulated) may actually be upthrusts, if vertical displacement has been great enough to cause the nearly vertical fault in the basement to cut through the sedimentary section (and flatten near the original ground surface).

The south flank of the Owl Creek Mountains in central Wyoming is bounded by the east-west trending (South) Owl

Creek thrust, which places Precambrian, Paleozoic, and Mesozoic rocks over Tertiary rocks of the Wind River basin to the south (fig. 113a). The canyon of the Wind River provides a north-south cross section through the fault (fig. 113b). The cross section is very similar to Sanford's (1959) "sandbox" model (figs. 18b, 19). The canyon exposes a series of normal faults on the hanging wall of the South Owl Creek thrust, where the surface dips reverse at the crest of the range (Wise, 1963); the prominent Boysen fault (see Relationship of Precambrian and Laramide Structures, section 5.12) dips 60 degrees to the south, with 1,500 feet (450 m) of offset on the Precambrian basement. The interpretation of downward steepening of the South Owl Creek thrust is predicated on the idea that extension accomplished by the Boysen and smaller normal fault has accommodated the upward flattening of the South Owl Creek thrust. This area has the best evidence for the extension necessary for development of upthrusts, of all foreland structures. A direct application of the model of the upthrust structure will be presented for Rattlesnake Mountain anticline in section 8.5 (The Corner Problem).

The east-west trending North Owl Creek thrust was discussed previously as a possible example of drape folding (see Uplift on Vertical Faults, section 7.41), but it was pointed out that the amount of vertical displacement (4,000 feet; 1,200 m) is excessive for passive drap-

ing of the sedimentary section. The upthrust model predicts that continued offset along the basement fault will result in flattening of the fault upward in the sedimentary section. The upthrown block is eroded to the Precambrian surface, with limited exposures of Paleozoic rocks. The depth of erosion may have removed the evidence of an upward fault-fold interchange (drape fold), or the upward flattening of an upthrust, as well as the normal faults which could have provided the extension needed for the development of either a drape fold or an upthrust. Tertiary volcanic rocks cover the western extent of this fault where such evidence would be anticipated to be preserved due to regional (northwest) plunge.

It is possible that the apparent thinning along the North Owl Creek thrust, indicated in the discussion of drape folds (section 7.41), may represent the initial development of a drape fold as an early stage in the formation of an upthrust along the east-west trending North Owl Creek. The possibility of lateral movement along the North Owl Creek fault will be disucussed in the sec- tion on crustal shortening and lateral movements (9.0).

In summary, upthrust structures appear to be present in the Wyoming foreland. However, as with drape folds, the evidence for them is along the east-west structural trends, not on the primary northwest trending Laramide

structures. The south flank of the Owl Creek Mountains, exposed in the canyon of the Wind River, displays the best documentation of extensional normal faulting on the hanging wall of a possible upthrust structure, anywhere in the foreland.

7.43 Thrust uplifts

The differences between the thrust uplift and fold-thrust uplift are in the details of the deformation, rather than the origin. The identification of a thrust uplift depends upon the determination that the basement fault zone is not a dual fault system, with an overturned flank, and that faulting was not preceded by folding.

Down-plunge views of some reverse faults on the State Geologic Map of Wyoming (Love and Christiansen, 1985) show no dual fault zones. However, it should be noted that the heave of most of these faults is small. Examples are exposed on the south flank of the Sweetwater uplift (fig. 97). The reverse faults exposed there trend in a west-northwest direction, oblique to the regional direction of shortening. In the case of reverse fault zones of larger scale, drilling through the hanging wall would be required in order to determine whether the movement was on a single or dual fault system, and whether an inverted (rotated) flank of Paleozoic (or younger) rocks was present under the basement overhang (see Model 4, section 7.24).

In conclusion, thrust uplift structures do occur in the foreland, but it is not clear whether they develop the large scale overhangs of basement rocks which are present along the the major uplifts.

7.44 Fold-thrust uplifts

There is strong evidence in support of the fold-thrust model in the Wyoming foreland. The evidence is from detailed mapping of surface structures, modern-day seismic reflection data, and a growing number of wells which have drilled structures which show the basic geometry of the model. Large individual fold-thrust structures of the Wyoming foreland develop overhangs which face either northeast or southwest (fig. 114). I interpret this bimodal distribution of overhangs to correspond to the development of a conjugate set of low angle reverse faults in the basement (Hafner, 1951), in response to the southwest to northeast directed regional compressive stress during the Laramide orogeny.

Brown (1983) has assembled examples of the sequential stages in the development of a fold-thrust. A northeast-southwest cross section of Zeisman dome (fig. 115), located on the east flank of the Bighorn basin, represents the first stage of the fold-thrust (see Model 4: Fold-thrust Uplift, section 7.24). This first stage is

typified by an asymmetric anticline in which the controlling fault dies out upward into a fault-fold interchange. Note that the direction of asymmetry in this case is directed away from the basin axis. Other structures typical of this stage of development can be found in areas such as Porcupine anticline (see figs. 25, 26, 27), which is eroded deeply enough to expose the single reverse fault in the basement core of the structure.

West Billy Creek anticline (fig. 116a) represents the second stage in the sequence of development. The reverse fault in the crestal position at the top of the basement, dies out upward into the fold as seen by the continuity of the Ordovician Big Horn Dolomite over the anticline (fig. 116b). A second reverse fault has formed along the synclinal axis, and dies out downward. These two faults represent the initial stage of the dual fault zone, which develops as the two faults extend through the section with continued deformation. The first fault formed (in the anticlinal core) moves up in the section, while the second fault (along synclinal axis) cuts down to the basement. Note that the second fault developed as the beds reached the point of overturning. This fault does not disrupt the underlying Big Horn Dolomite and the displacement increases upward in the sedimentary section, demonstrating that the fault originated high in the sedimentary section. The

section between the two faults shows the rotated flank in the early stage of development.

Experimental studies of so-called "drape folds" (Stearns and Weinberg, 1975) show the development of footwall imbricates off the pre-cut, or "first-formed reverse fault" (fig. 117a). Movement along footwall imbricates B-B' and C-C' accomplishes rotation of bedding surfaces between faults A and B, and B and C. This rotation may be analogous to the development of the upturned basement surface on the footwall of structures such as at Clarks Fork Canyon (see Geometry of Faulted Basement: Downthrown Blocks, section 5.42). Upward rotation of an imbricated basement block in the footwall (fig. 117b) may cause the overlying syncline to tighten, thus creating a volume problem which is accommodated by the development of the synclinal fault (lower) of the dual system. By inference, it is possible that the synclinal fault of the dual system is extended downward by intersecting an upward propogating footwall imbricate.

The dual fault zone is also present in the Deer Creek area (fig. 39) and the two faults are much closer together than in the West Billy Creek example. The sedimentary rocks between the two faults at Deer Creek are rotated more than those at West Billy Creek and, in the outcrop along the plunge of the structure, these units are thinner between the faults than in the footwall position. How-

ever, when measured parallel to the faults, the thicknesses of the units in the rotated flank are the same as those in the non-rotated, footwall position. This suggests that thinning in the dual fault zone takes place by shear during the overturning and rotation of the steep flank.

Brown (1983) suggested a minor addition to Berg's (1962b) model, based on observations of subsidiary folds present on the hanging wall of several fold-thrust structures (examples are: Five Springs area, section 5.41; northeast flank of Owl Creek Mountains, section 5.51). Development of this subsidiary feature (fig. 118) began in the early stage of the sequential development of the fold-thrust. The method of formation of the subsidiary ("rabbit ear") fold has been discussed previously (see Structures Related to Synclinal Adjustments, section 6.33). The final position of the subsidiary fold may be at any point on the steep limb above, within, or below, the dual fault zone (fig. 118c). The exact location depends upon the magnitude of the out-of-the-syncline movement.

Down-plunge views of fold-thrust structures. The four maps of the Tobacco Root Range of southwest Montana (fig. 119; Schmidt and Hendrix, 1981), show a complete sequential development (fig. 119a,b,c) of the fold-thrust model as postulated by Berg (1962b) when viewed down plunge (Mackin, 1959). The most complete example of a

fold-thrust structure is shown in the London Hills area (fig. 119d). The dual fault system is well developed, and the overturned and rotated flank is present. A well drilled through the London Hills structure would show the same geometry seen in the EA and Immigrant Trail areas which Berg (1962) used in defining his fold-thrust model (fig. 120).

In summary, the foregoing examples from Wyoming and Montana are all northwest trending structures, which show the fold-thrust model in different stages of development. It has been shown in an earlier section (Plate Convergence and Direction of Compression, section 4.31) that the direction of tectonic shortening determined for the Laramide orogeny is southwest-northeast, normal to these features. The conclusion to be drawn from this relationship is that the major Laramide structures are fold-thrust uplifts which trend northwest-southeast, and are either northeast or southwest vergent.

7.5 Conclusions

There is no single structural model which applies throughout the Wyoming foreland. The evidence presented in this section clearly leads to the conclusion that the orientation of a structural trend may determine which

structural model applies. Features displaying the basic characteristics of fold-thrust uplifts are the major northwest trending structures of the foreland. Thrust uplifts also trend generally northwest but may be at slight angles to the trends of the fold-thrusts. Those features which display the basic characteristics of the drape fold and upthrust structures are the east and northeast trending structures on the foreland which are parallel or sub-parallel to the regional direction of compression.

Northwest trending structures which have been interpreted as drape folds (i.e. Rattlesnake Mountain anticline, Stearns, 1971), or upthrusts, are structurally out of balance. The imbalance between the sediments and the basement surface, results from an absence of extensional mechanisms on the upthrown block. However, interpretations using the fold-thrust model are easily balanced.

8.0 CONCEPT OF COMPARTMENTAL DEFORMATION

8.1 Introduction

The northwest trending primary Laramide thrust and fold-thrust structures are often interrupted by less prominent east or northeast-trending cross faults (see General Geology of the Wyoming Foreland: Regional Foreland Structures; section 3.3). These cross faults segment mountain uplifts and/or terminate individual anticlines along plunge. Features such as the west-trending North Owl Creek thrust, Casper Mountain fault, Corral Creek fault, and the Tensleep fault segment various mountain ranges. The result is to divide these uplifts into "blocks" which are often bounded by faults on three sides (Piney Creek block, in the Bighorn Mountains), or monoclinal flexures (Pryor Mountains, in southern Montana). As discussed earlier, many of the cross fault trends were reactivated, from a Precambrian ancestry, during the Laramide orogeny (table 2; Precambrian Structural Trends, section 3.14; Relationship of Precambrian and Laramide Structures, section 5.12). I have chosen the term "compartmental deformation" to describe the process which produces this pattern (Brown, 1975).

These east and northeast trends have already been shown to be in the proper orientation for dominantly vertical differential displacement and are thus the

preferred location for the formation of drape folds and upthrusts (fig. 121; see Model 1: Uplift of Vertical Faults, section 7.21; Model 2: Upthrust Structures, section 7.22). In the compressional scheme of the Laramide orogeny, these faults may also have an oblique slip component of displacement as a result of their orientation with respect to the northeast-southwest direction of compression (see Plate Convergence and Direction of Compression, section 4.31; Orientation of Major Laramide Structures, section 3.32). The absence of well defined piercing points in the foreland stratigraphic section makes the identification of oblique slip along these faults difficult. This problem will be discussed more fully in a later section (see Crustal Shortening and Lateral Movements, section 9.0).

8.2 Early Concepts

Demorest (1941) described the changes in asymmetry of the Bighorn Mountains by dividing the range into the northern, central, and southern blocks (fig. 122). The northern and central blocks are separated by the Tongue River "lineament", which trends from southwest to northeast across the range (and is upthrown on the south). The central and southern blocks are separated by the east-west trending Tensleep fault which is upthrown on the north

(and displays a sense of left separation). Demorest also noted that the direction of vergence of secondary mountain flank structures varied from segment to segment.

Since Demorest's work, additional linear features crossing the Bighorn Mountains have been recognized. Hodgson (1965) described the Florence Pass lineament as part of an old Precambrian fault system, which is upthrown on the north as a Laramide fault zone. Hoppin and Jennings (1971) summarized previous work done on the range and defined the Thermopolis and Shell Creek lineaments. They also pointed out the consistency of the direction of asymmetry of flank structures within the various segments on the west flank of the range (fig. 123). North of Tongue River lineament, the general direction of asymmetry is directed northeast (out-of-the-basin); south of Tongue River to the Florence Pass lineament, the direction of asymmetry is to the southwest (toward the basin); between Florence Pass lineament and Tensleep fault, the flank structures are asymmetric toward the northeast; and south of Tensleep fault, the asymmetry is again directed to the southwest.

The term "compartment deformation" was used by Philcox (1964) in describing changes in fold asymmetry and style of faulting across tear faults in the Variscan fold belt in Southern Ireland. I prefer to restrict the term "tear fault" to the thin-skinned thrust belts (wherein the

tear faults separate fold trends which verge in the same direction), and have applied the term compartmental faults to the oblique-trending, high angle faults in the foreland, which segment the primary basement-involved structures which may verge in opposite directions across a compartmental fault. Stone (1969) has used the term wrench faults for all of the basement-involved foreland faults (including those which trend northwest), but for reasons to be discussed below (Length of Fault, Relative to Size of Uplift, section 8.31), I prefer to separate the faults which trend oblique or transverse to the uplifts from the primary thrust and fold-thrust faults. I refer to the former as "compartmental faults", and to the resulting "blocks" as compartments (after Philcox, 1964).

8.3 Characteristics of Compartmental Deformation

Examples of compartmental deformation in the foreland are found on all scales, from anticlines up to mountain ranges such as the Bighorn Mountains. The characteristics of compartmental deformation are described in this section. These characteristics are as follows:

1) Compartmental faults trend east, or northeast, and are only slightly longer than the width of the folds or uplifts they cross.

2) Abrupt changes in asymmetry may occur across compartmental faults.
3) Northwest trending structures may terminate against compartmental faults.
4) Structural balance is maintained from one compartment to another.

(Additional examples of compartmental deformation in the foreland are given in Examples From the Foreland, section 8.4).

8.31 Length of fault, relative to size of uplift

Many compartmental faults die out laterally within the folds which they cross. An example is the Casper Mountain fault (fig. 124) which dies out laterally, both east and west, in a fault-fold interchange. The short length of these faults (relative to the size of the structure on which they occur) places a limit on the magnitude of the lateral motion which can occur along them. This point is significant for the interpretation of foreland deformation

Stone (1969) has discussed some potential problems in the interpretation of two-dimensional cross sections which are transverse to a fault having a component of strike slip (fig. 125). The fault in this figure could be interpreted as a normal fault, reverse fault, or perhaps not even recognized, because of the oblique slip nature of the

displacement. Apparent change in direction of throw (from north side upthrown at the west end of the fault, to south side upthrown at the east end of the fault) is often quoted as evidence of strike slip motion. However it is clear from the figure that the fault has no regional significance as a strike slip fault, but merely accommodates the differential uplift on opposite sides of the fault. The fold amplitude could continue to grow with an increase in total crustal shortening across the block, but the ends of the fault would become closer together, indicating that the fault formed simultaneously with the folding.

8.32 Changes in asymmetry

Changes in direction of anticlinal asymmetry (reversal of inclination of their axial planes) on opposite sides of a compartmental fault have been noted by Hoppin and Jennings (1971). As indicated in figure 126, the change in asymmetry implies that the anticlines do not represent a single fold, which was offset by strike-slip movement. Instead, the folds probably result from reverse faults at depth, as at Hunt Mountain (see Downthrown Fault Blocks, section 5.42) which dip in opposite directions on either side of the compartmental fault. This can be interpreted as indicating that the two anticlines developed at the same time, in response to the same stress field, with a different direction of thrusting (and resulting asym-

metry of folding) in each compartment. Clearly, the compartmental fault must have been activated at an early stage in the folding.

An example of change in direction of asymmetry across a compartmental fault is shown by mapping along the east flank of the Bighorn Mountains (fig. 122). The Piney Creek basement block has been thrust eastward over the adjacent Powder River basin, along the Piney Creek thrust. It appears that the Piney Creek thrust is intersected by a compartmental fault (Piney Creek "tear fault") at the north end of the block. Two cross sections (fig. 127a, b) demonstrate the change in direction of asymmetry across the compartmental fault. South of the compartmental fault the Piney Creek thrust verges eastward, while to the north, the flank of the Bighorn Mountains dips gently eastward, with a basement-involved out-of-the-syncline thrust directed updip towards the west. The Piney Creek "tear fault" served as the compartmental fault which has allowed a change in direction of asymmetry along the mountain front. This indicates that each compartment deformed independently of the other, but both were contemporaneous with the development of the compartmental fault.

8.33 Termination of northwest trends

The intersection of the Pine Dome-Iron Mountain and Emmigrant Gap anticlinal trends with the Casper Mountain

fault (fig. 126) demonstrates the abrupt termination of many anticlines in the foreland. In this example, it is evident that these structural trends do not have a counterpart on the south side of the Casper Mountain fault. In other instances, anticlines may be present on opposite sides of the compartmental fault, but not match up with one another.

8.34 Structural balance maintained

If the rocks on opposite sides of a compartmental fault were deformed at the same time, but independently of one another, the magnitude of crustal shortening should be the same on both sides of the fault. This structural balance is readily apparent in figures 125 and 126. However, structural patterns are often significantly different on either side of a compartmental fault (fig. 128), and the balance of shortening may not be obvious.

It is also possible for the style of the structure to change completely and still maintain balance. For instance, an anticline on one side of a compartmental fault can be balanced by a syncline on the opposite side (fig. 129). This type of relationship provides good evidence that the compartmental fault formed early in the folding process, since the two compartments folded simultaneously, and in opposite directions of one another.

An example is the northeast trending Deep Creek fault which separates the northwest plunging Bighorn basin on the north, from the southeast plunging southern Bighorn Mountains-Casper arch on the south (fig. 130). This relationship demonstrates that structural balance may be maintained by an opposite sense of folding on a regional scale; the basin is balanced by the arch. Nichols (1965) has shown that the Deep Creek fault is parallel, and immediately adjacent to, a Precambrian dolerite dike which strikes northeast, suggesting that this is another Laramide feature which was controlled in its orientation by Precambrian structural trends.

8.4 Examples from the Foreland

The presence of buried compartmental faults may be inferred by the apparent offset of anticlinal axes, even though no faulting is observed on the surface. The Bonanza anticline-Zeisman dome trend (fig. 131) is an example. There, a northeast trend apparently offsets the south ends of the Bonanza, Paintrock, and Hyattville anticlines, and the north ends of Nowood anticline and Zeisman dome. Westward along the trend, contacts in the Cretaceous section strike northwest with no offset (fig. 132a) indicating the termination of the compartmental fault. To the east, a syncline which preserves Jurassic

rocks, plunges northwest across the projection of the compartmental fault limiting its extent in that direction (fig. 132b).

Two southwest-northeast cross sections (fig. 133) parallel to, but on opposite sides of the suspected compartmental fault, show the mismatch of structures across the trend. However, bed length measurements on the same horizon on both sections indicate that the two sets of folds are in structural balance. The larger folds of Nowood and Zeisman are balanced by three smaller folds, Bonanza, Paintrock, and Hyattville. As discussed earlier (Precambrian Structural Trends, section 3.14; and Relationship of Precambrian and Laramide Structures, section 5.12) several northeast trending Precambrian age shear zones were reactivated during the Laramide orogeny. Although no direct evidence is available, the northeast trend along which the folds have been terminated, may represent a Precambrian age basement shear zone which has been reactivated as a Laramide compartmental fault zone. On the sketch map of the interpreted compartmental fault zone (fig. 134a), note that the synclinal axes are not offset by the compartmental fault. This suggests the northeast-trending Laramide basement faulting was initiated by the uplift of the northwest-trending anticlines (see: The Corner Problem, section 8.5). The block diagram (fig. 134b) shows that the upward rotation of the basement

(in the core of the anticlines) is accomplished by movement along concave upward curvature of the reverse faults which control the various anticlines.

A similar analysis has been done across the Bighorn Mountains, parallel to the Tensleep fault (fig. 135), which Hoppin and others (1965) have shown to be a reactivated Precambrian fault zone. Bed length measurements along the Precambrian-Cambrian contact on cross sections on both sides of the fault are identical, demonstrating that structural balance is maintained on a regional scale.

8.5 The Corner Problem

Major objections to horizontal compression as the driving force during the Laramide orogeny has focused on the apparent absence of mappable strike-slip movement on the east or northeast-trending faults which terminate northwest-trending structures such as Rattlesnake Mountain anticline. As was noted above, the intersection of the northwest trending anticlines with the oblique or transverse faults results in segmentation of the foreland uplifts and anticlines into blocks. The structural relationships at the corners of these blocks are particularly important for the interpretation of horizontal versus vertical movements. The study of these relationships is referred to as the "corner problem" (Stearns, 1978).

If, as in the vertical uplift concept, the intersection of these trends results in a vertically rising "block corner", then drape folds would be formed on both sets of faults. In the compressional model, the northwest-trending faults should be a thrust or fold-thrust structure, and the east or northeast-trending faults should be high angle reverse, left oblique-slip faults. Stearns (1978) has contrasted the type of movements and fold styles which would occur on each of the two trends for both concepts (fig. 136). He has argued that no lateral offset is observed along the transverse trends in the foreland.

8.51 Experimental models of the "corner problem"

Experimental rock models have been used to study the "corner problem" (Logan and others, 1978). The model used in those studies (fig. 137a) consisted of a forcing block overlain by three thin rock layers (limestone, sandstone, and limestone). The forcing block was precut as shown in the figure. Cut #1 was vertical and parallel to the direction of loading to simulate the compartmental fault. Cut #2 was normal to the loading direction and dipped 65 degrees. It represents the main northwest trending reverse fault. With application of the load, the forcing block moved up the 65 degree cut and laterally along the ver-

tical cut. The deformed specimen (fig. 137b) shows the upthrown movement along both faults. Note that the lead confining jacket was not broken along the strike-slip fault. The rock layers (of the model) were offset by right lateral motion along cut #1, but apparently the ductility of the lead allowed the jacket to stretch and accommodate both the vertical and lateral components of offset.

The photomicrograph of the deformed model (fig. 137c) along section OB which shows a cross section of the compartmental fault (cut #1). The offset of the lower sandstone layer is the result of the forcing block moving up the 65 degree precut (#2), and towards the viewer. It also shows that the lower limestone layer broke cleanly along the vertical (#1) precut. However, the upper two layers formed a drape fold. Note the thinning of the sandstone layer (fig. 137c). The limestone layers thinned as much as 8.0% during deformation (fig. 138; Logan and others, 1978). The downward steepening of the faults in the model is similar to the geometry of the upthrust model.

The series of sections in figure 138 show the results of repetition of this experiment with increasing displacement. They show that the initial faulting along the compartmental trend (cut #1) did not reach the surface of the model. With increasing displacement the faults cropped out first at the lower hinge of the drape fold, and then

progressively up the flank of the drape fold toward the upper hinge. Thus, small lateral displacements may not result in surficial faulting, and faults appear first at the lower hinge of the drape fold, not over the compartmental fault.

8.52 Rattlesnake Mountain "corner"

Rattlesnake Mountain anticline is considered by many workers as the "type drape fold". It will be shown later in this section that the available information permits the interpretation that the south flank of Rattlesnake Mountain anticline is controlled by an east-west trending "buried" compartmental fault, which intersects the northwest-trending reverse fault (fault E, fig. 105) to the west. This intersection forms the "corner problem" referred to above (section 8.5). The index map of the area (fig. 139) shows that the northwest-southeast trend of Rattlesnake Mountain anticline changes abruptly to the east, around the southwest corner. Bedding along the trend of the compartmental fault dips south at greater than 60 degrees (fig. 140). Continuity of the sedimentary cover over, and around, the corner (fig. 141) has led Stearns (1978) to the conclusion that there is no lateral movement on the east-west trend.

My interpretation (fig. 105; section 5.52, Fault Cut-off Angles; Brown, 1984a) shows a component of hori-

zontal displacement (heave) on the reverse fault (E) of 2,250 feet (685 m). These results will be used in the interpretation of the "corner problem" at the south end of Rattlesnake Mountain anticline by applying the results of the experimental models discussed above.

An east-west trending fault (north side upthrown) is exposed in Triassic rocks along the south flank of Rattlesnake Mountain anticline (fig. 140). The fault dies out to the east (in the Triassic rocks) since the north-south striking Jurassic and Cretaceous units are not offset. To the west, the fault is covered by Quaternary colluvium (hill wash, Qc) at point "B". West of the Quaternary cover, the fault should be mappable in Jurassic and Cretaceous rocks, if present. Since the fault is not mapped, it either dies out to the west, or may have cut upsection through Jurassic and Cretaceous rocks where the outcrops are not sufficient to map it.

The fault is exposed near the lower hinge of the "drape fold" which plunges to the east and forms the "instant" south plunge (see section 8.53) of Rattlesnake Mountain anticline. The east-west trending fault (and associated drape fold) terminates the northwest trend of Horse Center anticline and the southeast trend of Rattlesnake Mountain anticline, which plunges abruptly into Dry Creek syncline on the south side (Structures Related to Synclinal Adjustments, section 6.33; figs. 58, 59). The

east-west trend of this fault, the change in structural style north and south of the fault, and termination of anticlinal trends are characteristic of compartmental faulting (section 8.3).

A north-south cross section (fig. 142) is drawn across the east-west trending drape fold and the fault which crops out in the Triassic rocks near the lower hinge. The fault dips northward and is interpreted to steepen downward into an upthrust geometry very similar to that of the compartmental fault shown in the rock models (figs. 137c, 138). The interpreted upthrust is in the proper position with respect to the south flank of the drape fold, and can be expected to connect with the basement level compartmental fault. The upthrust and basement compartmental fault are indicated to flatten abruptly with depth, and pass northward as a near horizontal fault which is the eastward (downdip) projection of reverse fault (E) shown in the transverse cross section (fig. 105; "T and A", for towards and away from viewer, represents movement normal or oblique to the plane of the cross section). The throw interpreted on the upthrust is relatively small (less than 500 feet; 150 m), but the total relief across the upthrust/drape fold combined is 4,000 feet (1,220 m) along this section.

The intersection of the east-west trending fault with the Triassic-Jurassic contact on the downthrown side

(footwall cut-off) is mapped at point "A". The fault intersection with this contact on the upthrown side (hanging wall cut-off) is covered by colluvium, but must be between points "B" and "C" (the length of the covered interval). Thus the strike separation (apparent, two dimensional map offset) of the Triassic-Jurassic contact along the fault is between 5,000 feet (1,520 m; A to B) and 8,000 feet (2,430 m; A to C). This separation includes any component of left-lateral slip (three dimensional net slip) and erosional shift of the outcrop.

The absence of recognized piercing points in the stratigraphic section, makes it impossible to prove left-lateral slip, but the east plunge of the drape fold requires that erosion not shift the Triassic-Jurassic contact hanging wall cut-off far to the west. It is evident from this relationship that movement on this fault can not be simple "dip slip", but must have some magnitude of left-lateral (strike) slip, which is also required by the west vergence of reverse fault E (fig. 105). Because the fault apparently dies out to the west (and to the east as well) it is required to be a rotational fault, with lateral changes in heave and throw (characteristic of compartmental faults).

As discussed earlier (Structural Balance Maintained, section 8.34) structural balance is maintained on both sides of compartmental faults. The profile of the folding

and faulting along a compartmental fault can magnify or suppress the apparent lateral offset along such trends. Differential folding, along with opposing asymmetries, and changes in the direction and amount of tectonic transport, will also affect the apparent offset of stratigraphic contacts (fig. 143) along compartmental faults. For example, Horse Center anticline, Dry Creek syncline, and Half Moon thrust together (fig. 59) maintain structural balance south of the Rattlesnake Mountain compartmental fault.

The abrupt changes in fold profiles and direction of tectonic transport, make it difficult to determine the location for reference lines for determining structural balance parallel to the compartmental fault south of Rattlesnake Mountain anticline (see APPENDIX C). Northeast-southwest cross sections (parallel to direction of regional shortening) drawn on the north and south sides of the compartmental fault illustrate the differential folding and faulting on either side. On the north side of the compartmental fault (fig. 144a), the large, singular uplift of Rattlesnake Mountain anticline verges toward the southwest, and contains a small rabbit ear fold which verges to the northeast; on the south side of the compartmental fault (fig. 144b), the Precambrian basement of Horse Center anticline has been transported to the northeast, and a large rabbit ear fold, detached in Mississippian limestones, verges to the southwest (see Fold-thrust Uplifts,

section 7.44). The Half Moon thrust has been generated as out-of-the-syncline "crowding" by constriction of the Dry Creek syncline between Horse Center and Half Moon anticlines (fig. 59).

These structures are located on the western rim of the Bighorn basin, and represent major zones of displacement transfer. The eastern reference line should be at the axis of the basin (six miles to the northeast of the right-hand side of the sections; 9 km), and the western reference line should be west of the left-hand side of the sections, to be assured of including all displacement transfer mechanisms. However, measurement of the lengths of the Precambrian basement surface, over the distance shown, reveals a reasonable balance of the cross sections in figure 144.

In summary, Rattlesnake Mountain anticline can be best interpreted as a fold-thrust controlled by a northwest trending reverse fault (fault E, fig. 105) which flattens with depth to the east. An east-west trending compartmental fault, matching the upthrust geometry of the experimental model, terminates Rattlesnake Mountain anticline on the southeast. The 5,000-8,000 feet (1,500-2,400 m) of left separation along this compartmental fault is sufficient to accommodate the 2,250 feet (680 m) of horizontal dip slip (heave) of reverse fault "E". I interpret the 5,000-8,000 feet (1,500-2,400 m) of left

separation to be a combination of erosional shift of the outcrop, and (at least) 2,250 feet (680 m) of net left slip, which defines the sense of motion along this fault as being reverse left-oblique slip.

8.53 Basement model of the "corner"

Most anticlines in the foreland are doubly-plunging; however, the geometry of the plunging ends of any one anticline may be different. Field observations show that often one end is blunt, or squared off, while the opposite end is tapered. A basement model of these geometries is exposed in the Livingston Peak area of southern Montana (Richards, 1975; fig. 145a). The northwest striking Suce Creek fault loses displacement gradually to the southeast, while to the northwest, the Stumbo Mountain fault intersects it at a right angle, giving the geometry of a "basement block corner".

A form-line contour map of a sedimentary unit restored over the basement block (fig. 145b) demonstrates that the tapered plunge end of the anticline could result from the gradual loss of displacement along the Suce Creek fault. The abrupt northwest plunge reflects the draping of the sedimentary section over the Stumbo Mountain fault and gives the "blunt" end of the anticline. I use the term "instant plunge" when a low plunge angle (0 to 20 degrees) changes to a high plunge angle (greater than 45 degrees)

in a short horizontal distance, as shown here. These results will be used in the interpretation of other anticlines in the foreland.

8.6 Application of Compartmental Deformation

The Derby-Winkleman dome line of folding in the western Wind River basin is a major northwest-trending structure which exhibits compartmental deformation. The surface geologic map (fig. 146) displays a series of structural closures, some of which are slightly en echelon to one another. The "tapered and blunt" plunge ends described above can be seen on several of the folds. The basement geometry is exposed up-plunge at point A (T.30 N., Rs.96 and 97 W.) where Precambrian and Paleozoic rocks are thrust westward over Cretaceous rocks (Gooldy, 1952). A series of sections across the trend (fig. 147) shows the increasing structural relief and constriction of the syncline on the steep flank. At Sage Creek anticline (SC; fig. 147b), a dual fault system with a rotated flank has been documented by well control (see Model 4: Fold-thrust Uplifts, section 7.24). Spang and others (1985) have interpreted this structure differently, but the basic model is the same as in figure 147. Using the one point of basement well control at Winkleman dome, and the cross sections in figure 147, a structure contour map on the top

of the basement has been constructed (fig. 148). This map has been interpreted to apply the concept of compartmental deformation to a major foreland fold trend. The "instant" plunges at the southeast ends of Dallas dome and Lander anticline, and the northwest ends of Sage Creek and Winkleman anticlines are interpreted as compartmental faults. The axis of the syncline between the fold trend and the regional dip slope of the Wind River Mountains is shown as deflected by the compartmental faults. However, it is still continuous, indicating that the compartmental faults are activated by the uplift of the anticlines (see: Bonanza-Zeisman trend, Examples From the Foreland, section 8.4).

The concept of compartmental deformation is especially useful in exploration for oil and gas reserves. The expectation that exploratory wells drilled as "stepouts" from a producing structure will find extensions of it, and thus the continuation of the oil field, should be tempered by the realization of the differences in structure which can exist on opposite sides of a compartmental fault.

The concept may have its greatest application in foreland basins which are filled with post-orogenic sediments, so that no outcrops are available for study. In such basins, seismic program to cross the regional trends are often arranged to cover large areas and the "turn-around" time for processing seismic data is usually long

enough that the entire field program is completed before the data are available for study. Thus, recognition that the anticipated structural pattern was not present usually comes after the field shooting is completed. Because most compartmental trends are transverse to the regional structures, one approach would be to shoot seismic "reconnaissance" lines parallel to regional strike. The "strike lines" would be normal to the compartmental faults, and in the optimum orientation for resolving the structural geometry with seismic reflection data. Subsequent lines could be programmed parallel to regional dip on each side of the compartmental fault, and in so doing, obtain maximum control on anticipated changes in structural continuity across the fault.

8.7 Summary

The concept of compartmental deformation can have a strong influence on the process of determining regional structural balance in the foreland. The recognition of simple offset of structural trends may lead to a variety of ideas regarding interpretation of the regional structural pattern. However, the existence of the concept of compartmental deformation should alert investigators to the possibility that structural trends intersected by compartmental faults may be offset, develop an opposed

sense of asymmetry, or be completely replaced by some other structural style across the fault, while overall structural balance is maintained. Compartmental faults often serve as regional "zones of displacement transfer".

Compartmental faults are not always exposed at the present level of erosion and their presence must often be inferred from interpretation of their characteristics. Mismatch of structural features across a linear trend is perhaps the most significant clue to recognition of the presence of compartmental faults.

Of primary interest in the interpretation of the foreland structural style is the knowledge that significant magnitudes of strike slip motion (combined with reverse dip slip) may have taken place along east, or northeast-trending compartmental faults with no surface expression, other than the development of drape folds. Other compartmental faults crop out as upthrusts (having reverse-oblique slip) at the lower hinge of the associated drape fold. Large lateral and vertical motions along drape fold and upthrust trends have resulted in major faults which have been eroded deeply into the sedimentary section, or down to the basement. These faults often display "drag" features which agree with the sense of lateral slip postulated along the compartmental fault. Structural balance is maintained on both sides of a

compartmental fault by differential folding and faulting in the two "compartments".

9.0 CRUSTAL SHORTENING AND LATERAL MOVEMENTS

9.1 Introduction

The term "crustal shortening", as applied to the foreland, refers to the shortening of the basement (to the depth of involvement). It is defined as the difference in distance between two reference points before (arc length), and after (map distance) deformation (see Calculation of Depth to Detachment-Appendix D; shortening equals arc length minus chord length). A comparison of magnitudes of shortening in overthrust belts around the world suggests a limit of approximately 50% shortening in such tectonic regimes (Bally and others, 1966; Dahlstrom, 1969b, 1970; Royse and others, 1975; and Boyer and Elliott, 1982). Only one comparable study (Kanter and others, 1981) has been published for the Wyoming foreland area.

Crustal shortening is measured in the direction of tectonic transport which is N40-50E in the Wyoming foreland (fig. 149; section 4.31, Plate Tectonic Setting of the Laramide Orogeny: Direction of compression). Thus total crustal shortening is the cumulative shortening of individual structures along a single line, parallel to the direction of tectonic transport (see Models of the Wyoming Foreland: Models 3 and 4).

Total crustal shortening along any cross section equals the heave of all reverse faults, plus the shor-

tening resulting from all folding (fig. 150), minus any measurable extension. Many of the major structures in the foreland are fold-thrust features which combine the heave of thrust faulting, with folding of the hanging wall and footwall (see Models of Structural Styles of the Wyoming Foreland, section 7.0; figs. 70, 87).

9.2 Consistency of Crustal Shortening

Structural balance must be maintained across the deformed foreland, therefore measurements along parallel lines across the foreland (fig. 149) should show essentially the same magnitude of crustal shortening (assuming end points are properly selected). A discrepancy in the shortening between adjacent profiles would indicate a change in the regional structural style between the profiles, or else possibly an error in interpretation.

The en echelon arrangement of faults and folds, as well as lateral fault-to-fold interchanges, and compartmental faults represent displacement transfer zones (Dahlstrom, 1969B) which maintain balance in shortening across a fold trend, along the strike of the fold trend. For consistency between cross sections, measurements of crustal shortening should be confined to the same strati-

graphic horizon (Dahlstrom, 1969b); in this study, the contact between the basement and sedimentary section is used.

The location of the profile lines in figure 149 is somewhat arbitrary, but specific geologic features were selected for the end points. The northeastern ends of the lines have been placed at the axis of the Powder River basin which serves as a null point, or reference line (see APPENDIX C: Technique of Structural Balancing; Appendix B: Characteristics of Parallel Folding). Lines oriented parallel to "regional structural strike" (northwest) may be drawn on the regional flank of a basin and used as "arbitrary" end points for lines of measurement (see discussion of arbitrary reference lines in Appendix C: Technique of Structural Balancing) when no "fixed" point is apparent. Selection of the southwestern end points presents a problem, because the western edge of the foreland is partially overridden by the thrust belt. However the axis of the Green River basin can serve as a reference line here.

9.3 Determination of Crustal Shortening

The distance along the top of the Precambrian basement in any profile represents the original length of that surface before deformation. The difference between the

original length of the surface and the map length of the profile gives the amount of shortening (fig. 150).

There are also shortcuts which can be used to estimate the total shortening in any profile. Spang and others (1985) have shown that the angle of dip of a basement reverse fault can be estimated from the geometry of the profile of the overlying, folded sedimentary section when seismic or drill hole data are not available to provide accurate measurements.

The heave of major reverse faults of the thrust and fold-thrust structures can be estimated from the dip of the fault and the structural relief (which is the vertical component of the dip slip). Assuming the dip of the fault plane is constant, the following relationship is obtained (Kanter and others, 1981):

$$\text{Heave} = \frac{\text{structural relief}}{\tan(\text{dip of fault plane})}.$$

The margins of several major uplifts in the foreland show no faulting at the surface, but apparently are faulted at depth, at least at the Precambrian level (fig. 29, Casper arch; fig. 101, Soda Lakes area). The shortening attributed to these features must be included in the overall summation to obtain the total crustal shortening. An

estimate of shortening can be made which will approximate the vertical height of a fold (fig. 151a), and the heave of a reverse fault which dips 45 degrees (fig. 151b). If an estimate of the magnitude of shortening is made from the height of a fold, without regard to the orientation of the axial plane, the estimate will usually be too small (fig. 152). In most instances, the dip of the axial plane can be determined from simple trigonometric considerations of the flank dips (fig. 153). The actual shortening (S) involved in the fold is equal to the height of the fold (Ht), plus the difference (X) between the measured length of the backlimb, and the length of its map projection.

Before discussing the actual values of crustal shortening determined for the foreland in this study, I need to briefly mention the concept of minimum displacement (Brown 1982). In drawing structural cross sections and making interpretations of outcrop and subsurface data, it is best to be as consistent in those interpretations as possible. One way to achieve this consistency is to interpret, and to draw, the smallest magnitude of fault displacement which will honor all the basic data. The actual magnitude of fault displacement may be much greater, but it can be no less than the minimum displacement. This makes it possible to compare displacements of different faults, or different interpretations of the same fault, without mixing "apples and oranges". In the following discussion,

the values of fault displacements used in the calculation of crustal shortening are minimum displacement values.

9.4 Values of Crustal Shortening for the Wyoming Foreland

I have measured the crustal shortening in each of the structural cross sections presented in this study and the results are tabulated on Table 11. These values demonstrate the range of crustal shortening in typical foreland structures. I have also constructed a continuous cross section along line A of figure 149, a map distance of approximately 235 miles (378 km). The shortening of the top of the Precambrian basement along this section (fig. 154) is 26.9 miles (43 km; 11.5% strain), and represents a minimum value.

To find the magnitude of shortening along lines B and C (fig. 149), I have used the values of shortening for structures along (or adjacent to) those lines, which are given on Table 11. For those structures along the lines which are not on table 11, I have estimated the shortening (fig. 155) using the various methods described earlier (section 9.3; figs. 151, 152, 153; Kanter and others, 1981; Spang and others, 1985).

The value of crustal shortening obtained for line B (fig. 149) is 28.6 miles (46 km; 12.5% strain). Measure-

TABLE 11. CRUSTAL SHORTENING ON INDIVIDUAL FORELAND STRUCTURES.

FIGURE	STRUCTURAL FEATURE	CRUSTAL SHORTENING
23	Five Springs area	1.00 miles
26a	Cow Creek-Porcupine	0.85 miles (4,500 ft.)
27	Hunt Mountain	0.38 miles (2,000 ft.)
29	Casper arch thrust	11.20 miles
34	Beartooth thrust	10.00 miles
39	Deer Creek area	0.21 miles (1,100 ft.)
42	Rattlesnake Mtn.	0.75 miles (3,960 ft.)
45	Bald Mountain anti.	0.60 miles (3,200 ft.)
50	Wildhorse Butte anti.	0.09 miles (500 ft.)
54	Goose Egg anticline	0.42 miles (2,200 ft.)
57	Spring Creek Anticline	0.72 miles (3,800 ft.)
59	Horse Center-Half Moon	1.10 miles
63	Pitchfork anticline	0.47 miles (2,500 ft.)
86	Red Canyon flexure	0.47 miles (2,500 ft.)
94	Oil Mtn.-Emigrant Gap	0.87 miles (4,600 ft.)
99	Wind River Mtns. (Berg)	11.80 miles
100	Wind River Mtns. (COCORP)	13.00 miles
101	Soda Lakes area, Colo.	2.00 miles
103c	Bellview dome, Colo.	0.60 miles (3,200 ft.)
110	Zeisman dome; N-S	0.15 miles (800 ft.)
112a	Tensleep fault (east)	0.19 miles (1,000 ft.)

TABLE 11. (CONT'D)		
112b	Tensleep fault (central)	0.15 miles (800 ft.)
112c	Tensleep fault (west)	0.09 miles (500 ft.)
113	Wind River Canyon	2.30 miles
115	Zeisman dome	0.15 miles (750 ft.)
116b	West Billy Creek	0.23 miles (1,200 ft.)
120a	EA thrust	5.68 miles
120b	Immigrant Trail thrust	4.00 miles
127a	East flank Bighorn Mtns.	1.81 miles
127b	Piney Creek thrust	4.16 miles
135a	E-W; Bighorn Mountains, north of Tensleep fault	1.90 miles
135b	E-W; Bighorn Mountains, south of Tensleep fault	1.90 miles
142	Rattlesnake Mtn. N-S	0.04 miles (200 ft.)
144a	Rattlesnake Mtn.	0.72 miles (3,800 ft.)
144b	Horse Center; north	0.76 miles (4,000 ft.)
144c	Horse Center; south	0.76 miles (4,000 ft.)
147a	Winkleman dome	0.66 miles (3,500 ft.)
147b	Sage Creek anticline	0.70 miles (3,700 ft.)
147c	Dallas dome	0.66 miles (3,500 ft.)
147d	Derby dome	0.63 miles (3,300 ft.)
149	Line B across foreland	28.60 miles
149	Line C across foreland	29.90 miles
154	Foreland regional line A	26.90 miles
159	Western Owl Creek Range	4.90 miles
162	Foreland regional section	28.00 miles

ment of a published section along line B (Petersen, fig. 2, 1983) yields a minimum value of 17 miles (27 km) of crustal shortening. There are two reasons for the smaller value. These are: 1) the scale of the published section (1 in = 100,000 ft or 30,000 m) which makes it difficult to be very accurate in the measurement, and 2) new well control on the northeastern end of the section which demonstrates at least three miles (5 km) of heave along the Piney Creek thrust (see section 8.32, Changes in Asymmetry; fig. 127) which is not shown on Petersen's (1983) section.

Kanter and others (1981) calculated shortening values for 15 regional lines across the Rocky Mountain foreland. Their line E-E' approximates the location and orientation of line B of this study. I determined the total value of crustal shortening along their line E-E' to be 28 mi (45 km). This was determined by adding the individual vectors which they had plotted as an example of their technique (Determination of Crustal Shortening, section 9.3; Kanter and others, fig.5, 1981).

The value of crustal shortening obtained for line C of this study (fig. 149) is 29 miles (46 km; 13% strain). The orientation of line C is such that it crosses a zone of displacement transfer. The decrease in shortening caused by the southeast plunge-out of the Wind River Moun-

tains is compensated for by the increase in shortening across the Granite Mountains and Casper arch structures.

I have also constructed another cross section (line D, fig. 162; Brown, 1987) which is in the same general area as cross sections B and C of figure 149, but is at a slightly different orientation (N40E). The value of crustal shortening on this section (fig. 162) is 28 miles (45 km; 13% strain).

In summary, values of crustal shortening determined for lines A, B, and C (fig. 149) and line D (fig. 162) are comparable (26.9, 28.6, 29, and 28 miles; 43, 46, 46, and 45 km) which indicates overall regional structural balance. Structural balance is maintained across the foreland, even when the major structures disappear by plunging-out and are replaced by many small structures, demonstrating the effectiveness of displacement transfer zones.

The values determined in this study are larger than those of Petersen (1983), but similar to those calculated by Kanter and others (1981). However, when Kanter and others applied the magnitude of shortening to the entire foreland, they calculated a total strain of only 5%. Inclusion of relatively undeformed areas of large extent (i. e. east flank of Powder River basin) in their calculations reduced the percentage value (5%) determined.

I would conclude that crustal shortening is pervasive throughout, and uniform across, the foreland. The data presented here support the concept that the reverse faults (and folds) shown in this study are the result of a regional compressional system. This system produced significant magnitudes of crustal shortening which can not be explained as local effects of dominantly vertical displacements.

9.5 Lateral Movements Related to Crustal Shortening

It is the purpose of this section to relate the magnitude of crustal shortening (discussed in the previous section) to the question of whether significant strike slip displacement has occurred in the foreland. It has been shown that east-west and northeast-trending compartmental faults may have components of lateral slip along them (see Concept of Compartmental Deformation, section 8.0).

The potential for large-scale lateral movements can be illustrated by considering the Five Springs area and the southeast plunge of the Wind River Mountains. Two northeast-trending compartmental faults are exposed in the Five Springs area of the Bighorn Mountains (fig. 156; Hoppin, 1970). Lateral offset of the overturned, east-dipping stratigraphic section, and the east-dipping re-

verse fault which bounds the Precambrian block, indicates approximately 7,000 feet (2,300 m) of left lateral slip along the East Medicine Mountain fault. Note that this compartmental fault is parallel, and immediately adjacent to a Precambrian igneous dike (see Relationship of Precambrian and Laramide Structures, section 5.12).

The Wind River Mountains uplift plunges southeast under Tertiary rocks and disappears (fig. 157). The 13 to 14 miles (20 to 22 km) of crustal shortening across this uplift (Table 11) must therefore be distributed to other structures in the area, by some manner. The loss of displacement at the southeast end of the range appears to be related to the change in strike of the mountain-bounding fault, from northwest-southeast, to more easterly.

Such a change in strike could result in a sense of left slip along the east-trending portion of the fault. The downwarp of the Red Desert basin may also have aided in maintaining structural balance by replacing anticlinal shortening (Wind River Mountains) with synclinal shortening (Red Desert basin; fig. 129; Concept of Compartmental Deformation, section 8.34).

The potential for such large displacement makes it surprising that there are so few areas which show the classic angularity of "drag folds" along suspected strike slip faults. Apparently, most of the potential lateral

movements are dissipated across small displacement compartmental faults and other displacement transfer zones.

There are two areas which show the typical angular relationship between anticlines and strike slip faults. These areas are: 1) the south flank of the Granite Mountains uplift (south-central Wyoming) and the associated Sheep Creek anticline (fig. 158), and 2) the north flank of the Owl Creek Mountains uplift (north-central Wyoming), and the associated Anchor anticline.

The south flank of the Granite Mountains uplift, which trends west-northwest (fig. 158), has been discussed in earlier sections (Model 3: Thrust Uplifts; sections 7.23, 7.43). Sheep Creek anticline (T.28 N., R.92 W.) is on the downthrown side of the northeast dipping Sheep Creek thrust (Berg, 1962b), and the axis makes an angle of approximately 15 degrees with the trace of the thrust. Sheep Creek anticline plunges northwest, under the Sheep Creek thrust, suggesting either: early strike slip movement along the fault, followed by overthrusting, or development of the Sheep Creek complex within a wrench fault system.

The relationship between Anchor anticline and the fault which bounds the north flank of the Owl Creek Mountains (figs. 35a, 38) has been discussed in earlier sections (Model 2: Upthrust Structures; sections 7.22, 7.42). Anchor anticline is a conical fold which is de-

tached in the Cambrian shales at the up-plunge end (figs. 80, 87). This change in longitudinal geometry, with the fold decreasing in amplitude to the up-plunge vertex, suggests that the fold formed at the same time as movement along the North Owl Creek fault. It is unlikely that the fault cut across, and offset, an earlier developed fold.

A northeast-southwest section across the Owl Creek uplift (fig. 159) displays over two and one-half miles (4 km) of crustal shortening accomplished by a series of southwesterly directed "back-thrusts" (Model 3: Thrust Uplifts, section 7.23; Appendix A) on the hanging wall of the North Owl Creek thrust. Thus at least two and one-half miles (4 km) of left slip may have occurred along the east-trending portion of the North Owl Creek fault. However, the absence of linear geologic features, which provide "piercing points" on fault planes, makes proof of such strike slip unlikely.

Stone (1969) has postulated a complete range of first and second order wrench faults for the origin of the primary folds and thrusts of the Rocky Mountain region (fig. 160). If the overall tectonic model for foreland deformation were primarily a wrench fault system, the structural style should be predominantly strike-slip faults, and en echelon folds. However, the style is predominantly fold-thrust structures and compartmental faults. It is simply a matter of what is the predominant style of de-

formation. The majority of the horizontal movement in the foreland was concentrated as reverse dip slip movement on individual northwest-trending thrust and fold-thrust structures (Model 3, section 7.23; Model 4, section 7.24). Compartmental faults were initiated early in the sequence of deformation of the northwest-trending folds (see Characteristics of Compartmental Deformation, section 8.3). Therefore, the lateral movement was distributed on short, individual compartmental faults, rather than on through going strike slip faults. A few areas had the potential for 10 to 15 miles (16 to 24 km) of strike slip, but such magnitudes of offset can not be demonstrated. In those areas where strike slip can be reasonably inferred (Five Springs area, Piney Creek tear faults, and North Owl Creek fault), the magnitudes which can be justified are considerably less (1 to 3 miles; 2 to 5 km). The absence of evidence for large-scale strike-slip movements argues against deformation by a pervasive wrench fault system.

9.6 Summary

The magnitude of crustal shortening across the Wyoming foreland during the Laramide orogeny is reasonably consistent when measured along three profiles parallel to the direction of tectonic transport. These measurements

give consistent values of shortening of 26 to 29 miles (41 to 46 km) which is equivalent to 11% to 13% strain.

The potential for large-scale lateral movements existed during the Laramide orogeny, as attested to by the values of crustal shortening which have been determined for individual structures, but it has been shown that most of the lateral movements were distributed along relatively short compartmental faults. Rather than accumulating large displacements on single strike slip faults, the regional shortening was distributed on individual structures. Major structures, having a definite form of large "crustal folds" which were oriented at right angles to the direction of tectonic transport, clearly indicate that the foreland was not deformed by a major wrench fault system, but rather by a fold and thrust system.

The values of crustal shortening determined in this study probably represent realistic measures of the total shortening involved in the deformation of the foreland during the Laramide orogeny. The application of the minimum displacement concept suggests that the values obtained (11.5-13%) should be considered minimum values. I believe the figure of 15% strain may represent a maximum value for the foreland. The central Wyoming portion of the foreland was at least 200 miles (320 km) in original width, thus the total amount of crustal shortening to be expected in that area (15% strain) would be approximately 30 miles

(48 km). This value should be used for comparison as an indication of whether future structural interpretation have accounted for sufficient crustal shortening to maintain consistent structural balance. For the maximum values to greatly exceed these, crustal shortening on major, unknown structural features must exist. The probability of such unknown structures existing is highly unlikely, given the widespread use of quality seismic data across the foreland.

10.0 STRUCTURAL SYNTHESIS OF THE WYOMING FORELAND

10.1 Introduction

The purpose of this chapter is to provide a synthesis of the structural development of the Wyoming foreland during the Laramide orogeny. This will be done by integrating results discussed in previous chapters (e.g. direction of compression, orientation of structural trends, styles of deformation, sequence of development, etc.) with addional data as needed.

10.2 Origin of the Laramide Orogeny

It was shown in sections 4.2 and 4.3 (Sevier Orogeny and Laramide Orogeny) that the transition from the thin-skinned deformation of the Sevier orogeny, to the thick-skinned, basement-involved deformation of the Laramide orogeny, coincided with a reorientation of the direction of convergence between the North American and Farallon plates (from N70E to N40E). The N40E direction of convergence is interpreted here to represent the direction of maximum compressive stress. This reorientation also coincided with an increase in the rate of plate convergence (section 4.32). It is my interpretation that the increase in plate convergence resulted in not only a lower angle of subduction and an eastward shift of the associated heat

flow, but also an increased magnitude of compressional stress directed into the basement of the Wyoming foreland.

10.3 Initial Deformation of the Wyoming Foreland

With the application of compressional stresses to the foreland along the N40E direction, the initial stages of Laramide deformation began in the west and progressed eastward through time (Time of Development of Major Structures, section 3.33). The area of the Owl Creek Mountains of Central Wyoming serves to demonstrate the nature of the onset of the Laramide orogeny (Keefer, 1965).

The initial response to Laramide compression in the area of the Owl Creek Mountains was of crustal downwarp (fig. 161). About 5,000 feet (1,500 m) of downwarp developed prior to the initial uplift of the range (Keefer, 1965, 1970). Ultimately, the magnitude of uplift (17,500 feet; 5,300 m) surpassed that of downwarping (16,000 feet; 4,800 m), resulting in a total structural relief of 33,500 feet (10,200 m) from mountain to basin. It is not known if crustal downwarping occurred at the site of all present-day mountain ranges, since studies such as Keefer's have not been published for other areas. However, total structural relief across the faulted margins of most other major foreland uplifts is of a similar order of magnitude.

A southwest-northeast cross section (fig. 162) across the central part of the foreland shows the Owl Creek Mountains as a structural positive located in the center of a basin-like depression, bounded by the Wind River and Bighorn Mountain uplifts. The axis of this depression coincides with the axis of depositional "thicks" shown on isopach maps of the Lower and Upper Cretaceous (fig. 6i, 6j). The Bighorn, southeastern Wind River, and Laramie basins lie along this same depositional axis. I suggest that this line was the axis of the initial crustal downwarping of the foreland, and that subsequent structural uplifts (e. g. Owl Creek Mountains and southeastern Granite Mountains) separated this depositional trough (crustal downwarp) into discrete foreland basins.

10.4 Basin Development and Flank Structures

Schmidt and others (1985) have determined the mean value of the spacing of "first-order" Laramide folds in the Wyoming foreland to be approximately 93 miles (150 km). Using these spacing values, experimental data concerning folding of a brittle layer above a ductile substrate, and regional heat flow analysis, they determined the depth to the brittle-ductile transition in the crust of the Wyoming foreland to be approximately 15-25 miles

(25-38 km). This suggests that the "first-order" structures of the Wyoming foreland were controlled (in part) by the brittle-ductile transition in the crust. They further suggested that structures with a spacing of less than approximately 25 miles (40 km) would not involve the entire crust, and were probably controlled by other factors, such as preexisting fault zones and/or variations in basement lithology.

Dallmus (1958) proposed that it is necessary to consider the initial downwarping of a basin as a flattening of the curvature of the Earth's surface, in order to fully understand the dynamic structural development of a basin. This flattening requires a shortening of the crust, which results in the generation of local compressive stresses, as long as the crust remains above the chord drawn from basin margin to basin margin (fig. 163). This is the same effect that causes the concave surface of a bent beam to be subject to compressive stresses (fig. 164).

I believe this concept can be applied to the initial development of foreland basins during the Laramide orogeny. Downbending of the crust would require shortening, and result in the development of local compressive stresses in the upper portion of the Precambrian basement. These structures would result in the development of a conjugate set of reverse faults (Hafner, 1951; fig. 165a; Rock Mechanical Properties of Foreland Basement: Summary,

section 5.23). If a sedimentary veneer is added to the model (fig. 165b), a series of reverse faulted anticlines, with out-of-the-basin asymmetry, could be developed. It is interesting to compare this model of basement-involved flank structures with the development of out-of-the-syncline crowd structures developed in the sedimentary section. Structures such as backlimb and rabbit-ear folds (Structures Related to Synclinal Adjustments, sections 6.33), and the modification of Berg's fold-thrust model (section 7.44), have their counterpart in these basement-involved structures. Both styles are apparently created by local compressive forces which are generated by the requirement of conservation of volume.

Such a model may be compared to the initial development of a single large-scale foreland basin, with the central uplift area representing a mid-basin uplift. It may also be compared to individual foreland basins which become asymmetric as shortening proceeds, and are surrounded by primary (first-order) mountain uplifts (compare fig. 165b to fig. 162.)

COCORP seismic data, combined with values derived for depth to the brittle-ductile transition zone (Schmidt and others, 1985), and depth-to-detachment calculations (Appendix D) suggest that major uplifts such as the Casper arch, and Wind River, and Beartooth Mountains represent first-order structures, which are probably controlled by

detachment at the brittle-ductile transition depth in the deep crust. Smaller-scale features, such as the Bighorn Mountains may represent intra-crustal detachment (Petersen, 1983). Even smaller-scale structures such as the Derby-Winkleman trend,and the Rattlesnake Mountain and Sheep Mountain anticlines are more likely to represent crustal "flakes" which result from downwarping of the crustal "beam".

Structures of this type are common in the foreland; for example, the anticlines on the gentle east flank of the Bighorn basin shown in figure 166. This seismic section shows the east-directed (out-of-the-basin) asymmetry of Bonanza and Paintrock anticlines (also see Examples From the Foreland, section 8.4). Similarly, the seismic section in figure 167 shows the west-directed (out-of-the-basin) vergence of flank structures on the steep west flank of the Powder River basin, across the Bighorn Mountains from the section in figure 166.

A modification of this style of basin flank structure is illustrated on the seismic section (fig. 168) of Oregon Basin uplift on the west flank of the Bighorn basin. The anticline is separated from the axis of the Bighorn basin by an east-directed reverse fault which forms part of the boundary of the basin. The fold form is accentuated by an antithetic, west-verging reverse fault. This style may be analogous to the "thrust/back-thrust" model discussed in

the section on lateral movements and crustal shortening (section 9.5). However, comparison with figure 167 suggests that features such as Oregon Basin anticline may have initially developed as out-of-the-basin, basement-involved, crowd structures (rabbit-ear style; section 6.33), which were isolated on the basin margin by later formation of the basin-bounding fault.

A basement "flake", which is thrust upward into the sedimentary section, becomes a "forcing block" (section 6.1) which, combined with the rotation of the upper basement surface of the footwall block to a synclinal curvature, serves as a "piston" to direct local compressive stresses into the sedimentary section at some low angle to the bedding surfaces.

10.5 Subsidiary Structures in the Sedimentary Section

Most "crowd structures" (back-limb and rabbit-ear folds, and cross-crestal structures) in the sedimentary section of the foreland, form because of volumetric crowding in synclines (section 6.33). Thus, they form in sequence with the large-scale structures.

Dating the development of the subsidiary folds effectively limits the age of the major fold. However, it is often difficult or impossible to accurately date the large primary folds because of the long period of tectonic ac-

tivity. However, it is often possible to date the time of formation of subsidiary folds, since they are more local- ized. Caution should be practiced in relating the age of formation of subsidiary folding to that of unrelated primary folds.

It is also important to realize that the orientations of crowd structures may not always be exactly parallel to the larger folds in the same area. Such variations in orientation have been used as evidence of changes in the regional direction of maximum compressive stress (Gries, 1983). However, subsidiary folds are late-stage features of a deformation process. They need not imply a "new tectonic pulse", nor should a change in their orientation relative to larger structures be taken as "proof" that a reorientation of the regional stress field has occurred. These features simply accomplish a volume adjustment within the space available.

10.6 Sequential Deformation of the Wyoming Foreland

10.61 Introduction

The purpose of this discussion is to trace a generalized sequence of deformation through time, from west to east, along the general line of section shown in figure 162. The development will be covered in the six time increments shown in figure 169 (Campanian, Maestrichtian, end of Cretaceous, end of Paleocene, early Eocene, post-

middle Eocene), and will emphasize three principal areas (Wind River, Owl Creek, and Bighorn Mountains) as representative of the foreland. Sequential diagrammatic cross sections (fig. 170) across the foreland, will show the areal relationships during the same time periods as in figure 169 (except for the omission of early Eocene).

It has been shown previously (Time of Development of Major Structures, section 3.33) that deformation of the foreland began during Campanian time in western Wyoming, and progressed eastward through time, ending in early or middle Eocene in the vicinity of the east flank of the Bighorn Mountains. Such a sequence of deformation requires that foreland structures have different ages across the region; however it should be kept in mind that the entire Laramide orogeny took place over a period of only 30 m. y. (75 m. y. a. to 45 m. y. a.).

10.62 Campanian

The Laramide orogeny began in Campanian time with horizontal compressive stresses transmitted through the crust along a southwest-to-northeast direction, from the zone of plate collision to the western margin of the Wyoming foreland. These stresses resulted in the initial buckling and folding of the crust along the Moxa arch (figs. 169a, 170a), west of which the crust was subsiding into the Cordilleran geosyncline in response to the tec-

tonic loading by emplacement of four major thrust sheets (Royse and others, 1975). Eastward, the foreland remained a stable platform of deposition, across which the Late Cretaceous Western Interior Sea reworked and redistributed synorogenic conglomerates which were shed from the rising thrust belt in the west. The present-day local structural basins and uplifts were not yet present, as shown by the regional facies distribution of Upper Cretaceous (fig. 6j) and the Mesaverde Group (fig. 7).

10.63 Maestrichtian

By late Campanian, or early Maestrichtian time, the Wind River-Gros Ventre-Teton-Targhee basement-involved fold-thrust trend had begun to develop perpendicular to the direction of maximum regional compressive stresses (figs. 169b, 170b). The crustal rotation associated with this major uplift, in part, controlled the eastward shift of the strand line of the Cretaceous sea; the last marine regression is marked by the top of the Lewis Shale in the Wind River and Bighorn basins. Initial crustal downwarp in the region of the Owl Creek Mountains was concomitant with, and probably facilitated by, the early stage of uplift of the Wind River Mountains to the west.

10.64 End of Cretaceous

By the end of Cretaceous, the steep southwest flank of the Wind River Mountains had been breached by erosion and was supplying sediment to the subsiding Green River basin. The gentle backlimb (dip slope) of the Wind River Mountains dipped northeast toward the axis of the Wind River basin, which had subsided approximately one mile by this time. The amount of the crustal shortening across the foreland which had developed by the end of Cretaceous (figs. 169c, 170c) is unknown. However, it is possible that as much as one-half of the total shortening accomplished by the Wind River fold-thrust system (table 11) had occurred by this time. The southwest-verging crustal shortening was probably accompanied by movement along east-west oriented compartmental faults (section 9.2) which transected the developing fold-thrust trends. Uplift of the Owl Creek Mountains had not yet begun. To the north and east, some local(?) structural warps had devel- oped in the Bighorn region, as evidenced by the slight unconformity at the top of Maestrichtian beds.

10.65 End of Paleocene

The Paleocene Fort Union Formation, deposited in the Green River basin southwest of the Wind River uplift, contains sedimentary fragments which indicate that the Precambrian basement in the core of the Wind River uplift was

subaerially exposed (figs. 169d, 170d). On the northeast side of the uplift, the Fort Union Formation was deposited on the gently dipping backlimb of the Wind River Mountains in angular unconformity with beds as old as Campanian. This unconformity suggests that the Derby to Winkleman line of folding (section 8.6) had been developed by this time, with the Precambrian basement thrust to the southwest, up the gentle dip slope of the Wind River Mountains (fig. 169d).

Subsidence of the stable craton continued along the axis of the Wind River basin during Paleocene time, and the Owl Creek Mountains were uplifted in the center of this downwarp. By the end of Paleocene, the Owl Creek Mountains had been uplifted 9,000 feet (2,700 m), and the Wind River basin downwarped 10,500 feet (3,200 m; Keefer, 1965; fig. 161). Left-lateral offset along the west-trending North Owl Creek fault (section 9.5), which probably exceeds two and one-half miles (4 km), occurred primarily in the late Paleocene as the initial shortening across the uplift developed.

Continued downwarp of the foreland, north and east of the Owl Creek uplift, spread deposition of the Paleocene Fort Union Formation throughout the Bighorn and Powder River basins. The latter two basins were probably quickly separated by initial uplift of the Bighorn Mountains. Paleocene sediments are found to be involved in tightly

folded synclines around the western flank of the Bighorn basin (fig. 90). The near sea level conditions in the northern area are demonstrated by the presence of large volumes of coal deposits in the northern Bighorn basin (southern Montana) and across the northern end of the Powder River basin. Development of the major anticlines around the flanks of the Bighorn basin had begun by this time, with compartmental deformation along such features as the Tensleep fault (section 8.4), Florence Pass lineament, the Bonanza-Zeisman trend (8.4), and along the south flank of Rattlesnake Mountain anticline (section 8.52). This allowed changes in the directions of asymmetry of the thrust and fold-thrust trends across these east- and northeast-trending features.

10.66 End of early Eocene

Lowermost Eocene beds are present in the subsurface beneath major thrust faults (i. e. Casper arch thrust) indicating that deformation in the region continued into early Eocene (fig. 169e). Deformation of the Wind River Mountains also must have continued into early Eocene with continued downwarp of the northeast flank. Deformation also continued along the Wind River basin/Owl Creek uplift, with cumulative uplift exceeding 15,000 feet (4,500 m) and over 12,000 feet (3,600 m) of downwarp.

10.67 Middle Eocene

Undeformed middle Eocene age sedimentary rocks unconformably overly Paleocene and older rocks around the margins of most foreland basins, indicating that most of the foreland deformation had ceased by this time. Middle (?) Eocene rocks also unconformably overly the thrusted southwest margin of the Wind River Mountains.

In the northwest Wind River basin, early (?) middle Eocene rocks occur in both the hanging wall and footwall of the "out-of-the-basin" Wind Ridge thrust (section 6.33), which was generated by final stages of deformation along the southwest flank of the Owl Creek uplift. This final adjustment brought the total displacement across the southern margin of the Owl Creek Mountains to over 33,000 feet (10,000 m), with uplift accounting for slightly more than half of the relief.

General quiescence returned to the foreland area at approximately middle Eocene, as shown by the deposition of organic-rich oil shales of the Green River Formation (Green River, Uinta, and Washakie basins) and Tatman Formation (Bighorn basin). The area bounded by Yellowstone Park and the Wind River and Owl Creek Mountains, and Bighorn basin, was covered with middle Eocene and younger volcanics and volcanoclastics, which have subsequently been eroded into the Absaroka Mountains (figs. 169f, 170f).

North of the Owl Creek Mountains, middle Eocene rocks are angularly unconformable on tightly folded Paleocene rocks along the west margin of the Bighorn basin. Northward, along the east flank of the Beartooth Mountains, rocks of the same age are dipping up to 40 degrees eastward into the Bighorn basin. Middle Eocene rocks also dip eastward away from the Bighorn Mountains (into the Powder River basin), indicating that the last, and minor, stages of deformation were post-middle Eocene (fig. 170f).

10.7 Summary

The Laramide orogeny was controlled by the direction and rate of collision between the North American and Farallon plates along the western margin of North America during the period 80-40 m. y. ago. The N40-50E direction of collision resulted in the formation of primary fold-thrust structures oriented northwest-southeast.

The initial deformation of the previously stable craton apparently began with crustal downwarp, at least in the area of the Owl Creek Mountains. Initially, downwarping was the dominant direction of crustal movement, but by the end of the Laramide, the component of uplift finally became dominant.

This crustal downwarp resulted in Laramide basins accompanied by the development of compressive stresses in

the upper portion of the Precambrian basement, as a result of flattening against the curvature of the Earth's surface. These compressive stresses forced "flakes" of basement rock upward into the overlying sedimentary section, along a conjugate set of low angle reverse faults. The resulting structures are the typical Laramide anticlinal folds displayed as flank structures around the margins of Laramide basins.

Primary Laramide structural features trend generally northwest, with subordinate trends of northeast, east, and north superimposed across the northwest grain. The superposition of these four structural orientations results in a block-like pattern of faults and folds. Basin-flank anticlines trend parallel, or subparallel, to the adjacent mountain uplifts. Many individual anticlines display a blunt, plunging end, which is controlled by steep, northeast- or east-trending compartmental faults.

The sequence of deformation of the foreland has been shown to have progressed across the foreland along a "tectonic front". This "front" began at the western margin of the foreland (Moxa arch) in Campanian time and formed the Wind River Mountain uplift (primarily) in Maestrichtian time, as indicated by the angular unconformity at the base of the Paleocene rocks on the northeast dip slope. The Owl Creek Mountains were uplifted primarily during the Paleocene and early Eocene. Further to the north, the

Bighorn and Beartooth Mountains were uplifted in early Eocene, with final movements occurring post-middle Eocene.

11.0 FINAL CONCLUSIONS

The following statements represent conclusions drawn from all my observations, and are presented in the order in which they were developed in the dissertation.

11.1 Plate Tectonic Setting

The plate tectonic setting of Western North America during the Laramide orogeny can be compared to the present day subduction zone along the Chile-Peru trench, and the Andean mountain belt (section 4.31). The direction of South American and Pacific plate convergence and the earthquake fault plane solutions are in agreement with eastwardly directed compression (section 4.5).

The direction of collision (N40E) between the North American and Farallon plates during the period from 80-40 m.a. represents the direction of maximum compressive stress during the Laramide orogeny. There is no apparent change in the direction of collision during the Laramide orogeny which would explain a shift to a north-south direction of compression, as envisioned by some workers.

The greatly increased rate of convergence at the onset of the Laramide orogeny resulted in a flattening of the subduction zone (section 4.32), which shifted the area of high heat flow hundreds of miles eastward under the crust of the Wyoming foreland. Displacement of the high

heat flow under the foreland resulted in a thermally weakened crust which yielded along low angle reverse faults when subjected to compressive forces. The major crustal structures which developed during the period of rapid convergence indicate that the direction of collision was the direction of compression (section 4.31). Therefore, the Wyoming foreland was under compression which acted along a line trending about N40E during the Laramide orogeny. Data derived from mapping small scale structures in the field (table 3) supports this conclusion.

Four principal orientations of foreland structures developed during the Laramide orogeny (section 3.32). These are: a) northwest, b) north-south, c) northeast, and d) east-west. Primary major foreland structures (i.e. Wind River, Bighorn, and Beartooth Mountains, etc.) developed at right angles to the maximum compressive stress, and thus trend northwest.

11.2 Basement Rocks

Data presented in section 5.11 demonstrate that the Precambrian basement of the Wyoming foreland is heterogeneous with respect to rock types and fabric orientation on the scale of individual outcrops (section 5.12). Anisotropies in the Precambrian basement complex do not appear to have controlled the location or orientation of the

primary, northwest-trending, Laramide structures (section 5.12). However, Precambrian age zones of weakness in the basement do control northeast and east-trending faults which segment the northwest and north-south trends. These faults are referred to as compartmental faults (section 8.0), and corners form at intersections of the northwest trends with the east and northeast trends (section 8.5).

Geometries observed on the upper surface of the basement are: a) horizontal planar, b) dipping planar, c) anticlinal curvature on upthrown fault blocks, and d) synclinal curvature on downthrown fault blocks (section 5.4). Folding of the upper basement surface (section 5.31) may have been accomplished by any or all of several mechanisms, including a) cataclastic deformation, b) microfracturing, d) rigid-body rotation, and e) flexural slip (section 5.32). Flexural slip may have taken place on remnant bedding surfaces, zones of metamorphic fabric, or along fractures which may have originated as relict sheeting joints or as sub-horizontal extension fractures (section 5.32).

There is a consistent relationship between the strike and dip of faults in the foreland, as follows (section 5.51): a) faults which strike to the northwest, dip at angles of 20 to 45 degrees, b) faults which strike north-northwest to north-northeast, dip at angles of 45 to 60 degrees, c) faults which strike east to east-northeast,

dip at angles of 60 to 80 degrees, and d) faults which strike northeast are generally nearly vertical. The northwest-striking, low angle reverse faults may be compared directly to Hafner's (1951) solution for horizontal compressive stresses (section 5.22).

11.3 Sedimentary Section

The Precambrian basement has acted as the dominant member and "forcing block" in the development of foreland structures (section 6.1). The upper basement surface may be planar, or folded into anticlinal and synclinal shapes in the cores of these structures (section 5.51). The form of Laramide structures in the sedimentary section was controlled by three factors which interacted during the time of deformation (section 6.21). These are: 1) the upward movement of a basement forcing block, 2) the deformational mechanisms active in the sedimentary section (which were controlled by lithology, depth of burial, and pore pressure), and 3) arrangement of "mechanical packages" (which are comprised of the same, or different lithologies). The preferred deformational mechanism of each package (section 6.22) was determined by the dominant lithology. Adjustments in fold shape were accomplished by detachments in the shales and shaly limestones.

Compressive loading of the sedimentary section caused flexural folding by bedding plane slip, which created parallel folds (section 6.31). A distinctive characteristic of parallel folds is the development of basal detachments beneath anticlines and upper detachments above synclines (section 6.32).

Multiple detachments (section 6.32) allowed anticlines to tighten downward, detach and pass into more open folds at depth, often changing directions of asymmetry as they did so. The possibility of multiple changes in direction of asymmetry within a single foreland fold urges caution when comparing directions of asymmetry between different structures. Any such comparison should be made at the same stratigraphic level.

Bedding-plane slip was translated into reverse faulting, which cut up section in the direction of tectonic transport. These faults died out upward by fault-fold interchange (section 6.32). Structures which resulted from this process are called: a) backlimb folds, b) cross-crestal structures, and c) rabbit-ear folds (section 6.33).

Duplication (or contraction) of strata (rather than extension or thinning), on the steep limb of an anticline suggests that horizontal compression, rather than vertical uplift is responsible for "crowd" structures. For example, the scale and location of the Windrock anticline

(section 6.32) suggests that structures such as this represent large-scale backlimb folds which were generated by volu-metric crowding which resulted from compressional folding of foreland basins.

11.4 Structural Styles of the Wyoming Foreland

There is no single uplift model which applies throughout the Wyoming foreland (section 7.5). The evidence presented in this study clearly leads to the conclusion that the orientation of a structural trend determines which structural model applies. Features displaying the basic characteristics of fold-thrust uplifts (section 7.24) are the major northwest-trending structures of the foreland. Low angle thrust uplifts (section 7.23) also trend generally northwest but may be at slight angles to the trends of the fold-thrusts. Those features which display the basic characteristics of the drape fold (section 7.21) and upthrust structures (section 7.22) are the east and northeast trending structures on the foreland which are parallel or sub-parallel to the regional direction of compression.

The fold-thrust model of Berg (1962) exhibits a dual fault zone and rotated flank (section 7.24). Several examples representing stages in the sequential development of fold-thrusts have been documented in this study from

both surface and subsurface (section 7.44). In addition, the recognition of subsidiary folds on the hanging walls of some fold-thrust structures has been added as a modification of Berg's original model (section 7.44).

Recognition of examples of low angle thrust uplift structures is dependent upon properly positioned subsurface well control (section 7.43). This is necessary to establish the presence, or absence, of the dual fault zone and rotated flank system.

Theoretical and experimental data support the viability of the drape fold and upthrust models (sections 5.22; 7.22). However, maintaining structural balance is a problem in the application of these two models to foreland structures. The drape fold is one stage in the sequential development of the upthrust geometry (section 7.21). Determination of the location and depth of penetration of extensional normal faults may be the key to separating upthrust structures from those which developed at right angles to horizontal compressive stresses (section 7.42).

Northwest-trending structures which have been interpreted as drape folds (section 7.33; i.e. Rattlesnake Mountain anticline, Stearns, 1971), or upthrusts (section 7.31; i.e. Soda Lake area, Colorado, Osterwald, 1961), are structurally out of balance. The imbalance between the sedimentary section and the upper basement surface results from an absence of extensional mechanisms on the upthrown

block (section 7.41). However, interpretations of these areas using a thrust or fold-thrust model are easily balanced (section 7.5).

East-west trending major foreland structures were formed on compartmental faults (section 8.0) at oblique angles to the direction of maximum compressive stress. This orientation permitted lateral slip on the compartmental faults, in addition to vertical uplift (section 9.5).

11.5 Compartmental Deformation

The interpretation of simple lateral offset of strucral trends along northeast and east-west trending faults may lead to a variety of ideas (section 8.2) regarding the regional structural pattern. However, the concept of compartmental deformation should alert investigators to the possibility that structural trends, intersected by compartmental faults, may be: a) offset, b) develop an opposed sense of asymmetry, or c) be completely replaced by some other structural style across the fault, while maintaining overall structural balance (section 8.3).

Compartmental faults are not always exposed at the present level of erosion. "Mismatch" of structural features across a linear trend, as well as abrupt plunge into it, are perhaps the most significant clues to recognition

of the presence of buried compartmental faults (section 8.4). Of primary interest in the interpretation of the foreland structural style is the recognition that significant magnitude of strike slip motion (combined with reverse dip slip) may have taken place along an east, or northeast-trending compartmental fault, with no surface expression, other than the development of a drape fold (section 8.51).

Other compartmental faults crop out as upthrusts (which have reverse-oblique slip) at the lower hinge of the associated drape fold (section 8.52). The geometry of these compartmental faults is in agreement with results of physical models of the "corner" problem (section 8.51). Examples of basement "corners" exposed in the foreland (section 8.53) serve to explain the development of the blunt plunging ends of many foreland anticlines, which display "instant" plunge across the steeply dipping compartmental fault (section 8.51).

11.6 Crustal Shortening

Structural balance in the Wyoming foreland is accomplished by: a) en echelon faults, b) en echelon folds, c) lateral fault-fold interchanges, and d) compartmental deformation (section 9.2). I have concluded that crustal shortening was pervasive, and uniform across the foreland.

Measurements for total shortening must be made along lines parallel to the northeast direction of maximum compressive stress (lines A, B, C of fig. 149; section 9.1).

Several methods exist which may be used to estimate the crustal shortening of individual structures (section 9.3). Most of these methods are related to: a) the horizontal heave component of reverse faults, and b) the vertical height of folds. Good agreement between estimations and measurements of crustal shortening has been demonstrated in this study.

The values of crustal shortening determined in this study (section 9.4) probably represent realistic measures of the total shortening involved in the deformation of the foreland during the Laramide orogeny. The application of the minimum displacement concept suggests that the values obtained in section 9.4 (26-29 miles; 41-46 km) should be considered minimum values. I believe the figure of 15% strain may represent a maximum value for the foreland.

Potential for large-scale lateral movements (section 9.5) existed during the Laramide orogeny, as attested to by the values of crustal shortening which have been determined. However, it has been shown that most of the lateral movements were distributed along compartmental faults and shared by individual anticlinal structures (section 9.5), rather than accumulating into large displacements on single strike slip faults. This is taken as indicating

that the foreland was not deformed by a major wrench fault system, but rather by a fold and thrust system (section 9.5).

The total amount of crustal shortening in the foreland is approximately 30 miles (48 km; section 9.6). This figure should serve as a "baseline" value in future interpretations.

11.7 Structural Synthesis

"Out-of-the-basin" vergence of basement-involved Laramide folds, is an indication that these structures are the result of the combined effects of a regional compressive stress, directed northeast-southwest, and local compressive stresses (section 10.4). The regional compressive stresses were the result of the convergence of the North American and Farallon plates along a N40E direction during the period of 80-40 m. y. a. (section 10.2).

The local stresses were generated by the basinal downwarping of the upper surface of the Precambrian basement (in opposition to the earth's curvature), as demonstrated by the bent beam model (section 10.4). The local anticlinal structures which parallel the flanks of the Laramide basins are cored by "flakes" of Precambrian basement (section 10.4). The flakes were forced upward into the overlying sedimentary section along low angle

reverse faults which form a northeast- and southwest-dipping conjugate set.

Deformation during the Laramide orogeny moved across the foreland as a "tectonic front" which began to deform the western margin of the region during Campanian time (section 10.62). Moving northeastward, deformation of the Wind River Mountains reached a climax during the Maestrichtian (section 10.63). During the same time period, the remainder of the foreland to the northeast of the Wind River uplift continued as a stable site of deposition along an axis which passed through the location of the Owl Creek Mountains (section 10.64).

Deformation progressed to the northeast of the Wind River Mountains in Paleocene with the uplift of the Owl Creek Mountains from the site of the earlier crustal downwarp (section 10.65). Paleocene rocks were spread to the northeast of the Owl Creek Mountains and may have been continuous across the site of the Bighorn Mountains, into the Powder River basin. Deformation in early Eocene in the Bighorn region is clearly demonstrated by the tightly folded Paleocene rocks along the western margin of the basin (section 10.66).

These folds are overlain unconformably by early or middle Eocene rocks. The post-middle Eocene age of the final pulse of the Laramide orogeny (section 10.67) is indicated by the basinward tilting of these Eocene age

rocks along the east flank of the Beartooth and Bighorn Mountains, and thrusting of middle Eocene age rocks along the Wind Ridge thrust in the northwest Wind River basin (section 6.33).

APPENDICES

APPENDIX A: GEOMETRY OF RICH-MODEL "RAMP ANTICLINES"

Rich (1934) described the control which stratigraphy has on the development of thrust geometries in the Appalachian overthrust belt (fig. A-1). In that province, thrust fault geometry is such that the fault plane is subparallel to bedding in incompetent units (shales), and cuts upward in the direction of tectonic transport across competent units (sandstones, limestones, dolomites). The change from gentle to steep dip upward is referred to as a ramp (fig. A-2a).

The angle between the bedding surfaces and the fault plane is called the cut-off angle (Brown, 1982). This cut-off angle generally does not change during deformation. When the fault plane flattens again in higher sedimentary layers, the cut-off angle will be rotated with the rock layers (fig. A-2b). The "ramp" portion of the fault plane generally dips in the direction of regional structural dip. The sedimentary layers, which are originally over the lower, bedding-parallel portion of the fault, will remain parallel to the fault plane as they are thrust up the ramp (fig. A2-b). This creates structural dip which is parallel to the ramp. Preservation of the cut-off angle, as the fault flattens at the top of the ramp, forces the sedimentary section to dip into the flattened fault plane ("critical dip"). Together, the regional structural dip (paral-

lel to the ramp) and the "critical dip" result in an anticlinal reversal called the ramp anticline. The process will be repeated for each ramp which is developed along the plane of the thrust (fig. A-3a). Therefore, a "ramp anticline" will be developed for each ramp in the fault plane (fig. A-3b).

The concept of ramps and associated ramp anticlines can be applied to the foreland because it is a geometric principle, not just related to compressional thrust tectonics. This application is discussed in the development of "crowd structures" of the back-limb and cross-crestal types, in section 6.33.

If a basement-involved reverse fault in the foreland has a "ramp" geometry (fig. A-4a), the same ramp anticline geometry would develop on the upper basement surface (fig. A-4b). The basement rock which occupies the wedge of the cut-off angle would not decrease in volume during deformation, but would rotate to conform to the fault plane. If the basement rock is not capable of deforming by flexural slip, some other mechanism (probably brittle) is required to force the rocks to conform to the flattened fault shape (fig. A-4b). The curved shape of the upper basement surface developed under these conditions is an induced geometry. A possible example of this may be exposed in Clarks Fork River canyon, and is discussed in section 5.41 (fig. 22).

The ramp geometry is also responsible for another structural feature referred to as the back-thrust. Morse (1977) created physical rock models of ramp anticlines which had "pre-cut" ramps, over which the rock layers were forced (fig. A-5b). Not only did the classic Rich-model ramp anticline develop (fig. A-5b; as described above), but also a series of thrust faults which dipped antithetically to the ramp. These thrusts developed at the lower hinge of the ramp and migrated up the ramp with increasing displacement. The relationship of ramp geometry to the development of back-thrusts is now applied to structural interpretations of "thin-skin" thrust belts world wide.

It is possible that the paired "thrust and back-thrust" geometry observed in the foreland may originate in a similar fashion, since this again is a geometric relationship. Such "thrust and back-thrust" occurrences are described in text sections 5.51, 7.23 and 9.5. It is therefore possible to interpret foreland basement-involved faults as flattening with depth, if the back-thrusts are present.

APPENDIX B: CHARACTERISTICS OF PARALLEL FOLDING

Parallel or "concentric" folds have characteristic features which are important in the interpretation of foreland structures in Wyoming. The purpose of this appendix is to describe these features as background for discussions in the text.

Folds in the foreland are typically asymmetric with inclined axial planes (fig. B-1). In cross section, the axial trace of an asymmetric fold separates the gently dipping back limb from the steeply dipping forelimb. A fold is described as being asymmetric (or verging) in the direction toward which the forelimb faces (to the right, in fig. B-1). The axial line (A. L.) is the intersection of the axial plane and any bedding surface. The orientation of the axial line in space defines the plunge of the fold. The crestal line is at the highest elevation on any bedding surface. It is often referred to as the "axis", but should not be confused with the axial line.

Parallel folds are formed primarily by the mechanism of flexural slip (fig. B-2) in which differential slip occurs along bedding planes, transferring volume from the synclinal trough towards the anticlinal crest. The relative magnitude of differential slip is indicated by the

overlap of the layers and the offset of the reference line in figure B-2.

Parallel folds tighten downward along the anticlinal axial trace and upwards along the synclinal axial trace. The tightening is described by the degree of folding (Fleuty, 1964; fig. B-3). The "degree of folding" is useful for comparing different folds, but it also applies to the variation in the shape of a single fold throughout the stratigraphic section. The downward tightening of anticlines (and upward tightening of synclines) implies that the folded sequence must be detached from the layers above and below it (fig. B-4; Dahlstrom, 1969a, 1970). Detachments which form beneath anticlines are called the basal detachment and those above synclines are called upper detachments. The development of two sets of detachments can be described as the formation of multiple detachments (fig. B-5; Dahlstrom, 1970).

Dip profiles through different levels of parallel folds (fig. B-6) reflect the downward tightening of anticlines (upward tightening of synclines) and can be used to indicate the structural level of the profile within the folded package. Broad anticlines and tight synclines indicate a high level, while the reverse indicates a deep level. Profiles of adjacent anticlinal and synclinal folds, with the same degree of folding at the same struc-

tural elevation, indicate a position midway through the fold.

Parallel anticlines can be divided into three zones, based on structural style (fig. B-7). These are: 1) an upper level of extensional deformation, commonly normal faulting, 2) a central level, called the "concentric zone" where there is neither strong extension nor compression, and 3) a lower level of compressional structures created by volumetric adjustments resulting from tightening of the fold. This three-fold zonation is recognized when the fold is buried to considerable depths. In most cases the normal faulting of the upper level extends upward to (or near) the surface. There are instances however, where the normal faulting does not appear to be well developed, suggesting that depth of burial may have overcome the effect of extensional stresses in the upper level.

Three general types of compressional structures are common at the lower zone (fig. B-8). These are: 1) crenulations (multiple folds), 2) complementary thrusts, and 3) decollement, or detachment on bedding planes. These same features may be observed in the core of a parallel anticline or the trough of a parallel syncline.

Differential movement away from the axial trace of the syncline results in development of drag folds on the flanks of anticline/syncline pairs (fig. B-9a). These drag

folds verge in the direction of transport, which gives them the form described as "S"- and "Z"-folds (fig. B-10).

Rock deformation experiments, which form asymmetric folds (Casarta, 1980), demonstrate that differential simple shear occurs on both flanks of an anticline. The greatest shear (and hence greatest rotation of reference lines) takes place on the forelimb of the structure (fig. B-9b).

Volumetric, bed-length adjustments in synclines are described as out-of-the-syncline movements (fig. B-11; Gair, 1950). Some of these adjustments take the form of reverse faults which sole out into bedding planes on the flank of the syncline. Out-of-the-syncline reverse faults die out downward, as the excess volume problem is transferred toward the anticline. Since all the movements are away from the synclinal trough, the axial plane of the syncline represents a null surface, across which material is not transferred.

APPENDIX C: TECHNIQUE OF STRUCTURAL BALANCING

The technique of "structural balancing" has been applied to areas of overthrust tectonics for many years (Dahlstrom, 1969b). The term "structural balancing", as used in this discussion, refers to conservation of rock volume during the process of deformation. Rock is neither created nor destroyed during deformation, therefore all cross sections should be susceptible to material balance.

The process of structural balancing is in reality a three dimensional (volume) problem. However, if it can be established that there is little or no material movement in or out of the plane of the cross section, then "balancing" is reduced to a two dimensional problem (cross sectional area). Furthermore, if it can also be established that thicknesses do not change during deformation, then "balancing" is further reduced to determining the consistency of lengths of lines, representing bedding surfaces. The idea of consistent bed lengths is what usually comes to mind when structural balance is mentioned.

The two dimensional approach is used in most areas of the foreland province, because experience has shown that cross sections drawn across the highest structural position of an anticline, and perpendicular to the plunge direction, are most likely to have maintained constant cross-sectional areas.

Figure C-1 demonstrates the concept of "consistency of bed thickness." In this example, the original thicknesses, whether constant ("layer cake"; fig. C-1a) or variable (stratigraphic wedge; fig. C-1b), are maintained during deformation. Therefore, original bed lengths also remain the same.

Figure C-2 illustrates the case of original thicknesses which do not remain consistent during deformation. In the case of shale flowage (fig. C-2a), the thickness increases in one area, and must therefore decrease in some other area. The bed length must change, for the area to remain constant. In the case of tectonic thinning (fig. C-2b), the original length of the upper bedding surface is increased to accommodate the shape of the fold. Therefore the stratigraphic unit must be thinned in order to maintain constant area.

In the Wyoming foreland, flowage of the rocks is not a major factor. Those areas which have been cited as having shale flowage are not unequivocal; the rocks present appear to have been faulted, but ductile flow structures have not been recognized. By far the most critical of the volumetric changes in the foreland is that of tectonic thinning. The drape fold and upthrust structures have been shown to require bed length adjustments such as this in order to preserve rock volume and to maintain structural balance.

The method of measuring bed length (to check for structural balance) is fairly straightforward. The most consistent measurements are made using synclinal axial traces as reference lines. These traces are chosen as reference lines because, in flexural slip folding, displacement is away from the synclinal axis, toward the anticlinal axis. Thus, material is less likely to move across the synclinal axial trace.

If the folds are symmetrical (fig. C-3a,b), the axial traces are both vertical, and perpendicular to bedding at the trough of the syncline and the crest of the anticline. However, if an anticlinal fold is asymmetric (axial trace is inclined), then the synclinal axial traces are inclined (fig. C-3c), to account for the differential slip along bedding planes (APPENDIX B). The lengths between the synclinal reference lines remain the same in all cases (fig. C-3a,b and C-3c), demonstrating that all of the stratigraphic units are in structural balance.

A problem may arise when an anticline has a long back limb which increases the distance to the adjacent syncline (or when the backlimb syncline is not developed; fig. C-4a). This raises the question of what should be used for a reference line on the backlimb. Consider the previous discussion of the asymmetric folds with the rotated axial traces (fig. C-3c). It can be seen that an arbitrary reference line drawn parallel to the inclined synclinal

axial trace, but located closer to the crest of the anticline, will result in similar, but shorter, measured bed lengths. These bed lengths will remain consistent between the reference line (drawn at the asymmetric syncline) and the arbitrary reference line (drawn on the backlimb of the anticline). Therefore, when the back limb of the anticline is very long (fig. C-4a), and it is impractical to draw the cross section to the adjacent syncline, it will suffice to construct an arbitrary reference line (fig. C-4b) parallel to the axial trace of the syncline (dip of the axial plane can be estimated; see section 9.3; arbitrary reference lines can also be approximated by drawing it parallel to the axial trace of the adjacent anticline).

When the bedding surfaces of a selected number of stratigraphic units (including the upper basement surface) are measured, a comparison of the measurements may be made. The differences in lengths of the various units are proportional to the volume of rock which has not been accounted for in the cross section. If a structural imbalance is present in the cross section, it is necessary to review the entire structural interpretation in order to determine what has led to the volume discrepancy.

APPENDIX D: DEPTH-TO-DETACHMENT CALCULATION

Parallel folding (Appendix B) requires the development of a basal detachment (Dahlstrom, 1970) under anticlines (fig. D-1). Therefore, it is desirable to be able to calculate the actual depth to the detachment for individual folds. Determination of the actual depth is important for several reasons. These are: 1) proper interpretation of structural cross sections, 2) assistance in locating zones of repetition for comparison to electric well logs, 3) prediction of depths of structural complications which might be encountered in drilling, and 4) determination of whether particular stratigraphic horizons (such as hydrocarbon reservoir rocks) are above a particular detachment horizon, and involved in the anticlinal closure.

Various methods for calculating the depth to the basal detachment have been published (Duska, 1961; De Sitter, 1964; Dahlstrom, 1969a). My preferred method is based on the concept that the depth to the basal detachment may be calculated from values of certain areas and bed lengths which may be obtained directly from cross sections.

Parameters (fig. D-1) which are necessary for the calculation are: 1) the arc length of the fold, 2) the chord length of the arc, and 3) the area between the arc and chord. The arc ac (fig. D-2) represents the original

unfolded length of the bedding surface. The arc length (ac) is measured between the axial traces of the adjacent synclines. The chord acrepresents the present map separation of the ends of the arc. (A) represents the area of rock which was transferred to (A') to create the fold. Area (A') can be measured on the cross section. The value (S) is obtained by subtracting the chord length from the arc length, and represents the amount of horizontal shortening required to create the anticline. The depth to the basal detachment (D) is also the vertical dimension of area A, and can be determined by simply dividing area A by the horizontal shortening (S). The depth-to-detachment (D) is then plotted perpendicular to the chord, and measured down from the mid-point of the chord.

Calculations using this technique have been useful in determining depth of involvement of various folds, some involving only the sedimentary section. Similar calculations have been made for some of the larger foreland anticlines which have the Precambrian basement faulted up into the core of the fold. The results of these calculations indicate that these folds are detached within the Precambrian basement, and suggest that the low angle reverse faults in the cores of the structures flatten downward.

LITERATURE CITED

Allison, M. Lee, 1983, Deformation styles along the Tensleep fault, Bighorn Basin, Wyoming, in Boberg, W. W., ed., Geology of the Bighorn Basin, 34th Annual Field Conference Guidebook: Wyoming Geological Association, p. 63-75.

Armstrong, Frank C. and Oriel, S. S., 1965, Tectonic development of Idaho-Wyoming thrust belt: American Association of Petroleum Geologists Bulletin, v. 49, no. 11, p. 1847-1866.

Armstrong, R. L., 1968, Sevier orogenic belt in Nevada and Utah: Geological Society of America Bulletin, v. 79, no. 4, p. 429-458.

Asquith, D. O., 1975, Petroleum potential of deeper Lewis and Mesaverde Sandstone in the Red Desert, Washakie and Sand Wash Basins, Wyoming and Colorado, in Bolyard, D. W., ed., Symposium on Deep Drilling Frontiers in the Central Rocky Mountains: Rocky Mountain Association of Geologists, p. 159-162.

Atwater, Tanya, 1970, Implication of plate tectonics for the Cenozoic tectonic evolution of western North America: Geological Society of America Bulletin, v. 81, no. 12, p. 3513-3536.

Bally, A. W., Gordy, P. L., and Stewart, G. A., 1966, Structure, seismic data, and orogenic evolution of southern Canadian Rocky Mountains: Canadian Petroleum Geologists Bulletin, v. 14, p. 337-381.

Barazangi, M., and Isacks, B. L., 1979, Subduction of the Nazca plate beneath Peru: Evidence from spatial distribution of earthquakes: Geophysics, J. R. Astron. Soc., v. 57, p. 537-555.

Beckwith, R. H., 1938, Structure of the southwest margin of the Laramie basin, Wyoming: Geological Society of America Bulletin, v. 49, p. 1515-1544.

_____ 1941, Structure of the Elk Mountain district, Carbon County, Wyoming: Geological Society of America Bulletin, v. 52, p. 1445-1486.

_____ 1942, Structure of the upper Laramie River valley, Colorado-Wyoming: Geological Society of America Bulletin, V. 53, p. 1491-1532.

Bell, W. G., 1956, Tectonic setting of Happy Springs and nearby structures in the Sweetwater Uplift area, central Wyoming, in Geological Record, Rocky Mountain Section: American Association of Petroleum Geologists.

Berg, R. R., 1961, Laramide tectonics of the Wind River Mountains; in Symposium on Late Cretaceous rocks: Wyoming Geological Association, 16th Annual Field Conference Guidebook, p. 70-80.

_____ 1962a, Subsurface interpretation of Golden fault at Soda Lakes, Jefferson County, Colorado: American Association of Petroleum Geologists Bulletin, v. 46, p. 704-707.

_____ 1962b, Mountain flank thrusting in Rocky Mountain foreland, Wyoming and Colorado: American Association of Petroleum Geologists Bulletin, v. 46, no. 11, p. 2019-2032.

Blackstone, D. L., Jr., 1940, Structure of the Pryor Mountains, Montana: Journal of Geology, v. 48, p. 590-618.

_____ 1947, Structural relationships of the Pryor Mountains; in Wyoming Geological Association Guidebook: Bighorn Basin Field Conference, p. 182-188.

_____ 1948, Structural relationships of northeast margin of the Laramie Mountains [abstract]: Geological Society of America Bulletin, v. 59, p. 1397-1398.

_____ 1949, Structural pattern of the Powder River basin, Wyoming; in Wyoming Geological Association Guidebook: 4th Annual Field Conference, p. 35-36.

_____ 1951, An essay on development of structural geology in Wyoming; in Wyoming Geological Association Guidebook; 6th Annual Field Conference, p. 15-18.

_____ 1956, Introduction to the tectonics of the Rocky Mountains; in Geological Record: American Association of Petroleum Geologists, Rocky Mountain Section, p. 3-19.

_____ 1963, Development of geologic structure in central Rocky Mountains; in Memoir 2, Backbone of the Americas, a Symposium: American Association of Petroleum Geologists, p. 160-179.

_____ 1970, Structural geology of the Rex Lake quadrangle, Laramie basin, Wyoming: Geological Survey of Wyoming Preliminary Report, no. 11, 17 p.

_____ 1977, The overthrust belt salient of the Cordilleran fold belt--western Wyoming, southeastern Idaho, northeastern Utah, in Heisey, E. L., Lawson, Don E., Norwood, Earl R., Wach, Philip H., and Hale, Lyle A., eds., Rocky Mountain Thrust Belt Geology and Resources, 29th Annual Field Conference: Wyoming Geological Association, in conjunction with Montana Geological Society and Utah Geological Society, p. 385-390.

_____ 1983, Laramide compressional tectonics, southeastern Wyoming: Contributions to Geology; v. 22, no. 1, p. 1-38.

Bonini, W. E., and Kinard, R. E., 1983, Gravity anomalies along the Beartooth front, Montana; in Boberg, W. W., ed., Geology of the Bighorn Basin: Wyoming Geological Association, 34th Annual Field Conference Guidebook, p. 89-95.

Borg, I., and Handin, J., 1966, Experimental deformation of crystalline rocks: Tectonophysics, v. 3, p. 249-368.

Boyer, S. E., and Elliott, David, 1982, Thrust Systems: American Association of Petroleum Geologists Bulletin; v. 66, no. 9, p. 1196-1230.

Brock, W. G., and Nicolaysen, Jerry, 1975, Geology of the Brady unit, Sweetwater County, Wyoming: in Bolyard, D. W., ed., Symposium on deep drilling frontiers in the Central Rocky Mountains; Rocky Mountain Association of Geologists, p. 225-238.

Brown, W. G., 1975, Casper Mountain area, Wyoming--a model of Laramide deformation [abstract]: American Association of Petroleum Geologists Bulletin, v. 59, no. 5, p. 906.

_____ 1981, Surface and subsurface examples of the Wyoming foreland as evidence of a regional compressional origin for the Laramide orogeny [abstract]: Contributions to Geology, v. 19, no. 2, p. 175-177.

_____ 1982, New tricks for old dogs--a shortcourse in structural geology: American Association of Petroleum Geologists, Southwest Sectional Meeting, 79 p.

---------- 1983, Sequential development of the fold-thrust model of foreland deformation in Lowell, J. D., ed., Rocky Mountain Foreland Basins and Uplifts: Rocky Mountain Association of Geologists, p. 57-64.

---------- 1984a, Rattlesnake Mountain Anticline--a reverse fault interpretation: The Mountain Geologist, v. 21, no. 2, p. 32-35.

---------- 1984b, Basement involved tectonics--foreland areas: American Association of Petroleum Geologists Continuing Education Course Note Series #26, 92 p.

_____ 1985, Overthrust faulting: in Course notes, Structural Geology School, American Association of Petroleum Geologists, 52 p.

_____ 1987, Laramide deformational style in the Wyoming foreland: in Perry, W. J. Jr., and Schmidt, C. J., eds., Interaction of Rocky Mountain foreland and Cordilleran thrust belt; [in press], Geological Society of America.

Bucher, W. H., 1920, The mechanical interpretation of joints: Journal of Geology, v. 28, p. 707-730.

Burchfiel, B. C. and Davis, G. A., 1975, Nature and controls of Cordilleran orogenesis, western United States--extensions of an earlier synthesis: American Journal of Science Bulletin, v. 275-A, p. 363-396.

---------- 1976, Compression and crustal shortening in Andean-type orogenesis: Nature, v. 260, p. 693-694.

Burke, Kevin and Dewey, J. F., 1976, Plume-generated triple junctions--key indicators in applying plate tectonics to old rocks: Journal of Geology, v. 81, p. 406-533.

Casarta, L. J., 1980, Effects of interlayer slip on multilayered folds: Unpublished Ms. Thesis, Texas A&M University, 100 p.

Chamberlin, R. T., 1925, The wedge theory of diastrophism: Journal of Geology, v. 33, p. 755-792.

_____ 1945, Basement control in Rocky Mountain deformation: American Journal of Science, v. 243-A, p. 98-116.

Chronic, B. John, McCallum, M. E., Ferris, C. S., Jr., and Egeler, D. H., 1969, Lower Paleozoic rocks in diatremes, southern Wyoming and northern Colorado: Geological Society of America Bulletin, v. 80, no. 1, p. 149-155.

Clark, Charles, 1978, West Poison Spider field, Natrona County, Wyoming: in Boyd, R. G., ed., Resources of the Wind River Basin: Wyoming Geological Association Guidebook 30th Annual Field Conference, p. 261-271.

Coney, P. J., 1978, Mesozoic-Cenozoic Cordilleran plate tectonics, in Smith, R. B. and Eaton, G. P., eds., Cenozoic Tectonics and Regional Geophysics of the Western Cordilleran: Geological Society of America Memoir 152, p. 33-50.

Cook, F. A., Albaugh, D. S., Brown, L. D., Kaufman, W., Oliver, J. E., and Hatcher, R. D., 1979 Thin-skinned tectonics in the crystalline southern Appalachians; COCORP seismic-reflection profiling of the Blue Ridge and Piedmont: Geology, v. 7, no. 12, p. 563-567.

Cook, R. A., and Stearns, D. W., 1975, Mechanisms of sandstone deformation: a study of the drape folded Weber Sandstone in Dinosaur National Monument, Colorado and Utah; in Bolyard, D. W., Deep Drilling Frontiers of the Central Rocky Mountains: Rocky Mountain Association of Geologists Symposium, p. 21-32.

Couples, Gary and Stearns, D. W., 1978, Analytical solutions applied to structures of the Rocky Mountain foreland on local and regional scales; in Matthews, V. III, ed., Laramide Folding Associated with Basement Block Faulting in the Western United States: Geological Society of America Memoir 151, p. 313-335.

Currie, J. B., Patnode, H. W., and Trump, R. P., 1962, Development of folds in sedimentary strata: Geological Society of American Bulletin, v. 73, no. 6.

Dahlstrom, C. D. A., 1969a, The upper detachment in concentric folding: Canadian Petroleum Geology Bulletin, v. 17, no. 3, p. 326-346.

---------- 1969b, Balanced cross sections: Canadian Journal of Earth Sciences, v. 6, no. 4, p. 743-757.

---------- 1970, Structural Geology in the eastern margin of the Canadian Rocky Mountains: Canadian Petroleum Geology Bulletin, v. 18, no. 3, p. 332-406.

Dallmus, K. F., 1958, Mechanics of basin evolution and its relation to the habitat of oil in the basin: American Association of Petroleum Geologist Habitat of Oil, p. 883-931.

Dana, J. E., 1895, Manual of Geology (4th. ed.): New York, 1078 p.

Darton, N. H., 1906a, Description of the Bald Mountain and Dayton, Wyoming Quadrangles: U. S. Geological Survey Folio No. 141, 15 p.

_____ 1906b, Geology of the Bighorn Mountains: U. S. Geological Survey Professional Paper No. 51, 129 p.

_____ 1906c, Description of the Cloud Peak and Ft. McKinney Quadrangles: U. S. Geological Survey Atlas Folio No. 142, 16 p.

De Chadenedes, J. Francois, 1975, Frontier deltas of the western Green River Basin, Wyoming, in Bolyard, D. W., ed., Symposium on Deep Drilling Frontiers of the Central Rocky Mountains: Rocky Mountain Association of Geologists, p. 149-157.

Demorest, M. H., 1941, Critical structural features of the Bighorn Mountains, Wyoming: Geological Society of America Bulletin, v. 52, p. 161-176.

Dennis, John G., 1967, International Tectonic Dictionary--English Terminology: American Association of Petroleum Geologists Memoir 7, 196 p.

De Sitter, L. U., 1964, Structural Geology: New York, London, and Toronto, McGraw-Hill, 551 p.

Dickinson, W. R., and Snyder, W. S., 1978, Plate tectonics of the Laramide orogeny; in Matthews, V. III, ed., Laramide folding associated with basement block faulting in the Western United States: Geological Society of America Memoir 151, p. 355-366.

Dockery, W. L, 1972, Pioneer Geologists of the American West: in Mallory, W. W., ed., Geological Atlas of the Rocky Mountain Region, United States of America: Rocky Mountain Association of Geologists, p. 13-22.

Donath, F. A. and Parker, R. B., 1964, Folds and folding: Geological Society of America Bulletin, v. 75, no. 1, p. 45-62.

Dunn, Sandra L. D., 1983, Timing of foreland and thrust belt deformation in an overlap area, Teton Pass, Idaho and Wyoming in Lowell, J. D., ed., Rocky Mountain Foreland Basins and Uplifts: Rocky Mountain Association of Geologists, p. 263-269.

Duska, L., 1961, Depth of basal shearing plane in cases of simple concentric folding: Journal of Alberta Society of Petroleum Geologists, v. 9, no. 1.

Eldridge, G. H., 1894, A geological reconnaissance in northern Wyoming: U. S. Geological Survey Bulletin, v. 119, 72 p.

Fanshawe, J. R., 1939, Structural geology of the Wind River Canyon area, Wyoming: American Association of Petroleum Geologists Bulletin, v. 23, p. 1439-1492.

_____, 1971, Structural evolution of the Bighorn basin in Renfro, Arthur R., ed., Symposium on Wyoming Tectonics and Their Economic Significance, 23rd Annual Field Conference: Wyoming Geological Association, p. 35-37.

Fleuty, M. J., 1964, The description of folds: Proceedings Geological Association England, v. 9, no. 1.

Foose, R. M., Wise, D. U., and Garbarini, G. S., 1961, Structural Geology of the Beartooth Mountains, Montana and Wyoming: Geological Society of America Bulletin, v. 72, no. 8, p. 1143-1172.

Gair, J. E., 1950, Some effects of deformation in the Central Appalachians: Geological Society of America Bulletin, v. 61, no. 8, p. 857-876.

Gingerich, Phillip D., 1983, Paleocene-Eocene faunal zones and a preliminary analysis of Laramide structure deformation in the Clarks Fork Basin, Wyoming, in Boberg, W. W., ed., Geology of the Bighorn Basin, 39th Annual Field Conference Guidebook: Wyoming Geological Association, p. 185-195.

Gooldy, P. L., 1947, Geology of the Beaver Creek-South Sheep Mountain area, Fremont County, Wyoming: Unpublished M. S. thesis, University of Wyoming.

Gries, Robbie, 1981, Oil and gas prospecting beneath the Precambrian of foreland thrust plates in the Rocky Mountains: Mountain Geologist, v. 18, p. 1-18.

_____ 1983a, Oil and gas prospecting beneath Precambrian of foreland thrust plates in the Rocky Mountains: American Association of Petroleum Geologists Bulletin, v. 67, no. 1, p. 1-26.

_____ 1983b, North-south compression of Rocky Mountain foreland structures, in Lowell, J. D., ed., Rocky Mountain Foreland Basins and Uplifts: Rocky Mountain Association of Geologists, p. 9-32.

Grose, L. T., 1972, Tectonics; in Mallory, W. W., ed., Geological Atlas of the Rocky Mountain Region, United States of America: Rocky Mountain Association of Geologists, p. 35-44.

Hafner, W., 1951, Stress distribution and faulting: Geological Society of America Bulletin, v. 62, p. 373-398.

Hamilton, Warren, and Meyer, W. B., 1966, Cenozoic tectonics of the western United States: Review of Geophysics, v. 4, p. 509-549.

Hedge, C. E., 1972, Age of major Precambrian rock units; in Mallory, W. W., ed., Geological Atlas of the Rocky Mountain Region, United States of America, p. 54-55.

Heimlich, R. A., 1969, Reconnaissance petrology of Precambrian rocks in the Bighorn Mountains, Wyoming: Contributions to Geology, v. 8, no. 1, p. 47-61.

Hennier, Jeff, and Spang, J.H., 1983, Mechanisms for deformation of sedimentary strata at Sheep Mountain Anticline, Bighorn Basin, Wyoming, in Boberg, W. W., ed., Geology of the Bighorn Basin, 34th Annual Guidebook: Wyoming Geological Association, p. 96-111.

Hennings, P. H., and Spang, J. H., 1985, Crystalline basement geometry from three dimensionally balanced cross-sections: Dry Fork Ridge, northeastern Bighorn Mountains, Wyoming [abs.]: Abstracts with Programs; The Geological Society of America, 98th Annual Meeting, p. 607.

Hewett, D. F., and Lupton, C. T., 1917, Anticlines in the southern part of the Bighorn basin, Wyoming: U. S. Geological Survey Bulletin No. 656, 192 p.

Hodgson, R. A., 1965, Genetic and geometric relations between structures in basement and overlying sedimentary rocks with examples from Colorado plateau and Wyoming: American Association of Petroleum Geologists Bulletin, v. 49, no. 7, p. 935-939.

Holden, G. S., and Fleckenstein, Martin, 1980, Geologic history of the Precambrian of the central Laramide Range, Wyoming: in Hollis, S., ed., Stratigraphy of Wyoming; Wyoming Geological Association, 31st Annual Field Conference, p. 17-22.

Hoppin, R. A., 1961, Precambrian rocks and their relationship to Laramide structure along the east flank of the Bighorn Mountains near Buffalo, Wyoming: Geological Society of America Bulletin, v. 72, no. 3, p. 351-367.

_____, 1970, Structural development of Five Springs Creek area, Bighorn Mountains, Wyoming: Geological Society of America Bulletin, v. 81, p. 2403-2416.

Hoppin, R. A., and Jennings, T. V., 1971, Cenozoic tectonic elements, Bighorn Mountain region Wyoming-Montana, in Renfro, Arthur R., ed., Symposium on Wyoming Tectonics and Their Economic Significance, 23rd Field Conference Guidebook: Wyoming Geological Association, p. 39-74.

Hoppin, R. A., and Palmquist, J. C., 1965, Basement influence on later deformation--the problem, techniques of investigation, and examples from Bighorn Mountains, Wyoming: American Association of Petroleum Geologists Bulletin, v. 49, no. 7, p. 993-1003.

Hoppin, R. A., Palmquist, J. C., and Williams, L. O., 1965, Control by Precambrian basement structure on the location of the Tensleep-Beaver Creek faults, Bighorn Mountains, Wyoming: Journal of Geology, v. 73, p. 189-195.

Houston, Robert S., 1971, Regional tectonics of the Precambrian rocks of the Wyoming province and its relationship to Laramide structure in Renfro, Arthur, R., ed., Symposium on Wyoming Tectonics and Their Economic Significance, 23rd Annual Field Conference Guidebook: Wyoming Geological Association, p. 19-28.

Houston, Robert S., and others, 1968, A regional study of rocks of Precambrian age in that part of the Medicine Bow Mountains lying in southeastern Wyoming--with a chapter on the relationships between Precambrian and Laramide structures: Geological Survey of Wyoming Memoir 1, 167 p.

Hudson, F. S., 1955, Folding of unmetamorphosed strata superjacent to massive basement rocks: American Associa- tion of Petroleum Geologists Bulletin, v. 39, p. 2038-2052.

Jenkins, O. P., 1943, Glossary of the Geologic units of California: California Division of Mines Bulletin, v. 118, no. 4, p. 667-687.

Jennings, T. V., 1967, Structural analysis of the northern Bighorn Mountains, Wyoming: PhD. Diss., University of Iowa.

Johnson, R. A., and Smithson, S. B., 1985, Thrust faulting in the Laramie Mountains, Wyoming from re-analysis of COCORP data: Geology, v. 13, no. 8, p. 534-537.

Jordan, T. E., Isacks, B. L., Allmendinger, R. W., Brewer, J. A., Ramos, V. A., and Ando, C. J., 1983, Andean tectonics: lateral segmentation in Central Andes, related to geometry of subducted plate: Geological Society of America Bulletin, v. 94, no. 3, p. 341-361.

Kanter, Lisa R., Dyer, Russ, and Dohmen, T. E., 1981, Laramide crustal shortening in the northern Wyoming Province: Contributions to Geology, v. 19, no. 2, p. 135-142.

Keefer, W. R., 1965, Stratigraphy and geologic history of the uppermost Cretaceous, Paleocene, and lower Eocene rocks in the Wind River basin, Wyoming: U. S. Geological Survey Professional Paper, 495-A, p. A1-A77.

_____ 1970, Structural Geology of the Wind River Basin, Wyoming. U. S. Geological Society Professional Paper, 495-D, 35 p.

Kraig, D. H., Wiltschko, D. V., and Spang, J. H., 1986, Interaction of the La Barge Platform with the western overthrust belt, southwestern Wyoming [abs.]: Abstracts with Programs; The Geological Society of America, 39th Annual Meeting of Rocky Mountain Section, p. 367.

_____ 1986, Interaction of the northern segment of the Moxa arch with the western overthrust belt, southwestern Wyoming [abs.]: Abstracts with Programs; The Geological Society of America, 39th. Annual Meeting of Rocky Mountain Section, p. 368.

Lamerson, P. R., 1982, The Fossil basin area, and its relationship to the Absaroka thrust fault system; in Powers, R. R., ed.,, Geologic Studies of the Cordilleran Thrust Belt, Volume 1: Rocky Mountain Association of Geologists, p. 279-340.

Lochman-Balk, C., 1972, Cambrian System; in Mallory, W. W., ed., Geologic Atlas of the Rocky Mountain Region, United States of America: Rocky Mountain Association of Geologists, p. 60-75.

Logan, J. M., Friedman, M., and Stearns, M. T., 1978, Experimental folding of rocks under confining pressure, part VI of Further studies of faulted drape folds, in Matthews, V., III, ed., Laramide folding associated with basement block faulting in the western United States: Geological Society of America Memoir 151, p. 79-99.

Long, Joe S., 1959, Geology of Phlox Mountain area, Owl Creek Mountains: Unpublished Ms. Thesis, University of Wyoming.

Love, J. D., 1974, Plate tectonics and foreland basement deformation: Geology, v. 2, no. 6 (June), p. 275-278.

_____, 1977, Foreland deformation, in Lowell, J. D., ed., Rocky Mountain foreland basins and uplifts: Rocky Mountain Association of Geologists, p. 1-8.

_____ , 1977, Summary of Upper Cretaceous and Cenozoic stratigraphy, and of tectonic and glacial events in Jackson Hole, northwestern Wyoming, in Heisey, E. L., Lawson, Don, E., Norwood, Earl R., Wach, Phillip H., and Hale, Lyle A., eds., Rocky Mountain Thrust Belt Geology and Resources, 29th Annual Field Conference: Wyoming Geological Association in conjunction with Montana Geological Society and Utah Geological Society, p. 585-593.

_____, 1982, A possible gap in the western thrust belt in Idaho and Wyoming; in Powers, R. B., ed.,, Geologic Studies of the Cordilleran Thrust Belt, Volume 1: Rocky Mountain Association of Geologists, p. 247-260.

_____, 1983, Foreland deformation; in Lowell, J. D., ed.,, Rocky Mountain Foreland Basins and Uplifts: Rocky Mountain Association of Geologists, p. 1-8.

Love, J. D., and Christiansen, A. C., 1985, Geologic Map of Wyoming: U. S. Geological Survey, scale 1:500,000.

Love, J. D., Weitz, J. L., and Hose, R. K., 1955, Geologic map of Wyoming: U.S. Geological Society, scale 1:500,000.

Luth, W. C., 1960, Mafic and ultramafic rocks of the Trailside area, Bighorn Mountains, Wyoming: Unpublished M. S. Thesis, University of Iowa.

MacLachlan, Marjorie E., 1972, Triassic system, in Mallory, W. W., ed., Geologic Atlas of the Rocky Mountain Region: Rocky Mountain Association of Geologists, p. 166-176.

McGooky, Donald P., 1972, Cretaceous system, in Mallory, W. W., ed., Geologic Atlas of the Rocky Mountain Region: Rocky Mountain Association of Geologists, p. 190-228.

Mackin, J. Hoover, 1959, The down-structure method of viewing geologic maps: Journal of Geology, v. 58, no. 1, p. 55-72.

Mallory, William W., ed.,, 1974, Geological Atlas of the Rocky Mountain Region: Rocky Mountain Association of Geologists, 331 p.

Matthews, V., III, and Work, D. F., 1978, Laramide folding associated with basement block faulting along the northeastern flank of the Front Fange, Colorado, in Matthews, V., III, ed.,, Laramide folding associated with basement block faulting in the western United States: Geological Society America Memoir 151, p. 101-124.

Mitra, G., and Frost, B. R., 1981, Mechanisms of the deformation within Laramide and Precambrian deformation zones in basement rocks of the Wind River Mountains: Contributions to Geology, v. 19, no. 2, p. 161-173.

Morse, J. D., 1977, Deformation in the ramp regions of overthrust faults: experiments with small-scale rock models; in Heisey, E. L., and Lawson, D. E., eds., Rocky Mountain Thrust Belt Geology and Resources: Wyoming Geological Association, 29th Annual Field Conference, p. 457-470.

Murray, F. E., 1960, An interpretation of the Hilliard thrust fault, Lincoln and Sublette Counties, Wyoming, in McGooky, D. P. and Miller, D. N., Jr., eds., Overthrust Belt of Southwest Wyoming and Adjacent Areas, 15th Annual Field Conference Guidebook: Wyoming Geological Association, p. 161-186.

Nelson, V. E., and Church, V., 1943, Critical structures of the Gros Ventre and northern Hoback Ranges, Wyoming: Journal of Geology, v. 51, no. 3, p. 143-166.

Nichols, C. E., 1965, Geology of a segment of Deep Creek fault zones, southern Bighorn Mountains, Wyoming: Ph. D. Diss., University of Iowa.

Osterwald, F. W., 1959, Structure and Petrology of the northern Bighorn Mountains, Wyoming: Geological Survey of Wyoming Bulletin, v. 48, p. 47.

_____, 1961, Critical review of some tectonic problems in Cordilleran foreland: American Association of Petroleum Geologists Bulletin, v. 45, no. 2, p. 219-237.

Palmquist, J. C., 1967, Structural analysis of the Horn area, Bighorn Mountains, Wyoming: Geological Society of America Bulletin, v. 78, p. 238-298.

_____ , 1978, Laramide structures and basement block faulting--two examples from the Bighorn Mountains, Wyoming, in Matthews, V., III, ed., Laramide Folding Associated with Basement Block Faulting in the Western United States: Geological Society of America Memoir 151, p. 125-138.

Petersen, F.A., 1983, Foreland detachment structures, in Lowell, J. D., ed.,, Rocky Mountain Foreland Basins and Uplifts: Rocky Mountain Association of Geologists, p. 65-77.

Philcox, M. E., 1964, Compartment deformation near Buttevant, County Cork, Ireland and its relation to the Variscan Thrust Front: Royal Dublin Society, 1964 Proceedings, v. 2, no. 1.

Phillips, Stephen T., 1983, Tectonic influences on sedimentation, Waltman Member, Fort Union formation, Wind River Basin, Wyoming, in Lowell, J. D., ed., Rocky Mountain Foreland Basins and Uplifts: Rocky Mountain Association of Geologists, p. 149-160.

Picard, M. D., Aadland, R. and High, L. R., 1969, Correlation and stratigraphy of Triassic Red Peak and Thaynes Formations, western Wyoming and adjacent Idaho: American Association of Petroleum Geologists Bulletin, v. 53, no. 11, p. 2274-2289.

Pierce, W. G., 1949, Heart Mountain and South Fork thrusts, Park County, Wyoming: American Association of Petroleum Geologists Bulletin, v. 25, p. 2021-2046.

_____, 1957, Heart Mountain and South Fork detachment thrusts of Wyoming: American Association of Petroleum Geologists Bulletin, v. 41, p. 591-626.

_____, 1965, Geologic map of the Deep Lake Quadrangle, Park County, Wyoming: U.S. Geological Society Geologic Quadrangle Map GQ-478,scale 1:62,500.

_____, 1966, Geologic map of the Cody Quadrangle, Park County, Wyoming: U.S. Geological Society Geologic Quadrangle Map GQ-542, scale 1:62,500.

_____, 1970, Geologic Map of the Devil's Tooth Quadrangle, Park County, Wyoming: U.S.Geological Society Geological Quadrant Map GQ-817, scale 1:62,500.

Pierce, W. G., and Nelson, W. H., 1968, Geologic map of the Pat O'Hara Mountain Quadrangle, Park County, Wyoming: U.S. Geological Society Geological Quadrangle Map GQ-755, scale 1:62,500.

_____, 1969, Geological map of the Wapiti Quadrangle, Park County, Wyoming: U.S.Geological Society Geological Quadrangle Map GQ-778, scale 1:62,500.

Poldevaart, Arie, and Bentley, R. D., 1958, Precambrian and later evolution of the Beartooth Mountains, Montana and Wyoming; in 9th. Annual Field Conference Guidebook, Billings Geological Society, p. 7-15.

Prucha, J. J., Graham, J. A., and Nickelsen, R. P., 1965, Basement-controlled deformation in Wyoming province of Rocky Mountain foreland: American Association of Petroleum Geologists Bulletin, v. 49, no. 7, p. 966-992.

Ramsay, J. G., 1962, The geometry and mechanics of formation of 'Similar' type folds: Journal of Geology, v. 70, no. 3, p. 309-327.

Renfro, H. B., and Feray, D. E., compilers, 1966, United States Geological Highway Map No. 5, Northern Rocky Mountain Region (Idaho, Montana, Wyoming): American Association of Petroleum Geologists, scale 1:1,875,000.

Rich, J. L., 1934, Mechanics of low-angle overthrust faulting as illustrated by Cumberland thrust block, Virginia, Kentucky, and Tennessee: American Association of Petroleum Geologists Bulletin, v. 18, no. 12, p. 1584-1596.

Richards, Paul W., 1957, Geology of the area east of, and southeast of Livingston, Park county, Montana: U.S. Geological Survey Bulletin, v. 1021-L, p. 385-438.

Robinson, Peter, 1972, Tertiary history in Mallory, W. W., ed., Geological Atlas of the Rocky Mountain Region: Rocky Mountain Association of Geologists, p. 233-242.

Royse, F., Jr., 1985, Geometry and timing of the Darby-Prospect-Hogsback thrust fault system, Wyoming [abs.]: Abstracts with Programs; The Geological Society of America, 38th. Annual Meeting of Rocky Mountain Section, p. 263.

Royse, F., Jr., Warner, M. A., and Reese, D. L., 1975 Thrust belt structural geometry and related stratigraphic problems, Wyoming, Idaho, north Utah in Bolyard, D. W., ed., Symposium on Deep Drilling Frontiers in the Central Rocky Mountains: Rocky Mountain Association of Geologists, p. 41-45.

Sales, J. K., 1968, Cordilleran foreland deformation: American Association of Petroleum Geologists Bulletin, v. 52, p. 2000-2015.

Sanford, A. R., 1959, Analytical and experimental study of simple Geologic structures: Geological Society of America Bulletin, v. 79, p. 19-51.

Schmidt, C. J., Evans, J. P., Fletcher, R. C., and Spang, J. H., 1985, Spacing of Rocky Mountain foreland arches and Laramide magmatic activity [abs.]: Abstracts with Programs; The Geological Society of America, 98th. Annual Meeting, Orlando, Florida, p. 710.

Schmidt, C. J., and Hendrix, T. E., 1981, Tectonic controls for Thrust belt and Rocky Mountain foreland structures in the northern Tobacco Root Mountains--Jefferson county area, southwestern Montana, in Symposium Guidebook to Southwest Montana: Montana Geological Society Field Conference Guidebook, p. 167-180.

Skeen, R. C., and Ray, R. R., 1983, Seismic models and interpretation of the Casper Arch Thrust--application to Rocky Mountain foreland structure, in Lowell, J. D., ed., Rocky Mountain Foreland Basins and Uplifts: Rocky Mountain Association of Geologists, p. 99-124.

Smith, A. G., and Briden, J. C., 1979, Mesozoic and Cenozoic Paleocontinental Maps: London, Cambridge University Press, 36 p.

Smith, A. G., Hurley, A. M., and Briden, J. C., 1981, Phanerozoic Paleocontintal World Maps: London, Cambridge University Press, 102 p.

Smithson, Scott B., Brewer, Jon, Kaufman, S., Oliver, Jack, and Hurich, Charles, 1978, Question of the Wind River thrust, Wyoming, resolved by COCORP deep reflection data and by gravity, in Boyd, Richard G., ed., Resources of the Wind River Basin, 30th Annual Field Conference Guidebook: Wyoming Geological Association, p. 227-234.

Spang, J. H., Evans, J. P., and Berg, R. R., 1985, Balanced cross sections of small fold-thrust structures: Mountain Geologists, v. 22, no. 2, p. 41-46.

Sprague, E. L., 1983, Geology of the Tepee Flats-Buffington Fields, Natrona County, Wyoming, in Lowell, J. D., ed., Rocky Mountain Foreland Basins and Uplifts: Rocky Mountain Association of Geologist, p. 339-343.

Stauder, W. J., 1975, Subduction of the Nazca Flats under Peru as evidenced by focal mechanisms and by seismicity: Journal of Geophysical Research, v. 80, p. 1053-1064.

Stearns, D. W., 1971, Mechanisms of drape folding in the Wyoming province, in Renfro, Arthur, R., ed., Symposium on Wyoming Tectonics and Their Economic Significance, 23rd Field Conference Guidebook: Wyoming Geological Association, p. 125-143.

_____ 1975, Laramide basement deformation in the Bighorn Basin--the controlling factor for structure in the layered rocks, in Exum, Frank A. and George, Gene R., eds., Geology and Mineral Resources of the Bighorn Basin, 27th Annual Field Conference Guidebook: Wyoming Geological Association, p. 149-158.

_____ 1978, Fault and forced folding in the Rocky Mountains foreland in Matthews, V., III, ed., Laramide Folding Associated with Basement Block Faulting in the Western United States: Geological Society of America Memoir 151, p. 1-37.

Stearns, D. W., Couples, Gary, and Stearns, M. T., 1978, Deformation of non-layered materials that affect structures in layered rocks, in Resources of the Wind River Basin, 30th Annual Field Conference Guidebook: Wyoming Geological Association, p. 213-225.

Stearns, D. W., Sacrison, W. R., and Hanson, R. C., 1975, Structural history of southwestern Wyoming as evidenced from outcrop and seismic: in Bolyard, D. W., ed., Deep drilling frontiers of the Central Rocky Mountains; Rocky Mountain Association of Geologists, p. 9-20.

Stearns, D. W., and Stearns, M. T., 1978, Geometric analysis of multiple drape folds along the northwest Bighorn Mountains Front, Wyoming: in Matthews, V., III, editor, Laramide folding associated with basement block faulting in the Western United States: Geological Society of American Memoir 151, p. 139-156.

Stearns, D. W. and Weinberg, D. M., 1975 A comparison of experimentally created and naturally formed drape folds, in Exum, Frank A. and George, Gene R.,eds., Geology and Mineral Resources of the Bighorn Basin, 27th Annual Field Conference Guidebook: Wyoming Geological Association, p. 159-166.

Stone, D. S., 1969, Wrench faulting and the Rocky Mountain Tectonics: Mountain Geologist, v. 6, no. 2, p. 67-79.

_____ 1975, A dynamic analysis of subsurface structure in northwestern Colorado; in Bolyard, D. W., editor, Symposium on Deep Drilling Frontiers in the Central Rocky Mountains: Rocky Mountain Association of Geologists, p. 33-40.

Stricker, Janna L., 1984, A structural and stratigraphic interpretation from the surface geology of Zeisman Dome, Bighorn Basin, Wyoming: Unpublished Senior Thesis, Baylor University, 66 p.

Suppe, J., 1985, Principles of Structural Geology, Prentice-Hall, Inc., Englewood Cliffs, New Jersey, 537 p.

Thom, W. T. 1923, Relationship of deep-seated faults to the surface structural features of central Montana: American Association of Petroleum Geologists Bulletin, v. 7, no. 1, p. 1-13.

Tomlinson, C. W., 1952, Odd Geologic structures of southern Oklahoma: American Association of Petroleum Geologists Bulletin, v. 36, no. 9, p. 1820-1840.

Wach, Philip H., 1977, The Moxa Arch, an overthrust model? in Heisey, E. L., Lawson, Don E., Norwood, Earl R., Wach, Phillip H., and Hale, Lyle A., eds., Rocky Mountain Thrust Belt Geology and Resources, 29th Annual Field Conference: Wyoming Geological Association in conjunction with Montana Geological Society and Utah Geological Society, p. 651-664.

Weinberg, D. M., 1978 Some two-dimensional kinematic analyses of the drape-fold concept, in Matthews, V., III, ed., Laramide Folding Associated with Basement Block Faulting in the Western United States: Geological Society of America Memoir 151, p. 51-78.

Weinberg, D. M., and Stearns, D. W., 1978, Kinematic analysis of drape folds in the Rocky Mountains foreland: some geological implications; in Boyd, R. G., ed., Resources of the Wind River Basin: Wyoming Geological Association 30th Annual Field Conference Guidebook, p. 199-212.

Wilson, C. W., Jr., 1934, A study of the jointing in the Five Springs Creek area, east of Kane, Wyoming: Journal of Geology, v. 42, p. 498-522.

Wise, Donald U., 1963, Keystone faulting and gravity sliding driven by basement uplift of Owl Creek Mountains, Wyoming: American Association of Petroleum Geologists Bulletin, v. 47, no. 4, p. 586-598.

_____ 1964, Microjointing in basement, middle Rocky Mountains of Montana and Wyoming: Geological Society of America Bulletin, v. 75, no. 4, p. 287-306.

Woodward, Lee A., 1976, Laramide deformation of Rocky Mountain foreland--geometry and mechanics: New Mexico Geological Society Special Publication, no. 6, p. 11-17.

STRUCTURAL STYLE OF THE LARAMIDE OROGENY, WYOMING FORELAND

(VOLUME 2: FIGURES)

A

THESIS

Presented to the Faculty of the University of Alaska

in Partial Fulfillment of the Requirements

for the Degree of

DOCTOR OF PHILOSOPHY

By

William G. Brown, B.S., M.S.

Fairbanks, Alaska

May 1987

LIST OF FIGURES

All figures are numbered sequentially in Volume II.

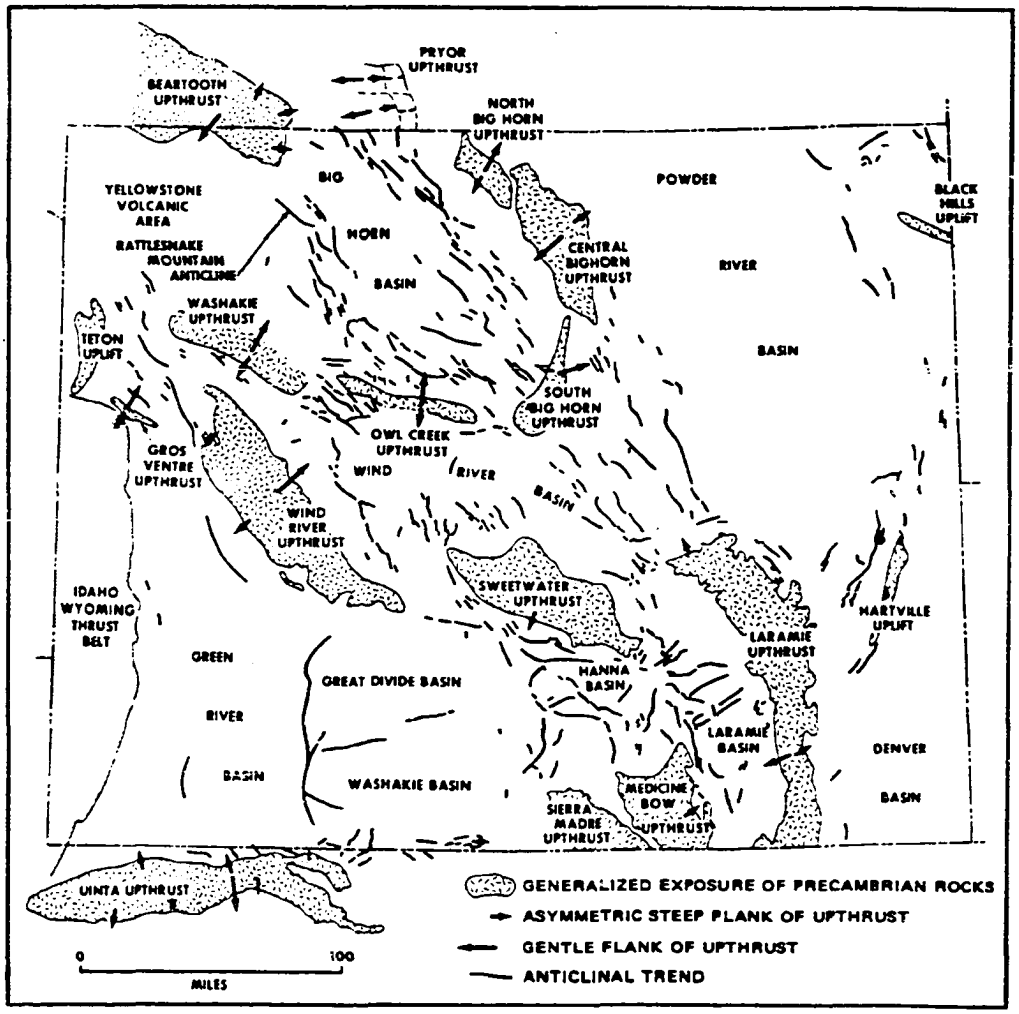

FIGURE 1. Index map of the Wyoming foreland showing distribution of exposed Precambrian-cored ranges (stippled), intervening basins, and trends of local anticlinal structures. (After Lowell, 1974).

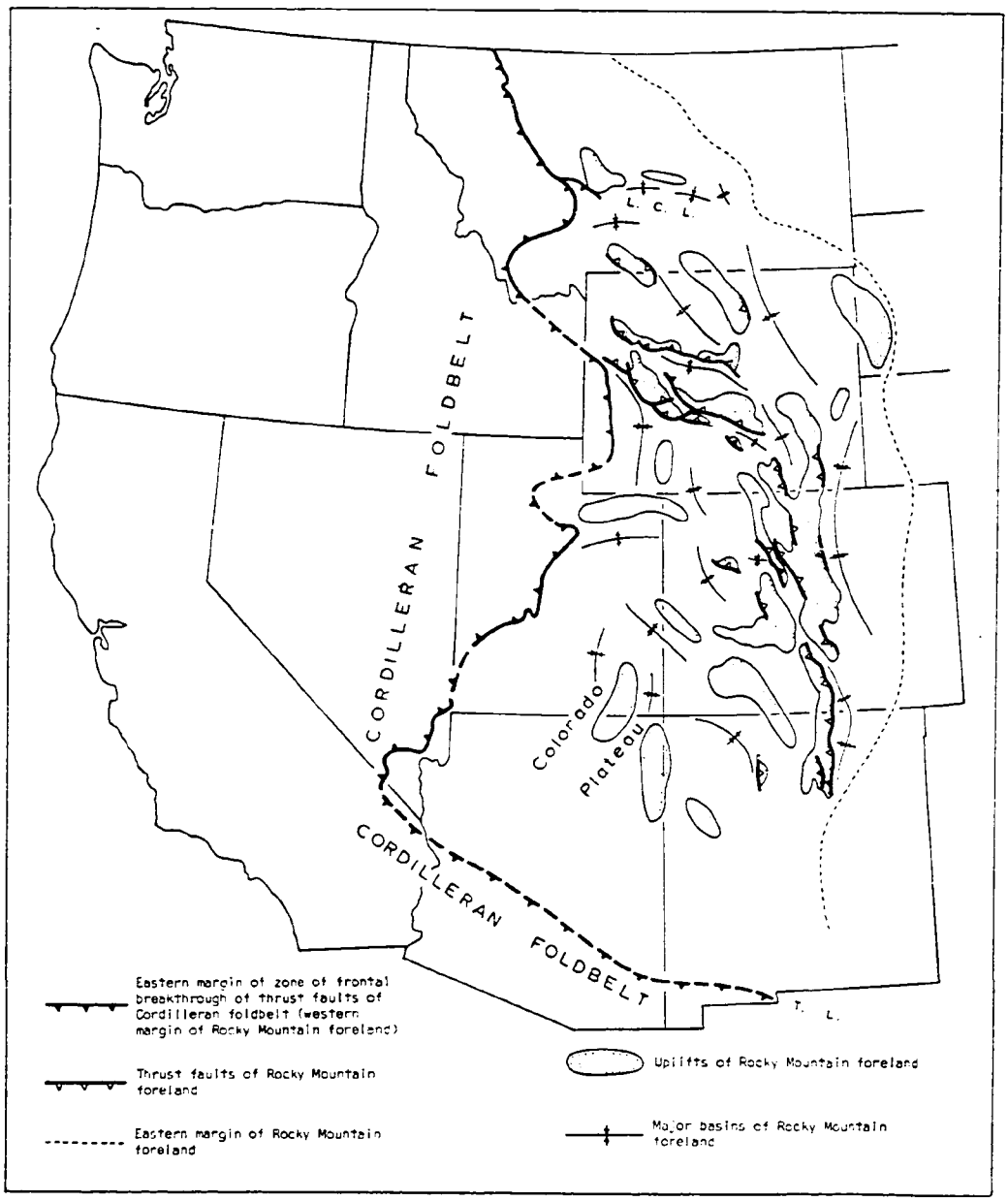

FIGURE 2. Index map of the Rocky Mountain foreland, of which the Wyoming foreland is a part. Cordilleran thrust belt (foldbelt) marks the western margin of the foreland province. (After Woodward, 1976).

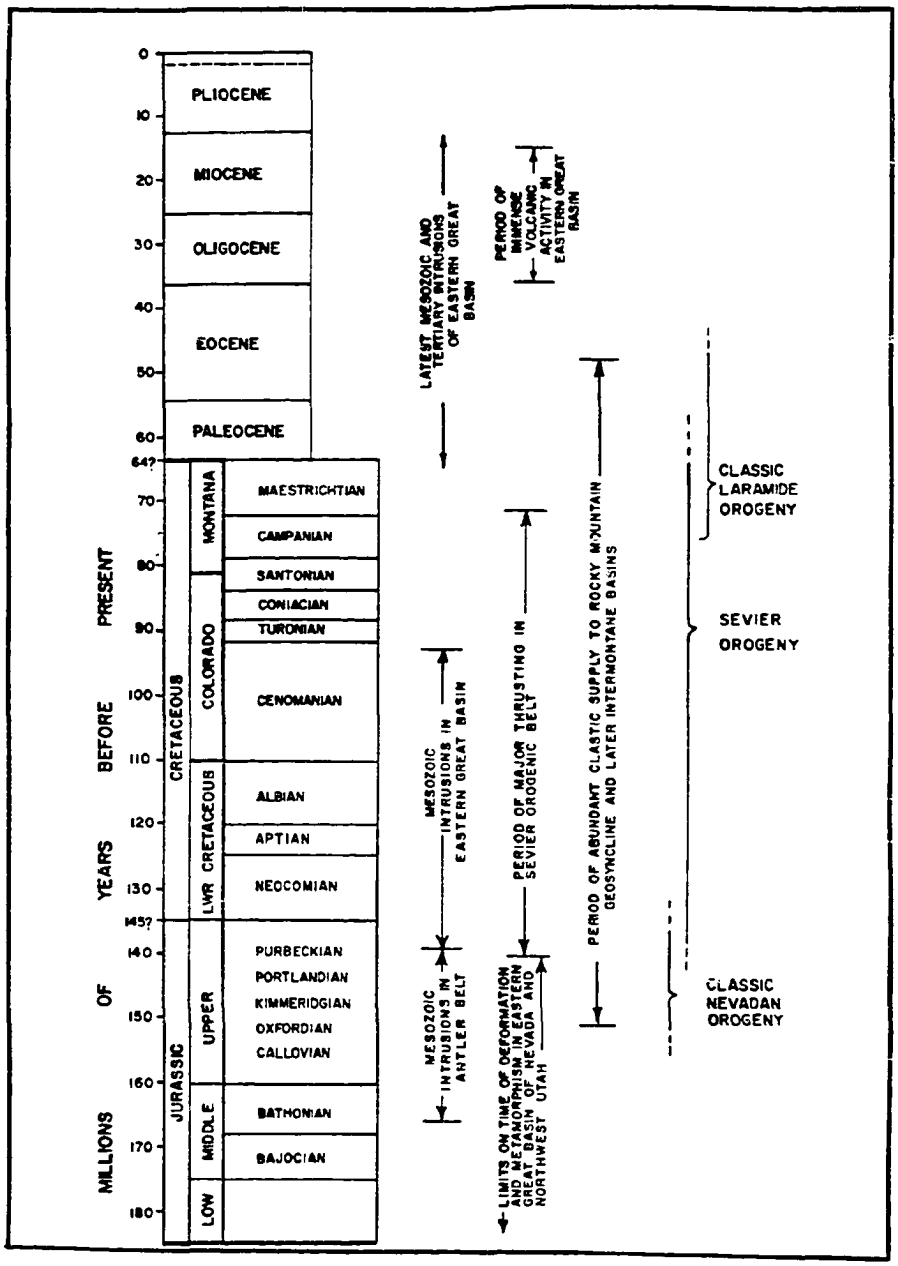

FIGURE 3. Mesozoic and Cenozoic geologic time scale showing onset and duration of tectonic events which have affected the western United States. Sevier and Laramide orogenies overlap in time during the Late Cretaceous. (After Armstrong, 1968).

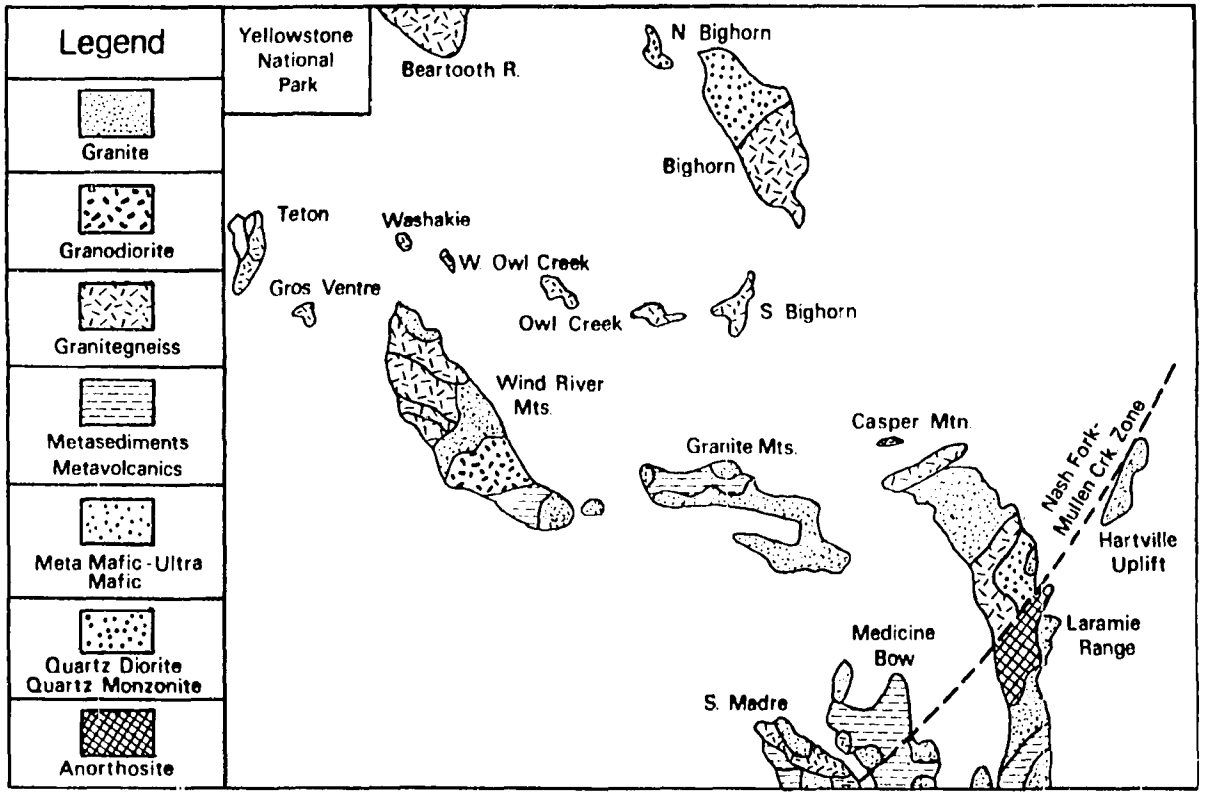

FIGURE 4. Distribution of age-dated Precambrian rocks in the Wyoming foreland. Nash Fork-Mullen Creek (NF) "shear zone" separates exposed older Precambrian rocks (2,000 m.y. and older) from younger Precambrian rocks (1,900 m.y. and younger) in the Medicine Bow Range of southeastern Wyoming. NF shear zone projects northeastward across Laramie basin, Laramie Mountains, and along the Hartville uplift, and is apparently equivalent in age and structural relationship to the "Mesabi iron trend" on the Canadian Shield.

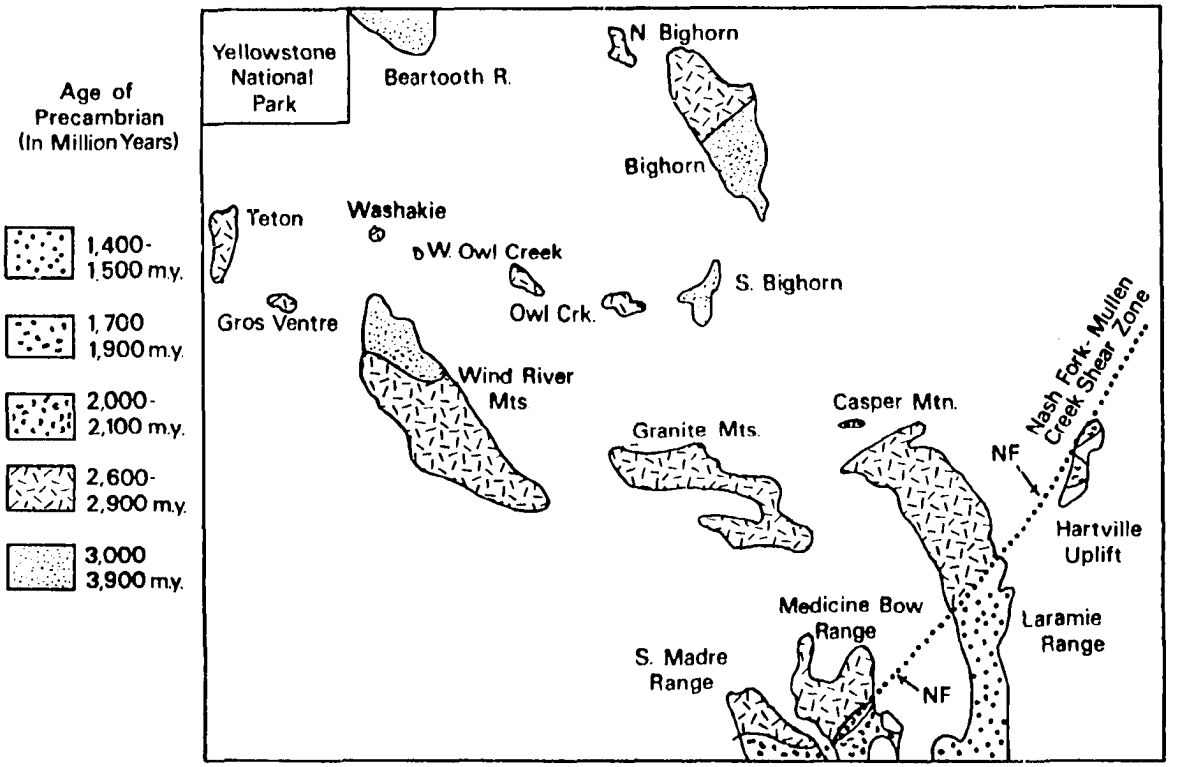

FIGURE 5. Distribution of exposed rock types of the Precambrian basement in the Wyoming foreland. Approximately 22% of the exposed basement is metasedimentary or meta-volcanic in origin.

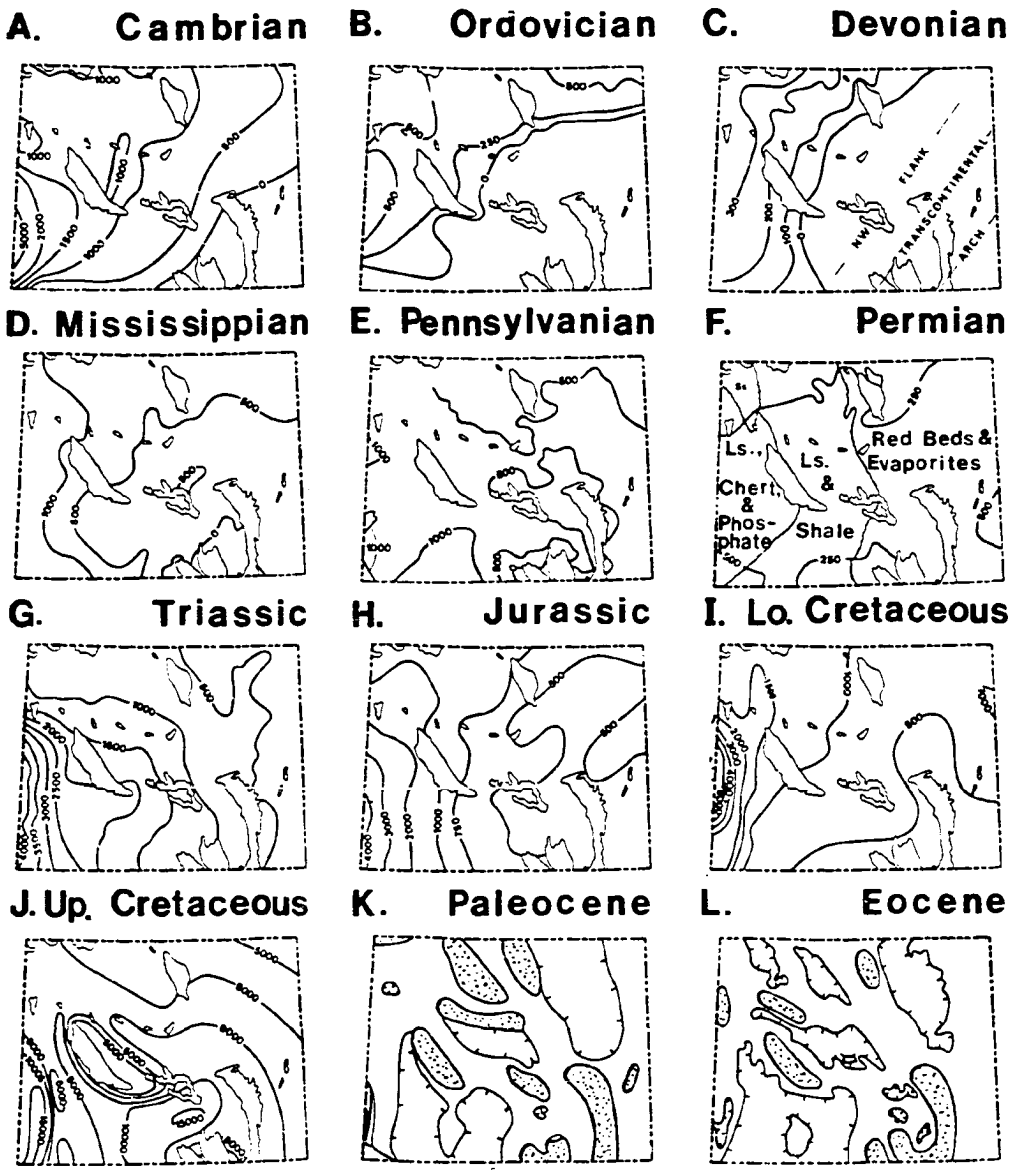

FIGURE 6. Montage of Paleozoic and Mesozoic isopachous maps and Cenozoic paleogeographic maps of the Wyoming foreland (after Mallory, 1972). A-Cambrian; B-Ordovician; C-Devonian; D-Mississippian; E-Pennsylvanian; F-Permian; G-Triassic; H-Jurassic; I-Lower Cretaceous; J-Upper Cretaceous; K-Paleocene; L-Eocene. Stippled areas exposed during deposition; hachured line is outcrop; present-day mountain ranges shown for reference.

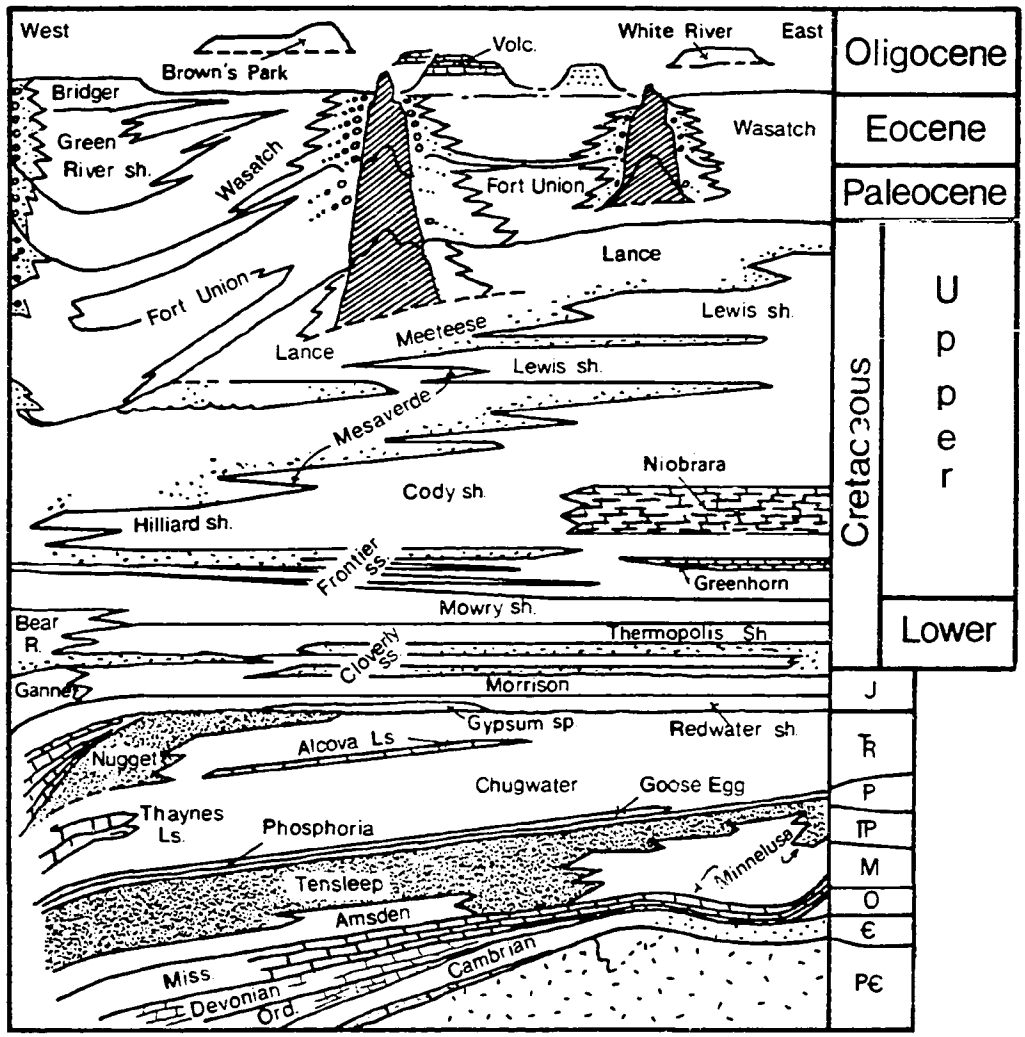

FIGURE 7. Stratigraphic cross section showing the west-to-east distribution of Phanerozoic stratigraphic units across the Wyoming foreland.

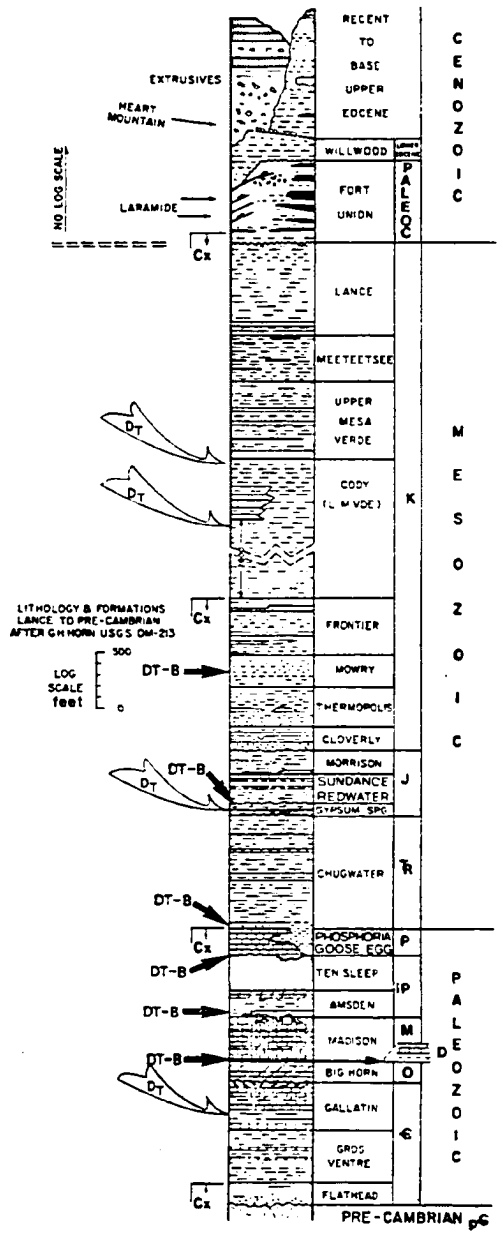

FIGURE 8. Stratigraphic column typical of the Bighorn basin, northern Wyoming, Cx = top of groups of structurally "competent" rocks; DT = detachment-prone stratigraphic horizons recognized by Fanshawe (1971); DT-B = additional detachment-prone stratigraphic horizons, as recognized in this study.

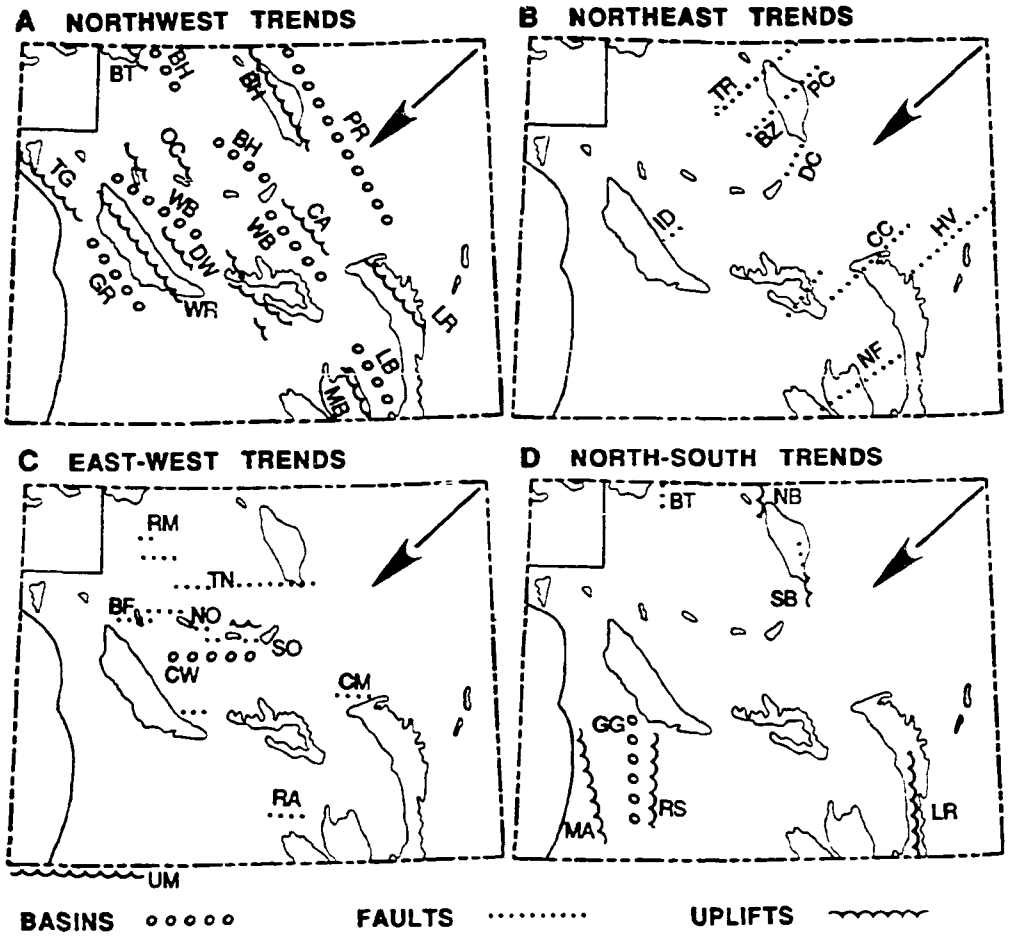

FIGURE 9. Montage showing the four principle orientations of Laramide structures on the Wyoming foreland. Letters refer to specific structural features: BF-Buffalo Fork; BH-Bighorn; BT-Beartooth; BZ-Bonanza/Zeisman; CA-Casper arch; CC-Corral Creek; CM-Casper Mountain; CW-central Wind River; DC-Deep Creek; DW-Dallas/Winkleman; GR-Green River; GG-Greater Green River; HV-Hartville; IT-Immigrant Trail; ID-igneous dike; LB-Laramie basin; LR-Laramie Range; MA-Moxa arch; MB-Medicine Bow; NB-northern Bighorn; NF-Nash Fork; NO-north Owl Creek; OC-Owl Creek; PC-Piney Creek; PR-Powder River; RA-Rawlins; RM-Rattlesnake Mountain; RS-Rock Springs; SB-southern Bighorn; SO-south Owl Creek; TG-Teton/Gros Ventre; TN-Tensleep; TR-Tongue River; UM-Uinta Mountains; WA-Washakie; WB-Wind River basin; WR-Wind River Mountains. Large arrow represents northeast-southwest direction of regional compression.

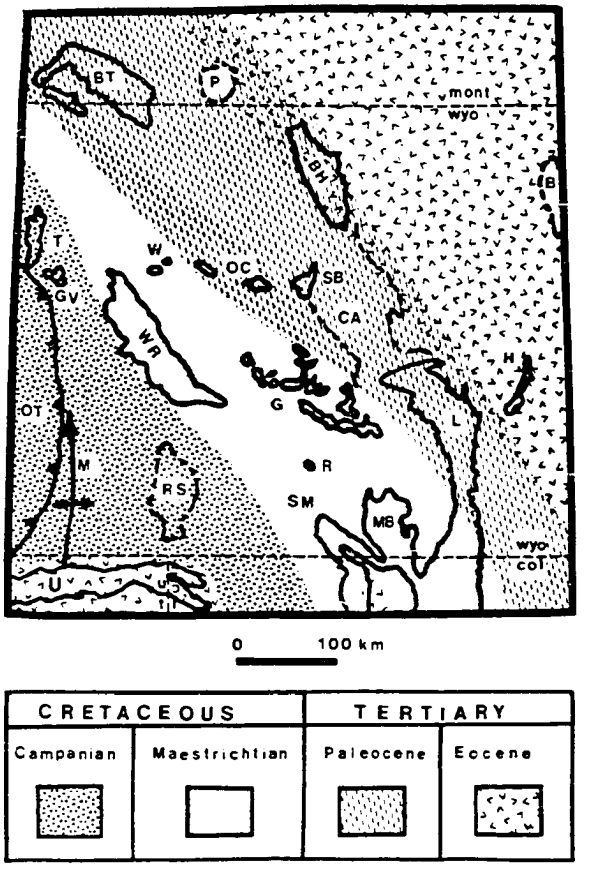

FIGURE 10. Index map showing west-to-east migration of the time of onset of the Laramide orogeny in the Wyoming foreland. Deformation began in Cretaceous (Campanian) and ended in Tertiary (Eocene). Areas of overlapping symbols indicate multiple periods of deformation attributed to the Laramide orogeny (modified from Gries, 1983). Effect of eastward shift of onset of Laramide orogeny can be considered a "tectonic front", which may have had weaker movements in front of and behind it. Letters refer to specific structural features: B-Black Hills uplift; BH-Bighorn Mountains; BT-Beartooth Mountains; CA-Casper arch; G-Granite Mountains; GV-Gros Ventre Range; H-Hartville uplift; L-Laramie Range; M-Moxa arch; MB-Medicine Bow Range; OC-Owl Creek Mountains; OT-Overthrust Belt; P-Pryor Mountains; R-Rawlins uplift; RS-Rock Springs uplift; SB-southern Bighorn Mountains; SM-Sierra Madre Mountains; T-Teton uplift; U-Uinta Mountains; W-Washakie Range; WR-Wind River Mountains.

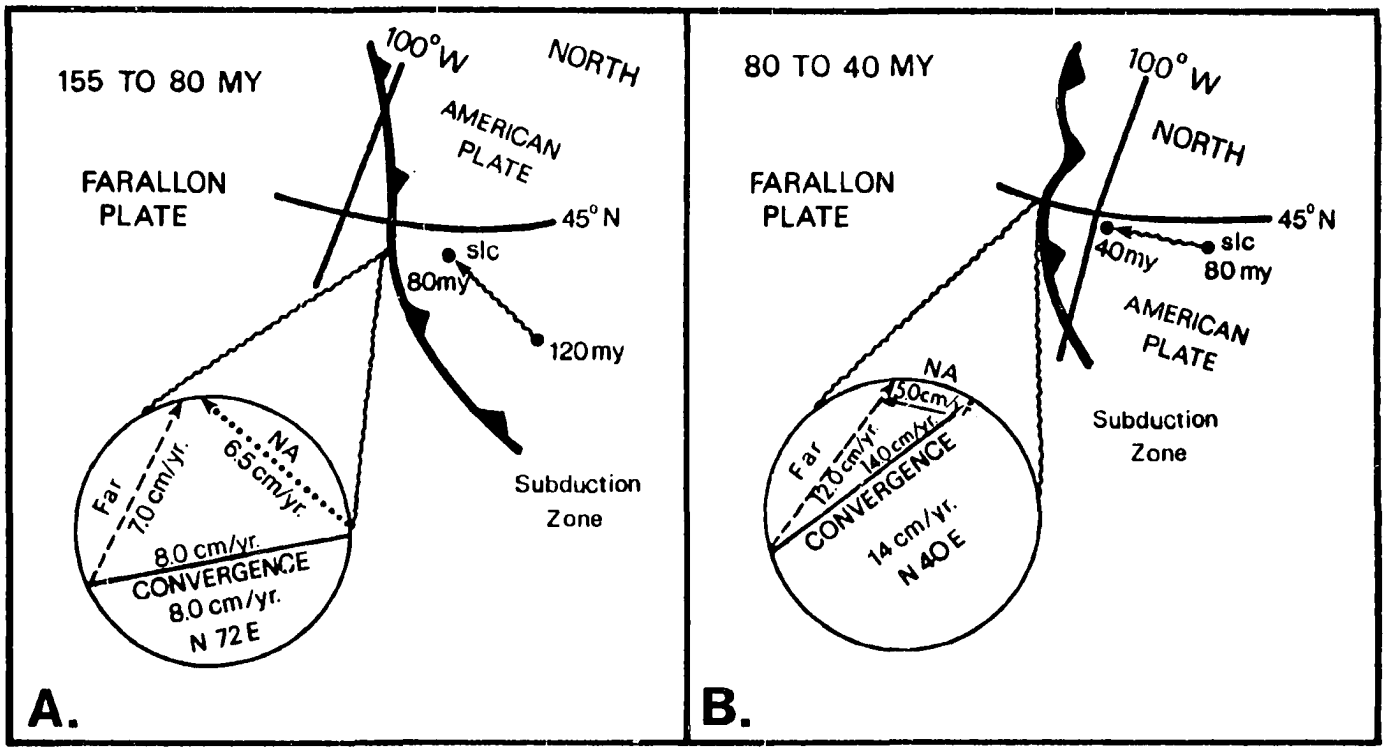

FIGURE 11. Plate tectonic setting of western North America relative to the Pacific (Farallon) plate, during the time of 155 m.y.a. to 40 m.y.a. (after Coney, 1978). Reference point slc = Salt Lake City. A) During Sevier orogeny (155-80 m.y.a.), North American (NA) and Farallon (Far) plates collided in a direction of N72E, at a rate of 8 cm (3 in) per year. B) During the Laramide orogeny (80-40 m.y.a.) North American and Farallon plates collided in a direction of N40E., at a rate of 14 cm (5.5 in) per year.

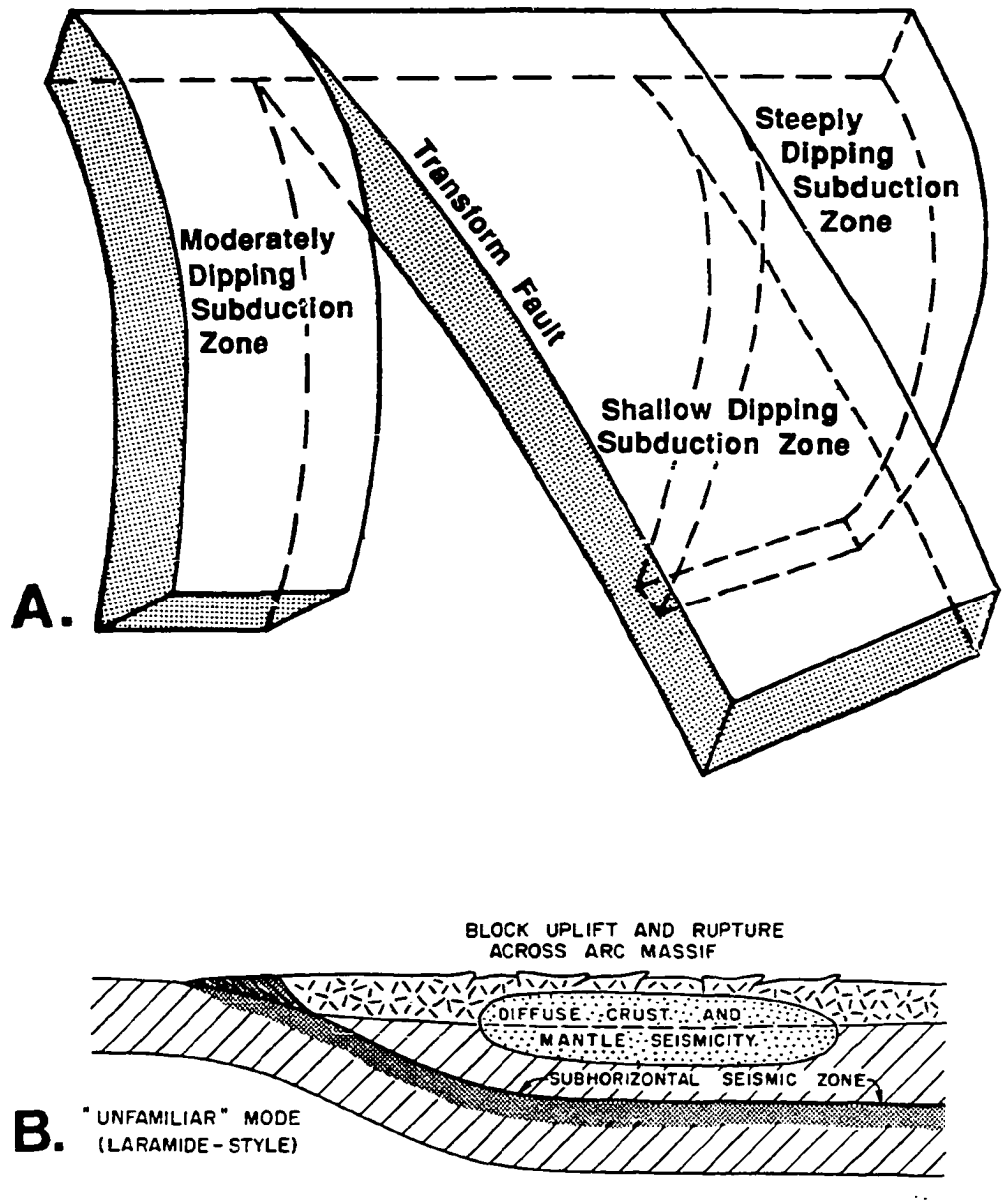

FIGURE 12. Concept of low-dipping subduction zone, which resulted from increased rate of subduction during the Laramide orogeny. A) Segmentation allowed shallow-dipping portion of the subduction zone to extend eastward farther under the Wyoming foreland than during Sevier orogeny. B) Presence of shallow-dipping subduction zone resulted in the eastward shift of seismicity and heat flow (after Dickinson and Snyder, 1978).

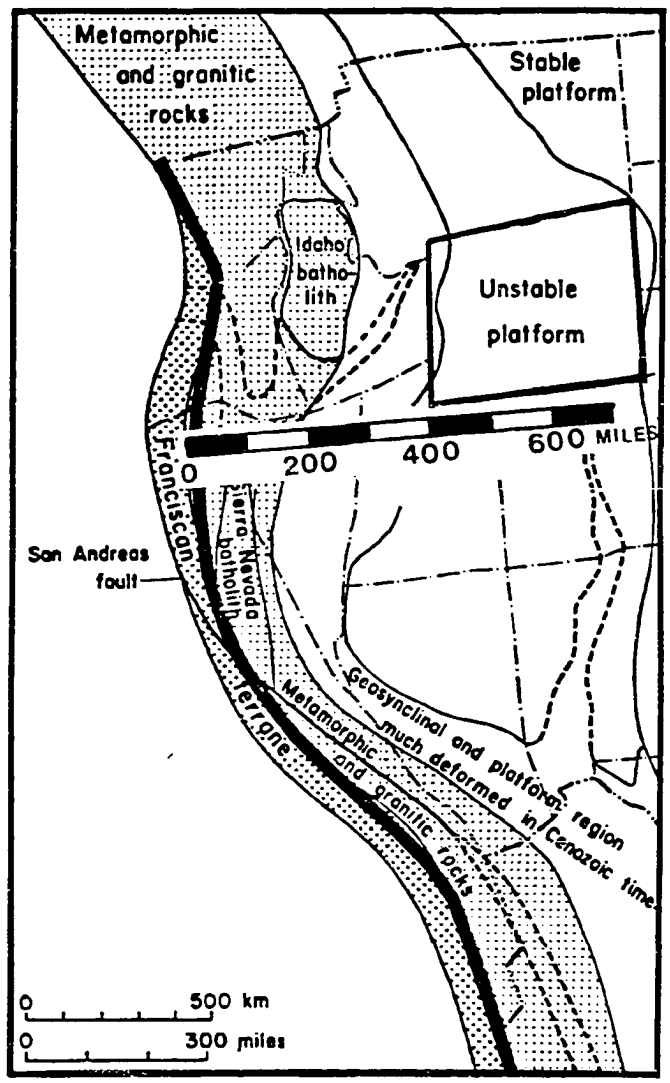

FIGURE 13. Palinspastic restoration of western North America to a time immediately after Laramide orogeny, and pre-Basin and Range taphrogeny (extension). Wyoming foreland was located approximately 500 to 700 miles (800 to 1100 km) east (inland) of the associated subduction zone during the Laramide orogeny. This is comparable to the location of the Andes mountain ranges and the Chile-Peru subduction zone today (modified from Hamilton and Meyer, 1966).

FIGURE 14. Shirley Mountain area, southcentral Wyoming. A) State Geologic Map (modified from Love and others, 1955) showing northeast-trending faults in the Precambrian basement which offset the northwest-striking mountain front with right-lateral separation. B) Aerial photograph shows the coincidence of northeast-striking faults in the basement, and Precambrian igneous dikes (indicated by the alignment of arrows.)

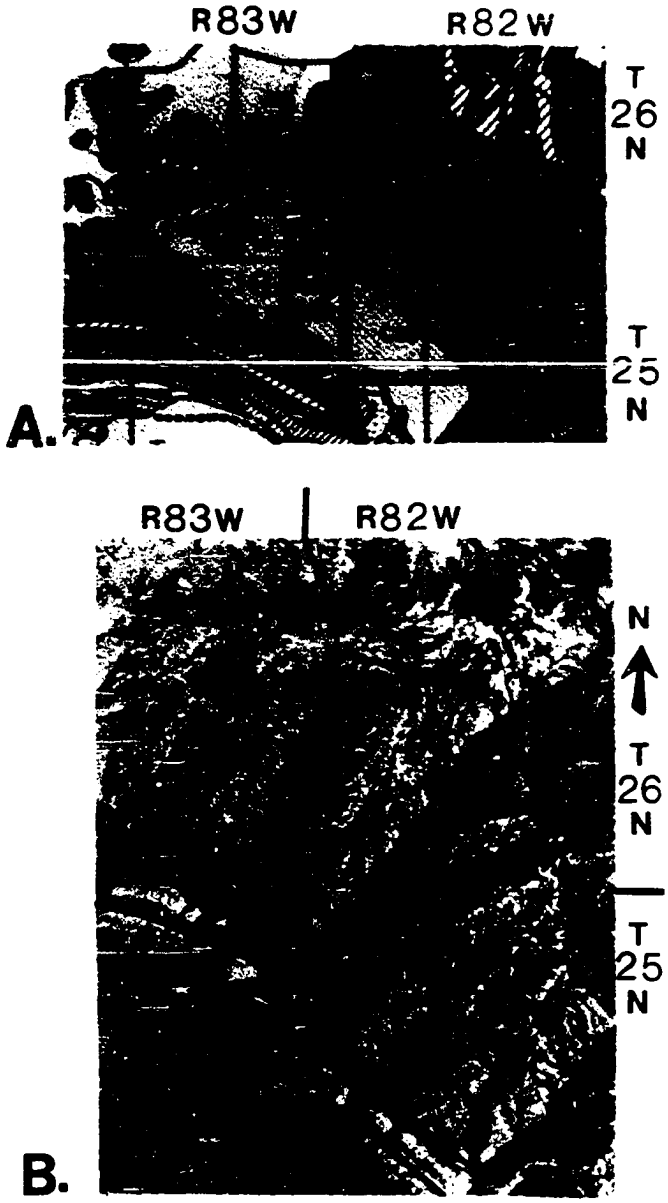

FIGURE 15. Outcrop of the Precambrian basement of the Owl Creek Mountains, exposed in the canyon of the Wind River (sec. 33, T.6 N., R.6 E, WRM). Basement rock is a garnet-grade schist (dark), intruded by pink granite pegmatite (light colored). The pegmatite is directly overlain by the Cambrian Flathead Sandstone. South of this outcrop the pegmatite is absent.

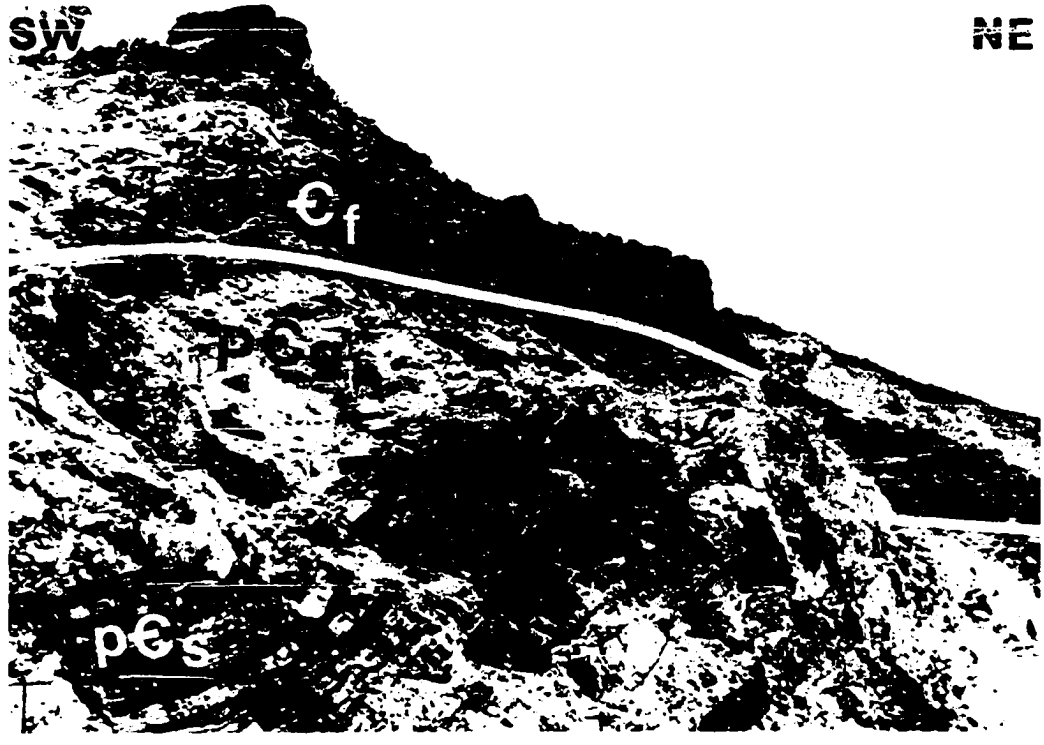

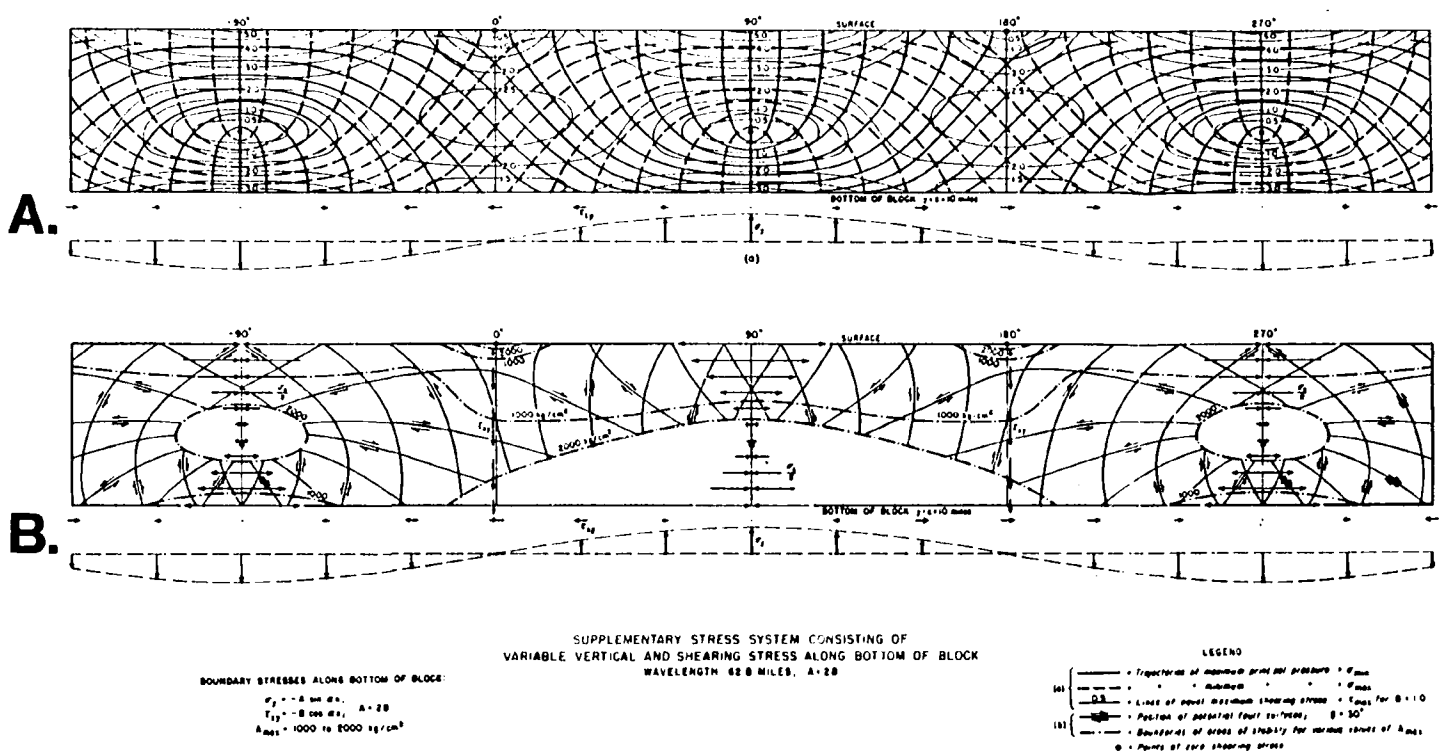

FIGURE 16. Mathematical model for stress distribution and fault plane orientations for differential vertical uplift (after Hafner, 1951). A) Stress trajectories calculated for a sinusoidal, differential vertical stress. B) Fault plane orientations interpreted from stress distribution in (A), above. Note that the uplifted portion (left side) of the model displays normal faulting, while the downthrown portion (right side) displays reverse faults. Downward steepening reverse faults (U) are classified as upthrust faults (after Hafner, 1951).

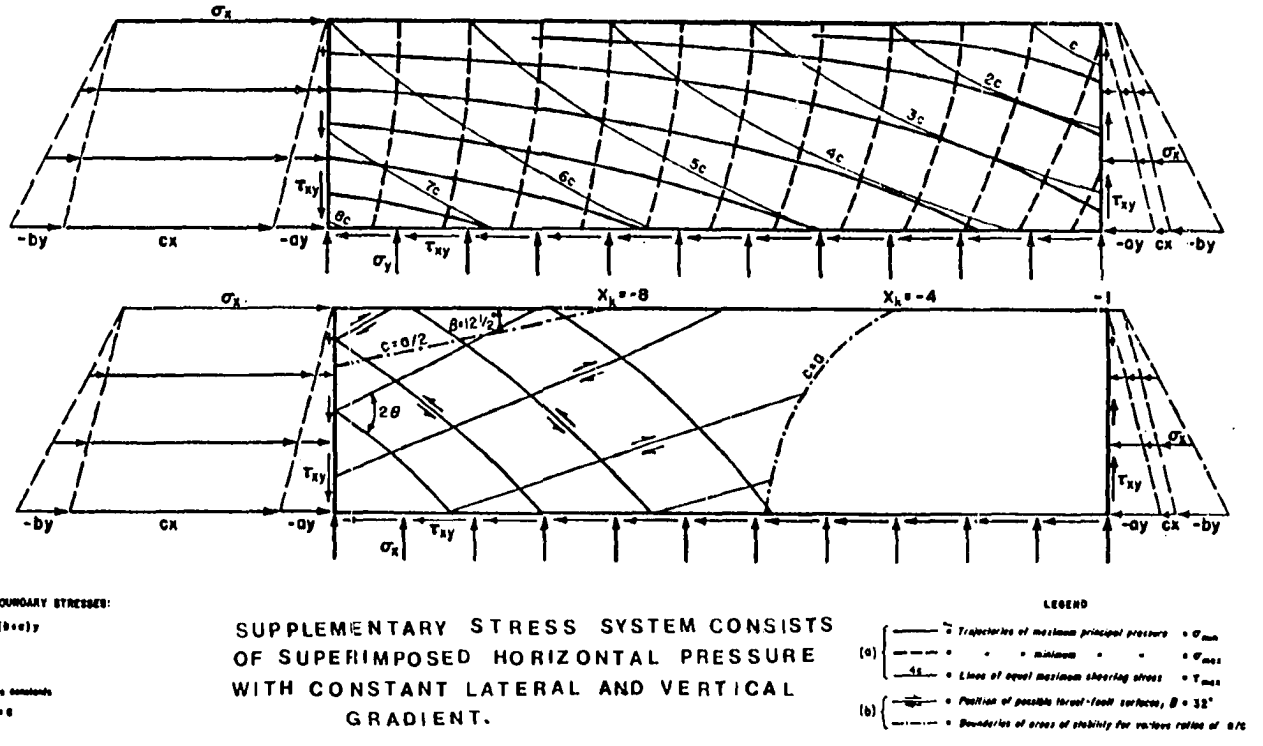

FIGURE 17. Mathematical model for stress distribution and fault plane orientations for horizontal compresssion (after Hafner, 1951). A) Stress trajectories calculated for horizontal compression. B) Fault plane orientations interpreted from stress distribution in (A), above. Note that resulting fault pattern is that of a conjugate set of reverse faults, both of which dip at less than 45 degrees, with the left-dipping fault being slightly concave upward (after Hafner, 1951).

FIGURE 18. Experimental models (Types I and II) employing the vertical uplift concept. A) Type I experiment displays crestal graben running parallel to the axis of the resulting model "anticline". B) Type II experimental model resulting in the development of the upthrust reverse fault geometry (concave downward), and associated normal faults on the upthrown block. (After Sanford, 1959).

No. 19 Material 2

(GRID LINES ARE 0.5 CM APART)

FIGURE 1. — TYPE I EXPERIMENT

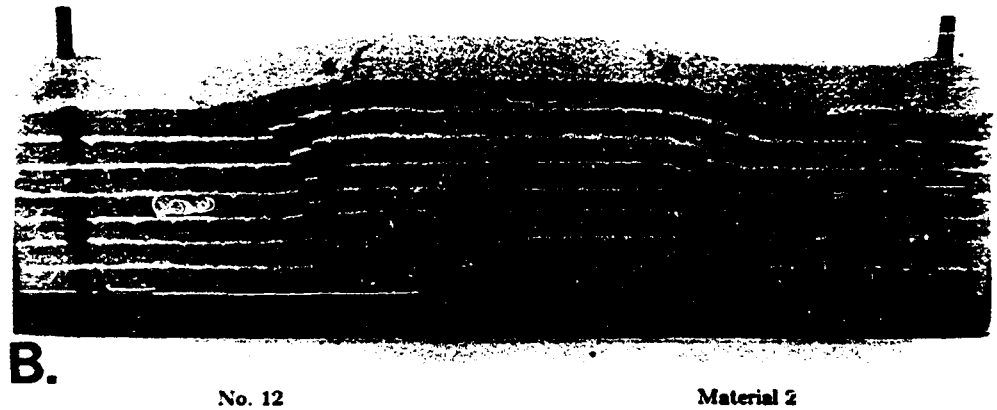

No. 12 Material 2

(GRID LINES ARE 0.5 CM APART)

FIGURE 2. — TYPE II EXPERIMENT

VERTICAL UPLIFT EXPERIMENT

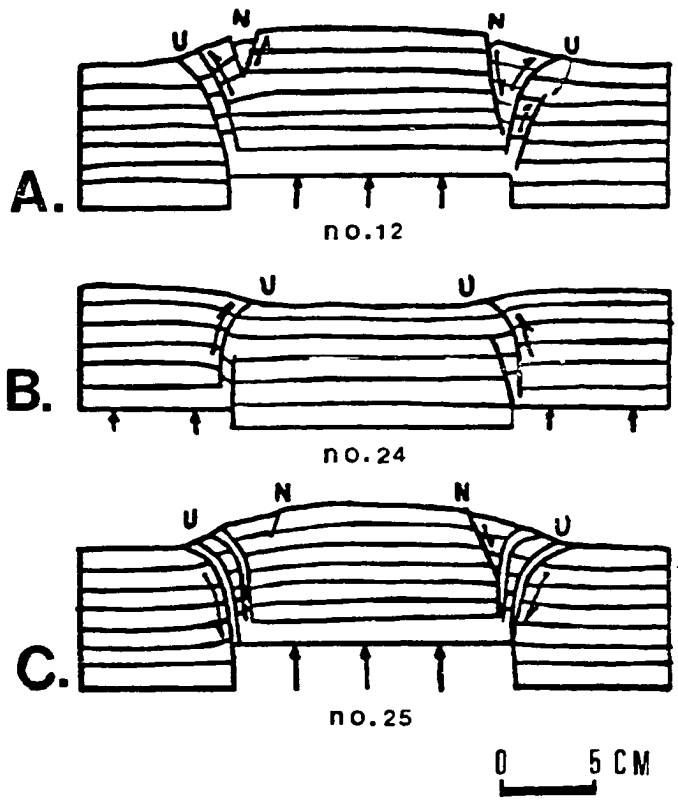

FIGURE 19. Line drawing of the Type II vertical uplift model shown in figure 18 (after Sanford, 1959). Horizontal lines are reference lines and do not represent true stratigraphic bedding. Vertical uplift along a discrete boundary (fault) resulted in development of an uplift bounded by upthrust faults in (A). Note development of prominent normal fault inboard of the right side upthrust fault, on the upthrown block in (A) and (C).

FIGURE 20. Outcrop of Precambrian granite pegmatite in Wind River canyon (T.6 N., R.6 E., WRM). Horizontal joints are probably relict sheeting joints which devel- oped due to erosional unloading of the granite during an extended period of erosion before depositon of Cambrian Flathead Sandstone. Material which fills the sheeting joints may be either weathered granite, or gouge, which could have developed as a result of differential slip of the granite along the pseudo-bedding planes during the Laramide orogeny.

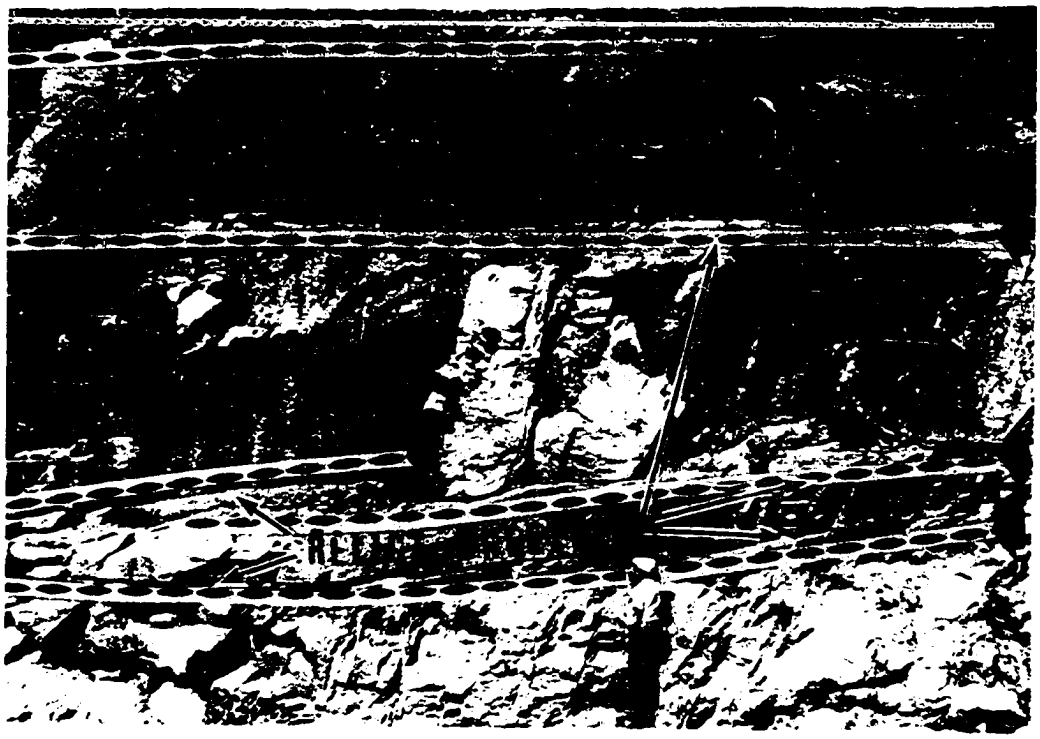

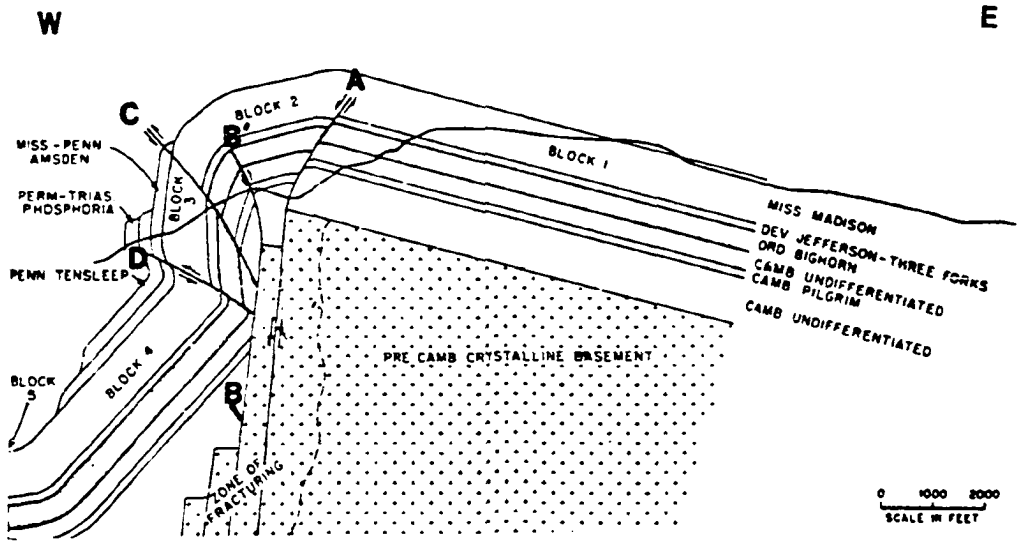

FIGURE 21. Vertical uplift interpretation of Rattlesnake Mountain anticline, (near Cody, Wyoming; T.52 N., R.103 W.) as a drape fold. Annotations (A, B, B', C, and D) added by this author and referred to in text (Brown, 1984).

FIGURE 22. View to the southeast of Precambrian basement surface exposed in the south canyon wall of the Clarks Fork River, southeastern Beartooth Mountains (T.56 N., R.103 W.). Basement surface is on the upthrown side of the East Beartooth fault, and dips progressively more steep towards the east as it approaches the reverse fault as indicated. Position of erosional gulleys (shown by white lines below basement surface) may be controlled by zones of cataclastic deformation in the basement. Approximately 1,000 feet (300 m) of vertical relief on the basement surface is visible in the photograph without any apparent faulting.

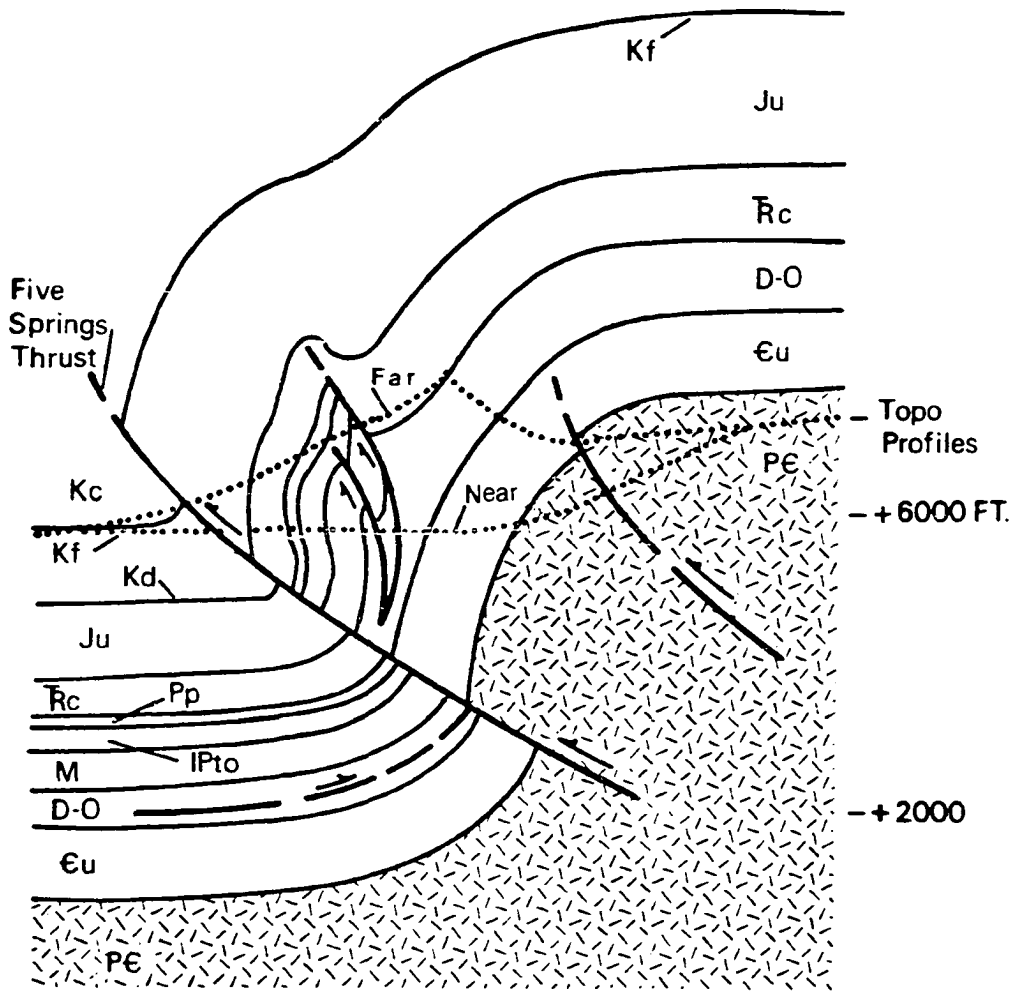

FIGURE 23. Precambrian basement exposed on the upthrown block of the Five Springs thrust on the west flank of the Bighorn Mountains (T.56 N., R.92 W.). The area between the two topographic surface lines is exposed in canyon of Five Springs Creek. Basement surface dips westward in conformity with the sedimentary section between the two reverse faults, while it displays flat, planar dip on the upthrown block at the east end of the section.

FIGURE 24. Precambrian basement surface exposed on the north canyon wall of the Clarks Fork River dips 45 degrees east (toward Bighorn basin) in conformity with the overlying sedimentary section. Exposure is on the downthrown side of the East Beartooth fault.

FIGURE 25. Porcupine Creek anticline, west flank of the Bighorn Mountains (T.55 N., R. 91 W.). Controlling reverse fault is exposed at Precambrian level with the basement surface being flat and planar on the upthrown (east) side. On the downthrown side, the basement surface and overlying sedimentary section dip west at approximately 45 degrees. Topographic fault scarp is visible at lower right corner of photograph.

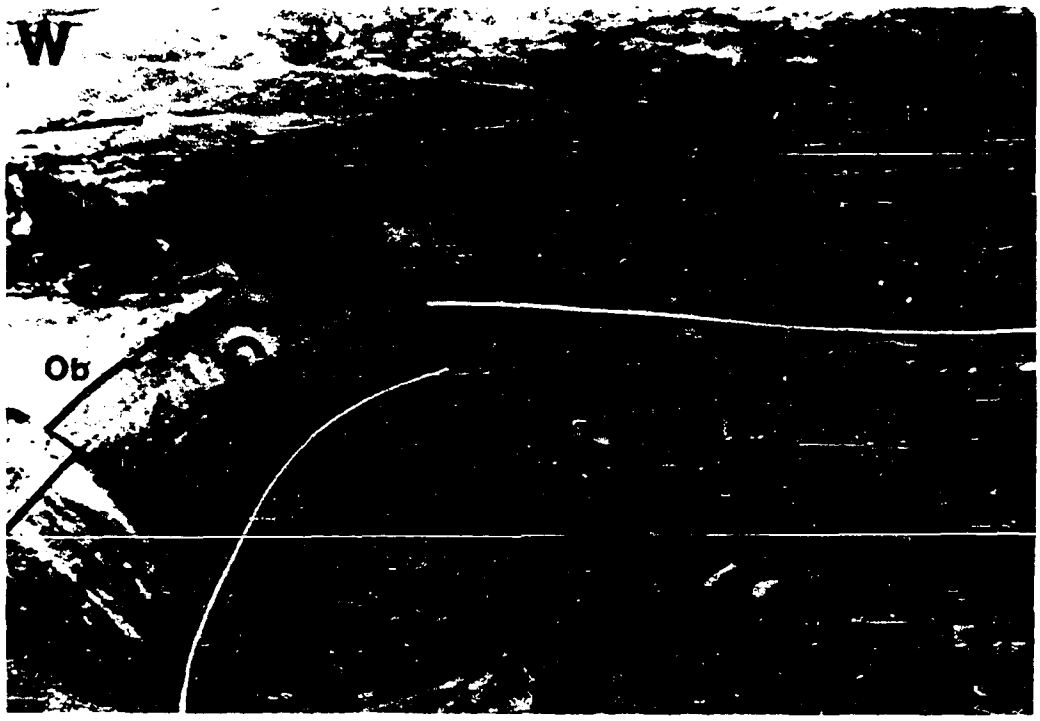

FIGURE 26. Cow Creek-Porcupine Creek area, west flank of Bighorn Mountains (T.55 N., R. 91 W.). A) Southwest to northeast cross section showing interpreted synclinal basement structure on the downthrown side of Porcupine Creek fault, and its relationship to mountain front. B) Photograph of exposed synclinal flexure on Precambrian basement (from Hoppin, 1970) surface approximately six miles (9 km) northwest along trend of Porcupine Creek structure (near Pete's Hole).

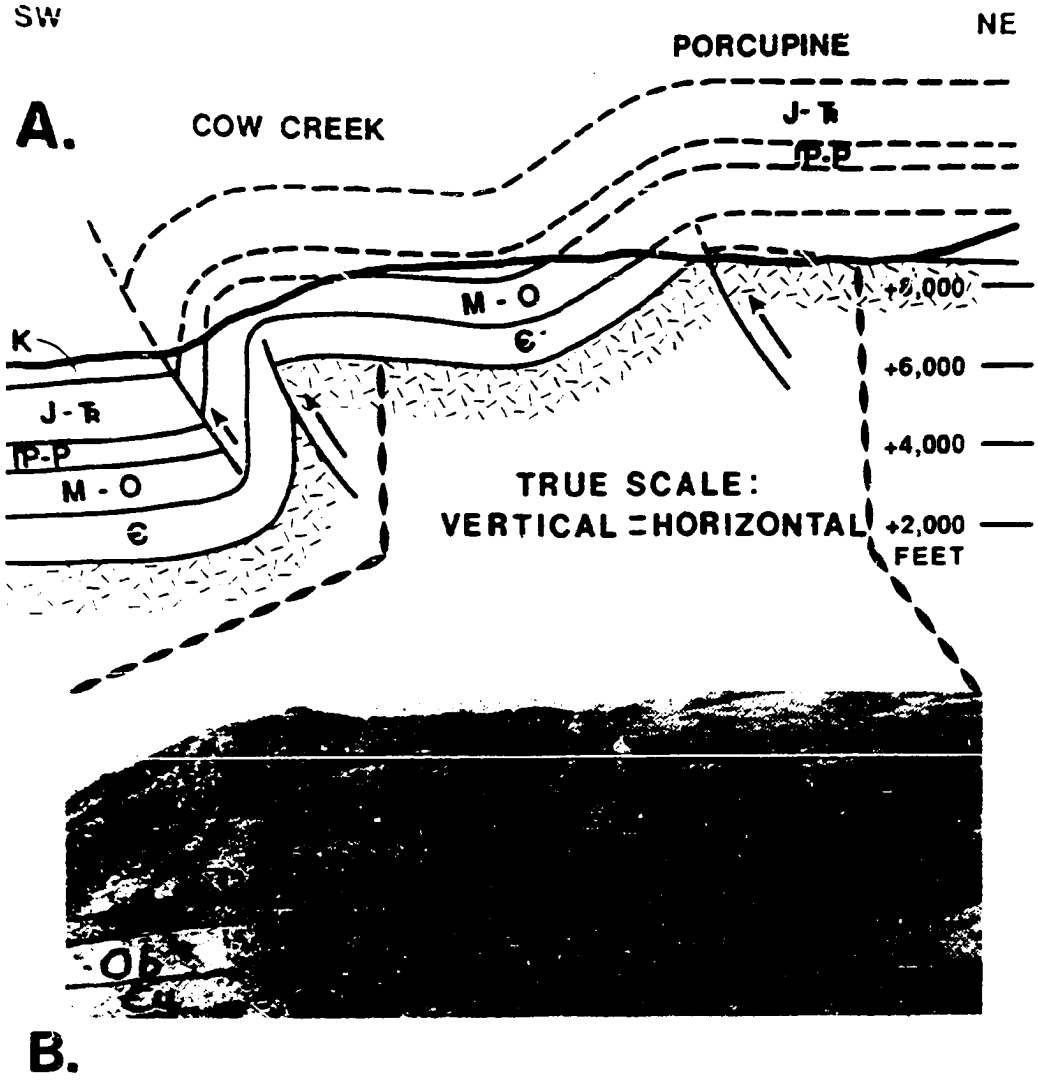

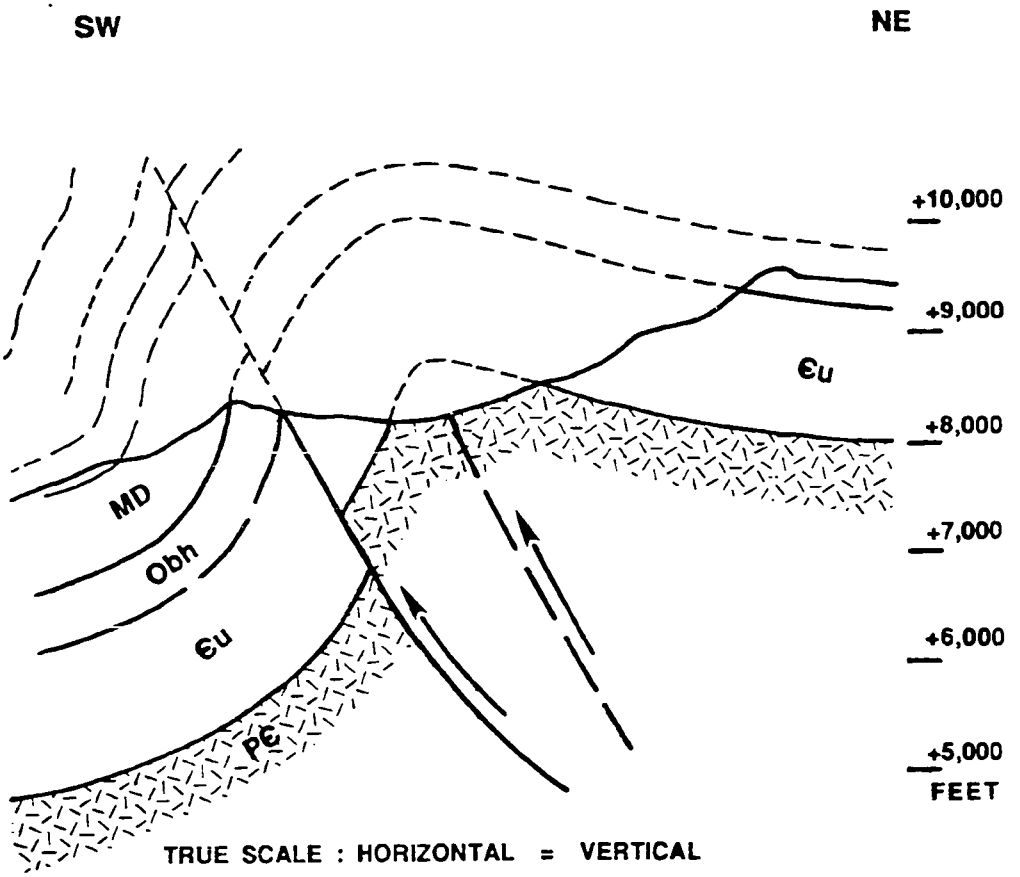

FIGURE 27. Core of Porcupine Creek anticline exposed in the Hunt Mountain area (T.55 N., R.91 W.) of the Bighorn Mountains displays approximately 4,500 feet (1400 m) of structural relief on basement surface by combined dip and fault offset. If fault offset is palinspastically removed, basement anticlinal form remains, indicating folding and/or rotation of basement surface preceded fault offset at that level.

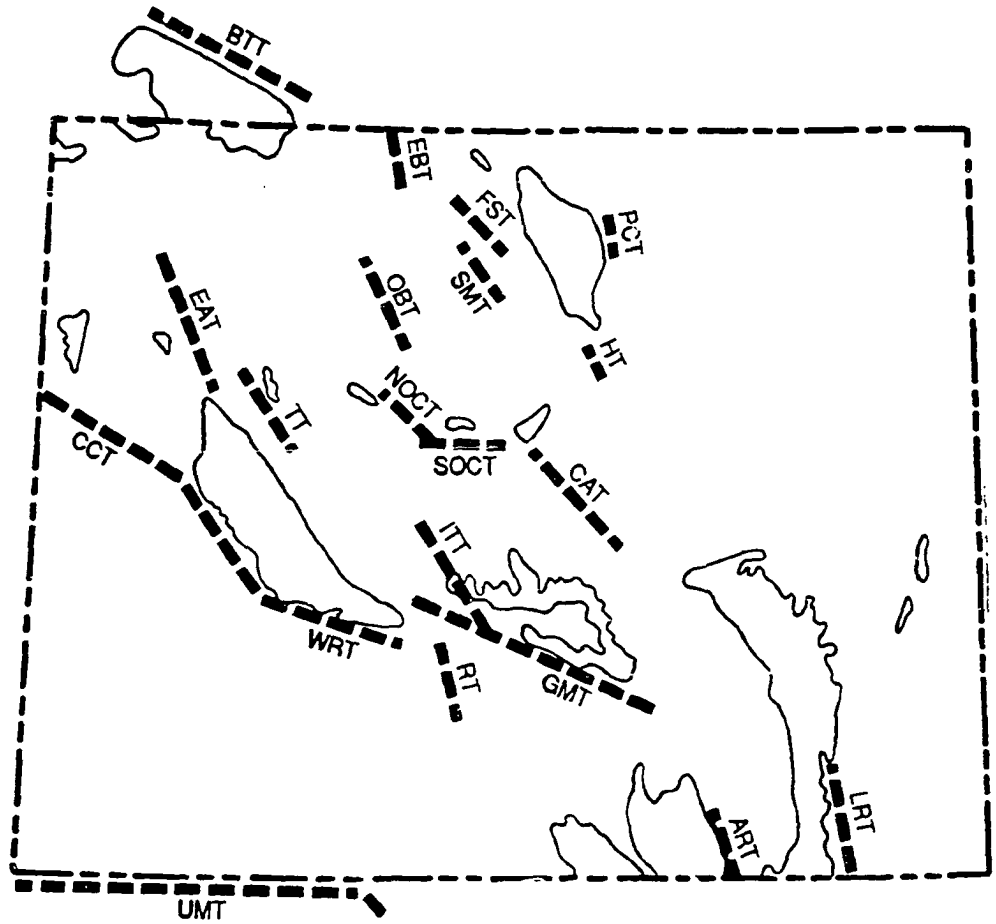

FIGURE 28. Index map of Wyoming foreland showing location and orientation of low angle (45 degrees, or less) reverse faults. Symbols: ART-Arlington thrust; BTT-Beartooth thrust; CAT-Casper arch thrust; CCT-Cache Creek thrust; EAT-EA thrust; EBT-Elk Basin thrust; FST-Five Springs thrust; GMT-Granite Mountains thrust; HT-Horn thrust; ITT-Immigrant Trail thrust; LRT-Laramie Range thrust; NOCT-North Owl Creek thrust; OBT-Oregon Basin thrust; PCT-Piney Creek thrust; RT-Rawlins thrust; SMT-Sheep Mt. thrust; SOCT-South Owl Creek thrust (shallow); TT-Tripod thrust; UMT-Uinta Mountain thrust; WRT-Wind River thrust.

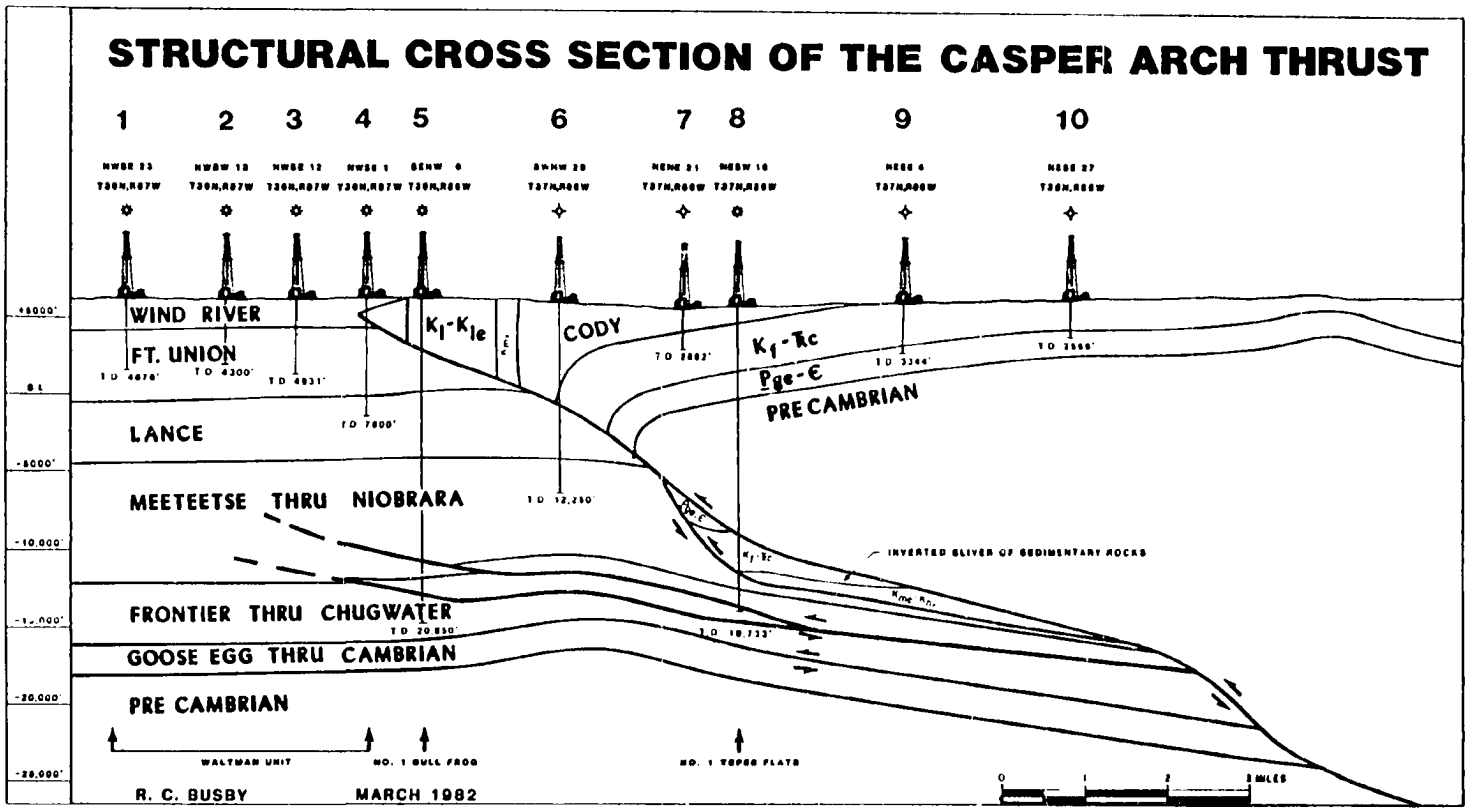

FIGURE 29. Structural section across west flank of Casper arch. Geometry of Casper arch thrust determined from well control and reflection seismic data. Numbering of wells added for discussion in text (modified from Skeen and Ray, 1983).

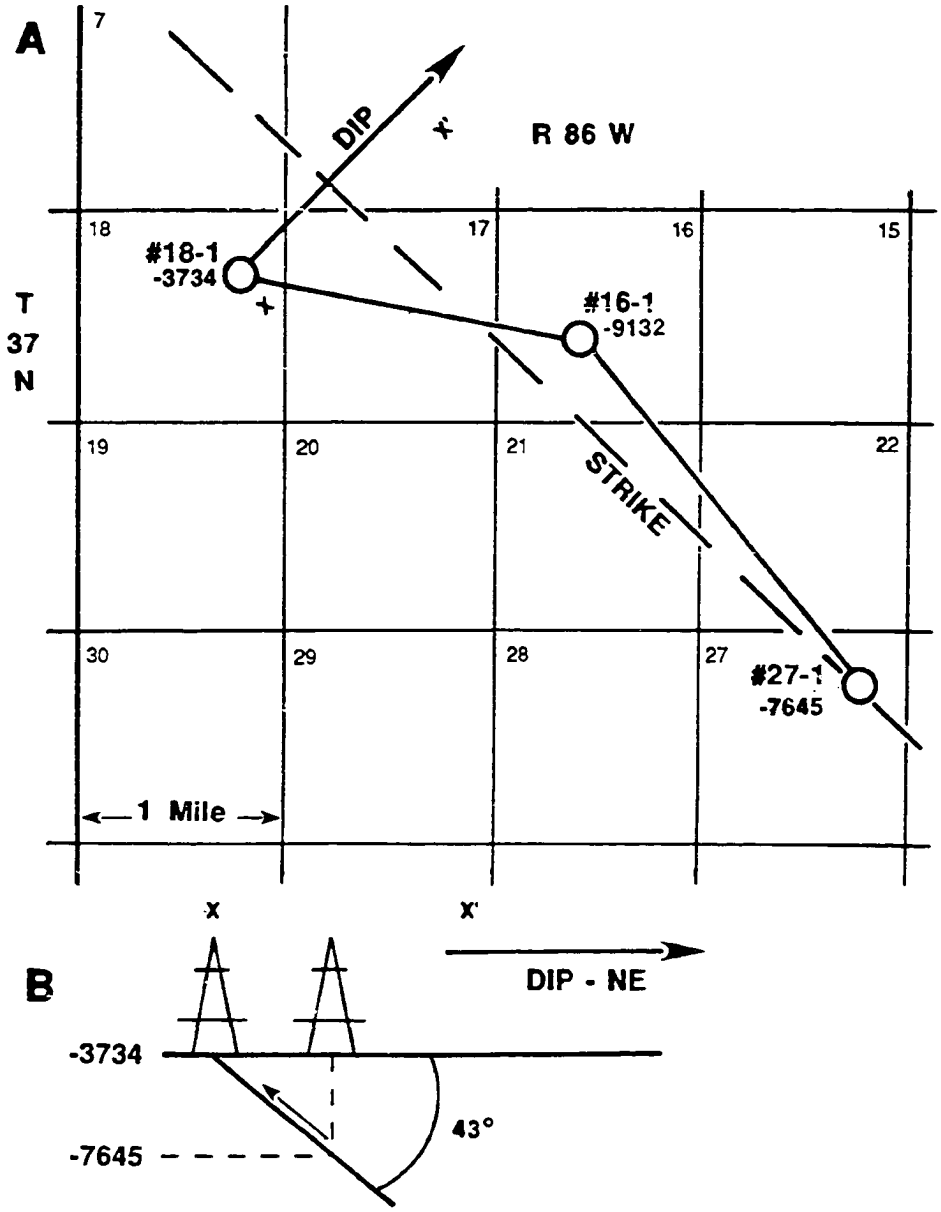

FIGURE 30. West flank of Casper arch (T.37 N., R.86 W.). A) Three-point calculation of dip of Casper arch thrust, using wells which cut the fault plane after drilling through the Precambrian basement overhang. B) Casper arch thrust dips 43 degrees to the northeast under the Precambrian basement.

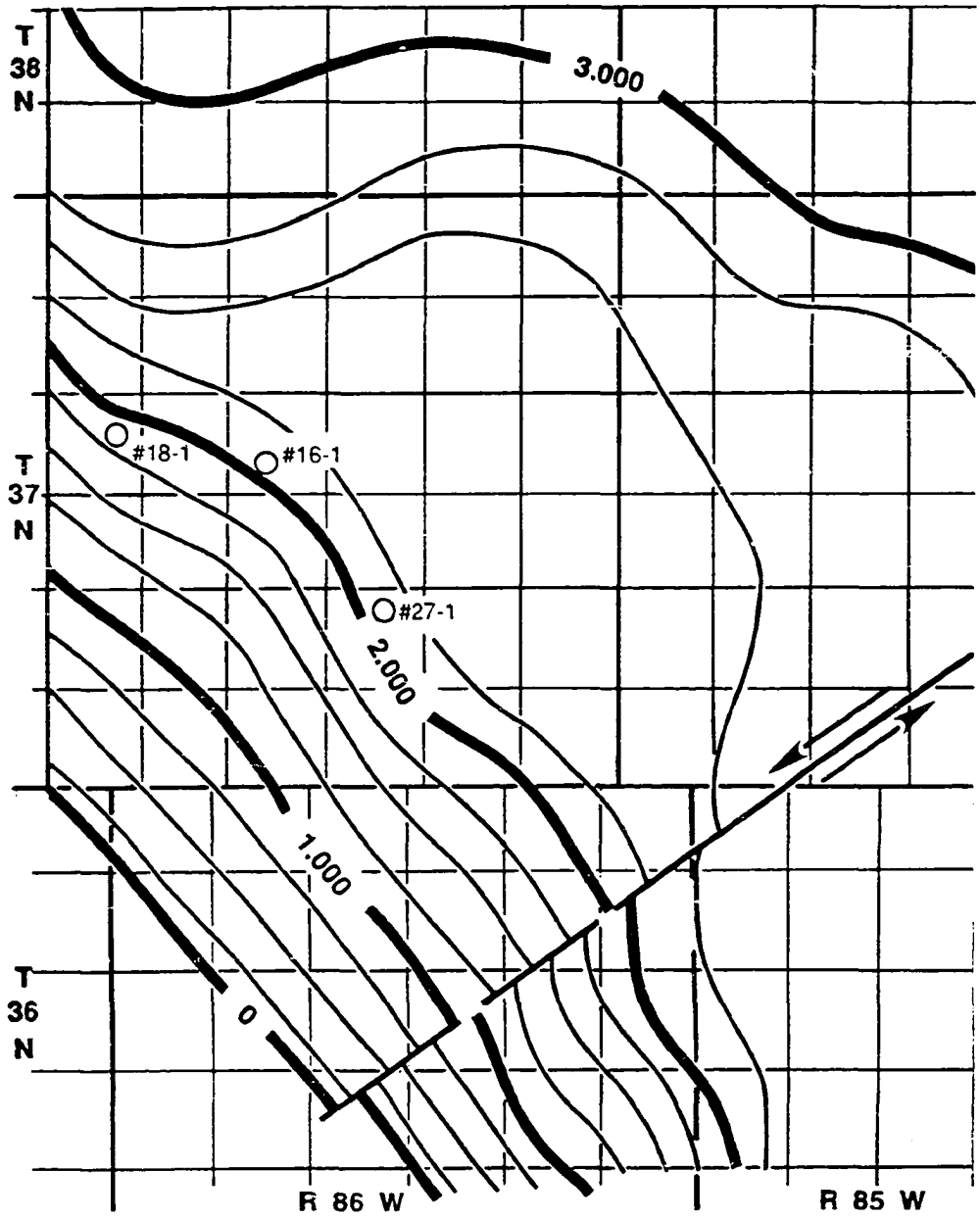

FIGURE 31. Seismic time-structure contour map of the Casper arch thrust. Flattening of thrust plane to the northeast is indicated by wider spacing of contours. This flattening of the fault plane takes place northeast of (and under) the Precambrian overhang indicated in figure 30, and indicates a stair-step arrangement of the fault (after Skeen and Ray, 1983).

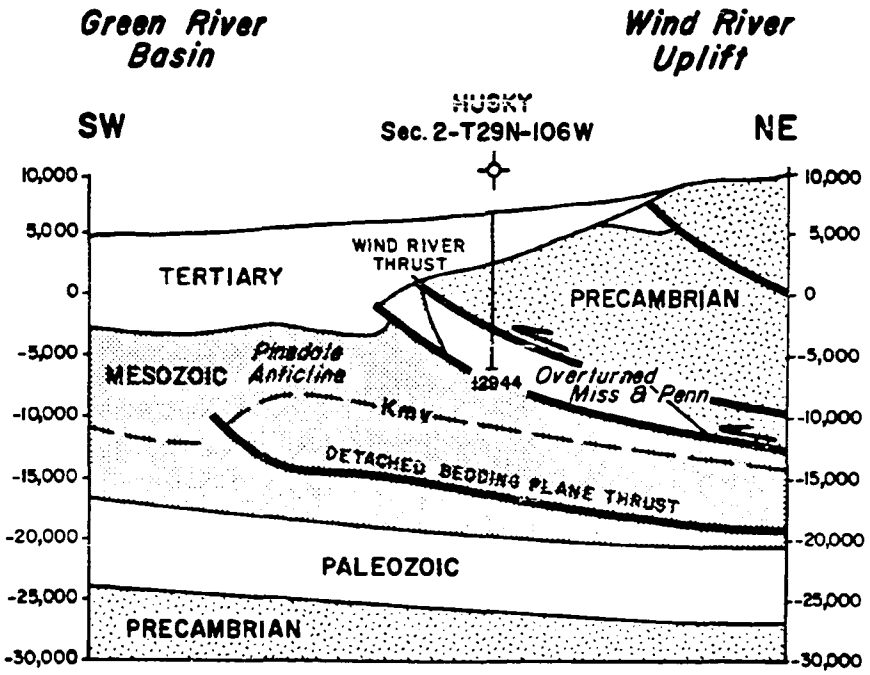

FIGURE 32. Southwest flank of the Wind River Mountains uplift (T.29 N., R.106 W.). Husky Oil drilled the first well to penetrate the Precambrian basement overhang of this major foreland uplift. Well drilled through 6,247 feet (1900 m) of basement rock before faulting into overturned Paleozoic sedimentary rocks (after Gries, 1983).

FIGURE 33. Reflection seismic line across the southwestern margin of the Wind River Mountain uplift. Husky Oil well has been projected into line of section at position where it drilled through the Precambrian overhang. The mountain-bounding fault is a low angle reverse fault which flattens to the northeast, at the right-hand end of the section. Note the seismic velocity "pull-up" under the Precambrian basement overhang which results from higher seismic velocities through the granite (after Lowell, 1983).

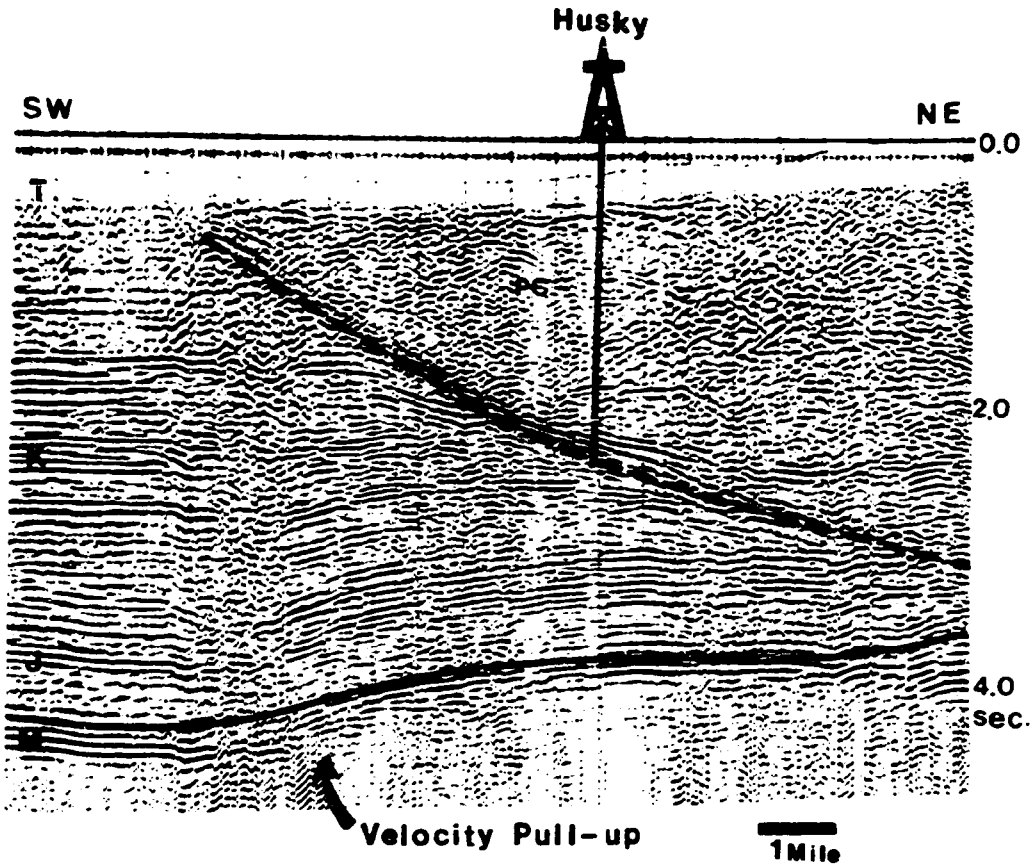

FIGURE 34. Gravity study of the northeast flank of the Beartooth Mountains uplift (T.8 S., R.20 E., Montana). A) observed Bouguer gravity profile across the mountain flank near Red Lodge, Montana. B) Structural model 1 using the vertical block uplift concept (after Foose and others, 1961). C) Structural model 2 using a low angle thrust (after Thom, 1955, 1957). D) Comparison of gravity profiles calculated for models 1 and 2 show that model 2 (low angle thrust) provides the "best-fit" to the observed gravity. Basement overhang determined from model 2 is approximately 7.5 miles (12 km; after Bonini and Kinard, 1983).

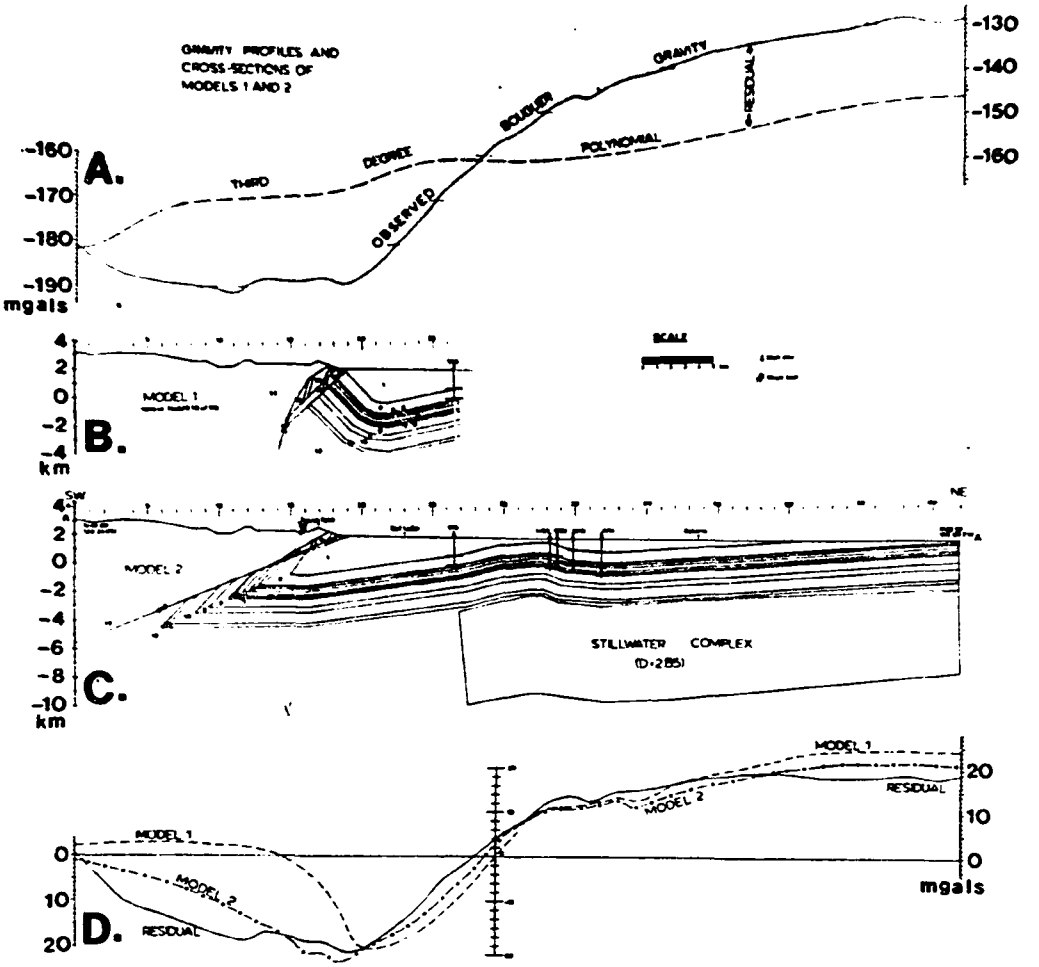

FIGURE 35. North flank of the Owl Creek Mountains, central Wyoming. A) Geologic map (modified from Love and Christiansen, 1985) showing the internal structures, and the North Owl Creek fault (NOCF) which bounds the uplift. NOCF changes strikes from northwest, to west in T.8 N., R.2 E. (WRM), where it appears to truncate several Precambrian cored anticlines on the south side of the fault. Locations for photographs in figures 35b and 38, and cross section in figure 159 are shown. B) Photograph of NOCF along its northwest trend shows Paleozoic rocks thrust to the northeast over overturned Triassic beds, along a low angle reverse fault which dips 20 degrees to the southwest.

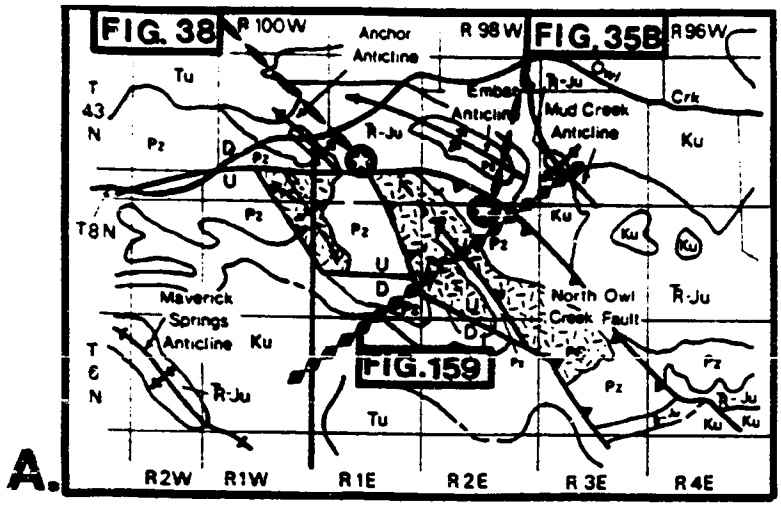

FIGURE 36. New road-cut exposures of Precambrian basement in the hanging wall of the Five Springs thrust fault (T.56 N., R.92 W.). Fractures with shallow dip to the right are small displacement (2-3 feet; 1 m) reverse faults which dip 30 degrees to the northeast.

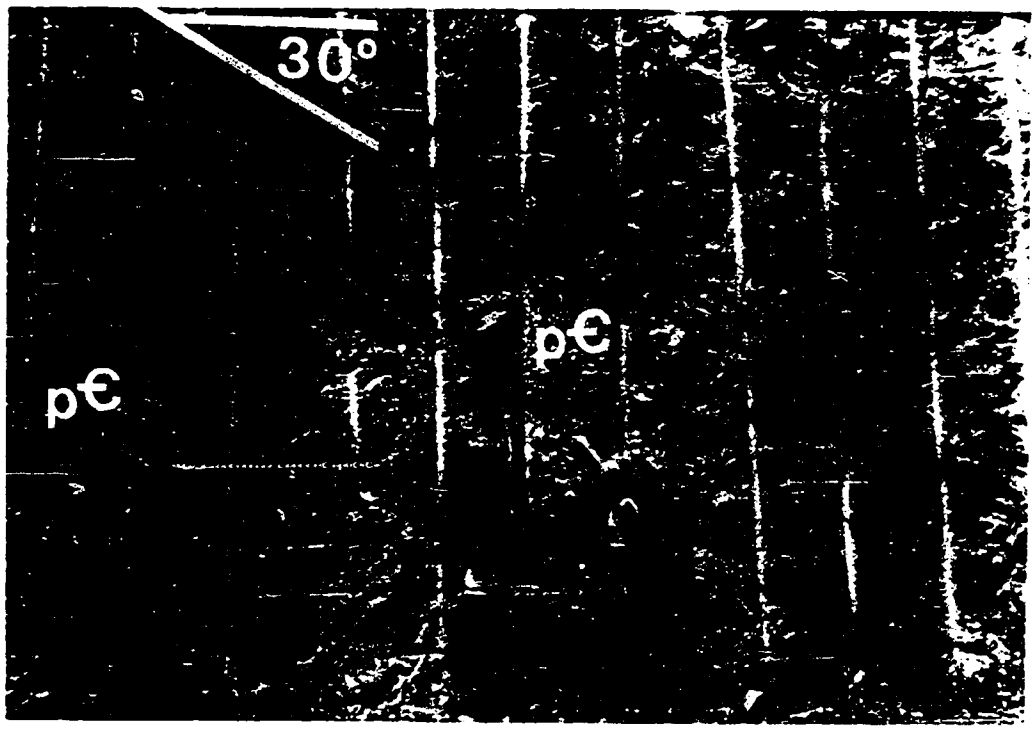

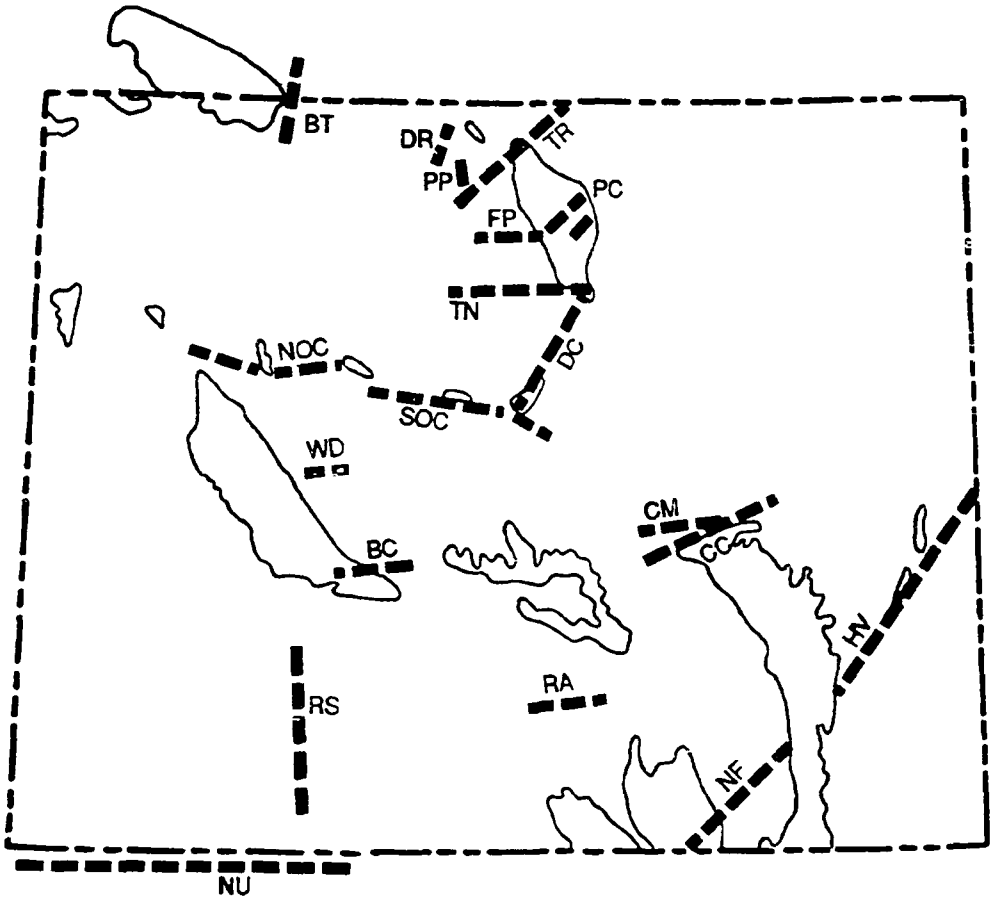

FIGURE 37. Index map of Wyoming foreland showing location and orientation of high angle (45 degree and greater) reverse faults. Symbols: BC-Beaver Creek fault; BT-East Beartooth fault; CC-Corral Creek fault; CM-Casper Mountain fault; DC-Deep Creek fault; DR-Deer Creek fault; FP-Florence Pass fault; HV-Hartville fault; NF-Nash Fork fault; NOC-North Owl Creek fault; NU-North Uinta fault; PC-Piney Creek faults; PP-Porcupine Creek fault; RA-South Rawlins fault; RS-Rock Springs fault; SOC-South Owl Creek fault (deep); TN-Tensleep fault; TR-Tongue River lineament; WD-Winkleman fault.

FIGURE 38. West view of north flank of Owl Creek Mountains, along trend of North Owl Creek Fault (NOCF) in T.8 N., Rs.2 E. to 1 W. (WRM). Fault is high angle reverse (dips 60 to 80 degrees south) with south side (left) upthrown, placing Precambrian basement against Triassic and Upper Paleozoic rocks. Several Precambrian cored anticlines terminate against this fault on the upthrown side. Anchor anticline plunges away from the fault (northward) on the downthrown side, making an acute angle with the NOCF, which suggests left-lateral movement along the fault.

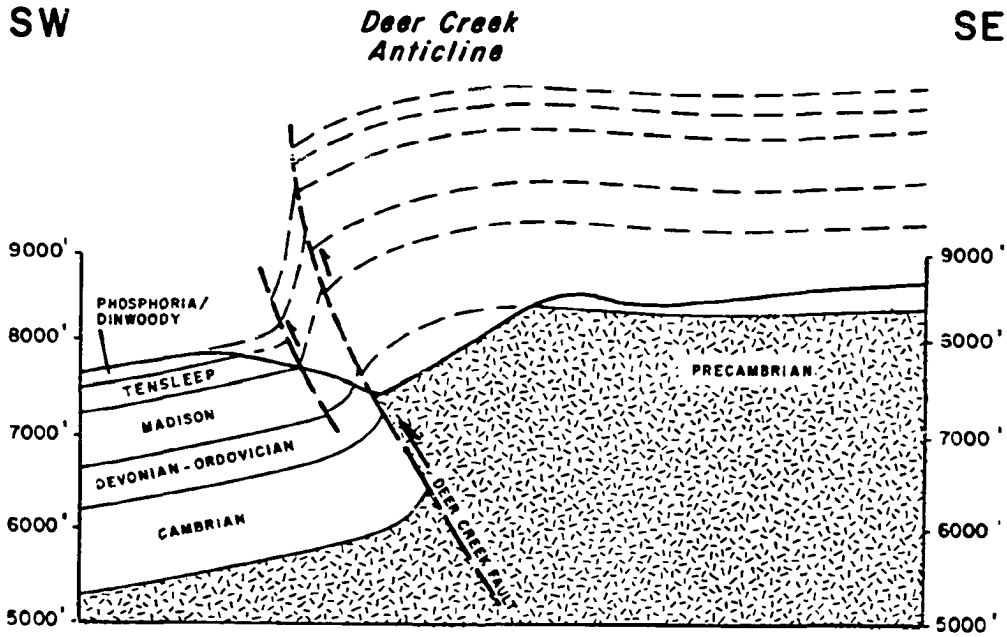

FIGURE 39. Deer Creek anticline, northwest Bighorn Mountains (T.57 N., R.92 W.). Precambrian basement is thrust to west over Devonian to Cambrian beds along the 45-60 degree, east-dipping Deer Creek fault. A second reverse fault is located southwest of Deer Creek fault, and creates a dual fault zone. The sedimentary section between the two faults is rotated and thinned in exposures located down-plunge (Brown, 1983).

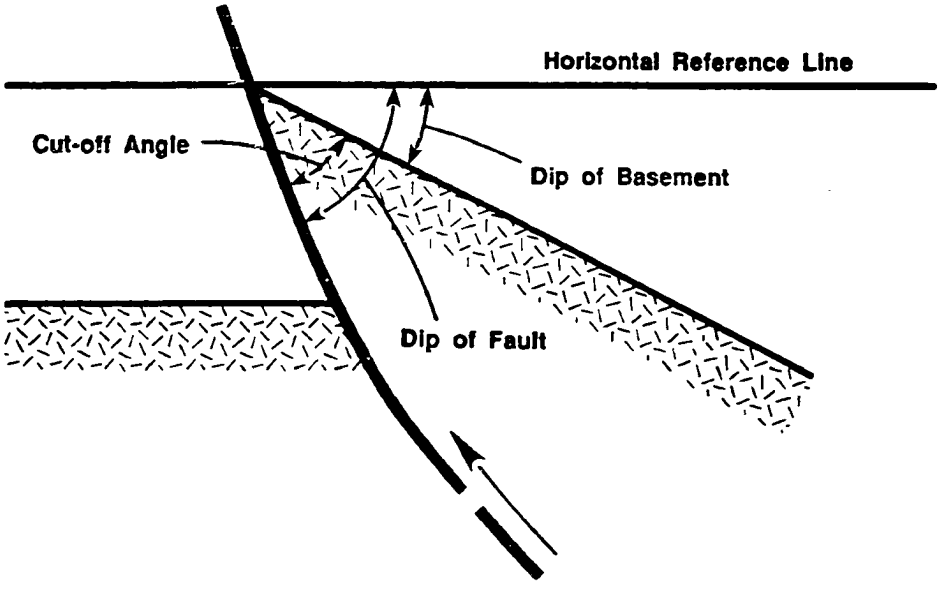

FIGURE 40. Geometry of fault cut-off angle. In this example the cut-off angle is measured between the fault plane and the upper surface of the Precambrian basement. The cut-off angle represents the dip of the fault plane at the time when the basement surface was horizontal, and just before the fault offsets the basement surface. It can also be seen from the diagram that the present-day dip of the fault, minus the present-day dip of the basement surface, equals the basement cut-off angle.

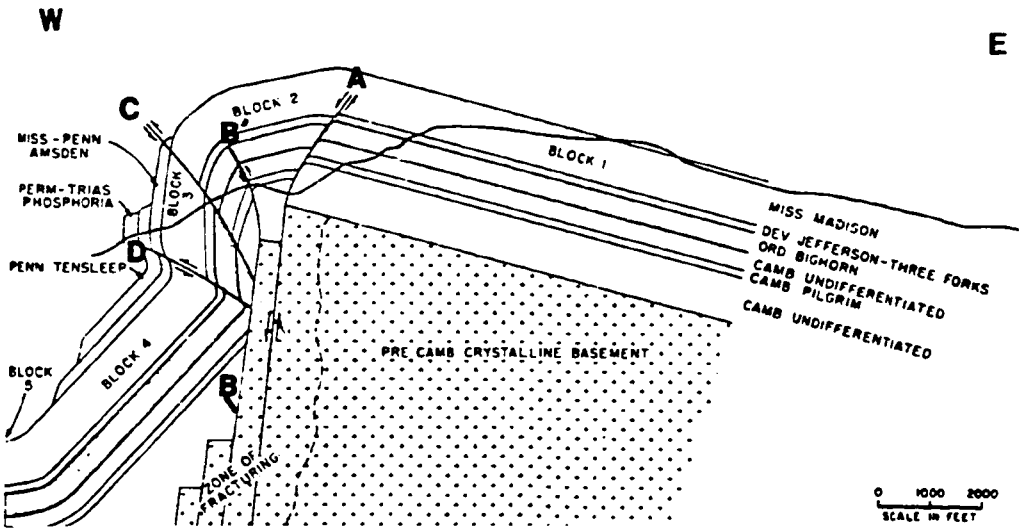

FIGURE 41. Drape fold interpretation of Rattlesnake Mountain anticline (Stearns, 1971; same as figure 21). Normal fault (A) is exposed at the Buffalo Bill dam site. and is considered by many workers to the the controlling fault of the structure. Note that fault (B) has much greater throw than fault (A), but is shown to die out upward into reverse faults (B'and C).

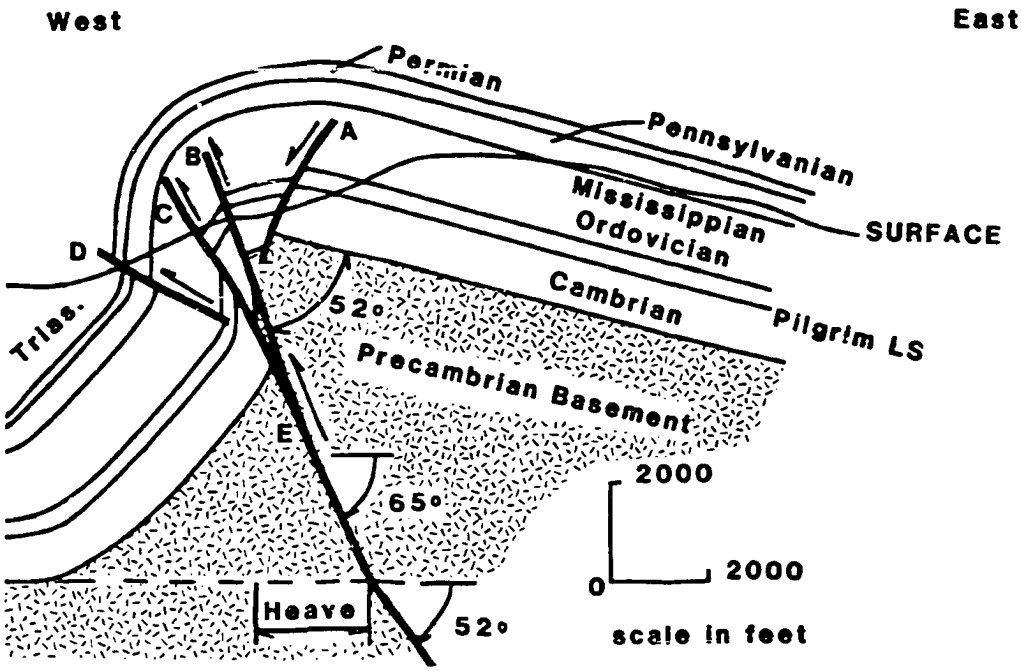

FIGURE 42. Reverse fault interpretation of Rattlesnake Mountain anticline located in T.52 N., R.102 W. (Brown, 1984a; modified from Stearns, 1971). Annotations A, B, C, D, and E refer to fault planes, while X, X', and X'' represent positions along the surface of the Precambrian basement. The controlling reverse fault E is measured to have a dip of 65 degrees to the east, and a heave of 2,250 feet (680 m). Fault E dies out upward into faults B and C. Normal fault A developed from fracturing of the basement block corner. Fault D accommodates volume problems developed by oversteepening of the west flank of the anticline. The fault cut-off angle (52 degrees), measured between fault E and the basement surface, represents the dip of fault E at X''.

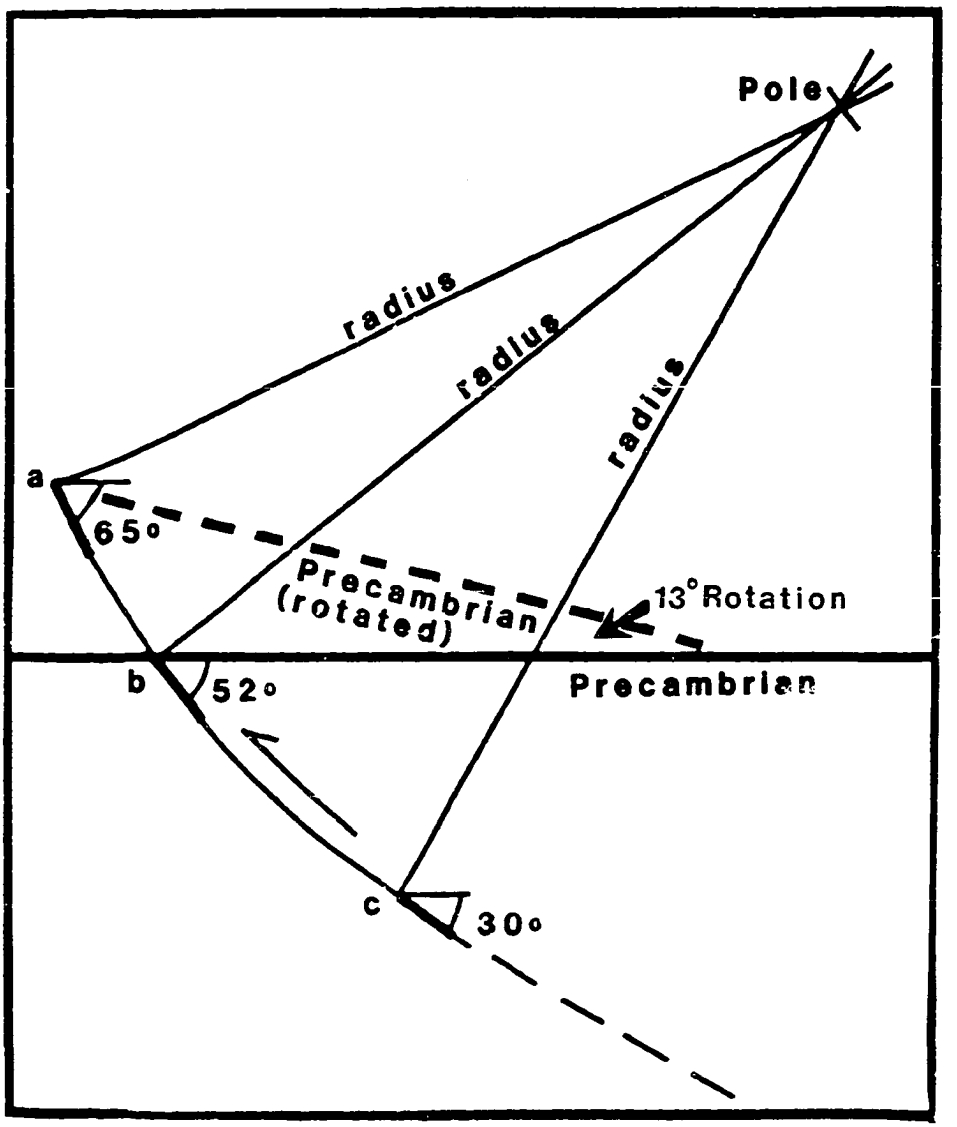

FIGURE 43. Graphic reconstruction of reverse fault geometry at Rattlesnake Mountain anticline. Lines drawn normal to the dip of reverse fault E at the points of present-day dip (65 degrees), and the restored basement cutoff angle (52 degrees), intersect at a pole of rotation. These normals serve as radii, with the pole as the center of curvature, to produce an arc of which reverse fault E is a portion. Movement along fault E with the curvature of the arc shown would have accomplished the 13 degree dip (and rotation) of the basement surface.

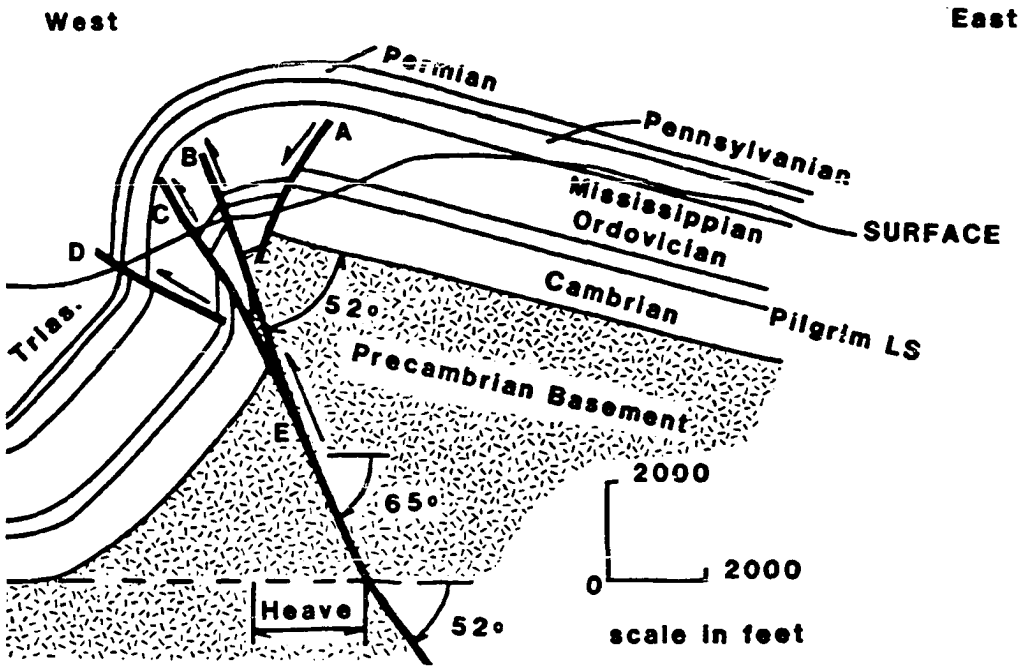

FIGURE 44. Rattlesnake Mountain anticline (Brown, 1984a; same as figure 42) displays a stratigraphic section typical of a "nonwelded, nonthinning" structural-stratigraphic unit (Stearns, 1971, 1978). Cambrian shales act as the nonwelded unit, which separates the nonthinning Paleozoic carbonates from the Precambrian basement.

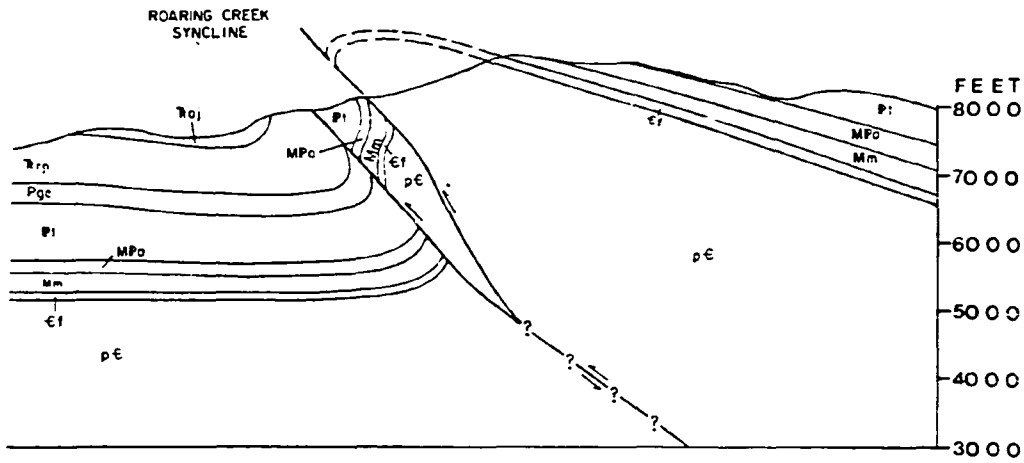

FIGURE 45. Bald Mountain anticline (T.25 N., R.81 W.; Blackstone, 1983) displays a stratigraphic section typical of a "welded, nonthinning" structural-stratigraphic unit (Stearns, 1971, 1978). The Cambrian shales have undergone a facies change into sand which, when combined with the basal Flathead Sandstone, serves to "weld" the overlying "nonthinning" Paleozoic carbonates to the basement.

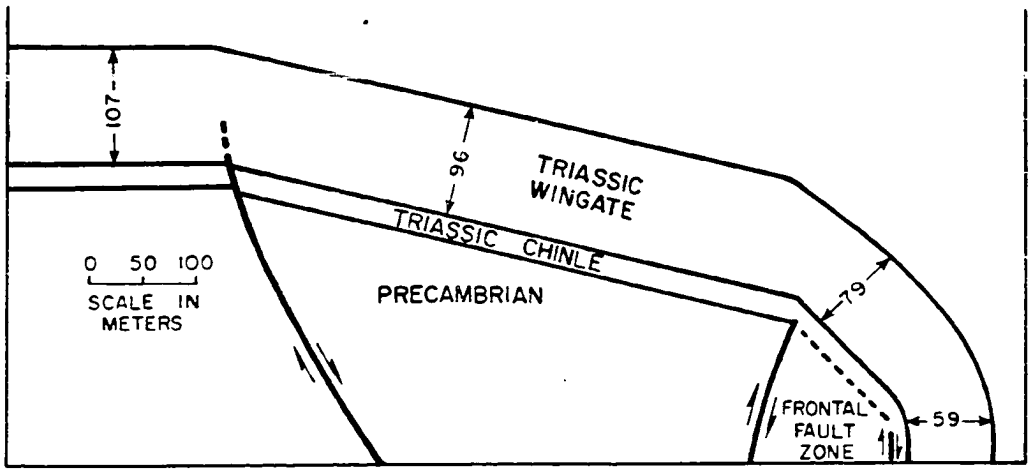

FIGURE 46. Uncompaghre uplift (northwest Colorado) displays a stratigraphic section typical of a "welded, thinning" structural-stratigraphic unit. The Triassic Chinle Formation welds the Wingate Sandstone to the Precambrian basement. The Triassic Wingate Sandstone reacts in a "ductile" manner, thinning by cataclastic flow. Examples of this structural-stratigraphic response in Wyoming have not been published.

COMPOSITE FORELAND STRUCTURE

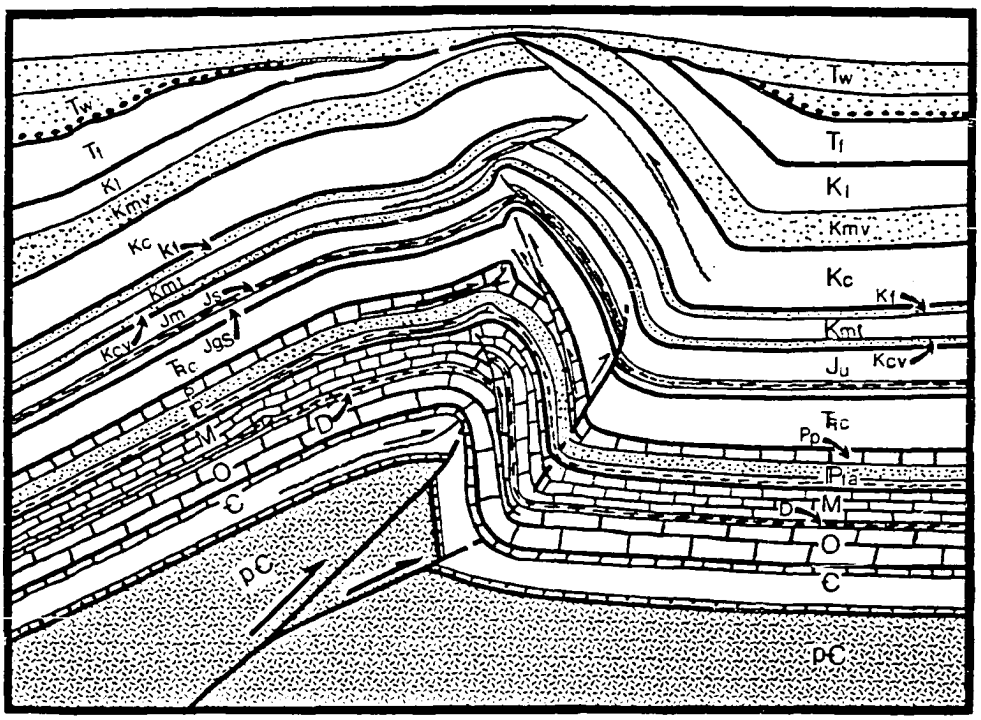

No Scale

FIGURE 47. Composite foreland structure, illustrating multiple zones of detachment, changes in direction of asymmetry, and development of volumetric adjustments such as rabbit-ear and cross-crestal structures. Each of the various features illustrated above may be found on individual structures within the Wyoming foreland. In some cases, all of these may be found on a single structure.

FIGURE 48. Evidence of flexural slip folding at Sheep Mountain anticline (T.54 N., R.94 W.). A) Slickensides on bedding-plane surfaces of Mississippian Madison Limestone. (Pencil on surface of slicks for scale.) B) Small displacement reverse fault in Mississippian Madison Limestone, located on steep east flank of anticline, rises out of bedding-plane slip, and cuts upsection in the direction of tectonic transport.

FIGURE 49. Rabbit-ear fold developed in Mississippian Madison Limestone on the steep east flank of Sheep Mountain anticline (T.54 N., R.94 W.). The ear is developed just below crest of main anticlne, which lies to the west. Limestone beds beneath rabbit-ear dip steeply to the east. (Photograph from Hennier and Spang, 1983.)

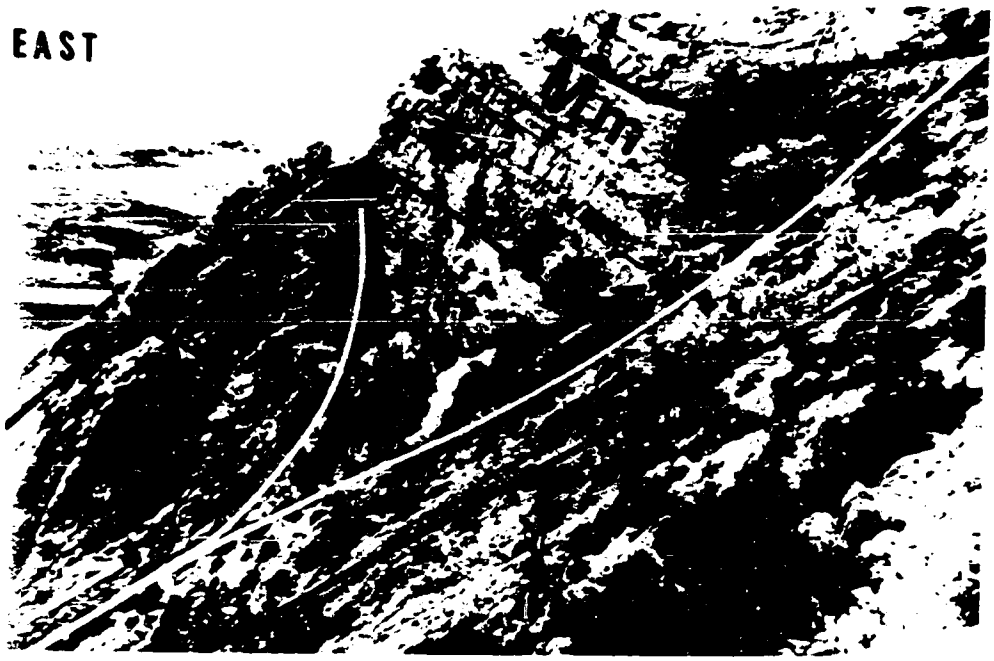

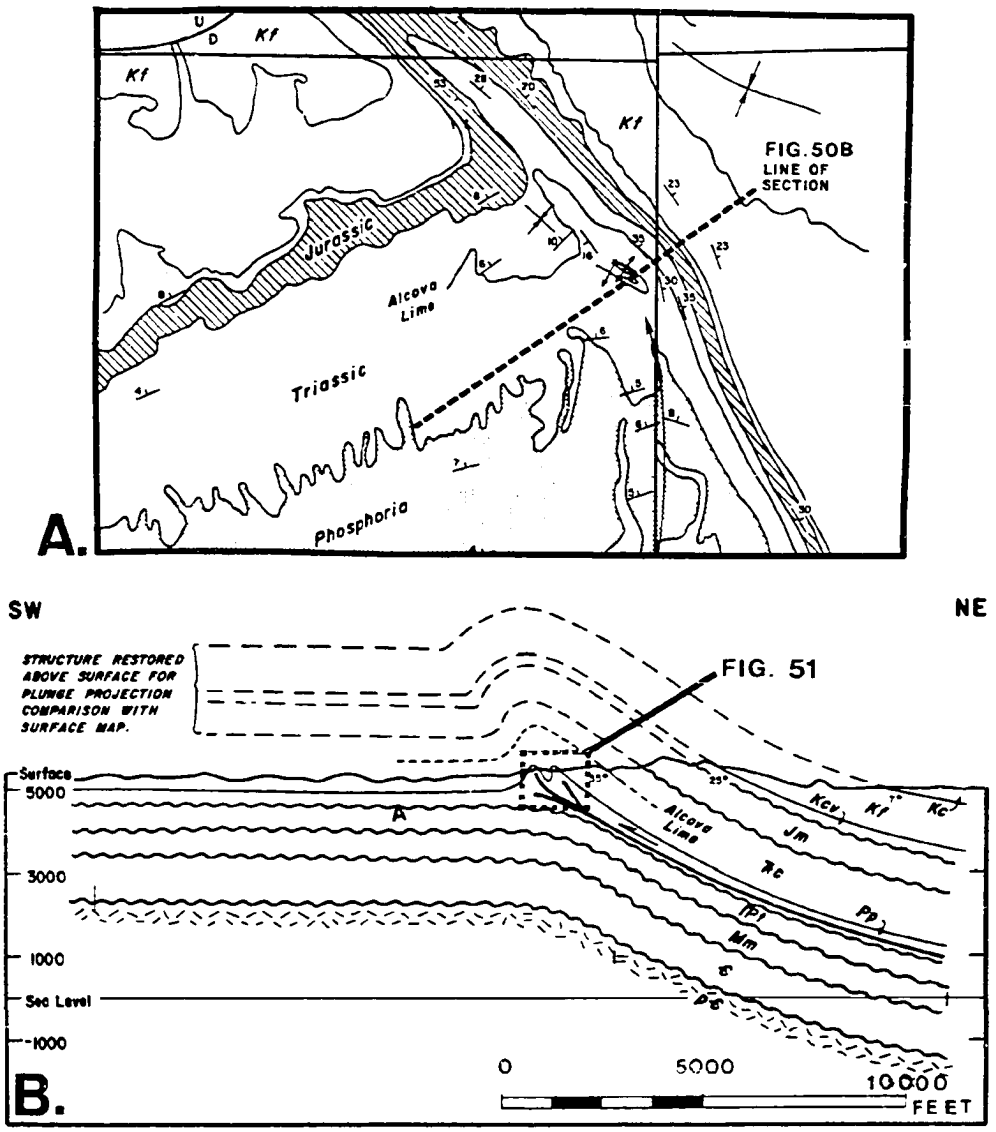

FIGURE 50. Wildhorse Butte anticline (T.42 N., R.92 1/2 W.) is a crowd structure (rabbit-ear) on the flank of the Owl Creek Mountains/Bighorn basin (after Petersen, 1983). A) Geologic map shows the change in strike (from northeast to southwest) in the Permian Phosphoria Formation, forming a "corner" which localizes the rabbit-ear fold. Line of cross section in figure 50b is indicated. B) Structural cross section indicates detachment of the rabbit-ear fold in the Permian carbonates; however, detachment may be at the base of the Pennsylvanian Tensleep Sandstone (in the Amsden Shale). Area of figure 51 is indicated on the cross section.

FIGURE 51. Outcrop of the carbonates of the Permian Phosphoria Formation in the core of Wildhorse Butte anticline. A) Core is comprised of two anticlinal folds, with a thrust-faulted syncline between. The folds and faulting represent volumetric adjustments in the core of a downward-tightening parallel anticline. B) The cherty limestones of the Phosphoria Formation are highly fractured in the tightly folded core of the eastern-most anticline.

A.

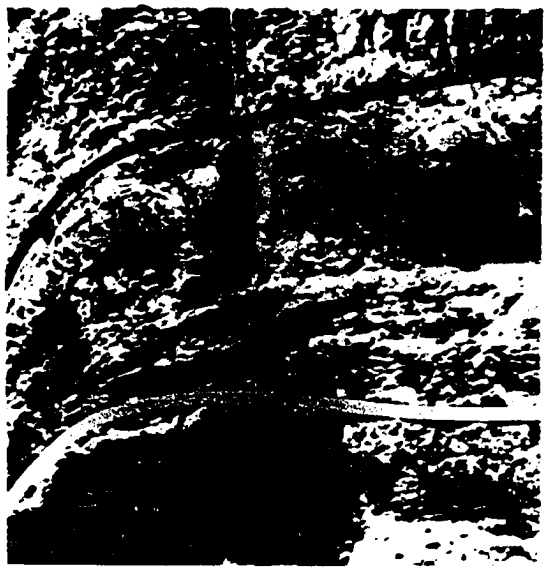

B.

FIGURE 52. Tightly folded and faulted core of West Mud Creek anticline (T.8 N., R.2 E., WRM) is exposed in the Permian Phosphoria Formation. Fold has tightened downward in the parallel manner and volumetric adjustments in the form of thrust faults, can be traced into bedding planes. At the bottom center of the photograph, the fold can be seen to return to a more open degree of folding.

FIGURE 53. A subsidiary rabbit-ear fold is developed on the northeast flank of Goose Egg anticline in the northeast Bighorn basin (T.55 N., R.95 W.). A) The tightly folded rabbit-ear provides the northeast flank of a syncline which separates the ear from the crest of Goose Egg anticline. This syncline tightens upward (parallel fold- ing) and develops multiple folds in the Cretaceous Mowry and Thermopolis Shales, as volumetric adjustments. The syncline develops an upper detachment, and returns to a more open syncline above, as shown by the Frontier Sandstone. B) Rabbit-ear fold tightens downward into an isoclinal fold, which must detach at a very shallow depth.

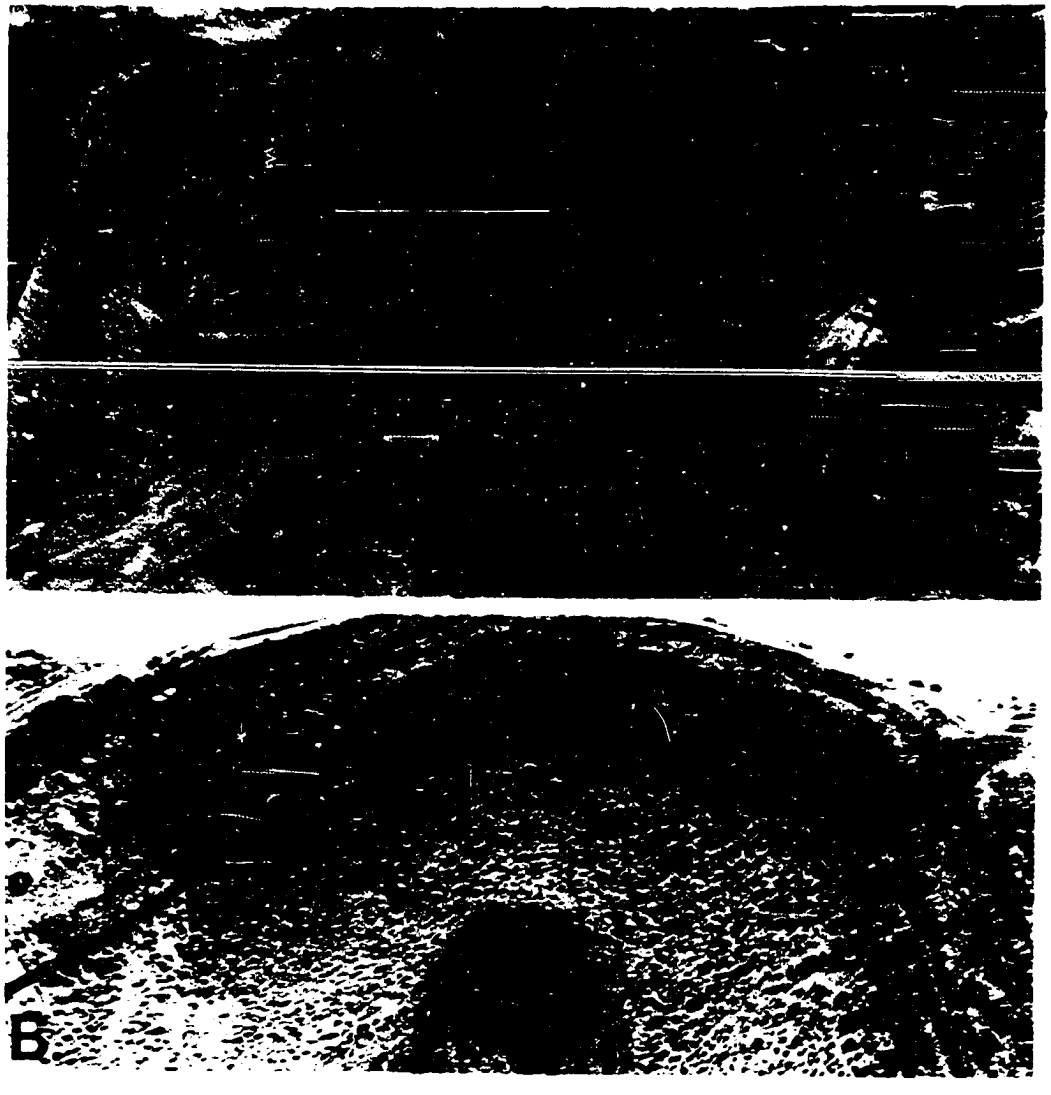

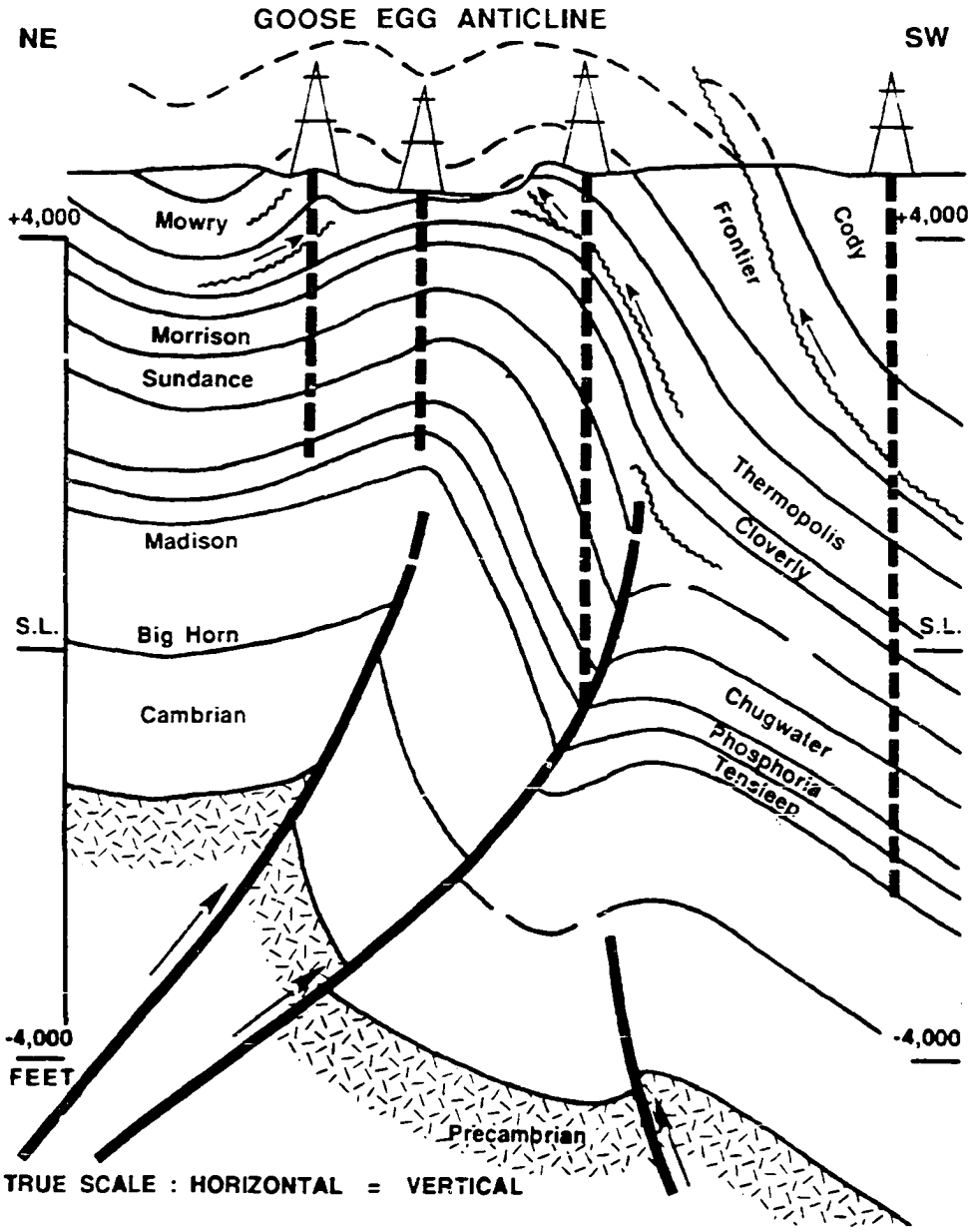

FIGURE 54. True scale structural cross section across Goose Egg anticline. Line of flexure into Bighorn basin appears to be controlled by a southwest-verging reverse fault in the basement, with a northeast-verging thrust coming out of the Bighorn basin. Associated changes in direction of asymmetry generate and localize detachment structures up through the stratigraphic section.

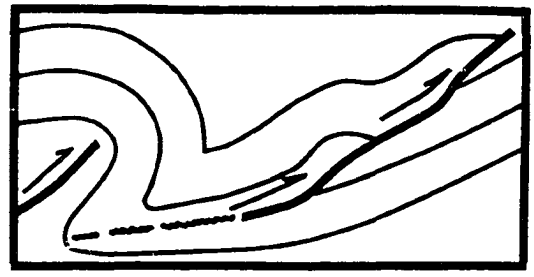

A. Back Limb Fold

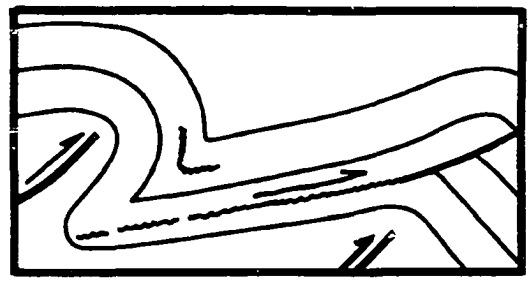

B. Cross Crestal Fold

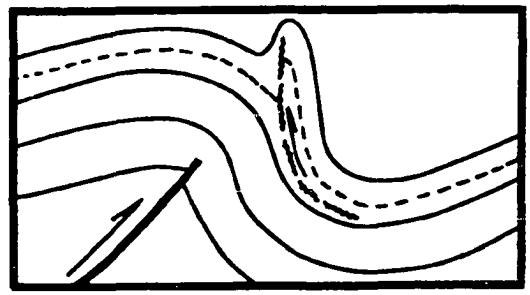

C. Rabbit Ear Fold

FIGURE 55. Three models of volumetric adjustments developed by parallel-folded synclines. A) Back-limb folds which travel up the gentle limb of the structure may develop ramp anticlines by moving upward across ramps in the more competent rocks. B) Cross-crestal structures develop as bedding plane slip moves up the gentle limb of the structure, and overrides the top of the adjacent anticline, offseting the shallow and deep crests. C) Rabbit-ear folds are similar to A and B above, but develop on the steep limb of the structure.

FIGURE 56. Southwest flank of the Virgin anticline in Utah (T.42 S., R.14 W.) displays a syncline exposed in the Triassic Chinle Formation. A) Asymmetric syncline is formed between oppositely verging reverse faults. B) Line drawing of photograph in (A) above shows the deepest beds (1) pass around the synclinal axial trough (lower right) unfaulted. Ash beds (2) above, however, are offset along a reverse fault which occupies the position of the axial plane. The overlying thicker white bed (4) is not offset along the axial trace, but instead is reverse faulted on the northeast flank of the syncline. Reverse faulting at the two different positions is apparently linked by bedding plane slip between, and parallel to, beds 2 and 3.

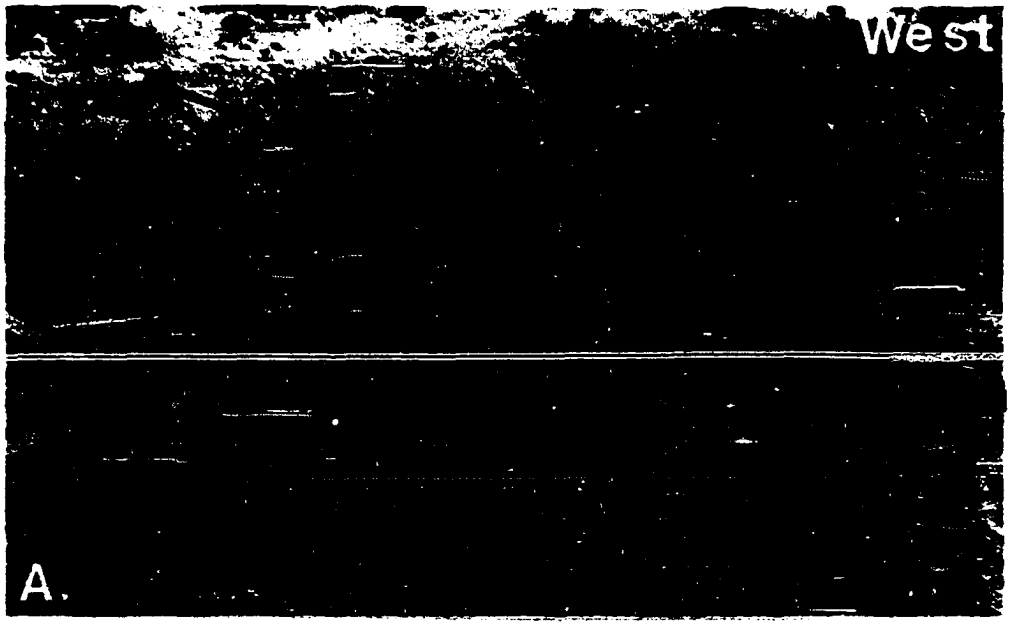

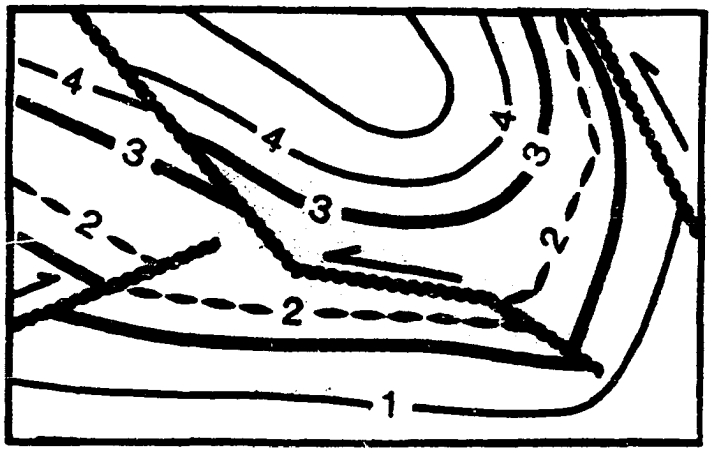

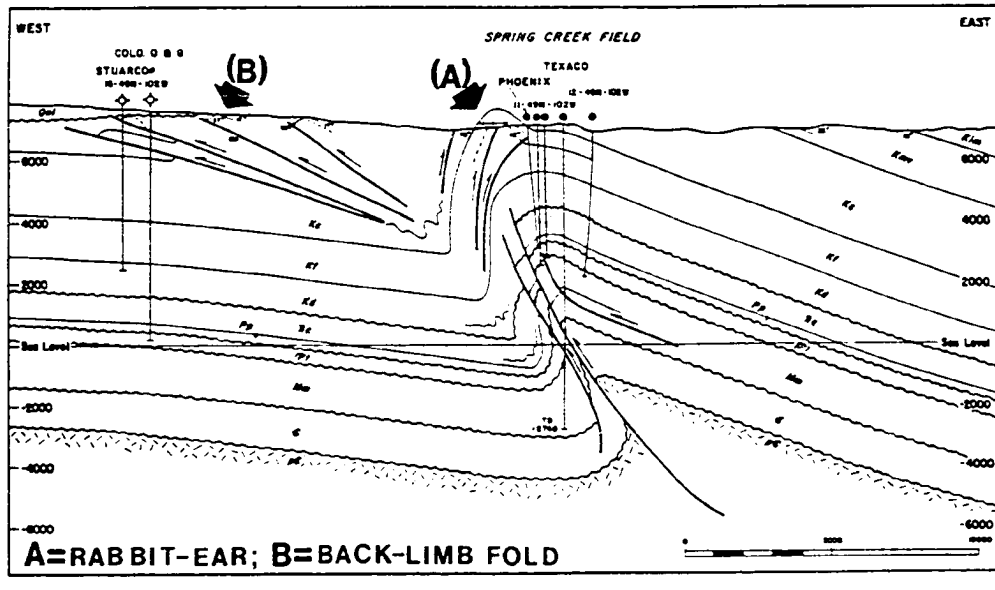

FIGURE 57. Spring Creek anticline western Bighorn basin (T.48 N., R.102 W.). Out-of-the syncline crowd structures of both the back-limb and rabbit-ear styles develop from volume problems in the same syncline adjacent to the steep flank of the anticline. Well control on the west end of the section encounters repeated Upper Cretaceous rocks, but an unpublished seismic section shot up to the steep limb of Spring Creek anticline shows that the underlying Cretaceous Frontier and deeper beds are nearly flat, as shown (modified from Petersen, 1983).

FIGURE 58. Surface geologic map of the Horse Center and Half Moon anticlines (modified from Pierce, 1970). Line of cross section for figure 59 trends northeast-to-southwest across the southeast plunge end of Horse Center anticline, Dry Creek syncline, and Half Moon anticline and thrust. The distance between the two anticlines is 3.5 miles (5.6 km).

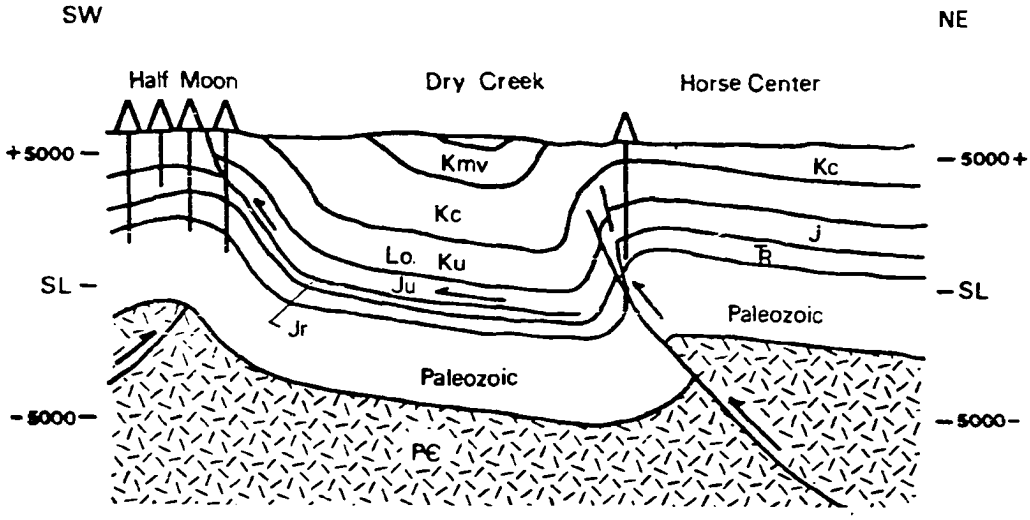

FIGURE 59. Horse Center-Half Moon cross section. Volume problems created at the trough of the asymmetric Dry Creek syncline are translated to the west flank of the syncline via bedding-plane slip in the Jurassic Redwater Shale. On the west end, the bedding-plane slip is directed up the steep flank of the deep Half Moon anticline and cuts to the surface as the Half Moon thrust fault. Repetition of Cretaceous rocks is observed in the electric logs of the wells at the crest of the structure as the bedding-plane slip changes upward into reverse faulting. The horizontal distance of this transfer of rock volume is 3.5 miles (5.6 km; modified from unpublished data by F.A. Petersen). Compare this interpretation with that of figure 56.

FIGURE 60. Windrock anticline (Sec. 31, T.41 N, R.105 W), located on the northeast flank of the Wind River Mountains, represents a large scale, out-of-the-syncline (Wind River basin) crowd structure (back-limb fold). A) Photograph shows the close degree of folding exposed in the Lower Jurassic Sundance Formation. B) Cross section is interpreted to show the detachment in the Redwater Shale, as determined by a depth-to-detachment calculation.

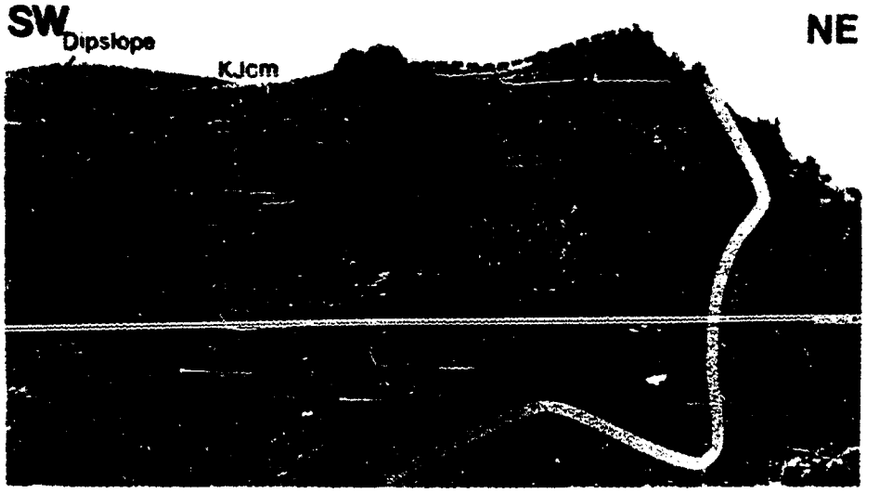

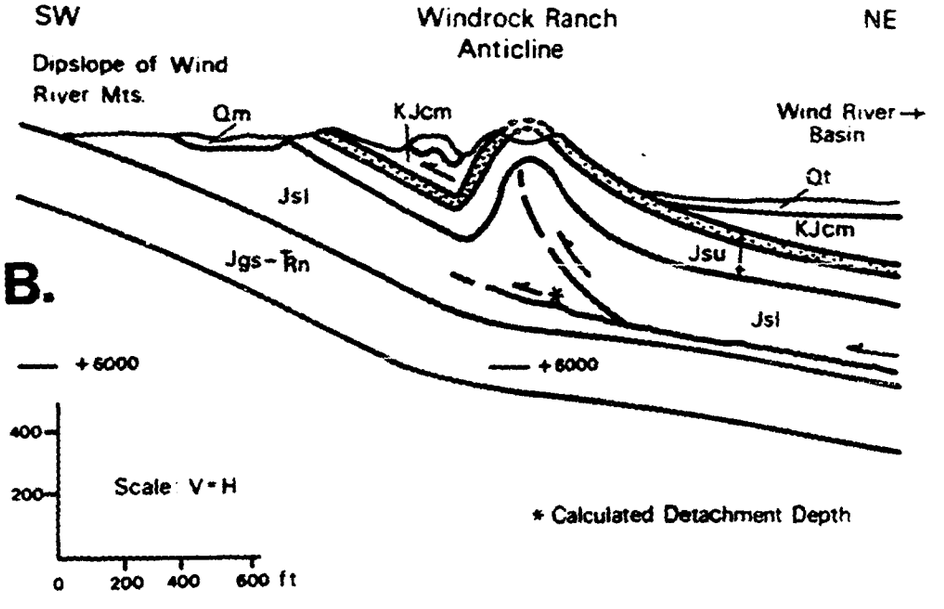

FIGURE 61. Seismic reflection line recorded on the northeast flank of the Wind River Mountains displays a large scale back-limb fold approximately ten miles (16 km) northeast (down-dip) of Windrock anticline (fig. 60). Identified reflections originate from: 1) the basal Cretaceous sandstones, 2) top of Triassic Chugwater Formation, and 3) top of Mississippian Madison Limestone. The anticline is interpreted to detach in the Jurassic Sundance Formation. (Permission to publish this section was granted by Donald Stone, President, Sherwood Exploration Company; Denver, Colorado.)

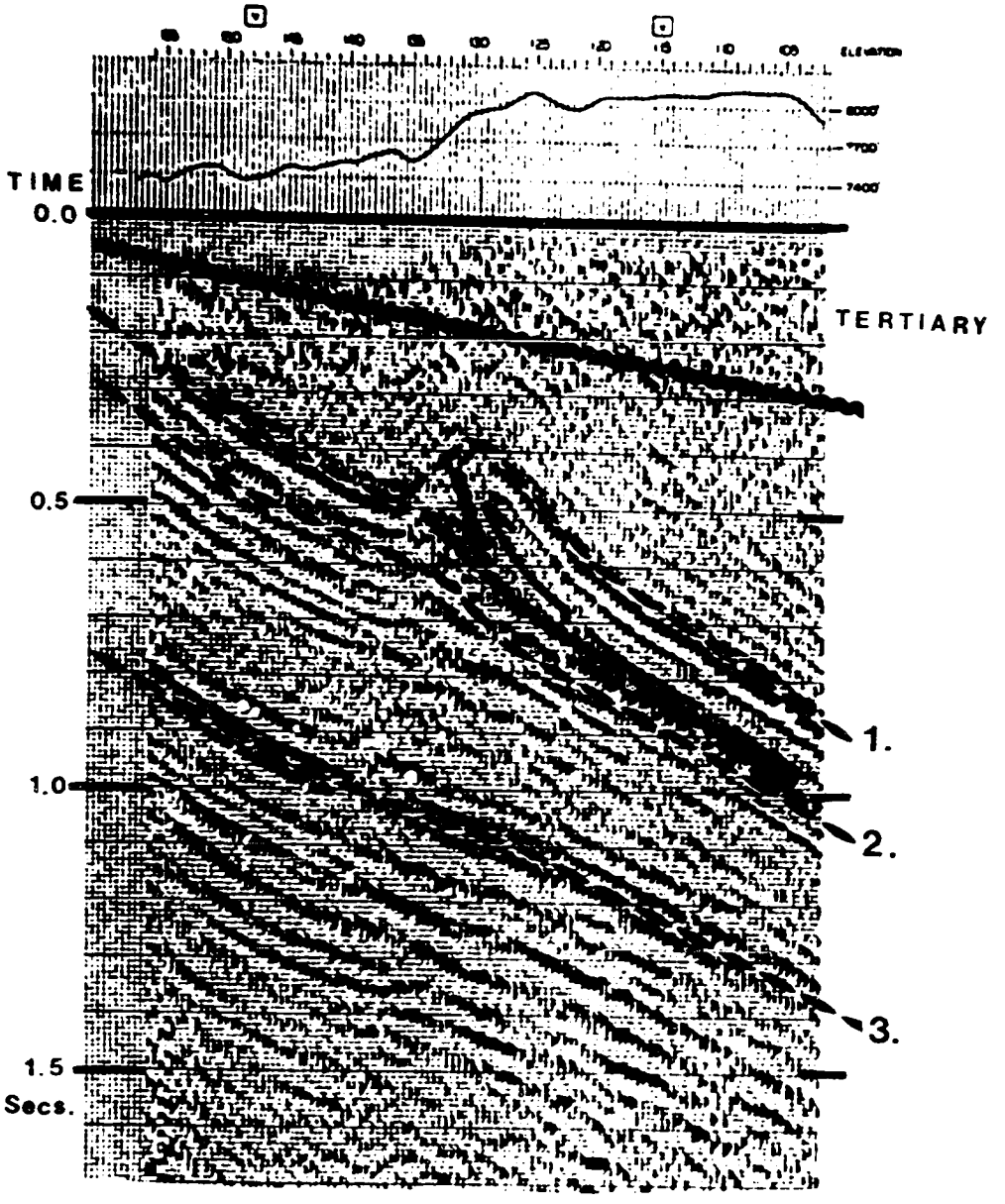

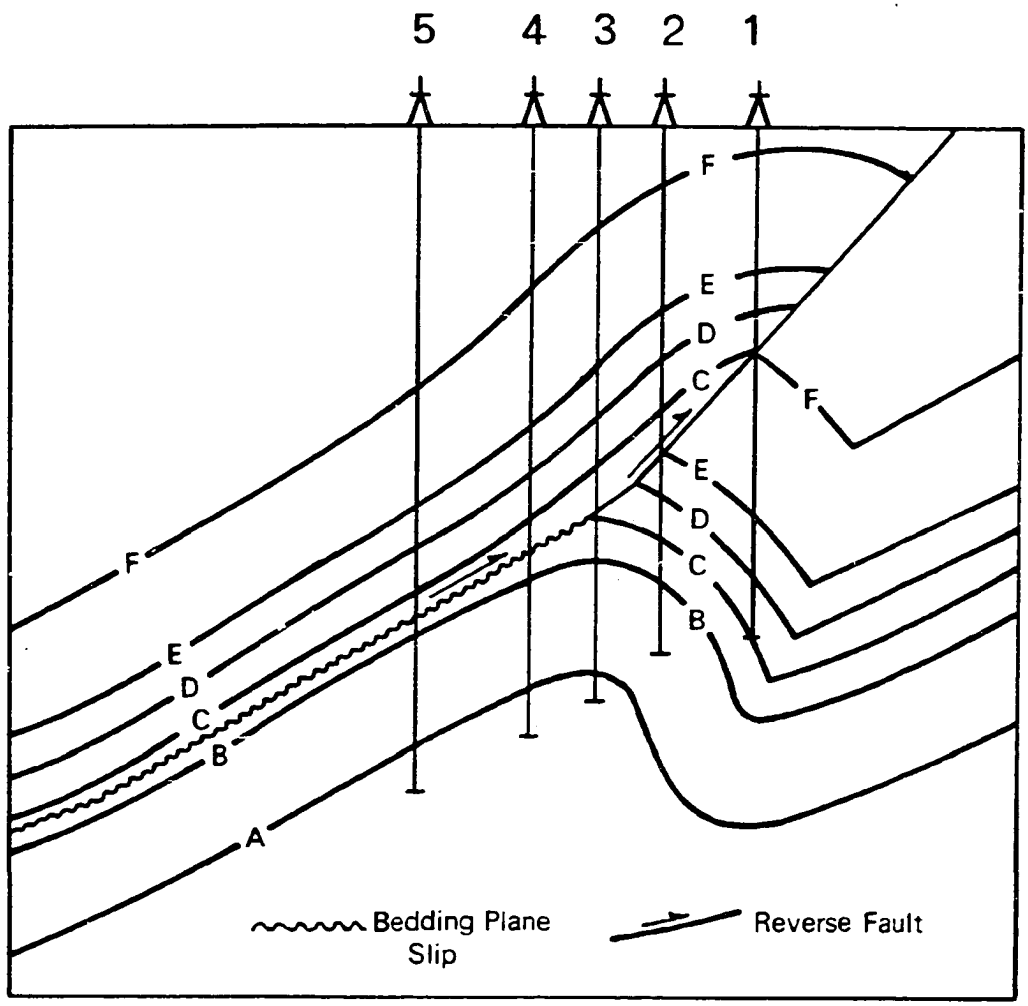

FIGURE 62. Diagrammatic cross section depicting the development of a cross-crestal structure, and its identification from electric well logs. Well 1 will show maximum amount of repeated stratigraphic section (C over F), while well 2 will show a decrease (C over E). Well 4 will show a normal stratigraphic section (C over B), but the character of the electric log in this interval will be "stretched and elongated" which is interpreted to result from bedding-plane slip. Well 5 may show no indication of structure at all.

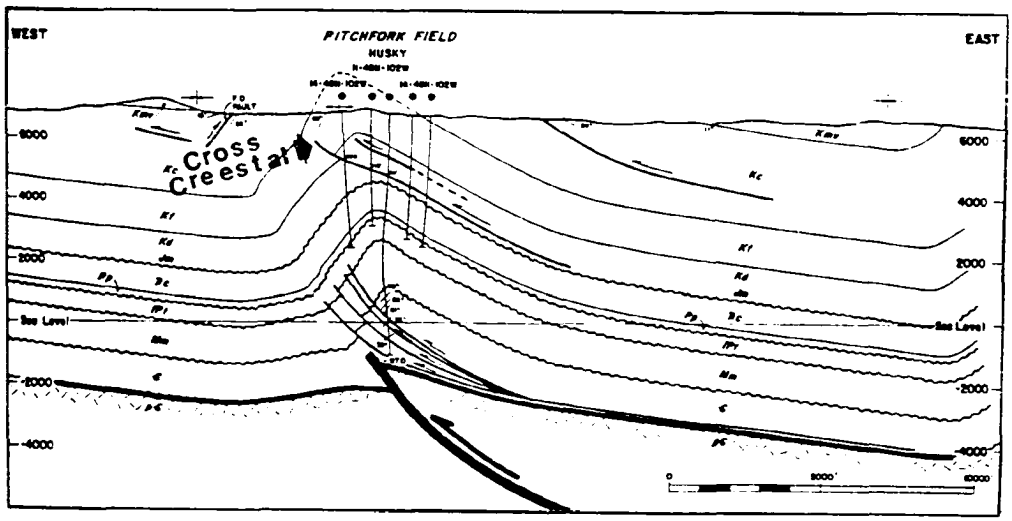

FIGURE 63. Pitchfork anticline (T.47 N. R.101 W) displays a cross-crestal structure developed by bedding-plane slip in the Jurassic Redwater Shale, from the syncline at the right side of the section. Structural repetition is best documented in the Lower Cretaceous Clovery Group (modified from Petersen, 1983).

FIGURE 64 Horse Center anticline (Tps.51 and 52 N., Rs. 101 and 102 W). A) Geologic map (same as figure 58) is rotated to approximate a down-plunge view to the south. The mapped fault labeled (X) is a cross-crestal fault, which originates as bedding-plane slip in the Jurassic Sundance Formation (Js) on the east flank of Horse Center anticline (left side of map). The bedding-plane slip cuts upsection and displaces the crest of the structure westward (to the right) at the Cretaceous-Jurassic Clovery-Morrison (KJcm) level. B) The crest at the Triassic Chugwater level is seen in the aerial down-plunge view. The dotted crestal trace shows the offset.

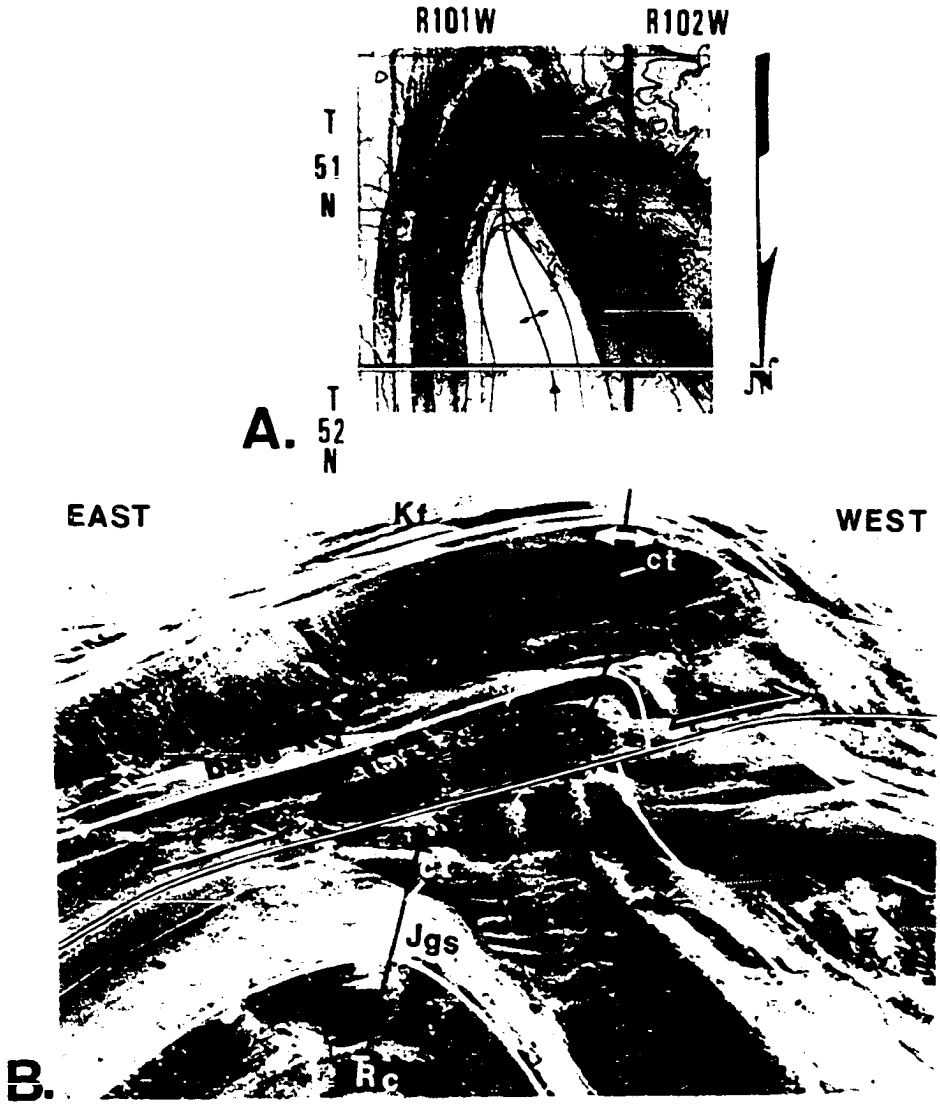

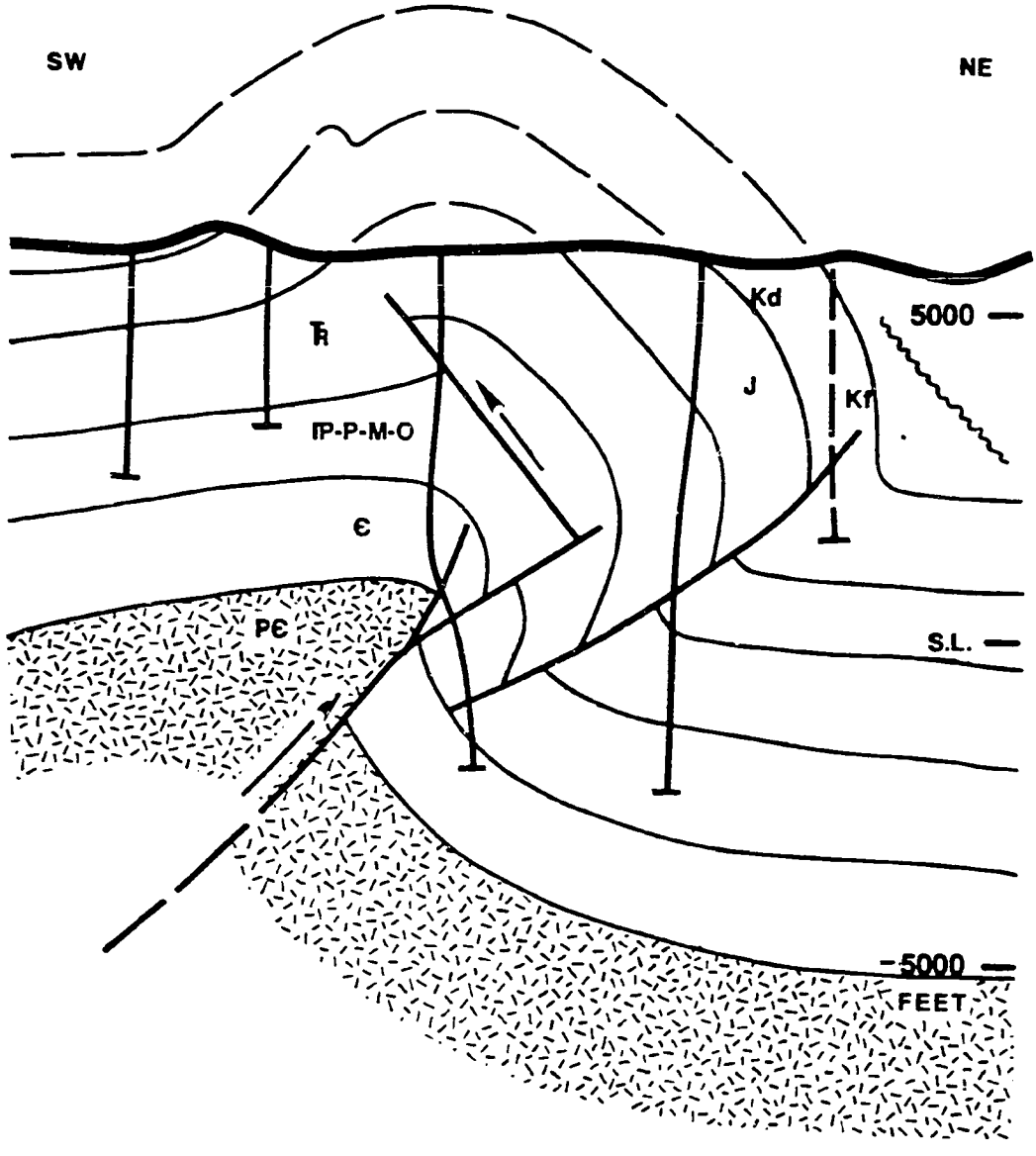

FIGURE 65. Schematic cross section of Horse Center anticline showing the relationship of the shallow cross-crestal and the deeper structure. Cross section is oriented opposite the down-plunge view of figure 64. Control of the deep structure is shown in figure 144c.

FIGURE 66. Vertical aerial photograph of Wildhorse Butte anticline (T.42 N., R.93 W.). White Jurassic Gypsum Springs Formation outlines the form of a rabbit-ear fold. Permian Phosphoria carbonates are exposed in the tight core of the fold (see figures 50, 51).

FIGURE 67. Big Trails anticline is located in the southeast portion of the Bighorn basin (T.44 N., R.87 W.). A) The rabbit-ear fold exposed in the Permian Goose Egg Formation (red bed facies) is located on the steep east limb. A white gypsum bed outlines the form of the fold, which is west-vergent. Beds exposed in the core of the rabbit-ear are very tightly folded, suggesting close proximity to the basal detachment. B) The Pennsylvanian Tensleep Sandstone is exposed in the core of the main fold, approximately one mile up-plunge from (A). This deeper anticline is faulted at the crest of the structure, and is east-vergent.

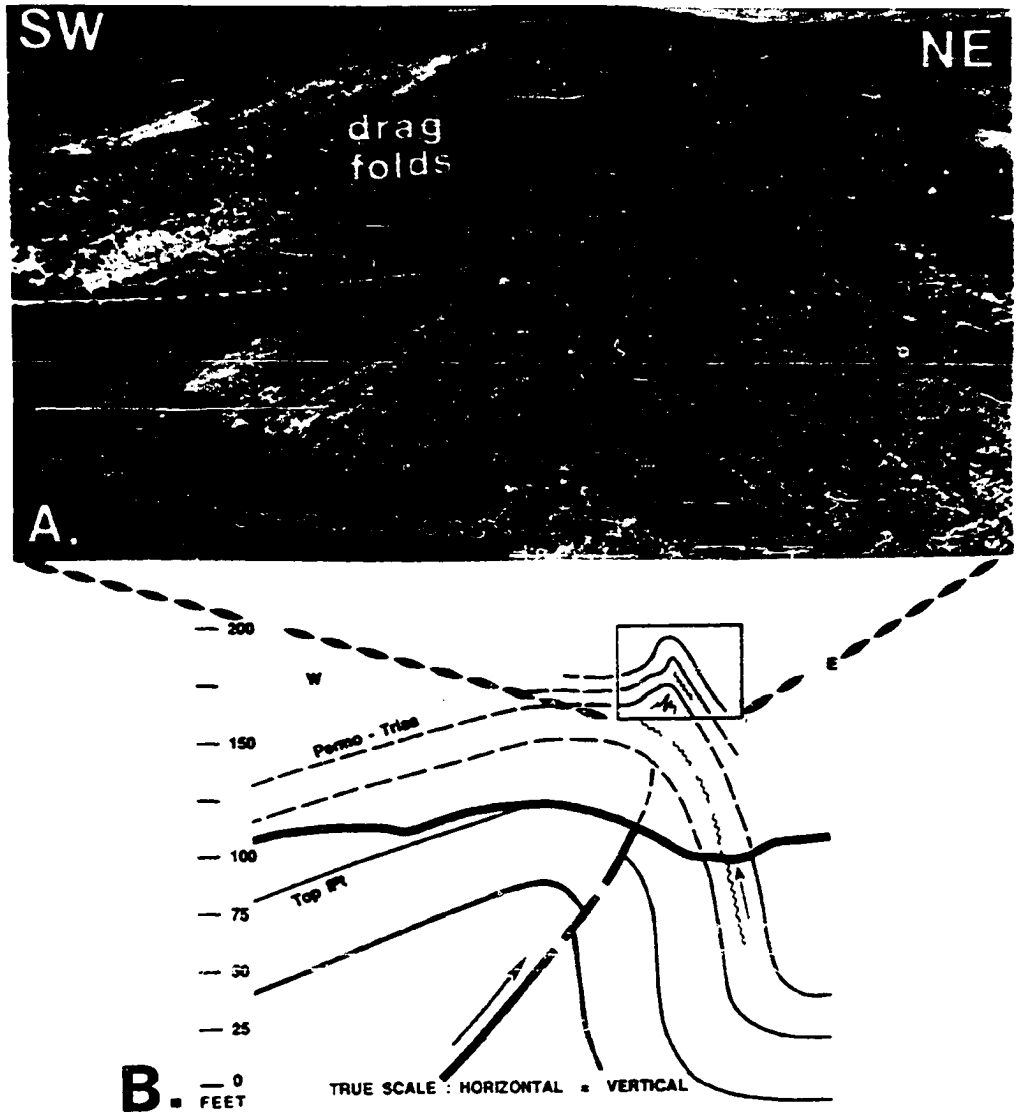

FIGURE 68. L-shaped syncline developed in Mississippian carbonates on the northeast flank of the Wind River Mountains (Tps.1 and 2 S., R.2 W., WRM). A) Outcrop photograph shows the abrupt flattening of the carbonates at the synclinal hinge (bottom center). Above the axial trace of the syncline, the Mississippian carbonates can be seen to have been repeated by a reverse fault which verges up the steep flank. B) Line drawing of (A) shows how the reverse fault develops in response to volumetric problems in the L-shaped syncline.

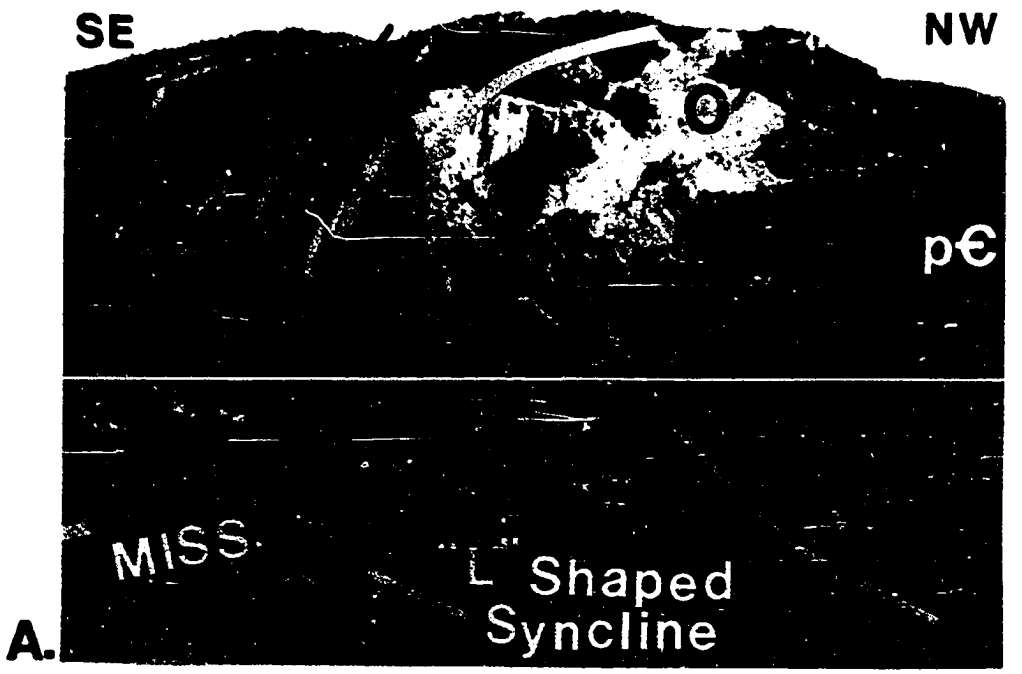

A.

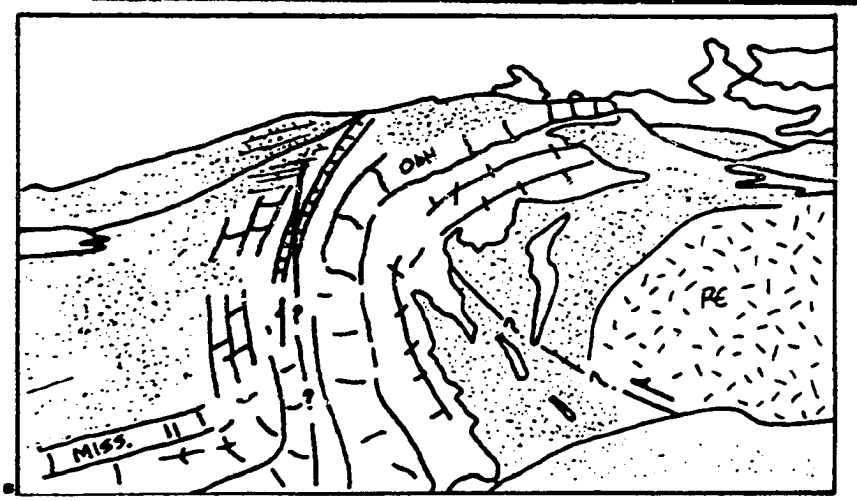

B.

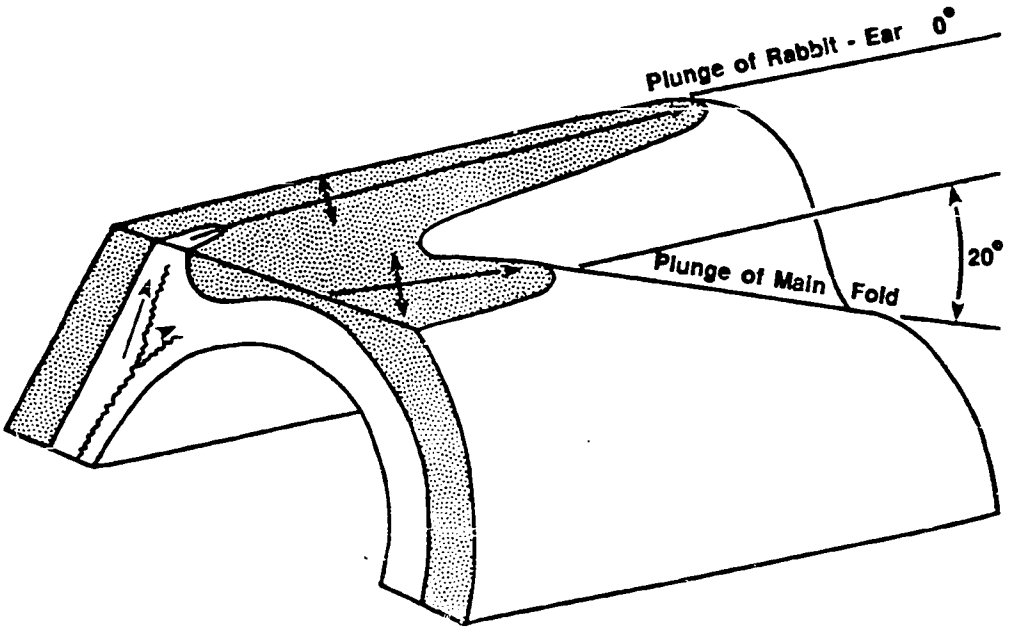

FIGURE 69. Perspective diagram showing the relationship between rabbit-ear and main fold as a function of different rates of plunge. Often, the main fold has a steeper plunge than the associated rabbit-ear fold. Erosion of the structures causes an elongated outcrop pattern of the ear, versus a shortened map pattern of the main fold, emphasizing the characteristic "ear" of the rabbit-ear fold.

FIGURE 70. Rattlesnake Mountain anticline near Cody, Wyoming (T.52 N, Rs.102 and 103 W.). A) Vertical aerial photograph is rotated to approximate a down-plunge view of subsidiary fold. Cross section along line A-A' is shown in (B). The rabbit-ear fold (expressed by the Pennsylvanian-Mississippian contact) is controlled by reverse faulting exposed in the Ordovician Big Horn Dolomite (Ob).

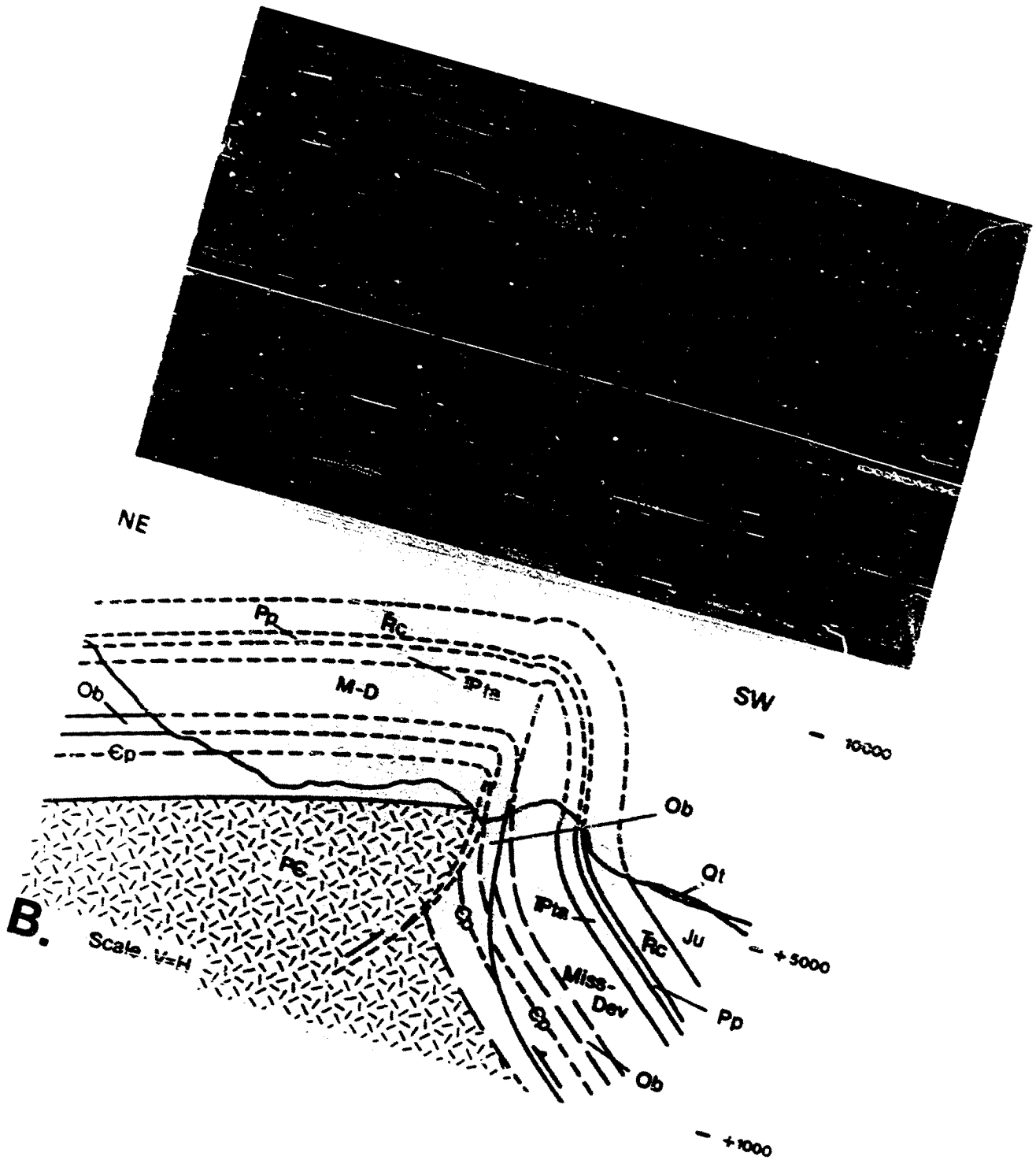

FIGURE 71. Duplication of Ordovician Big Horn Dolomite on steep southwest flank of Rattlesnake Mountain anticline. A) Top of Big Horn Dolomite is clearly repeated by a thrust fault which verges up the steep flank. B) South view of fold illustrates that the duplication of the Big Horn Dolomite is apparently linked to the rabbit-ear with the reverse fault becoming parallel to bedding upsection and displacement dying out upward into the fold.

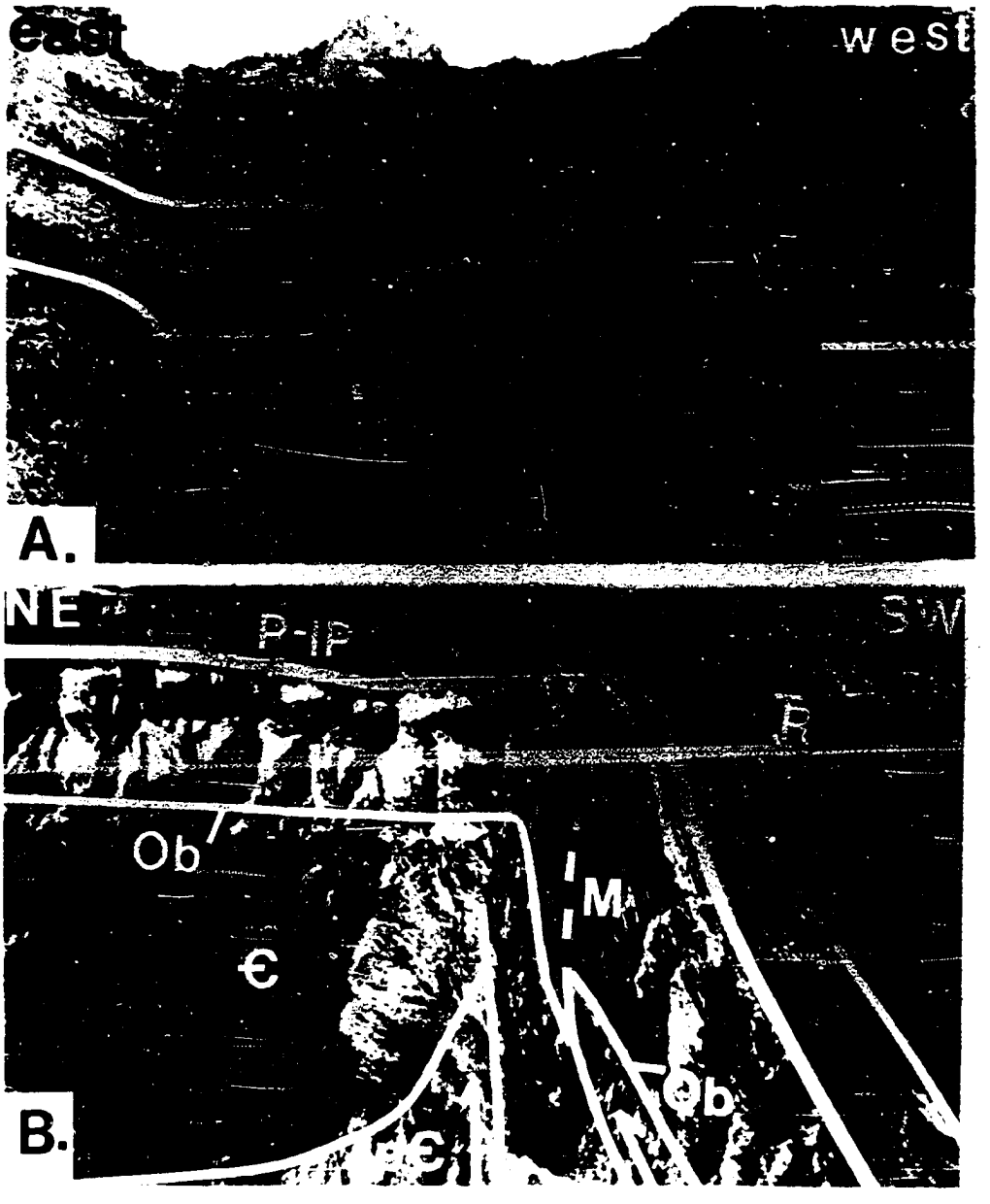

FIGURE 72. Down-plunge (north) view of Sheep Mountain anticline, located on the east flank of the Bighorn basin (T.54 N., R.94 W.). Rabbit-ear fold is localized on the northeast flank and expressed in the Lower Cretaceous Cloverly Group. Controlling reverse fault changes into bedding-plane slip downward into the Jurassic Sundance Formation. The white Gypsum Springs Formation is continuous over the crest of the main fold.

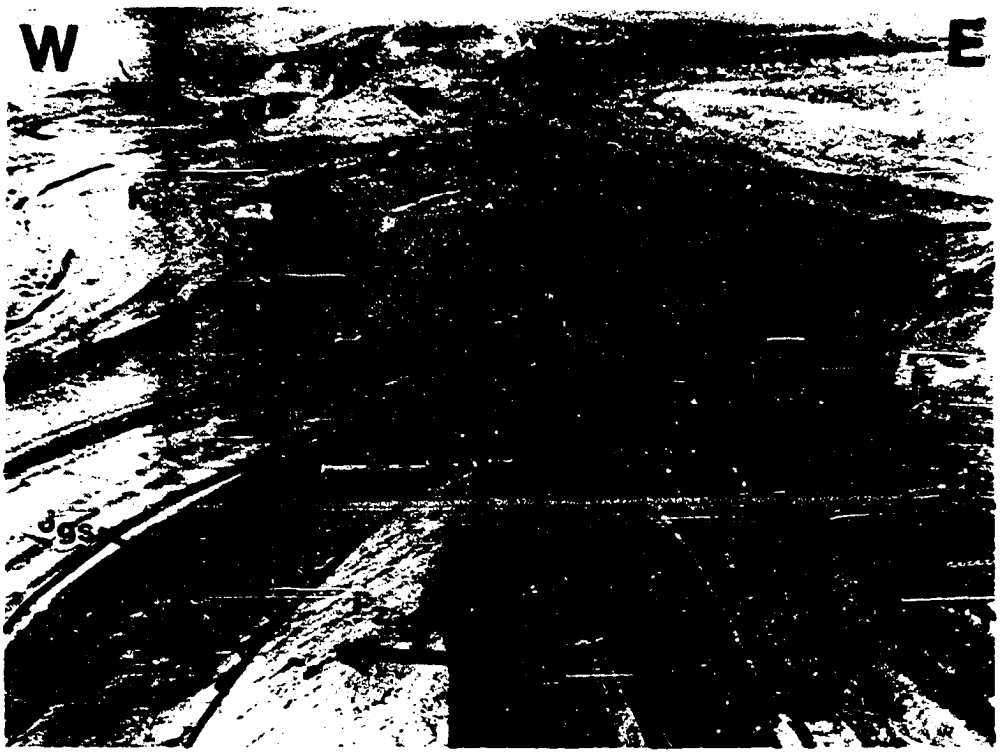

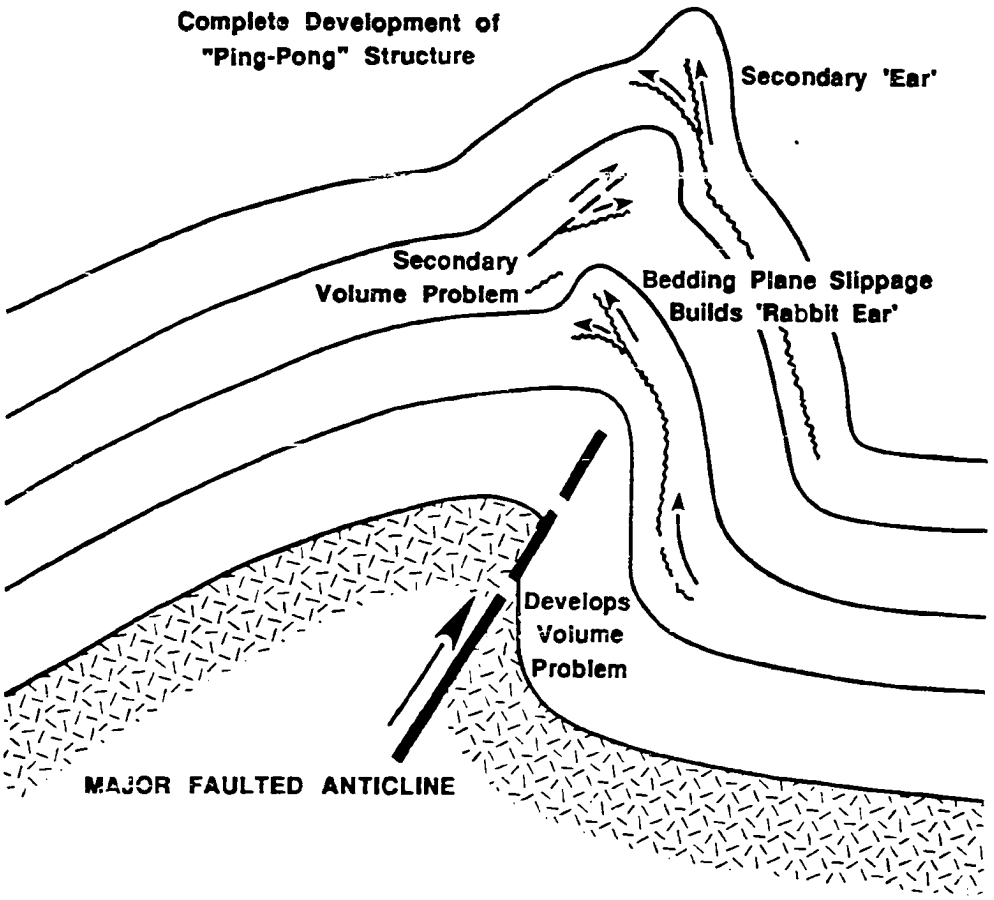

FIGURE 73. Diagrammatic cross section depicting the development of "multiple detachments", with associated "ping pong" changes in direction of asymmetry of the multiple rabbit-ear and backlimb folds. The right-facing asymmetry of the major fold creates an "L" shaped syncline which develops volume problems as it tightens upward. Resulting rabbit-ear fold verges to the right, resulting in secondary "L" shaped syncline (facing right). Secondary syncline responds to volumetric crowding by developing a secondary rabbit-ear, which verges to the left. The process is repeated up through the stratigraphic section.

FIGURE 74. Vertical aerial photograph of Chabot anticline in the southeast end of the Bighorn basin (Tps.42 and 42 N., R.88 W.). Chabot anticline plunges 14 degrees to the northwest at the top of the Paleozoic section (Pz). Rabbit-ear is expressed at the upper Triassic contact.

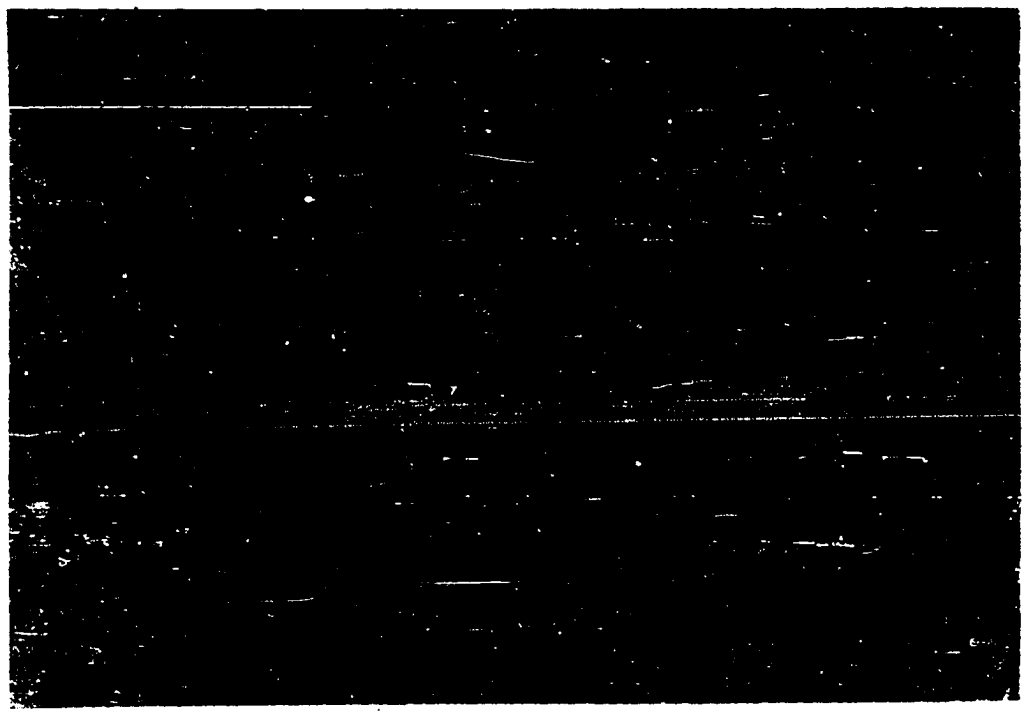

FIGURE 75. Aerial plunge view of Chabot anticline. Permian Goose Egg Formation is duplicated by out-of-the-syncline faulting which verges to the west. Faulting dies out upward into Triassic rocks, forming the classic rabbit ear, whose asymmetry is opposite to that of the deeper structure. Change in asymmetry in overlying Jurassic and Cretaceous rocks can be observed down-plunge to the northwest.

FIGURE 76. Detail of development of rabbit-ear fold at Chabot anticline. A) Bedding-plane slip occurs in the Permian Goose Egg Formation on the steep east flank, with the sense of shear showing vergence up the flank. B) Bedding-plane slip is replaced by a west-verging thrust which cuts upsection, repeating the upper limestones of the Permian Goose Egg Formation, which dies out upsection in the Triassic Chugwater Formation.

sw ne

FIGURE 77. Development of "ping-pong" change in direction of asymmetry at Chabot anticline. A) Main rabbit-ear fold is asymmetric towards the southwest at the top of the Triassic section. Poor outcrops in the secondary syncline obscure the development of northeast-verging detachment which dies out upsection in the Lower Cretaceous. B) East-facing asymmetry described in (A) is displayed in the Lower Cretaceous Thermopolis Shale, with a secondary rabbit-ear developed in the overlying Lower Cretaceous Mowry Shale.

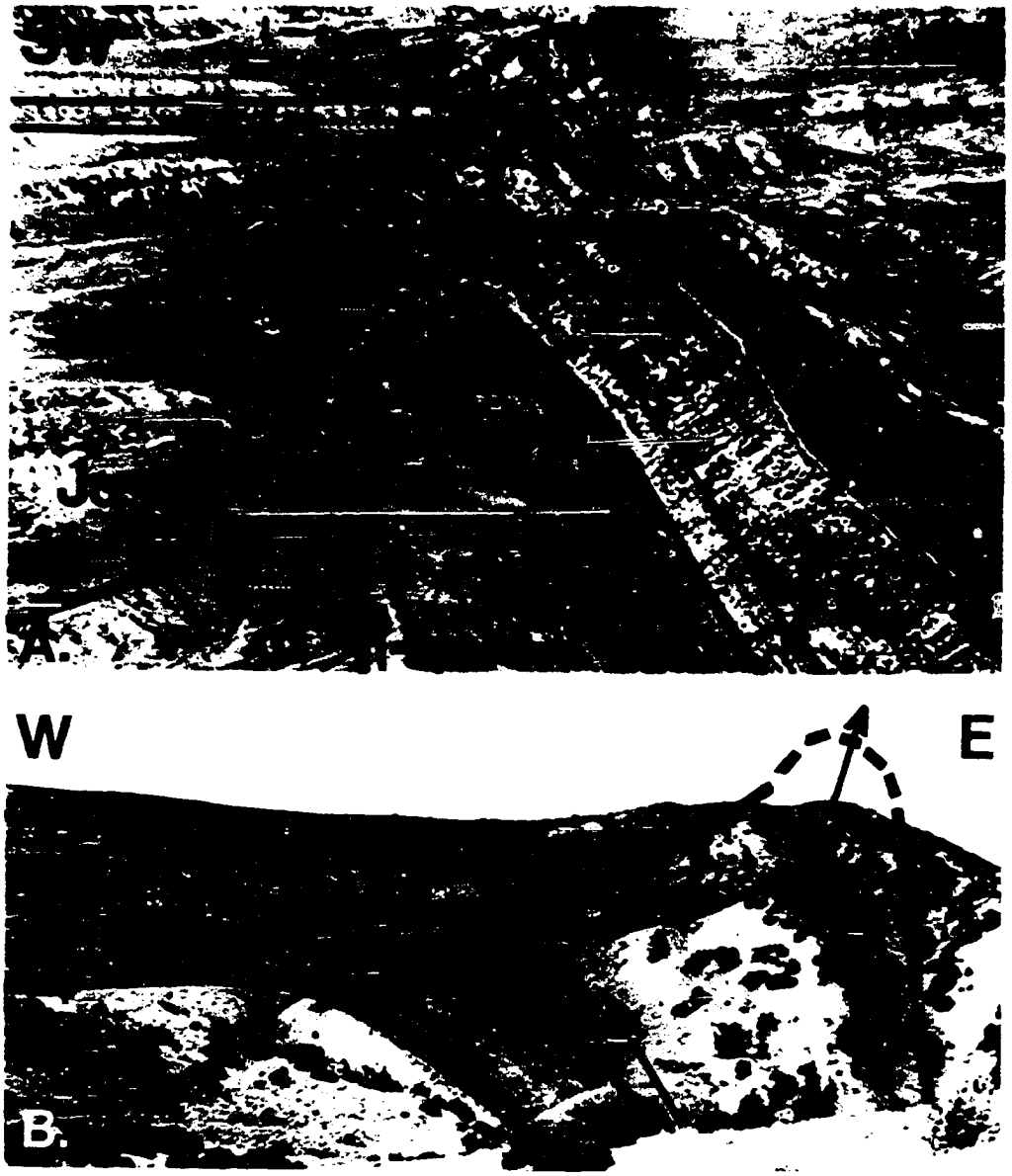

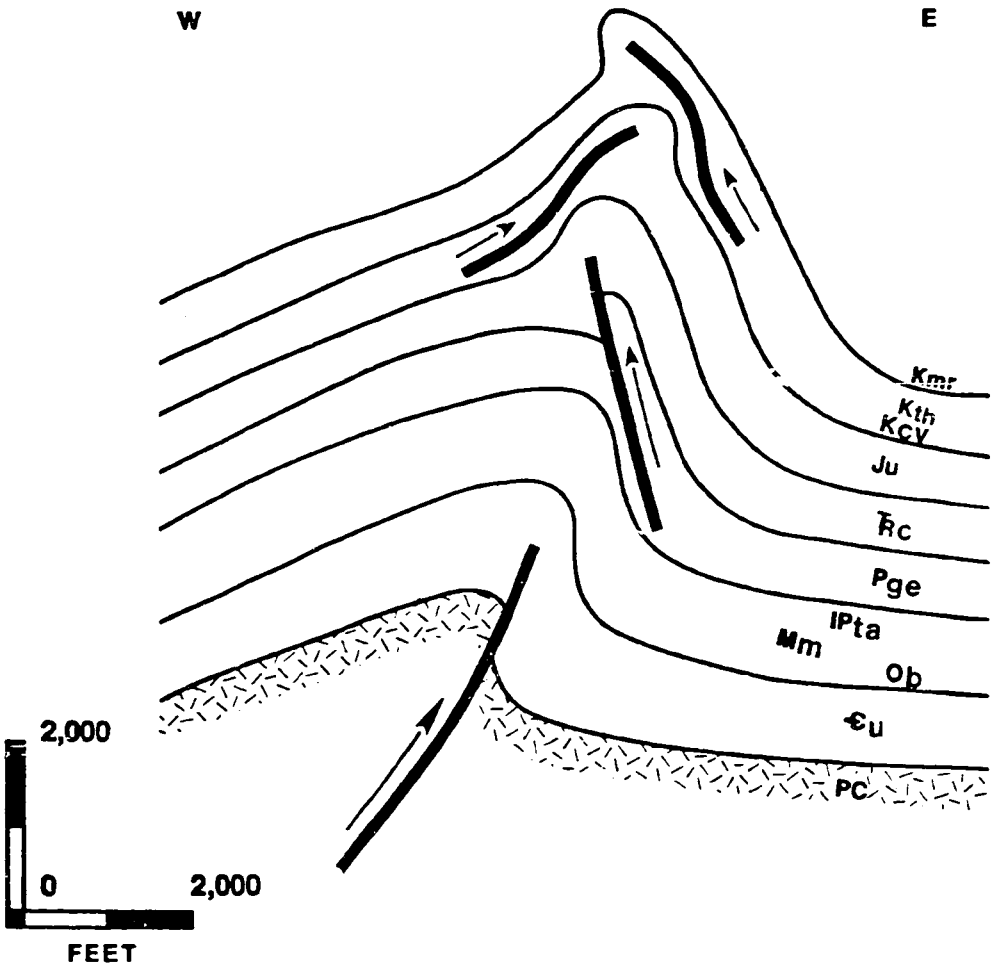

FIGURE 78. Diagrammatic structural cross section of Chabot anticline showing the complete development of multiple detachments, rabbit-ear and backlimb folds. Symbols: Kmr-Mowry Shale; Kth-Thermopolis Shale; Kcv-Clovyerly Group; Ju-Jurassic undivided; Trc-Triassic Chugwater Formation; Pge-Permian Goose Egg Formation; lPta-Tensleep/Amsden; Mm-Mississippian Madison Formation; Ob-Ordovician Big Horn Dolomite; Cu-Cambrian undivided; pC-Precambrian basement.

FIGURE 79. Lodge Grass Creek anticline located on the north plunge of the Big Horn Mountains (T.58 N., R.91 W.). A) Photograph is printed in reverse (actual south view) to approximate cross section shown in (B). Base of Ordovician Big Horn Dolomite (Obh) is continuous over crest of anticline, which is asymmetric towards the west. Valley floor is developed on the gentle east-dipping, nonfolded basal Cambrian Flathead Sandstone. B) Anticline tightens downward and detaches in the Cambrian Gros Ventre Shales which are covered. Dashed line is schematic representation of the fault cutting upsection.

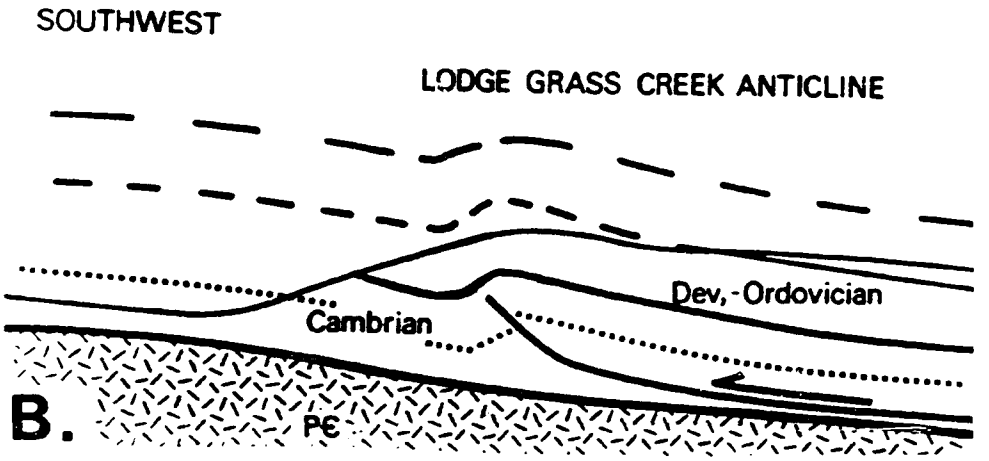

FIGURE 80. Up-plunge exposure of Anchor anticline, on north flank of Owl Creek Mountains (T.8 N., R.1 E.). Rock in the extreme lower left corner is Precambrain basement (pC) and north-dipping Cambrian Flathead Sandstone (Cfh). Cambrian Pilgrim Limestone (Cp) is folded in disharmony with the underlying Flathead Sandstone and the overlying Gallatin Limestone (Cg).

FIGURE 81. Mississippian limestones are eroded to show circular arcs because the beds are folded continuously through a 90 degree angle over the crest of Rattlesnake Mountain anticline (T.53 N., R.103 W.).

FIGURE 82. Erosion of "L"-shaped syncline to the level of the Mississippian limestones reveals a broad, curved, circular shape as the steep limb flattens to the gentle dip at the base of the "L".

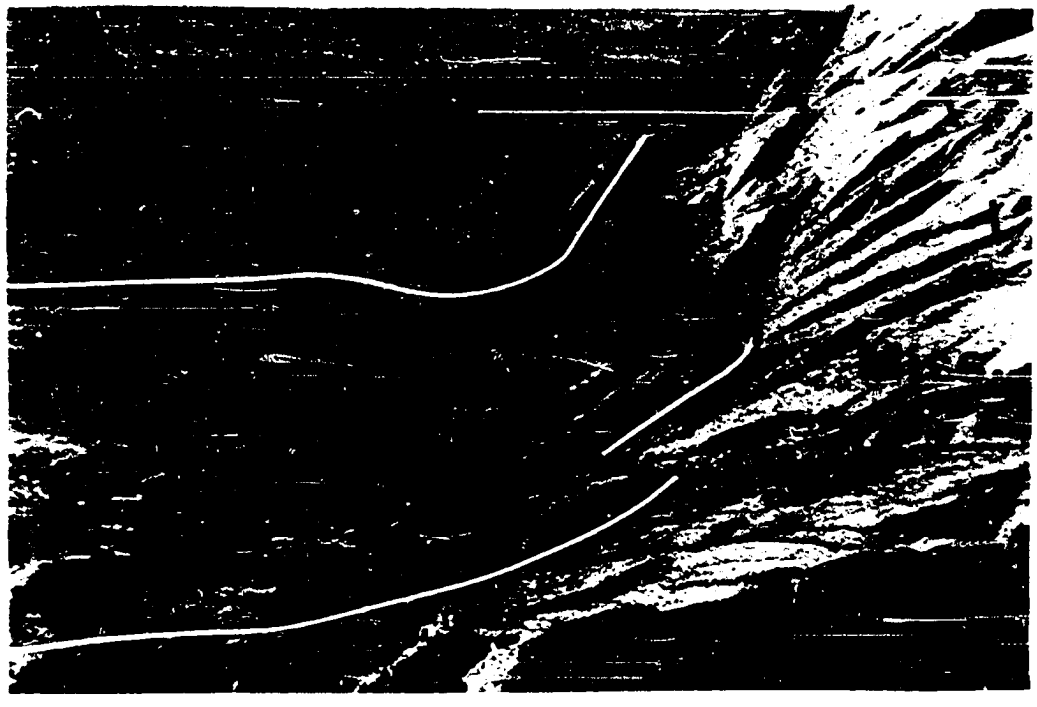

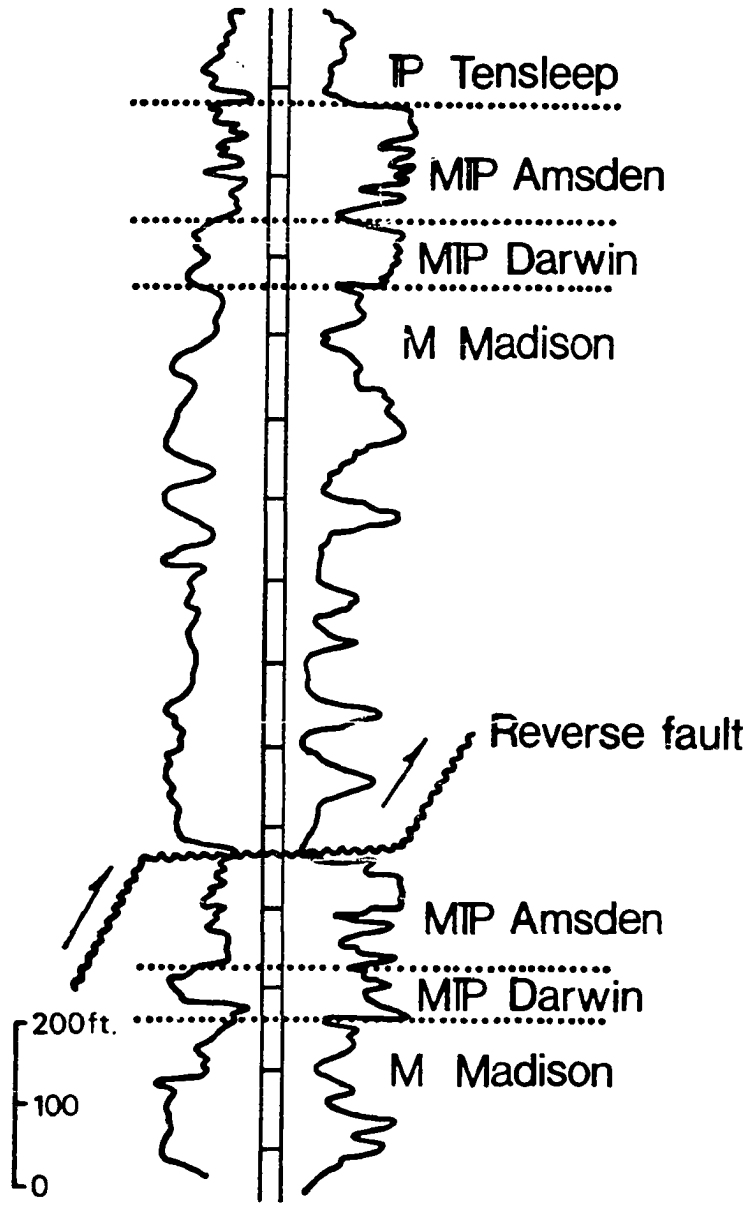

FIGURE 83. Portion of the electric log from the Superior #1 Government well, drilled on the crest of Horse Center anticline (sec. 31, T.52 N., R.101 W.). Pennsylvanian and Mississippian rocks are repeated by a reverse fault which originates as bedding-plane slip in the upper portion of the Devonian shaly limestones.

FIGURE 84. Ordovician Big Horn Dolomite exposed in the tight anticlinal hinge of Shell Canyon flexure (T.53 N., R.90 W.). The dolomite is continuous across the kink-like hinge of the fold.

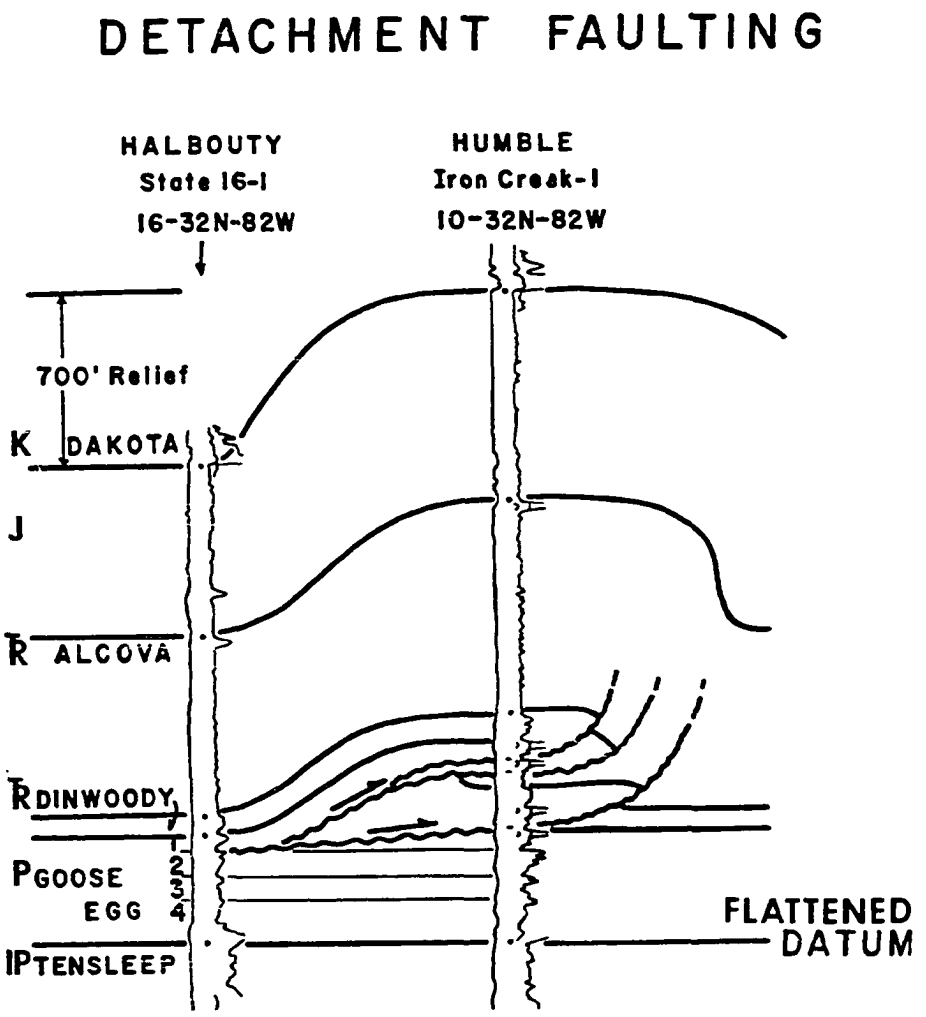

FIGURE 85. Portions of the electric logs from the Humble Iron Creek #1 well, drilled on the crest of Iron Creek anticline, on the Casper arch, and the Halbouty State #16-1 well drilled on the flank of Iron Creek anticline. A limestone in the Permian Goose Egg Formation has been repeated three times by reverse faulting in the core of the structure.

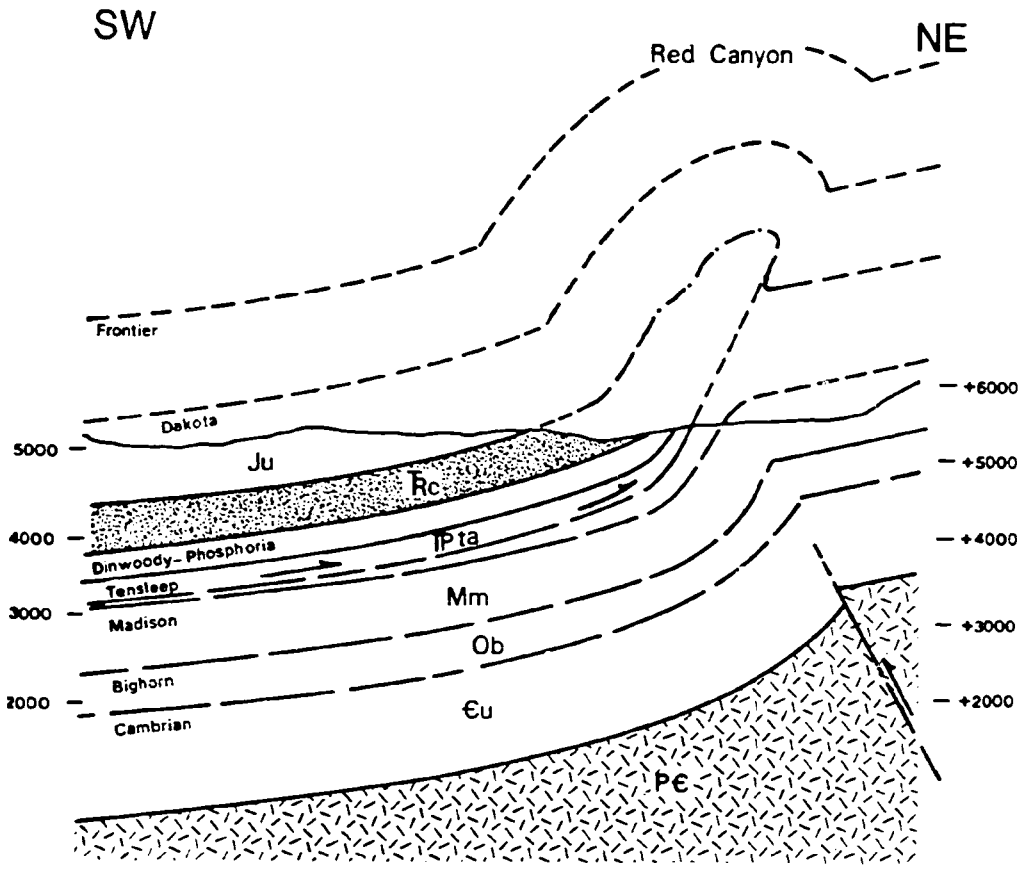

FIGURE 86. Duplication and disharmonic folding of the Pennsylvanian Tensleep Sandstone (with respect to the underlying Mississippian carbonates) by a detachment developed in the Pennsylvanian-Mississippian Amsden Shale, at Red Canyon (T.54 N., R.91 W.), on the flank of Shell Canyon flexure. Also, note the kink-like hinge of the Shell Canyon flexure, as the fold tightens downward from the broad, circular shape of the Mississippian carbonates.

FIGURE 87. The carbonates of the Permian Phosphoria Formation fold conformably over the crest of Anchor anticline (T.8 N., R.1 E., WRM) as the faulting at the top of the Tensleep Sandstone dies out upward.

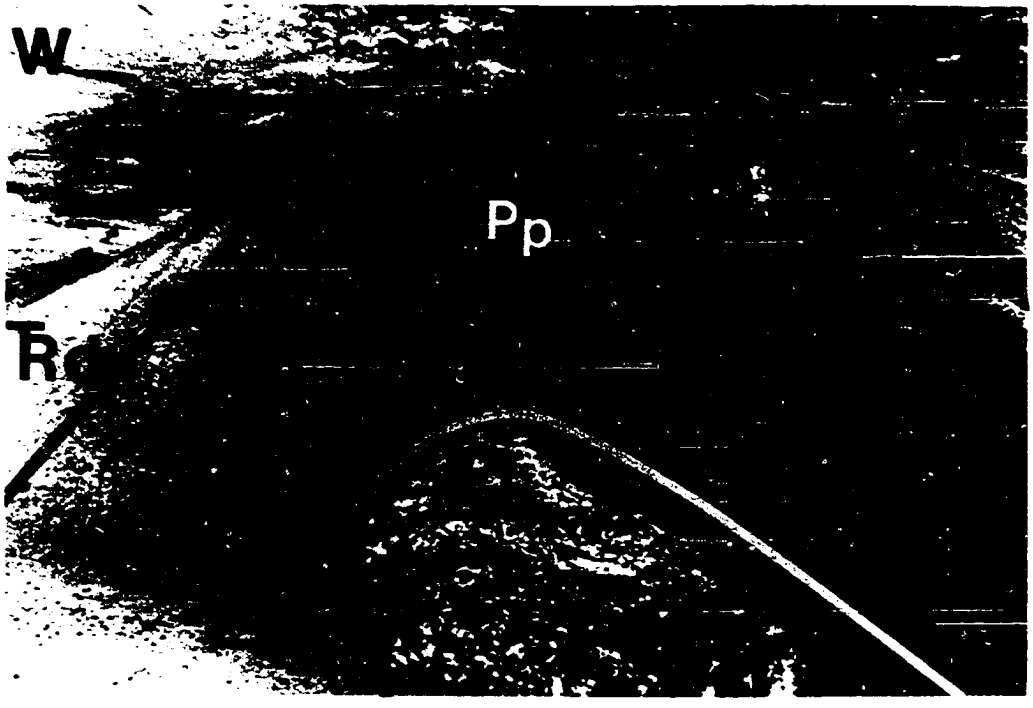

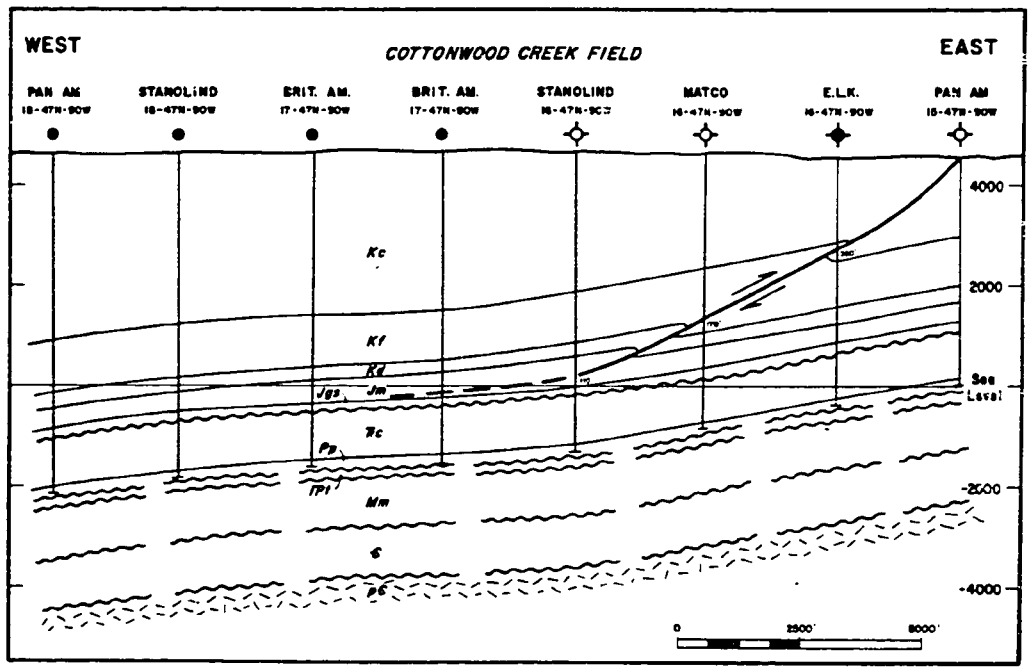

FIGURE 88. Faulting which results in repetition of the Lower Cretaceous Frontier Sandstone in the Cottonwood Creek field (T.47 N., R.90 W.), dies out downward as the fault plane flattens and soles out in Jurassic shales (after Petersen, 1983). Cottonwood Creek field has no structural closure, and production is from a stratigraphic trap in the Permian carbonates.

FIGURE 89. Subsidiary folds developed in the Lower Cretaceous section. A) Rabbit-ear fold exposed in the Frontier Formation (Kf) is developed on the southwest flank of Maverick Springs anticline (T.5 N., R.1 W., WRM) by detachment and thrusting in the Mowry Shales (Kmr). B) Subsidiary drag fold in the Mowry Shale is developed on the northeast flank of Horse Center anticline (T.52. N., R.101 W.) by faulting in the underlying Thermopolis Shale (Kth).

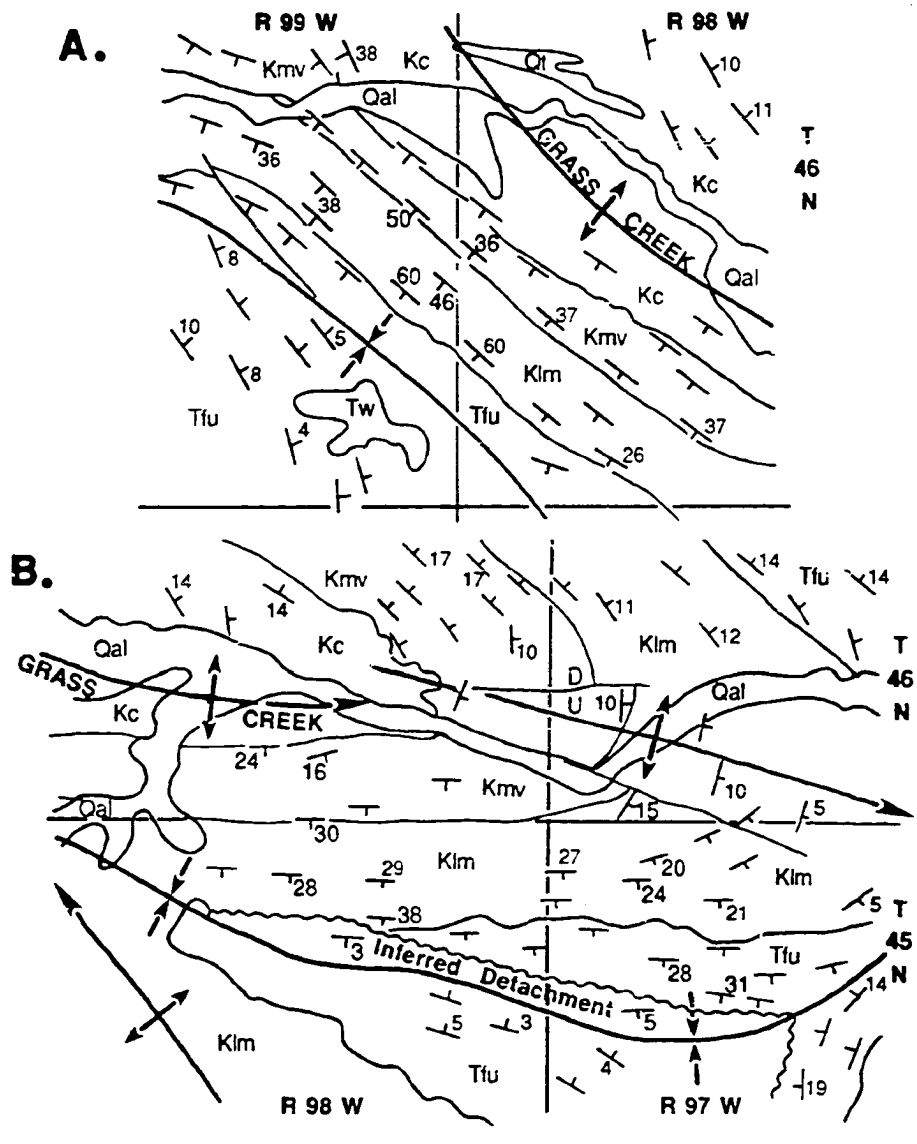

FIGURE 90. Upward-tightening synclines involving Paleocene Fort Union Formation (Tfu). A) Syncline on the southwest flank of Grass Creek anticline (T.45 N., R.98 W.) displays progressive steepening of dips toward the axis of the syncline, indicating upward-tightening of parallel-folded beds. B) To the southeast, the plunging syncline also tightens upward, until an abrupt lessening of the dip rate occurs within the Fort Union Formation. This change in dip rate is interpreted to represent the upper detachment of parallel-folded synclines.

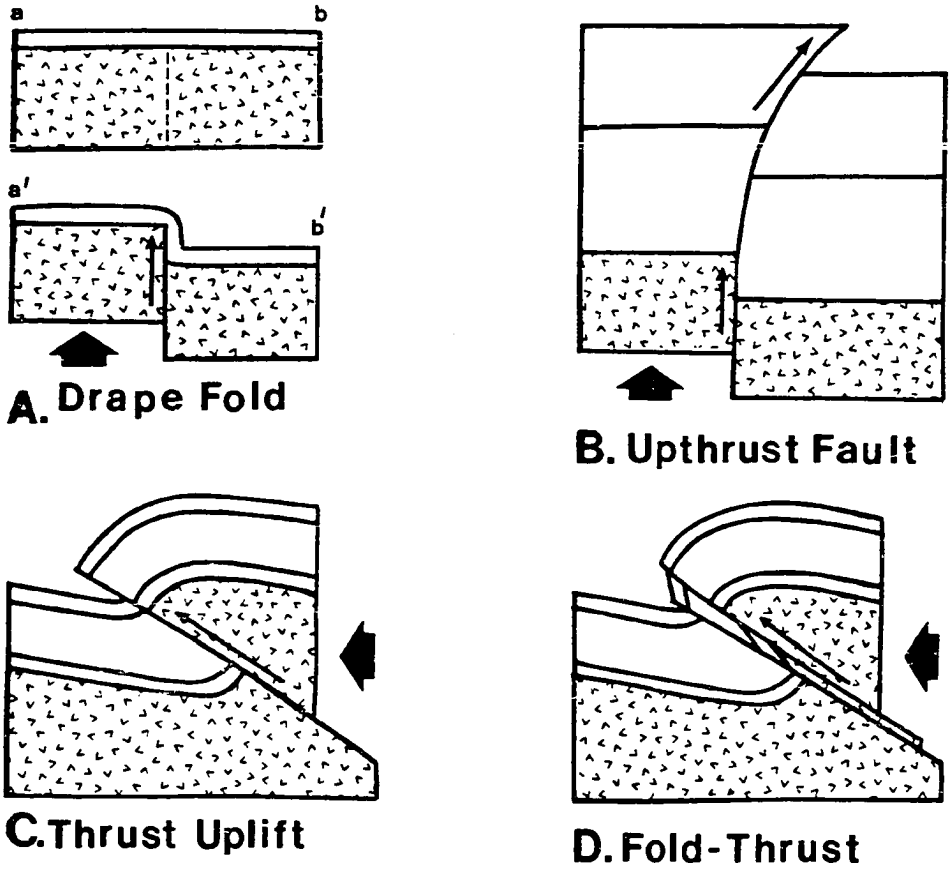

FIGURE 91. Four models of the structural style of the Wyoming foreland. A) Vertical faulting with draping of the sedimentary section (drape fold). B) Upthrust faulting. C) Thrust uplift. D) Fold-thrust. (A) and (B) (after Prucha and others, 1965) are variations of the differential vertical uplift concept, while (C) and (D) (after Berg, 1962) are variations on the horizontal compression concept.

DRAPE FOLDS

Bed-Length Accommodations

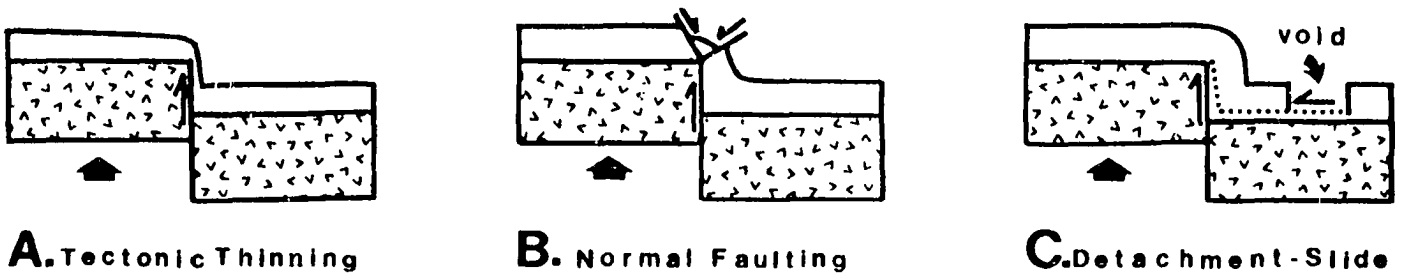

FIGURE 92. Bed-length (volumetric) accommodations necessitated by vertical uplift and draping of the sedimentary section. A) Tectonic thinning, or stretching of the sedimentary units. B) Extension of bed length by normal faulting. C) Movement of sedimentary section laterally into the fold on a detachment developed above the basement creating a void in adjacent area.

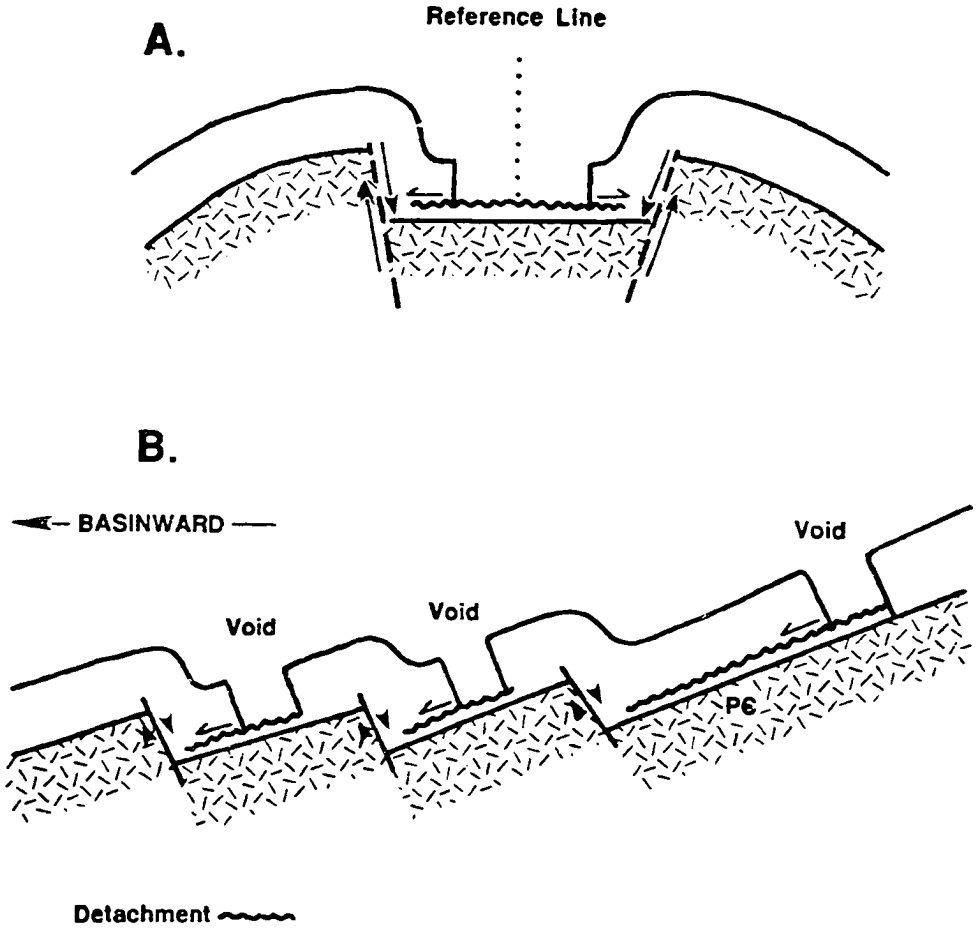

FIGURE 93. Problems associated with application of the "detachment" mechanism to maintain volumetric balance (bed length) in "drape folds". A) Two asymmetric "drape folds" facing one another (as shown) would require rock from the same area, resulting in a much larger sedimentary void than that required for a single drape fold. B) Asymmetric drape folds developed in line on the flank of a mountain uplift would result in either multiple "voids" or a single void of major dimensions. In both cases above, no such voids are detectable throughout the foreland area.

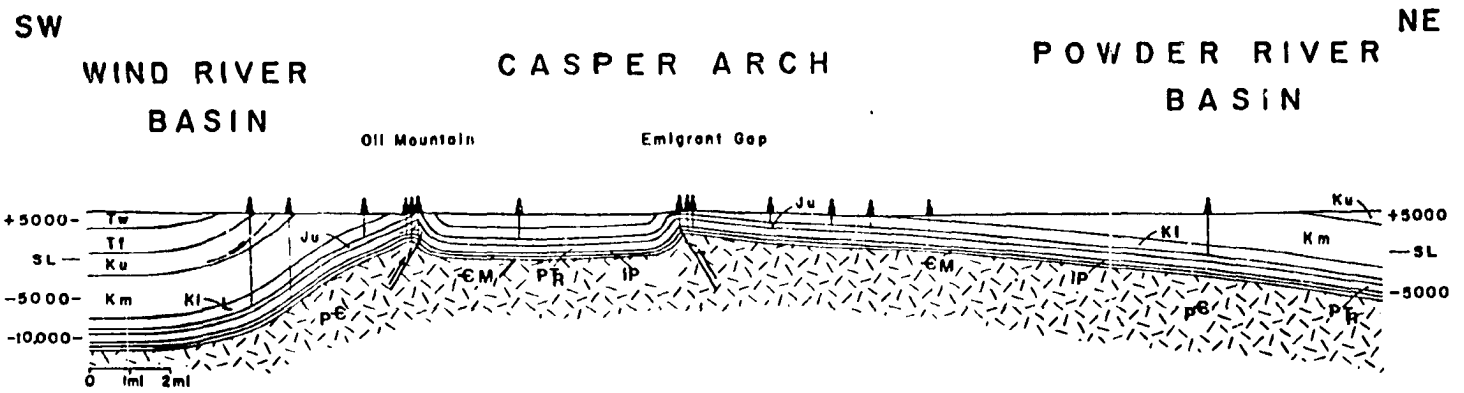

FIGURE 94. An example of asymmetric structures which face each other are the Oil Mountain and Emigrant Gap lines of folding on the Casper arch (T.33 N., Rs.81 and 82 W.). The presence of Cretaceous (and older) rocks in the syncline between the two structures indicates that a void has not developed in that position.

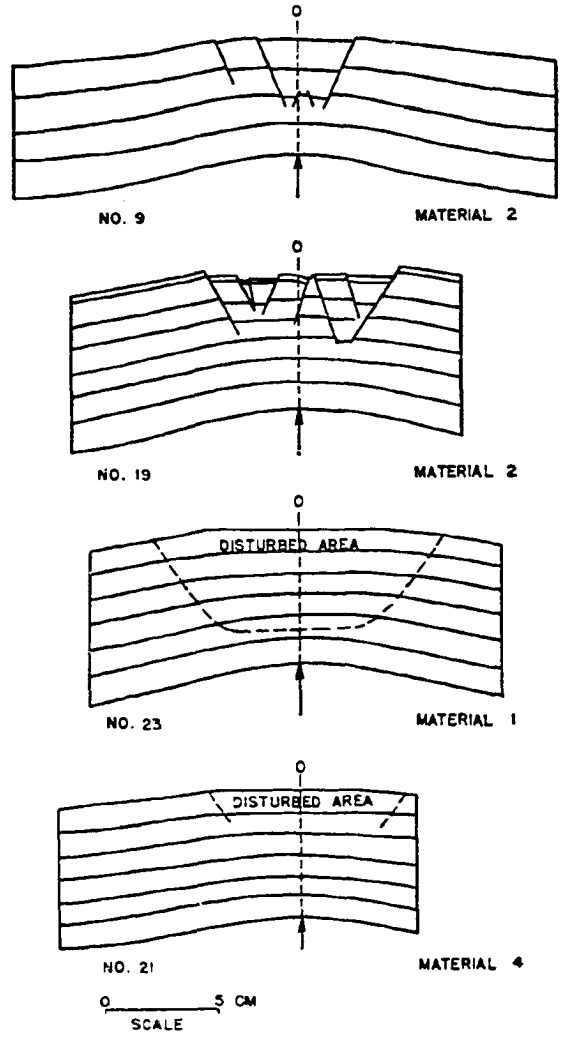

FIGURE 95. Experimental fracturing and folding created by the application of a broad curve in the vertical displacement along the lower boundary (Type I, after Sanford, 1959). Type of deformation developed depends upon the material used in the experiment. Extensional graben developed over center of fold, which widened with progressive folding. Disturbed areas are characterized by thinning of material, flattening of upper surface, and blurring of "bedding" lines.

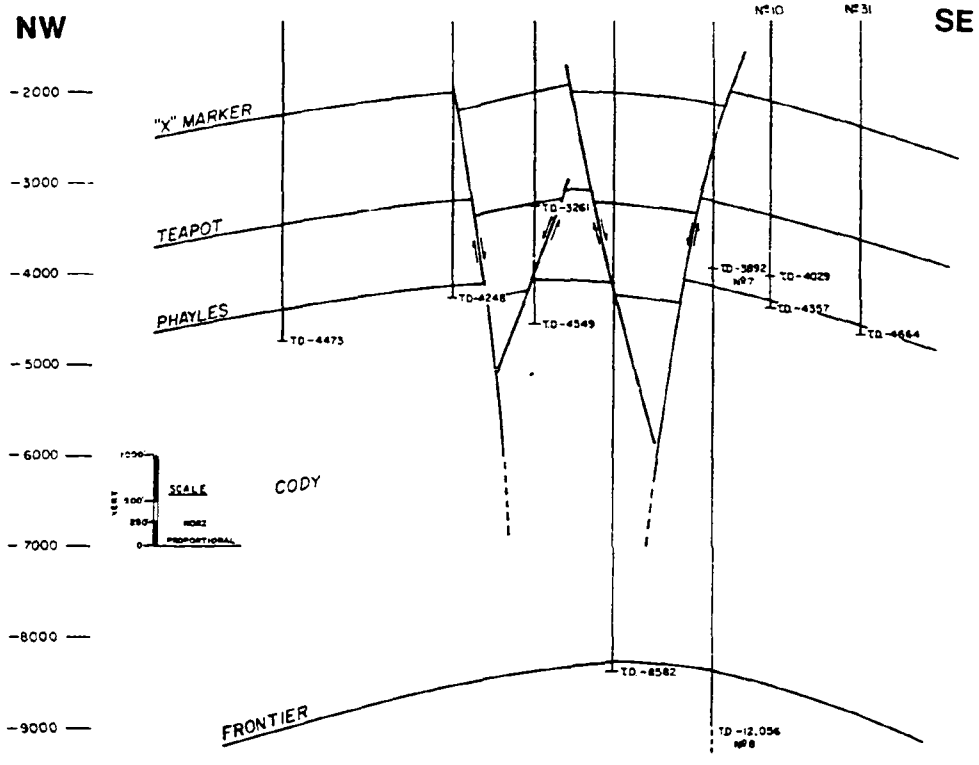

FIGURE 96. Example of extension by development of crestal graben on West Poison Spider anticline, southeast Wind River basin (T.33 N., R.84 W.; after Clark, 1978).

FIGURE 97. Thrust uplift geometry at Precambrian basement level, exposed on the south flank of the Granite Mountains uplift (T.25 N., Rs.84 and 85 W.). State Geologic Map (Love and others, 1955), is rotated 180 degrees to approximate a down-plunge view, or true cross section.

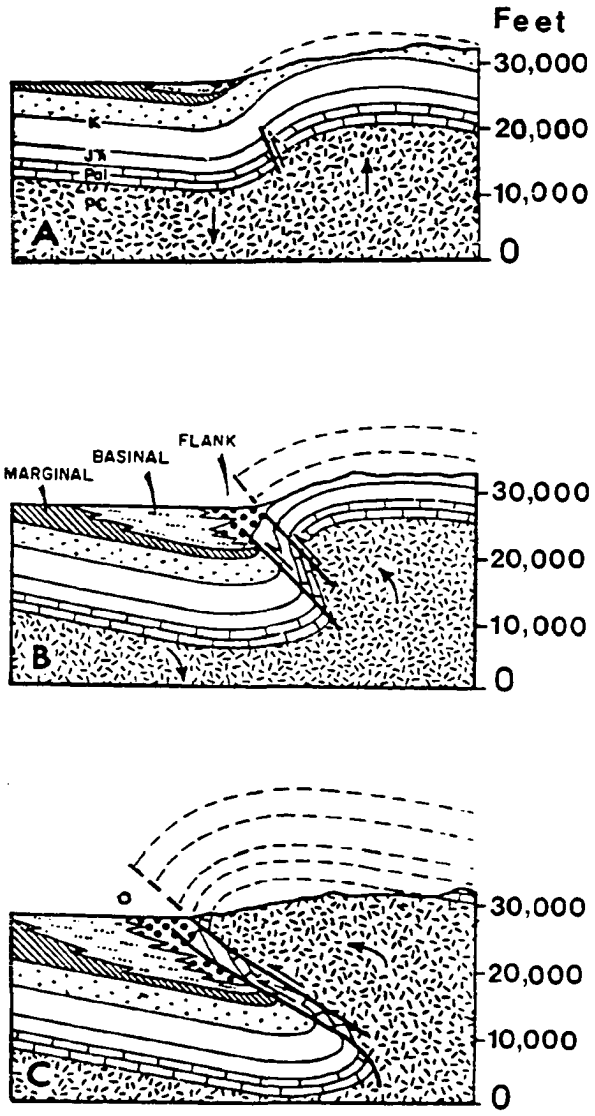

FIGURE 98. Sequence of development of fold-thrust structure (after Berg, 1962). A) Stage 1 represented by asymmetric anticline, probably controlled by deep faulting. B) Stage 2 represented by continued uplift and development of two reverse faults on the steep flank of the structure, which has begun to rotate and become overturned. C) Stage 3 represented by large scale transport and development of major basement overhang, along with extreme rotation and thinning of flank caught between the two reverse faults.

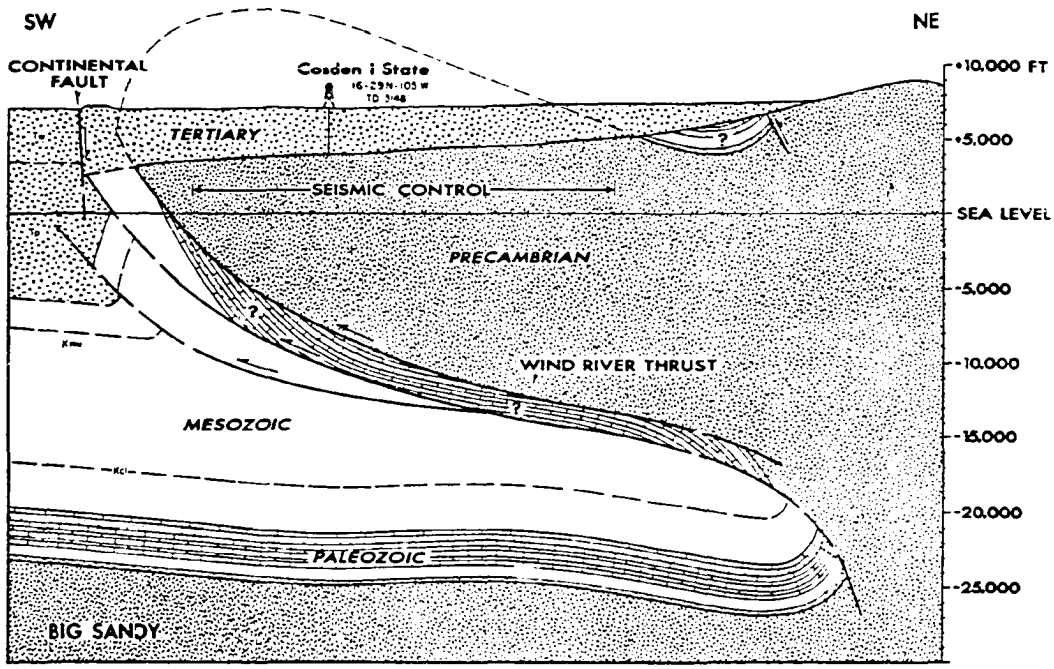

FIGURE 99. Fold-thrust model applied to the Wind River Mountains of west-central Wyoming (after Berg, 1962). Interpretation was based upon reflection seismic data available at the time, and well control on other mountain uplifts. Berg predicted a large basement overhang of approximately eight miles (13 km), an inverted section of Paleozoic rocks caught between two low angle reverse faults, which ultimately steepened with depth, and a normal stratigraphic section of Mesozoic and Paleozoic rocks overlying basement in the footwall.

FIGURE 100. COCORP (Consortium for Continental Reflection Profiling) seismic interpretation of the Wind River Mountains uplift (after Smithson and others, 1978). A) Portion of reflection profile (in time) across the Wind River uplift. B) Line drawing interpretation of reflection data in (A) above, shows approximetely 13 to 14 miles (22 kilometers) of Precambrian basement overhang developed on a reverse fault which does not steepen with depth.

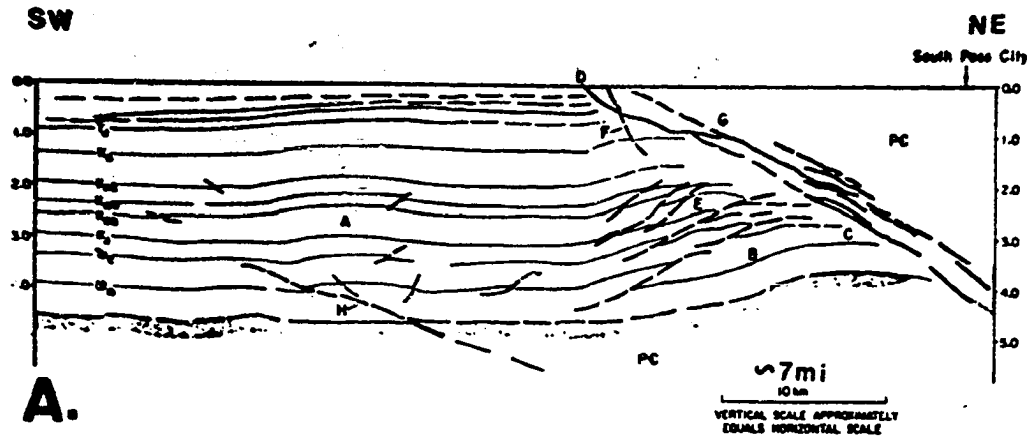

A.

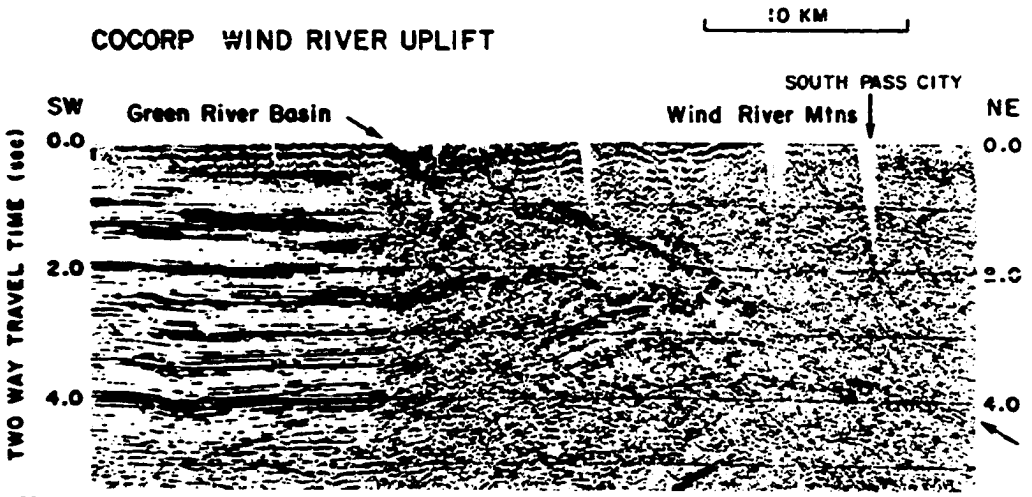

B.

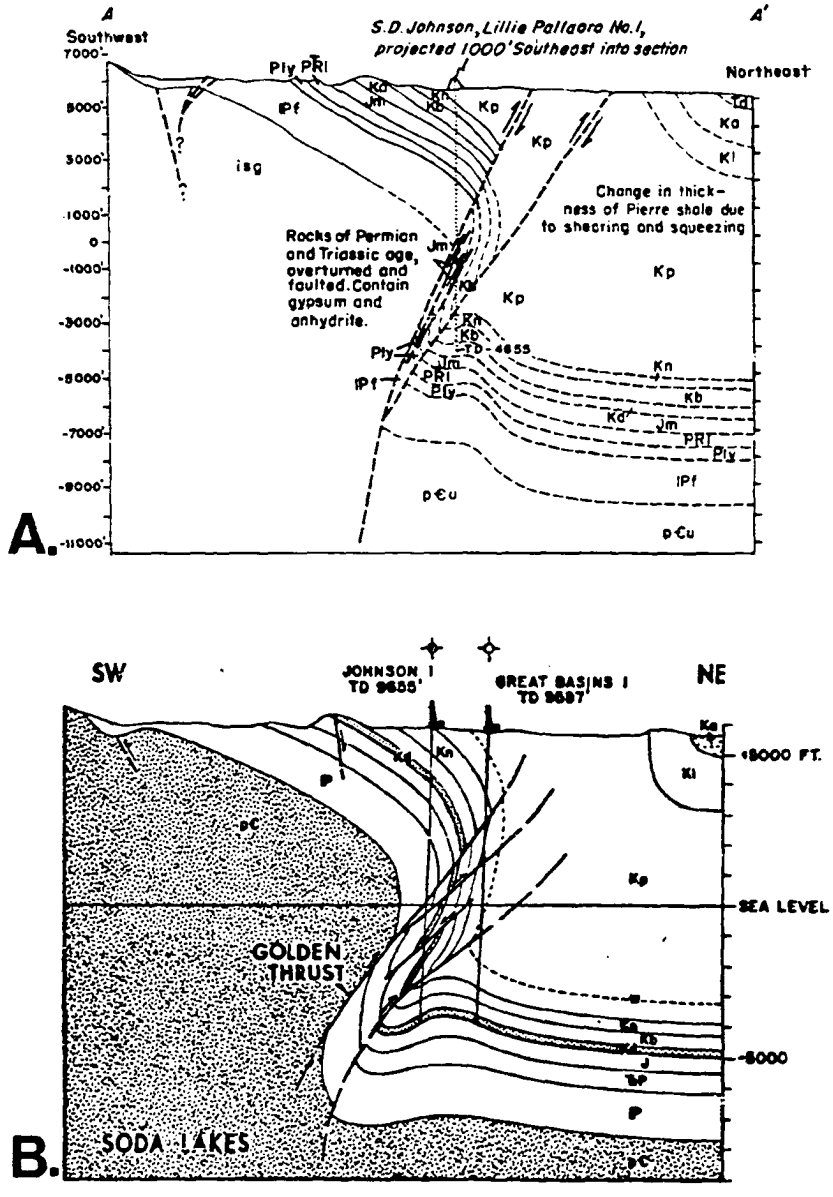

FIGURE 101. Comparison of upthrust and fold-thrust interpretations of the Soda Lakes area, Colorado (T.5 S., R.69 W.). A) Upthrust interpretation (after Osterwald, 1961) shows high angle reverse fault(s) and planar basement surface on hanging wall. B) Fold-thrust interpretation (after Berg, 1962) shows lower angle reverse faults and curvature on upper basement surface on hanging wall.

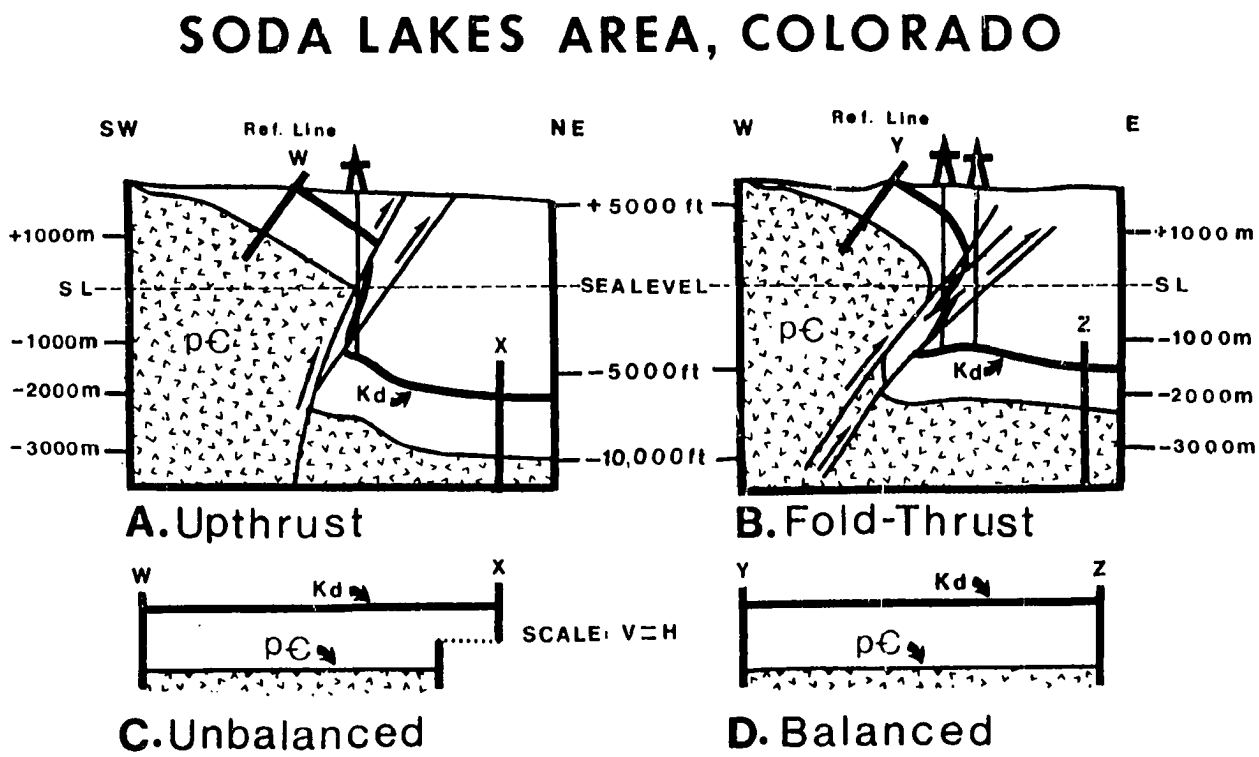

FIGURE 102. Application of structural balance concept to Osterwald's and Berg's interpretations of Soda Lakes area (same as figure 101). A) Comparison of lengths of the Cretaceous Dakota (Kd) and upper surface of the Precambrian basement for Osterwald's interpretations shows the basement to be 25% shorter than the Dakota. B) Comparison of the same surfaces for Berg's interpretation shows the basement to be only 5% shorter than the Dakota.

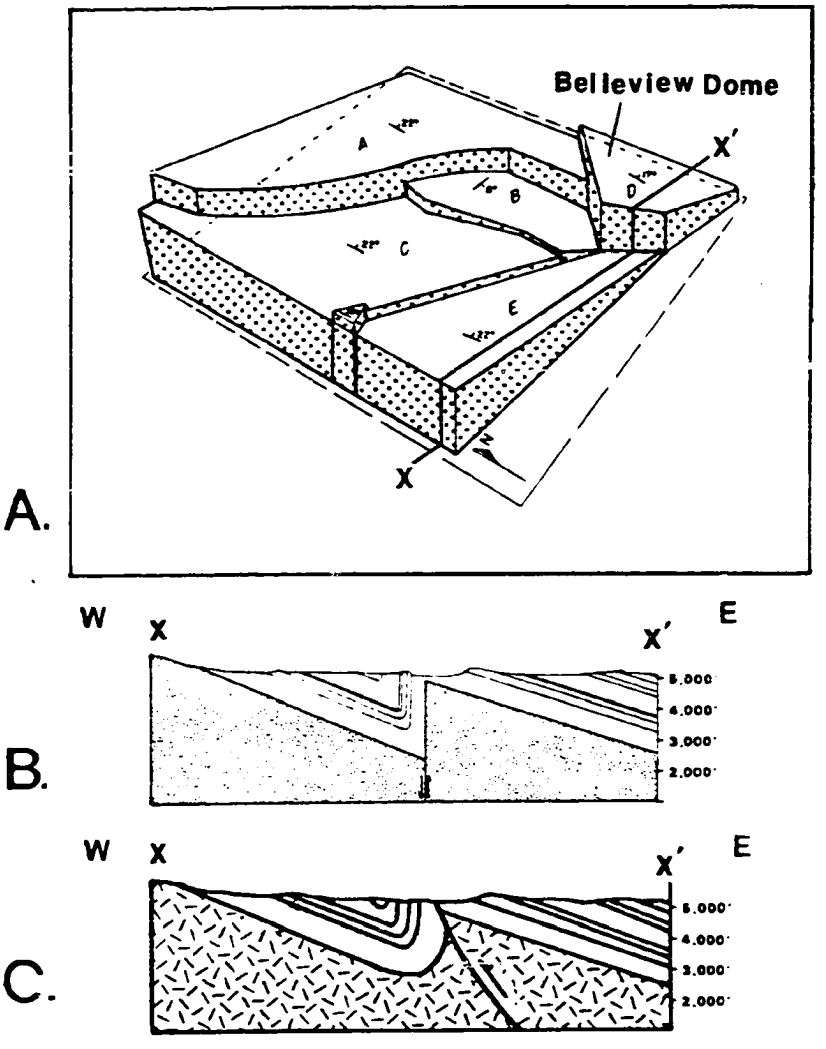

FIGURE 103. Comparison of interpretations of Belleview dome area, Colorado (T.8 N, Rs. 69 and 70 W.) using models of vertical uplift and horizontal compression. A) Block diagram of upper basement surface (after Matthews and Work, 1978). Indicated line of cross section A-A' used in comparisons. B) Drape fold interpretation (after Matthews and Work, 1978) employs a vertical basement fault, with the sedimentary section draping continuously over the block edge. Upper surface of basement is planar on both fault blocks. C) Compressional reverse fault interpretation (after Brown, 1982), employs a low angle reverse fault, which dies out upward into a fault-to-fold interchange, along with folding or rotation of the basement surface on the footwall block.

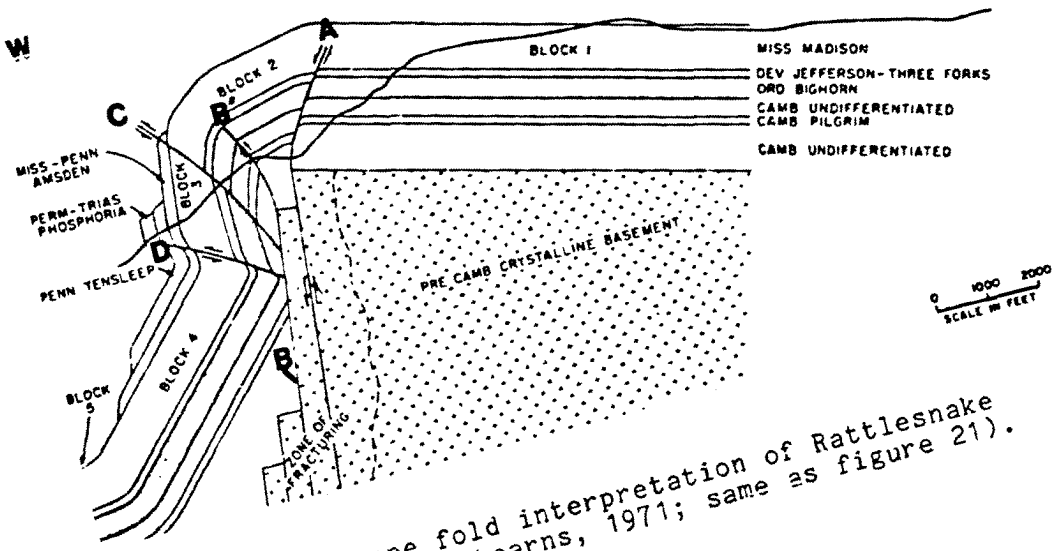

FIGURE 104. Drape fold interpretation of Rattlesnake Mountain anticline (Stearns, 1971; same as figure 21).

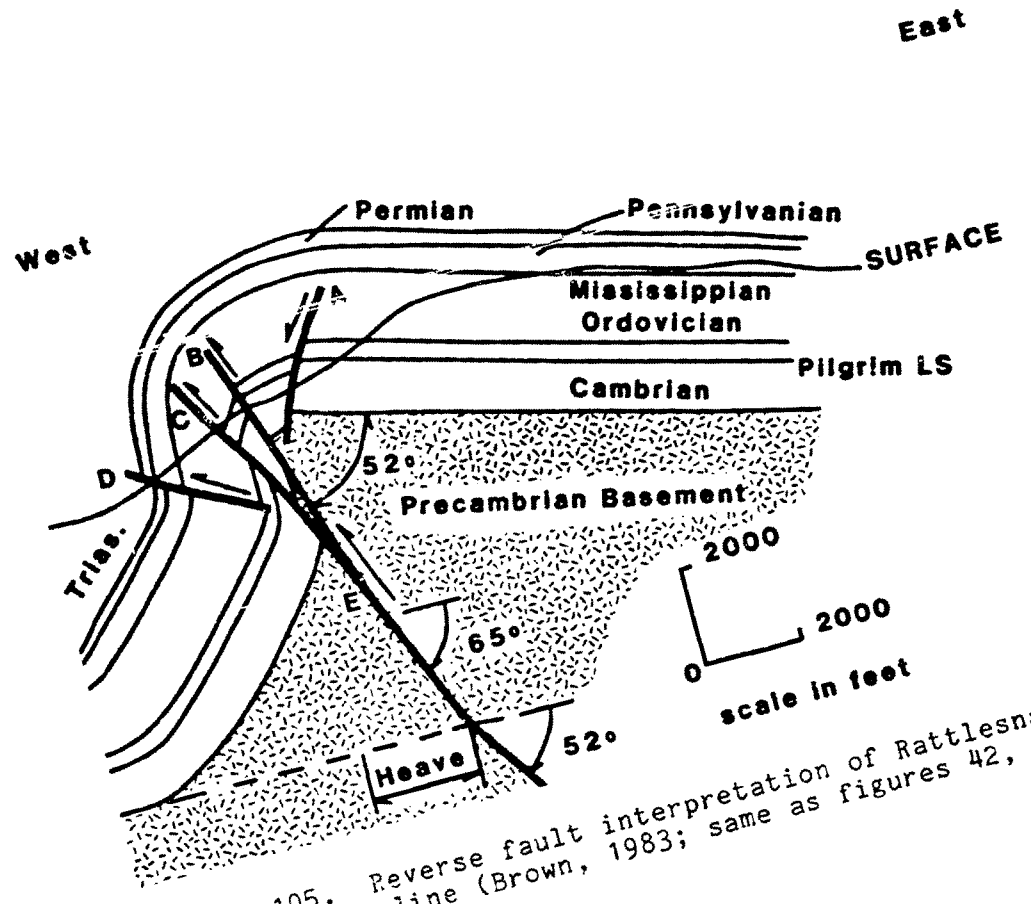

FIGURE 105. Reverse fault interpretation of Rattlesnake Mountain anticline (Brown, 1983; same as figures 42, 44).

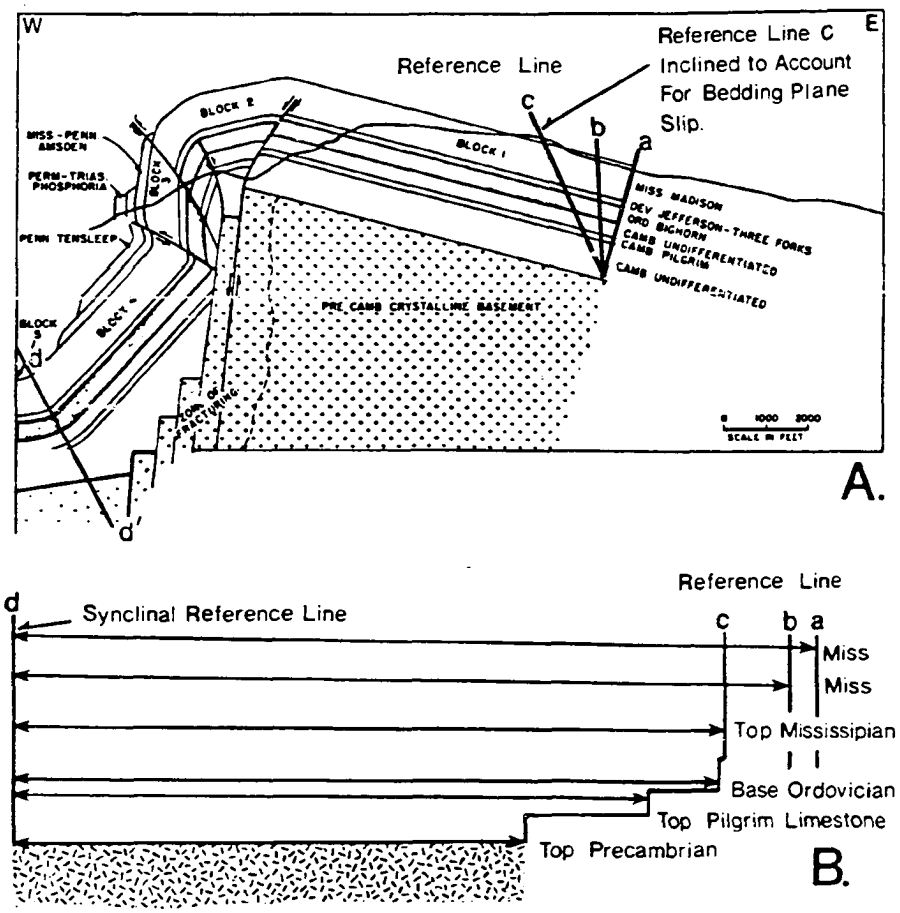

FIGURE 106. Concept of structural balance as applied to drape fold interpretation of Rattlesnake Mountain anticline. A) Cross section (same as figure 104) with reference lines a, b, c, and d, added and basement surface extended on lower left side of cross section (modified from Stearns, 1971). B) Variations in bed length measurements (between reference lines a-d, b-d, and c-d) made on top of Mississippian Limestone demonstrates importance in selecting proper orientation of reference lines. Reference line (c) is considered to be proper orientation. Measurement of bed length for base of Ordovician Big Horn Dolomite, Cambrian Pilgrim Limestone, and upper basement surface (between lines c & d) yield good agreement between the Mississippian and Ordovician lengths, but the Pilgrim Limestone and upper basement surface are approximately 2,000 feet (600 m) and 5,000 feet (1500 m) shorter, respectively, than the Mississippian.

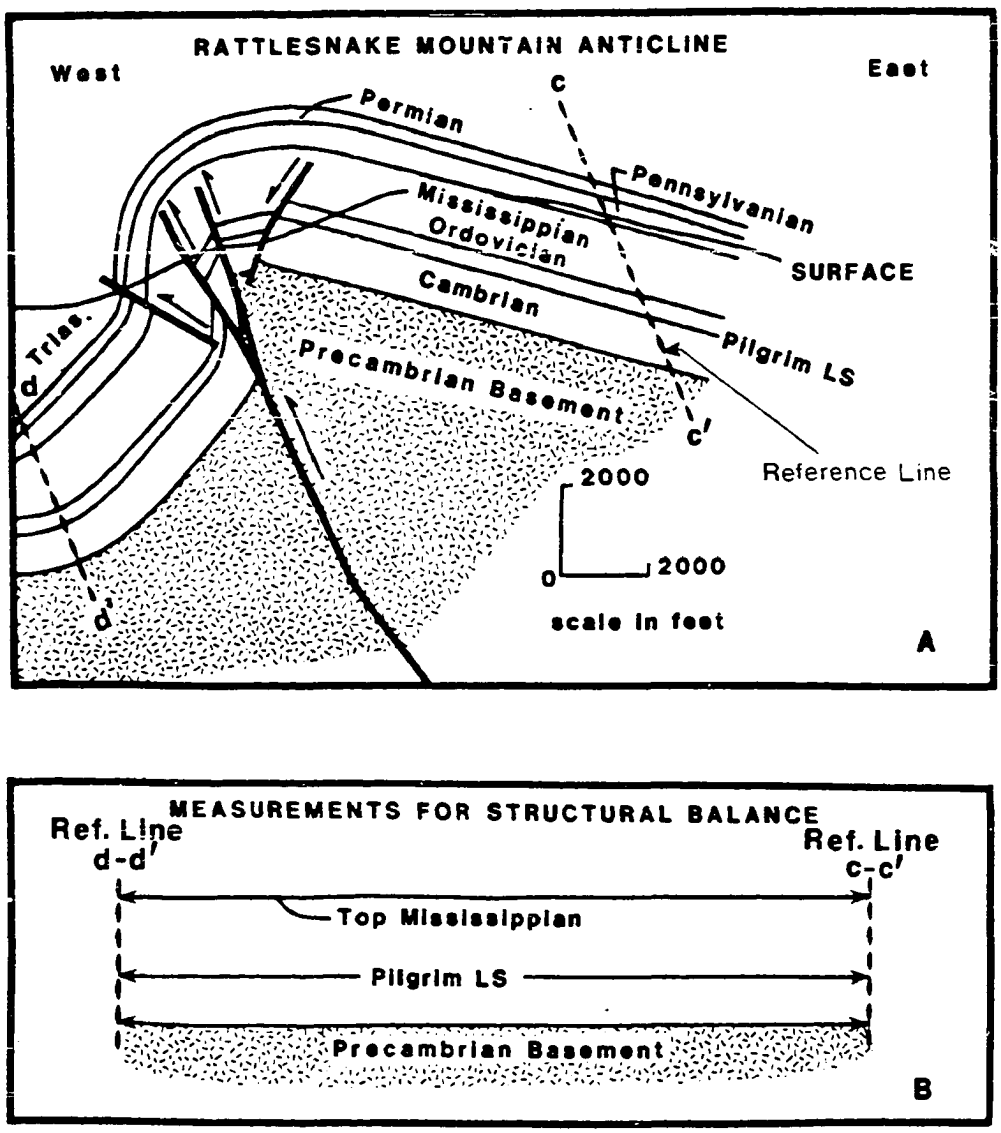

FIGURE 107. Concept of structural balance as applied to reverse fault interpretation of Rattlesnake Mountain anticline. A) Cross section (same as figure 105) with reference lines c and d, same as in figure 106. B) Measurements for top Mississippian Limestone, Cambrian Pilgrim Limestone, and upper basement surface shows good agreement in all bed lengths (modified from Brown, 1983).

FIGURE 108. Extensional faulting exposed in Cambrian shales on steep flank of Rattlesnake Mountain anticline. A) One set of faults is nearly horizontal. Sense of drag and offset indicate upper block has moved to the right (towards the crest of the fold). B) Second set of faults dips strongly to the west. Sense of offset indicates hanging wall has moved up to the right (towards crest of fold). Classical definition of this set of faults would be "reverse", but extension, or lengthening of the beds is being accomplished.

A.

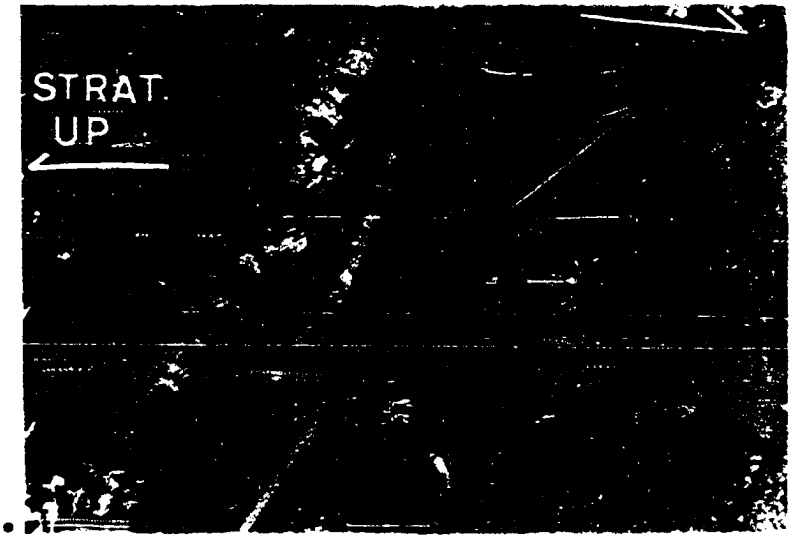

B.

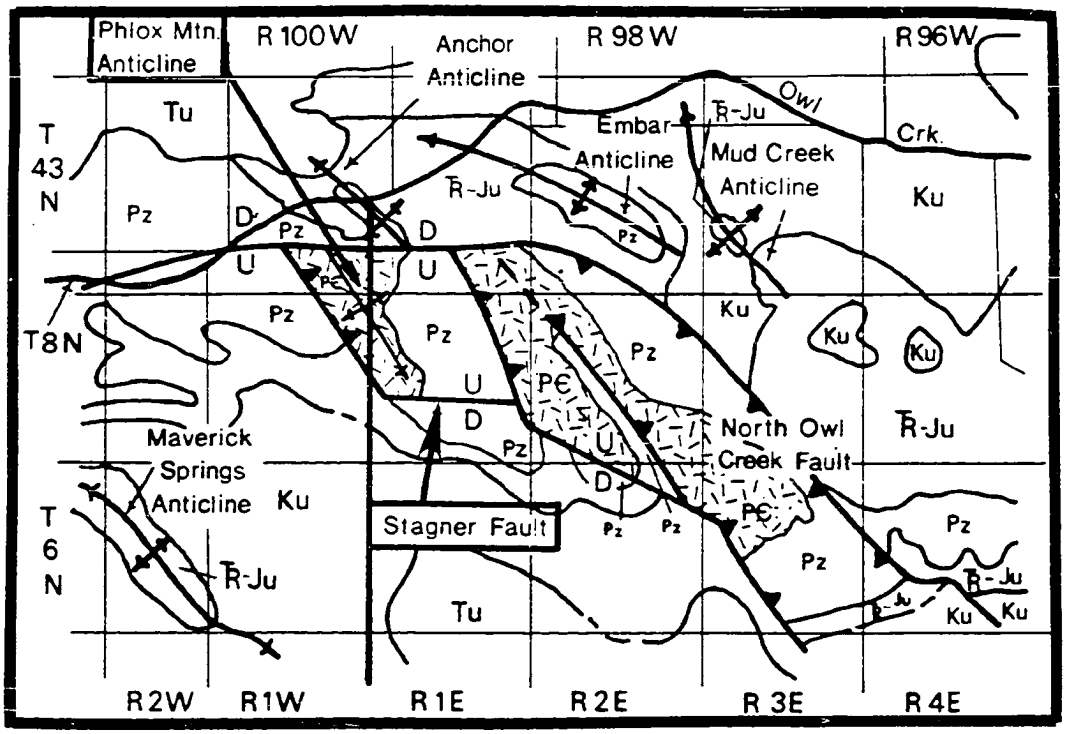

FIGURE 109. Geologic map of the Owl Creek Mountains (modified from Love and Christiansen, 1985). Phlox Mountain anticline (Tps.7 and 8 N., R.1 W.) plunges to the southeast, where it is transected by the east-trending Stagner fault (north side upthrown) in T.7 N., R.1 E.. On the south side of the Stagner fault, Phlox Mountain anticline continues to plunge southeastward, but at a lower structural elevation. Field study of the Stagner fault area should provide data concerning thinning of the stratigraphic section associated with drape folding.

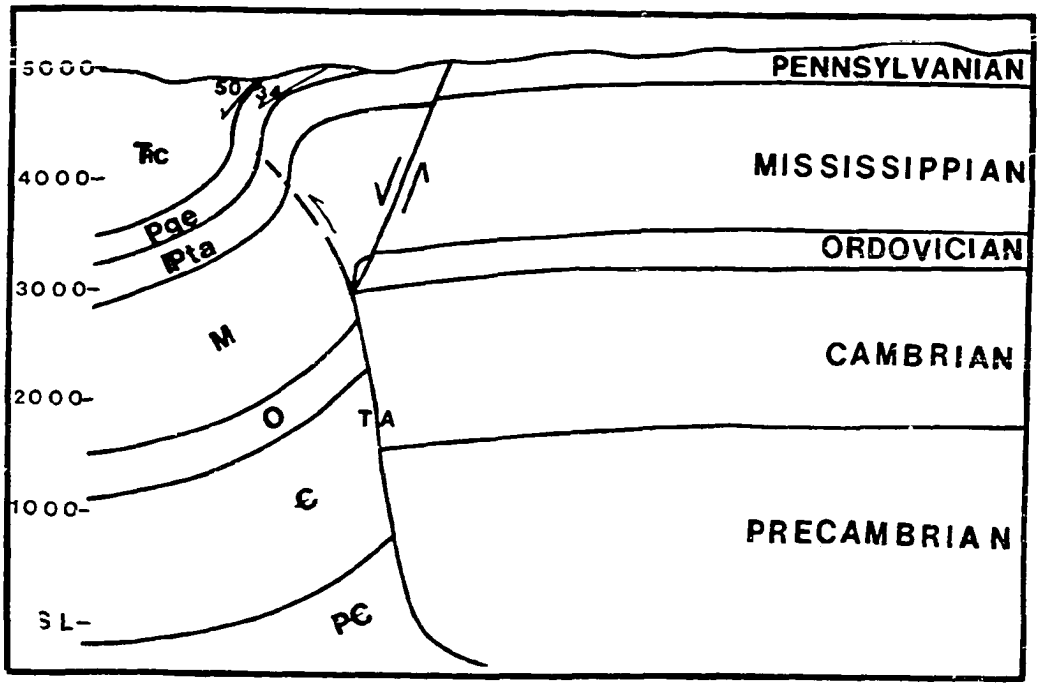

FIGURE 110. Extension by normal faulting on the north flank of Zeisman dome (T.49 N., R.89 W.) may indicate a drape fold (or early stage upthrust) along this zone (after Stricker, 1984).

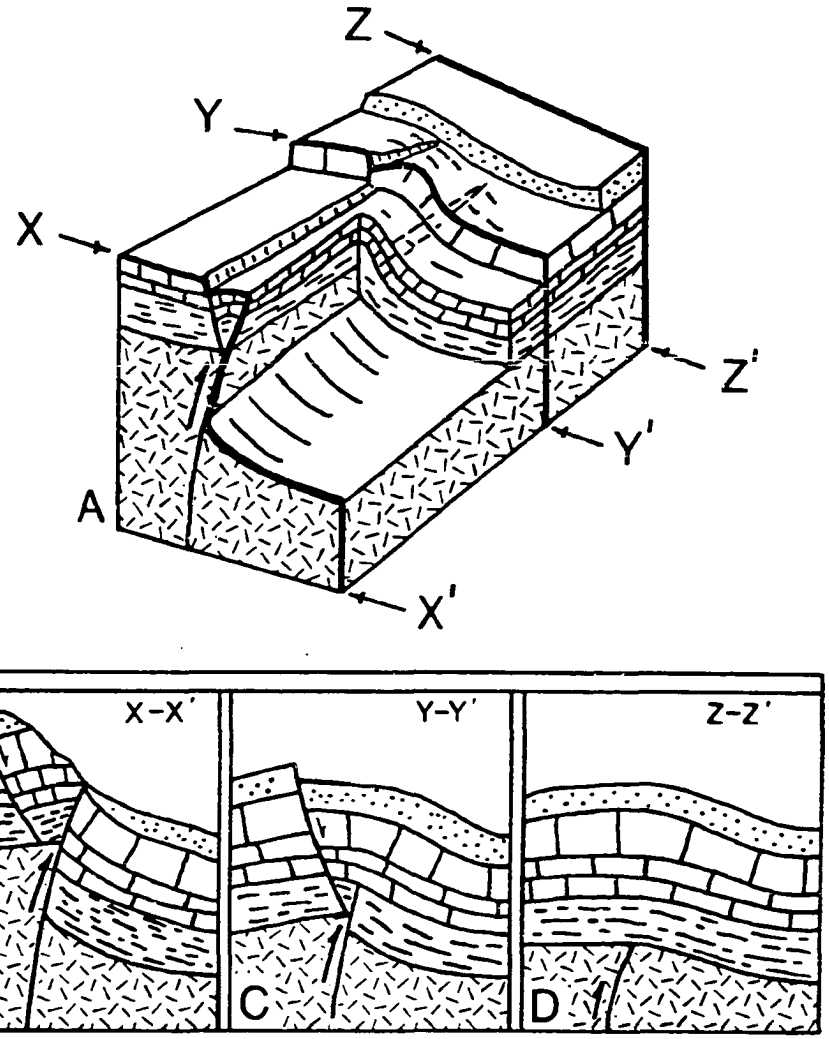

FIGURE 111. Development of drape fold by progressive loss of displacement along a high angle reverse fault. A) Block diagram illustrates lateral change in displacement, which eventually develops a drape fold. B) Cross section X-X' shows a high angle reverse fault, which cuts through the entire stratigraphic section. C) Cross section Y-Y' shows decrease in displacement to the point that only the upper basement surface is offset, with the sedimentary layers forming an overlying drape fold. D) In cross section Z-Z', all fault displacement is absent; the flexure which remains at the uppper basement surface is a function of the upturned basement surface in (B) and (C). The cross sections can be considered sequentially (in reverse order:D, C, B) as the process through which the high angle reverse fault (in B) developed.

FIGURE 112. Development of the Tensleep fault trend (T.47 N., Rs. 83 to 90 W.). A) Wyoming State Geologic map (modified from Love and others, 1955). All three cross sections are drawn north-to-south across the fault, and spaced approximately 15 miles (24 km) apart. B) Greatest displacement (the north side up) places Precambrian basement against Ordovician Big Horn Dolomite near the crest of the Bighorn Mountains (R.85 W.). C) Displacement decreases progressively towards the west until (R.87 W.) the Mississippian carbonates are faulted opposite the Pennsylvanian Tensleep Sandstone (basement against lower Cambrian). D) In R.90 W., fault displacement has decreased to the point where there is no offset at the top of the Pennsylvanian Tensleep, and by reconstruction, it is interpreted that the upper basement surface is not offset.

FIG. 112D

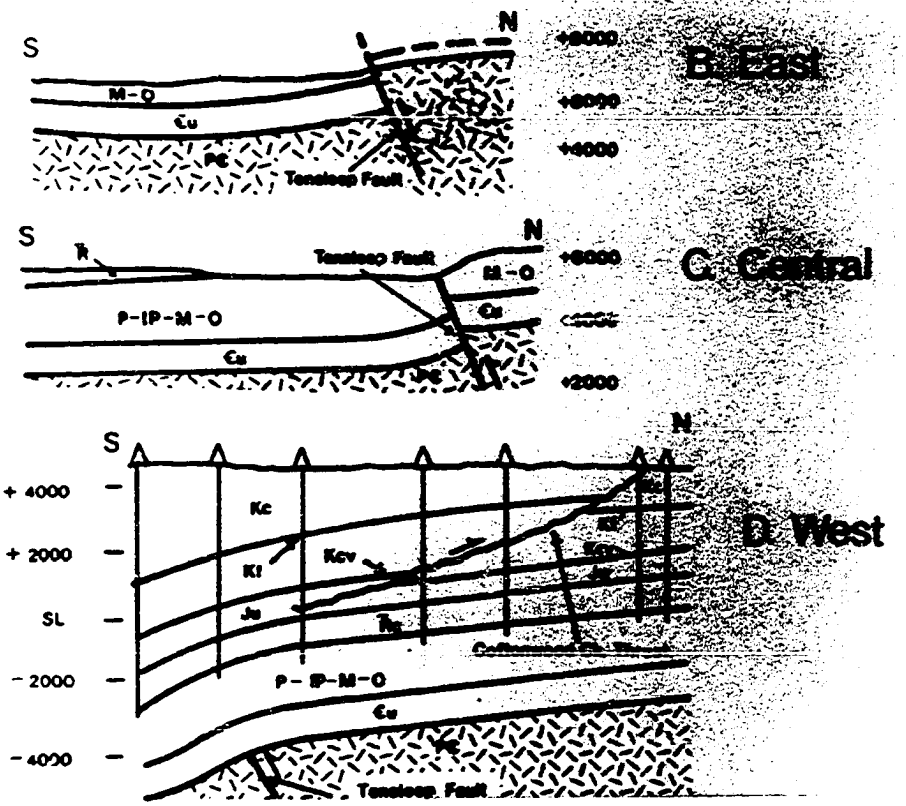

FIGURE 113. Owl Creek Mountains, central Wyoming. A) Geologic map showing the trace of the Boysen normal fault and the buried South Owl Creek fault (modified from Love and others, 1955). Line of section crosses crest of uplift at the canyon of the Wind River. B) South flank of the Owl Creek Mountains is interpreted as an upthrust structure, with required extension provided by the east-west trending Boysen normal fault, and associated smaller normal faults on the hanging wall of the South Owl Creek fault (after Brown, 1983). "Towards and away" notation indicates concept of oblique-slip on the east-west trending South Owl Creek fault.

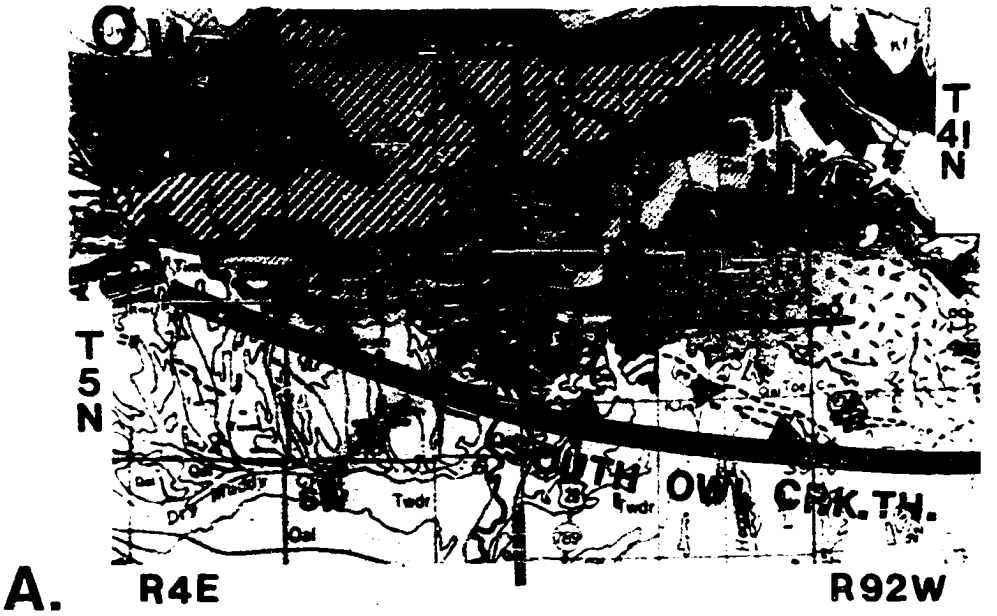

A.

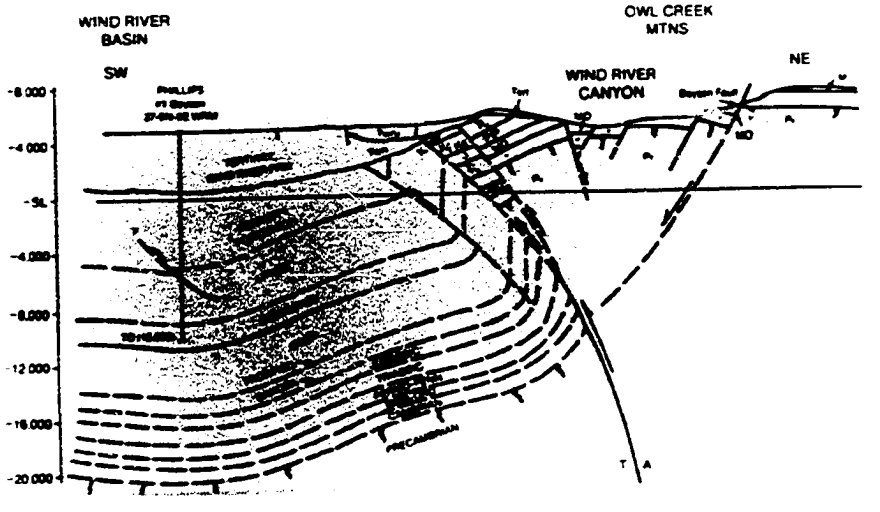

B.

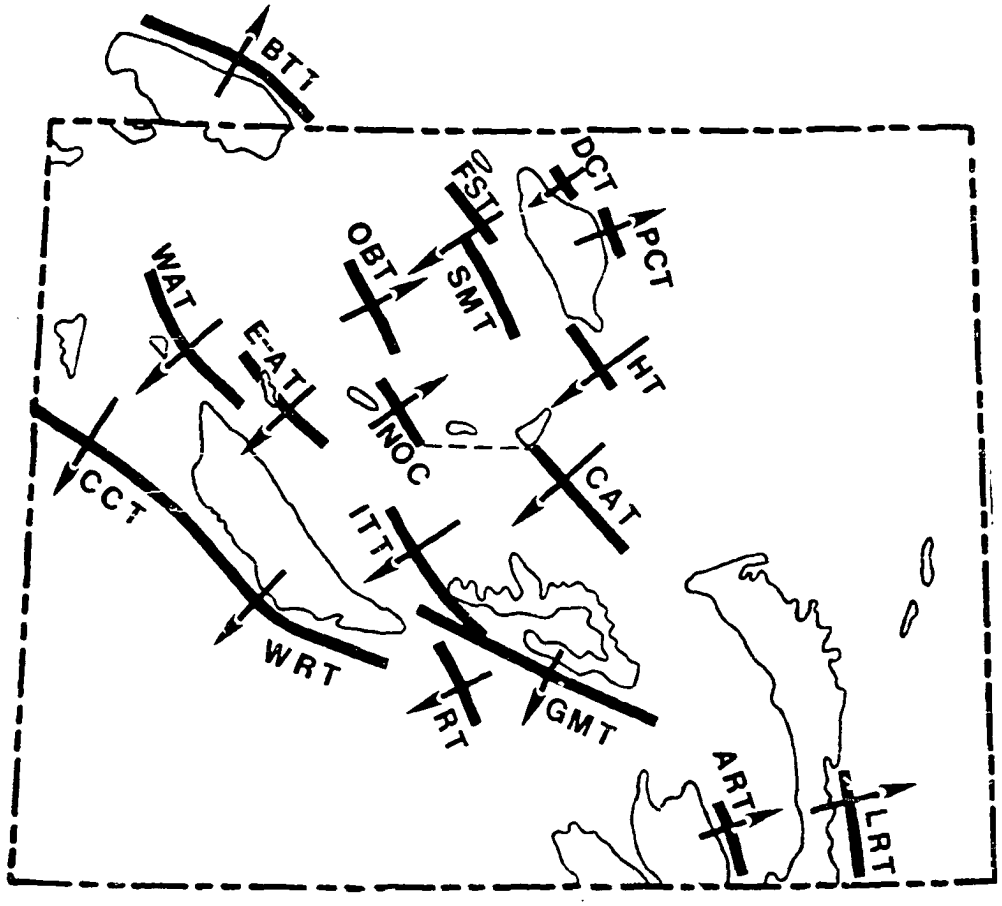

FIGURE 114. Index map of the Wyoming foreland showing directions of vergence of fold-thrust structures. The northeast and southwest directions of tectonic transport may be interpreted as representing a conjugate set of basement reverse faults. Symbols refer to specific faults: ART = Arlington thrust; BTT = Beartooth thrust; CAT = Casper arch thrust; CCT = Cache Creek thrust; DCT = Deer Creek thrust; E-AT = E-A thrust; FST = Five Springs thrust; GMT = Granite Mountains thrust; HT = Horn thrust; ITT = Immigrant Trail thrust; LRT = Laramie Range thrust; NOC = North Owl Creek thrust; OBT = Oregon Basin thrust; PCT = Piney Creek thrust; RT = Rawlins thrust; SMT = Sheep Mountain thrust; WT = Washakie thrust; WRT = Wind River thrust.

FIGURE 115. Zeisman dome area on the east flank of Bighorn basin (T.49 N., R.89 W.). A) East-facing asymmetry of Zeisman dome is controlled by a west-dipping reverse fault, which dies out upward in the sedimentary section, representing a very early stage in the development of a fold-thrust (Brown, 1963). B) Aerial view shows the east vergence of Zesiman dome with the abrupt termination of northwest plunge by a southwest-trending panel of steep dip, which was shown in figure 110.

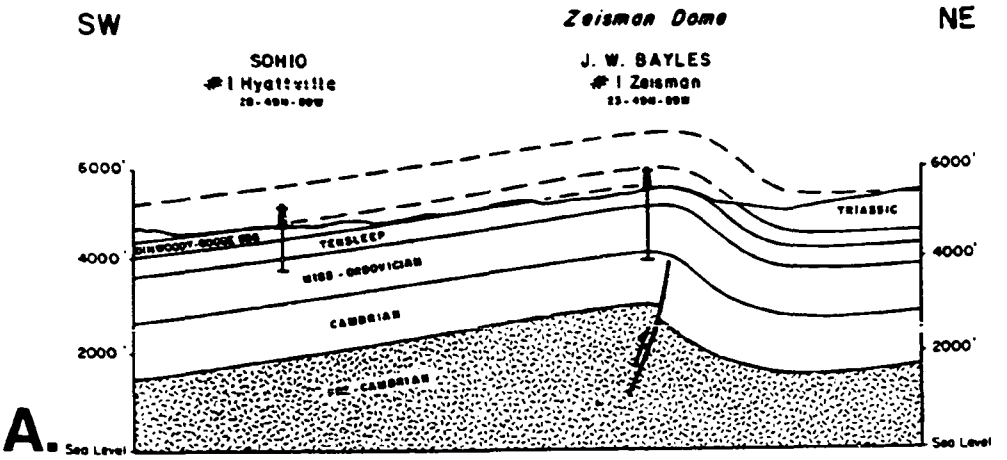

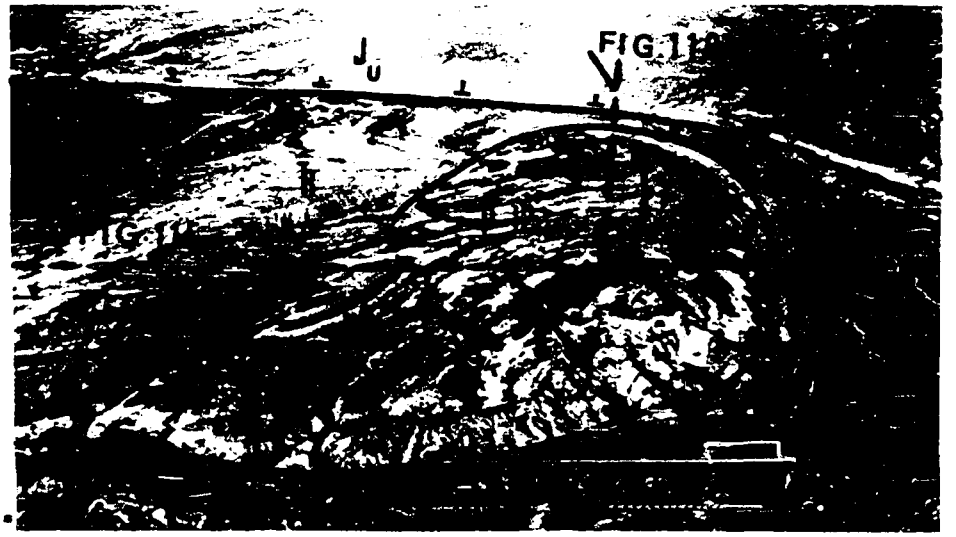

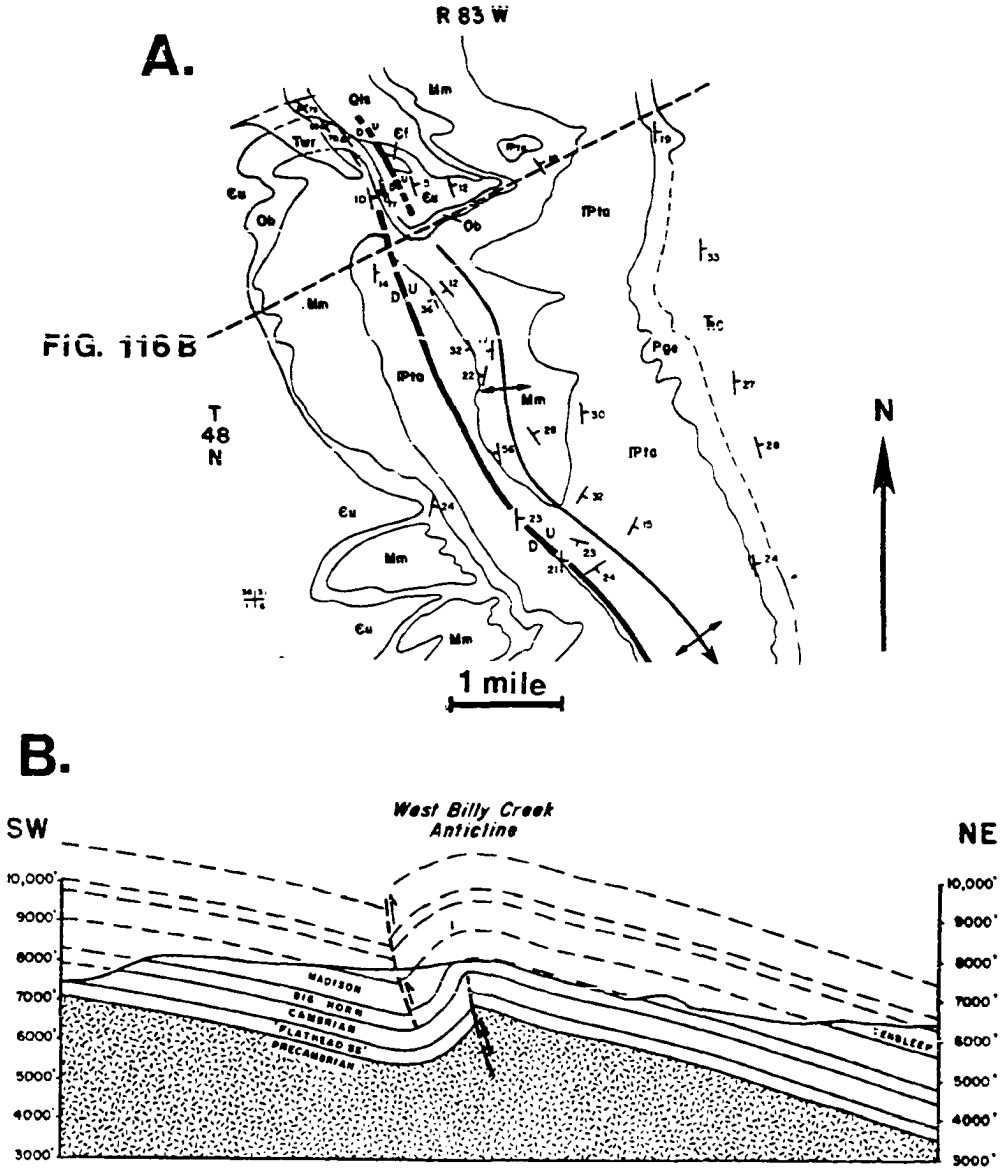

FIGURE 116. West Billy Creek anticline on the east flank of the Bighorn Mountains. A) Geologic map (Brown, 1983) shows that the faulting in the core of the anticline dies out upward at the Cambrian level, while the faulting in the syncline dies out downward in the Mississippian and Ordovician carbonates. Presence of two faults represents the dual fault system, with rotation of the intervening sedimentary section indicating a second stage in the development of a fold-thrust.

FIGURE 117. Development and propagation of dual fault system. A) Experimental rock model showing footwall imbrication of controlling fault (A-A') which causes rotation of bedding surfaces in the fault slivers (Brown, 1983). B) Rotation shown in model is applied to foreland models (fault E) to explain rotation of upper basement surface, which in turn causes tightening of syncline above. Synclinal fault (C) in the sedimentary section may propagate downward to join fault (E), developing the lower fault of the dual fault system.

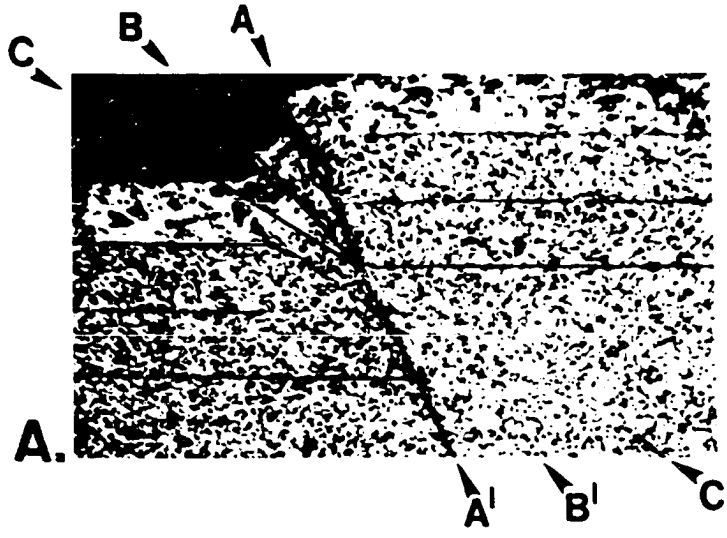

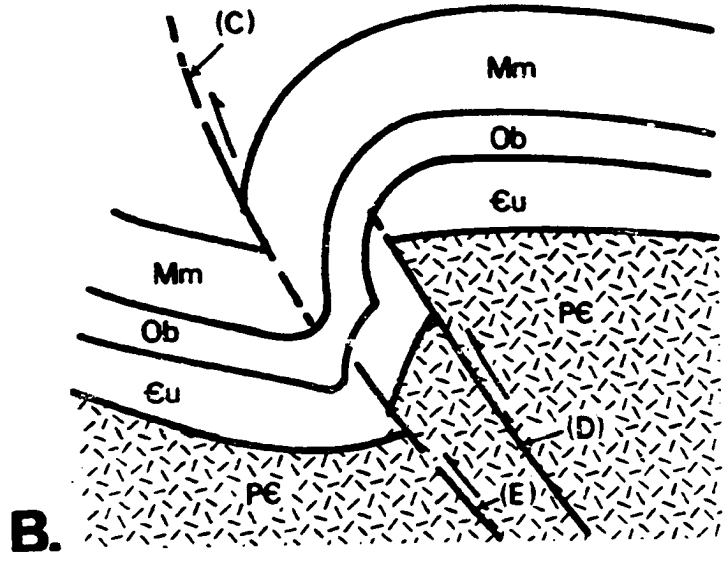

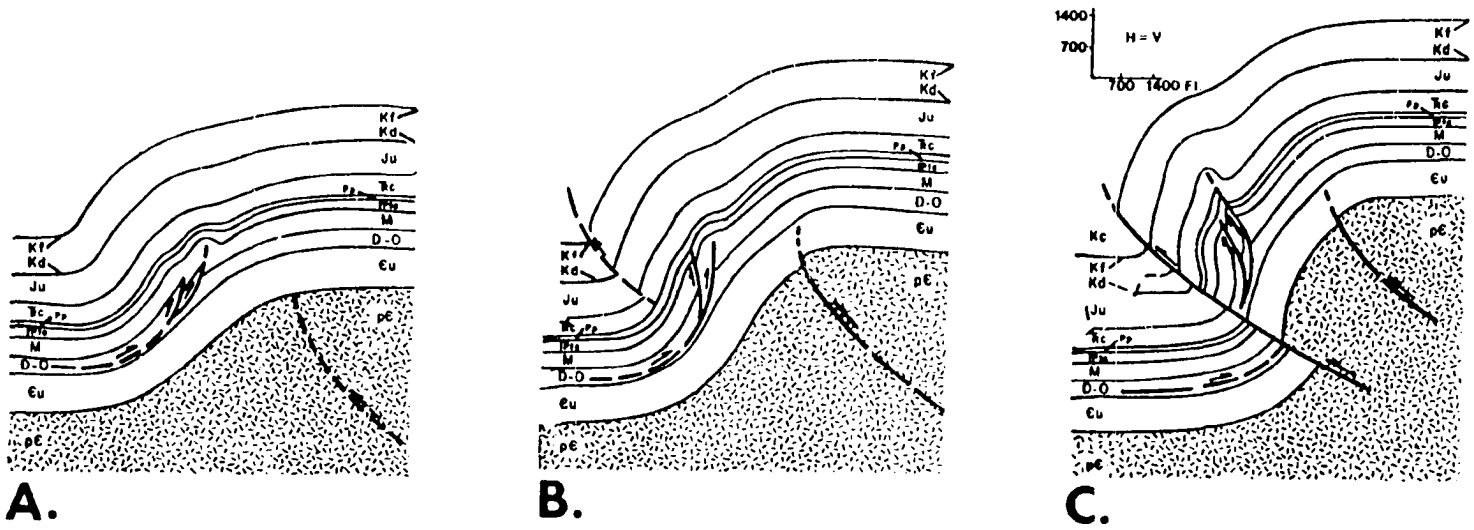

FIGURE 118. Sequential development of fold-thrust, with development of subsidiary folding on hanging wall (Brown, 1983). A) Sequence develops as demonstrated by Berg (1962), but with recognition that volumetric problems in adjacent syncline will result in the development of rabbit-ear folds on the steep flank of the uplift. B) Continued shortening causes progressive development of rabbit-ear, plus development of dual fault system with reverse fault at synclinal hinge. C) Ultimately, fold-thrust is transported over the sedimentary section in adjacent syncline, and rabbit-ear fold is isolated on the steep flank of the uplift.

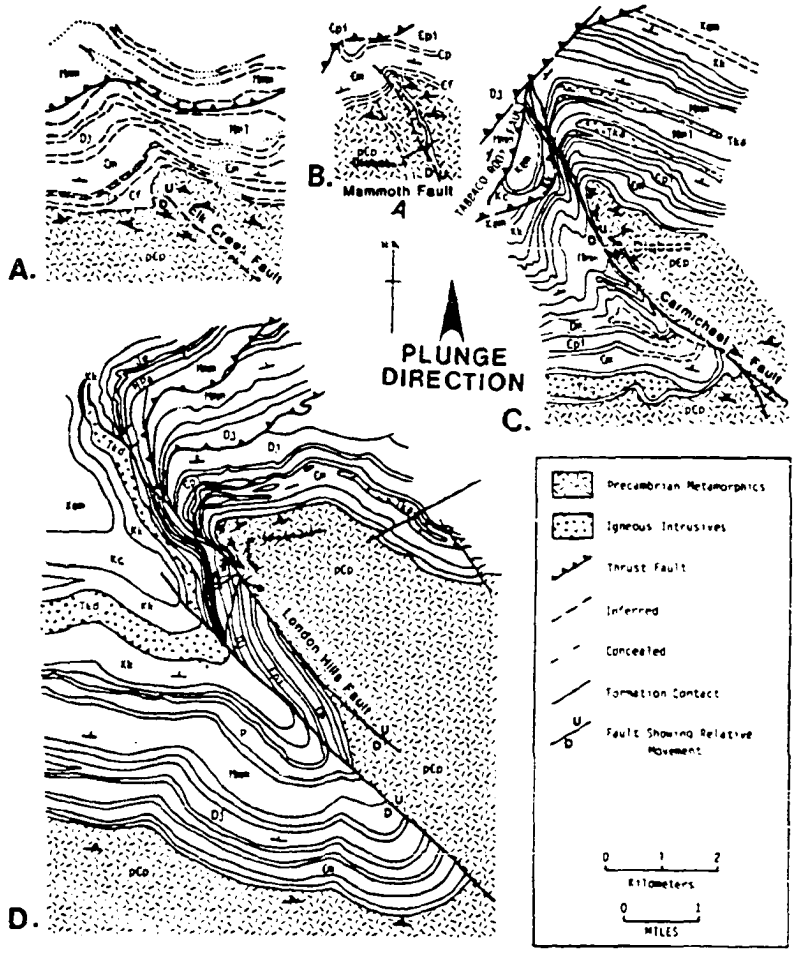

FIGURE 119. Montage of geologic maps from the Tobacco Root Range, southern Montana (modified from Schmidt and Hendrix, 1981). All four structures plunge in a northerly direction, so that each map approximates a cross section (by down-plunge viewing) of a stage in the sequential development of a fold-thrust. A) Upper basement surface is folded, but not faulted. B) Upper basement surface is faulted and folded. C) Basement overhang has developed. D) Complete development of dual fault system, rotated flank, and basement overhang.

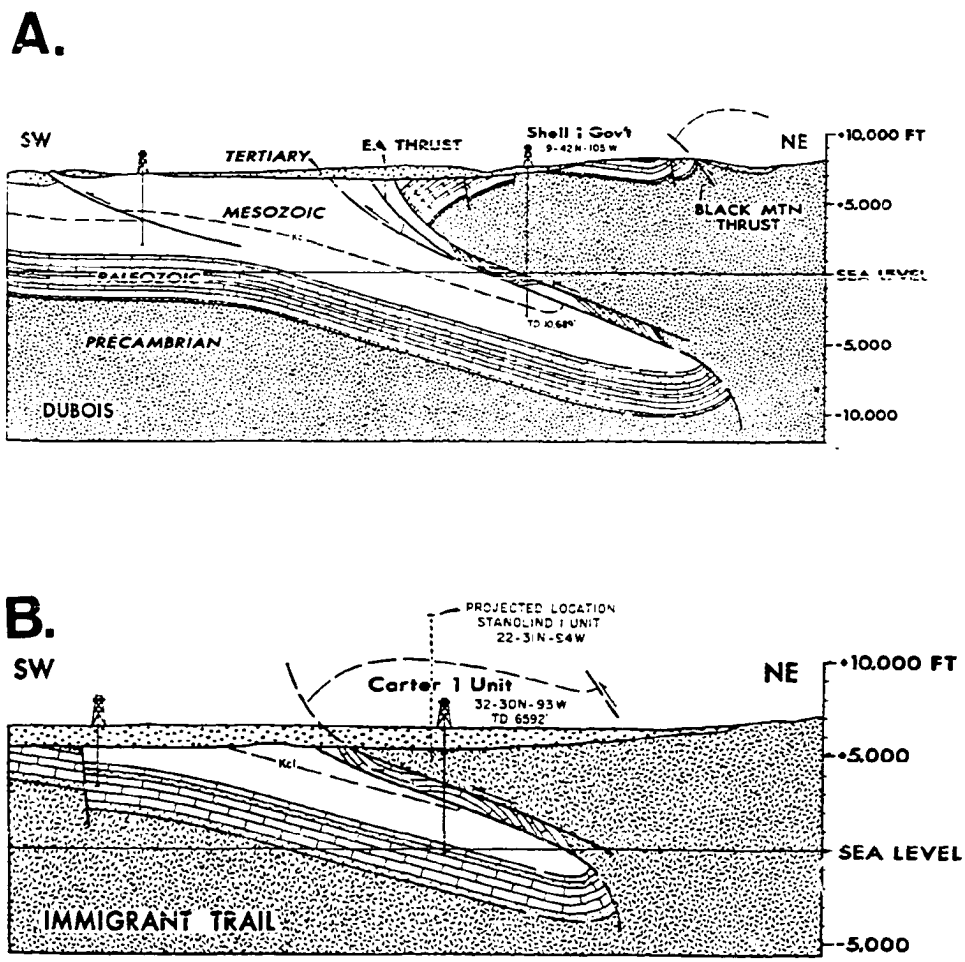

FIGURE 120. Earliest fold-thrust interpretations by Berg (1962). A) EA thrust, in the Washakie Range (T.42 N., R.103 W.). B) Immigrant Trail thrust, in the Granite Mountains of central Wyoming (T.30 N., R.93 W.). Both examples were documented by wells which drilled several thousands of feet of Precambrian basement, and drilled into the dual fault zone containing overturned, but recognizable, Paleozoic rocks, and finally into right-side up Mesozoic rocks dipping under the uplift.

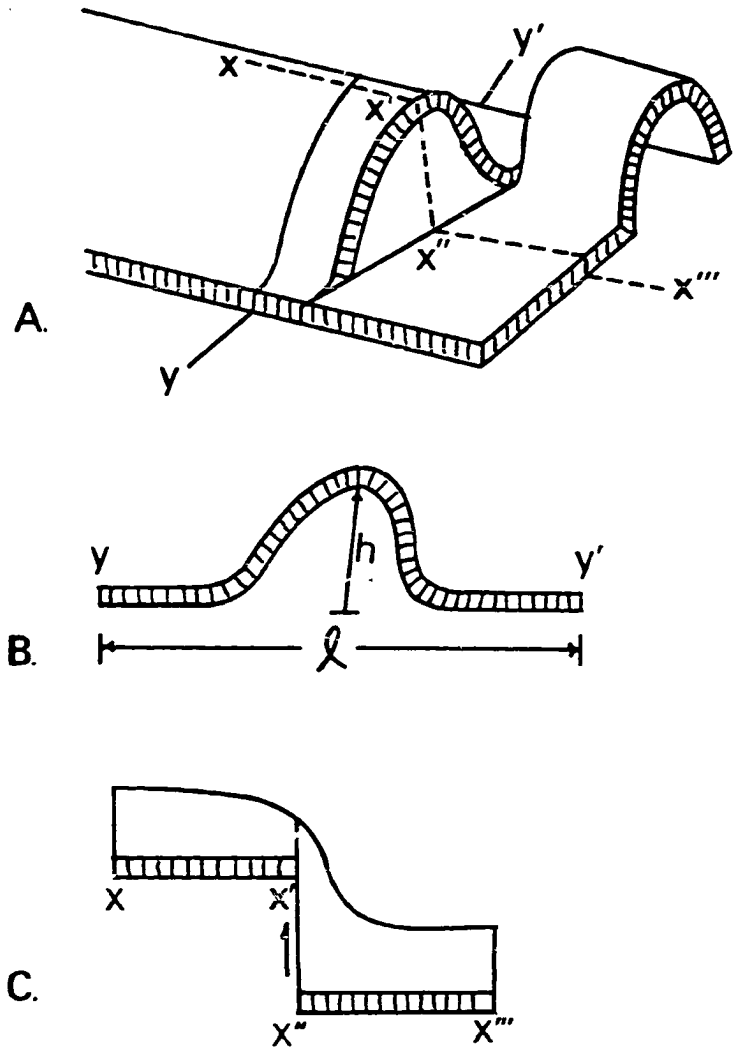

FIGURE 121. A) Northwest-trending Laramide folds are often transected (and seemingly terminated) by east or northeast-trending faults. Structural balance is maintained through the development of different fold profiles, which place the anticlinal crest on one profile adjacent to relatively unfolded rocks on the other profile. B) The sense of vertical movement at the anticlinal crest is accentuated, as seen on cross section Y-Y'. C) A longitudinal profile (X-X''') displays the vertical offset (X-X'') of a particular horizon. Often the fault dies out upward, resulting in a local drape fold which terminates the northwest-trending anticline.

FIGURE 122. The Bighorn Mountains are segmented into large structural blocks by a series of east-west, and northeast-trending compartmental faults. The major faults are (north to south): TRL-Tongue River Lineament; SCL-Shell Creek Lineament; FPL-Florence Pass Lineament; TF-Tensleep Fault. In addition to these, the Deep Creek Fault (DCF) is a major north-northeast trending fault. Relation-ships between cross sections A-A', B-B', PCT-Piney Creek Tear, and Piney Creek Block will be shown in figure 127. (Map modified from Love and others, 1955).

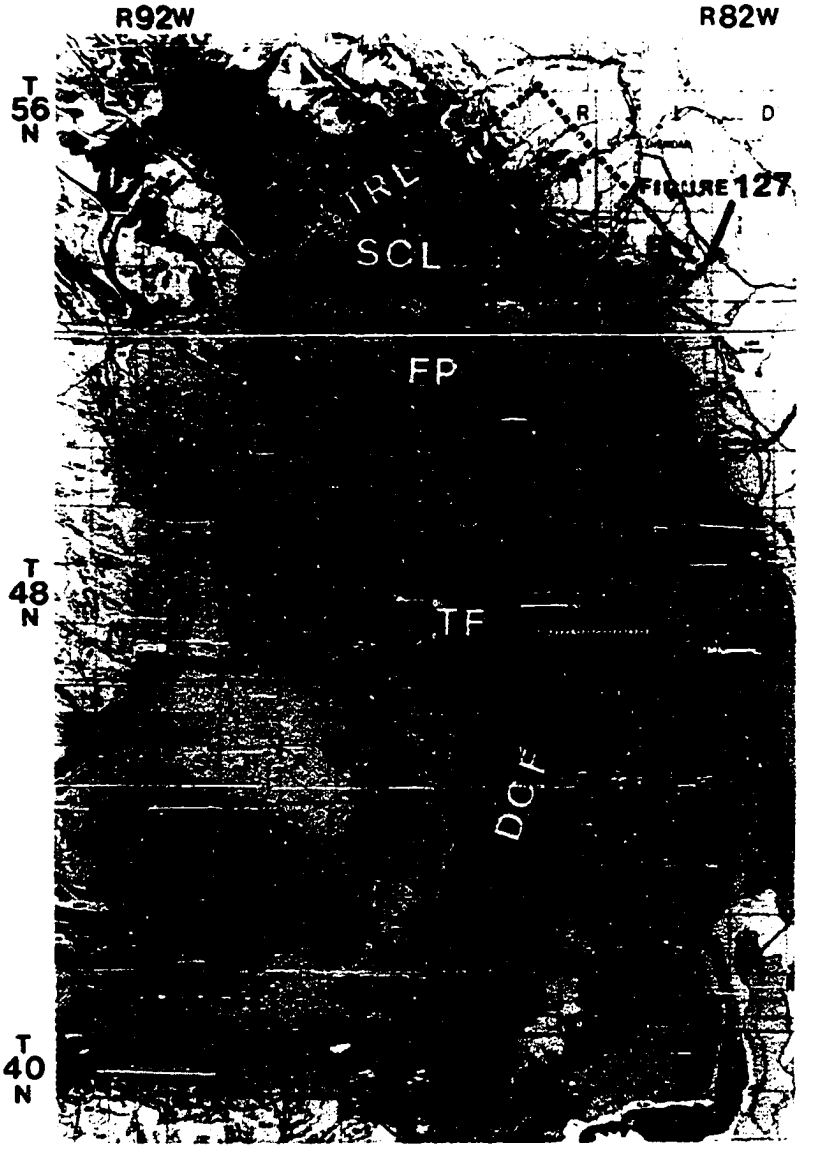

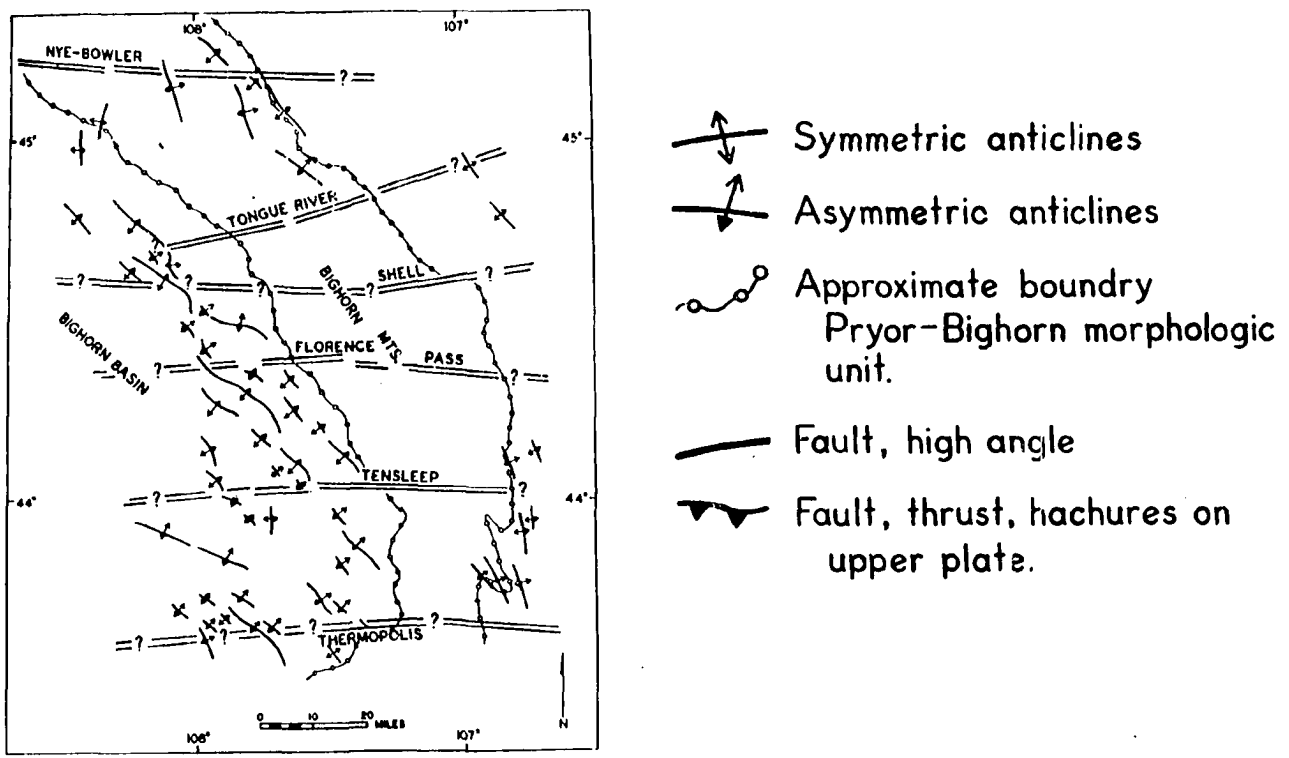

FIGURE 123. Direction of asymmetry of mountain-flank folds changes from one mountain segment (compartment) to another, as shown by Hoppin and Jennings (1971).

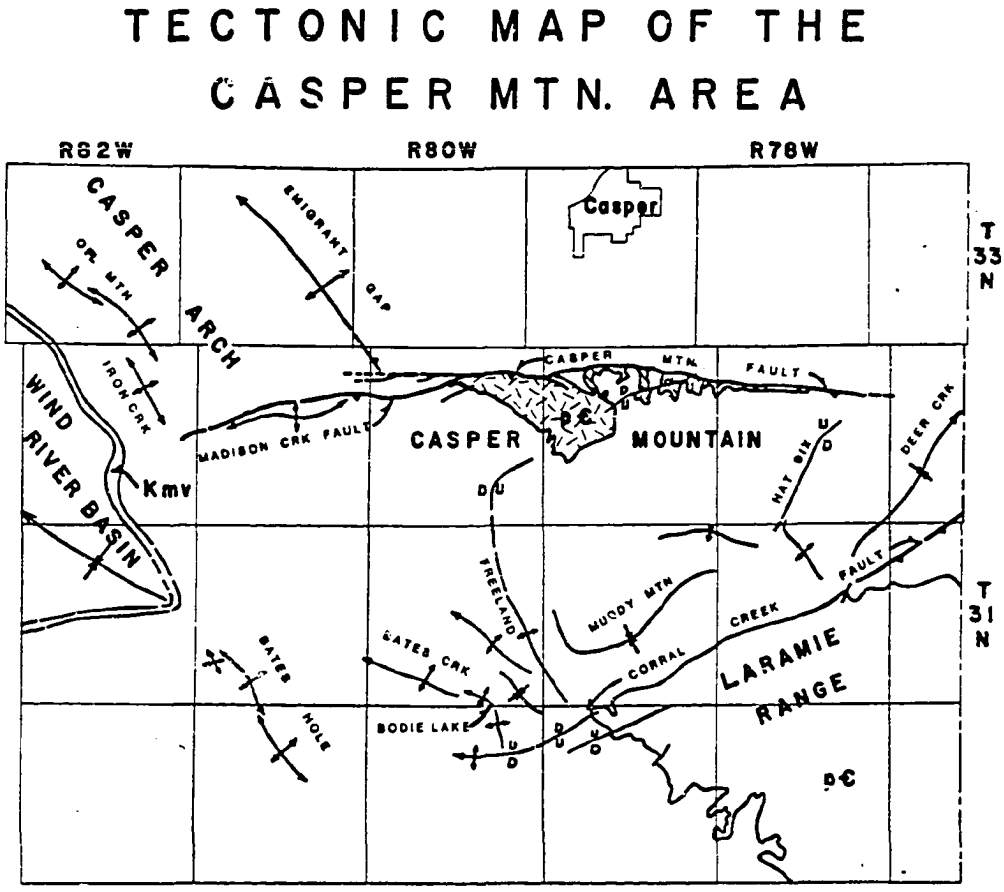

FIGURE 124. The Casper Mountain area displays abrupt termination of the Emigrant Gap and Oil Mountain-Iron Creek lines of folding at the Casper Mountain-Madison Creek compartmental fault. Also the Bates Creek-Bodie Lake and Freyeland lines of folding are terminated at the Corral Creek compartmental fault. Abrupt terminations of folds is a major characteristic of compartmental deformation (after Brown, 1975).

FIGURE 125. Concept of compartmental deformation. (A) Length of fault is small, relative to size of the structure on which it occurs. Limited strike-slip offset can occur on such faults. (B) Apparent offset of anticlinal axes versus synclinal axes indicates different sense of slip along the fault. (C) Movement on fault plane is oblique slip, and folds developed independently of one another, which results in potential problems of interpreting two-dimensional cross section across the fault (modified from Stone, 1969, who described the model as a wrench fault).

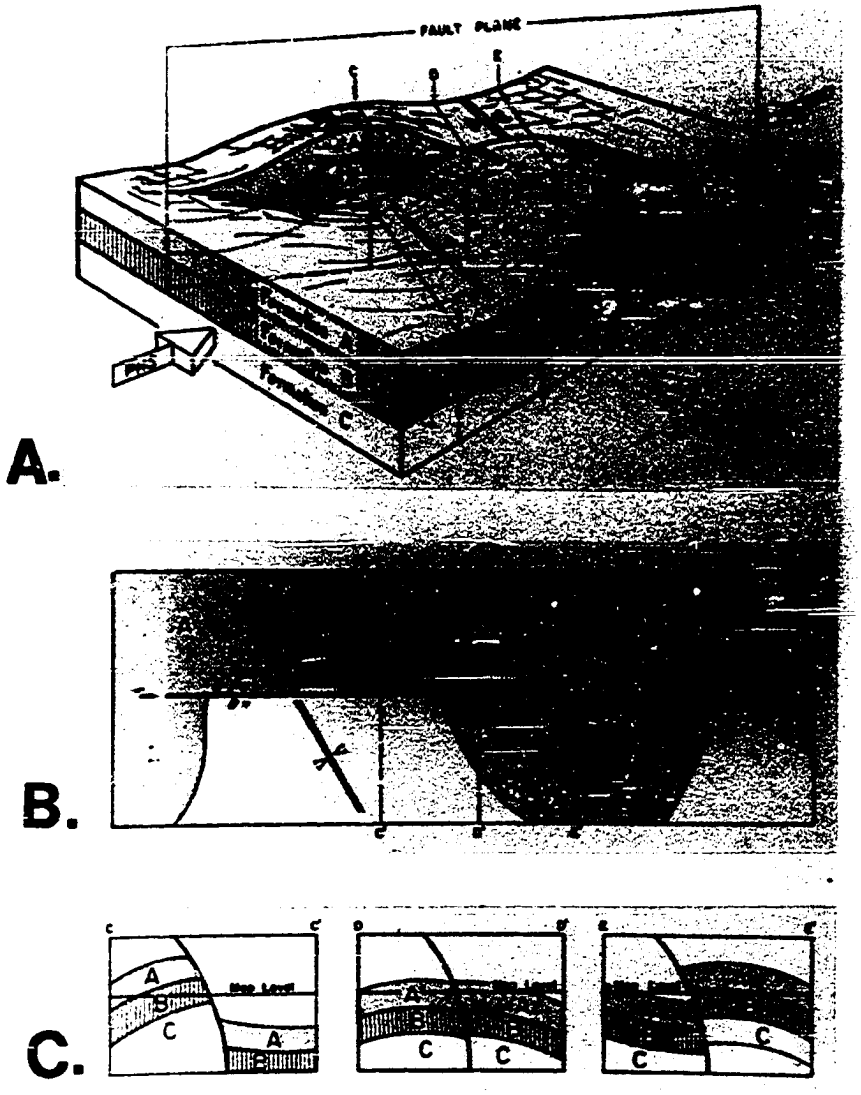

FIGURE 126. Abrupt change in direction of asymmetry may occur across a compartmental fault. Opposed dips of reverse faults indicate that the two anticlines developed independently of one another, and were never a singe line of folding. Compartmental fault must develop early in the sequence of deformation (Brown, 1975).

COMPARTMENTAL DEFORMATION

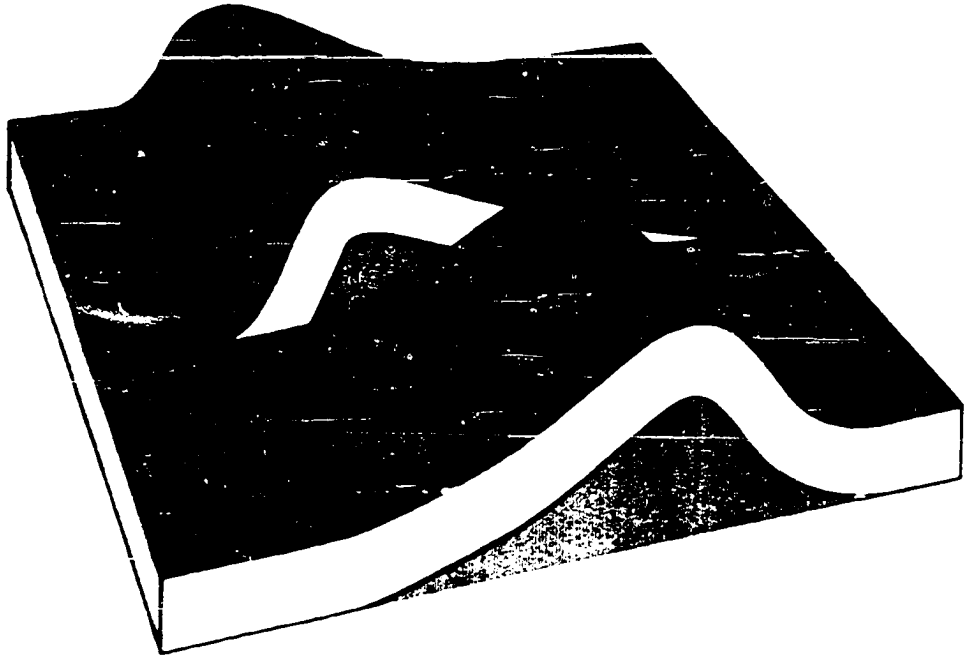

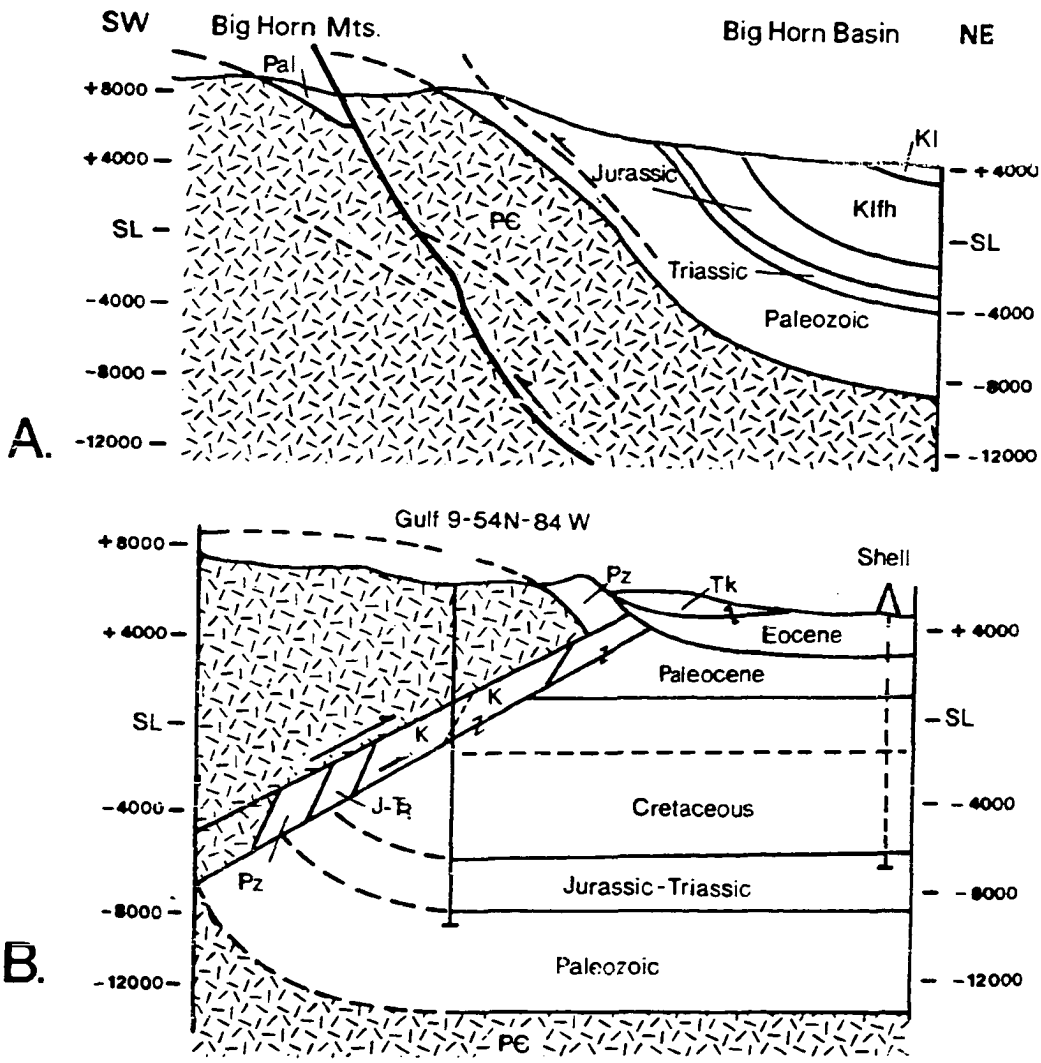

FIGURE 127. Change in structural style across the Piney Creek compartmental fault, east flank of the Bighorn Mountains (T.53 N., R.84 W.; location of cross sections shown on figure 122). A) The east-dipping flank of the Bighorn Mountains north of the Piney Creek "tear" fault is modified by an out-of-the-basin thrust, which involves the Precambrian basement. B) The Piney Creek "block" has been thrust eastward over the adjacent Powder River basin.

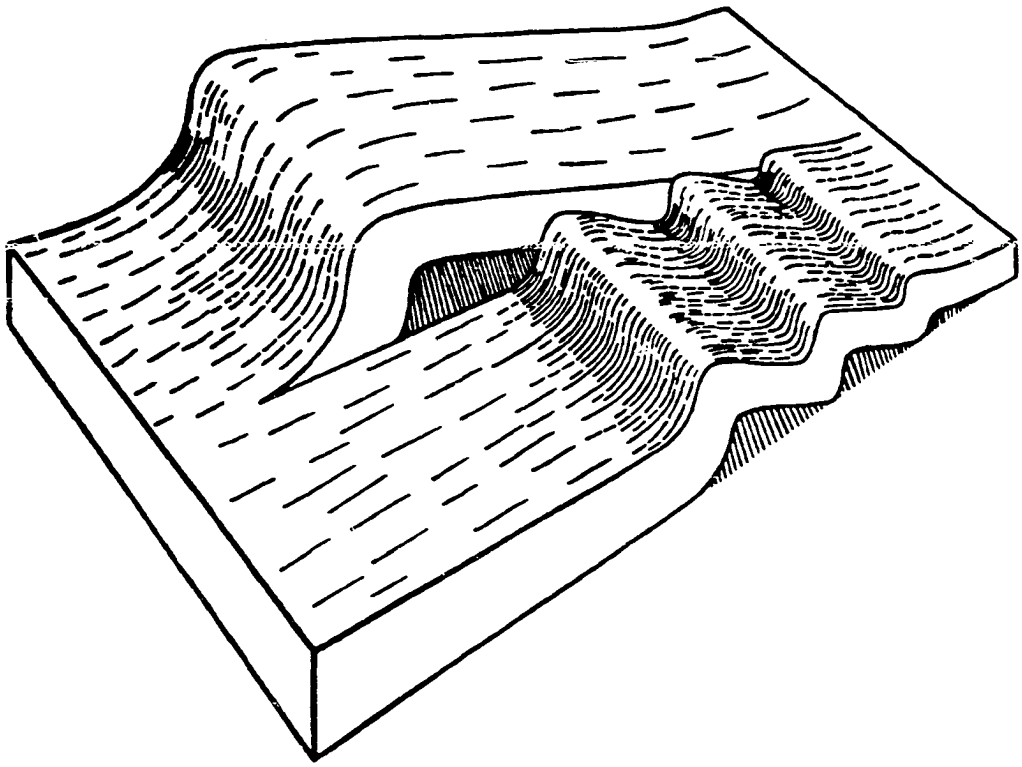

FIGURE 128. Structural balance is maintained from one compartment to another. One large anticline may be balanced by several smaller anticlines in the adjacent compartment (after Bell, 1956).

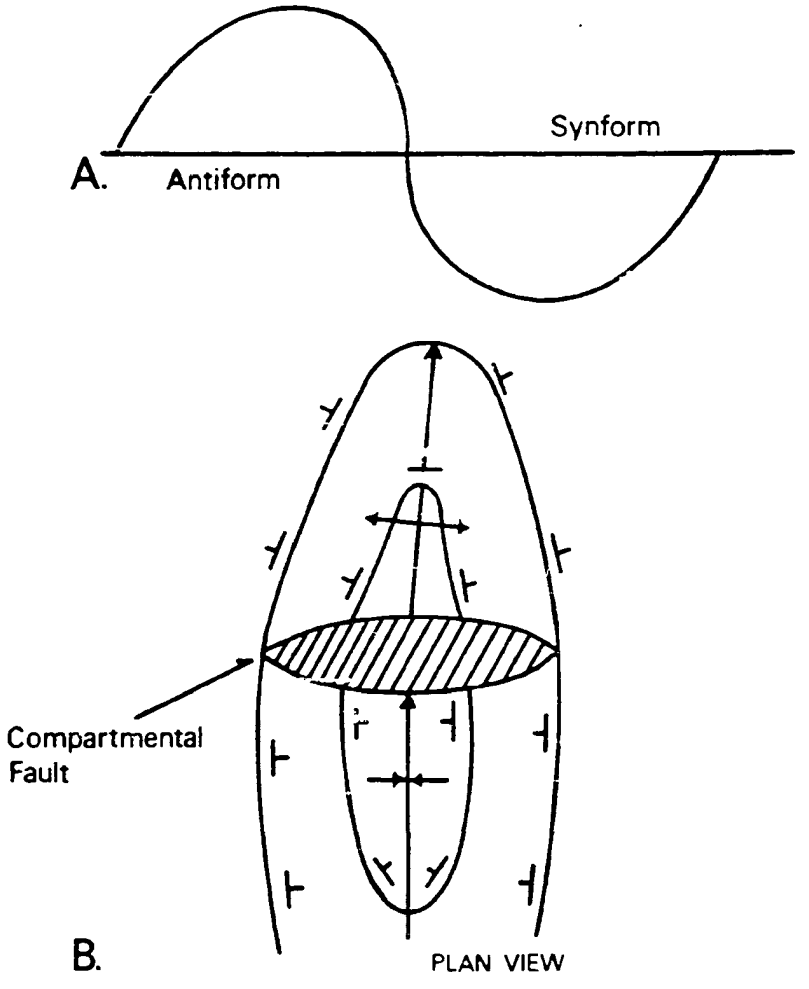

FIGURE 129. A) Equal crustal shortening may be achieved by both anticlinal and synclinal folding. B) A compartmental fault may separate anticlinal and synclinal fold profiles, each displaying the same amount of crustal shortening.

FIGURE 130. Deep Creek fault serves as a compartmental fault in the southern Bighorn Mountains. Structural balance is achieved between the northwest-plunging Bighorn basin, and the southeast-plunging southern Bighorn Mountains (modified from Love and others, 1955).

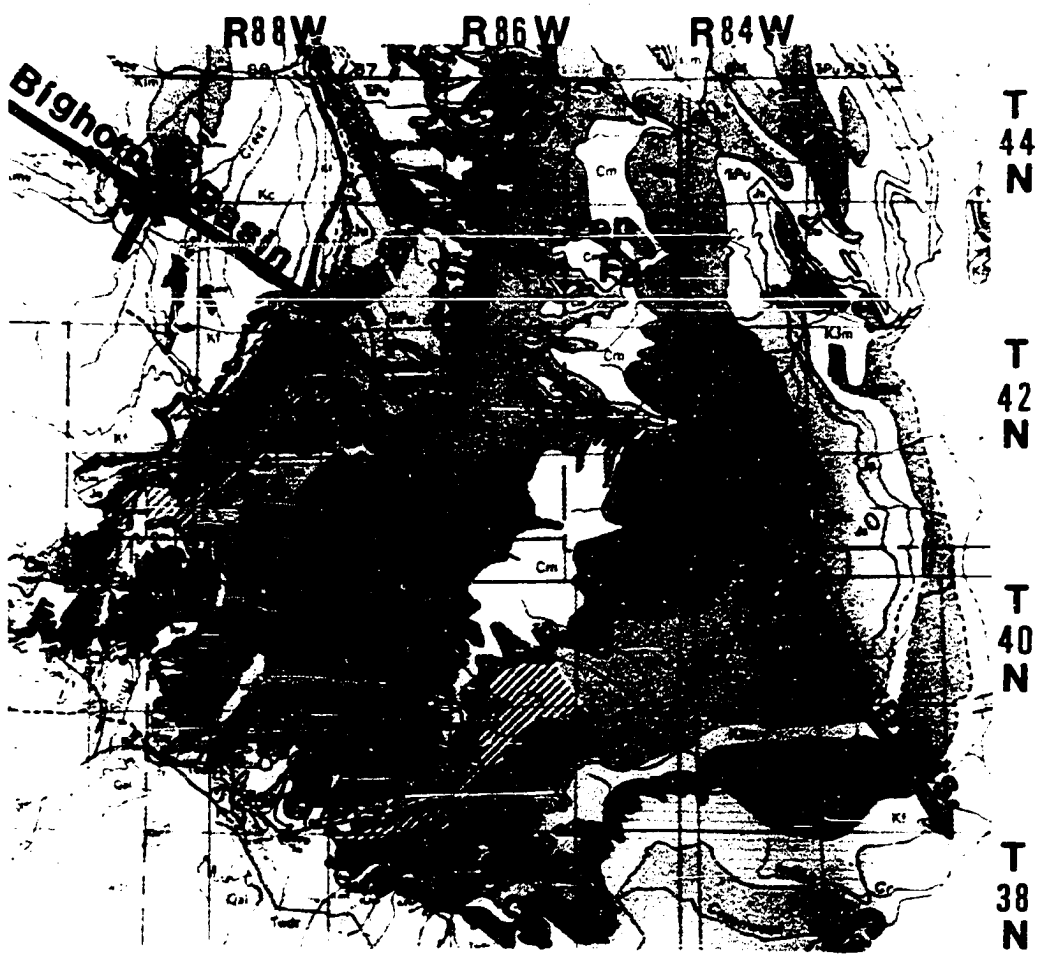

FIGURE 131. Possible buried basement compartmental trend. Line X-X' indicates trend of possible buried fault, against which several anticlines are terminated (B-Bonanza; PR-Paint Rock; HV-Hyattville; NW-Nowood; ZD-Zeisman dome). Structural balance is maintained by three anti- clines on the north side (B, PR, HV), and two larger anticlines on the south side (NW, ZD). Southwest termination of the compartmental fault is indicated by unfaulted Frontier (Kf) outcrop at X; while northeast termination is indicated by undeflected synclinal axis at X'. Basement compartmental fault dies out upward into the sedimentary section. Location of figure 132a and b, and cross sections Y and Z in figure 133, are shown.

FIGURE 132. Aerial views of Bonanza-Zeisman compartmental trend. A) Down-plunge view (northwest) along trend of Bonanza and Nowood anticlines shows apparent offset across compartmental fault. Continuity of Cretaceous outcrops at the left-center of the photo marks western termination of basement fault. B) View to southeast shows northwest termination of Zeisman dome as indicated by steeply dipping Jurassic Gypsum Springs (straight white outcrop). Northeastern termination of basement compartmental fault is indicated by undeflected synclinal axis in upper-left portion of photograph. BCF = buried compartmental fault.

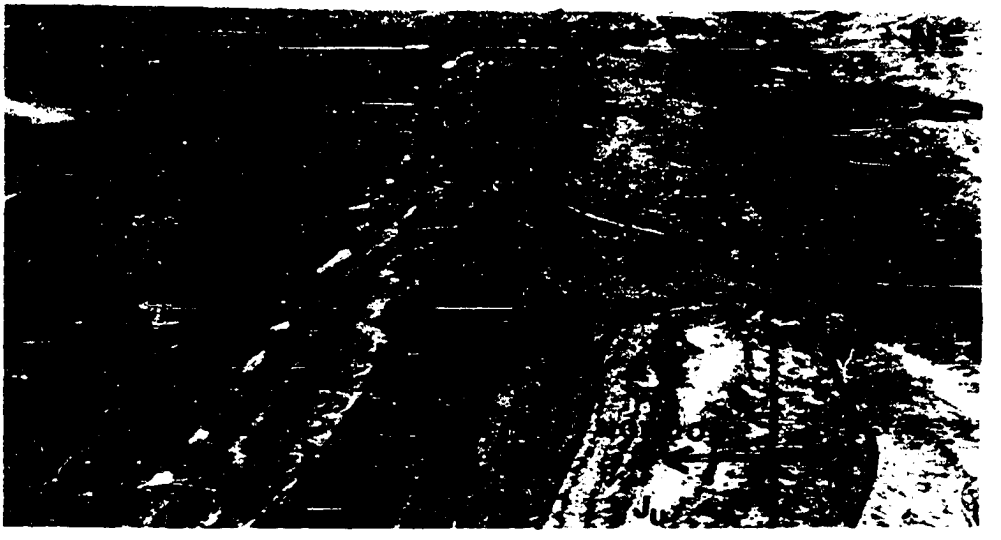

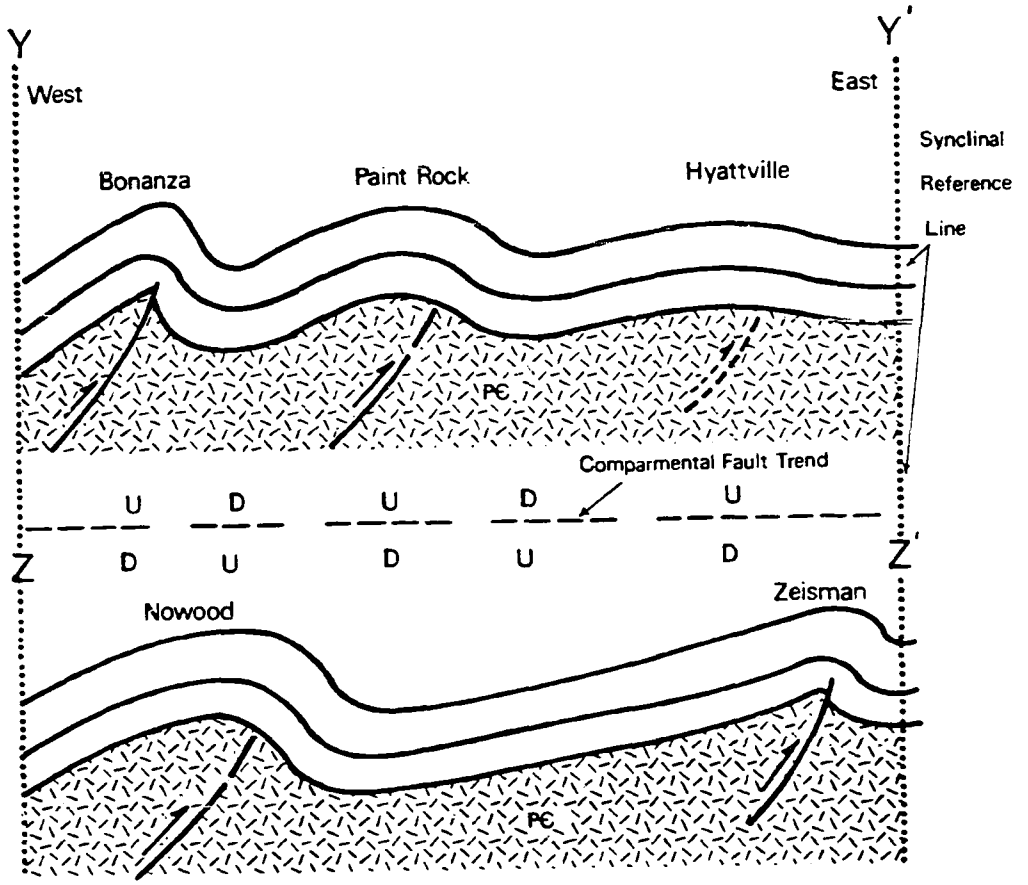

FIGURE 133. Profiles north (Y-Y') and south (Z-Z') of the Bonanza-Zeisman compartmental trend demonstrate maintenance of structural balance by non-paired anticlinal structures of varying sizes.

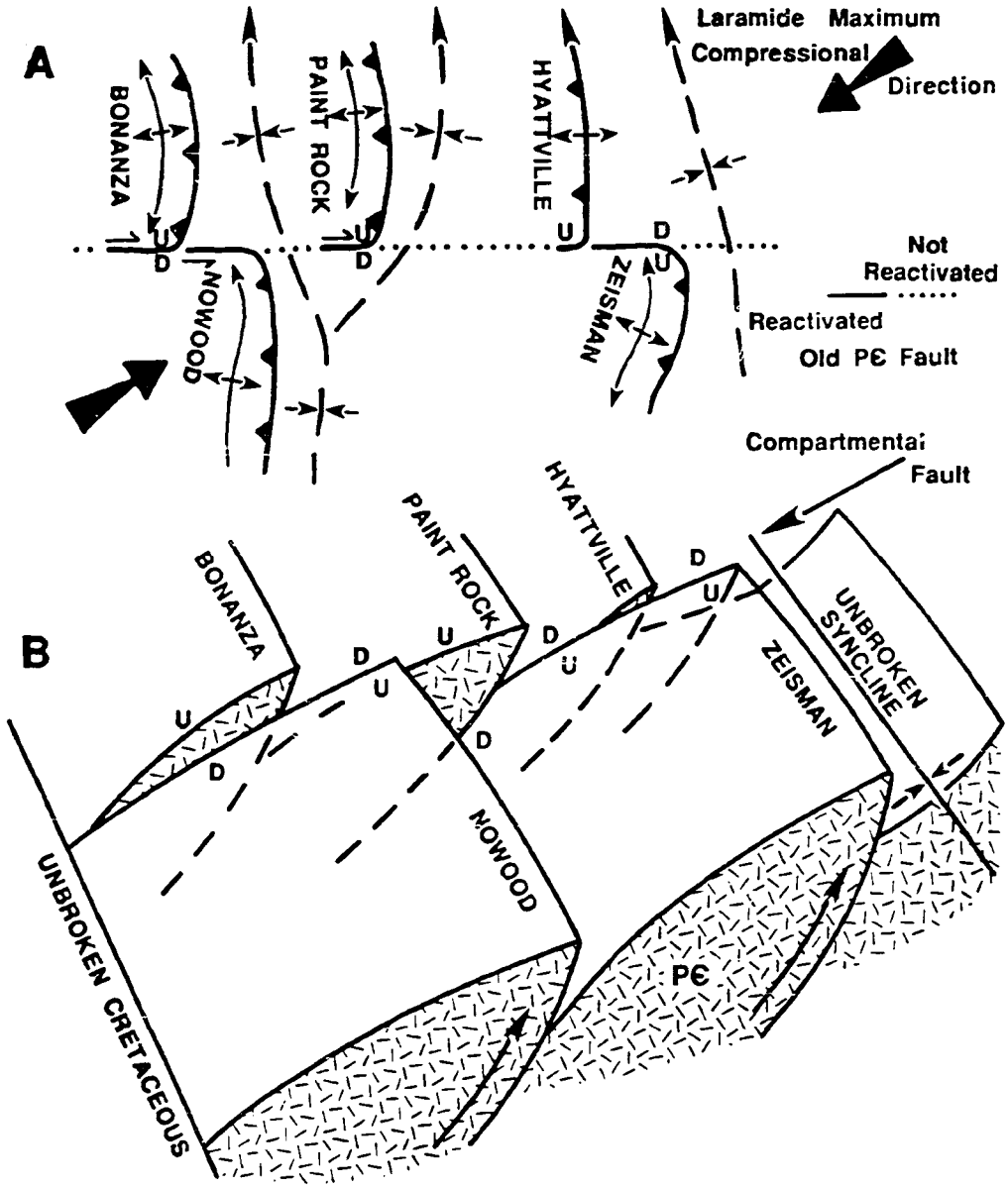

FIGURE 134. Map and block diagram of the buried Bonanza-Zeisman compartmental fault. A) Laramide maximum principal stress oriented obliquely to the compartment fault may have reactivated a Precambrian line of weakness. The synclines between these anticlines are deflected slightly, but are continuous across the compartmental fault, indicating that the upward movement of the basement blocks in the cores of the anticlines reactivated only selective portions of the older fault (B).

FIGURE 135. Demonstration of regional structural balance across the Tensleep compartmental fault. A) Geologic map (modified from Love and others, 1955) shows extent of Tensleep fault, which outcrops in the Bighorn Mountains (east). Unpublished seismic data, and well control, indicate the fault continues to the west flank of the Bighorn basin (dashed). B) The cross section north of the Tensleep fault indicates a large Bighorn Mountains uplift, modified only slightly by flank faulting. C) South of the Tensleep fault, the Bighorn uplift is more subdued, with an increase in faulting on both flanks. Lengths of the upper basement surface, measured from the axis of the Powder River basin (east) to the axis of the Bighorn basin (west), are identical, demonstrating structural balance across a major foreland uplift.

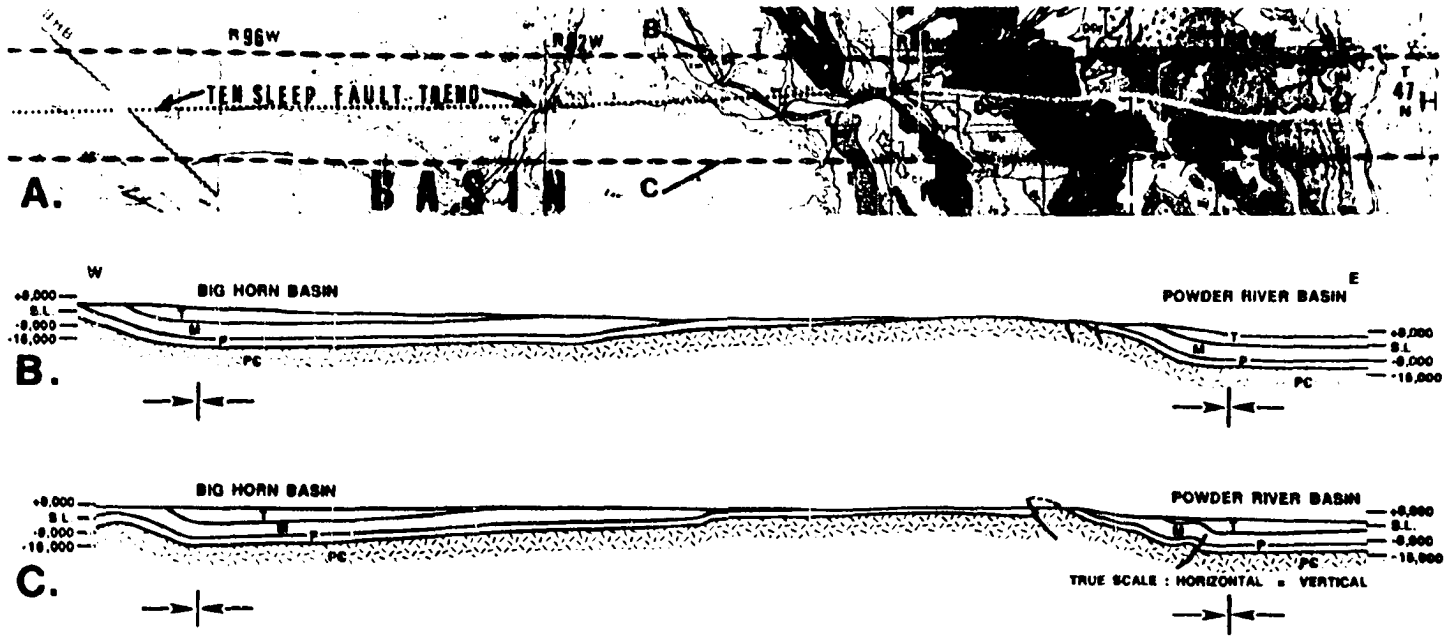

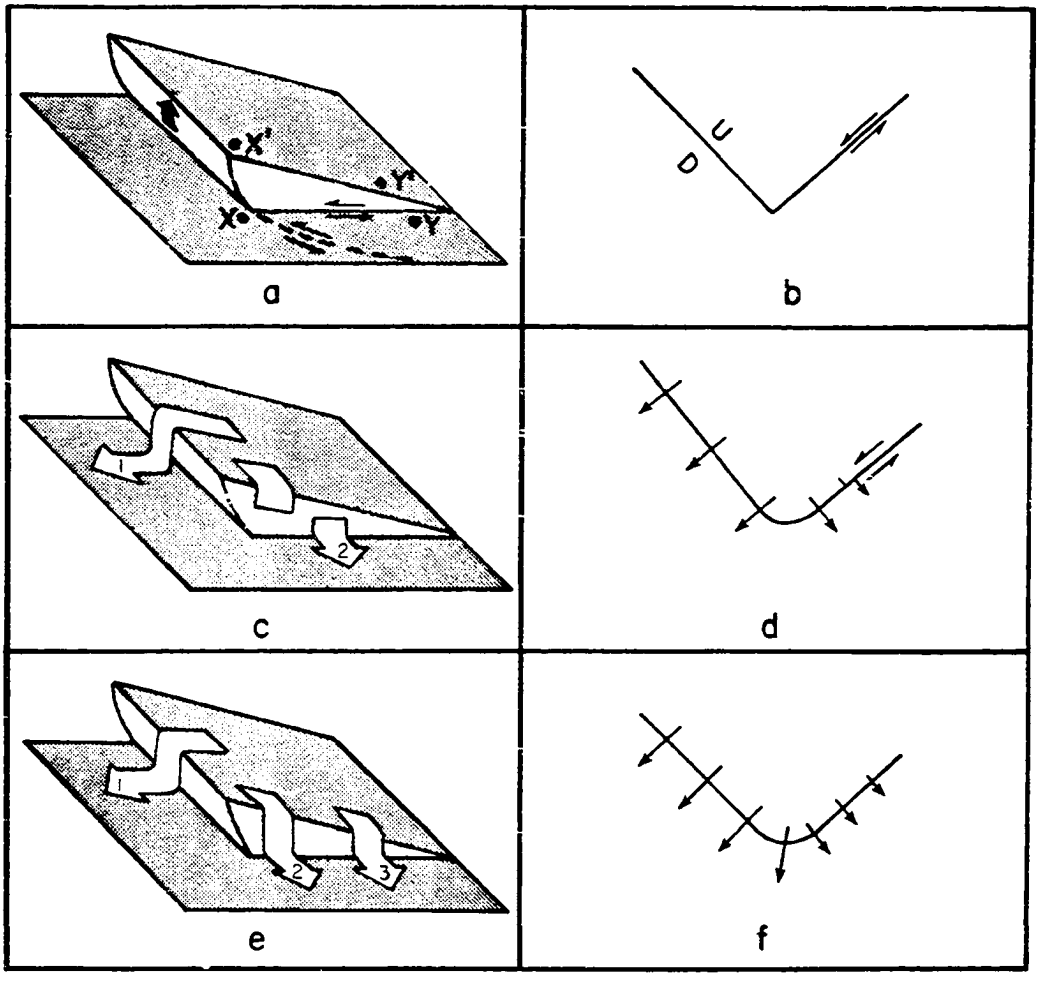

FIGURE 136. Block diagrams and map patterns of different concepts of the "corner problem" (after Stearns, 1978). A) Block diagram and B) map pattern of low angle thrust concept. C) and D), same as (A) and (B), with large arrows to indicate continuity of sedimentary section over the trace of the thrust, but which is offset along the "tear" fault which forms the "corner". E) and F) demonstrate continuity of the sedimentary section over, and around the "corner" as envisioned for the drape fold model.

FIGURE 137. Experimental model designed to study problems associated with the "corner" problem in the Wyoming foreland (modified from Logan and others, 1978). A) Physical model is comprised of a sandstone forcing block (2.0 cm thick, 3.0 cm wide, 10.0 cm long) which is precut at angles of 90 degrees (#1) and 65 degrees (#2) to the top of the block. The forcing block is overlain by a veneer comprised of intact layers of limestone, sandstone, limestone (each 0.3 cm in thickness). Total model dimensions are: 2.9 cm x 3.0 cm x 10.0 cm.. The assembled model is covered on four sides by thin strips of Lead, and jacketed with heat-shrink tubing. B) Deformed model (with heat-shrink tubing removed) shows the uplift of the forcing block along the 65 degree cut (#2). Section OB is oriented across the 90 degree cut (#1), along which right-lateral oblique slip has occurred. C) Photomicrograph of thin-section along OB shows offset of sandstone forcing block, and overlying limestone, sandstone, limestone veneer. T and A, and arrow indicate right-lateral oblique slip along 90 degree cut #1.

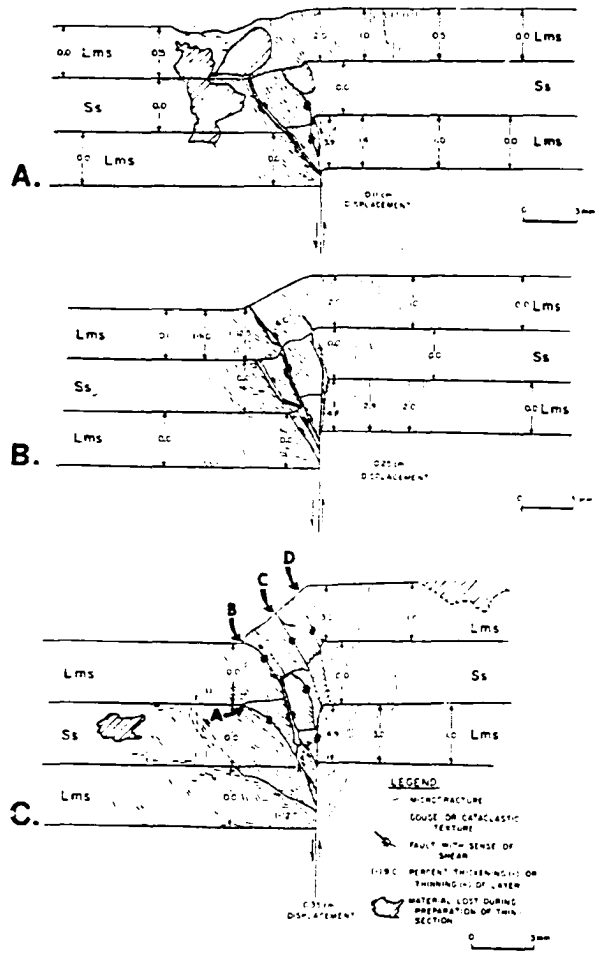

FIGURE 138. Results of three runs of the drape-corner experiment show sequence of deformation related to increased displacement of model faults. All sections are oriented along line OB, figure 136. A) Initial displacement (0.11 cm vertical; 0.046 cm horizontal) created faults (a and b) on the downthrown block, at an angle to the vertical precut, which did not reach the surface of the model. B) Increasing displacement (0.25 cm vertical, 0.105 cm horizontal) resulted in additional faulting in the downthrown block. Fault (b) reached the model surface, but at the lower hinge of the drape fold, while a third fault (c) began to develop above fault (b). C) With maximum displacement (0.33 cm vertical, 0.139 cm horizontal), fault (c) propagated to the model surface and fault (d) developed above it. (All values of horizontal displacement were calculated by the author for a 65 degree precut.)

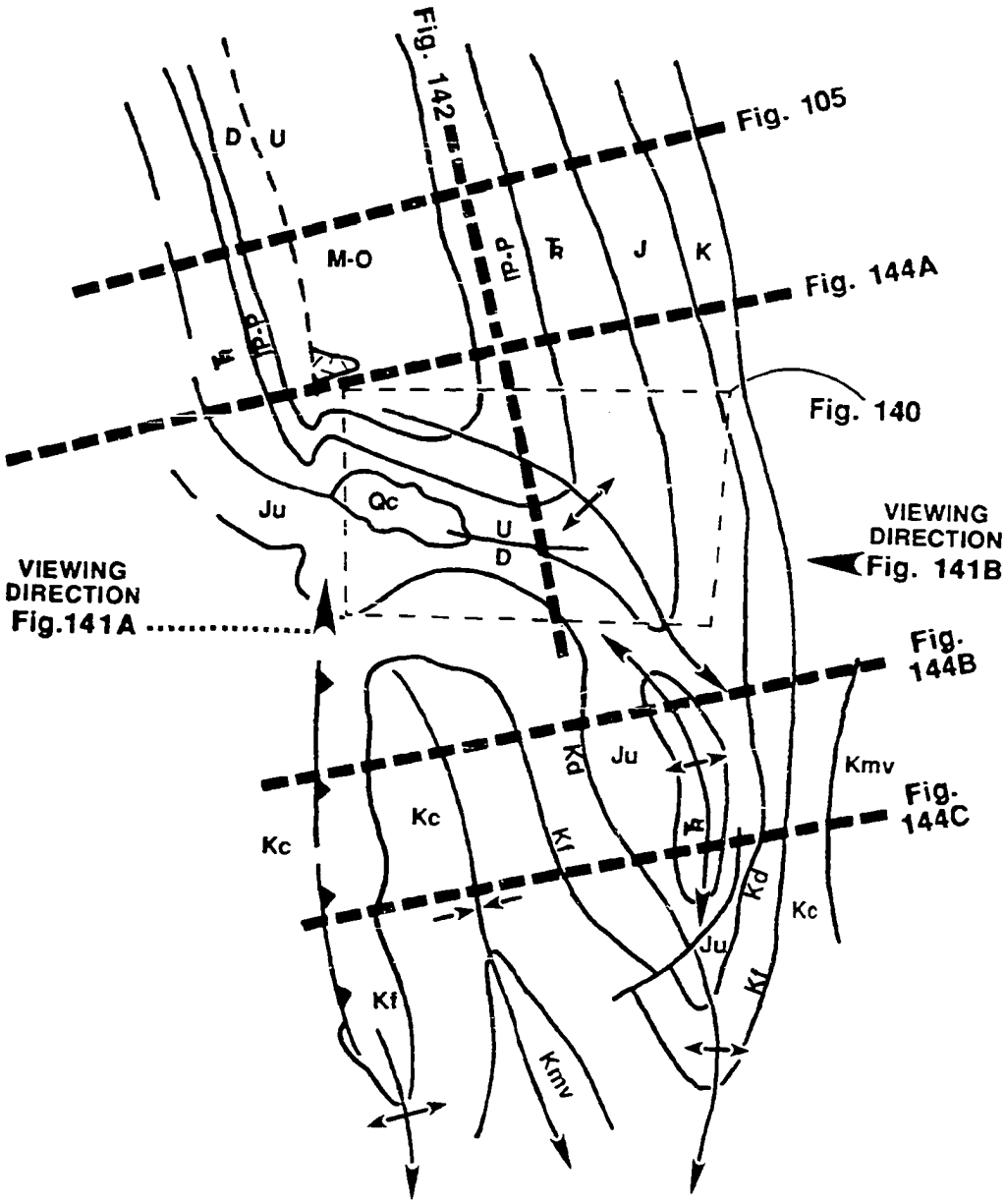

FIGURE 139. Index map of Rattlesnake Mountain-Horse Center-Half Moon area (modified from Pierce, 1966, 1970). Area in figure 140 is shown by fine dashed line, as well as location of the cross section shown previously in figure 105. Viewing directions for photographs in figure 141a, b, as well as those cross sections to be shown in figures 142, and 144a, b, c are also indicated.

FIGURE 140. Surface geologic map along south plunge of Rattlesnake Mountain anticline (modified from Pierce, 1970). Point A is footwall cut-off of the Triassic-Jurassic contact on an east-west compartmental fault. Hanging wall cut-off is covered under Quaternary (Qc), but must be located between points B and C. Lateral separation (two dimensional) created by compartmental fault is at least 5,000 feet (1500 m; A to B) and may be up to 8,000 feet (2400 m; A to C). North-south line of cross section in figure 142 is shown.

FIGURE 141. "Corner" of Rattlesnake Mountain anticline. A) Northwest view of panel of steep south dip on hanging wall of compartmental fault. Note the continuity of sedimentary section around corner, and over crest of west-east trending drape fold. B) East view of drape fold over steep south plunge of Rattlesnake Mountain anticline. Note lack of faulting at upper hinge of drape fold and presence of faulting at lower hinge.

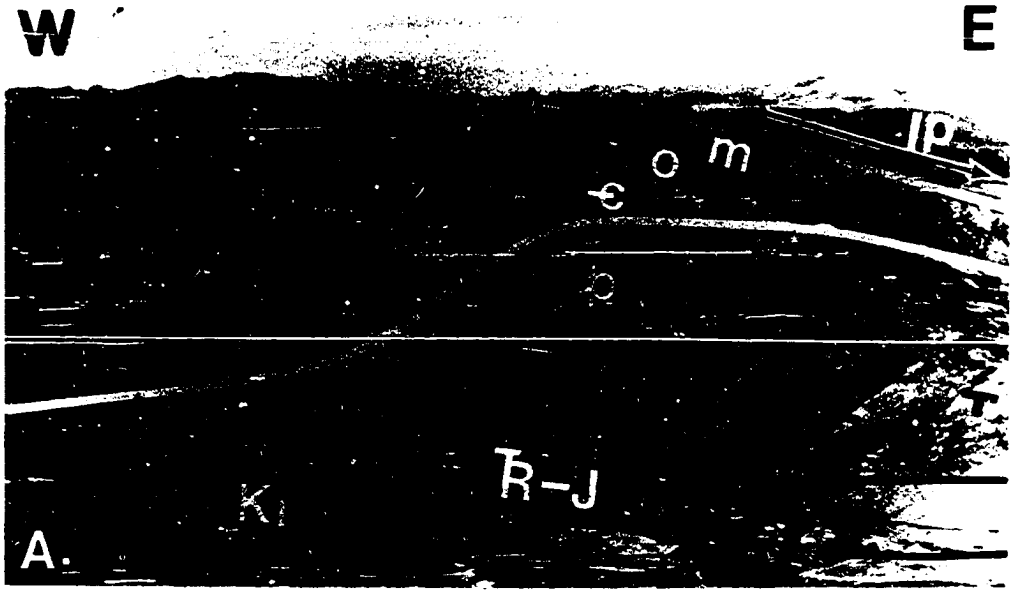

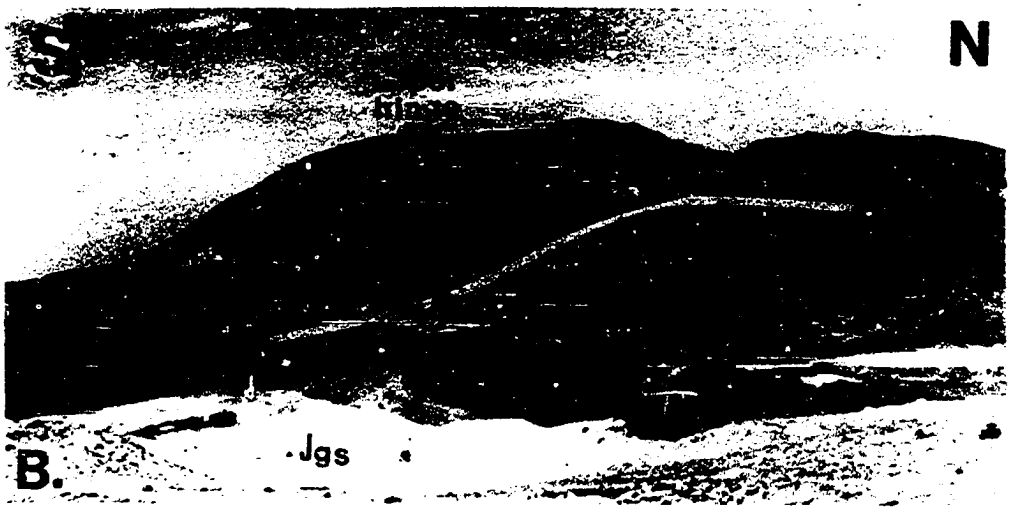

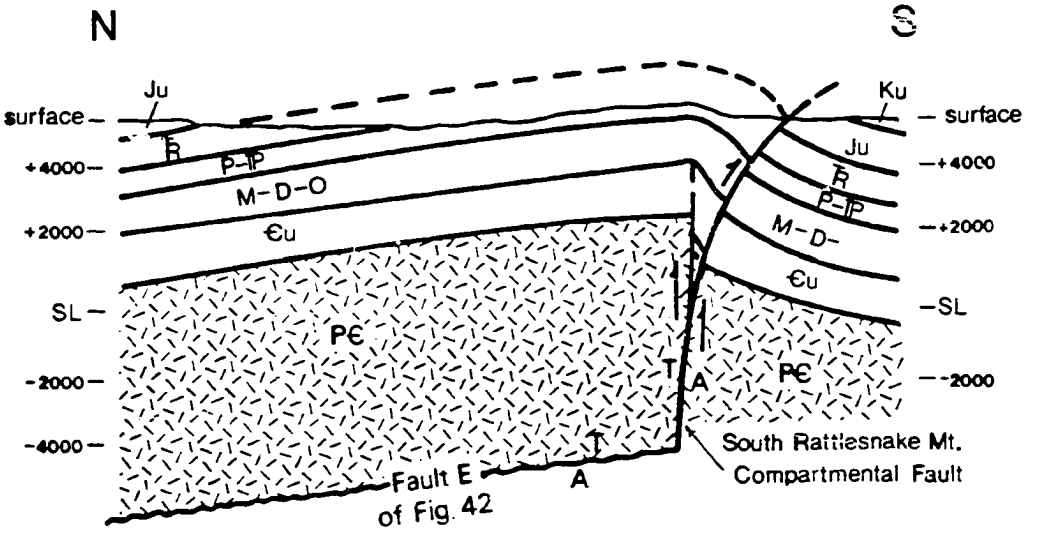

FIGURE 142. North-south structural section over steep south plunge of Rattlesnake Mountain anticline. Plunge is created by draping over a basement compartmental fault. Geometry similar to that created with experimental models. Horizontal fault is projection (into this line of section) of reverse fault (E) in figure 105, which has a heave component of 2,250 feet (680 m) and creates the uplift of Rattlesnake Mountain anticline.

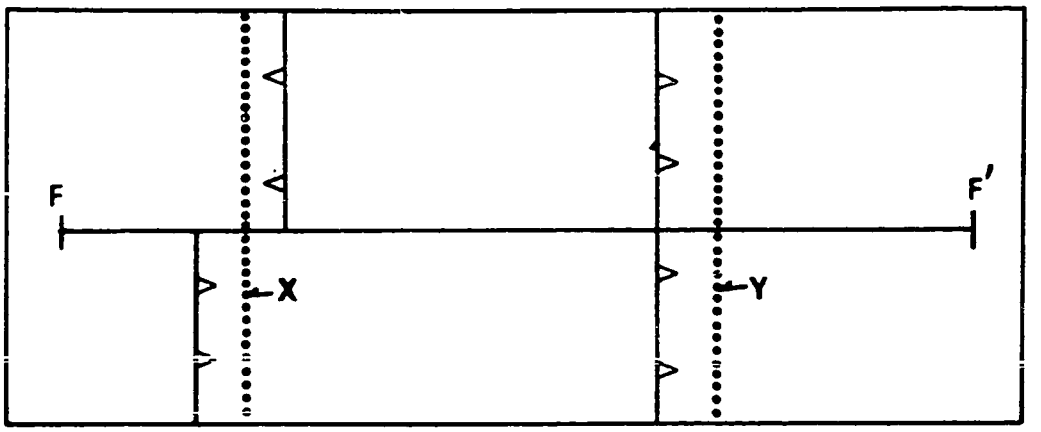

A.

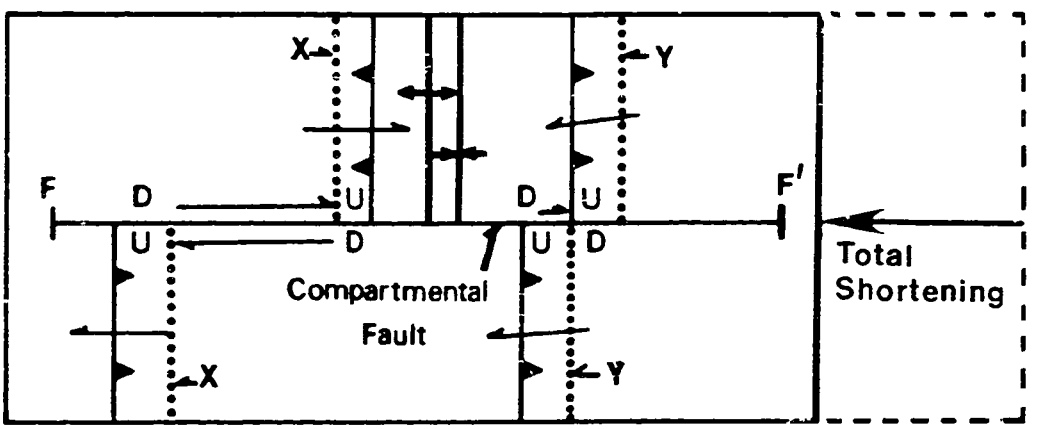

B.

FIGURE 143. Diagrammatic illustration showing variability in apparent lateral offsets created by differential faulting and folding along a compartmental fault. A) Before faulting linear geological features X and Y are continuous across incipient compartmental fault F-F'. Incipient reverse faults are shown with open "barbs". B) Application of horizontal compression parallel to compartmental fault (F-F') activates the reverse faults (shown with solid barbs). Geological features X and Y are offset by differing amounts as a function of heave and sense of vergence. Folding in the northern "compartment" balances the difference in fault shorteing north and south of compartmental fault F-F'. Differential uplift caused by faulting and folding results in oblique slip along fault F-F'.

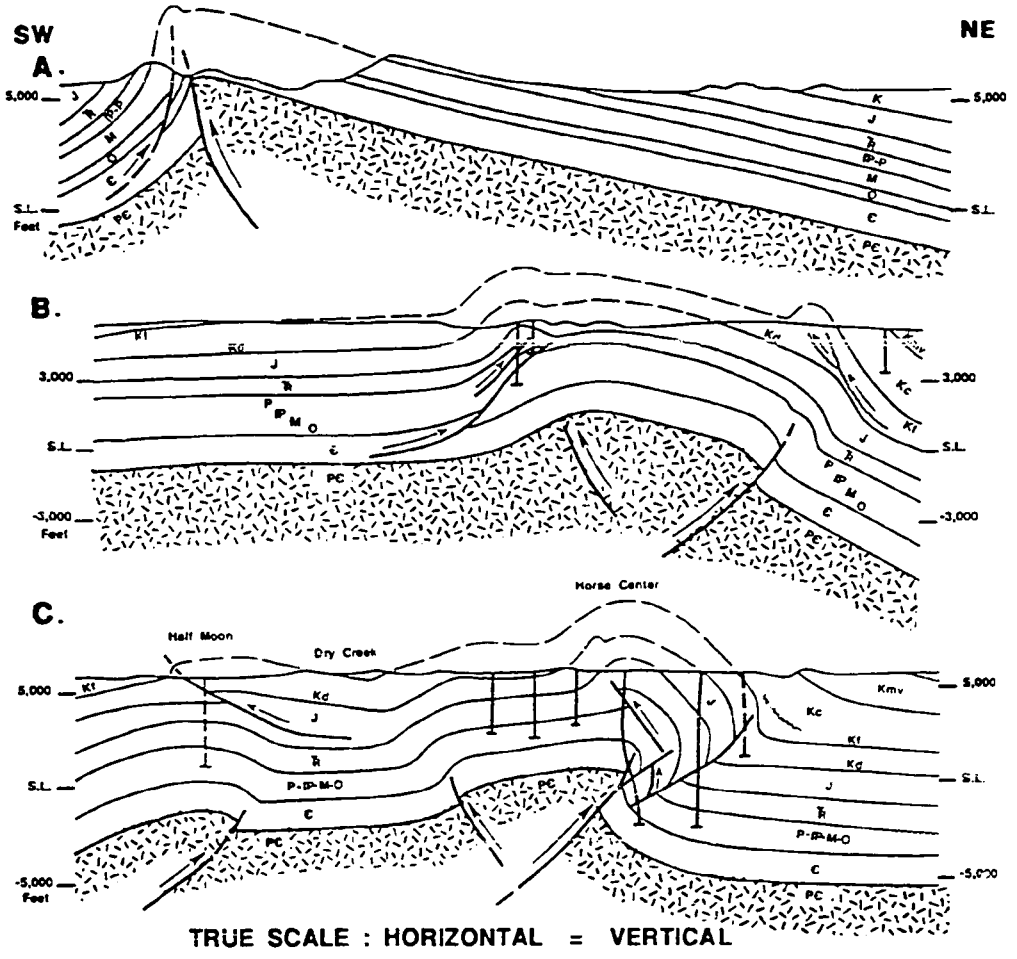

FIGURE 144. Demonstration of preservation of structural balance north and south of the Rattlesnake Mountain compartmental fault. Location of cross sections shown on figure 140. A) Southwest-northeast section on north side of compartmental fault showing west-verging Rattlesnake Mountain anticline with minor detachment faulting on steep west flank. B) Cross section immediately south of the compartmental fault (in the by-pass area between Rattlesnake Mountain and Horse Center anticlines) shows an east-verging structure, with several areas of detachment on both flanks, and some indication of a west-verging back-thrust. C) Cross section from Half Moon anticline, across Dry Creek syncline and Horse Center anticline shows increase in deformation over a shorter area along basement faulting, with more severe detachment faulting in the sedimentary section; thus structural balance is maintained.

FIGURE 145. Livingstone Park area, southern Montana. A) Geologic map (after Richards, 1957) displays geometry of basement block corner, created by intersection of Suce Creek and Stumbo Mountain faults. B) Form-line contour map (Brown, 1982) showing gentle, tapered, southeast plunge developed as Suce Creek fault fault dies out laterally. "Instant" plunge in the sedimentary section is created by draping over the Stumbo Mountain compartmental fault.

A.

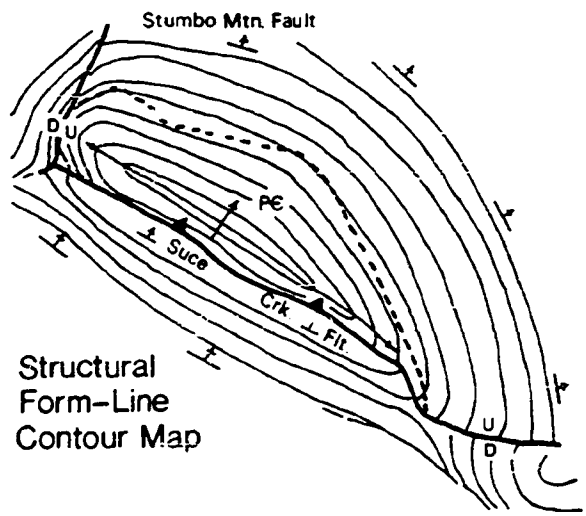

B. Structural Form-Line Contour Map

FIGURE 146. Geologic map of the Derby-Winkelman dome line of folding (after Love and others, 1955). Basement geometry is exposed up-plunge at point A. Local structural closures are: SM-Sheep Mountain; DB-Derby dome; DS-Dallas dome; LD-Lander anticline; SC-Sage Creek anticline; WD-Winkleman dome. The entire line of folding is asymmetric towards the west (out-of-the-basin).

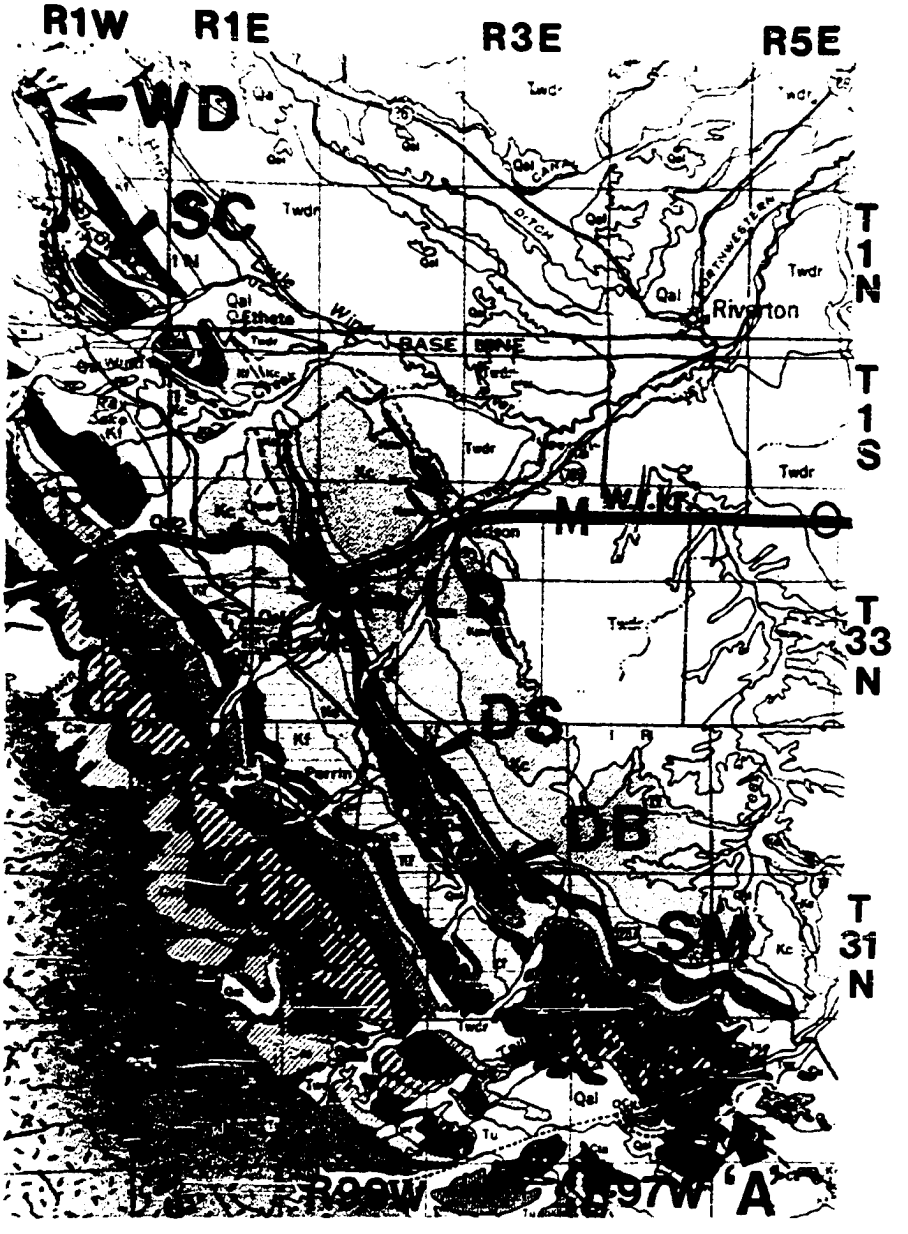

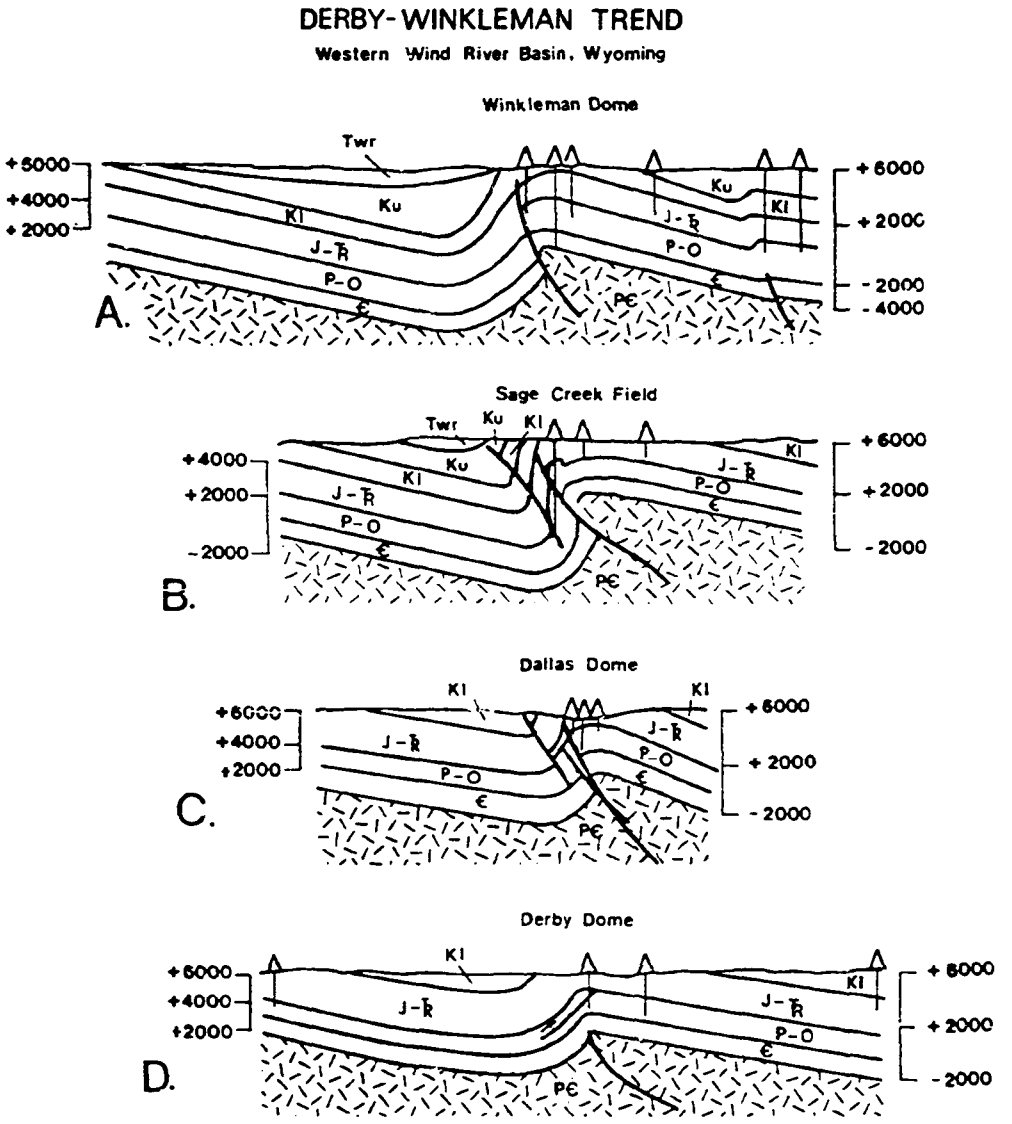

FIGURE 147. Montage of structural sections across the Derby-Winkleman line of folding. A) Winkleman dome contains the only well control which encounters Precambrian basement. B) Well control on Sage Creek anticline establishes the presence of the dual fault system, and a rabbit-ear fold isolated on the hanging wall block. C) Dallas dome displays early stage of the dual fault zone as well as a cross-crestal fault. D) Derby dome, like Winkleman, is less tightly folded than Sage Creek anticline, and thus the dual fault system has not developed; however the rabbit-ear and cross-crestal structures have developed.

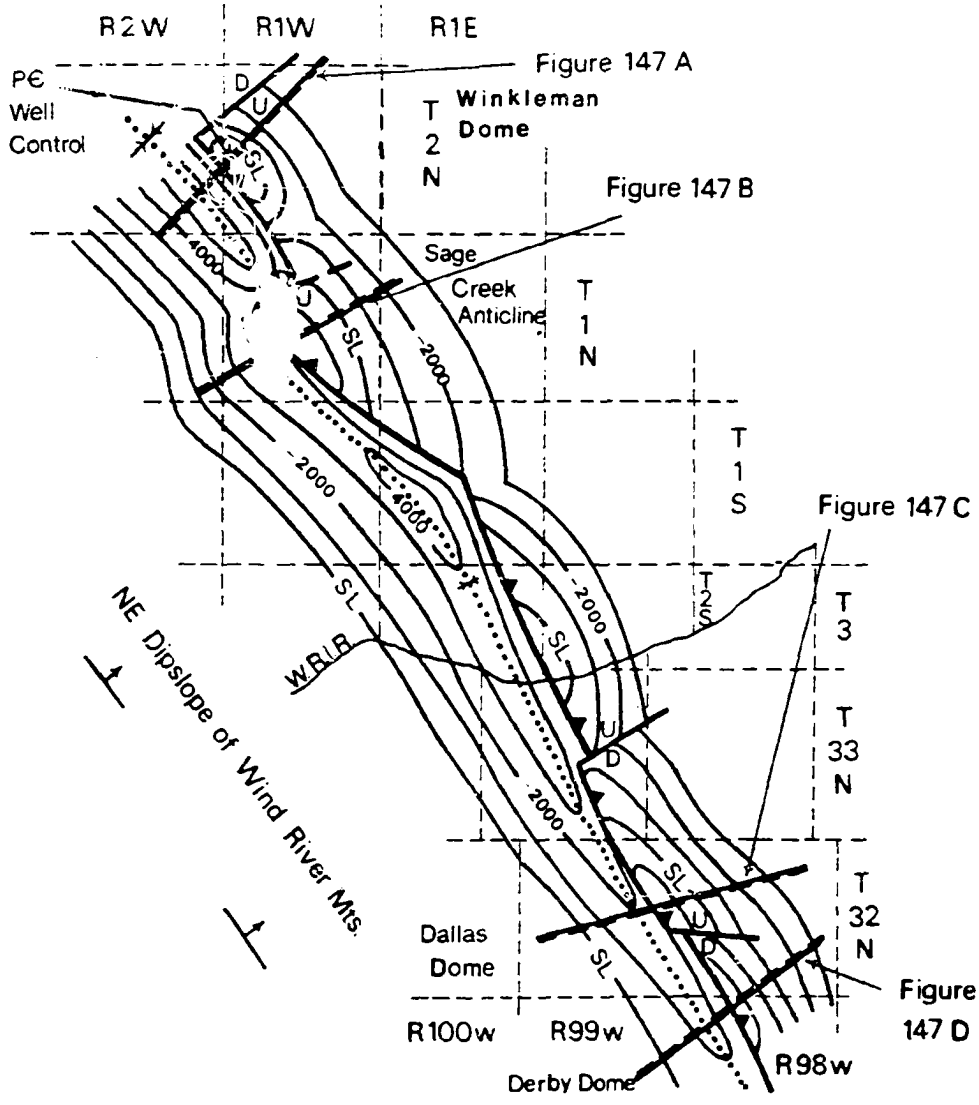

FIGURE 148. Structure contour map on the upper surface of the Precambrian basement along the Derby-Winkleman line of folding. Elevations of the basement taken directly from cross sections in figure 147, and the single point of well control at Winkleman dome. Southeast plunge of Dallas and Lander structures, plus the northwest plunge of Sage Creek and Winkleman dome, are controlled by northeast-trending compartmental faults. The syncline on the steep flank of the line of folds is continuous, indicating that the compartmental faults were activated by the uplift of the anticlines.

FIGURE 149. Index map of the Wyoming foreland (modified from Renfro and Feray, 1966) showing the location of three lines (A, B, and C) along which values of crustal shortening have been determined in this study. Cross section along line A is shown in figure 154. Values of crustal shortening have been estimated for the two lines B and C.

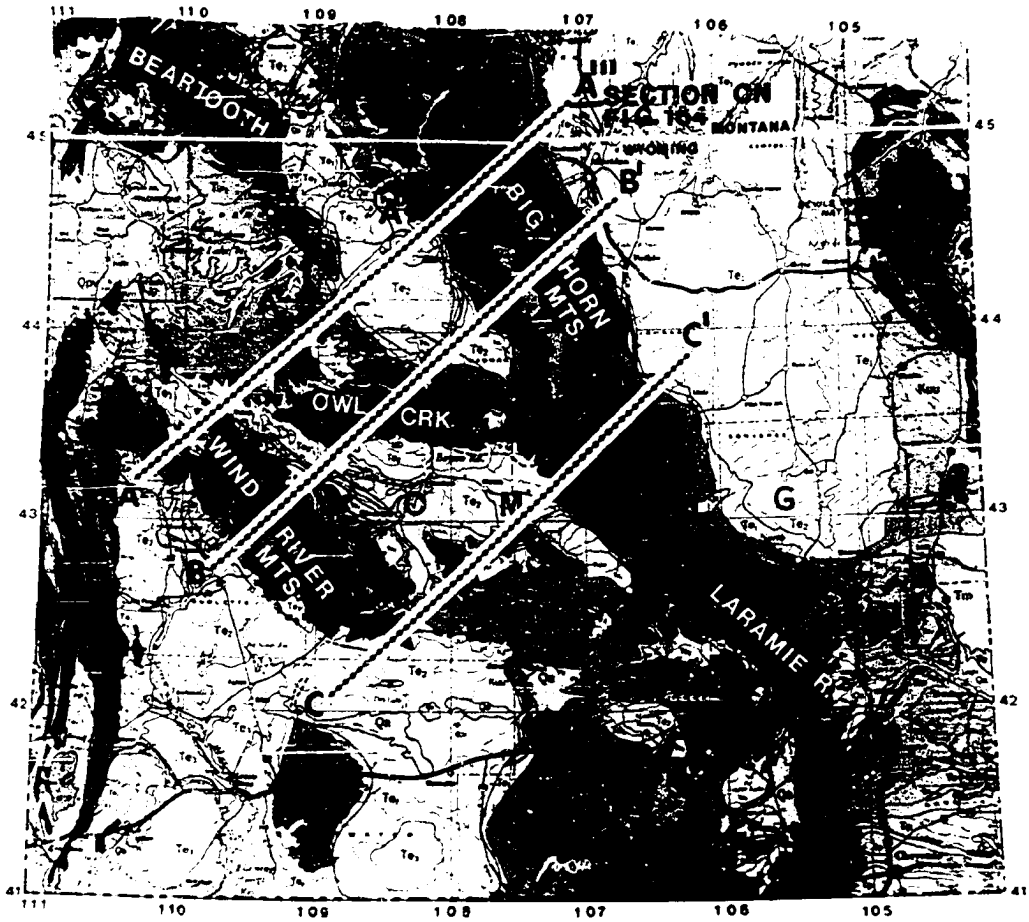

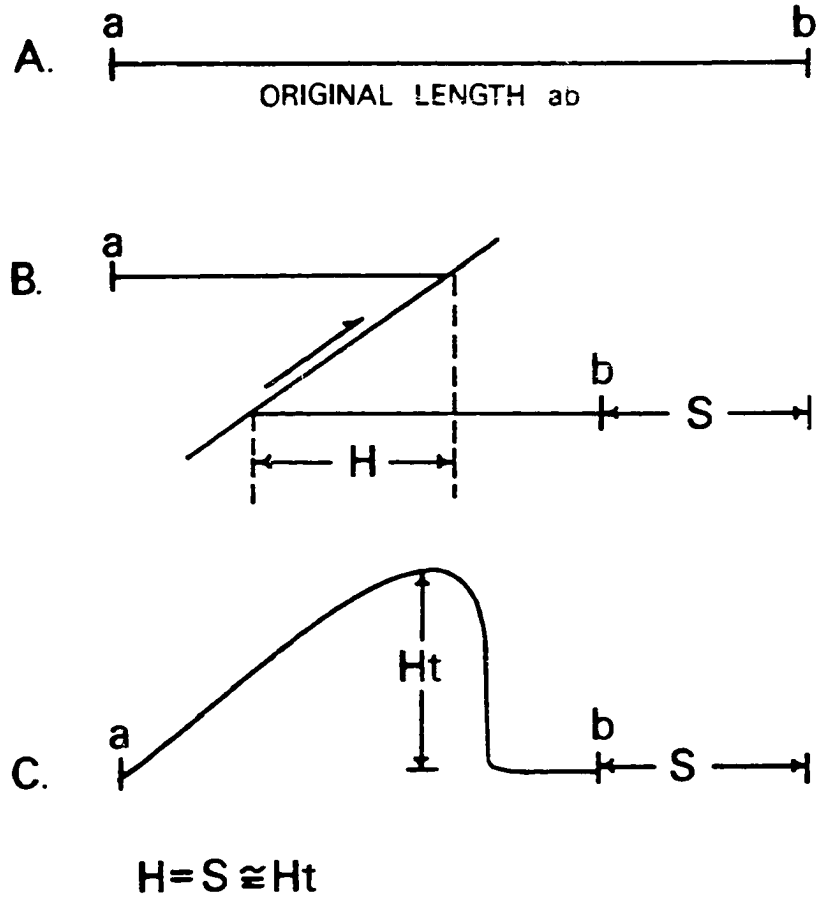

FIGURE 150. Two methods of estimating crustal shortening which can be accomplished by either faulting or folding. A) Line length (a-b) represents original, undeformed bed length. B) Heave component (H) of a reverse fault represents the amount of crustal shortening (S). C) Vertical height (Ht) of fold approximates amount of crustal shortening (S).

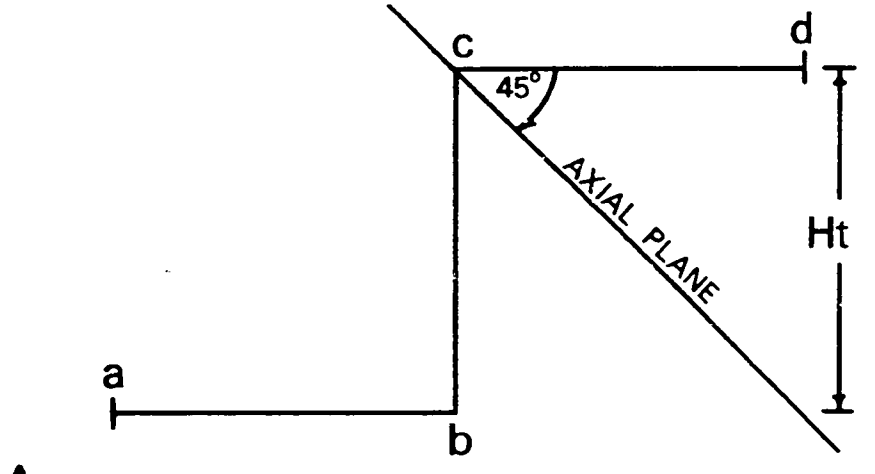

A.

$S = Ht = cb$

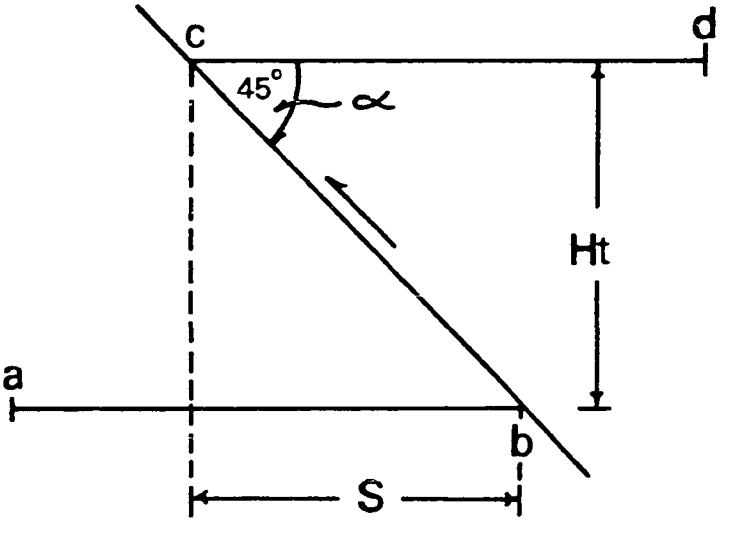

B.

$S = \tan \propto (45) = Ht$

FIGURE 151. A) Estimated crustal shortening of a fold with a 45 degree dipping axial plane: shortening (S) equals vertical height of fold (Ht). B) Uplift with a reverse fault dipping 45 degrees: shortening equals vertical height (Ht) of uplift.

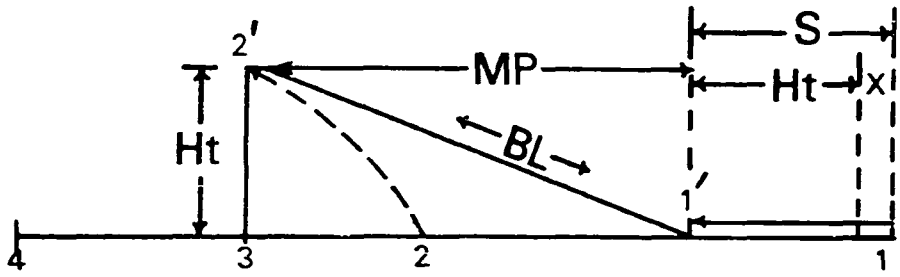

MP = Map Projection of 1'-2'
BL = Line 1'-2'
X = MP-BL
Ht = 2'-3
S = Ht + X

FIGURE 152. Estimation of shortening by folds with axial planes dipping other than 45 degrees. Initial bed length equals 1-2-3-4, and deformed length equals line 1'-4. (BL) equals back limb of fold. (MP) equals map projection of back limb. (S) equals total shortening by folding. (Ht) equals height of vertical limb. (X) equals amount by which total shortening (S) is underestimated. X = BL-MP; S = Ht + X.

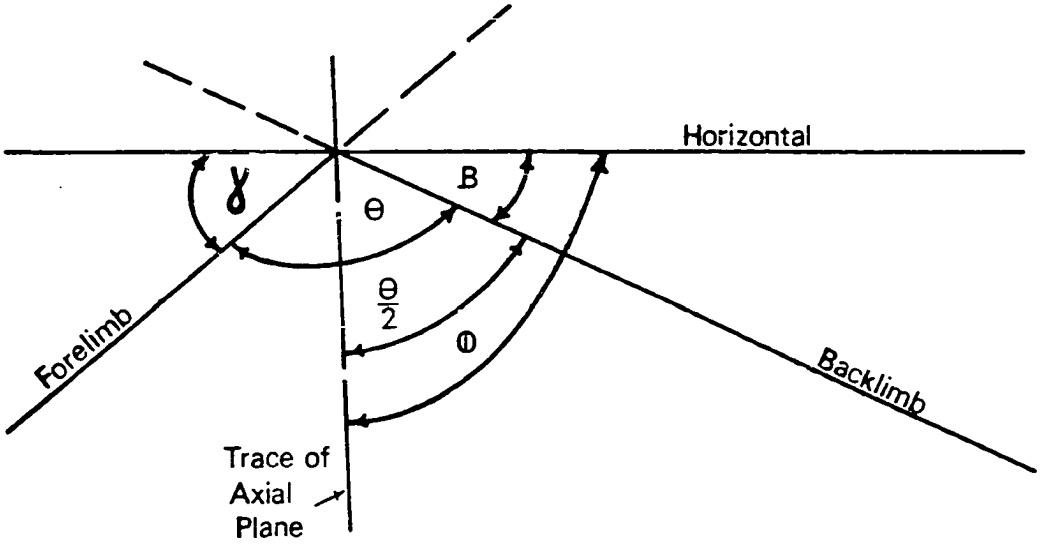

B = Dip of Backlimb

γ = Dip of Forelimb

Θ = Fold Angle or Degree of Folding
$= 180^{\circ} - [\gamma + B]$

Φ = Dip of Axial Plane
$= \frac{\Theta}{2} + B$

$$\Phi = B + \left[\frac{180 - (B + \gamma)}{2}\right]$$

FIGURE 153. Method of estimating dip of axial plane of a fold, using dips on flanks of the structure.

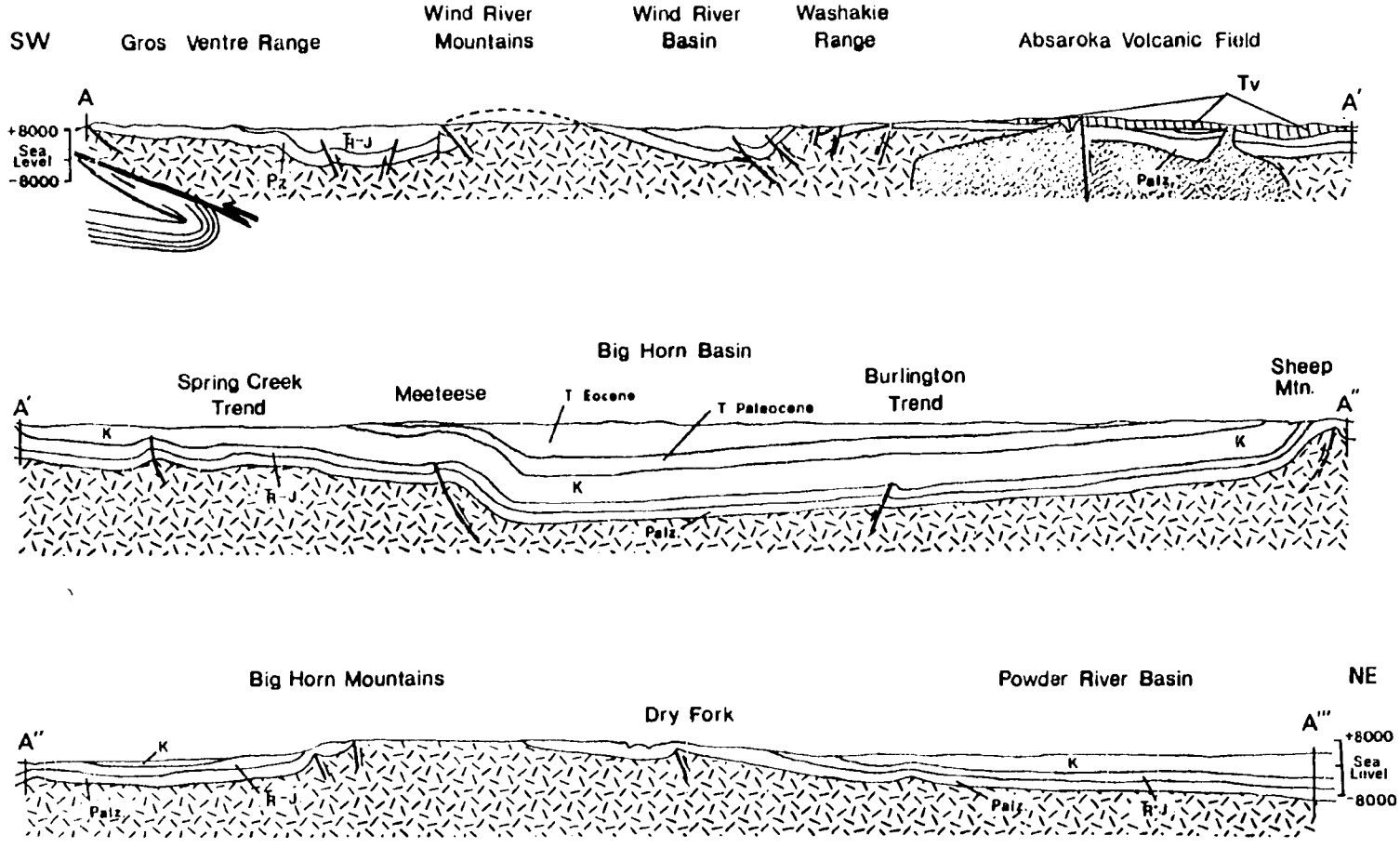

FIGURE 154. Structural section across the Wyoming foreland, along line A of figure 149. Shortening measured along the upper basement surface is 26.9 miles (43km).

FIGURE 155. Index map of the Wyoming foreland (modified from Renfro and Feray, 1966) showing locations of structures used in estimating values of crustal shortening along lines B and C of figure 149. Figure numbers shown refer to structures listed in Table 11.

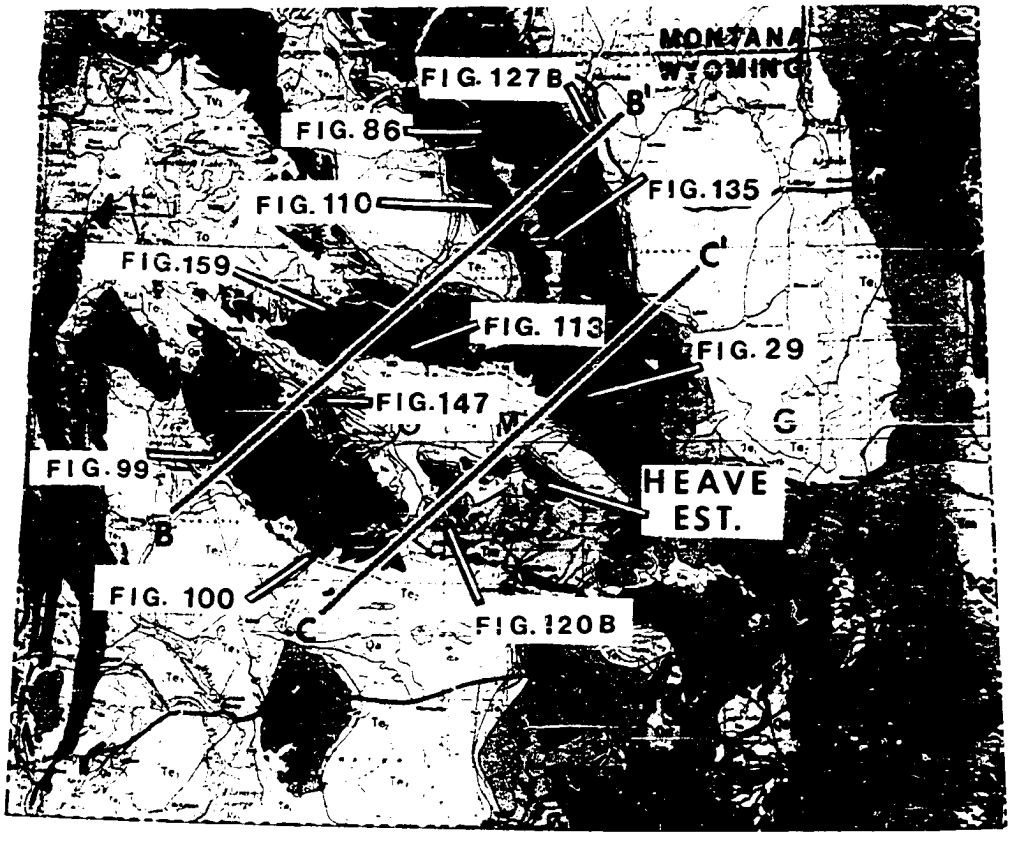

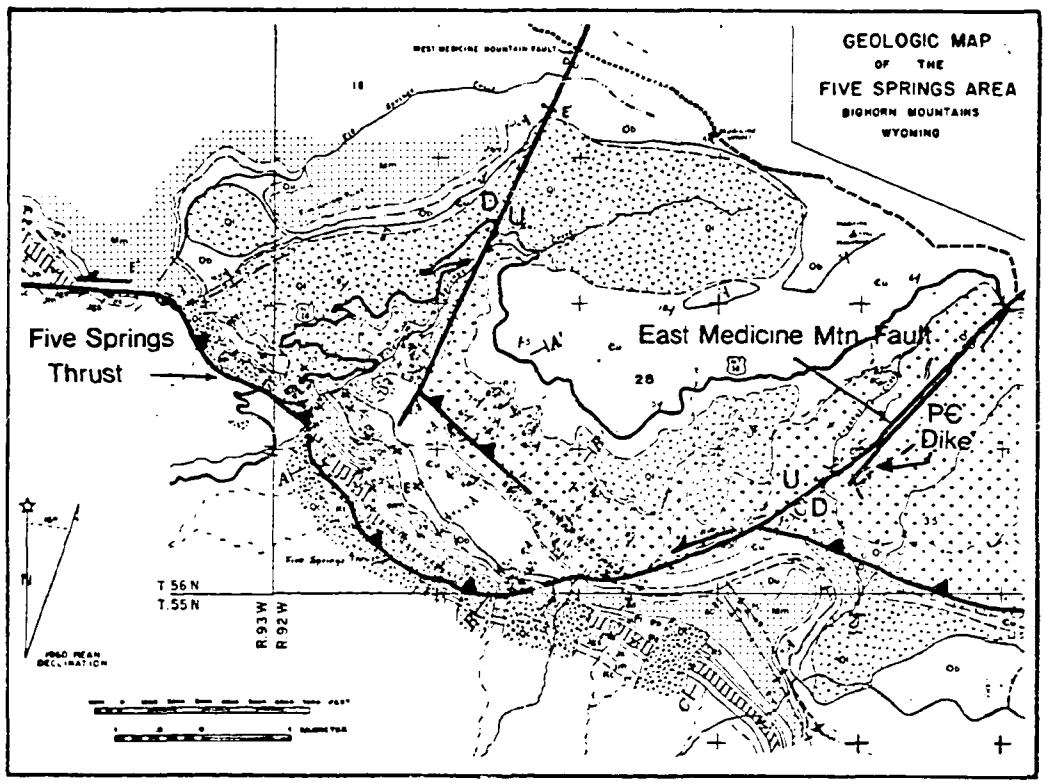

FIGURE 156. Geologic map of the Five Springs area, Bighorn Mountains (after Hoppin, 1970). East and West Medicine Mountain faults are northeast-trending compartmental faults. East Medicine Mountain fault strikes parallel, and adjacent to a Precambrian igneous dike. Left-lateral strike slip along the East Medicine Mountain fault equals 7,000 feet (2100 m).

FIGURE 157. Geologic map of Wyoming (modified from Love and others, 1955) showing the southeast plunge of the Wind River Mountains uplift. Change in strike to a more easterly trend suggests a component of left-lateral slip on the Wind River thrust. Loss of crustal shortening indicated by plunge-out of uplift requires a transfer of displacement to other structural features in the region.

FIGURE 158. A) Geologic map of Wyoming (modified from Love and others, 1955) showing the south flank of the Granite Mountains uplift. B) Enlargement of geologic map showing Sheep Creek anticline (SCA) which plunges northwest under the Sheep Creek thrust (SCT). Regional tectonic transport (RTT) direction (large arrow) and the angular relationship between Sheep Creek anticline and Sheep Creek thrust suggests a component of left-lateral slip along that fault.

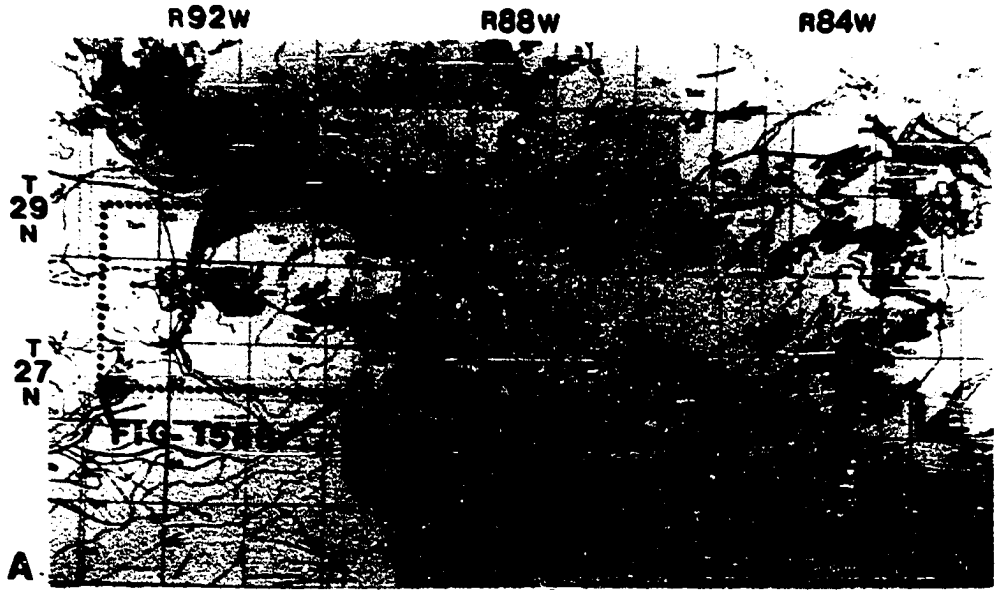

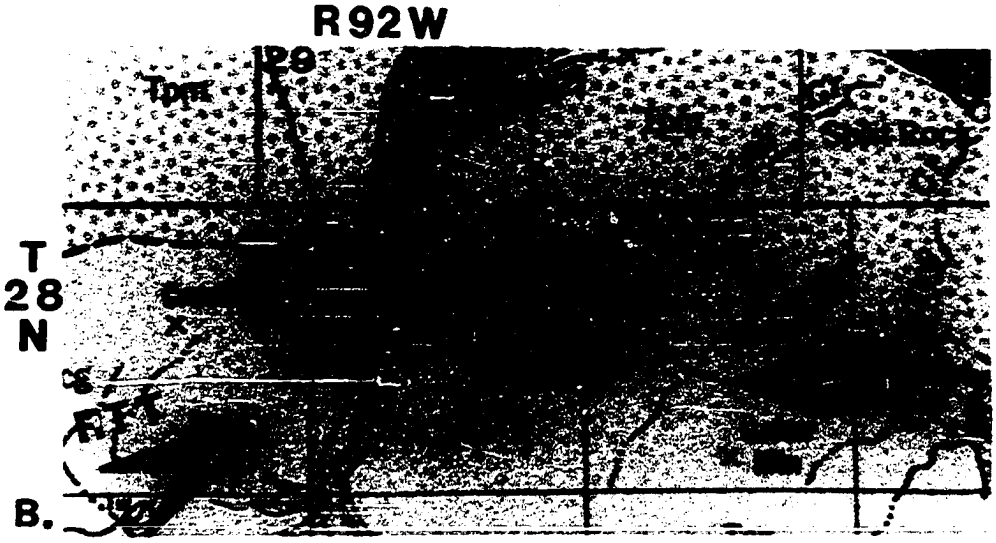

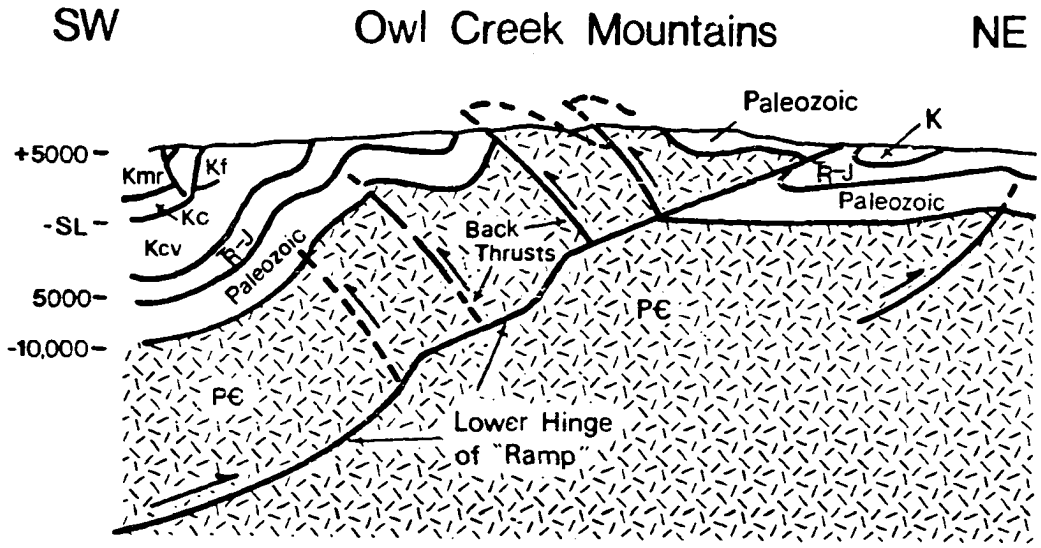

FIGURE 159. Structural section across the Owl Creek Mountain uplift (line of section is shown on figure 109), displays multiple back-thrusts which are antithetic to the North Owl Creek fault (NOCF). Two and one-half miles (4 km) of crustal shortening is accomplished by the NOCF and associ- ated back-thrusts. The NOCF is interpreted to flatten southwestward to form ramps which may have originated the back-thrusts.

FIGURE 160. A) Wrench fault concept applied to the Wyoming foreland (after Stone, 1969). B) Development of primary fold trend (1), primary thrust (2), first-order left wrench faults (3), first-order right wrench faults (4), and drag fold (5a); PHS = principal horizontal stress.

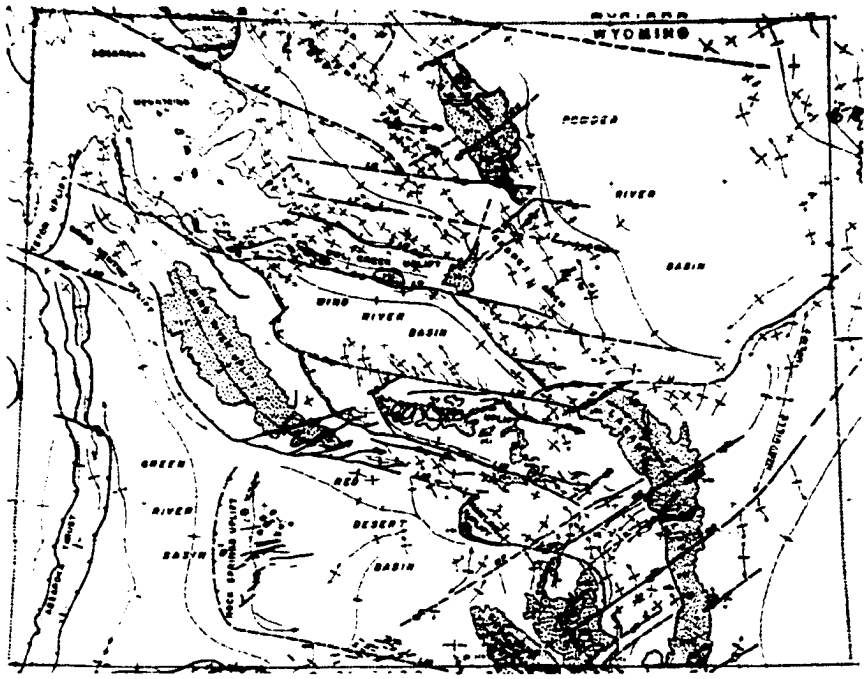

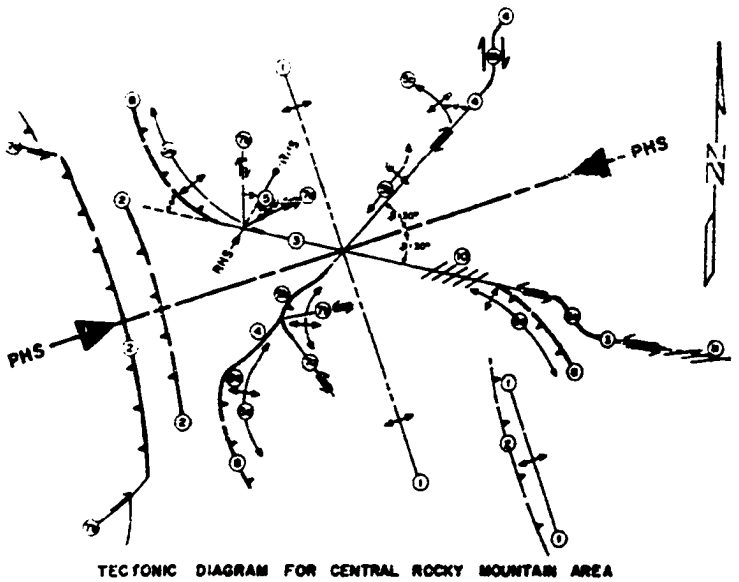

TECTONIC DIAGRAM FOR CENTRAL ROCKY MOUNTAIN AREA

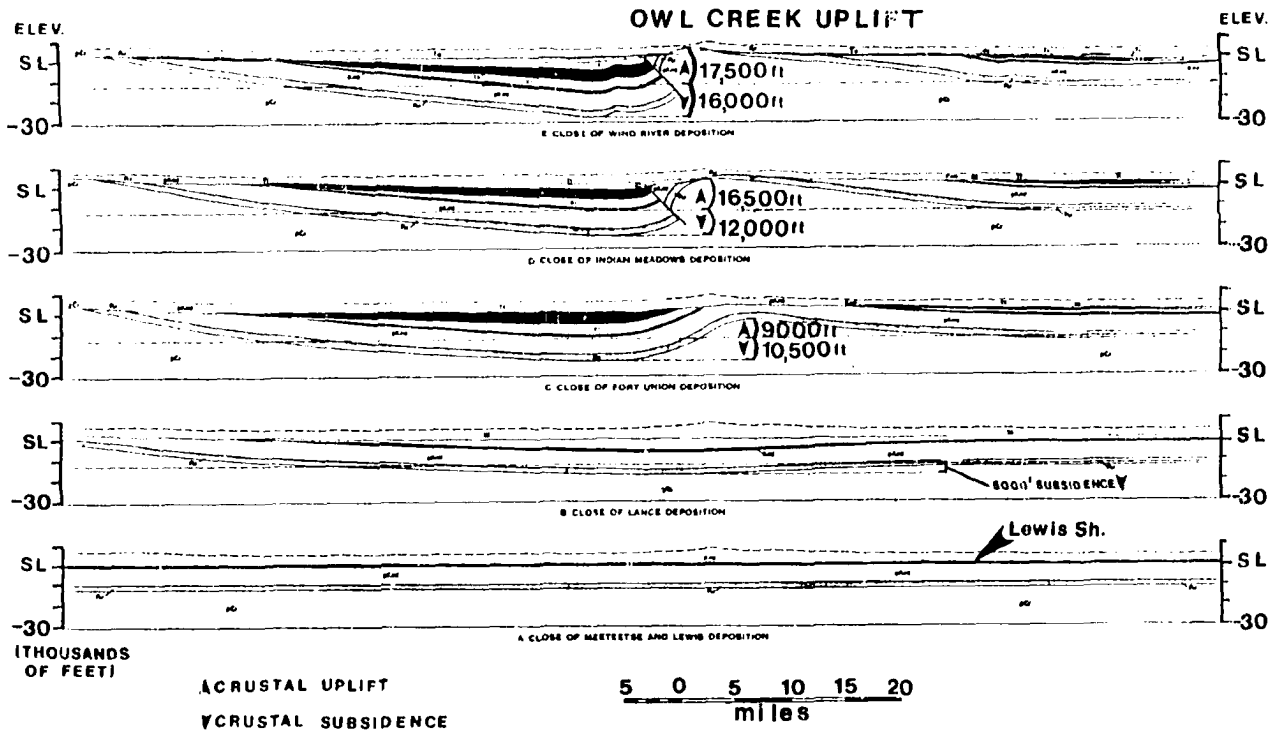

FIGURE 161. Sequential diagram showing initial deformation of Wyoming foreland at beginning of Laramide orogeny (after Keefer, 1965). A) Stage 1 (end of deposition of marine Lewis Shale) shown relative sea level marker. B) Stage 2 (end of Cretaceous) shows initial crustal downwarp. C) Stage 3 (end of Paleocene), crustal uplift of 9,000 ft has occurred, but crust has been downwarped 10,500 ft. D) Stage 4 (close of Indian Meadows deposition-early Eocene) both crustal downwarp and uplift continue. E) Stage 5 (close of Wind River depositon in middle Eocene) 33,500 feet of structural relief had been created, with uplift (17,500 ft) finally overcoming downwarp (16,000 ft).

FIGURE 162. Structural section across the Wyoming foreland along line A of index map. Owl Creek Mountain uplift arose where initial crustal downwarp commenced in Upper Cretaceous. Total crustal shortening along this line of section is approximately 28 miles.

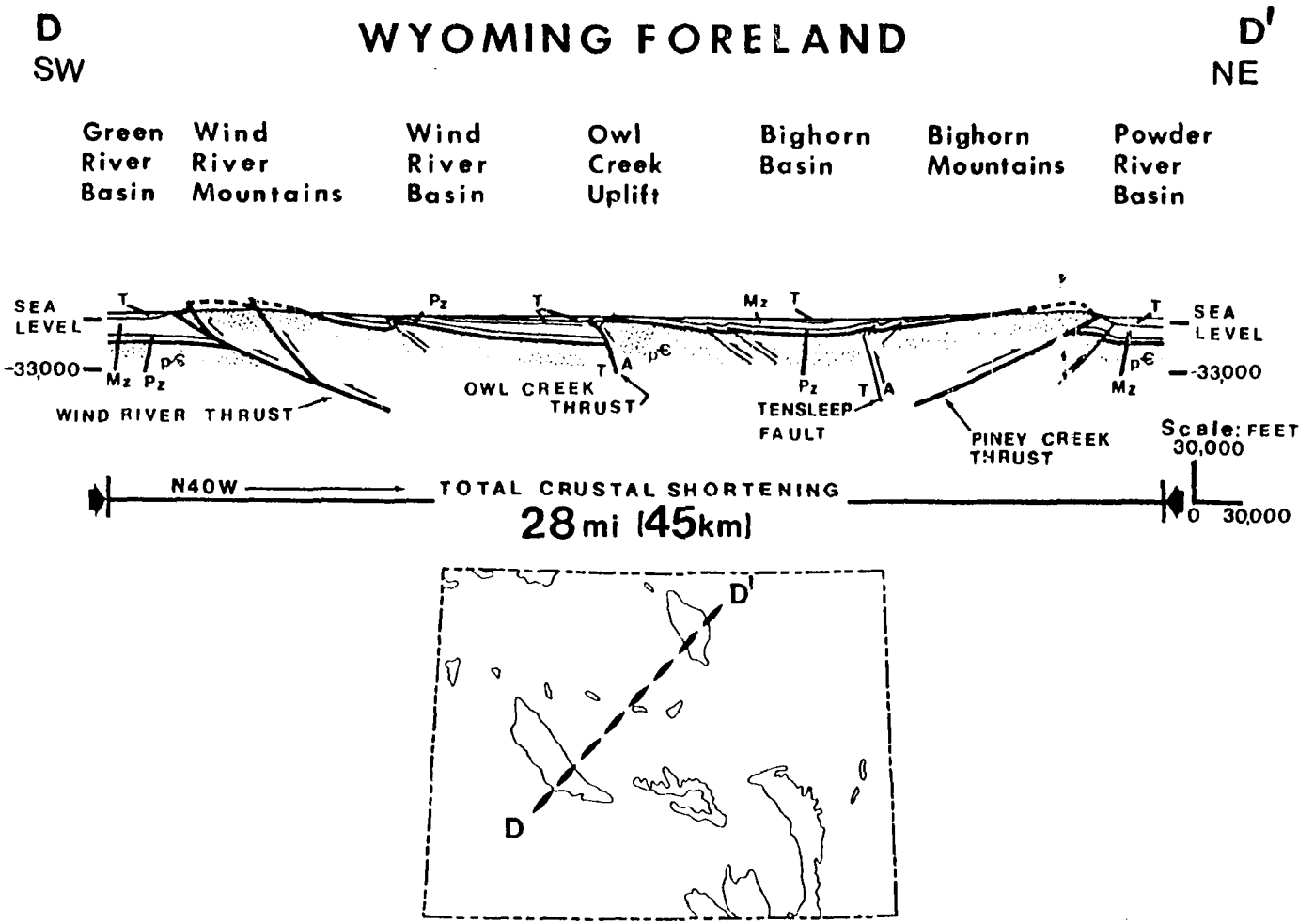

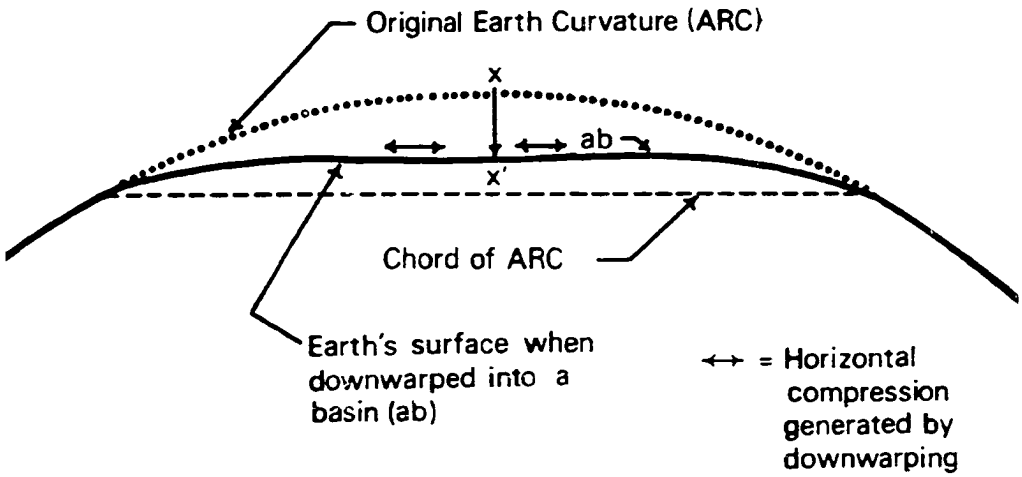

FIGURE 163. Diagram demonstrating Dallmus' (1958) concept of basin formation as represented by flattening of Earth's curvature. Crustal downwarp (X-X') of a basin (line ab) against the curvature of the Earth, will result in volumetric problems in the crust and generation of horizontal compressive stresses.

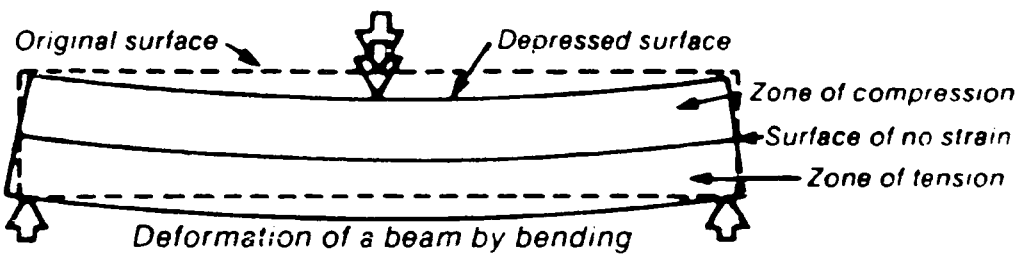

FIGURE 164. Compressive stresses are generated in the concave portion of a bent beam, as long as that portion of the beam has not passed through the chord of the arc. Extensional stresses are generated in the convex portion of the beam, and a neutral surface separates the two zones.

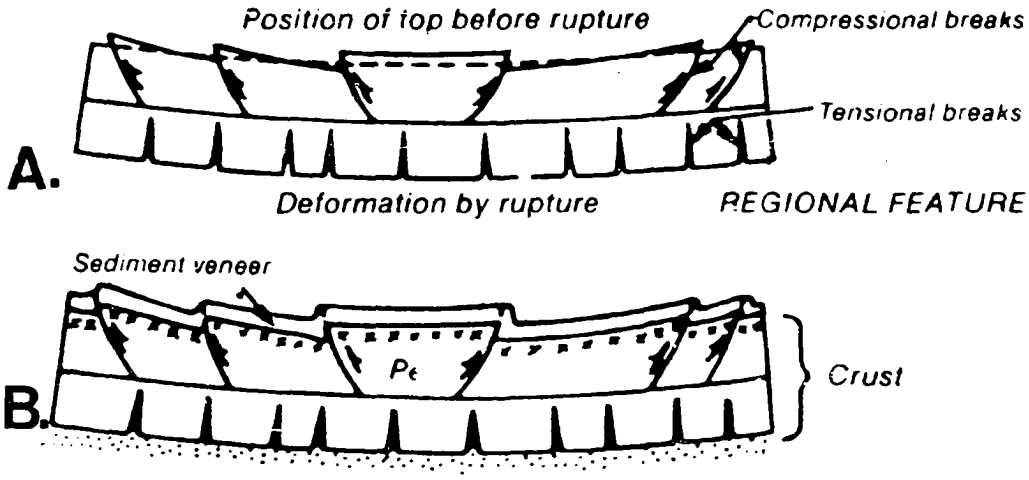

FIGURE 165. Application of the "bent beam" concept to deformation of the Wyoming foreland during the Laramide orogeny (Brown, 1984b). A) Equating the "beam" to the Earth's crust, the upper portion of the Precambrian basement (above the neutral surface) will be under compression during basin downwarping. Reverse-faulted basement flakes may be formed which could have an "out-of-the-basin" sense of vergence. B) The addition of a sedimentary veneer over the upper basement surface would allow for upward "fault-to-fold" interchanges, producing a model of the foreland structures described in this study.

FIGURE 166. Seismic section (scaled time) of a portion of the east flank of the Bighorn basin (modified from Stone, 1985). Bonanza and Paintrock anticlines (T.49 N, Rs.90-91 W) demonstrate "out-of-the-basin" vergence which is controlled by reverse-faulted basement "flakes". Continuity of reflections down to the Precambrian basement also shows the lack of a "void" which would be needed if these structures were drape folds and the "detachment" mechanism was called upon to compensate for bed volume (see figure 92).

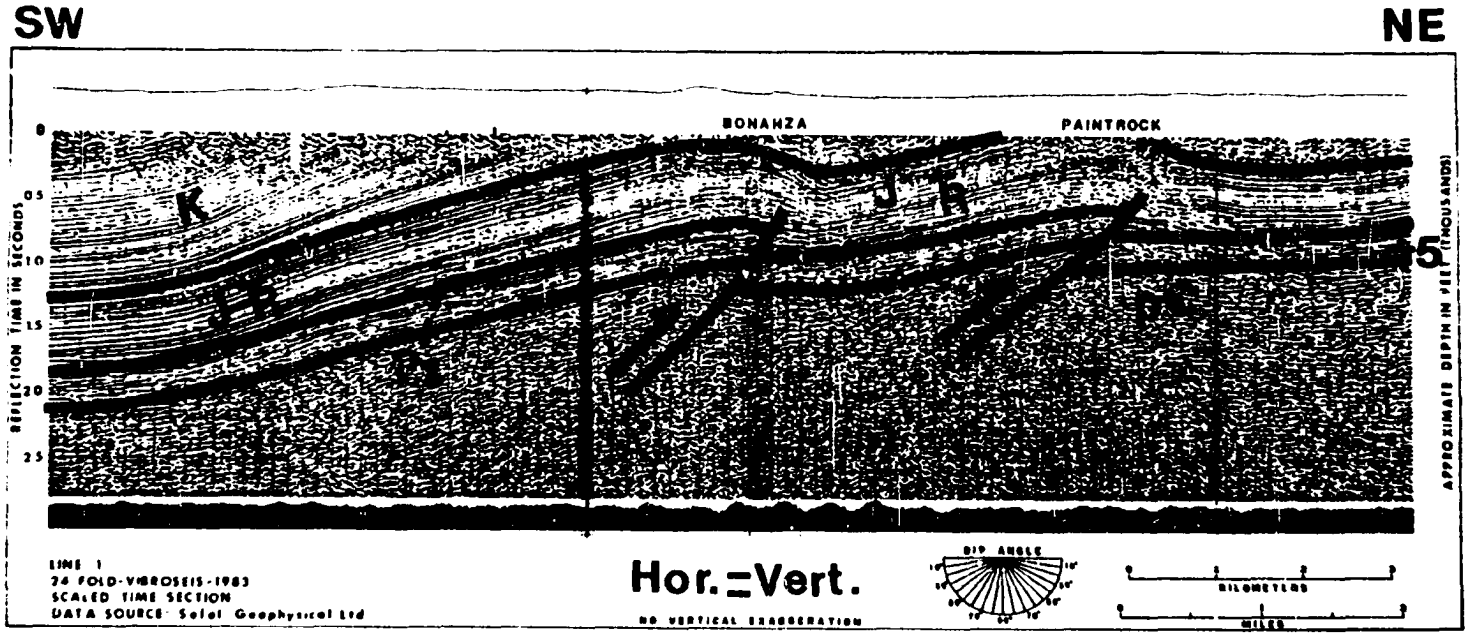

FIGURE 167. Reflection seismic section (migrated time) of a portion of the west flank of the Powder River basin (modified from Sacrison, 1978). Out-of-the-basin direction of tectonic transport has developed two anticlinal structures (location unknown) which are thrust onto the east flank of the Bighorn Mountains.

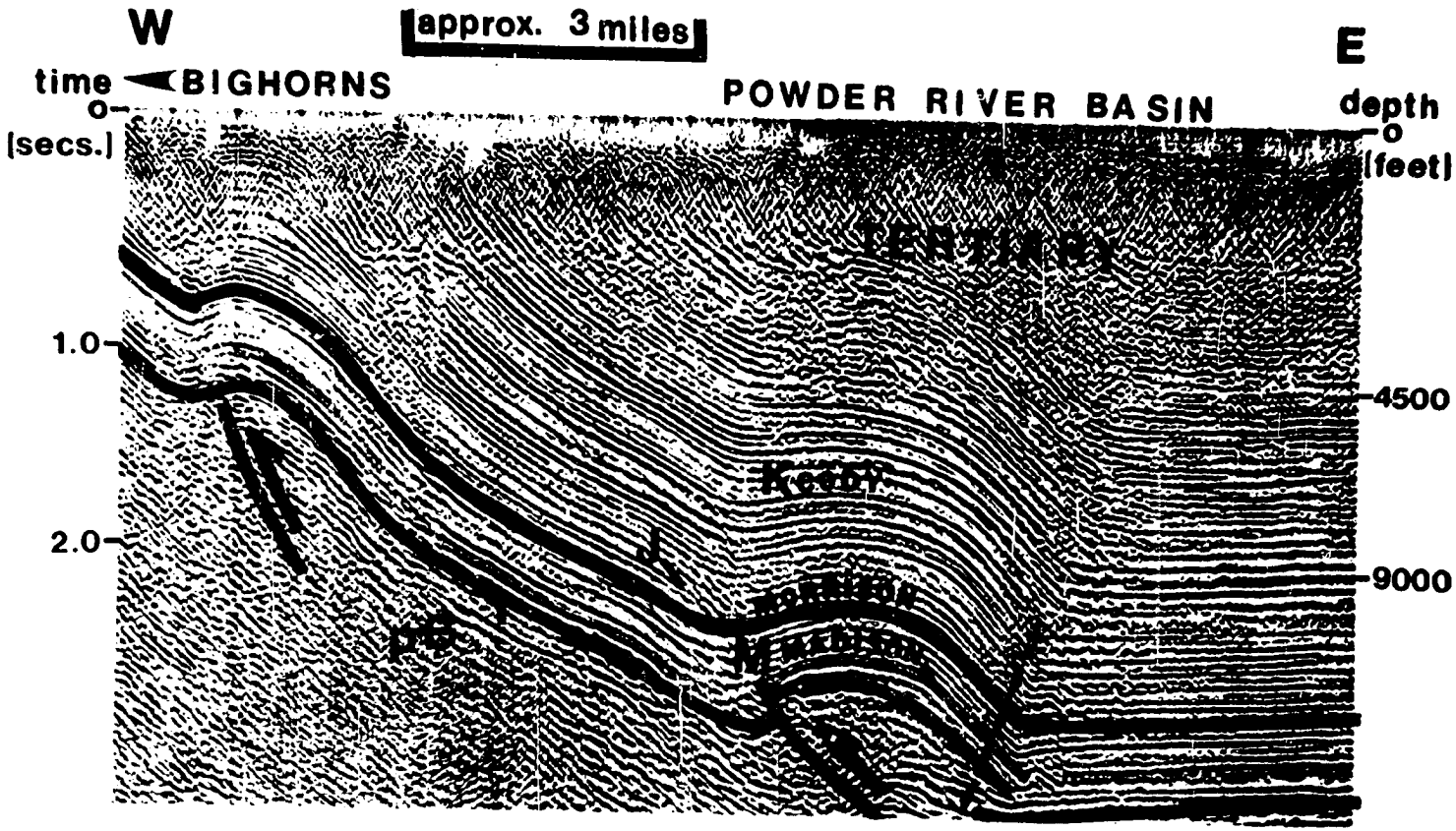

FIGURE 168. Reflection seismic section (scaled time) over Oregon Basin anticline (T.52 N., Rs.99-101 W) on the west flank of the Bighorn basin (modifed from Stone, 1985). The Oregon Basin "thrust" and associated "back-thrust" may be interpreted as an original out-of-the-basin vergence on the "back-thrust", with later offset along the basin-bounding Oregon Basin "thrust".

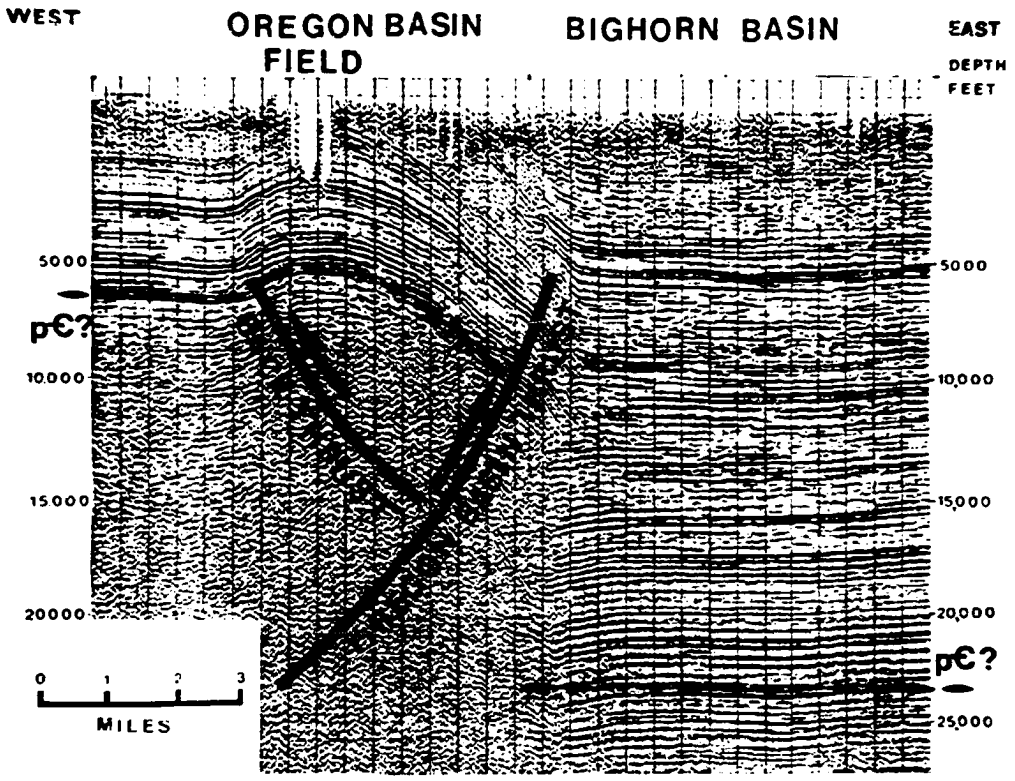

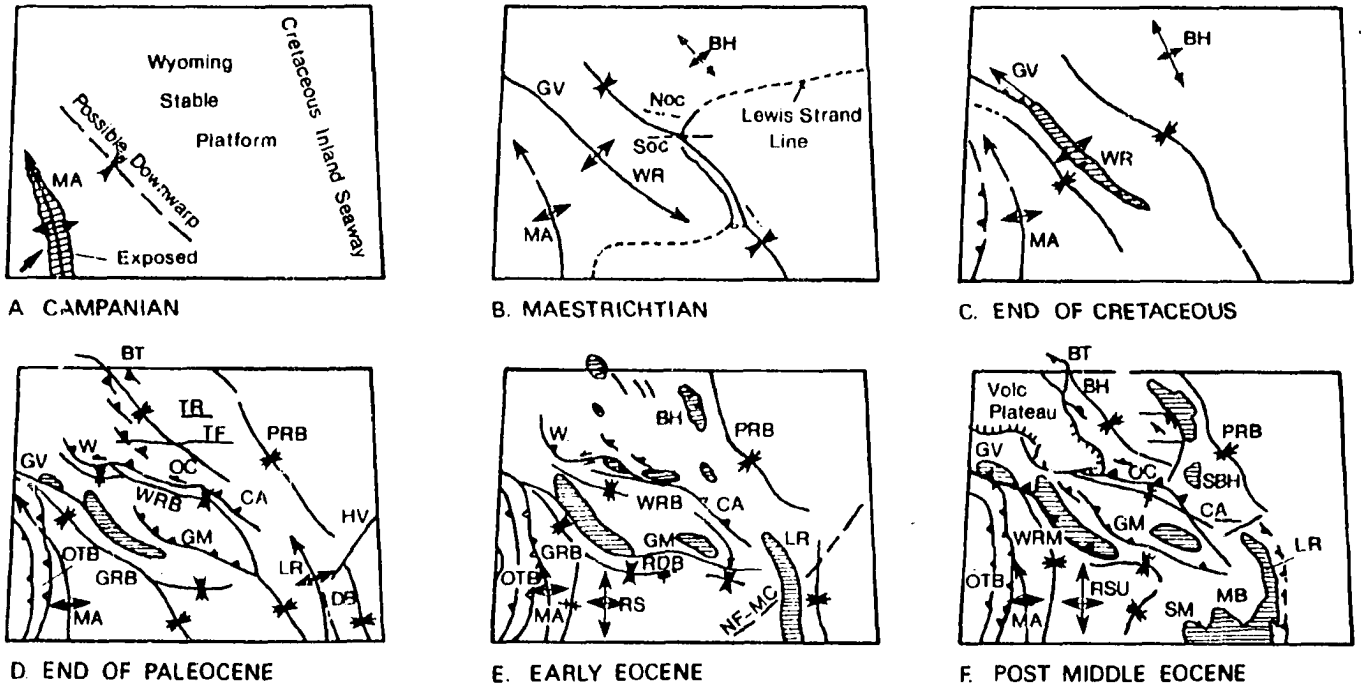

FIGURE 169. Montage of paleotectonic and paleogeographic maps which demonstrate the sequential deformation of the Wyoming foreland through time. A) Campanian: deformation began along Moxa arch, western margin of foreland, with regional downwarp to the northeast. B) Maestrichtian: deformation shifted to site of Wind River Mountains, with continued downwarp to northeast. C) End of Cretaceous: Wind River Mountains were being eroded, with gentle local uplifts to the northeast. D) End of Paleocene: uplift of Owl Creek Mountains and breakup of inital downwarp; uplift of local structures (W) in Wind River basin. E) Early Eocene: accentuation of Owl Creek uplift, with exposure of local areas in Bighorn region. F) Middle Eocene: late-stage movements along east flank of Beartooth, Bighorn, and Laramide Mountains.

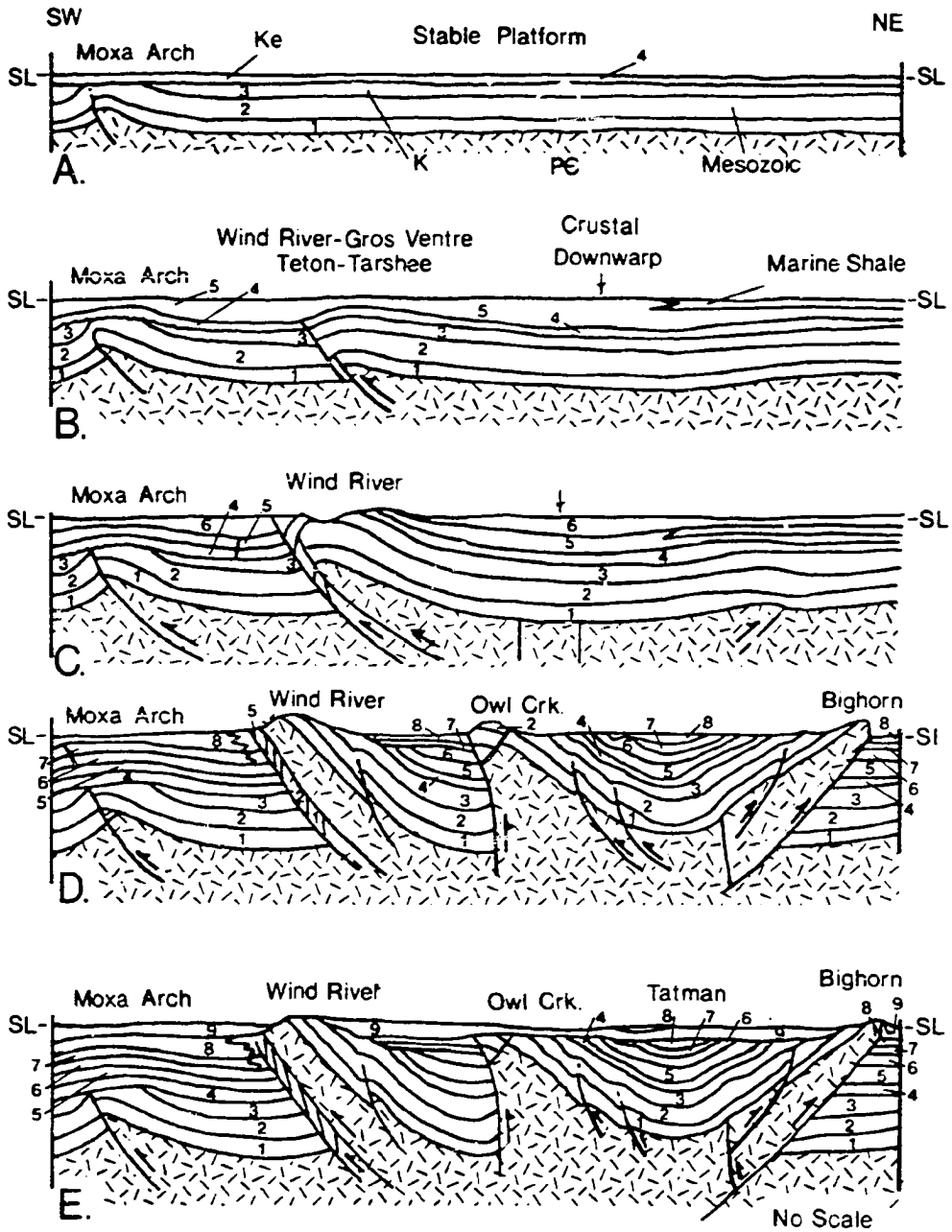

FIGURE 170. Montage of sequential, diagrammatic structural sections across the foreland along line A of figure 162. Sequence is the same as in figure 169, except for omission of early Eocene sequence (fig. 169e). Key to age of rocks: 1 = Paleozoic; 2 = Triassic-Jurassic; 3 = Lower Cretaceous; 4 = Erickson Formation (Upper Cretaceous); 5 = Upper Cretaceous (Meeteetse-Lewis); 6 = Upper Cretaceous (Lance); 7, 8 = Paleocene (Fort Union); 9 = Eocene (Wasatch).

APPENDIX FIGURES

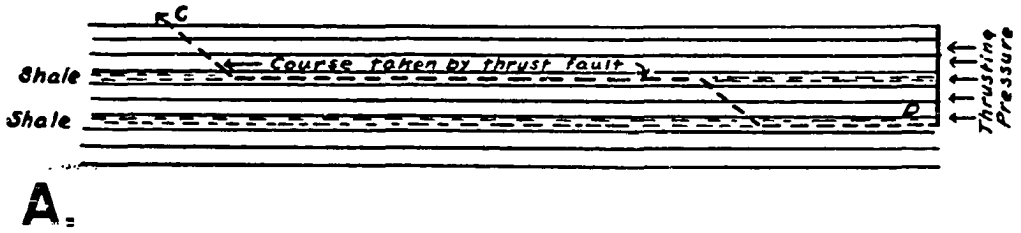

A.

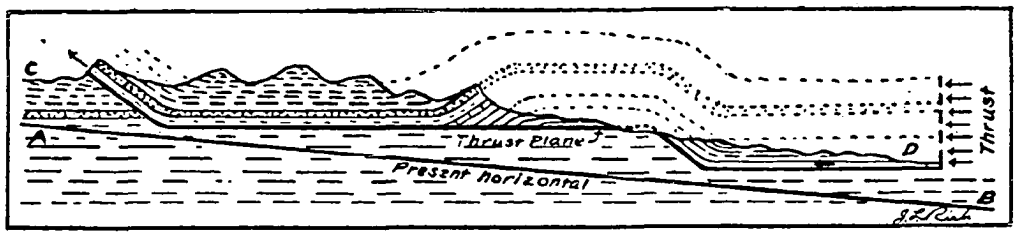

B.

FIGURE A-1. Concept of Rich-model ramp anticline (after Rich, 1934). A) Incipient thrust plane develops parallel to bedding in easy-gliding shales, and breaks diagonally across more brittle beds, creating a series of ramps as the fault cuts up to the surface. B) Structural section across Cumberland Plateau follows this ramp-type geometry.

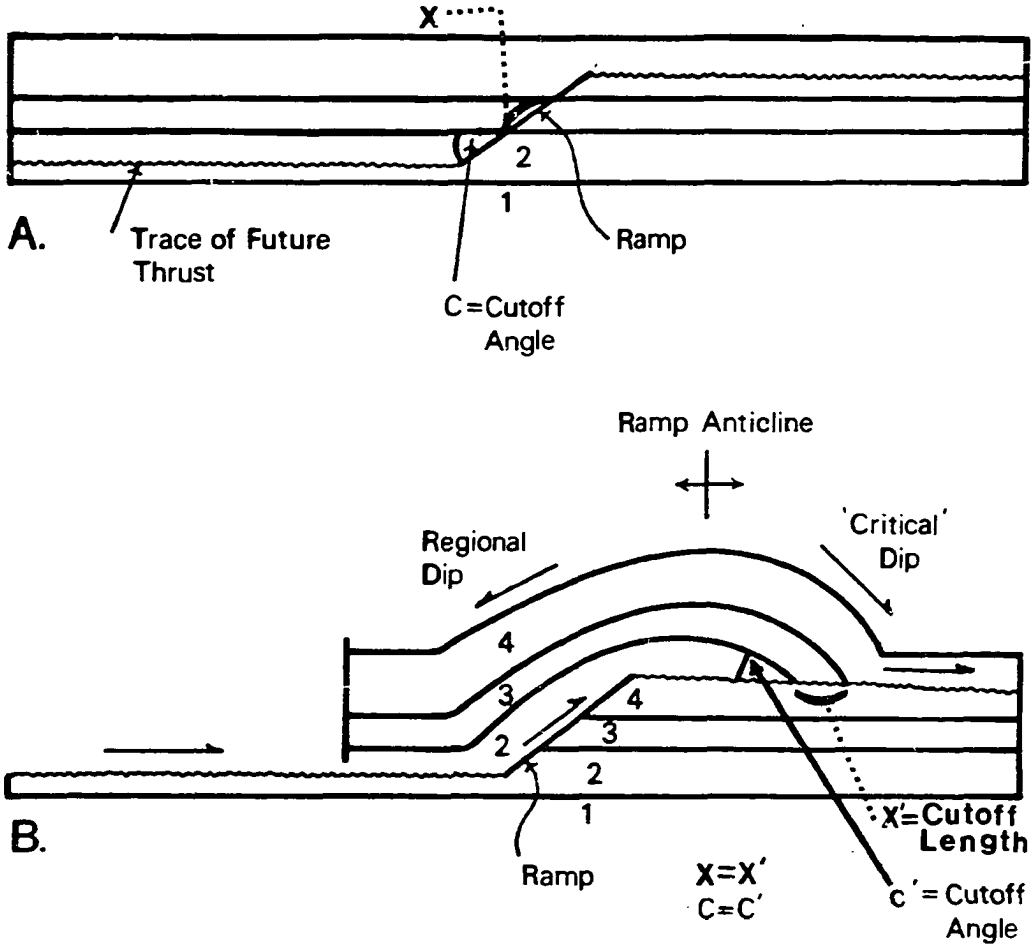

FIGURE A-2. Geometry of Rich-model ramp anticline. A) The upward break (diagonally) across more competent, or brittle layers of rock, results in the formation of a ramp, which in this case is followed by another bedding-parallel flattening of the thrust plane. The incipient fault will develop cut-off angles (e.g. C) and cut-off lengths (e.g. X) as it breaks across bedding. B) The movement of rock layers from one flat to another, up and over the ramp, will create the "ramp anticline" which results from the flattening of the thrust. Preservation and rotation of fault cut-off angles (C) and lengths (X) creates the "critical" dip down the ramp, against "regional" dip.

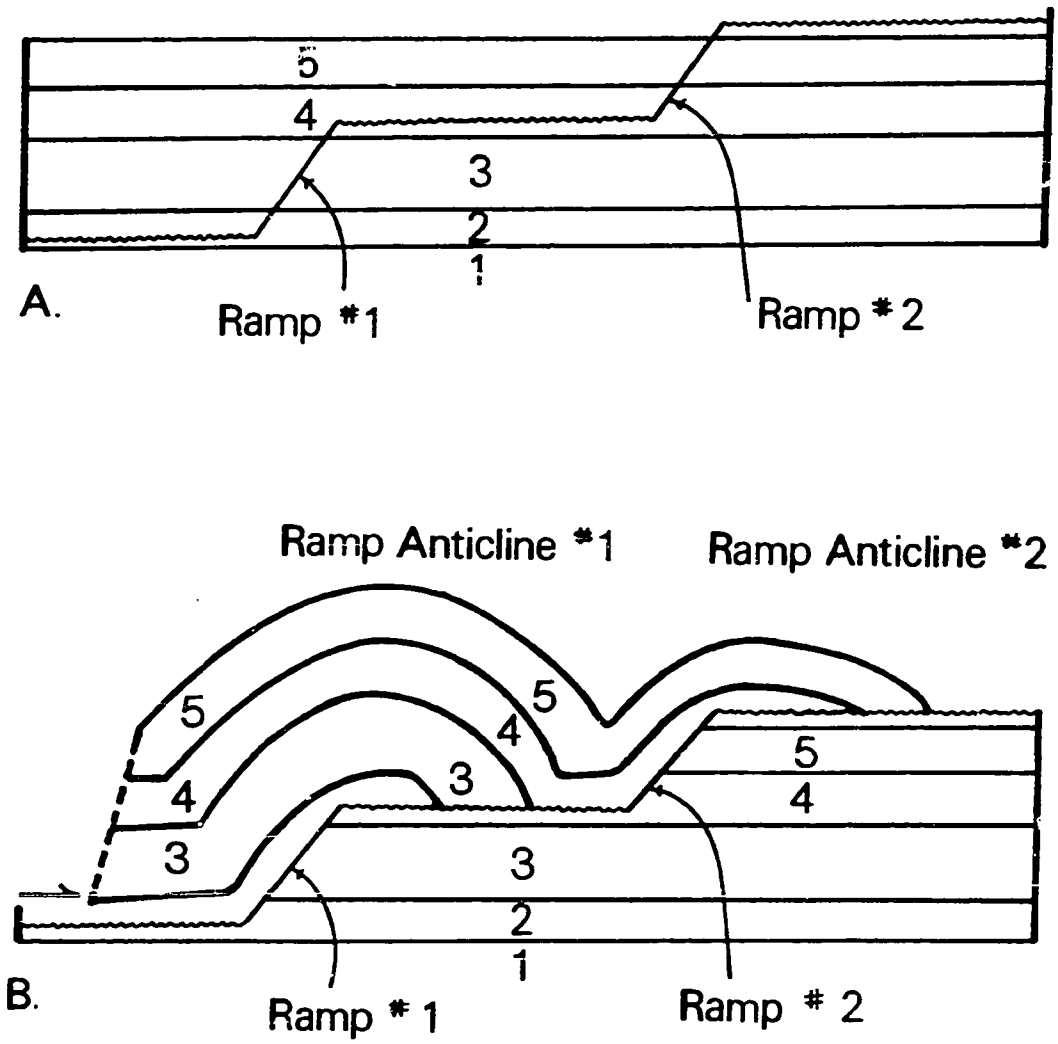

FIGURE A-3. Development of multiple ramp anticlines. A) Geometry of ramp is repeated in higher stratigraphic units. B). A ramp anticline will form for each ramp over which the rocks have moved.

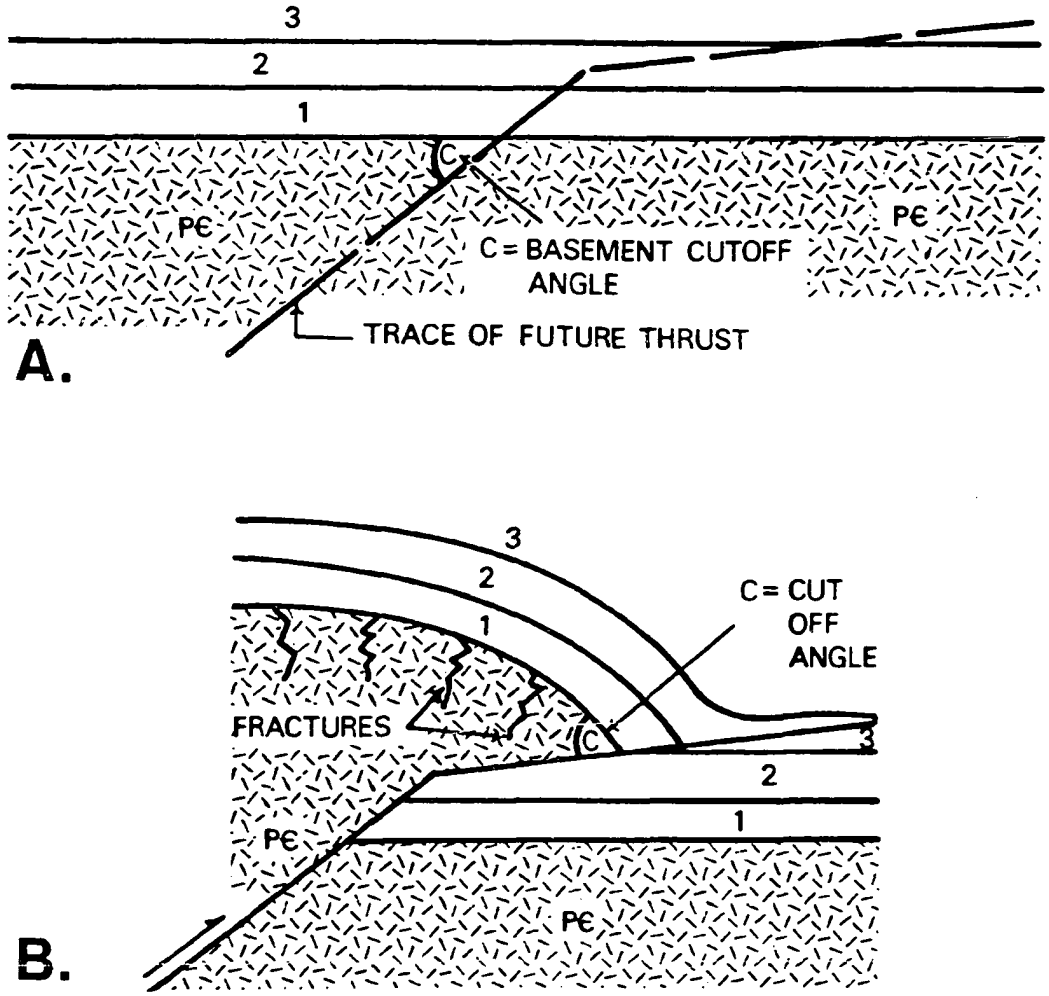

FIGURE A-4. Application of ramp anticline geometry to basement-involved foreland reverse faults. A) Ramp is developed as fault breaks through the upper basement surface (along with cut-off angle "C"), and "flattens" to some lesser degree of dip in the sedimentary section. B) As upper basement surface moves across the ramp and passes onto the low-dipping portion of the fault, rotation of the cut-off angle (C) causes dip into the fault plane, resulting in an anticlinal shape on the upper basement surface.

FIGURE A-5. Experimental rock model which creates Rich-model ramp anticline (after Morse, 1977). A) Configuration of model is such that compression parallel to arrows causes bottom layer on upper block to move from the lower hinge of the ramp, up and onto the flattened portion of the "fault". B) Geometry in deformed layers is that of a Rich-model ramp anticline, but note also that "back-thrusts" (large arrows) develop at the lower hinge of the ramp, and migrate passively up the ramp with continued displacement along the thrust plane.

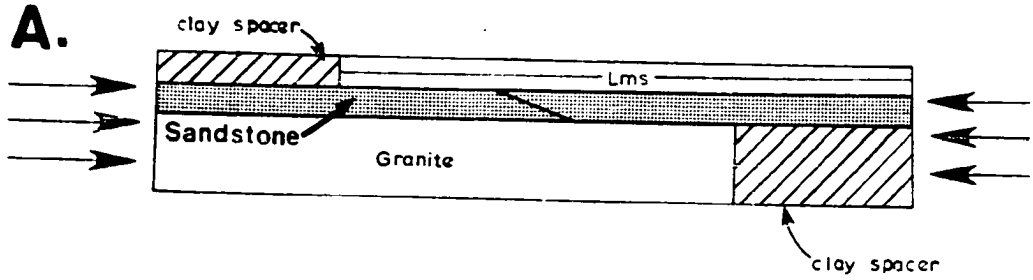

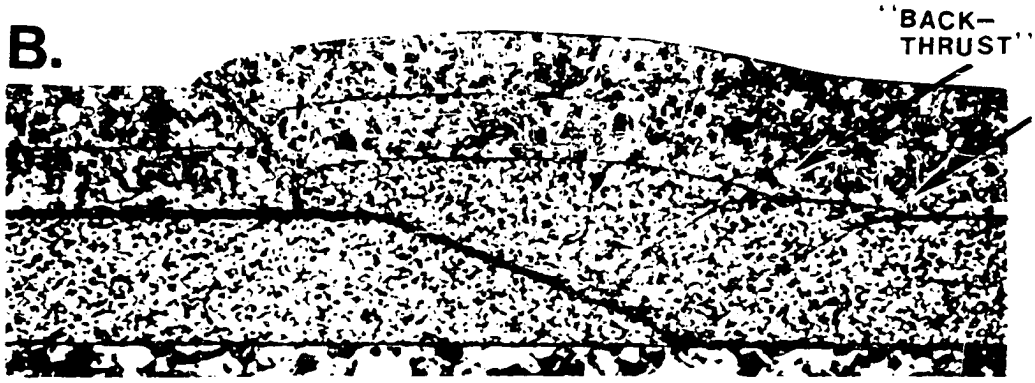

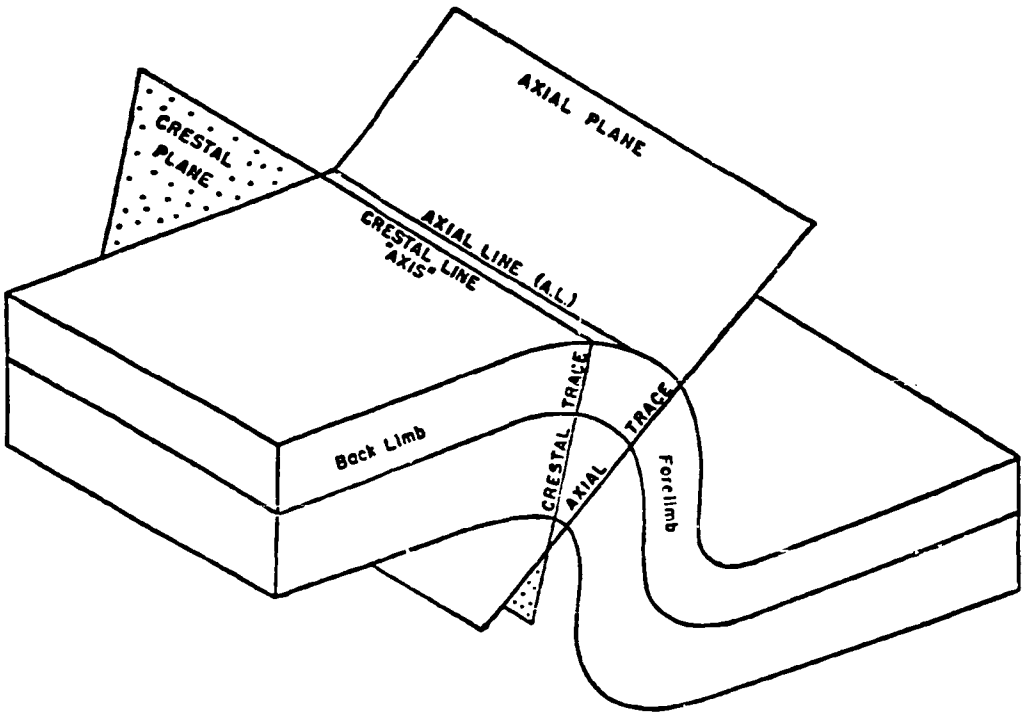

FIGURE B-1. Terminology used to describe asymmetric anticlines. Axial plane divides fold into equal geometric halves. The axial plane intersects bedding surfaces in the axial line, and is intersected by a transverse section as the axial trace. The crestal plane connects the structurally highest points on all bedding surfaces along the length of the fold. The crestal plane is intersected by a transverse section as the crestal trace, and intersects the bedding surfaces as the crestal line, which is often referred to as the "axis" of the fold. The gentle flank of the fold is the back limb, while the steep flank is the forelimb. Direction of asymmetry "faces" in the direction which the forelimb faces.

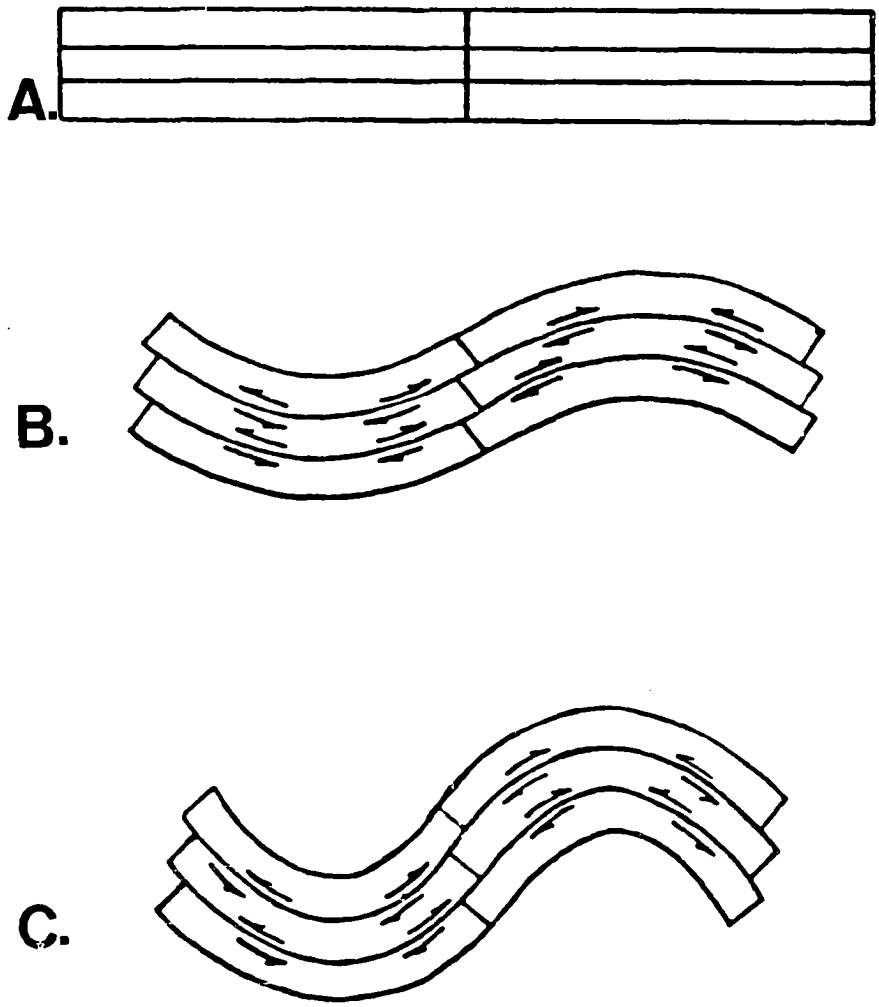

FIGURE B-2. Nature of bedding-plane slip in flexural slip folding. A) Original attitude of bedding with a reference line perpendicular-to-bedding. B) Flexing of the layers results in classic out-of-the-syncline bedding-plane slip is indicated by arrows and offset of reference line. C) Magnitude of bedding-plane slip is indicated by the "shingling effect" of edges of layers, demonstrating the volume transfer of material from synclinal axis toward the anticlinal axis.

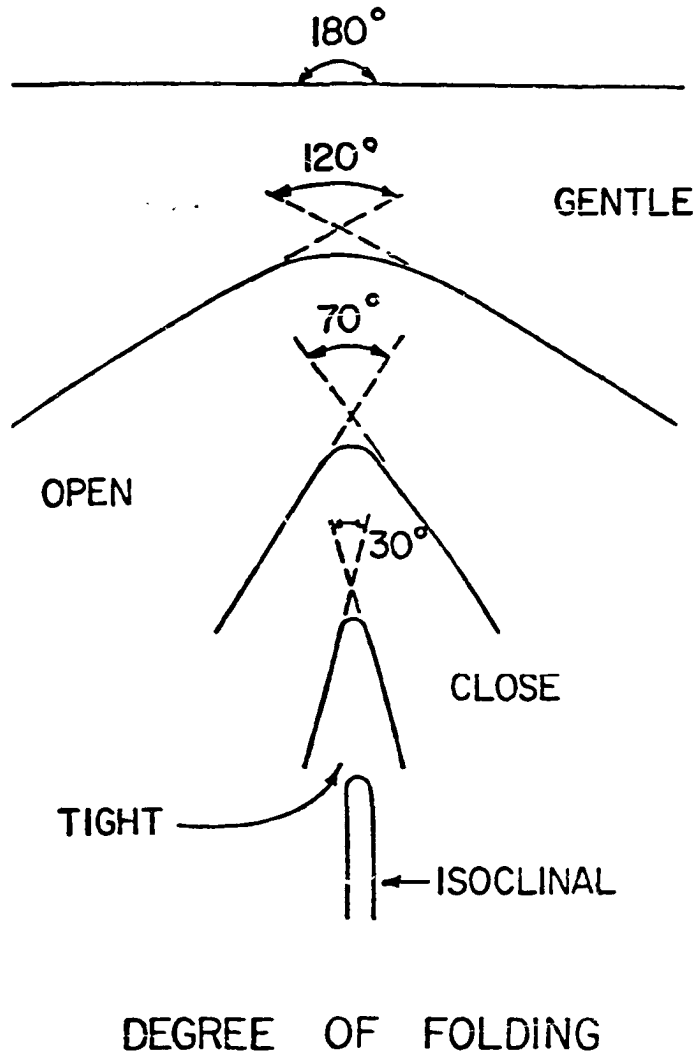

FIGURE B-3. Description of folds using the "degree of folding" shown by the interlimb angles (after Fleuty, 1964).

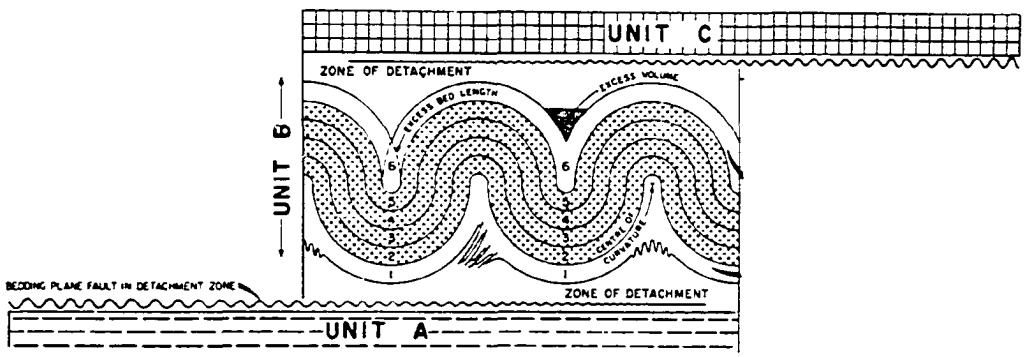

FIGURE B-4. Development of "upper" and "basal" detachments related to parallel folding of rock layers via flexural slip mechanism. Parallel folding results in tightening of the fold down the anticlinal axial trace, and up the synclinal axial trace. Ultimately, the volume of rock can not be maintained within the fold arc, and a detachment develops by bedding-plane slip and allows the fold to become disharmonic with adjacent layers (Dahlstrom, 1970).

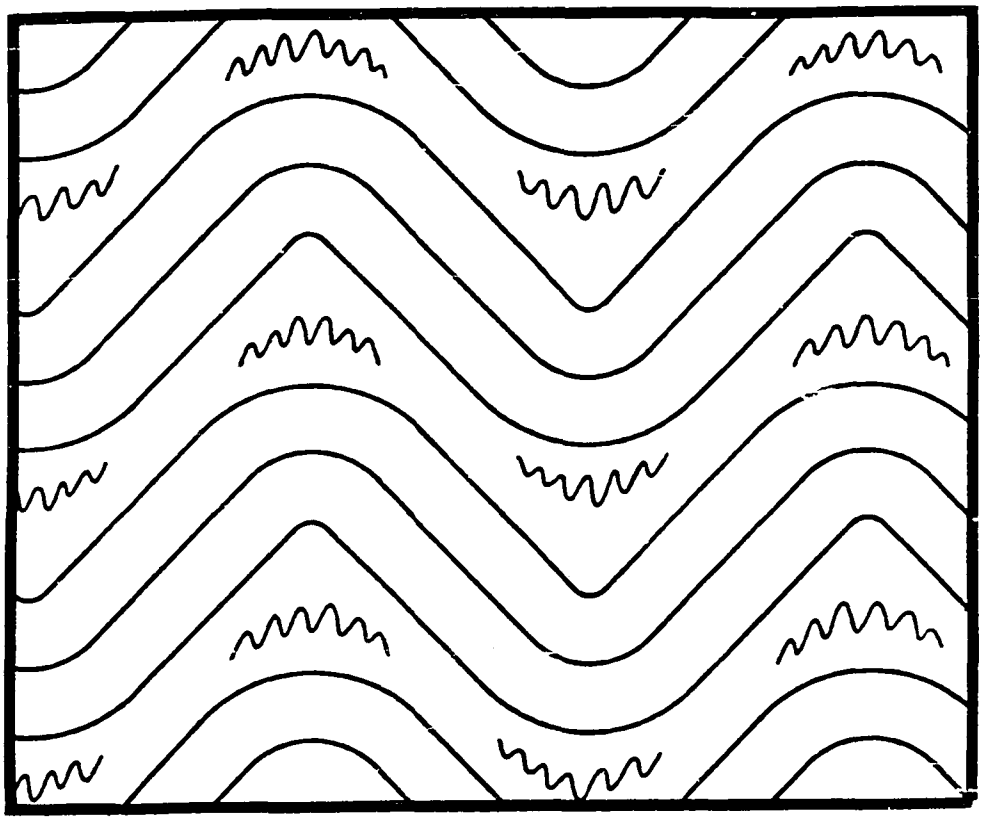

FIGURE B-5. Concept of multiple detachments (after Dahlstrom, 1969a). Folds which develop detachments as a consequence of volume problems may, in turn, pass back into more open folds beyond the detachment. The more open fold may then tighten and ultimately detach, and repeat the process time and again. The result is a parallel-folded structure which propagates to greater depths than normally expected, and contains numerous detachments scattered throughout the stratigraphic section.

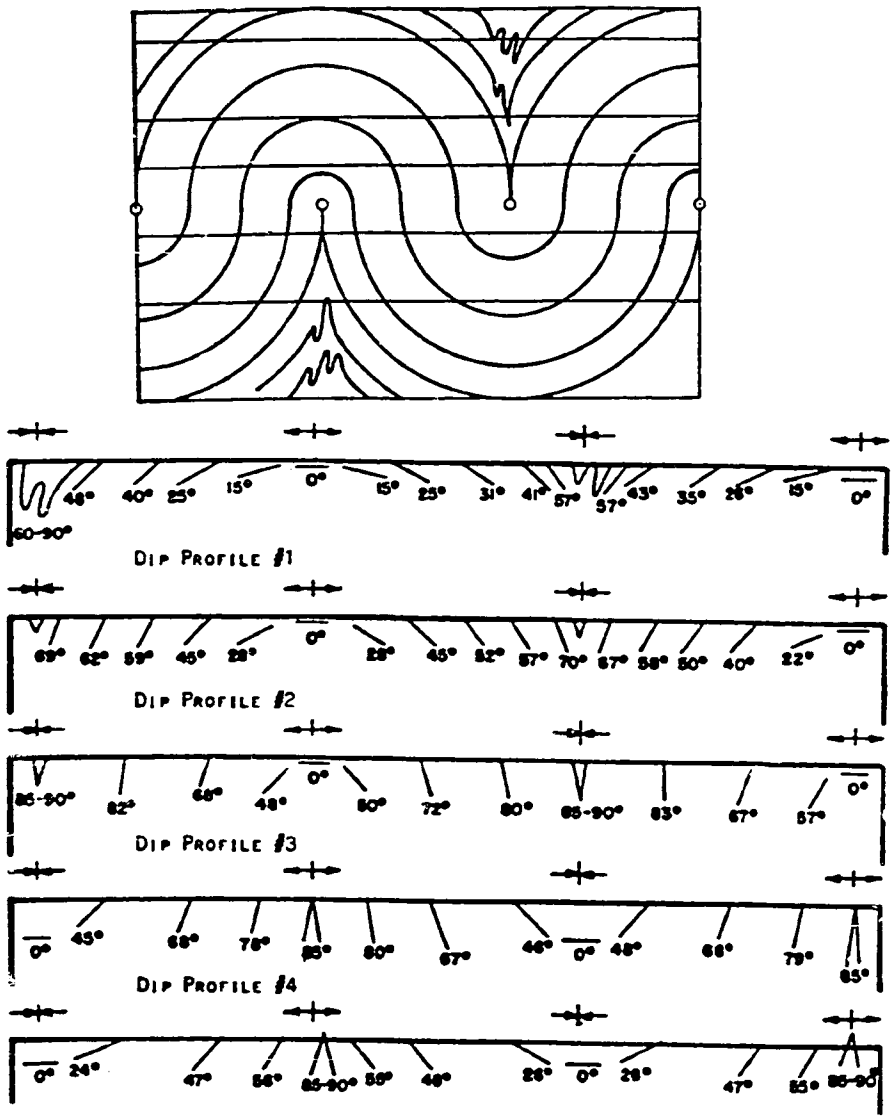

FIGURE B-6. Ideal parallel folds. A) Five structural levels through ideal parallel anticline and syncline. B) Dip profiles at each of five structural levels demonstrate how the folds tighten along their axial traces. Relative position within a parallel fold (level 1 to 5) can be ascertained by the recognition of: level 1- broad anticlinal form and tight, disharmonically folded synclines; level 3 to 4- approximately equal shapes of anticline and syncline at the centers of curvature; level 5- tightly folded, disharmonic anticlines, and broad, open-folded synclines.

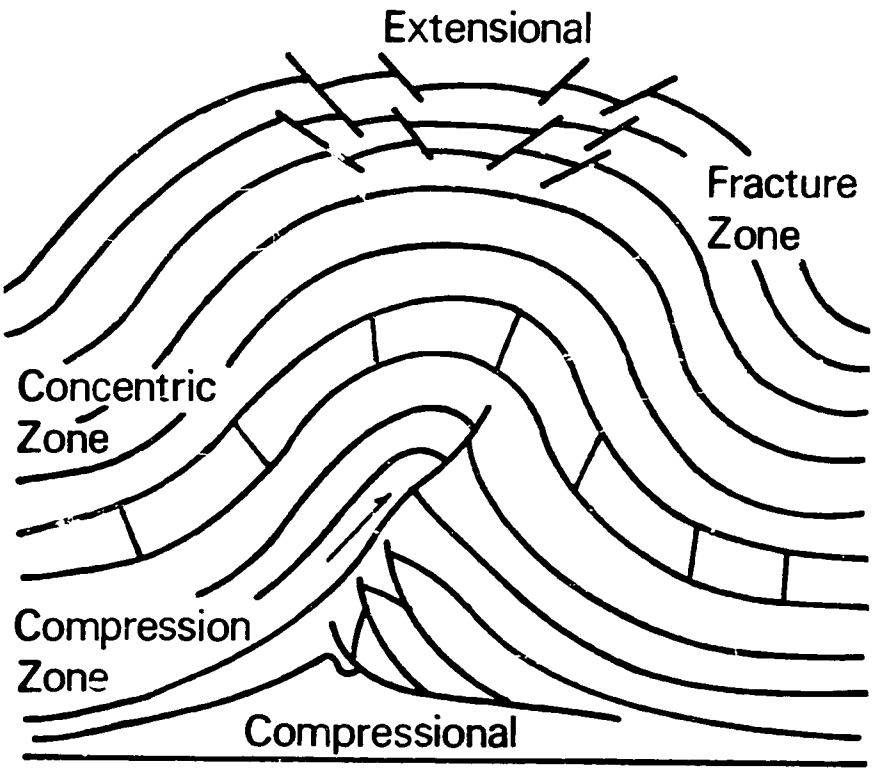

FIGURE B-7. Zoning of the ideal parallel fold. Fracture zone: extension accomplished by normal faults which die out downward at shallow depths. Compressional zone: shortening accomplished by complimentary thrusts and fold crenulations. Concentric zone: neither extension nor shortening, equates to neutral surface in beam (after De Sitter, 1964).

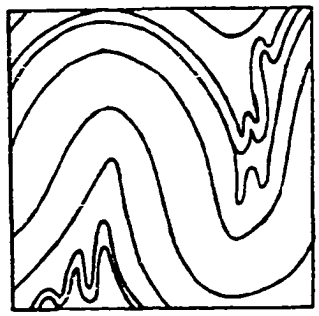

CRENULATION

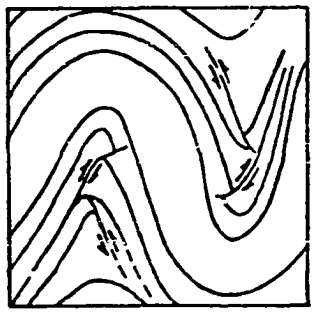

COMPLEMENTARY THRUSTING

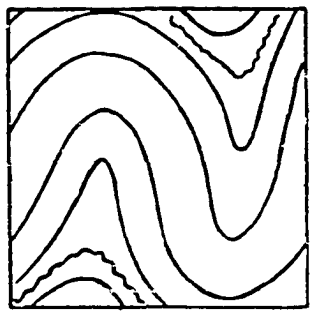

DECOLLEMENT
(DETACHMENT ALONG BEDDING PLANE)

FIGURE B-8. Three methods of bed-length accommodation beyond the center of curvature in parallel-folded anticlines and synclines. A) Crenulation, or development of disharmonic folds. B) Complimentary thrusting in the core of the folds. Synclinal faults are referred to as out-of-the-syncline thrusts.

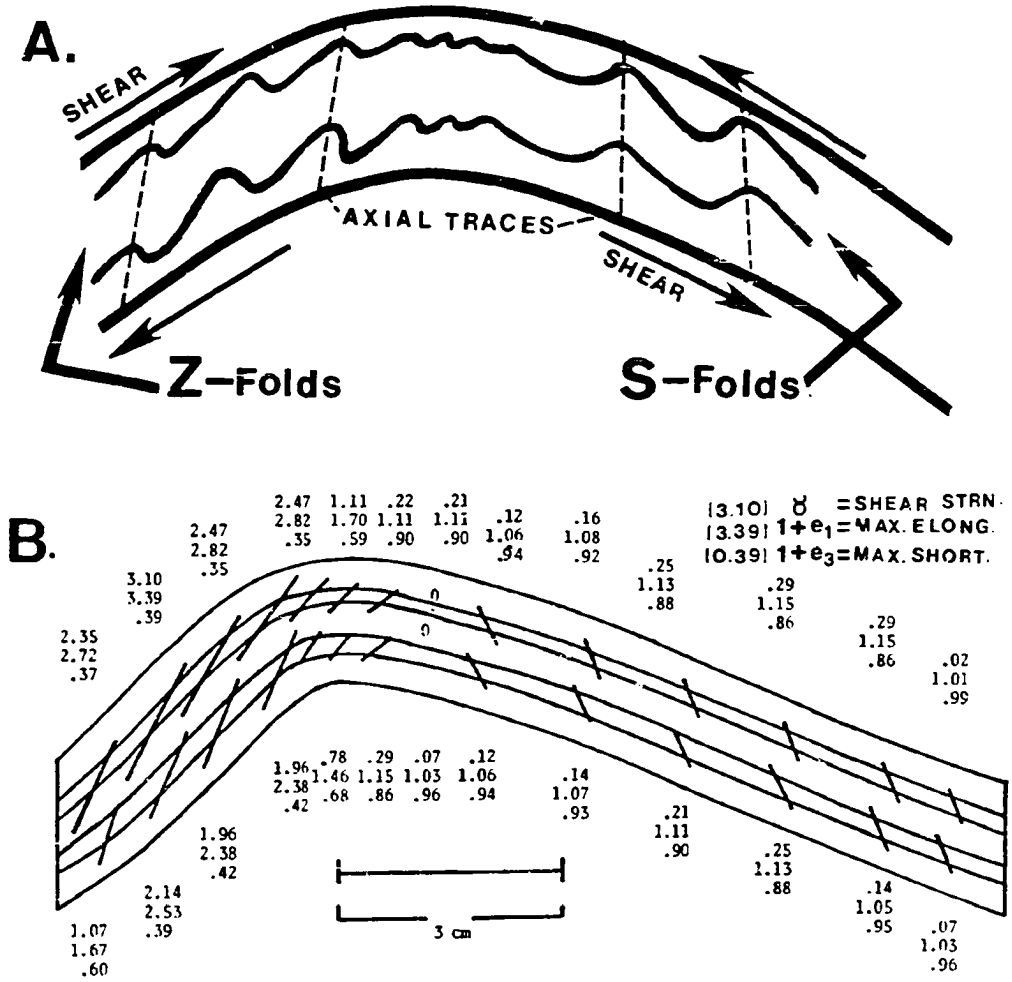

FIGURE B-9. Development of S- and Z-drag folds, by bedding-plane slip. A) Sense of vergence develops the classic snape of drag folds. B) Experimentally derived values of magnitude, and orientation of the finite shear strain (top no.), maximum finite elongation (middle no.), and maximum finite shortening strain (bottom no.) in asymmetric folds (after Casarta, 1980). Inclined short lines indicate sense and magnitude of bedding-parallel shear developed in the flexural slip folding. Note that the anticlinal axial trace does not represent a neutral surface, with respect to bedding-plane slip, as does a synclinal axial trace. Cross-crestal and rabbit-ear structures are foreland examples of bedding-plane slip which crosses the anticlinal axial trace.

FIGURE B-10. Outcrop examples of S- and Z-folds. A) An S-fold formed on the right-hand flank of a subsidiary fold within the core of Goose Egg anticline (in Cretaceous Mowry Shale). B) A Z-fold formed on the northwest plunge of Chabot anticline (in Permian Goose Egg Formation).

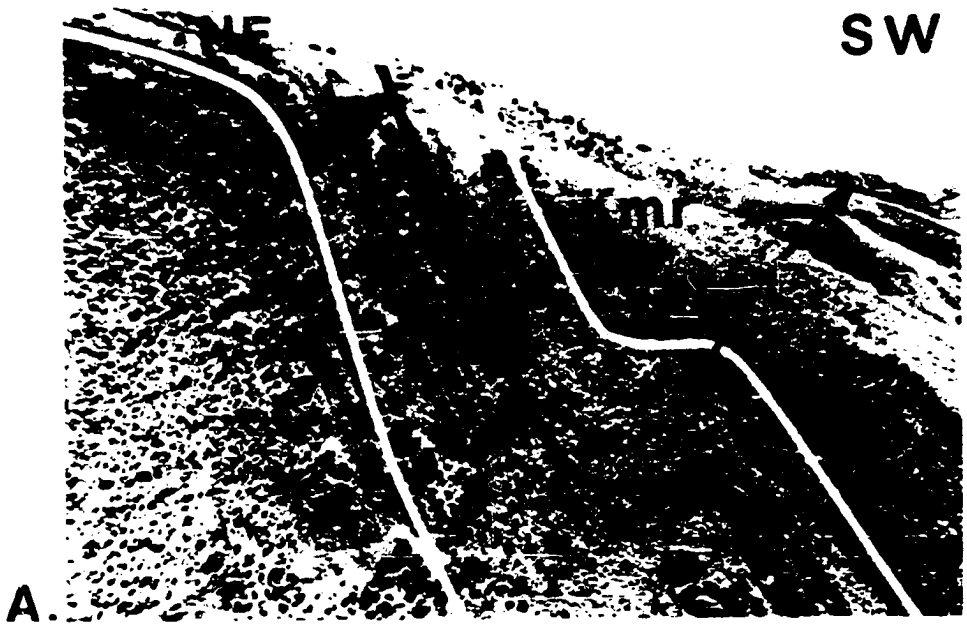

A.

B.

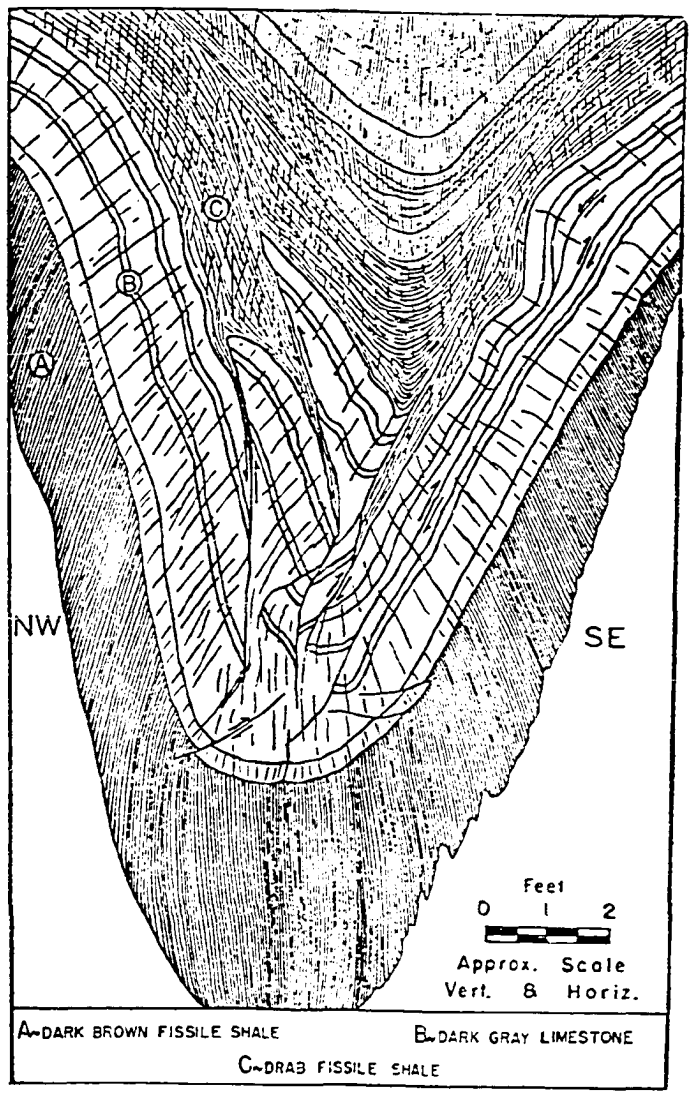

FIGURE B-11. Example of out-of-the-syncline thrust faults. Faults die out downward in the syncline, but display repetition by thrusting on the flank of the structure. Faults may be unrecognized further up the flank, as they pass into bedding-parallel orientation. Ultimately the fault will die out upward into a drag fold (S or Z), or cut upsection again as a thrust fault (Gair, 1950).

CONSISTENT BED THICKNESS

CONSTANT ORIGINAL BED THICKNESS

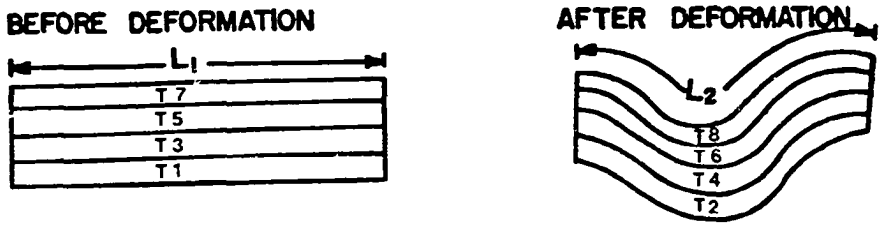

A. T1=T2, T3=T4, T5=T6, T7=T8; L1=L2

VARIABLE ORIGINAL BED THICKNESS

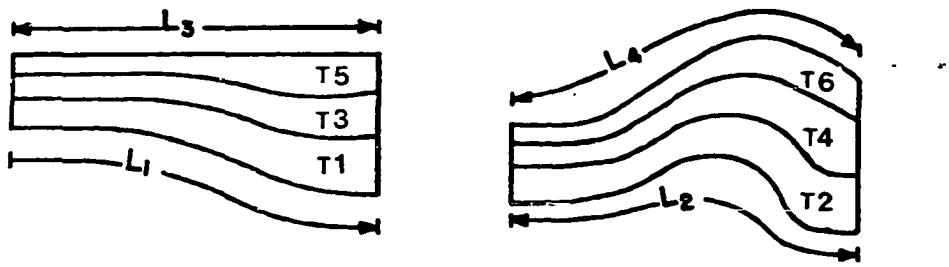

B. T1=T2, T3=T4, T5=T6; L1=L2, L3=L4

FIGURE C-1. Concept of consistent bed thicknesses in structural balance. A) Constant original bed thickness remains consistent during deformation, so that original bed-lengths also remain consistent. B) Variable original bed thickness (stratigraphic wedge) remains consistent during deformation and original bed-length also remains consistent.

CHANGING BED THICKNESS

A. SHALE FLOWAGE

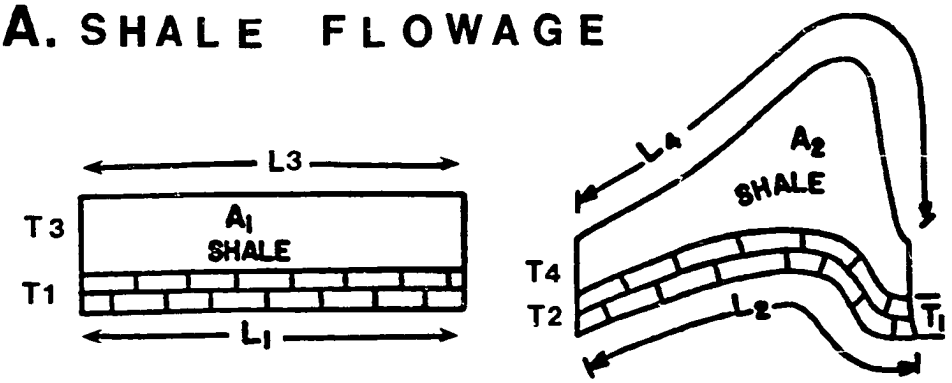

T1=T2; L1=L2; A1=A2; T3≠T4; L3<L4

B. TECTONIC THINNING – ATTENUATION

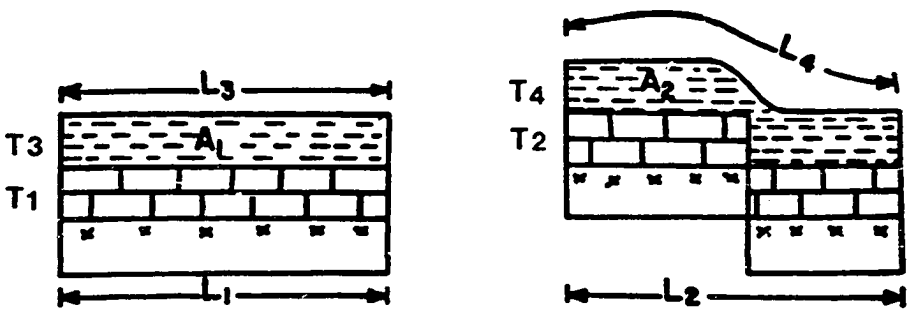

T1=T2; L1=L2; A1=A2; T3≠T4; L3<L4

FIGURE C-2. Concept of changing bed thicknesses in structural balance. A) Area remains constant (A1 = A2), therefore bed lengths must change (L4 longer than L3). Shale flowage is an example of changing bed thickness during deformation. B) Tectonic thinning, or attenuation, is another example of changing bed thickness during deformation.

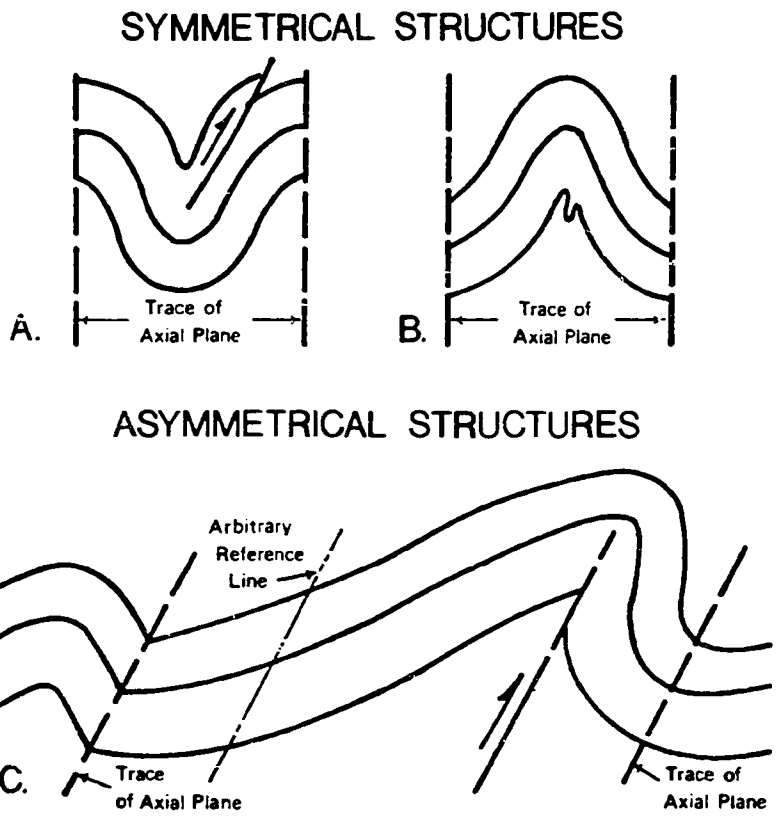

FIGURE C-3. Selection of reference lines for use in determination of bed lengths in symmetric and asymmetric folds. A) Bed-length measurement of a syncline requires the use of anticlinal axial traces as reference lines. Caution must be taken to account for any cross-crestal or rabbit-ear structures which transfer synclinal volume across anticlinal axial trace. B) Bed-length measurement of an anticline is made between neutral surfaces which are the synclinal axial traces. C) Bed-length measurements of asymmetric structures are best made between inclined synclinal axial traces. Note that an arbitrary reference line could be drawn parallel to the synclinal axial trace, at a position closer to the crest of the anticline. This does not alter the relative lengths measured. For cases in which a "back-limb" thrust develops out of the adjacent syncline, the arbitrary reference line should be at a position which is down-dip from the thrust.

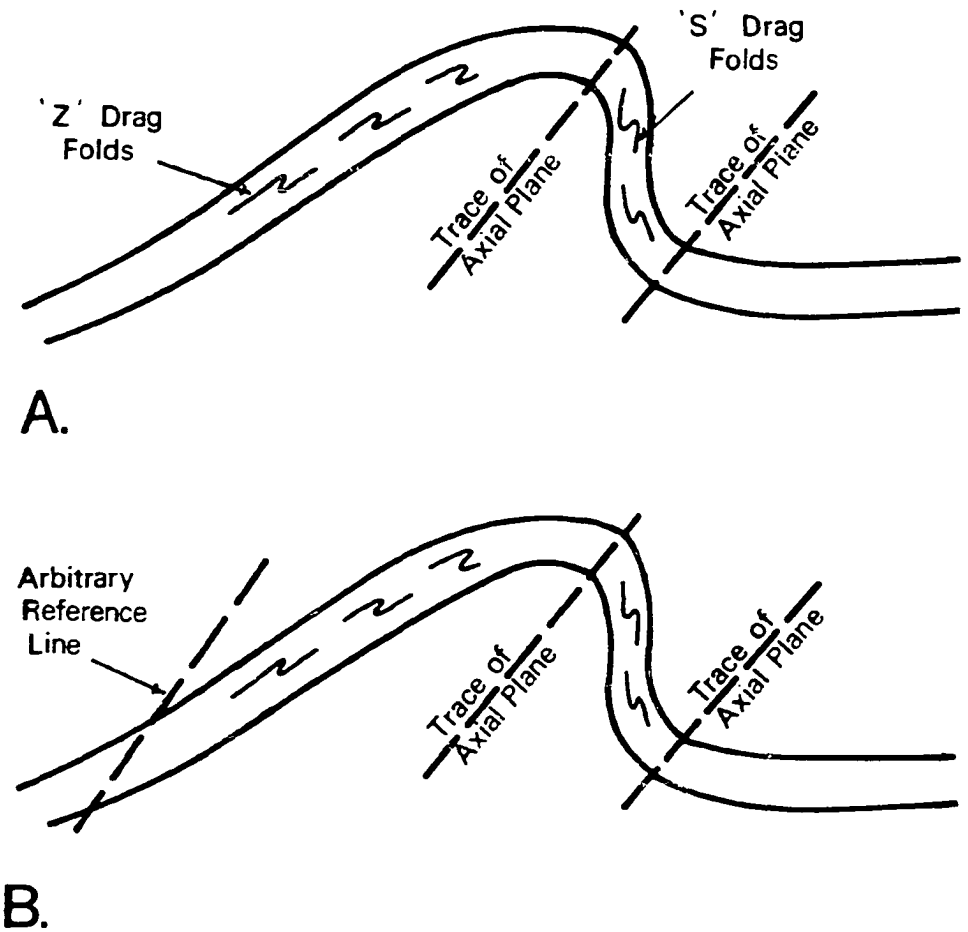

FIGURE C-4. Selection of reference lines for use in determination of bed lengths of structures where a back-limb syncline is not present. A) Fold asymmetry is accompanied by development of drag folds on the back limb, indicating bedding-plane slip on that flank. The back limb may be too long to justify drawing a section all the way to the adjacent syncline. B) The arbitrary reference line described in figure C-3, may be drawn parallel to the trace of the back limb syncline on a shorter cross section, and measurements made between this and the trace of the forelimb syncline.

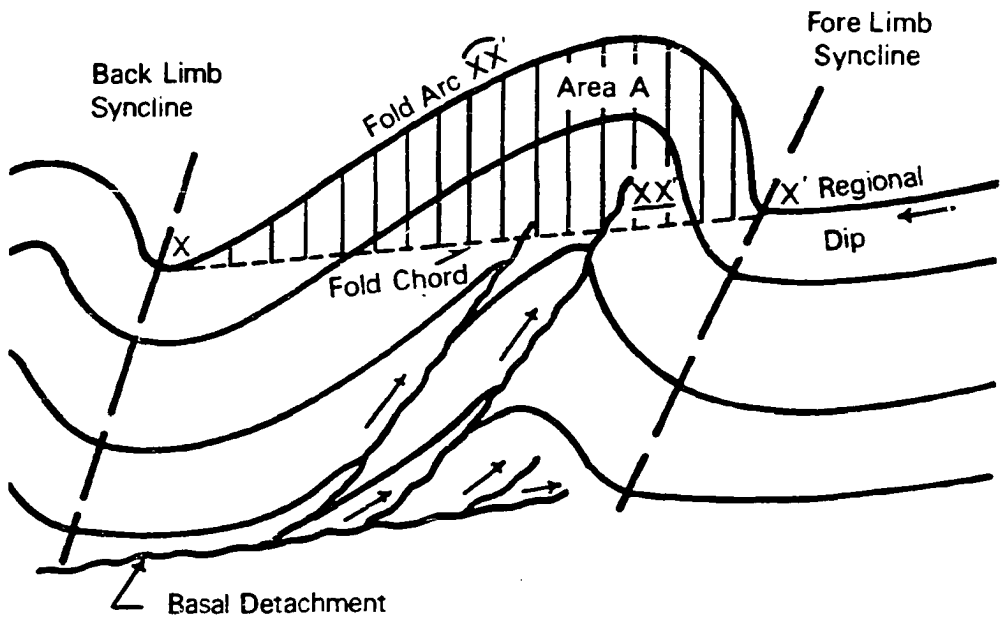

FIGURE D-1. Diagrammatic structural cross section illustrating the basal detachment required by a parallel-folded anticline. Measurement of lengths of fold arc, fold chord, and area between are needed to calculate depth-to-detachment.

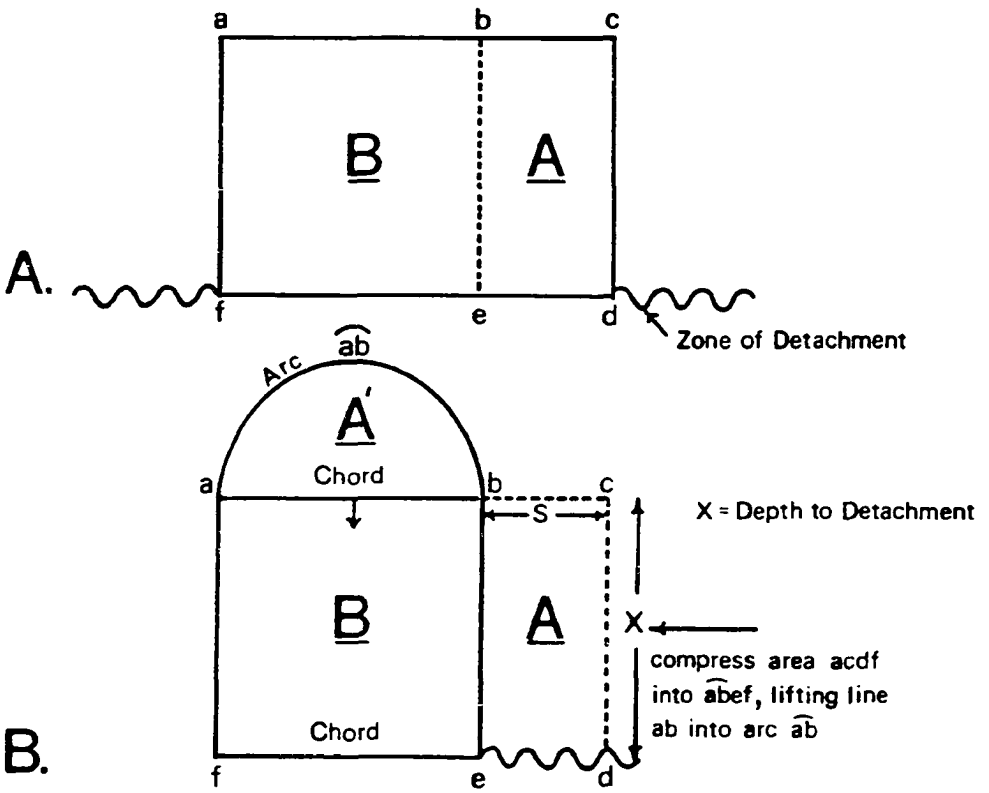

FIGURE D-2. Method for calculation of depth to basal detachment under anticline. A) Line abc represents orignal, pre-deformational length of bedding surface. Area (abcdef) represents the volume of rock above potential basal detachment def. B) Area (abcdef) is compressed into area [befa(Arc ab)] to create the fold. Line abc is lifted into Arc ab, and area (A) is transferred into area (A'). Area (B) remains constant. Amount of shortening (S) is equal to the difference between the original bedding surface length (line abc, or arc ab), and the length of the chord (ab, or ef). Area (A') equals original area (A), and also equals bc times cd (depth to detachment). Depth to the basal detachment equals area (A') divided by bc, the value of shortening (S). Depth to the basal detachment is then plotted below the midpoint of the chord, and perpendicular to it.